

HUNGARIAN

Journal of

INDUSTRIAL

CHEMISTRY

Edited by

the Hungarian Oil & Gas Research Institute (MÁFKI),
the Research Institute for Heavy Chemical Industries (NEVIKI),
the Research Institute for Technical Chemistry of the
Hungarian Academy of Sciences (MÜKKI),
the Veszprém University of Chemical Engineering (VVE).
Veszprém (Hungary)



Volume 4.

1976

Number 1.

CODEN: HJICAI

Editorial Board:

R. CSIKÓS and Gy. MÓZES

Hungarian Oil & Gas Research Institute
(MÁFKI Veszprém)

A. SZÁNTÓ and M. NÁDASY

Research Institute for Heavy Chemical Industries
(NEVIKI Veszprém)

T. BLICKLE and O. BORLAI

Research Institute for Technical Chemistry
of the Hungarian Academy of Sciences
(MÜKKI Veszprém)

A. LÁSZLÓ and L. PÉCHY

Veszprém University of Chemical Engineering
(VVE Veszprém)

Editor-in Chief:

E. BODOR

Assistant Editor:

J. DE JONGE

Veszprém University of Chemical Engineering
(VVE Veszprém)

The "Hungarian Journal of Industrial Chemistry" is a joint publication of the Veszprém scientific institutions of the chemical industry that deals with the results of applied and fundamental research in the field of chemical processes, unit operations and chemical engineering. The papers are published in four numbers at irregular intervals in one annual volume, in the English, Russian, French and German languages.

Editorial Office:

Veszprémi Vegyipari Egyetem
"Hungarian Journal of Industrial Chemistry"
H-8201 Veszprém, P.O. Box: 28
Hungary

Felelős szerkesztő: Dr. Bodor Endre
Kiadásért felelős: Dr. Nemecz Ernő, a VVE rektora
Készült a Váci ÁFESZ nyomdában, Felelős vezető: Kiss János

STUDIES ON THE DYNAMICS OF DOWNWARD COCURRENT GAS-LIQUID
FLOW IN PACKED-BED REACTORS

R. MOHILLA, B. FERENCZ, Mrs. M. VARGA and M. BAKOS

(Veszprém University of Chemical Engineering,
Veszprem, Hungary)

Received: October 4, 1975.

This paper presents the mathematical model describing the dynamic behaviour of a co-current gas-liquid system flowing downward in a packed-bed reactor. Based on the parameters of the reactor, the frequency response characterizing the dynamic behaviour, can be calculated from the mathematical model developed if the disturbing function is a change occurring in input concentration. The way to create this mathematical model, the algorithm used to calculate the characteristic frequency responses, the critical comparison of the calculated and experimental results are presented here.

INTRODUCTION

Packed-bed catalytic reactors with downward flowing gas and liquid phases are not at all uncommon in the practice of chemical industry. However, there are only a few papers dealing with the dynamic behaviour of such operation units although this knowledge is indispensable to design appropriate control for such systems. Previous experiments revealed that the reaction taking place, and even more so, the pore-diffusion process, has little - if any - effect on the dynamic behaviour. Hydrodynamics play the controlling role. Therefore, it seemed worthwhile to develop the mathematical model of an operation unit featuring convective, conductive

and transfer flows. The model was then compared to the experimental results. An attempt was made to obtain the results of both the model and the experiments in such a mathematical form that readily fitted those used in process control calculations. Therefore, the logarithmic amplification vs. angular frequency and the phase vs angular frequency diagrams (Bode-plots) were calculated, respectively.

THE MATHEMATICAL MODEL

The concentration response of a change, carried out in the input concentration, was sought under constant feed conditions. The following assumptions were made to develop the mathematical model:

- a) Mixing in the respective phases of the operation unit can be described by the axially dispersed piston-flow tubular model [1].
- b) Transfer takes place between the fluid phases.
- c) There are two components in the system. One of the components is present in infinite dilution and its transfer has no observable effect on the mass-flow rates of the respective phases.
- d) Only small deviations from the steady state conditions, adequately described by the linearized, constant coefficient differential equation systems, are considered.
- e) Feed and other physical parameters are constant, although they can be functions of the steady state conditions (set-points).
- f) The relationship describing the distribution of the components in question between the two phases is linear within the range studied.
- g) As in the case of the majority of practical problems, it is assumed that the transfer process is controlled at the liquid phase side; and that the transfer can adequately be described by the two-film theory.

It should be noted that it is easy to show that the model can also be applied to describe counter-current and/or gas phase controlled systems, and by appropriate selection of the coefficients, heat-transfer is also implied.

The extended Damköhler equation, relating to the gas phase reads as follows:

$$\begin{aligned} A \epsilon_g D_g \frac{\partial^2 c_g(z,t)}{\partial z^2} - B_g \frac{\partial c_g(z,t)}{\partial z} - \beta \Omega A (c_f^*(z,t) - c_f(z,t)) = \\ = \epsilon_g A \frac{\partial c_g(z,t)}{\partial t} \end{aligned} \quad (1)$$

while to the liquid phase:

$$\begin{aligned} A \epsilon_f D_f \frac{\partial^2 c_f(z,t)}{\partial z^2} - B_f \frac{\partial c_f(z,t)}{\partial z} + \beta \Omega A (c_f^*(z,t) - c_f(z,t)) = \\ = \epsilon_f A \frac{\partial c_f(z,t)}{\partial t} \end{aligned} \quad (2)$$

Distribution of the components between the phases is as follows:

$$c_g = m c_f^* \quad (3)$$

Rearranging Equation (3), c_f^* can be eliminated from Equations (1) and (2).

Considering only small deviations from the steady state condition, it can easily be proved that the equation system is invariant relative to the steady state setting-point conditions. That is to say, it holds even if c_g and c_f are considered as small deviations from the steady state values.

To obtain relationships that are also readily applicable in process control, the Laplace-transformed versions of Equations (1) and (2) are derived, having eliminated c_f^* under zero initial conditions. Introducing appropriate coefficients, the two equations obtained are as follows:

$$\begin{aligned}
 -h_g H_g \frac{d^2 c_g(z,s)}{dz^2} + H_g \frac{dc_g(z,s)}{dz} + (sT_g + 1) c_g(z,s) - \\
 -mc_f(z,s) = 0
 \end{aligned}
 \tag{4}$$

$$\begin{aligned}
 -h_f H_f \frac{d^2 c_f(z,s)}{dz^2} + H_f \frac{dc_f(z,s)}{dz} + (sT_f + 1) c_f(z,s) - \\
 -\frac{c_g(z,s)}{m} = 0
 \end{aligned}
 \tag{5}$$

and the coefficients:

$$h_g = \frac{D_g}{v_g} = \frac{\epsilon_g A D_g}{B_g};$$

$$h_f = \frac{D_f}{v_f} = \frac{\epsilon_f A D_f}{B_f}$$

$$H_g = \frac{mB_g}{\beta \Omega \epsilon_g}$$

$$H_f = \frac{B_f}{\beta \Omega A}$$

$$T_g = \frac{m\epsilon_g}{\beta \Omega}$$

$$T_f = \frac{\epsilon_f}{\beta \Omega}$$

The h and H characteristic length and T characteristic time constants can be traced back to well-known dimensionless numbers, and to the average residence time as follows:

$$Bo_g = \frac{v_g H}{D_g} = \frac{H}{h_g};$$

$$Bo_f = \frac{v_f H}{D_f} = \frac{H}{h_f}$$

$$\frac{St_g}{m} = \frac{\beta \Omega H}{m v_g \epsilon_g} = \frac{H}{H_g};$$

$$St_f = \frac{\beta \Omega H}{v_f \epsilon_f} = \frac{H}{H_f}$$

$$\bar{t}_g = \frac{H}{v_g} = T_g \frac{St_g}{m}; \quad \bar{t}_f = \frac{H}{v_f} = T_f \cdot St_f$$

The solution of equation systems (4) and (5) yields the transfer function of the operation unit at any z length, taken axially from its feed point.

A solution of the form

$$c_g(s) = p(s) e^{\gamma(s)z} \quad (6)$$

$$c_f(s) = q(s) e^{\gamma(s)z} \quad (7)$$

is sought, where $p(s)$ and $q(s)$ are the function of the Laplace variable. Substituting the solutions assumed for equations (4) and (5) and observing that $c_g(s)$ and $c_f(s)$ should suffice them, a fourth-order algebraical equation is obtained for $\gamma(s)$. Let its solutions subsequently be $\gamma_i(s)$, where $i = 1, \dots, 4$.

Let us introduce the formula:

$$p_i(s) = -h_g H_g \gamma^2(s) + H_g \gamma_i(s) + s T_g + 1$$

The general solution is then obtained as:

$$c_g(z, s) = \sum_{i=1}^4 p_i(s) e^{\gamma_i(s)z} \quad (8)$$

$$c_f(z, s) = \frac{1}{m} \sum_{i=1}^4 p_i(s) \cdot p_i(s) e^{\gamma_i(s)z} \quad (9)$$

Let us introduce the following four boundary conditions [2];

$$c_{g0}(s) = c_g(+0, s) - h_g \left(\frac{dc_g(z, s)}{dz} \right)_{z=+0}$$

$$\left(\frac{dc_g(z, s)}{dz} \right)_{z=H} = 0$$

$$z = H$$

$$c_{f0}(s) = c_f(+0, s) - h_f \left(\frac{dc_f(z, s)}{dz} \right)_{z=+0}$$

$$\left(\frac{dc_f(z, s)}{dz} \right)_{z=H} = 0$$

$$z = H$$

Substituting functions (8) and (9) into these four boundary conditions, a linear equation system is obtained and the four unknown $P(s)$ values can be determined from it.

Theoretically, doing so, the transfer function is obtained.

Therefore, the Laplace transforms of the c_g and c_f response functions, corresponding to any c_{g0} , c_{f0} disturbances, be generated in the following form:

$$c_g(z, s) = c_{gg}(z, s) + c_{gf}(z, s)$$

$$c_f(z, s) = c_{fg}(z, s) + c_{ff}(z, s)$$

It is hopeless to attempt the inverse transformation of that expression. Fortunately, as far as the goal is concerned, it is unnecessary. Applying the $s=j\omega$ substitution, the frequency function can be determined at any one point of the operation unit concerned.

The dynamic behaviour of the operation unit studied is characterized by the following four frequency functions:

$$F_1(z_1, j\omega) = \frac{c_{gg}(z_1, j\omega)}{c_{go}(j\omega)} \Big|_{c_{fo} = 0} \quad (10)$$

$$F_2(z_1, j\omega) = \frac{c_{gf}(z_1, j\omega)}{c_{fo}(j\omega)} \Big|_{c_{go} = 0} \quad (11)$$

$$F_3(z_1, j) = \frac{c_{fg}(z_1, j\omega)}{c_{go}(j\omega)} \Big|_{c_{fo} = 0} \quad (12)$$

$$F_4(z_1, j) = \frac{c_{ff}(z_1, j\omega)}{c_{fo}(j\omega)} \Big|_{c_{go} = 0} \quad (13)$$

where the subscript 1 refers to any - distinguished - set-point.

It is obvious from the previous discussion, that there is no theoretical difficulty in calculating the values of the four frequency functions, but a considerable amount of calculation is required.

A computer programme was therefore compiled to calculate the points of the frequency functions or rather, for the sake of direct comparison with the experimental results, the respective points of the corresponding Bode-diagrams.

THE COMPUTING ALGORITHM

The schematics of the computing algorithm is shown diagrammatically on Figure 1. Only a few details of the calculations, requiring special care, are reviewed here.

Such a part of the algorithm is the solution of the characteristic equation of the differential equation systems (4) and (5).

Solutions of a fourth-order equation can be derived either from the appropriate root-formula or by any approximating method. In this case, the problem of selecting the appropriate initial values in the previous case, the not-always-sufficient accuracy of the values computed from the root-formula, arise. Therefore, an improvement can be achieved taking the solutions derived from the root-formula as initial values, assessing their relative errors and refining them to the required level employing the Newton-method.

Special care must be taken not to exceed the permitted (determined) magnitudes of the numbers that the computer is able to process. Note, for example, the equation systems relating to the $p_i(s)$ coefficients of the expressions (8) and (9), Employing appropriate normalization measures, it is possible to keep each of the coefficients and the subtotals of the computation within the permitted range, without deforming the results of the computation, for example, without making them equal to computer-zero due to the fact that their relatively small value is carelessly normalized.

EXPERIMENTAL

A brief outline of the experimental setup and the measurements taken to check the validity of the model developed, are presented here. A detailed account of the experimental procedure will soon follow in another publication.

Experiments were carried out in a vertical tube (i.d. 0.11 m, length, $H=0.91$ m) packed with glass beads (diameter: 3mm) or porous alumina beads of the same size. The specific volume fraction occupied by the liquid phase was characterized from the liquid hold up and the specific void volume fraction values. The specific surface area (Ω) was determined experimentally. The mass transfer coefficient (β) was calculated according to Kafarov [3], and the Bodenstein number according to Hofmann [4]. The phase system studied was an air-water system. Gaseous sulphur dioxide was used as a tracer injected into the gas flow entering the system. Respective sulphur

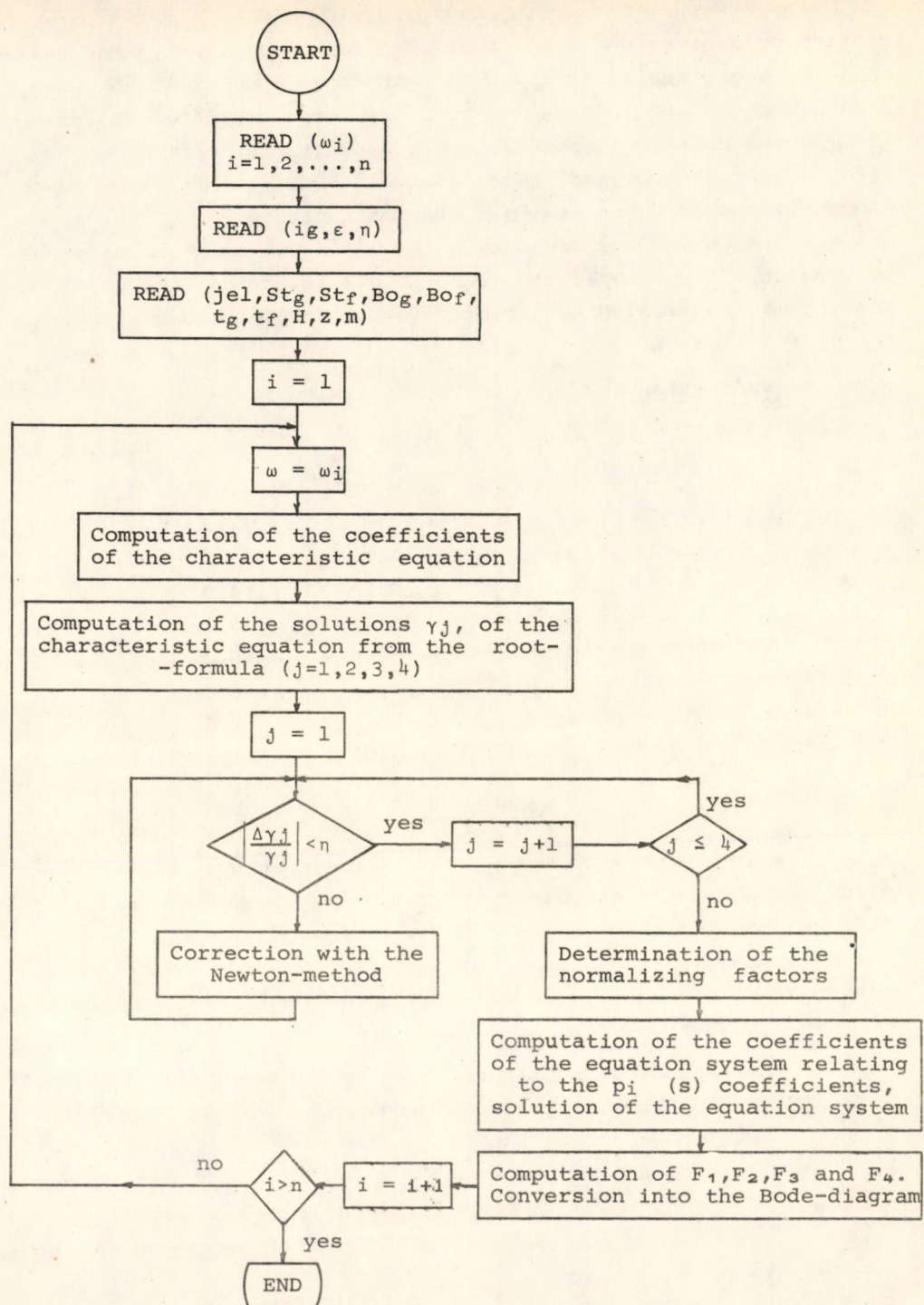


Fig. 1.

dioxide concentrations were monitored at the outlet in the gas-phase by a gas analyzer, and by a conductivity meter in the liquid phase. Signals from these two monitors were amplified and passed to a potentiometric recorder, after appropriate - if necessary - zero offset. A coupled potentiometer, built into the potentiometric recorder, was fed by a constant voltage level, the attenuated voltage was monitored by an RFT 3518.000 data collector and punched onto paper tape. The selected gas injection time was 1 second, it was controlled by a switch-timer, simultaneously triggering the data collector.

Measurements were made in the following range:

Code	J	J
	kg m ⁻² s ⁻¹	kg m ⁻² s ⁻¹
1.	0.1	5.0
2.	0.1	14.0
3.	0.1	25.0
4.	0.5	5.0
5.	0.5	14.0
6.	1.0	2.0
7.	0.01	14.0
8.	1.0	14.0

Data interpretation was made by a computer programme compiled for the ODRA 1024 computer, its computing algorithm was first published by HUSS and DONEGAN [5]. Raw data was taken from the punched tapes. The programme computed the respective points of the Bode-diagram. The results obtained were analysed according to the following points:

- a.) A previously published method [6] was used to predict the duration of the tracer impulse; experiments verified, that the 1 second long pulse can, in practice, be considered as a Dirac impulse.

- b.) Based on experimental values it was concluded that the time constants of the conductivity meter and the potentiometric recorder do not appreciably distort the signal.
- c.) The arithmetic mean values of repeated experiments were used.
- d.) Experiments were carried out to determine the time delays caused by the dead volumes in the gas analyzer and operation unit; these delays were later applied to correct the measured values.
- e.) A computer algorithm, based on a three-successive-points approximation, was used to smooth the flow of data.

Experimental results were compared to those obtained the model. When there is a difference between the time delays of operation unit and measuring system, the experimental results very well fit the computed ones. If the time delays mentioned are approximately of the same magnitude, the results should be viewed in a critical manner, for the dynamics of the analyzer significantly distort the numerical values subjected to numerical correction. In such cases, analyzers of a shorter response time would be desirable

SYMBOLS USED

- A cross section of the operation unit, (m^2)
- B volumetric flow rate, (m^3s^{-1})
- D axial dispersion coefficient of the component, (m^2s^{-1})
- F frequency function
- H length of the operation unit, (m)
- J mass flow density, ($kg\ m^2\ s^{-1}$)
- P general polynomial expression
- T time constant, (s)
- c concentration, ($kg\ m^{-3}$)
- h length, characterizing the dispersion, (m)
- j $\sqrt{-1}$
- m dimensionless Henry coefficient
- p coefficient in general

- q coefficient in general
s variable of the Laplace transformation, (s^{-1})
t time, (s)
 \bar{t} average residence time, (s)
v linear velocity of the convective flow, ($m\ s^{-1}$)
z length co-ordinate, (m)
 β mass transfer coefficient, ($m\ s^{-1}$)
 γ solution of the characteristic equation (m^{-1})
 ϵ specific void volume coefficient
 ω angular frequency, ($rad\ s^{-1}$)
 Ω specific surface area in unit volume, (m^{-1})

SUBSCRIPTS

- g quantity in the gas phase
f quantity in the liquid phase
o initial value
x equilibrium value

Dimensionless quantities

- Bo Bodenstein number
St Stanton number

REFERENCES

1. BAKOS M., MIDOUX N., CHARPENTIER, J.C.: Magyar Kémiai Folyóirat 78, 367 (1971)
2. MOHILLA R., FERENCZ B.: Vegyipari folyamatok dinamikája, (The Dynamics of Chemical Processes) Műszaki Könyvkiadó. Budapest. 1972. 158 pp.
3. KAFAROV, V.V.: Az anyagátadás alapjai. (The Fundaments of Mass Transfer) Műszaki Könyvkiadó. Budapest, 1967.
4. HOFMANN, H.: Chem. Eng. Sci. 14, 193 (1961)
5. HUSS, C.R., DONEGAN, I.I.: NACA Technical Note. 3598. Washington, 1956.
6. MOHILLA R.: Mérés és Automatika. 17, No. 6. 209 (1969)

РЕЗЮМЕ

В настоящей статье излагается математическая модель, описывающая динамическое поведение системы газ-жидкость, стекающей в реакторе с неподвижным слоем катализатора. Зная параметры реактора, с применением представленной математической модели можно вычислить частотную функцию в этом случае, если изменение входной концентрации играет роль воздействия. В статье показывается метод написания математической модели, алгоритм вычисления характерных частотных функций, и дается оценка результатов, полученных при вычислении и экспериментально.

σ -ORGANO TUNGSTEN DERIVATES AS OLEFIN METATHESIS CATALYSTS III*
STUDIES ON CATALYTIC PROPERTIES

L. BENCZE, L. MARKÓ, R. OPITZ** AND K.-H. THIELE**

(Department of Organic Chemistry, Veszprém University
of Chemical Engineering and ** Technische Hochschule
für Chemie, "Carl Schorlemmer", Leuna Merseburg,
Sektion Verfahrenschemeie)

Received: November 12. 1975.

MBz₄ (M=W, Mo, Zr, Ti, U), WBz₃Cl and WPhCl₃ were tested as catalysts in the olefin metathesis reaction alone, and in combination with AlCl₃, EtAlCl₂, AlBr₃ and FeCl₃. All the tungsten compounds, combined with the aluminium containing cocatalysts were active. The activity of the catalytic system was significantly enhanced under CO atmosphere and the formation of tungsten carbonyl derivatives was observed. WPhCl₃ was found to be active in the disproportionation of 2-pentene without any cocatalyst, however, the rate of the reaction was low due to the low solubility of the catalyst. Application of FeCl₃ as cocatalyst, and the tetrabenzyl derivatives of Mo, Zr, Ti and U as catalysts gave catalytically inactive systems in either combination.

INTRODUCTION

Homogeneous catalytic systems used for olefin disproportionation reactions generally consist of a transition metal compound as catalyst, a cocatalyst and a solvent. Occasionally, an activator can also be included. The catalysts applied are mainly molybdenum

*

For Part II see Reference [3].

and tungsten (complex) halides; the cocatalysts are aluminium compounds of marked Lewis-acid character; while the most frequently applied solvents are benzene or chlorobenzene [1-3,7,8].

According to the previous observations [2,3], a few organometallic compounds containing carbon-tungsten σ bonds, are appropriate catalysts for the disproportionation reactions of straight-chain olefins [2,3]. To continue this work, the effect of a limited set of the experimental parameters on the properties of the catalyst was investigated. The parameters studied included the type of starting organometallic transition metal compound, the type of cocatalyst, solvent, cocatalyst/catalyst molar ratio and the application of a carbon monoxide atmosphere.

EXPERIMENTAL

Experiments were carried out in either an argon or carbon monoxide atmosphere. Hydrocarbons were dried refluxing them over sodium-potassium alloy and freshly distilled immediately before use.

Chlorobenzene was dried and stored over phosphorous pentoxide. Experiments were carried out with freshly distilled chlorobenzene.

Tetrabenzyl tungsten and phenyl tungsten trichloride were prepared according to previously described methods [4,5].

Tribenzyl tungsten chloride was prepared, treating tetrabenzyl tungsten with hydrochloric acid. Its purity was as high as 95 per cent [6].

Catalytic experiments were carried out with $1 \cdot 10^{-4}$ moles of the organometallic compounds and the corresponding amounts of cocatalysts, with 15 mls of solvents, 5 mls of the olefin and 5 mls of an internal standard. To follow the conversion rate of the olefin, the reaction mixture was sampled at appropriate time intervals. Methanol was applied to stop any further progress of the reaction in the samples taken.

Experimental parameters are summarized in Table I.

Tetrabenzyl Derivates of Transition Metals (MBz_4)

Tetrabenzyl tungsten alone was inactive within the ranges of the experimental parameters studied. However, in benzene or chlorobenzene solutions, WBz_4 combined with aluminium halides acts as an active disproportionating catalyst. Catalytic activity was observed at an aluminium/tungsten molar ratio as low as $\text{Al/W}=1.5$; which is an unusually low value. The characteristic "S" shape of the conversion vs. time diagrams refer to a definite induction period, including the time required for the catalyst formation. An increase in the molar ratio shortens the duration of the induction period and eventually at an Al/W ratio of 10, the induction period completely disappears. In the midrange, between the 10 to 40 per cent conversion values, the curves ran fairly parallel, which means, that apart from the induction period, catalytic activity of the systems studied was fairly constant once the $\text{Al/W}=4$ value was exceeded (Figure 1).

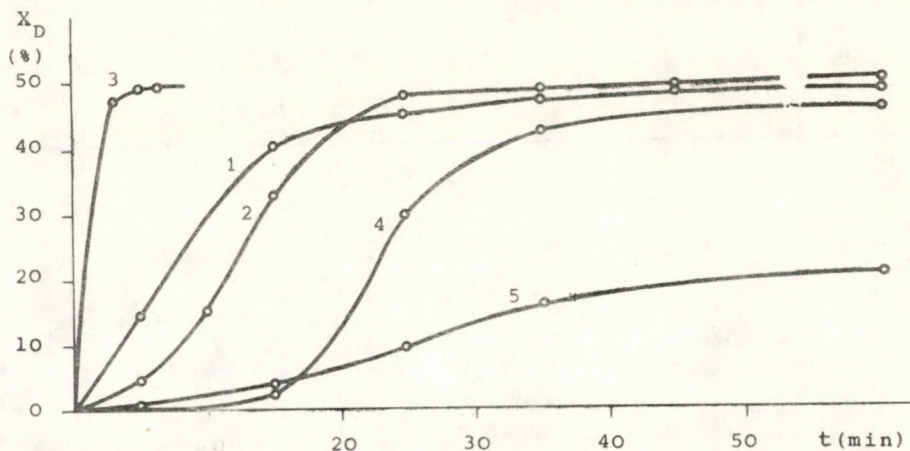


Fig.1. Effect of the molar ratio on the disproportionation rate of 2-pentene in the $\text{WBz}_4\text{-AlCl}_3$ -chlorobenzene system.
1 - N°2; 2 - N°5; 3 - N°8; 4 - N°6; 5 - N°7.

Table 1. Summary of the experimental conditions

N°	Catalyst	Cocatalyst	Molar ratio Al(Fe)/W	Activator	Olefin	Solvent	Internal standard
1	W(CH ₂ C ₆ H ₅) ₄	-	-	-	2-pentene	benzene	n-pentane
2	W(CH ₂ C ₆ H ₅) ₄	AlCl ₃	10	-	2-pentene	benzene	n-pentane
3	W(CH ₂ C ₆ H ₅) ₄	AlCl ₃	8.5	-	2-pentene	benzene	n-pentane
4	W(CH ₂ C ₆ H ₅) ₄	AlCl ₃	8.3	-	2-pentene	benzene	n-pentane
5	W(CH ₂ C ₆ H ₅) ₄	AlCl ₃	5.8	-	2-pentene	benzene	n-pentane
6	W(CH ₂ C ₆ H ₅) ₄	AlCl ₃	4.4	-	2-pentene	benzene	n-pentane
7	W(CH ₂ C ₆ H ₅) ₄	AlCl ₃	1.5	-	2-pentene	benzene	n-pentane
8	W(CH ₂ C ₆ H ₅) ₄	AlCl ₃	6.4	CO	2-pentene	benzene	n-pentane
9	W(CH ₂ C ₆ H ₅) ₄	AlCl ₃	2.9	-	2-pentene	chlorobenzene	n-pentane
10	W(CH ₂ C ₆ H ₅) ₄	AlCl ₃	5.9	-	2-pentene	chlorobenzene	n-pentane
11	W(CH ₂ C ₆ H ₅) ₄	EtAlCl ₂	6.2	-	2-pentene	benzene	n-pentane
12	W(CH ₂ C ₆ H ₅) ₄	AlBr ₃	3.2	-	2-pentene	benzene	n-pentane
13	W(CH ₂ C ₆ H ₅) ₄	AlBr ₃	3.0	-	2-pentene	chlorobenzene	n-pentane
14	W(CH ₂ C ₆ H ₅) ₄	AlBr ₃	5.0	-	2-pentene	chlorobenzene	n-pentane
15	Mo(CH ₂ C ₆ H ₅) ₄	-	-	-	2-pentene	benzene	n-pentane
16	Mo(CH ₂ C ₆ H ₅) ₄	AlCl ₃	8.0	-	2-pentene	benzene	n-pentane
17	Mo(CH ₂ C ₆ H ₅) ₄	AlCl ₃	10.0	-	2-pentene	benzene	n-pentane
18	Mo(CH ₂ C ₆ H ₅) ₄	AlCl ₃	10.0	CO	2-pentene	benzene	n-pentane
19	Mo(CH ₂ C ₆ H ₅) ₄	EtAlCl ₂	10.0	-	2-pentene	benzene	n-pentane
20	Mo(CH ₂ C ₆ H ₅) ₄	FeCl ₃	10.0	-	2-pentene	benzene	n-pentane

Table 1. (continued)

No	Catalyst	Cocatalyst	Molar ratio Al(Fe)/W	Activator	Olefin	Solvent	Internal standard
21	Ti(CH ₂ C ₆ H ₅) ₄	AlCl ₃	10.0	-	2-pentene	benzene	n-pentane
22	Ti(CH ₂ C ₆ H ₅) ₄	EtAlCl ₂	10.0	-	2-pentene	benzene	n-pentane
23	Zr(CH ₂ C ₆ H ₅) ₄	AlCl ₃	10.0	-	2-pentene	benzene	n-pentane
24	Zr(CH ₂ C ₆ H ₅) ₄	EtAlCl ₂	10.0	-	2-pentene	benzene	n-pentane
25	U(CH ₂ C ₆ H ₅) ₄	AlCl ₃	10.0	-	2-pentene	benzene	n-pentane
26	WCl(CH ₂ C ₆ H ₅) ₃	-	-	-	2-pentene	benzene	n-pentane
27	WCl(CH ₂ C ₆ H ₅) ₃	FeCl ₃	10.0	-	2-pentene	benzene	n-pentane
28	WCl(CH ₂ C ₆ H ₅) ₃	AlCl ₃	9.0	-	2-pentene	benzene	n-pentane
29	WCl(CH ₂ C ₆ H ₅) ₃	AlCl ₃	8.0	-	cyclohexene	benzene	cyclohexane
30	WCl ₃ Ph	-	-	-	2-pentene	benzene	n-pentane
31	WCl ₃ Ph	AlCl ₃	7.0	-	2-pentene	benzene	n-pentane
32	WCl ₃ Ph	AlCl ₃	6.4	-	2-pentene	benzene	n-pentane
33	WCl ₃ Ph	AlCl ₃	6.7	CO	2-pentene	benzene	n-pentane
34	WCl ₃ Ph	AlCl ₃	1.9	CO	2-pentene	benzene	n-pentane
35	WCl ₃ Ph	EtAlCl ₂	10.0	-	2-pentene	benzene	n-pentane
36	WCl ₃ Ph	EtAlCl ₂	4.0	-	2-pentene	benzene	n-pentane
37	WCl ₃ Ph	AlBr ₃	10.0	-	2-pentene	benzene	n-pentane
38	WCl ₃ Ph	AlBr ₃	3.7	-	2-pentene	benzene	n-pentane
39	WCl ₃ Ph	FeCl ₃	10.0	-	2-pentene	benzene	n-pentane

Increasing the amount of the aluminium chloride decreased the selectivity of the reaction. This decrease was especially marked above the 40 per cent conversion values (Figure 2.)

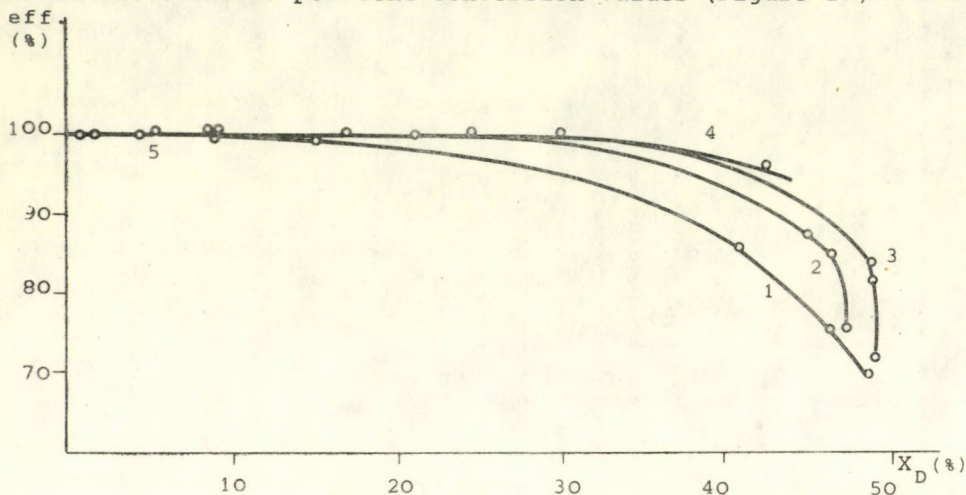
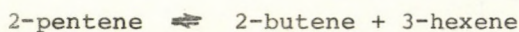


Fig.2. Change of the selectivity of the reaction as a function of 2-pentene conversion
1 - N°2; 2 - N°4; 3 - N°5; 4 - N°6; 5 - N°7.

Having reached the equilibrium conversion of the reaction:



the cis/trans isomer ratios of the initial and the produced olefins are in agreement with the thermodynamical value. If the cocatalyst applied was EtAlCl_2 , the disproportionation reaction started with a rather high reaction rate, but at about 8 per cent conversion of the 2-pentene, the reaction came to a halt. In such systems even the cis/trans isomerization reaction was blocked and the cis isomer content of the olefin produced was considerably higher than the corresponding thermodynamical value. The explanation probably lies in the transalkylation reactions of the metal compounds, in which tungsten compounds are formed, having neither disproportionation, nor cis/trans isomerization catalytic activity.

The catalytic disproportionate activity and the selectivity of the catalyst combinations containing AlBr_3 is much poorer than

of those containing AlCl_3 . This effect was especially marked at higher (over about 10) molar ratios. The alkylating activity of the catalyst significantly increased while the rate of the disproportionation remained low. When the more stable chlorobenzene was used as a solvent, the alkylation rate was somewhat repressed but the disproportionation rate was still poorer than in the systems containing AlCl_3 (Figure 3).

Studying the effect of solvents no significant difference was found between benzene and chlorobenzene, except that the induction period was somewhat longer if the solvent was chlorobenzene (Figure 4).

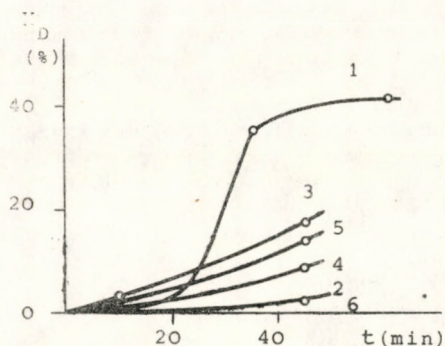


Fig. 3 Effect of AlBr_3 on the reaction rate

(1 - N°9; 2 - N°12;
3 - N°13; 4 - N°14;
5 - N°37; 6 - N°38)

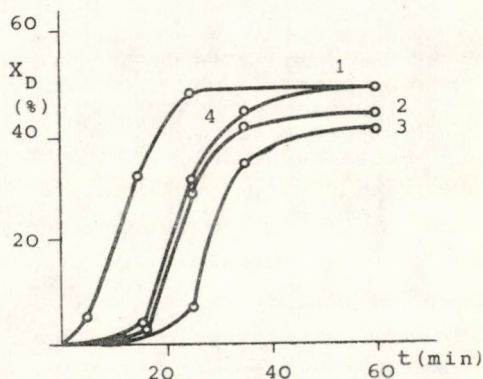


Fig. 4. Effect of the solvent on the reaction rate

(1 - N°4; 2 - N°6;
3 - N°9; 4 - N°10)

Tetrabenzyl derivatives of Mo, Zr, Ti and U were also studied and were found to exhibit no activity at all. In this respect the inactivity of the Mo compound was somewhat surprising since the molybdenum nitrosyl complexes are widely used components of disproportionating catalyst combinations [7].

Tribenzyl tungsten chloride (WBz_3Cl)

Based on the assumption that catalytically active derivatives are formed in the transalkylation reaction of tetrabenzyl

tungsten and AlCl_3 , experiments were initiated to produce a tungsten organometallic compound of higher halogenid content and to test its catalytic activity.

Tribenzyl tungsten chloride alone did not catalyse the disproportionation of 2-pentene, however, in combination with AlCl_3 , it proved to be more active than the tetrabenzyl tungsten combination at the same molar ratios (Figure 5).

The "ring opening" polymerization reaction of cyclohexene was also attempted with that catalyst. However, in a similar manner to any other catalyst known so far, the system studied, failed.

Phenyl tungsten trichloride (WPhCl_3)

Applying phenyl tungsten trichloride as a catalyst, the first linear olefin disproportionation system was obtained, consisting of a single, organic transition metal compound, that required no activation by a cocatalyst or UV irradiation. Benzene and chlorobenzene solubility of the catalyst was rather low, therefore, the relatively low conversion values (10 per cent in 18 hours) detected, in fact corresponded to a rather high catalytic activity. The addition of AlCl_3 increased the solubility of the compound and obviously also the catalytic activity of the solution obtained. The induction period of the conversion vs. reaction time curves practically disappeared and the curves closely approached those obtained with tetrabenzyl tungsten at higher molar ratios ($\text{Al/W}=10$), plotted on Figure 5. With EtAlCl_2 as a cocatalyst, a catalytically inactive system was obtained. The reaction product of the metallic compound settled out from the system as a black precipitate. Due to its high alkylating activity, the composition containing AlBr_3 was unsuitable as a disproportion catalyst. Measurable disproportion activity could be detected only at low molar ratios ($\text{Al/W}=3-4$), but even then, the selectivity of the reaction never exceeded the 10 per cent level. Attempts were made to substitute FeCl_3 for the AlCl_3 as a cocatalyst, but no catalytic activity was ever observed with any of the compounds tested.

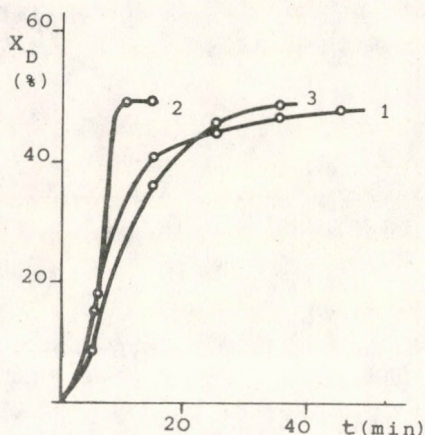


Fig. 5 Effect of the type of the tungsten derivative on the reaction rate
(1 - N°2; 2 - N°28
3 - N°32)

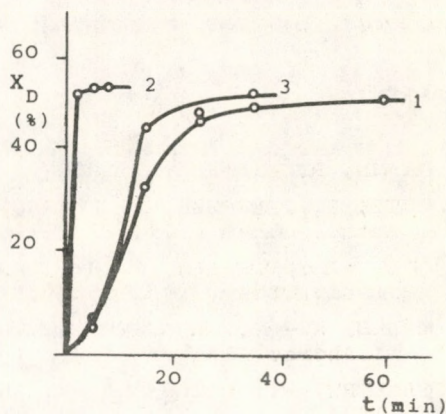


Fig. 6 Effect of the carbon monoxide atmosphere on the reaction rate
(1 - N°30; 2 - N°33;
3 - N°34)

Carbon monoxide activation of the catalysts

Previously it was found that carbon monoxide significantly enhanced the activity of the olefin disproportionating catalyst combinations, consisting of tungsten (carbonyl) halogenid complexes and alkyl aluminium halides [8]. The conclusion that the activating effect of carbon monoxide was valid over a much broader field, can be drawn from the results presented here. Namely, the catalytic activity of any combinations consisting of a sigma-organo-tungsten derivative and of AlCl_3 , is significantly enhanced in CO atmosphere (Figures 1 and 6). Carbon monoxide activation is of major significance, because, while maintaining high activity, lower molar ratios can be applied, thereby the rate of olefin consumption side reactions, requiring higher Lewis-acid concentrations, can be decreased. In the IR spectra of CO activated reaction mixtures prepared from either WBz_4 or WPhCl_3 , a strong absorption band can be

observed at 1980 cm^{-1} . This band is assigned to the $\text{Wo}(\text{CO})_6$, formed in the reaction mixture. A few weaker absorption bands occurring in the carbonyl region, also indicate the presence of other carbonyl compounds. However, attempts to identify them failed.

REFERENCES

1. HAINES, R. J. and LEIGH, G.J.: Chem Soc. Rev., 4, 155 (1975)
2. OPITZ, R., BENCZE, L., MARKÓ, L. and THIELE, K.-H.: J. Organometal. Chem., 71, C3 (1974)
3. OPITZ, R., THIELE, K.-H., BENCZE, L. and MARKÓ, L.: J. Organometal. Chem., 96, C53 (1975)
4. THIELE, K.-H., ROUSSEK, A., OPITZ, R., MOHAI, B. and BRÜSER, W.: Z. Anorg. Allg. Chem., 412, 11 (1975)
5. GRAHLERT, W., MIŁOWSKI, K. and LANGBEIN, M.: Z. Chem., 14, 287 (1974)
6. THIELE, K.-H.: unpublished results
7. ZUECH, E. A., HUGHES, W. B., KUBICEK, D. H. and KITTELMAN, E.: J. Amer. Chem. Soc., 92, 528 (1970)
8. BENCZE, L. and MARKÓ, L.: J. Organometal. Chem., 28, 271 (1971)

РЕЗЮМЕ

Соединения MBz_4 ($\text{M} = \text{W}, \text{Mo}, \text{Zr}, \text{Ti}, \text{U}$), WBz_3Cl и WPhCl_3 были изучены в качестве катализатора при реакции обменного разложения олефинов и отдельно и в комбинации с соединениями AlCl_3 , EtAlCl_2 , AlBr_3 и FeCl_3 . Все соединения вольфрама в сочетании с комбинированными катализаторами, содержащими алюминий оказались активными. Активность каталитических систем значительно повышалась в атмосфере CO , и наблюдалось образование карбонильных производных вольфрама. WPhCl_3 оказался активным при диспропорционировании 2-пентена без некоторого вспомогательного катализатора, однако же скорость реакции была низка, соответственно низкой растворимости катализатора. С применением FeCl_3 в качестве вспомогательного катализатора и тетрабензильных производных Mo , Zr , Ti и U в качестве катализатора комбинирующие друг с другом каталитические системы не получились.

ANWENDUNGSBEREICH UND WIRTSCHAFTLICHKEIT DER ROTATIONS-
DÜNNSCHICHTAPPARATE

I. GRESZ

(CHEMIMAS, Budapest)

Eingegangen am 1. August 1975

Mit der Verbreitung der Rotations-Dünnschichtapparate verbreiten sich nicht gleichmäßig die Kenntnisse über die optimalen Betriebsmöglichkeiten, Wirtschaftlichkeit der Apparate, die zweifellos vielseitig sind, und zahlreiche vorteilhaften Eigenschaften aufweisen können.

Es ist den erwähnten Mangelhaftigkeiten anzurechnen, daß eine hohe Zahl von Investitions- und Betriebsfachleuten entweder "für die Dünnschichtapparate" oder "gegen die Dünnschichtapparate" sind, während die Ersteren die Dünnschichtapparate - mit der Überspitzung der Vorteile, für jeden Zweck, die Letzteren mit dem Aufwerfen von grundlosen Problemen, für keinen Zweck anwenden wollen.

In diesem Vortrag möchte ich - auf Grund der ungarischen Entwicklungs-, Forschungs- und Betriebserfahrungen - mindestens teilweise die folgenden Fragen beantworten:

- in welchem Anwendungsbereich
- auf welchen Gebieten
- mit welchem Kostenaufwand

lohnt sich Dünnschichtapparate in Betrieb zu setzen?

ANWENDUNG UND WIRTSCHAFTLICHKEIT DER ROTATIONS-DÜNNSCHICHTAPPARATE

Auf mehreren Gebieten der chemischen Industrie ist es endlich soweit gekommen, daß die Rotations-Dünnschichtapparate nun nicht mehr mißtraurisch abgelehnt werden.

Heute geht es nicht mehr um die Frage, ob diese Apparate eingesetzt werden sollen, sondern eher darum, zu welchem Zweck und mit welchem Kostenaufwand sich der Einsatz der Rotations-Dünnschichtapparate vertreten läßt.

EINSATZBEREICH

Im Zusammenhang mit den Rotations-Dünnschichtapparaten stellen Betriebsingenieure vor allem die Frage nach der Leistung. Diese Frage ist offen gestanden durchaus berechtigt: ihre Beantwortung scheint aber lediglich in Kenntnis des zu verarbeitenden Materials möglich zu sein. Aus dem Gesichtspunkt der Wirtschaftlichkeit wäre es aber durchaus notwendig, die Leistung des Apparates bereits in der ersten Phase der perspektivischen Planung mitzuberechnen. Um den geschilderten Widerspruch aufzulösen, seien hier vorerst einige Begriffe geklärt. Betrachten wir erstens einmal den Ersatzbereich.

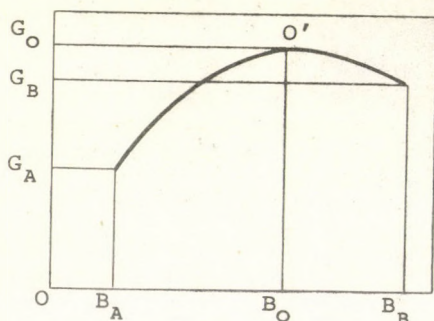


Abb. 1. Anwendungsbereich des Rotations-Dünnschichtapparates, $G = f(B)$

sowie auch von den Eigenschaften des verarbeiteten Materials um 0,5 - 0,7 festlegen.

Der Zusammenhang $G = f(B)$ verläuft bei den für Verdampfungszwecke eingesetzten Rotations-Dünnschichtapparaten etwa wie es in Abbildung 1 dargestellt ist. - Obwohl der Kurvenverlauf von der Skalenteilung der Koordinatenachsen stark beeinflusst wird, - läßt sich der Wert von $\frac{G_0}{B_0}$ anhand von zahlreichen Messergebnissen (eigenen, sowie aus der Fachliteratur genommenen Daten) abhängig von der Betriebsart, (im Vakuum oder beim atmosphärischen Druck)

Es kann ferner festgestellt werden, daß der Kurve $G = r(B)$ im Punkt "A" $B_A = G_A$ ist. Das bedeutet mit anderen Worten, daß die eingespeiste Flüssigkeitsmenge restlos evaporiert wurde. Bei trocken-substanzhaltigen oder in Form von Schmelzen ausgetragenen Endkonzentraten ist der Punkt "A" vom ausgehenden Gewichtsprozent K_0 des Trockensubstanzgehaltes abhängig, der nur angenähert aber nicht erreicht werden kann. Den Punkt "B" kann man theoretisch auf jeder beliebigen Stelle aufnehmen, in der Praxis muß er aber bei etwa $\frac{G_B}{B_B} \approx 0,47 - 0,5$ liegen um das Überfluten (flooding) des Gerätes vermeiden zu können.

Die für die Einspeisung - Verdampfung zwischen $0 - B_B$ und $G_0 - G_A$ - gegebene Grenzwerte bestimmen den Einsatzbereich laut meiner Interpretation.

Zwecks ausführlicherer Untersuchung der Funktionen Typ $G = f(B)$ wurden die Ergebnisse von etwa 35 Versuchserien für Verdampfung von Wasser, Obstsaften, Enzymlösungen - unter Vakuum und in atmosphärischem Druck - verglichen. Die Untersuchungen habe ich mit graphischer Methode durchgeführt; so, daß - in einem beliebigen Koordinatensystem - die aus den Ergebnissen der Versuche sich ergebenden Punkte $B_0 - G_0$ immer auf den identischen Ort gelegt wurden. Bei dem Aufzeichnen wurde die Skalenteilung der Koordinatenachsen geändert.

Auf die so erhaltene Kurvenschar läßt sich die Hüllkurve

$$y = \frac{x}{x^3 + 1}$$

aufzeichnen, beziehungsweise bei atmosphärischer Verdampfung deren mit 15° verdrehte Abbildung, bei der die Maximumwerte ebenfalls bei dem schon erwähnten $B_0 - G_0$ Punkt festgelegt sind.

Aus dieser Erkenntnis ausgegangen habe ich meine annähernde Rechnungsmethode entwickelt.

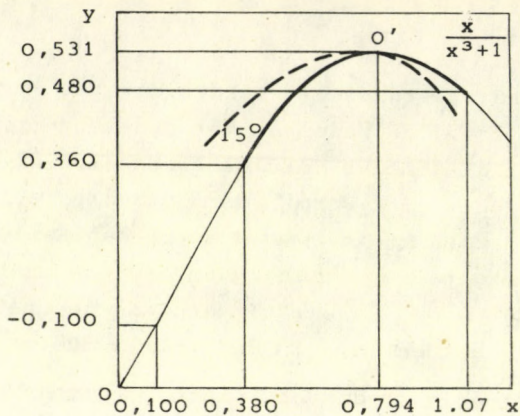


Abb. 2. Die Funktion $y = \frac{x}{x^3+1}$

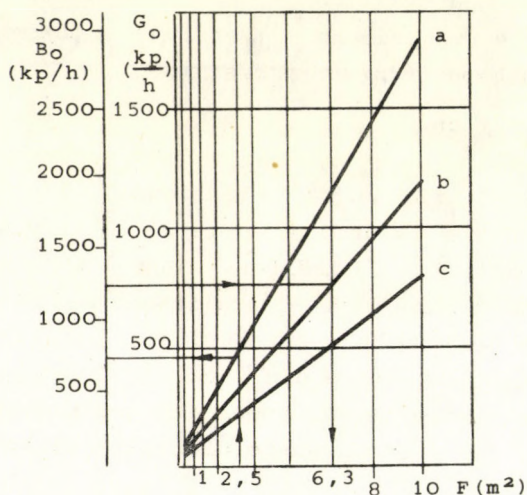


Abb. 3. Die Relation zwischen der maximalen Dampfmenge und dem ihr zugehörigen Einspeisungswert, B - G zusammengehörige Wertpaare.

"a" - Obere Leistungsgrenze des Dünnschichtapparates im Vakuumbetrieb, für wasserartige Stoffe, Δt 70 °C. Umfangsgeschwindigkeit des Rotors mit beweglichen Wischern $\sim 6/\text{sec}$.

"b" - Untere Grenze der Vakuumverdampfung, obere Grenze der atmosphärischen Verdampfung; im ersteren Falle für dicke, klebrige, schwer verdampfende Stoffe, im letzteren Fall für wasserartige Stoffe. Betriebsparameter wie oben.

"c" - Untere Grenze der atmosphärischen Verdampfung von dicken, klebrigen, schwer verdampfenden Stoffen. Betriebsparameter, wie oben.

Im diesen Fall soll die Funktionsverbindung also nicht bedeuten, daß die Werte B und G aus der mit entsprechenden Einsetzungen berechnet werden können, sondern nur das, daß sie durch ihren Verlauf ein geeignetes Hilfsmittel für die Verfolgung des in einem Dünnschichtverdampfer sich abspielenden Verdampfungsprozesses ist.

Der Verlauf des funktionellen Zusammenhanges, sowie sein Nutzwertbereich sind in Abbildung 2 dargestellt.

Die Funktion kann auch zur Veranschaulichung von atmosphärischen Verdampfungsprozessen herangezogen werden: sie ist lediglich um ihren Höchstpunkt P (0,794; 0,531) in Uhrzeigerrichtung um 15° zu verdrehen. Die so erhaltene Kurve ist in Abbildung 2 mit gestrichelter Linie dargestellt.

Die soeben erörterten Zusammenhänge sind zur Zeit nur empirisch erarbeitet worden: sie liefern aber einen sehr einfachen Behelf für die graphische Darstellung des Zusammenhanges $G = f(B)$ bei Dünnschichtapparaten verschiedener Kapazität, und somit für die Vorausberechnung des optimalen Betriebspunktes ebenfalls.

In Abbildung 3 sind die zusammengehörigen Wertpaare $B_0 - G_0$ für die Rotations-Dünnschichtapparate mit beweglichen Wischern "UNIFILM" in Funktion ihrer Heizflächen und Verarbeitungsart angeführt.

Anhand der Abbildung 3 können folgende Fragen beantwortet werden:

- welche Einspeisungs- und Verdampfungsvolumina bei einem gegebenen Apparat, bei Spitzenleistung, im Laufe der Verarbeitung eines gegebenen Materials zu erwarten sind?

(Hilfslinie Nr. 1)

- Welche Apparatgröße für die Verarbeitung einer gegebenen Materialmenge mit gegebenen Eigenschaften zu wählen ist?

(Hilfslinie Nr. 2)

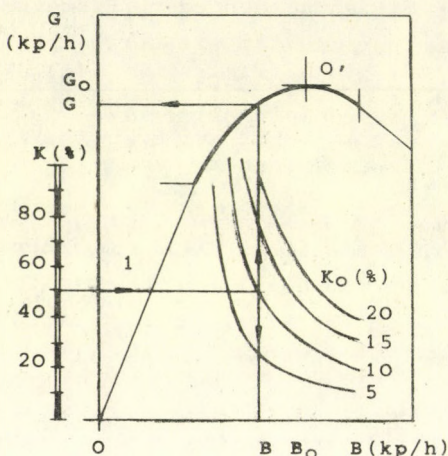


Abb. 4. Nomogrammformular
für $G = f(B)$ in Vakuum-
betrieb

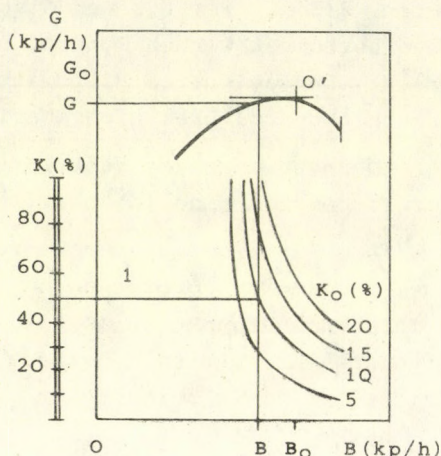


Abb. 5. Nomogrammformular
für $G = f(B)$ in atmosphä-
rischem Betrieb

Anhand der aus Abbildung 3 gewonnenen Angaben wird eine in beliebigem Maßstab konstruierte Kurve $\frac{x}{x^3+1}$ aufgrund der Strecken $O-B_0$ und $O-G_0$ aus Abbildung 4 und 5 kalibriert. Aus den gewonnenen Angaben ergibt sich mit guter Annäherung der Einsatzbereich des gewählten Apparates.

Abbildung 4 bezieht sich auf Vakuumverdampfung, und Abbildung 5 gilt für den Fall der atmosphärischen Verdampfung.

Zu den Abbildungen 4 und 5 sei bemerkt, daß die Abweichung der Kurven vom Verlauf des reellen Verdampfungsprozesses ausgehend von Punkt "O" in Richtung der größeren Einspeisungswerte hin zunimmt, und zwar darum, weil im reellen Verdampfungsverfahren nach einem, dem Punkt "O" entsprechenden Maximum anschließend eine kurze, etwas abfallende aber nahezu gerade Strecke folgt. Da aber diese gerade Strecke in allgemeinen nur bei verhältnismäßig selten vorkommt, läßt sie sich ohne weiteres auch vernachlässigen.

Die Hilfslinien, welche in den Abbildungen unten gezeigt sind, werden dann benützt, wenn es um die Trochensubstanzerhöhung des verarbeiteten Materials geht.

(Das Einzeichnen der Hilfslinien erfolgt aufgrund des Zusammenhanges $G \propto B \left(1 - \frac{K_0}{K}\right)$ mittels Werttabelle.)

Zum Beispiel:

Es soll die Verdampfungsfähigkeit eines Dünnschichtapparates mit beweglichen Wischern und einer Heizfläche von $2,5 \text{ m}^2$ für das leichtflüchtige, wasserähnliche Medium unter Vakuum bestimmt werden.

Der Schnittpunkt der Hilfslinie 1 (Abbildung 3) mit der Linie "a" gibt das gewünschte Ergebnis:

$$G_0 = 460 \text{ kp/h, wenn } B_0 = 570 \text{ kp/h}$$

Wenn man für atmosphärische Verarbeitung eines Mediums ähnlicher Eigenschaften, und mit einer gegebenen Menge (z.B. $B_0 = 1250 \text{ kp/h}$) die nötige Heizfläche des Dünnschichtapparates sucht; dann ergibt's sich für die erwartende Leistung: $G_0 = 760 \text{ kp/h}$.

Auf Grund der erhaltenen Ergebnisse kann die aus dem Zusammenhang $G = f(B)$ eines Dünnschichtapparates sich gegebene Kurve folgenderweise aufgetragen werden; die Strecke $O-B_0$ der Koordinatenachse der Abbildungen wird als 570, beziehungsweise 1250, die Strecke $O-G_0$ als 460, beziehungsweise 760 Einheit betrachtet werden.

Auf solcher Weise sind die Wertepaare G, B für den ganzen Betriebsbereich eines gegebenen Dünnschichtapparates bekannt.

Somit verfügen wir nun über die Angaben, welche unter Heranziehung von einigen zweckgerechten Behelfen bereits genügen um die Berechnungen über die Wirtschaftlichkeit des Dünnschichtapparates mit guter Annäherung zu erstellen und die eingangs gestellte Frage nach der Leistung zu beantworten.

WIRTSCHAFTLICHKEIT

Wird den Investitionsfachleuten die Information über Leistung und Kaufpreis eines Dünnschichtapparates auf den Tisch gelegt, so kommt es häufig, daß sie das Vorhaben kurz und bündig mit dem Urteil ablehnen: es ist "zu teuer".

Diese Feststellung trifft zwar zu, doch steckt dahinter oft ein Irrtum: entscheidend ist dabei nämlich stets der gegebene Anwendungszweck, sowie die herangezogene Vergleichsbasis.

Wird lediglich der Kaufpreis an sich berücksichtigt, so ist es klar: zu dem Preis kann man einen viel größeren herkömmlichen Röhreneindampfer beschaffen. Es bedarf keiner weiteren Auseinandersetzung, daß ein Dünnschichtapparat für die Verarbeitungszwecke, welche auch mit einem Röhreneindampfer durchgeführt werden können, überflüssig ist. Die beiden Apparate gehören nicht in dieselbe Kategorie: sie lassen sich einfach nicht vergleichen.

Die Rotations-Dünnschichtapparate sind Sondereinrichtungen, deren Einsatz in der chemischen Industrie nur in gewissen Fällen zweckgerecht ist. In diesen gewissen Sonderfällen sind sie aber, außerordentlich wirtschaftlich.

Bevor eine Erörterung der meines Erachtens wichtigen Kriterien der Wirtschaftlichkeit aufgeführt würde, möchte ich anhand einiger konkreten Investitionsangaben und informativen Kostenfaktoren eine Grundlage für die vorherige Investitionsplanung liefern.

Der wichtigste Gesichtspunkt, der nicht nur aus geschäftspolitischen, sondern auch aus technischen Gründen wesentlich ist, lautet wie folgt:

Es ist durchaus nicht gerechtfertigt einen Einzel-Dünnschichtapparat nur darum zu kaufen, um Einsparungen bei der einmaligen Investition erreichen zu können.

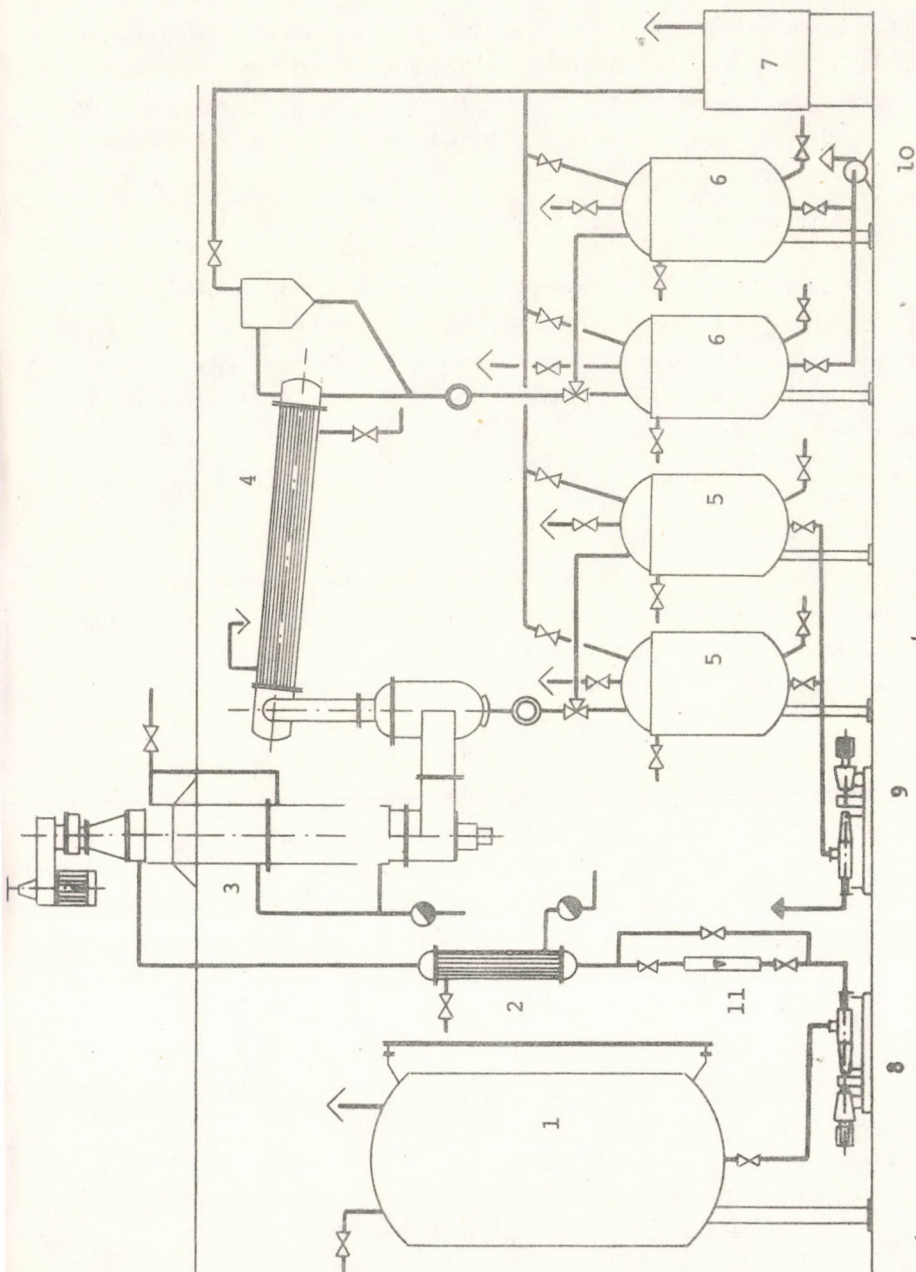


Abb. 6. Komplette Dünnschichtanlage UNIFILM, für Gleichstrom, mit Fallfilm.

- 1 - Behälter; 2 - Vorwärmer; 3 - UNIFILM-Apparat; 4 - Kondensator;
 5 - Konzentratsammler; 6 - Kondensatsammler; 7 - Vakuumpumpenaggregat;
 8 - Dosierpumpe; 9 - Konzentratpumpe; 10 - Kondensatpumpe;
 11 - Dosierungskontrolle

Die mit großer Fachkenntnis ausgelegten Hilfseinrichtungen sichern die Kontinuität und die optimale Leistung des Betriebs. Die Auffassung, wonach die Hilfseinrichtungen auch selbst gebastelt werden können, führt nur zu oft zu Fehllösungen, und nach einem halben Jahr kann z.B. durch einen zu kleinen Kondensator auf der Vakuumseite so viel Lösungsmittel verschwindet werden, daß die Kosten einer kompletten Dünnschichtanlage allein daraus bereits amortisiert wären.

In Abbildung 6 wird eine schematische Darstellung aller bestandteile einer kompletten Anlage gezeigt, so wie sie in unserem Lande am häufigsten vorkommt; Abweichungen sind möglich, dennoch soll hier an diesem Beispiel eine Erörterung der Investitionskosten vorgenommen werden.

Ein weiterer wesentlicher Faktor aus der Sicht der Investitionsplanung liegt in der Wahl der Betätigung: ob sie von Hand aus, halbautomatisch oder automatisch durchgeführt werden soll. Aus Abbildung 8 ist es klar und deutlich zu sehen, daß die Mehrkosten der eingebauten automatischen Steuerung aus den Einsparungen an zusätzlichen Kosten amortisiert werden, - und dabei sind die aus dem höheren Gütestandard und der geringeren Störanfälligkeit herführenden Vorteile noch gar nicht berücksichtigt. (Der Berechnungen wurden vorhandene Versorgungsleitungen und Gebäude zugrunde gelegt: die Montage kann mittels einiger einfachen Stahlkonstruktionen erfolgen. Die automatischen Steuerelemente regeln vor allem die wichtigsten Parameter: den Heizdampf, beziehungsweise die Dosiereinrichtung, um die Temperatur des Konzentrats oder die konstante Viskosität zu sichern. Das Wechseln der Sammelbehälter oder das Anlassen und Einstellen der Entnehmpumpen gelten als Nebenprozesse.)

Die Angaben der Abbildung 8 sind ausdrücklich von informativem Charakter; die Gegebenheiten, die ortsbedingten Eigenheiten, Amortisationsnormen sind ja bei den verschiedenen Betrieben so (4) vielfältig und abweichend, daß die Möglichkeit für eine allgemein gültige Kostenfeststellung ausgeschlossen ist.

Es scheint Zweckmäßig zu sein, in jedem Anwendungsfall die gegebenen Istzahlen der ermittelten eigenen Regie- beziehungsweise Amortisationsschlüsselwerte, mit Rücksicht auf die Investitionskosten und Arbeitskraftversorgung einzusetzen und somit die Hilfslinien 2 und 3 der Abbildung 8 der jeweiligen Aufgabe anzupassen. Es war bestrebt, die ungünstigsten Verhältnisse der Kalkulation zugrunde zu legen: allein bei den "Angaben über die verarbeiteten Stoffmengen" der Abbildung 3 wurde eine Ausnahme gemacht, um sie laut Linie "b" zu berücksichtigen.

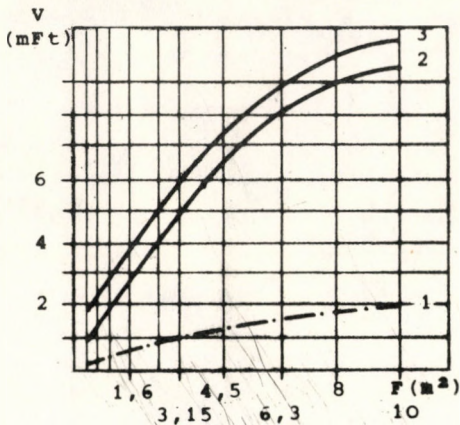


Abb. 7. Investitionskosten einzelner Rotations-Dünnschichtapparate UNIFILM und kompletter Anlage. (Basis: Preisniveau 1975)

- 1 - Investitionskosten individueller Apparate UNIFILM
- 2 - Investitionskosten kompletter Anlage, mit Handsteuerung
- 3 - Investitionskosten kompletter Anlage, mit automatischer Steuerung

Der Berechnungen wurde vorhandene Versorgungsleitungen und Gebäude zugrunde gelegt.

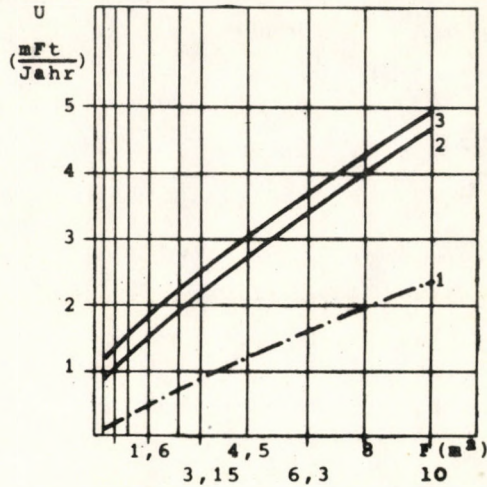


Abb. 8. Informative Betriebskostenangaben der Rotations-Dünnschichtanlagen (Energiekosten + allgemeine Regiekosten + Amortisation). (Basis: Preisniveau 1975)

- 1 - Effektive Regiekosten (Dampf, Wasser, Strom)
- 2 - Betriebskosten im Jahresdurchschnitt, bei automatischer Steuerung
- 3 - Betriebskosten im Jahresdurchschnitt, bei Handsteuerung

Die Betriebsparameter der Dünnschichtanlage wurden unter Voraussetzung von $B_0 - G_0$ berücksichtigt.

Aufgrund dieses Kapitels kann die eingangs gestellte Frage, mit welchem Kostenaufwand, beantwortet werden.

VORSCHLÄGE FÜR DIE ANWENDUNGSGEBIETE

Wie aus den bisherigen Erwägungen und Berechnungen ersichtlich, sind die Verarbeitungsvolumina bei den Dünnschichtapparaten wegen der aus maschinenbautechnischen Gründen beschränkten Heizflächenabmessungen verhältnismäßig gering, spezifisch aber, auf 1 m^2 berechnet ganz besonders groß [2]. Aus diesem Grund lassen sich die Wirtschaftlichkeitsparameter der Rotationsdünnschichtapparate nur binnen ihrer Typengruppen, praktisch also allein "untereinander" vergleichen.

Der Einsatz von Dünnschichtapparaten ist daher in den folgenden Fällen zu vertreten:

- Bei Stoffen, welche sich auf anderen Apparaten überhaupt nicht oder nur mit großen Verlusten verarbeiten lassen (wärmeempfindliche Stoffe, Enzyme, Vitamine, Proteinerzeugnisse).
- bei Stoffen, deren Abfälle nach der Verarbeitung mit anderen Methoden noch so reich an Wirkstoffen sind (kleberige, dicke, Abfälle von schlechter Wärmeleitfähigkeit), daß die Rekuperation an sich schon die Wirtschaftlichkeit des Apparates sichert [1];
- bei Produkten, deren Genießbarkeit durch andere Verarbeitungsmethoden beeinträchtigt wird (Obstsäfte und sonstige Nahrungsmittel)
- schließlich in den Fällen, wo die Reinheit des Konzentrates ausschlaggebend ist (Lösungsmittelentfernung bei Kunstharzen für die elektrische Industrie).

Der Einsatzbereich und die "Leistung" der verschiedenen Bautypen von Rotations-Dünnschichtapparaten mit beweglichen Wischern läßt sich nach der beschriebenen Methode ermitteln, und auch die Angaben hinsichtlich der Investitions- beziehungsweise Betriebskosten der Dünnschichtapparate UNIFILM liegen vor. Alles in allem läßt es sich also feststellen, daß die Anschaffung des Rotations-Dünnschichtapparates rentabel ist, wenn:

- das im Jahresdurchschnitt am Dünnschichtapparat verarbeitete Produkt dem Installateur einen größeren Nutzen bringt, als die in Abbildung 8 angegebene jährliche Gesamtbetriebskostenziffer;
- das mit dem Dünnschichtapparat zu verarbeitende Produkt in keiner anderen Weise hergestellt werden kann, aber zur Erzeugung eines weiteren hochwertigen Produktes unerlässlich ist, und aus dem Gewinn am letzteren die Betriebskosten des Dünnschichtapparates gedeckt werden;

die Verwertung der sonst nicht nutzbaren Abfälle die jährlichen Betriebskosten laut Abbildung 8 decken.

Diese Angaben und Methoden ersetzen nicht die eingehende und konkrete Prüfung, welche in allen Einzelfällen nach wie vor notwendig sein wird: sie liefern aber eine Grundlage zur vorherigen Berechnung der Leistung und der Investition.

ZEICHENERLÄUTERUNG

B	Einspeisungsvolumen	kp/h
B ₀	der maximalen Dampfmenge zugehörige Einspeisungswert	kp/h
G	Menge des verdampften Mediums	kp/h
G ₀	Maximale Dampfmenge	kp/h
F	nominale Heizfläche	m ²

Δt	Differenz zwischen dem Siedepunkt des Heizmediums und dem des zu verarbeitenden Stoffes, unter verwendetem Betriebsdruck	$^{\circ}\text{C}$
K_0	Anfangstrockensubstanzgehalt des zu verarbeitenden Stoffes	Gewicht %
K	Trockensubstanzgehalt nach der Verarbeitung	Gewicht %
V	Investitionskosten	Mio Ft
\ddot{U}	Betriebskosten	Mio Ft

LITERATURVERZEICHNIS

1. MUTZENBERG, A.B.: Chem. Eng., 72, 19 (1965)
2. FRANK - PALL : Chem. Prum. 24, 49 (1974)
3. UJHIDY A.: Filmbepárlók, filreaktorok (Filmverdampfer, Filmreaktoren), Műszaki Könyvkiadó, Budapest, 1967
4. Verzeichnis der Amortisationsnormen. Staatl. Plankommission, Budapest, 1974
5. S.M.S. Bericht, 1971.

РЕЗЮМЕ

Ротационные пленочные аппараты широко распространены. Но знания, с помощью которых можно оптимально и экономично эксплуатировать эти многосторонние аппараты, имеющие исключительно выгодные свойства, не известны так широко.

Вследствие этого по вопросу применимости ротационных пленочных аппаратов мнения специалистов, занимающихся инвестицией и эксплуатацией, разделяются. Некоторые из них, переоценивая преимущества, предлагают аппараты для выполнения любой задачи, а другие, ставя необоснованные проблемы вообще не советуют их применение.

В настоящей статье - на основе опытов по развитию, исследованию и эксплуатации - излагаются следующие вопросы:

- в какой рабочей области
- при каких задачах
- при каких затратах

стоит применять пленочные аппараты.

A CONTINUOUS METHOD FOR PRODUCING ZnS_2O_4 SOLUTIONS

M. SZABÓ and P. KÁLDI*

(Department of Chemical Process Engineering

*Department of Chemical Technology

Veszprém University of Chemical Engineering)

Received: February 1975.

The following investigations and experiments were carried out:

a) Mass transfer between phases on sulphur-dioxide- H_2O -Zn metal powder system with the following equipment:

- 1) falling film column
- 2) well mixed semibatch reactor
- 3) continuous cocurrent tube reactor

The main purposes were to determine the principal relationships among the hydrodynamic conditions, the mass transfer, and the reaction conditions.

b) On the basis of the investigations mentioned above a suitable reactor type could theoretically be worked out.

c) Measurements were carried out to determine the most important technological parameters. A suitable reactor type and technological parameter system were developed to ensure the ZnS_2O_4 solution, the free of Zn-powder and siede products, in a concentration demanded by industry.

From the beginning of the 20th century Na-dithionite and other by-products have been used on an industrial scale, and its technological production was reported on [1] a long time ago. The consumption of dithionite and by-products has been constantly

growing in industry. During the last decades some new technological methods were developed, but today the semibatch reactor type is mainly used for producing ZnS_2O_4 solutions.

According to this method SO_2 gas is absorbed into the water Zn powder suspension. So far only one continuous method was developed by the BASF company [2]. Considering this surprising fact, it can be considered that there are many problems in gaining ZnS_2O_4 solutions having practically any Zn powder and byproducts.

The rate of decay of dithionite in water can reach a very high value near the saturation of SO_2 and above 50°C . A very detailed paper about this field was presented by LOBANOV and others [3]. They did not analyse the SO_2 concentration in solution, but determined the pH value as a parameter of the rate constant of the decay processes. It is unknown the relationship existing between the pH value and SO_2 concentration in solutions at various temperatures and the ZnS_2O_4 concentrations.

For industrial purposes the required concentrations has to reach $400 \text{ (kg m}^{-3}\text{)}$ value. The changes in the pH value during time using an industrial example in a well mixed semibatch type reactor is presented in Figure 1.

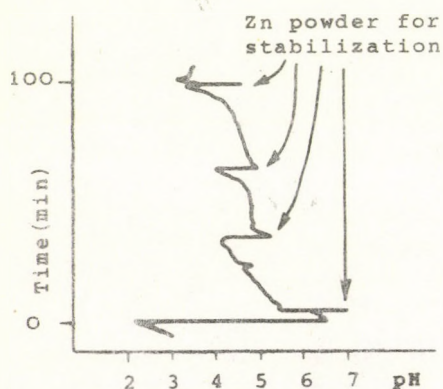


Fig. 1. How the pH changes with time

The Zn powder was added in three portions, and the volume rate of SO_2 fed in was constant.

The big change of SO_2 concentration in the solution can be assessed when it is considered that the decrease of one pH value is equal to 10 times greater SO_2 concentration in solutions. At the end of the process, when the Zn powder is totally used up there is a sharp decrease in pH value causing considerable decay damage.

Concerning the technology of this product which ensures optimum conditions for the yield to be attained, the entire system, including the suitable reactor type, had to be investigated.

For this purpose, the mass transfer between phases, the hydrodynamics of the system and some theoretical examinations were carried out.

Theoretically and economically the use of such a SO_2 gas is advantageous which has been obtained by the burning of sulphur and the oxygen of air. The use of this SO_2 gas mixture is widespread in industry.

The chemical composition and the grain size distribution of the Zn powder are as follows:

Zn content of metal = 94.1 %

total Zn content = 98.0 %

$\frac{\text{metallic Zn}}{\text{total Zn}} = 0.96$

GRAIN SIZE	%	Diameters of grain fractions	%
10^{-6} m	-	10^{-6} m	-
1	1.0	13	9.0
3	2.0	15	8.5
5	4.5	17	8.0
7	8.0	19	7.0
8	9.0	21	6.0
9	10.0	23	4.5
10	9.5	25	3.0
11	9.0	27	1.0

The grain size distribution was measured by a BOUND-BROOK type photo-sedimentometer.

MASS TRANSFER BETWEEN PHASES

Mass Transfer between Gas and Liquid Phases in a Falling Film Column

A glass tube was used with an inside diameter of 17×10^{-3} m, and a length of 1.34 m. The tests were carried out in a counter current of the phases consisting of $200 \text{ kg m}^{-3} \text{ ZnS}_2\text{O}_4$, $125 \text{ kg m}^{-3} \text{ Zn}$ powder in liquid phase, and pure SO_2 and N_2 gases were taken from cylinders. The concentrations of both phases were measured by classical iodometry [4].

The value of the mass transfer coefficient was calculated from the total pressure of SO_2 in gas phase.

$$\beta_g (1/22.4) \text{ mol SO}_2 / \text{m}^2 \times \text{h} \times \text{Hgmm}$$

According to the experimental results, the value of the mass transfer coefficient was controlled by the hydrodynamic conditions of the liquid phase. The following parameters were kept $t = 25^\circ \text{C}$, the volume rate of the liquid feed: $0.200\text{--}0.350 \text{ m}^3 \text{h}^{-1}$ SO_2 conc. = 20%. In one series of the experiment the SO_2 concentration was changed from 10 to 60 %, while the total gas volume rate at the inlet was constant $0.300 (\text{m}^3 \text{h}^{-1})$. Characterizing the liquid volume rate by the Reynolds number of the film, the main results of this experiment can be seen in Fig. 2.

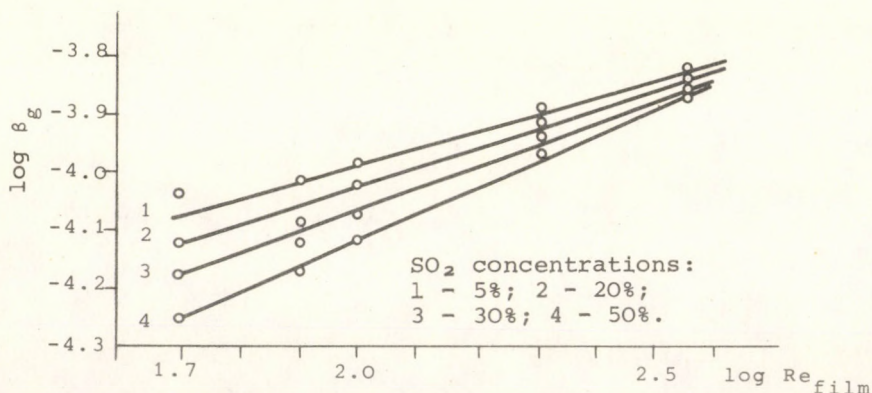


Fig.2. The alteration of the mass transfer coefficient with the flow rate of the film

The results can be summarized as follows:

a) The relationship existing between the Re number of the film and the mass transfer coefficient can be described by an equation having two parameters.

$$\log \beta_g = -3.589 - 0.842 \log(\text{SO}_2 \%) + [-0.106 + 0.33 \log(\text{SO}_2 \%) \log Re_F] \quad (1)$$

There are a few remarkable phenomena:

a) The smaller the value of the SO_2 concentrations, the greater is the independence from the Re_F under these circumstances.

b) The value of the mass transfer coefficient becomes independent from the SO_2 concentration at 470-500 Re_F . The investigation of this phenomena is of interest, but it should be stressed that the falling film becomes turbulent in the whole cross-section at 500 Re_F . Good mixing circumstances ensure the same SO_2 concentration on the liquid film cross section if the film diffusional time is much less than the reaction time. The reaction taking place between absorbed SO_2 and Zn powder, begins on the liquid film surface, and in the course of liquid film mixing continues in the core. The ratio of apparent rate coefficients of reaction and diffusion, regulate the measure of SO_2 concentration in the liquid film and the depth of penetration. Without giving any detailed interpretation of this phenomena, it should be mentioned, that in the industrial semibatch type reactor the measured p_H value corresponds to a SO_2 concentration in the liquid phase.

According to some authors [5,6,7] the turbulent effect begins inside the film at 150 Re_F , but others [8,9,10,11,13,14,15,16,17] report that this critical number occurs at 300 Re_F .

The experimental results of DUKLER [18] ZHIVAJKIN and VOLGIN [12,19] agree with our results, as they found continuous transition from the laminar region to the turbulent one.

Experiments in a Well Mixed Semi-Batch Tank Reactor

The experimental reactor of one litre volume using a high speed rotating (1000 min^{-1}) mixer is illustrated in Figure 3. The suspension filled in consisted of $100 \times 10^{-6} \text{ m}^3$ water and $16 \times 10^{-3} \text{ kg}$ Zn powder.

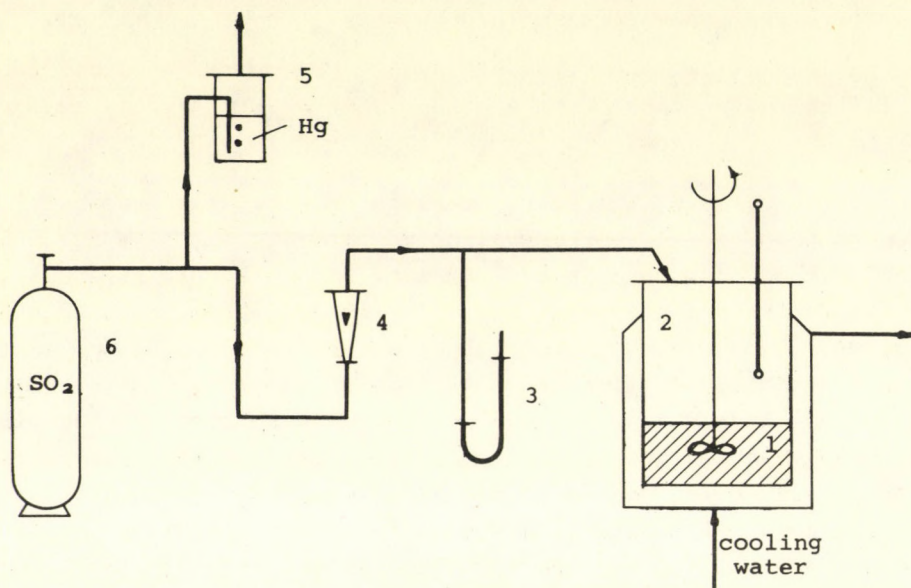


Fig. 3. The experimental set-up.

1 - suspension; 2 - gas phase; 3 - manometer; 4 - rotameter.
5 - manostat; 6 - SO_2 cylinder

Tests with a Constant SO_2 Pressure

The temperature was maintained at 60°C and the SO_2 pressure at a constant value during one experiment, as 30, 50, 75, 100, 150 Hg mm. After the O_2 was removed by pure N_2 , a small pressure equivalent to the wanted SO_2 pressure was created. The gas was fed through a rotameter in a regulated volume rate which ensured a constant partial pressure of SO_2 inside the reactor.

The gas volume rate was regulated by making the inside total pressure equivalent to the atmospheric one. So the measured gas volume rate could be taken into consideration and the value consumed by the chemical reaction if we did not take the changes of absorbed gas concentration into account. The rate of dissolution of the Zn powder was calculated by the following equation:



During the dissolution of Zn powder its specific surface was assumed to be constant, calculated from the measured distribution.

The rate of dissolution of Zn powder as a function of the partial pressure of SO_2 can be seen in Figure 4.

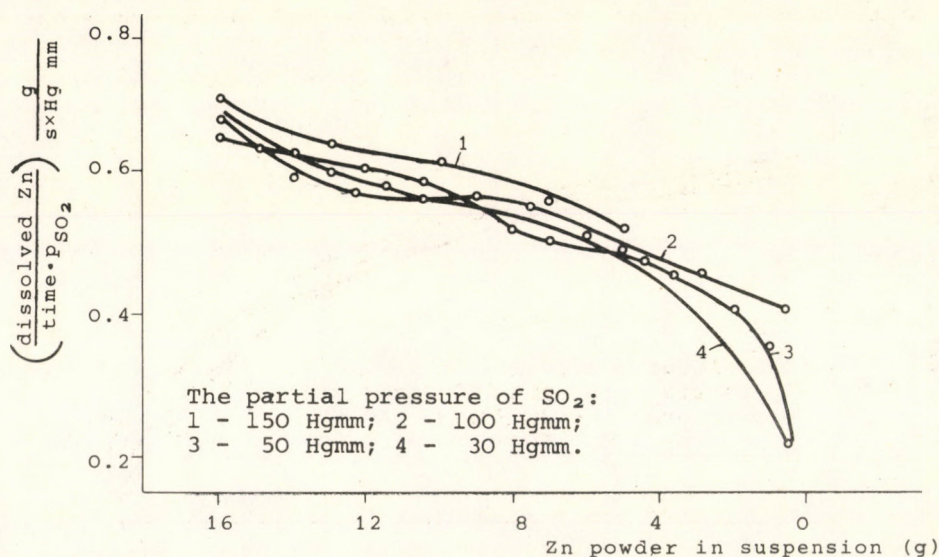


Fig. 4. Zn powder dissolution rate

It was very remarkable that the rate of dissolutions as a function of the partial pressure of SO_2 gas had only a small dependence from the actual mass of Zn powder in the suspension. This means that the greater the mass of Zn powder in the liquid, the less the absorbed SO_2 concentration and vice versa if the mixing level is sufficient.

Tests for Determining the Influence of Temperature on the Dissolving Rate

To determine the influence of temperature on the rate of dissolution of Zn powder, the partial pressure of SO_2 was kept at 150 Hgmm, and the temperature was changed from 30 to 60 °C. The results are presented on Figure 5. The change of temperature had no remarkable influence on the rate of dissolution. The relationships existing in the concentration of aqueous ZnS_2O_4 solution, the temperature and SO_2 pressure were unknown. Accordingly only qualitative investigations and notes could be made about the mechanism of the process of dissolution.

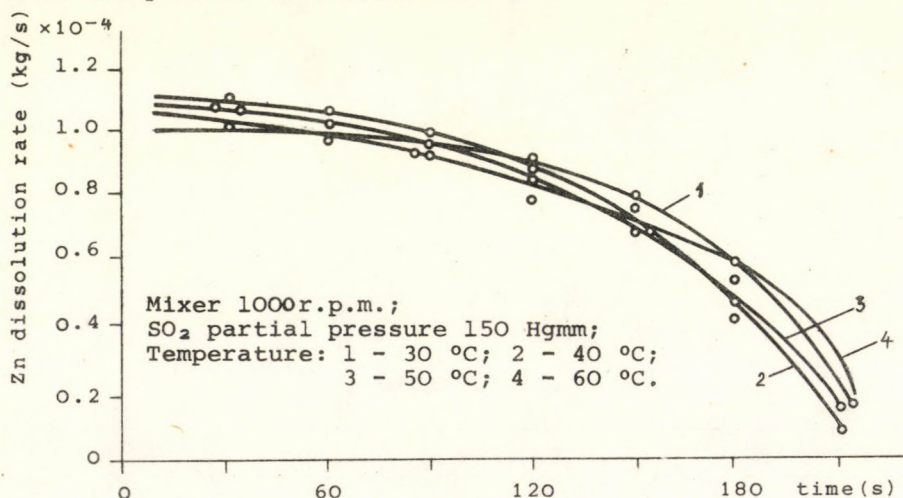


Fig. 5. The dissolution rate of Zn powder

In all cases the dissolution was diffusion controlled under the investigated circumstances.

Theoretical Considerations on Mass Transport Processes between the Phases

Considering this investigated three phase system, a consecutive process scheme can easily be imagined for describing it. As the over all process is diffusion controlled its kinetics degenerate to the first order.

a) Let the apparent rate coefficient of the mass transfer between gas and liquid and solid phases be k_1 and k_2 :

$$k_1 = \beta_g \omega_g \epsilon_g \quad (1/s) \quad (3)$$

$$k_2 = \beta_l \omega_l \epsilon_l \quad (1/s) \quad (4)$$

b) The diffusion process and mass transfer between liquid and solid phases co-exist in the liquid phase.

In the well mixed system the value of the turbulent diffusion coefficient is 2 or 4 times greater in the exponent than in the molecular one. It is appropriate to use the following rate coefficient for the rate coefficient of the diffusion process:

$$k_3 = D_{eff} \omega_l^2 \quad (5)$$

The reciprocal values of the rate coefficients give the time of reaction and diffusion.

In literature e.g. ASTARITA [32] introduced the concept of the equivalent diffusion time which was based on the value of the molecular diffusion constant. Some deficiencies can be pointed out in ASTARITA's theory:

- 1) It does not contain the value of D_{eff} .

2) The characteristic length (in our case it was the reciprocal value of the specific surface of the regarded phase) does not contain the reality of the system.

Let the value of D_{eff} be: $D_{eff} = 10^3 D$ and the following equality and inequalities exist in the system:

$$k_1 > k_2, \text{ or } k_1 \gg k_2$$

when the suspension contains a relatively large amount of Zn powder:

$$k_1 \sim k_3$$
$$t_R > t_D, \text{ or } t_R \gg t_D.$$

These facts mean, that $C_{SO_2l} \neq 0$ in the whole liquid phase and

$$C_{SO_2s} = 0 \text{ on the surface of the Zn grains.}$$

This facilitates the calculation of mass transfer between the liquid and solid phases.

THE CALCULATION OF MASS TRANSFER BETWEEN THE LIQUID AND SOLID PHASES IN THE SUSPENSION. THE DISSOLUTION OF Zn POWDER

As previously mentioned, the rate of dissolution of Zn powder was the slowest step in the process, similar to the hydrogenation of oils with suspended catalyst, when the whole liquid volume has some value of absorbed H_2 .

The SO_2 absorbed by water may be:

- a) dissolved physically
- b) hydrated
- c) dissociated forms

With regard to the state of equilibrium existing among these forms, some papers were published by EIGEN and co-workers [20], who pointed out that the physically dissolved form is overwhelming.

According to LYNN [22] and NIJSING [23], the equilibrium state among the forms enters instantaneously.

At the boundary surface of the liquid, the equilibrium state is established at less than 0.003 second.

The value of the molecular diffusion constant of SO_2 in water at 20 °C, determined by TOOR and CHIANG is:

$$D = 1.41 \times 10^{-9} \text{ (m}^2 \cdot \text{s}^{-1}\text{)}$$

This value was taken into account for calculating other temperature or physical properties by CHIANG's reports [25].

Among the absorbed SO_2 forms in the water the physically absorbed one is active for dissolving the Zn metal based on electron theory. It was verified by experiment that the Zn powder suspended in pure (free of water) alcohol or oil, did react with physically absorbed SO_2 [26].

Trough experiments KING [27] pointed out that the dissolution of Zn and Mg metal rods rotated in dilute strong mineral acids with a depolarizator for inhibiting the formation of H_2 , was diffusion controlled.

Generally, the mass transfer coefficient for a submerged spherical solid body and liquid phase can be estimated by the well known equation [28],

$$\frac{\delta_{dp}}{D} = 2 + 0.6 \text{Re}_p^{0.5} \text{Sc}^{0.5} \quad (6)$$

In a mixed suspension, the relative speed of particles changes in time and space. To calculate this relative speed, SCHWARZBERG and TREYBAL [29] proposed a complicated equation based

on their experimental results but its use is very limited. Others proposed equations for calculating mass transfer coefficients on the basis of dissipated energy [33].

It can be assumed that the speed, existing between the entrained particles and liquid, must be higher than the value calculated by STOKES' equation. Examining the mass transfer process on dispersed ion exchange resin, NYERS [30] measured the values of co-efficients and the relative speed of particles which depended on the intensity of the mixing.

The particle speeds had 2-20 times greater values than those calculated by STOKES' equation.

HARIOT [31] reported the same results in his papers.

The mechanism of the dissolution of Zn powder is a complicated unstable process, as the salt concentration, the viscosity of the salt concentration, the viscosity of the solution, the value the diffusion co-effecient and the distribution of Zn powder diameters change.

For calculating the distribution of Zn powder diameters and the SO_2 concentration in the liquid, the strategy was built up by the following steps.

1) The starting distribution of Zn powder size was divided into 16 fractions and the following data were calculated for each fraction:

- a) the surface
- b) the mass
- c) the number of particles

2) For each fraction the mass transfer co-efficient was calculated by Equation (3). Supposing that the relative speed of the particle was 10 times greater than the value calculated by STOKES'

equation on the basis of previous experiments, the value of the density, the concentration and the viscosity in the liquid were calculated by polynoms.

3) From the value of the mass transfer co-efficients of each fraction, an average was calculated.

4) In the knowledge of the experimentally determined value of the Zn dissolution rate and the whole surface of the Zn powder, it is easy to compute the SO_2 concentration in the liquid.

5) For a chosen time interval, the dissolved Zn mass was calculated in each fraction.

6) At the end of the time interval, the new distribution of the particle diameters, the mass, the surface values belonging to each fraction and the ZnS_2O_4 concentration in the liquid were calculated.

7) With these new data the calculation was continued. The distribution of Zn powder sizes during the dissolution process is given in Figure 6.

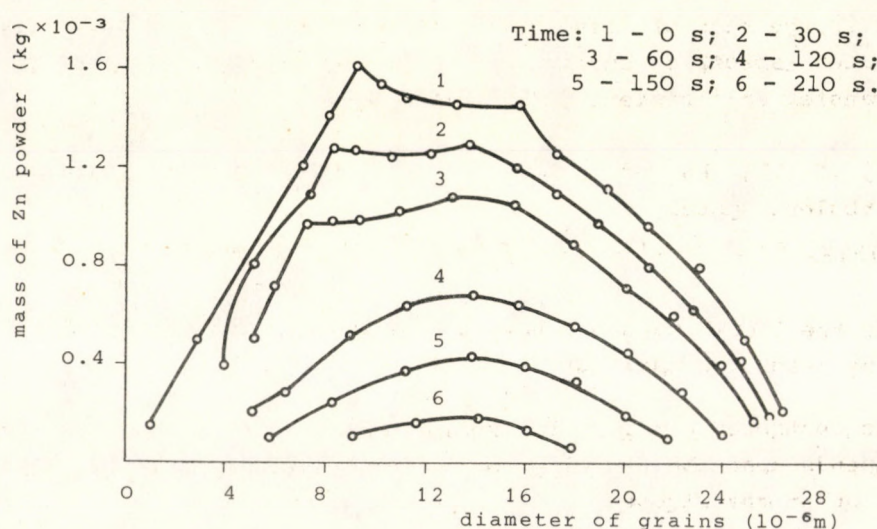


Fig. 6. The change of particle size distribution during the dissolution.

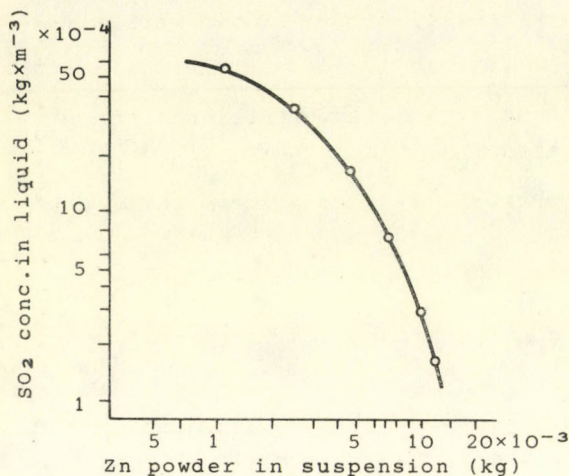


Fig. 7. The dependence of SO₂ concentration in liquid on the content of Zn powder in suspension.

In Figure 7. the SO₂ concentration vs. Zn powder content both in liquid is presented (well mixed batch-reactor, pressure of SO₂ = 150 Hgmm, the revolution of impeller 1000 min⁻¹, the dispersion consisted of 16 × 10⁻³ kg Zn powder, and 100 × 10⁻³ kg water).

Investigating the results presented on Figures 6. and 7, the following can be verified:

a) under the same conditions, the smaller the diameter the greater is the rate of dissolution. This derives on one hand from the greater specific surface and from the greater value of the mass transfer co-efficient on the other hand.

b) If $k_1 > k_2$ or $t_r \gg t_D$ conditions are fulfilled in a turbulent system,

$$C_F \neq f(x, y, z) ; \quad C_F = f(\text{Zn powder content of suspension})$$

If the liquid does not have any Zn powder content, the value of C_F may reach the equilibrium value.

As mentioned earlier, the ZnS₂O₄ decays in solution, and its rate depends upon the p_H value, or in our system upon the SO₂ concentration in the liquid.

To avoid this decay, the SO₂ concentration in the liquid has to be maintained on the lowest possible level. This question is very important for the design of a technological unit.

THE DEVELOPMENT AND TESTS OF THE CONTINUOUS TECHNOLOGICAL UNIT

According to the experimental results it is advantageous to maintain strong turbulent conditions in the unit, and in the whole system the next circumstance to be ensured is:

$$k_1 > k_2$$

Considering the specific surfaces between the gas-liquid phases with reference to the liquid volume, their values in the investigated reactors can be shown:

Falling film column $3000 < \omega_{g-1} < 7000 \text{ (m}^{-1}\text{)}$

well mixed reactor $500 \omega_{g-1} < 1500 \text{ (m}^{-1}\text{)}$
(liquid in froth pool)

For industrial purposes, those types are advantageous in which froth or foam can be formed. As the wanted ZnS_2O_4 concentration is about 400 kg m^{-3} in solutions without any or with the least amount of Zn powder, the following difficulties have to be taken into account:

- a) the counter current flow of the phases should be avoided
- b) it is advantageous in the technological unit to avoid backmixing,
- c) it is desirable that the SO_2 concentration in the liquid be on a lower level.
- d) In the case of a cocurrent unit the feeds of components in stoichiometric rates demand a very long residence time. To avoid this the feed of SO_2 has to have some surplus.

Taking into consideration all those questions, the steady-state cocurrent plug flow reactor type can be used for the following reasons:

a) When the SO_2 concentration is greater in the gas phase the Zn powder mass is greater in suspension.

b) These circumstances maintain the lowest level of SO_2 concentration in the liquid phase.

c) The rate of ZnS_2O_4 formation is inversely proportional to the ZnS_2O_4 concentration.

Using a gas mixture containing about 21 % SO_2 , endeavours were made to calculate the residence time of liquid and gas. First of all an attempt was made to carry out the process in an empty tube. Choosing a tube 27×10^{-3} m in diameter, and 2 m in length, the measure of backmixing of the liquid phase was investigated at various speeds in both phases that created foam of a froth pool. The investigations were extended to gas linear speeds up to $6 \text{ (m s}^{-1}\text{)}$ and the liquid one $0.5 \times 10^{-2} - 3.5 \times 10^{-2} \text{ (m s}^{-1}\text{)}$.

The values of turbulent diffusion co-efficients of the liquid phase could be written by a simple equation:

$$K = k^* + m V_L$$

where k^* is an interpolated value without liquid feed.

The results are presented in Figure 8. It was a remarkable fact that the values of the turbulent diffusion co-efficients presented a maximum and later decreased. The measure of backmixing at $6 \text{ m} \cdot \text{s}^{-1}$ linear flow rate did not make it possible to produce a solution free from Zn powder. To avoid the back-mixing of the liquid, discs for locally tightening the cross-section of the tube were used. This means a plug flow reactor consisting of well mixed cascade elements. The experimental equipment was suitable for continuously investigating the whole technological process. The plug flow or tubular reactor had an outside cooling tube up to 1 m and holes at various intervals for thermometers and drawing samples from gas and liquid phases.

The main results can be summarized as follows:

- 1) The rate of ZnS_2O_4 formation, and the yield on a metal base were the same between 40-60 °C
- 2) The maximum yields of ZnS_2O_4 with reference to metal Zn were 0.95 in 2.0 m long column
1.00 in 2.5 m long column,

when the concentration reached 400 kg m^{-3} and the mass of unreacted Zn powder was $0.5 - 1.0 \text{ kg m}^{-3}$.

- 3) The average values of the ZnS_2O_4 concentration along the column obtained in 15 experiments are shown in Figure 9.
- 4) The concentrations of SO_2 in the solution along the length of column were calculated from the experimental results. The results are presented on Figure 10. There are two graphs:

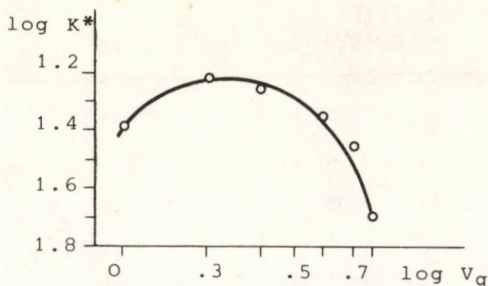


Fig.8. How the turbulent diffusion coefficient changes with the gas flow rate in an empty tube

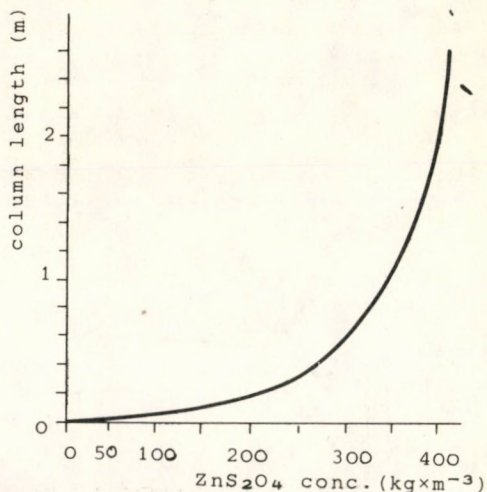


Fig.9. The change of the ZnS_2O_4 concentration along the column

1. graph: with regard to stoichiometrical SO_2/Zn ratio
2. graph: shows the case when 5 % Zn powder was fed in surplus.

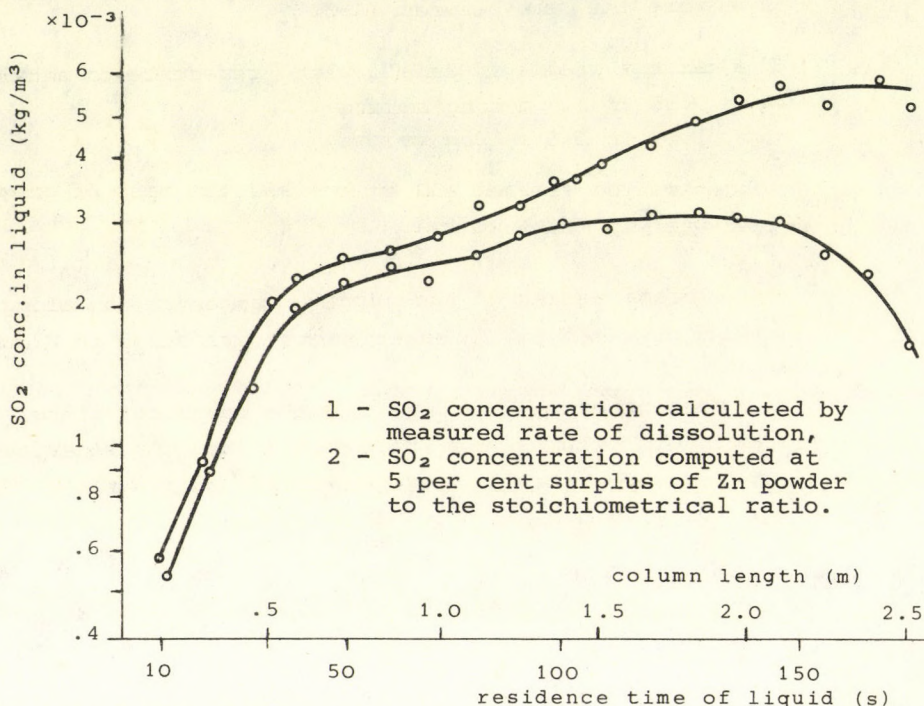


Fig. 10. The change of SO_2 concentration in liquid along the length of the column

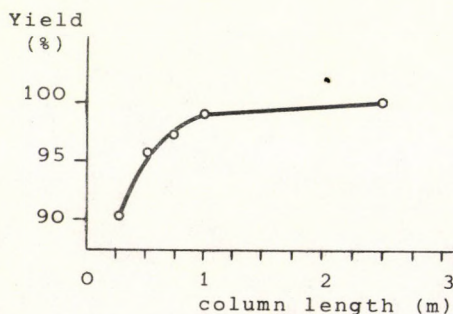


Fig. 11. The yield of ZnS O on metal base along the length of column

5) The ZnS_2O_4 yields on a metal base along the column were shown on Figure 11.

According to the results the yields had lower values in the neighbourhood of the entrance. This derived from the fact that the ZnO content of Zn powder settled about 5 % on the surface and this layer was first dissolved by SO_2 .

6) Finally the experiments should be mentioned, when only the water feeding was cut to half and the concentration increased to 800 kg m^{-3} . The yield decreased to 0.93.

By the method developed for continuously producing ZnS_2O_4 solutions, it was possible to obtain the theoretical yield. This method is suitable for industrial purposes by increasing the size.

SYMBOLS USED

C_L	- concentration in liquid phase	$\text{ML}^{-3} \text{mole L}^{-3}$
d	- characteristic length	L
D	- diffusion constant	$L^2 \text{ t}^{-1}$
j	- mass flux	$\text{ML}^{-2} \text{ t}^{-1}$
k	- apparent rate of reaction (first order)	t^{-1}
K	- turbulent diffusion coefficient	$L^2 \text{ t}^{-1}$
m	- linear coefficient	dimensionless
n	- rotation	t^{-1}
t_r	- reaction time	t
t_D	- diffusion time	t
x, y, z	- spacial co-ordinates	L
v	- superficial velocity	$L \text{ t}^{-1}$
β	- mass transfer co-efficient	$\text{mole} \cdot \text{t} \cdot L^{-3} \cdot M^{-1}$
β	- mass transfer co-efficient	$L \cdot \text{t}^{-1}$
ω	- specific surface	$L^2 \cdot L^{-3}$
ϵ	- volume fraction of dispersed phase	dimensionless

REFERENCES

1. JELLINEK, K.: Das Hydrosulfit. Verlag von Ferdinand Enke, Stuttgart, 1911
2. DRP. 753.614
3. LOBANOV, T.N., KUNIN, G.M., SMIRNOVA, J.J.: Himiya Khimicheskaya Tekhnologiya, 2, 189 (1963)

4. Specification of production of hydrosulfite. Chemical Works of Peremarton, 1963
5. SCHOOKLITSCH, A., SITZBER : Akad. Wiss. Wien. Math.-Naturw.Kl. Abt. II. a. 129, 895 (1920)
6. STIRBA, C., HURT, D.M.: A.I.Ch.E.J.; 1, 178 (1955)
7. KUKATELADZE, S.S., STYRIKOVICH, M. A.: Hydraulics of Gas Liquid Systems, Casenergoizdat, Moscow, 1959
8. HOPF, L.: Ann. Physik, 32, 777 (1910)
9. JEFFREYS, H.: Phil. Mag.,49, 793 (1925)
10. MONRAD, C.C. BADGER, W.L.: Ind. Eng. Chem., 22, 1103 (1930)
11. SCHMIDT, E., SCHURIG, W. and SELSCHOPP, W.: Techn. Mech. Thermodyn. 1, 53 (1930)
12. ZHIVAJKIN, L. J. A., VOLGIN, B. V.: Zh. Prokl. Khim., 34, 1236 (1961)
13. GRIGULL, U.: Forsch. Gebiete Ingenieurw., 13, 49 (1942)
14. GRIGULL, U.: Forsch. Gebiete Ingenieurw., 18, 10 (1952)
15. EMMERT, R. E. and PIGFORD, R. L.: Chem. Eng. Progr., 50, 87 (1954)
16. FULFORD, D. G.: Gas-Liquid Flow in an Inclined Channel. Ph. D. Thesis, Univ. Birmingham, England, 1962
17. SZÁNYA, T.: B. Sc. Thesis. Veszprém Univ. of Chemical Engineering Veszprém, 1970
18. DUKLER, A. E.: Chem. Eng. Progr., 55, (10) 62 (1959)
19. ZHIVAJKIN, L. J. A., VOLGIN, B. V.: Intern. Chem. Eng., 4, 80 (1964)
20. EIGEN, M., KUSTIN, K. und MASS, G.: Zeitschrift für Phys. Chem. N.F., 30, 131 (1961)
21. TOOR, H. L. and CHIANG, S. H.: A.I.Ch.E.J., 5, 343 (1959)
22. LYNN, S., STRAATEMIER, J. R. and KRAMMERS, H.: Chem. Engng. Sci. 4, 49 (1955)

23. NIJSING, R. A. O., HENDRKSZ, R. H. and KRAMMERS, H.: Chem. Engng. Sci., 10, 88 (1959)
24. TOOR, H. L. and CHIANG, S. H.: A.I.Ch.E.J., 5, 339 (1959)
25. WILKE, C. R. and CHIANG, S. H.: A.I.Ch.E.J., 1, 264 (1955)
26. BERNTHSEN, J.: Lieb. Ann., 208, 136 (1882)
27. KING, C. V.: Trans. New York Acad. Sci., 10, 262 (1948)
28. BIRD, R. B., STEWART, W.E. and LIGHTFOOT, N. E.: Transport Phenomena. John Wiley and Sons, New York, 1960
29. SCHWARTZBERG, A. G. and TREYBAL, R. E.: Ind. Eng. Chem. Fund., 7, 89 (1968)
30. NYERS Á.: B. Sc. Thesis, Veszprém Univ. of Chemical Engineering, Veszprém, 1970
31. HARRIOT, P.: A.I.Ch.E.J., 8, 94, 97 (1962)
32. ASTARITA, G.: Mass Transfer with Chemical Reaction. Elsevier Publishing Comp., Amsterdam (London) New York, 1967
33. UHL, W. V. and GRAY, B. I.: Mixing Theory and Practics. Academic Press, New York and London, 1967

РЕЗЮМЕ

Были проведены следующие испытания и эксперименты:

- а., Массопередача между фазами пылевидной системы двуокиси серы - H_2O - металлический Zn в следующих установках:

- 1., Колонна с падающей пленкой
- 2., Смешанный реактор полунепрерывного типа
- 3., Непрерывный прямоточный реактор трубчатого типа

Главной целью работы является определение основных соотношений между гидродинамическими условиями, массопередачей и условиями реакций.

- б., На основе испытаний теоретически излагается возможность конструирования реактора выгодного типа.
- в., Были проведены измерения с целью определения самых значительных технологических параметров. Наконец, были разработаны реактор выгодного типа и система технологических параметров обеспечения свободного от пыли Zn и содержащий побочные продукты в допустимой промышленностью концентрации раствор ZnS_2O_4 .

ALGORITHM SEARCH METHOD TO SOLVE MATHEMATICAL
MODELS OF COMPLEX SYSTEMS

L. PLEVA and B. NOVÁK

Department of Mechanics,
Veszprém University of Chemical Engineering,
Veszprém, Hungary

Received: November 8, 1975.

A method used to determine the algorithms of simple and complex chemical as well as energetic systems is presented. Even nonlinear algebraic, differential and integral equations occurring in the equation set are readily handled. The manual method developed is presented in connection with the occurrence evaporator, obtained by the computerized algorithm search is also presented.

INTRODUCTION

In determining the characteristics of simple and complex chemical as well as energetical systems, the solution of nonlinear equations with given initial conditions is commonly required.

In this paper a method is presented, using this the algorithm can be prepared by manual calculators. The algorithms of complex and extensive problems are similarly obtained, but here a computer is preferred.

The method developed can be used to determine the algorithm of the solutions of equation systems. The algorithm determines only the economical order of the computation or the solution. Linear and nonlinear, algebraical equations, ordinary differential equations, as well as integral equations are readily handled [1].

The method presented is, first of all, of considerable importance in the case of nonlinear equation systems.

PROBLEM INVOLVING A SINGLE STEP EVAPORATOR

This example presents the case of a single step evaporator, which is the element of a complex evaporator system. The evaporator unit is considered as an operation unit. The description of this element is considered first. The inputs and outputs of this operation unit are such that they can readily be connected to several systems. The description of this evaporator unit is of medium complexity. The model presented in Figure 1 shows that it consists of readily separable and separately describable elementary operation units (i.e. of an embranchement in the vapour line and of the evaporator unit proper).

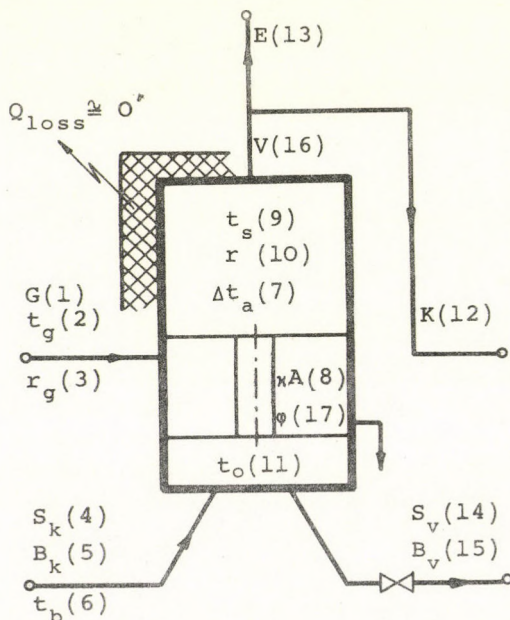


Fig. 1

The latter one, in fact, is a composite unit, but for the purposes of the present study its detailing can be neglected. This means that the model in fact consists of two models built together because steam take off is rather frequent in this case. Thus there is no need to create a new model in every case from the elementary models of the embranchment and the evaporator unit proper. If the embranchment is not required, it can be eliminated by specifying $E = 0$.

In case of $E < 0$ (negative off-take value) extra steam is introduced into the system externally. When the mathematical description of the system is made, i.e. when the model is generated, no reference is made to the number of elements the system is composed of.

Therefore an equation or equation set can be assigned in studying the mathematical model that does not describe any particular operation unit. These equations, restricting us to the field of the mathematical model, can then be considered as the mathematical models of an imaginary operation unit. The equations can be manipulated just as if they referred to particular operation units. That is, each of the equations can be considered to be the equivalents of elementary mathematical models of which the overall, more extended systems are composed of.

EQUATIONS DESCRIBING THE STEADY-STATE OPERATION OF THE OPERATION UNIT

Additional conditions relating to particular equations are presented in joined comments. Figure 1 presents the unit with the numbered coded variables.

1. $V = K + E$

The mass flow balance of the embranchment (vapour is considered to be pure steam, i.e. liquid droplets carried out are neglected).

$$2. \quad \varphi = G/V$$

A characteristic feature of real practical use is the specific steam consumption.

$$3. \quad \Delta t_a = 63.5 \cdot B_V^{1.5}, \quad 0 < B_V < 0.25$$

The rise of the boiling point of the sodium hydroxide solution in the $B_V < 0.25$ weight ratio range. Based on a nomogram [2], the equation was determined by the least square method. Within the specified range the equation can accurately be used (with a close to unity correlation coefficient and small standard deviation).

Assuming perfect mixing in the solution block of the evaporator, the boiling point rise can be calculated from the concentration of the solution leaving the unit, if, for the sake of simplicity, $t_o = 100^\circ\text{C}$ is assumed.

$$4. \quad G \cdot r_g = V \cdot r + S_k (t_o - t_b)$$

The above equation is the heat flow balance of the perfectly isolated evaporator body. Specific heat of the dilute aqueous solution is considered to be unity, $c = 1$, the dissolution heat is neglected, the heating steam is supposed to be dry, saturated steam.

$$5. \quad B_V \cdot S_V = B_K \cdot S_K$$

This is the dry material balance equation of the solution. Assuming that the solution does not carry off solution droplets, the equation satisfies the practical needs.

$$6. \quad r_g = 603 - 0.64 \cdot t_g, \quad 50 \leq t_g \leq 150^\circ\text{C}$$

This is the equation describing the enthalpy of the water in the range specified.

$$7. \quad r = 603 - 0.64 \cdot t_g$$

This equation yields the enthalpy of the water taken at the temperature of the solution. In Equation 6 the enthalpy of water was calculated at the temperature of the heating steam and of the vapour-heating-steam in between the subsequent stages, respectively. In Equation 7 this calculation is carried out at the temperature of the solution, because due to the rise in the boiling point temperature, vapour is formed at this level. In general, aqueous solutions are brought to boil with steam-heating. Occasionally, the first stage is heated by steam, while the further stages are heated with certain organic solvent vapours. The enthalpy of water was built into the mathematical model of the operation unit, however, occasionally that single equation in itself is considered as a mathematical model. Substituting the enthalpy equation of another solvent for that of the water, which can, for example, also be introduced into the mathematical model of the appropriate operation unit.

$$8. \quad t_o = \Delta t_a + t_s$$

This equation describes the boiling point of the solution.

$$9. \quad S_v = S_k - V$$

This is the mass flow balance equation of the evaporation

$$10. \quad \kappa A(t_g - t_o) = S_k(t_o - t_b) + V \cdot r$$

This is the heat transfer equation of well mixed systems

The above equations give a mid-depth description of the evaporator unit 1, a more or a less detailed description being also feasible. It is the user who must decide what depth he wants to achieve considering the requirements and the possibilities, as well as the problem to be solved.

This description does not take into consideration the momentum flows. Furthermore it contains neglections which are indicated at the corresponding equations. Because the mathematical model does not directly make use of the momentum data, the model can only be used to calculate the pressure in the unit and in the whole evaporator system as well indirectly through the boiling point. Therefore, if boiling points are specified as input parameters, the pressure should be independently checked.

The equations derived can be rearranged into the form of $\bar{F}(\bar{x}) = \bar{O}$. Each of the equations is then differentiated and non-zero elements are marked in a table containing the variables and the equations. Thus a so called occurrence matrix is obtained, showing what variable occurs in what equation.

If the matrix is constructed in such a way that its rows correspond to the equations and its columns to the variables, then for example, the occurrence matrix of the mathematical model of the evaporator body described by the previous equations, takes the form shown in Figure 2.

E \ V	1	2	3	4	5	6	7	8	9	10	11	12	13	14	15	16	17
	G	t _g	r _g	S _k	B _k	t _b	Δt _a	κA	t _s	r	t _o	K	E	S _v	B _v	V	φ
1												X	X			X	
2	X															X	X
3							X								X		
4	X		X	X		X				X	X					X	
5				X	X									X	X		
6		X	X														
7									X	X	X						
8						X			X		X						
9				X										X		X	
10	X		X		X		X		X	X						X	

Fig. 2.

$$S_{zf} = L - M = 17 - 10 = 7$$

Mid-depth
description

There are several known methods to calculate the degree of freedom of the system [3]. However, the independency of the equations remains questionable even if the degree of freedom of the mathematical model is determined. Should the equation system be linear, the independency test would not present any problem. However, the systems studied generally require nonlinear equation systems.

After this point the trial and error method is applied. It is advisable at first to seek the solution taking the input data independent from the complex operation unit as the initial input data. If this approach is successful, i.e. if the mathematical equation system representing the physical model can be solved, then the number of variables, taken in the cost of the degree of freedom, satisfies the independent equation system. Error can appear if an unused equation and/or an unknown remains. This means, that though the degree of freedom was correctly calculated, interdependent equations were included into the equation system. Therefore the theoretical solution subtracting the degree of freedom from the numbers of unknowns results in as many unknowns as equations becomes more secure or of higher degree if the ordered occurrence matrix results in a formal solution. That is, the algorithm belonging to a given input system is found and no unnecessary unknown and equation is left behind. In final analysis, only the numerical solution based on the formal solutions means unquestionable solubility, because the convergence of the iterative methods, generally required, is tested at first only here.

If this test was carried out on an operation unit and its mathematical solution could be obtained then no similar test would be required for those systems composed of operation units alike. In cases like that it is sufficient to test the theoretical and the formal solution. It is worthwhile to note that there is a possibility that the former one depends on the structure of the system, while the latter on the input system selected.

ALGORITHM SEARCH

The following operations are carried out on the occurrence matrix.

a) Vertical lines or some other marks are drawn to the input variables (input parameters). Because these are already known they are not computed. We have to specify as many input variable values as the degree of freedom requires.

b) If manual solution is sought, it is advisable to search with a straight-edge for those equations in each of the lines that contain only a single unknown variable. If such a row is found, then this equation (row) and variable (column) is crossed out. The number of this equation and the sign of the variable is noted. Doing so, the algorithm writing process has started up. For example, the following: V3 from E6 means that from the column of E equations, from the sixth equation the third variable from the line of the variables, that is in this case, r_g , should be computed. Meanwhile, it can be noted, that crossing out a column of the variables, the hitherto unknown value is crossed out from other, momentarily not treated equations as well. Therefore again and again the lines are to be re-searched to see if another case, with only one variable in it appeared.

Having repeated this search, until no further line containing one variable is found, the columns are examined (c). End of the operation b) indicates the point at which the cycle starts; until this point the algorithm is written in a direct order.

c) The columns are tested as follows. Where there is only one mark in a column, that is, the corresponding unknown occurs only in one equation, this equation and variable is also marked already showing the end of our algorithm. These equations and variables together are written into the algorithm in reverse order, just opposite to the order in which they were found. Then a cycle should be initiated (d) but to keep the number of equations inside the cycle

and the time of the iterations at minimum, the former operation (c) is employed. Thus in the algorithm, the (d) cycle is enclosed between the algorithm part (b) written in the forward order and part c), written in the reverse order.

d) Initiation of the iterative cycle. It should be noted that cycle-free matrix can also occur, but generally having gone through the previous steps, the occurrence matrix also contains rows (equations) with two or more unknown variables. That is, there is still no algorithm constructed to compute them.

Let us now find a line containing two variables, then cross out the column of one of the variables and the variable "selected" this way should be noted. (If there are more than two unknowns, use of the computerized algorithm is proposed). Such an algorithm can, for example, be found on page 233 of ref. [1]. From this point on the search is continued according to operation b). If during that phase a row is found where all the variables are crossed out except the row itself, the "selected" variable is then computed from that equation. If the cycle does not return to its start point the other variable should be selected. Thus the iteration forms a single loop, which starts with the selection of a single variable there is no need to select more variables within the iterative step and the number of equations involved is also kept to a minimum. That means that none of the equations enclosed in that iteration loop, which is terminated by the equation used to calculate the selected variable, can be eliminated. The following step is the checking of the errors. The guessed value of the selected variable taken should be compared to the value computed with the numerical solution. In fortunate cases the appropriate value could immediately be obtained and the iteration loop could be abandoned and the following computation step initiated. Generally, however, the computation must be repeated several times until the value of the unknown is obtained within the error limits specified, assuming that the iterative process is convergent.

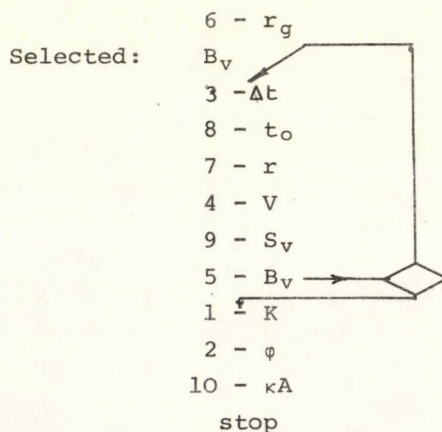
If the iterative process is divergent then the alculation of another unknown should be attempted from the initial equation of the iteration loop. In this case, however, the iteration loop enclosed in the algorithm shold also be rearranged. If convergence is still lacking, then it is possible that the mathematical model constructed does not describe the state of the system with the given input data set.

If two or more variables have to be selected for the algorithm search, the search becomes more complicated. This field already calls for the application of the computer. There are several programmes compiled specifically for the treatment of large, complex systems.

The final step of the algorithm search consists of the use of each of the equations listed and the formulation of the computation order of the unknowns not included in the input system. Thus:

Input: $G \ t_g \ S_k \ B_k \ t_b \ t_s \ E$

Algorithm:



Having completed this, it is advantageous to rearrange the occurrence matrix according to the main diagonal (Figure 3). Computations starts in this case from the lower right corner of the

quadratic pattern. Equations are entered into the rows according to the order of the algorithm from the bottom upward. Unknowns are entered into the matrix at the upper side from the right to the left. the sign which is shown in the field under the main diagonal means an iteration process, e.g. $E3 - B_v$.

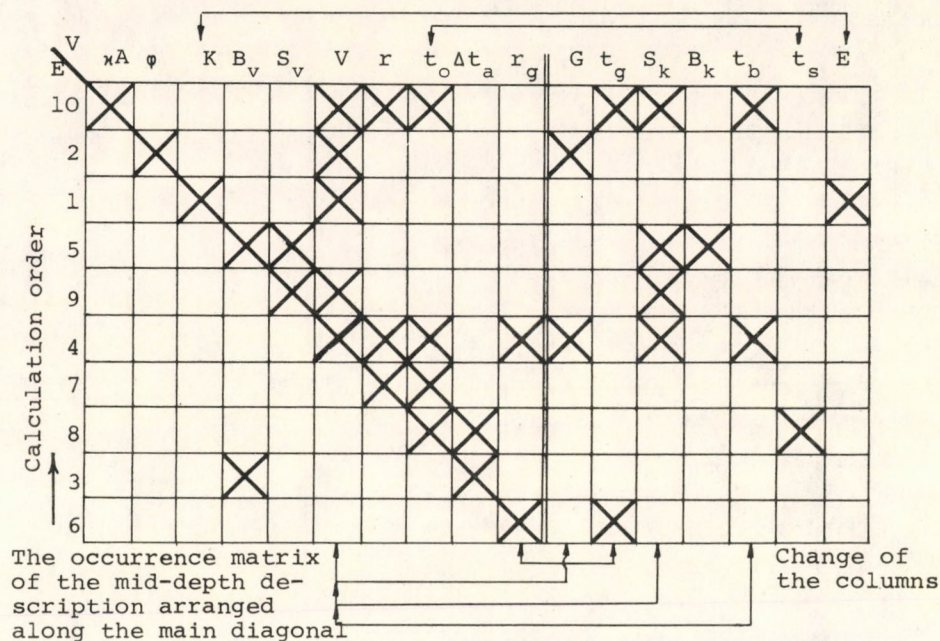


Fig. 3.

EXAMPLE OF THE EVAPORATOR SYSTEM

Let us now compose a three stage cocurrent evaporator system with steam offtake form three of the evaporator bodies shown in Figure 1.

If complex operation units are composed into a system, the physical and mathematical model becomes more complicated. Output

data of the previous unit becomes the input data of the following unit throughout the entire system. This can be noted in the occurrence matrix, arranged along the main diagonal, describing the three stage, cocurrent evaporator system with steam off-take (Figure 4). Here the relationships of the number-coded variables (input-output variables) written in the L1, L2 and L3 rows are shown in this manner that under the V11 of row L1 comes V6 of row 2, that is, the t_o solution temperature of the first evaporator becomes equal to the t_b input temperature of the second evaporator, ect.

Manually it is very difficult - if at all feasible - to solve such systems. The example presents the occurrence matrix of a three-stage evaporator system with steam off-take. The matrix is arranged along the main diagonal. A special input system was applied to demonstrate that the iteration is not strictly bound to the description of the system. In this case there is no iteration at all. The input system applied is such a variable set which can easily be measured on evaporator systems. In the columns M1, M2 and M3, the serial number of the equations, describing the unit is also given. This method of presentation was selected to aid those who choose the manual method.

Generally, it can be concluded that the necessity of iteration mainly depends on the manner the system is connected (e.g. feedback, and counter-current flows, etc.) on the depth of the description, and on the selected input system.

CONCLUSIONS

Advantages of the algorithm searching method are as follows.

The term "degree of freedom" is easily visualized, that is to say, that under a given degree of freedom and system studied, the ease of the solutions of different input systems can readily be compared.

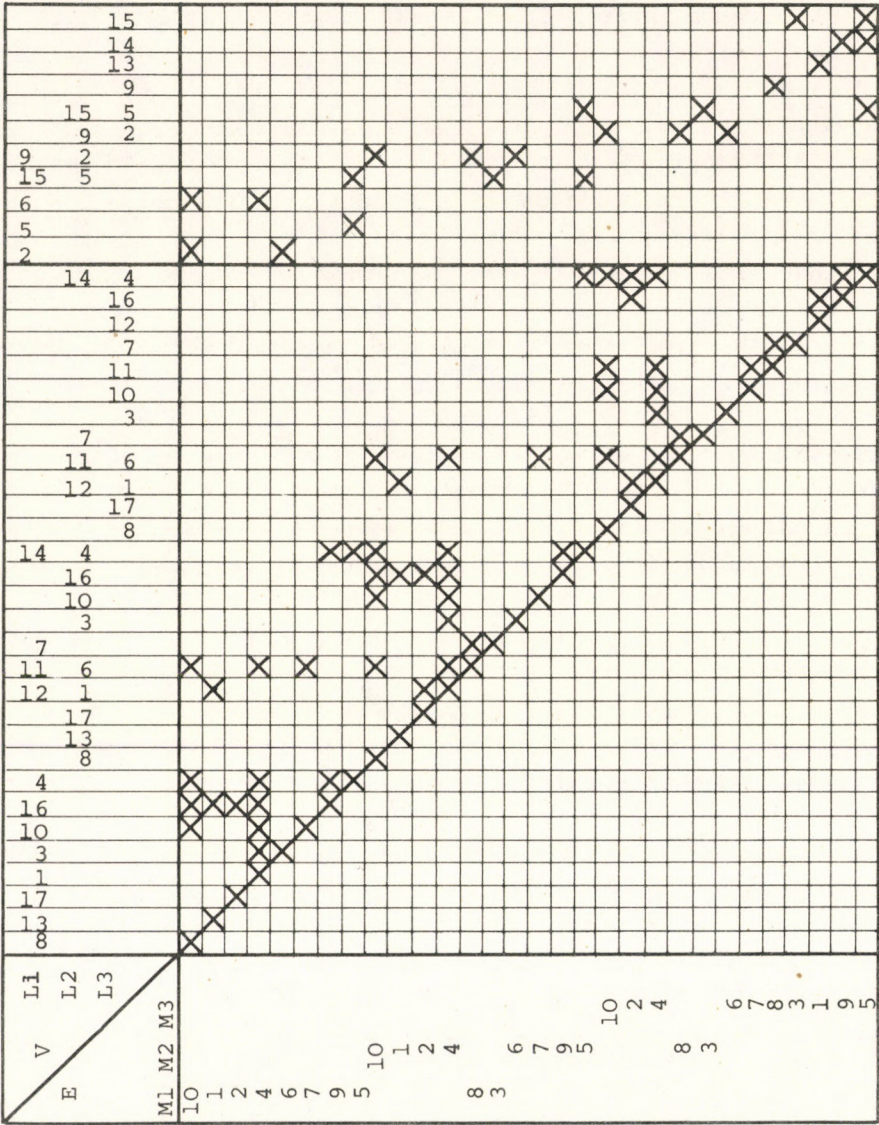


Fig. 4.

Thus, besides the routine inputs of the systems, other, just as useful input systems can also be derived. If a few trials resulted in real (numerical) solutions, the method can well be used to determine the reality of different input systems selected.

Several new solutions can be obtained (cf. Figure 3) by carrying out appropriate column changes in the occurrence matrix arranged along the main diagonal, giving a solution corresponding to some input system. This means that once a solution is obtained, by investing some additional work, further useful solutions can also be obtained. If a column belonging to a cycle is changed it may result in extinguishing that very cycle, because a new input system was created. Thus the method is very productive.

If the method outlined is employed, the number of equations occurring in the cycle is kept to a minimum; these equations, as well as those derived from them, can separately be studied, independently from the other, already solved equations.

Thus, for example, if the cycle turns out to contain only linear equations, then this cycle is a virtual cycle because there are numerous well known methods to solve linear equation systems. This can happen either by chance caused by the selected input system, or by the "mechanical" application of the method.

If nonlinear equations occur, then, especially in the manual method, the test is advantageously carried out in the reversed order of the solution of the cycle. In the case of the single evaporator unit this order of the equations is: 5 - 9 - 4 - 7 - 8 - 3.

$$B_v = \frac{B_k S_k}{S_k - \frac{G(603 - 0.64 t_g) - S_k(63.5 B_v^{1.5} + t_s - t_b)}{603 - 0.64(63.5 B_v^{1.5} + t_s)}}$$

The equations built into each other result in a transcendent relationship. Then this, if wanted, can be plotted and doing so, the change of variables suggested to secure convergency, can be

justified. If identity is obtained during this process, the equations involved are not independent.

The method can be applied to study both simple and complicated systems. This feature allows us to compare different systems because the characteristics of the systems are well indicated by the occurrence matrix.

The method outlined is primarily suggested for engineers and researchers working on practical problems. Numerous, so far unrevealed possibilities lie in this method. Undoubtedly, it can be concluded that the description of the solution of any system is greatly simplified.

SYMBOLS USED

A	surface area of the evaporator, (m^2)
B_k	concentration of the solution entering the unit, (weight %)
B_v	concentration of the solution leaving the unit, (weight %)
E	mass flow of steam off-take, (kg/h)
G	mass flow of heating steam input, (kg/h)
K	mass flow of the vapour after the steam off-take point, (kg/h)
r_g	enthalpy of the heating steam, (kcal/kg)
S_k	overall mass flow of the solution entering the unit, (kg/h)
S_v	overall mass flow of the solution leaving the unit, (kg/h)
Δt	rise of the boiling point of the solution, ($^{\circ}C$)
t_b	temperature of the solution entering the system ($^{\circ}C$)
t_g	temperature of the heating steam, ($^{\circ}C$)
t_o	temperature of the solvent in the evaporator, ($^{\circ}C$)
t_s	temperature of the vapour formed, ($^{\circ}C$)
V	overall mass flow rate of the vapour formed, (kg/h)
φ	specific steam consumption, (kg/h)
κ	heat transfer coefficient, (kcal/ $m^2h^{\circ}C$)

REFERENCES

- 1 LEDET, W.P. and HIMMELBLAU, D.M.: Adv. Chem. Eng., 1970, No.8
- 2 PERRY, J.H.: Vegyész mérnökök kézikönyve. Chemical Engineers' Handbook Vol.1, p. 1019, Műszaki Könyvkiadó, Budapest, 1968.
- 3 BENEDEK P. and LÁSZLÓ A.: A vegyész mérnöki tudomány alapjai. Fundamentals of Chemical Engineering, Műszaki Könyvkiadó, Budapest, 1964

РЕЗЮМЕ

Авторами излагается метод, применимый для определения алгоритмов простых и сложных систем химической промышленности и энергетики. Алгебраические, дифференциальные и интегральные уравнения, содержащиеся в системе уравнений могут быть и нелинейными. Ручной метод, применимый при небольших системах представляется на примере матрицы Якоби однокорпусного выпарного аппарата. Излагается и решение многоступенчатой выпарной системы, полученное при определении алгоритма на вычислительной машине.

MATHEMATICAL MODEL OF THE PARTIAL OXIDATION
FLAME-REACTION OF METHANE

P. BENEDEK, A. LÁSZLÓ*, A. NÉMETH and P. VÁCZI

(Computer Application R. & D. Center, Budapest, Hungary and

*Department of Chemical Process Engineering, Veszprém
University of Chemical Engineering, Veszprém, Hungary)

Received: December 8, 1975.

Increased knowledge of the elementary reactions involved and the development of computer technology permitted the construction of the reaction mechanism based adiabatic model of acetylene production by partial oxidation of methane. The role of the possible elementary reactions was studied and a mechanism, sufficient to describe the process, was determined. The effect of a change in the composition and temperature of the gas fed in upon the process was modelled and agreement was found between the data computed and measured in an actual flame reactor. Competition of the pyrolysis, i.e. the acetylene producing and oxidation reactions was analysed and the progress of the process was explained.

Although commercial scale acetylene production based on the partial oxidation of methane is rather widespread, a more profound theoretical treatment has for a long time remained unchallenged. Due to the lack of detailed information on the reaction mechanism involved and appropriate computation technology, it was commonly believed that at first the greater part of the methane was reacted with the oxygen present, then due to the heat evolved, the remainder of the methane was pyrolysed (through ethane and ethylene) into acetylene [1,2,3].

A comparatively long time ago, the experimental results attained indicated that a mechanism existed, which was different from that outlined above. To demonstrate this statement, composition data from a 100 Nm³/hour experimental flame reactor obtained along the axis of the flame, are presented in Figure 1 [4]. From the figure it is obvious that acetylene, the pyrolysis product already appears at that point where a considerable amount of unreacted oxygen is still present. Later on other authors reported similar data [5,6]. This indicated that the oxidation and pyrolysis processes are not so much of a consecutive, but of a competitive nature.

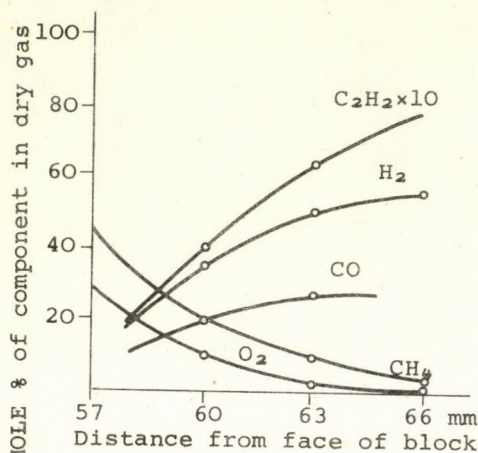


Fig.1. Flame room gas composition data

Following the development of computation technology and model construction, adiabatic models of the process appeared as first approximations. One of these models was established by the authors [7], where the source term, representing the reaction mechanism, contained the CO, CO₂, H₂ and H₂O concentrations calculated from the water-gas equilibrium; as well as empirical relationships describing the pyrolysis products as functions of the initial methane-oxygen ratio and the temperature.

Stepanov and his co-worker published another model [8], describing the pyrolysis process with a reaction mechanism consisting of four reactions and substituting the oxidation reactions with an empirical, overall expression. The rate constants of the reaction mechanism were determined from measured values by a curve fitting method.

Intensive research activity has been carried out in recent years to establish the reaction mechanism of the high temperature methane oxidation and pyrolysis occurring in the flames. Due to

the inherent experimental difficulties, the data available relate only to the oxidation of hydrocarbon mixtures in oxygen rich flames or the oxygen-free pyrolysis of hydrocarbon mixtures. In both cases, the reaction mechanisms involved, have been more or less clarified. Existing knowledge permits us to summarize the results of the kinetical studies in a single mechanism, based on the principle of the transfer of reaction parameters. Taking advantage of our expertise in computation technology, we can examine how far the kinetical results obtained can be utilized in the rather special case of partial oxidation.

The following assumptions were made:

a) Oxidation and pyrolysis reactions are not consecutive, but competitive reactions and the consecutive or competitive character of the carbon containing species is indicated in Figure 2.

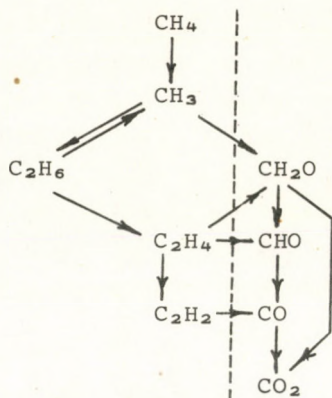


Fig. 2. Scheme of oxidation and pyrolysis routes

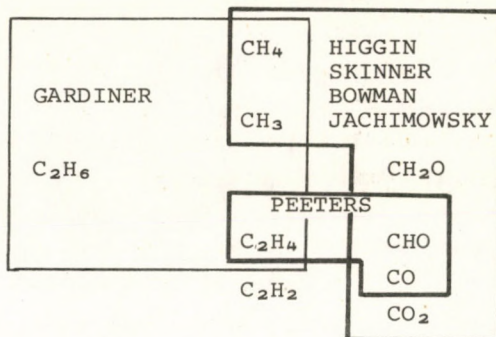


Fig. 3. Sources of elementary reaction parameters

b) There is no hydrocarbon formation from oxygen containing species; there is merely a unidirectional transfer from the pyrolytic reaction chain into the oxidation reaction chain.

Consequently, elementary reactions satisfying these assumptions were compiled from published literature. Because reaction mechanisms and reaction parameters, in published literature, belong to each other - for, both are fitted to measured data - an attempt was made to build the more extended reaction mechanisms into the overall mechanism to be used in the mathematical model of the partial oxidation of methane. Three more extensive studies, dealing with

- a - the oxidation of methane
- b - the oxidation of ethylene
- c - the pyrolysis of methane in an oxygen-free atmosphere, respectively, were considered (cf Figure 3).

Table 1 presents the reaction mechanisms, their corresponding pre-exponential coefficients, activation energies, and the respective reference numbers.

In fact, not only elementary reactions, but occasionally, their linear combinations are also included. If, due to the rapid decomposition of the radical, the radical formation reaction acts as a rate controlling reaction, then the linear combination of these two reactions results in an overall reaction containing no radical at all. Such reactions are the reactions No. 20 and 21, their details are shown at the foot of the table.

Overall reactions are also incorporated in those cases in which their reaction parameters are more credible than those of the elementary reactions. Such a reaction is, for example, the dehydrogenation reaction of ethylene (No. 18 reaction). There are a few reactions shown in Table 1, which were finally not included in the adequate mechanism. (The selection method employed will be outlined in more detail later.) The mechanism proposed here contains an important amendment compared to the previously published mechanism [9], namely, that ethylene and acetylene formed in the pyrolytic step can also be oxidized.

Table 1. Reactions and rate constant coefficients used in computer analysis

No	A s, kmole, m ³	E J. kmole ⁻¹		ref
1. CH ₄	1.30exp14	4.31exp8	CH ₃ + H	13
2. CH ₄ + OH	7.24exp10	2.49exp7	H ₂ O + CH ₃	13
3. CH ₄ + O	3.20exp10	3.33exp7	CH ₃ + OH	13
4. CH ₄ + H	4.14exp10	4.86exp7	CH ₃ + H ₂	13
5. CH ₃ + H	2.52exp10	0	CH ₄	17
6. CH ₃ + H	3.17exp 9	4.18exp7	CH ₄ + H	16
7. CH ₃ + O ₂	8.00exp 6	0	CH ₂ O + OH	13
8. CH ₃ + O	1.90exp10	0	CH ₂ O + H	13
9. CH ₂ O + OH	2.30exp10	0	H ₂ O + CHO	19
10. CH ₂ O	2.84exp11	1.47exp8	CO + H ₂	19
11. CH ₁ O	2.84exp11	1.47exp8	H + CO	19
12. 2xCH ₃	2.00exp13	1.60exp8	C ₂ H ₄ + H ₂	15
13. C ₂ H ₆	8.45exp14	3.35exp8	2xCH ₃	16
14. C ₂ H ₆ + H	1.26exp11	4.10exp7	C ₂ H ₄ + H + H ₂	16
15. C ₂ H ₆ + CH ₃	2.00exp 8	4.40exp7	C ₂ H ₄ + H + CH ₄	16
16. 2xCH ₃	6.00exp10	4.00exp7	C ₂ H ₄ + 2xH	15
17. 2xCH ₃	8.43exp 9	0	C ₂ H ₆	15
18. C ₂ H ₄	2.20exp 9	1.67exp8	C ₂ H ₂ + H ₂	8
19. O + C ₂ H ₄	2.26exp10	1.13exp7	CH ₃ + CHO	20
20. O ₂ +O+C ₂ H ₄	2.50exp10	2.09exp7	2xH +CH ₂ O+CO ₂	20*
21. O ₂ + O+C ₂ H ₂	5.20exp10	1.55exp7	2xH +CO +CO ₂	20**
22. H ₂ O + H	1.15exp11	8.42exp7	OH + H ₂	18
23. H ₂ + O ₂	2.53exp11	7.03exp7	OH + O	13
24. OH + H ₂	3.68exp10	2.30exp7	H ₂ O + H	13
25. CO + OH	2.32exp 9	2.39exp7	CO ₂ + H	14
26. H + CO ₂	4.80exp11	1.06exp8	OH + CO	14
27. O ₂ + CO	1.60exp10	1.73exp8	O + CO ₂	19
28. O + H ₂	1.27exp10	3.94exp7	OH + H	13
29. OH + OH	8.60exp 9	4.19exp6	H ₂ O + O	13
30. H+OH+H ₂ O	1.20exp11	0	2H ₂ O	18
31. H+H+H ₂ O	4.00exp 9	1.15exp7	H ₂ O + H ₂	18

* C₂H₄+O CH₂+CH₂O; CH₂+O₂ CO₂+H+H

** C₂H₂+O CH₂+CO ; CH₂+O₂ CO₂+H+H

Even in this step, decomposition reactions of the acetylene leading to homologues or charcoal, were not included in the model mechanism because of their minor importance at the present stage of the investigations.

Most probably, there are not only longitudinal components of the convective flow of the preheated, premixed homogeneous reaction mixture in the flame reactor, mixing nevertheless, although its importance is duly acknowledged, is not considered in the present model. Counter-current convective heat transfer of heat radiation is also neglected. This neglect leads to a reactor model in which the adiabatic gas mixture follows the plug flow mechanism because the radial heat transfer is not considered. Applying the Gallilei transforms, the length co-ordinate of the reactor is transformed into a time co-ordinate and the isobaric, adiabatic transient of the gas mixture enclosed in a piston is computed instead of the steady-state tube reactor. This results in a differential equation relating to each of the species of Table 1:

$$\frac{dc_j}{dt} = \sum_i v_{ij} \left[A_i e^{-\frac{E_i}{RT}} \prod_l c_l^{n_{il}} \right] - c_j \frac{d \ln V}{dt} \quad (1)$$

The differential equation of the temperature is derived from balance equation of the enthalpy:

$$\frac{dT}{dt} = - \frac{\sum_j \frac{dc_j}{dt} \sum_k a_{jk} T^k}{\sum_j c_j \sum_k k a_{jk} T^{k-1}} \quad (2)$$

The differential equation describing the total volume of the isobaric reaction mixture reads as follows:

$$\frac{d \ln V}{dt} = \frac{\sum_{i,j} v_{ij} \left[A_i e^{-\frac{E_i}{RT}} \prod_l c_l^{n_{il}} \right]}{\sum_j c_j} + \frac{d \ln T}{dt} \quad (3)$$

The detailed derivation of these differential equations is outlined in our previous publications [10, 11]. It should be noted however, that differential equations (1) to (3) are not adequately conditioned, therefore their numerical integration presents considerable difficulties. According to our knowledge, no faster computing algorithm has been proposed than the Gear Algorithm which we used [12]. The coefficients of the enthalpy polynomial in Equation (2) are listed in Table 2.

Based on the data presented in Tables 1 and 2, as well as on further restrictions (isothermic or adiabatic and isochoric or isobaric case) our programme system generates the particular differential equation system and then solves it within the given initial conditions (temperature, pressure, and mole per cent composition data). The functions obtained as the solutions or other characteristics derived from these functions are then printed-according to the user's wishes - on the line- printer as tables or function-plots.

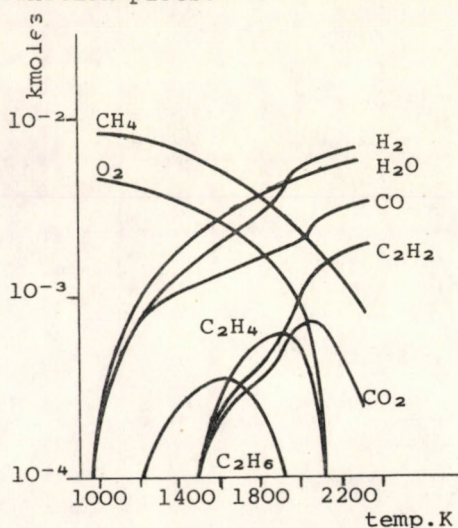


Fig. 4. Main product distribution. $\text{CH}_4 = 63 \text{ Vol.}\%$; $\text{O}_2 = 37 \text{ Vol.}\%$; $T_0 = 900 \text{ K}$

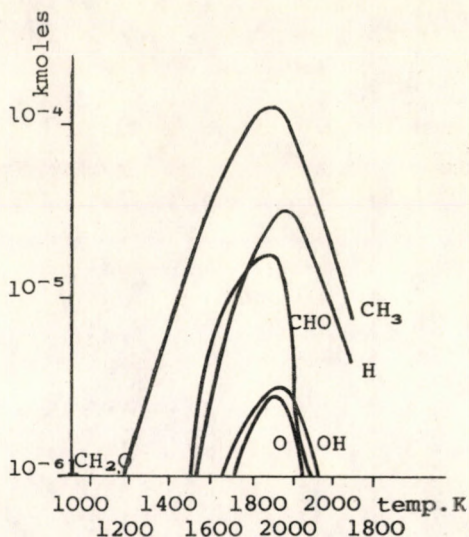


Fig. 5. Radical distribution. $\text{CH}_4 = 63 \text{ Vol.}\%$; $\text{O}_2 = 37 \text{ Vol.}\%$; $T_0 = 900 \text{ K}$

As an example, Figure 4 presents the increase of the concentrations of the main products along with the decrease of the amounts of the reactants computed.

Table 2. Enthalpy functions

C O N S T A N S					
SPECIES	a_0	a_1	a_2	a_3	a_4
CH ₄	-6.6725x10 ⁷	2.9479x10 ⁴	6.6252	1.9184x10 ⁻²	-7.0131x10 ⁻⁶
CH ₃	2.6700x10 ⁸	2.9479x10 ⁴	6.6252	1.9184x10 ⁻²	-7.0131x10 ⁻⁶
H	2.0000x10 ⁸	1.4126x10 ⁴	4.0237x10 ⁻¹	-3.8717x10 ⁻⁵	8.0600x10 ⁻⁸
O ₂	0.0000	2.8459x10 ⁴	6.9999x10 ⁻¹	3.5735x10 ⁻³	-1.3971x10 ⁻⁶
CH ₂ O	-1.1388x10 ⁸	1.8090x10 ⁴	2.9313x10 ⁻¹	-4.3704x10 ⁻³	-4.3939x10 ⁻⁷
OH	4.1836x10 ⁷	2.9984x10 ⁴	-1.4292	1.2976x10 ⁻³	-8.8817x10 ⁻⁸
O	2.4000x10 ⁸	1.4229x10 ⁴	3.5000x10 ⁻¹	1.8767x10 ⁻³	-6-9850x10 ⁻⁷
H ₂ O	-2.3904x10 ⁸	3.2889x10 ⁴	-5.3643x10 ⁻¹	5.1647x10 ⁻³	-1.5005x10 ⁻⁶
CO	-1.1394x10 ⁸	2.9391x10 ⁴	-2.3257	4.7794x10 ⁻³	-1 4687x10 ⁻⁶
H ₂	0.0000	2.8253x10 ⁴	8 0474x10 ⁻¹	-7.7435x10 ⁻⁵	1.6121x10 ⁻⁷
C ₂ H ₄	6.1027x10 ⁷	2.1414x10 ⁴	4.5101x10 ⁻¹	-2.4330x10 ⁻³	-2.3762x10 ⁻⁶
C ₂ H ₆	6.8863x10 ⁸	2.1492x10 ⁴	5.9641x10 ⁻¹	-1.0528x10 ⁻³	-3.6685x10 ⁻⁶
C ₂ H ₂	2.2735x10 ⁸	2.1641x10 ⁴	4.7295x10 ⁻¹	-2.3483x10 ⁻²	5 2212x10 ⁻⁶
CO ₂	-3.9347x10	2.3977x10 ⁴	2.7653x10 ⁻¹	-1.0511x10 ⁻²	1.6748x10 ⁻⁶
CHO	0.0000	0.0000	0.0000	0.0000	0.0000

Temperature, rather than time plotted along the x co-ordinate, characterises how far the reaction has proceeded. This manner of presentation makes it obvious that in agreement with the hypothesis, oxidation and pyrolysis reactions are of a competitive nature, which will be discussed later in more detail.

It can be seen from Figure 5, that the concentrations of the radicals and atoms rise steeply, and except for the CH_2O (both in the magnitude of the concentration and time of the maximum value), stop at about the same time value. The maximum is rather sharp. Rapid concentration is followed by rapid freezing-in, and steady-state concentrations, which are so familiar in the isothermic case, are not at all observed.

Further computations were also carried out to follow the reaction. The contribution of each of the elementary reactions to the concentrations of each of the 15 species of the reaction mixture was calculated in 10-15 time moments. The results obtained in one of these calculations are presented in Table 3. The results are summarized in Figure 6. The horizontal line drawn to any of the reactions indicates that the reaction proper accounts for the formation or decomposition of at least one of the species in greater amounts than 5 %. The changes of the roles of those reactions depend on the changes of the temperature and the concentrations.

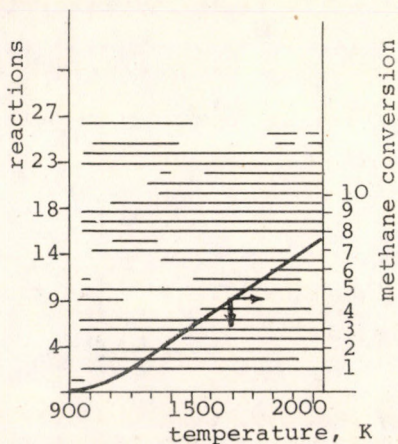


Fig. 6. Effect of elementary reactions on the process

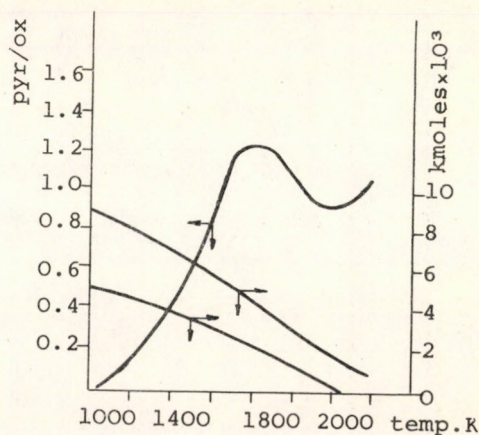


Fig. 7. Pyrolysis-oxidation ratio and feed consumption (case: 63 % CH_4 + 37 % O_2)

Table 3. Integrated weight of elementary reactions (formation)

No of reactions	CH ₄	CH ₃	H	O ₂	CH ₂ O	OH	O	H ₂ O	CO	H ₂	C ₂ H ₄	C ₂ H ₆	C ₂ H ₂	CO ₂	CHO
1.	-	0	1	-	-	-	-	-	-	-	-	-	-	-	-
2.	-	32	-	-	-	-	-	76	-	-	-	-	-	-	-
3.	-	9	-	-	-	21	-	-	-	-	-	-	-	-	-
4.	27	29	-	-	-	-	-	-	-	45	-	-	-	-	-
5.	27	-	-	-	-	-	-	-	-	-	-	-	-	-	-
6.	72	-	35	-	-	-	-	-	-	-	-	-	-	-	-
7.	-	-	-	-	82	20	-	-	-	-	-	-	-	-	-
8.	-	-	1	-	7	-	-	-	-	-	-	-	-	-	-
9.	-	-	-	-	-	-	-	0	-	-	-	-	-	-	-
10.	-	-	-	-	-	-	-	-	61	15	-	-	-	-	-
11.	-	-	3	-	-	-	-	-	12	-	-	-	-	-	-
12.	-	-	-	-	-	-	-	-	-	2	7	-	-	-	-
13.	-	28	-	-	-	-	-	-	-	-	-	-	-	-	-
14.	-	-	-	-	-	-	-	-	-	10	39	-	-	-	-
15.	0	-	0	-	-	-	-	-	-	-	1	-	-	-	-
16.	-	-	28	-	-	-	-	-	-	-	53	-	-	-	-
17.	-	-	-	-	-	-	-	-	-	-	-	100	-	-	-
18.	-	-	-	-	-	-	-	-	-	17	-	-	100	-	100
19.	-	2	-	-	-	-	-	-	-	-	-	-	-	22	-
20.	-	-	4	-	12	-	-	-	21	-	-	-	-	65	-
21.	-	-	12	-	-	-	-	-	-	12	-	-	-	-	-
22.	-	-	-	-	-	18	98	-	-	-	-	-	-	-	-
23.	-	-	16	-	-	39	-	24	-	-	-	-	-	6	-
24.	-	-	1	-	-	-	-	-	-	-	-	-	-	-	-
25.	-	-	-	-	-	2	-	-	5	-	-	-	-	-	-
26.	-	-	-	-	-	-	-	-	-	-	-	-	-	-	-
27.	-	-	-	-	-	-	2	-	-	-	-	-	-	7	-

This test was used to select the adequate overall mechanism. The convention accepted was that any one of the reactions contributing to the formation of at least one of the species to a smaller extent than 5% can correctly be excluded from the reaction mechanism. Therefore, as few as 27 of the 31 reactions included in the Table 1 are sufficient to describe the process. These 27 reactions form the adequate mechanism of the partial oxidation of methane and further calculations were carried out considering only these 27 reactions.

The term pyrolysis module is introduced to make the analysis of the competition of the oxidation and pyrolysis easier. The numerator of that term in any one instant is equal to the quantity of carbon, found in the form of ethane, ethylene, or acetylene, the denominator equals the amount of carbon found in the species CO_2 . That term, i.e. the pyrolysis module shows how the carbon content of methane is shared between the pyrolysis and oxidation reaction paths.

Figure 7 presents the pyrolysis module as a function of the actual temperature characterizing the extent of the reaction in the previously described case. The methane and oxygen concentration functions are also included in the Figure.

Analysing this plot it is found that at the beginning, i. e. at low temperatures, the overall reaction is started with oxidation. Because under adiabatic circumstances this results in rising temperature, and the pyrolytic reactions are speeded up along with the increasing extent of oxidation and rising temperature. This is indicated by the increasing steepness of the rising initial part of the pyrolysis module. This trend continues until the maximum point is reached. The maximum means that the amount of the pyrolysis products is equal to the amount of the oxidized species. However, pyrolysis products ethylene and acetylene are subject to quick oxidation, therefore their concentration drops while the quantity of the oxidation products increases. This is demonstrated

by the falling part of the pyrolysis module curve. When the total oxygen reserve is consumed, the second part of the overall reactions ends and the remaining methane starts to decompose. This is the third part of the overall reaction resulting once again in the rise of the pyrolysis module.

To illustrate the mechanism just described, Figure 8 presents the carbon balance as a Shankey diagram. This diagram presents the integrated quantity of each of the species formed or consumed until that point where the oxygen concentration falls to zero. Two important facts should be noted. The first one is the recirculation around the methyl radical, the other is the ratio of the oxidation products formed through the methyl radical to those formed from ethylene, as well as acetylene species. It is easy to note that the oxidation paths. It can also be noted that more than one fourth of the acetylene and ethylene formed is lost throughout the oxidation mechanisms.

Initial conditions of the partial oxidation process of methane can be changed. Holding the original initial temperature and pressure values, but employing an increase of oxygen (42 per cent oxygen, 58 per cent methane), faster oxidation should be witnessed in the first part of the overall reaction, where dimerisation and oxidation reactions of the methyl radical are in competition. The competition of the methyl radical and the pyrolysis products around the maximum of the pyrolysis module cannot be significantly changed. Correspondingly, when the oxygen is completely consumed, the pyrolysis module is lower than in the previous case, but the quantity of the unreacted methane is already low. This computed result agreed with the previous experimental observations (Table 4).

Keeping the initial pressure and composition values unchanged, and rising the initial temperature 100 °K higher no significant change was observed in the final gas composition. Previous experimental results of the authors indicated a slight, but nevertheless significant rise in the acetylene yield.

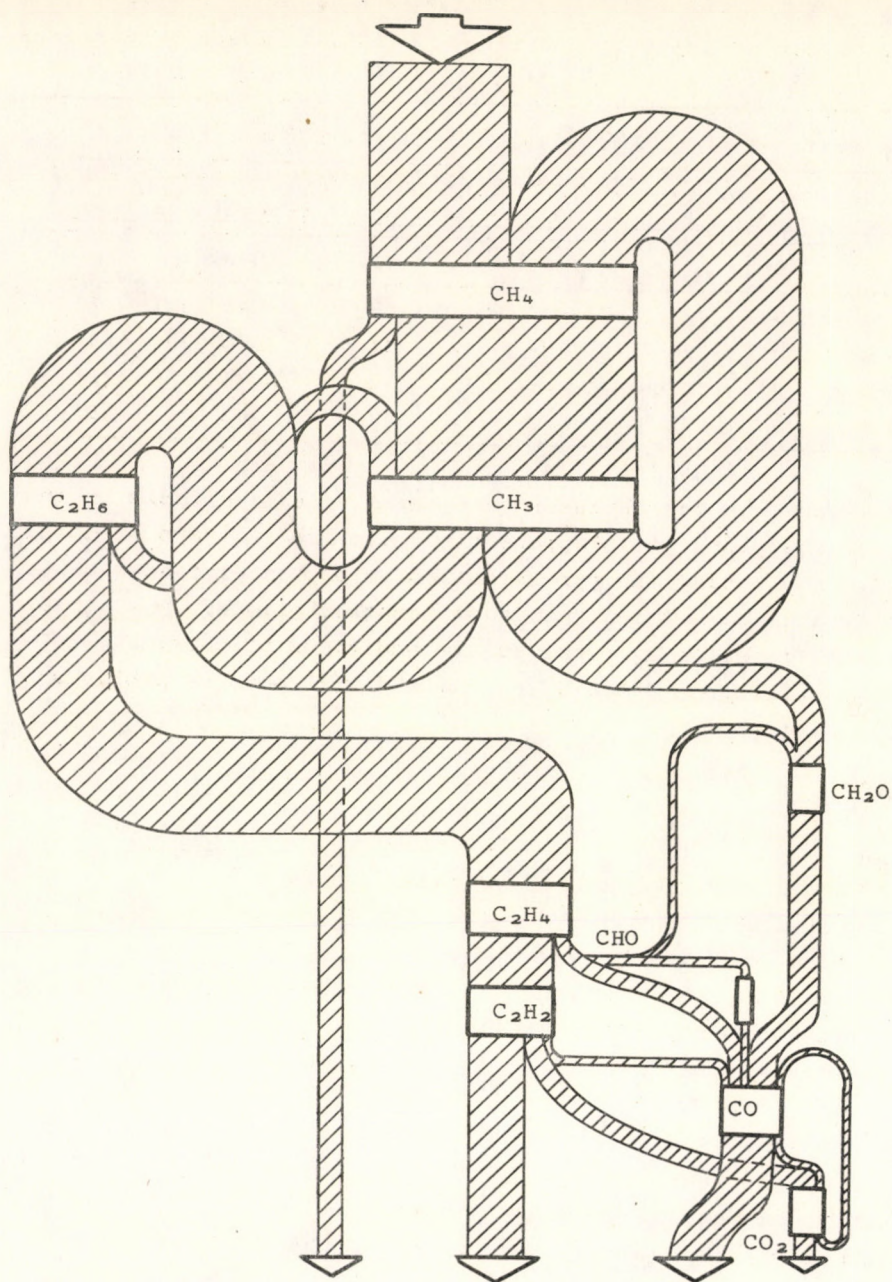


Fig. 8. Carbon diagram at 99.9 % O_2 consumption (case: 63 % CH_4 + 37 % O_2 ,) $T = 900 \text{ K}$

Table 4. Effect of initial conditions (at 99.9% oxygen conversion)

Feed (vol. %)				Initial temperature (K)	Carbon balance (%)		
CH ₄	C ₂ H ₆	C ₂ H ₄	oxygen		oxidation products	pyrolysis products	residual methane
63	0	0	37	900	42	43	15
58	0	0	42	900	53	45	2
63	0	0	37	1000	41	46	13
53	10	0	37	900	42	37	21
53	0	10	37	900	43	42	15

The question thus arises: what means are available to increase the acetylene yield? Apparently, there are two ways of doing so: one is separating the pyrolysis and oxidation processes as it is already done commercially in dual chamber plants. The other, the overall reaction by appropriate additions of chemical additives. The results obtained in this field will soon be published in a following paper.

SYMBOLS USED

- c concentration of any of the species, (kmole m⁻³)
- t reaction time, (s)
- v stoichiometric coefficient
- A pre-exponential coefficient, (s, kmole, m³)
- E activation energy, (J kmole⁻¹)
- V total volume, (m³)
- p pressure, (Nm⁻²)
- T temperature, (K)
- n order of the reaction
- a coefficients of the enthalpy polynomial
- k index of the exponent of the enthalpy polynomial
- j, l index of the species
- i index of the reaction

REFERENCES

1. SACHSSE, H.: Chem. Ing. Technik, 26, 245 (1954)
2. BARTHOLOMÉ, E.: Chem. Ing. Technik, 26, 253 (1954)
3. Van TIGGELEN, A., NANQUIN, G.: Ind. Chim. Belge, 24, 349 (1958)
4. BENEDEK, P., LÁSZLÓ, A., NÉMETH, A.: MÁFKI 186. kiadvány, 1958
5. TESNER, A.: Brit. Chem. Engng. 72 (1958. Febr.)
6. GLASS, A., COOPER, W., BODY, J.: Chem. Engng. Prog. 61 (8), 49 (1965)
7. NÉMETH, A., DOBAY, S.: Proc. 2nd Conf. on Applied Physical Chemistry, Vol. 2. pp. 539, Akadémiai Kiadó, Budapest, 1971
8. STEPANOW, A.W., MACHORIN, K.E.: Chem. Techn. 24, 135 (1972)
9. BENEDEK, P., LÁSZLÓ, A., NÉMETH, A., VÁCZI, P.: Deuxième Symposium European sur la Combustion. Vol. I. pp. 54. The Combustion Institute, 1975
10. BENEDEK, P., VÁCZI, P.: Magyar Kémikusok Lapja, 28, 623 (1973)
11. NÉMETH, A., BENEDEK, P., VÁCZI, P.: Magyar Kémikusok Lapja, 29, 100 (1974)
12. GEAR, C.W.: Communications of the ACM, 14, 176, 185 (1971)
13. HIGGIN, R.M.R., WILLIAMS, A.: 12th Symp. on Combustion, Pittsburgh, pp. 579, The Combustion Institute, 1969
14. VANDOORE, J., PEETERS, J., Van TIGGELEN, D.J.: 14 th Symp. on Combustion, Abstract, Pittsburgh, pp. 141. The Combustion Institute,
15. GARDINER, W.C., OWEN, J.H., CLARK, T.C., DOVE, J.E., BAUER, S.H., MILLER, J.A, Mc LEAN, W.J.: ibid pp. 161
16. EISENBERG, B., BLISS, H.: Chem. Engng. Progr. Symp. Ser. No. 72. 63, 3 (1967)
17. TROTMAN-DICKENSON, A.F., MILNE, G.S.: Tables of Bimolecular Gas Reaction, NSDS-NBS9, U.S. Department of Commerce (1967)
18. DENIS, G.H., DAUBERT, T.E.: AICRE Journal, 20, 720 (1974)
19. SKINNER, G.B.: J. Chem. Phys.; 56, 3853 (1972)
20. JACHIMOWSKI, C.J.: Comb. a. Flame, 23, 223 (1974)
20. PEETERS, J., MAHNEN, G.: Combustion Institute European Symposium, 1973. pp. 53. Academic Press, London, 1973

РЕЗЮМЕ

Расширение знаний, связанных с отдельными реакциями и развитие вычислительной техники позволили составление адиабатической модели получения ацетилена неполным окислением метана, основанной на механизме реакции. С помощью ее было изучено значение отдельных реакций предполагаемого механизма реакции, и был определен удовлетворительный для описания процесса механизм. Было смоделировано влияние изменения состава и температуры входного газа, и получено соотношение, совпадающее с данными, измеренными в реакторе пламенного типа. Была обсуждена последовательность пиролизических (т.е. производящих ацетилен) и окислительных реакций, и на основе этого обсуждения истолковалось прохождение процесса.

СТРУКТУРА ОРГАНИЗОВАННОГО ТРЕХФАЗНОГО ПСЕВДООЖИЖЕННОГО СЛОЯ.
ЭКСПЕРИМЕНТАЛЬНАЯ ЗАВИСИМОСТЬ СОДЕРЖАНИЯ
ТВЕРДОЙ ФАЗЫ ОТ СКОРОСТЕЙ ПОТОКОВ

А. ЕРМАНОВА, Й. ХОЛДЕРИТ, Е. Ф. СТЕФОГЛО, В. И. ПЬЯНОВ

(Институт Катализа СО АН СССР, г.Новосибирск)

Поступила в редакцию: 1. декабря 1975 г.

Проведено экспериментальное исследование структуры трехфазного псевдоожигенного слоя газ-жидкость - твердый материал (ТПС) в присутствии насадочной насадки. Показано, что наличие насадки в слое приводит к выравниванию его структуры, к устранению пространственных неоднородностей. Экспериментально изучен фазовый состав ТПС без насадки и в присутствии насадки. На основании известных в литературе подходов к описанию порозности двухфазного псевдоожигенного слоя жидкость-твердые частицы, предложена приближенная модель для описания зависимости объемной доли твердой фазы от скорости жидкости.

Известно, что структура трехфазного псевдоожигенного слоя газ-жидкость-твердый материал (ТПС) является существенно неоднородной в широком диапазоне линейных скоростей фаз. Исследование механизма образования, роста и всплывания пузырей в ТПС [1-5] показало, что основной причиной, вызывающей появление неоднородностей в ТПС, является более высокая склонность газовых пузырей к коалесценции, чем в двухфазном барботажном слое. Крупные пузыри,

поднимаясь с относительно большой скоростью, увлекают с собой часть жидкости, практически не содержащей твердой фазы.

В работах [6-7] указывается на возможность перехода от режима неоднородного к режиму однородного псевдооживления путем увеличения скорости жидкости при постоянной скорости газа. Режим однородного псевдооживления визуально можно характеризовать равномерным распределением мелких газовых пузырей по объему реактора. Вследствие этого наблюдается рост газосодержания [8] и скорости массопереноса через границу раздела фаз газ-жидкость [9] при переходе от неоднородного к однородному ТПС.

К сожалению, режим однородного псевдооживления в ТПС наступает лишь при тех линейных скоростях жидкости, при которых слой сильно расширен, и концентрация твердых частиц мала. С целью создания однородной структуры ТПС во всем интервале его существования, мы использовали внутри слоя специальные распределительные устройства (насадки) [27], способствующие диспергированию крупных газовых пузырей и равномерному распределению их по объему реактора. В предварительных экспериментах сравнивали несколько насадок различных размеров, видов и типов, среди которых наилучшей оказалась т.н. "каркасная" насадка (рис. 1), представляющая собой цилиндр обечайку с перфорированной боковой поверхностью в виде полосок - радиусов, отогнутых внутрь, и внешним диаметром, равным внутреннему диаметру аппарата. Объем насадки занимает 3% объема реактора.

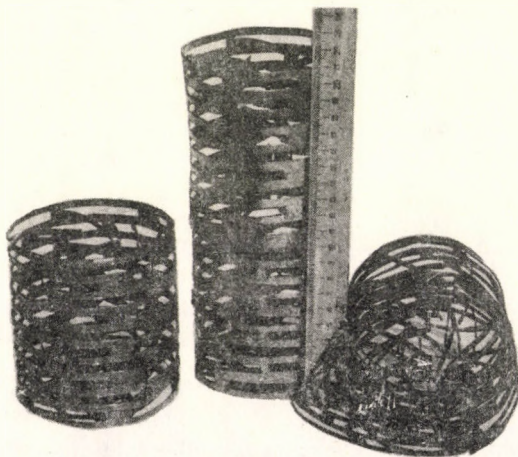


Рис. 1. Общий вид каркасной насадки

Настоящая работа посвящена изучению влияния этой насадки на среднюю объемную долю твердой фазы в ТПС. В дальнейшем ТПС без на-

садки будем называть "свободным" (СТПС), а ТПС с насадкой "организованным" (ОТПС).

Проведение экспериментов

С целью сопоставления, свободный и организованный ТПС исследовали в одной и той же колонне диаметром 100 мм, высотой 1000 мм при восходящем прямотоке воды и воздуха. Твердой фазой служили стеклянные шарики диаметром 0,75 мм и узкие фракции песка средним диаметром 0,2 и 0,45 мм. Фиктивную линейную скорость (Объемный расход, деленный на полное сечение аппарата) воды и воздуха варьировали в пределах 0,28-8,7 см/сек и 2-7 см/сек соответственно.

Объемные доли фаз определяли следующим образом: после загрузки в колонну определенного количества твердого материала установили заданные расходы воздуха и воды. При этом слой расширился до перелива колонны. После установления стационарного состояния (т.е. после прекращения уноса избытка твердых частиц) одновременно прекратили подачу воды и воздуха. После осаждения слоя измеряли суммарную высоту твердой и жидкой фаз (H_1) и высоту двухфазного неподвижного слоя (H_2). Объемные доли воздуха, воды и твердых частиц рассчитывали по следующим формулам:

$$\varphi_1 = 1 - \frac{H_1}{f \cdot H}, \quad \varphi_2 = 1 - \varphi_1 - \varphi_3, \quad \varphi_3 = \frac{(1 - \epsilon_0) H_2}{f \cdot H} \quad (1)$$

где H - полная высота колонны; ϵ_0 - порозность двухфазного неподвижного слоя, множитель $f=0,97$ учитывает объем насадки в ОТПС, а для СТПС $f=1$.

Результаты эксперимента

Визуальные наблюдения показали, что нарнасная насадка действительно приводит к диспергированию и равномерному распределению газовых пузырей во всем диапазоне существования ОТПС. Режим неод-

Таблица 1

Фазовый состав свободного трехфазного псевдооживленного слоя
воздух-вода-твердые частицы (СТПС)

$d_3=0,20$ мм, песок					$d_3=0,45$ мм, песок					$d_3=0,75$ мм, стеклянные шарики				
W_1 см/сек	W_2 см/сек	φ_1	φ_2	φ_3	W_1 см/сек	W_2 см/сек	φ_1	φ_2	φ_3	W_1 см/сек	W_2 см/сек	φ_1	φ_2	φ_3
2,0	0,50	0,02	0,68	0,30	2,0	0,28	0,04	0,49	0,47	2,0	0,61	0,02	0,58	0,48
	1,70	0,02	0,80	0,18		0,68	0,04	0,61	0,35		1,73	0,02	0,71	0,33
5,0	0,50	0,05	0,66	0,29		3,72	0,05	0,80	0,15		3,83	0,02	0,74	0,24
	1,70	0,05	0,79	0,16	5,0	0,38	0,05	0,53	0,42		5,72	0,03	0,80	0,17
7,0	0,50	0,07	0,65	0,28		0,90	0,05	0,64	0,31		8,64	0,03	0,84	0,13
	1,70	0,07	0,78	0,15		1,66	0,05	0,73	0,22	5,0	0,61	0,05	0,51	0,44
						1,42	0,05	0,75	0,20		1,73	0,05	0,65	0,30
						6,67	0,08	0,83	0,09		3,83	0,05	0,72	0,23
						9,96	0,08	0,86	0,06	7,0	0,61	0,07	0,51	0,42
											1,73	0,07	0,63	0,30
											3,83	0,07	0,72	0,21

Таблица 2

Фазовый состав организованного трехфазного псевдооживленного слоя
воздух-вода-твердые частицы (ОТПС)

$d_3=0,20$ мм, песок					$d_3=0,45$ мм, песок					$d_3=0,75$ мм, стеклянные шарики				
W_1 см/сек	W_2 см/сек	φ_1	φ_2	φ_3	W_1 см/сек	W_2 см/сек	φ_1	φ_2	φ_3	W_1 см/сек	W_2 см/сек	φ_1	φ_2	φ_3
2,0	0,75	0,05	0,62	0,33	2,0	0,60	0,03	0,46	0,51	2,0	1,2	0,03	0,48	0,49
	0,88	0,05	0,73	0,22		2,0	0,04	0,76	0,20		4,1	0,05	0,72	0,23
	0,89	0,07	0,77	0,16		3,3	0,07	0,84	0,09		5,6	0,05	0,83	0,12
	1,02	0,06	0,76	0,18	3,5	0,60	0,06	0,47	0,47	3,5	1,2	0,06	0,51	0,43
	1,58	0,07	0,83	0,10		2,0	0,08	0,72	0,20		4,0	0,08	0,72	0,20
	1,91	0,07	0,86	0,07		2,7	0,11	0,74	0,15		5,6	0,08	0,80	0,12
5,0	0,75	0,05	0,75	0,30		3,3	0,13	0,79	0,08	5,0	1,2	0,09	0,46	0,45
	0,89	0,05	0,73	0,22	5,0	0,60	0,09	0,44	0,47		4,0	0,10	0,71	0,19
	1,96	0,06	0,84	0,10		2,0	0,12	0,77	0,11		5,6	0,16	0,76	0,08
	1,91	0,07	0,87	0,06		2,4	0,16	0,69	0,15					
	2,90	0,07	0,91	0,02		2,7	0,15	0,78	0,07					

народного псевдооживления, характерный для СТПС, в организованном ТПС не наблюдается.

Результаты экспериментов по определению фазового состава ТПС представлены в таблицах 1 и 2. Очевидно, что при прочих равных условиях объемная доля твердой фазы является функцией фиктивных линейных скоростей воздуха и воды: $\varphi_3 = \varphi_3(W_1, W_2)$. Однако, если в качестве независимых переменных вместо фиктивных выберем средние истинные линейные скорости воздуха и воды, определяемые соотношениями:

$$U_1 = \frac{W_1}{\varphi_1}, \quad U_2 = \frac{W_2}{\varphi_2} \quad (2)$$

то оказывается, что объемная доля твердой фазы будет зависеть лишь от скорости воды (U_2), т.е. $\varphi_3 = \varphi_3(U_2)$. Независимость функции $\varphi_3(U_2)$ от W_1 наблюдалась нами в диапазоне скоростей воздуха $2 \leq W_1 \leq 7$ см/сек. При более высоких скоростях газа эта закономерность нарушается.

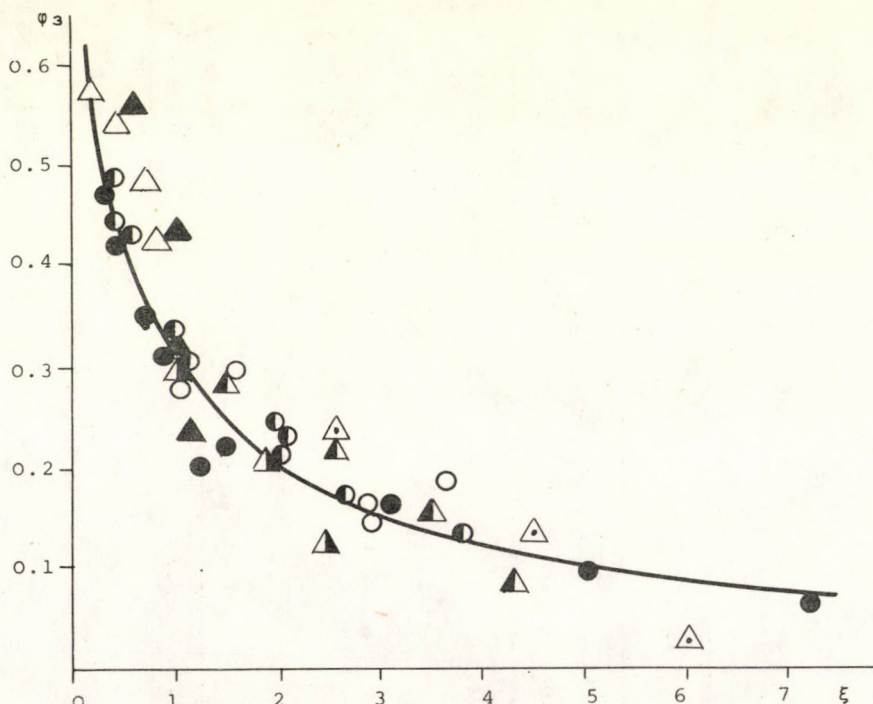


Рис.2. Зависимость объемной доли твердой фазы от безразмерной скорости жидкости. Свободный ТПС.

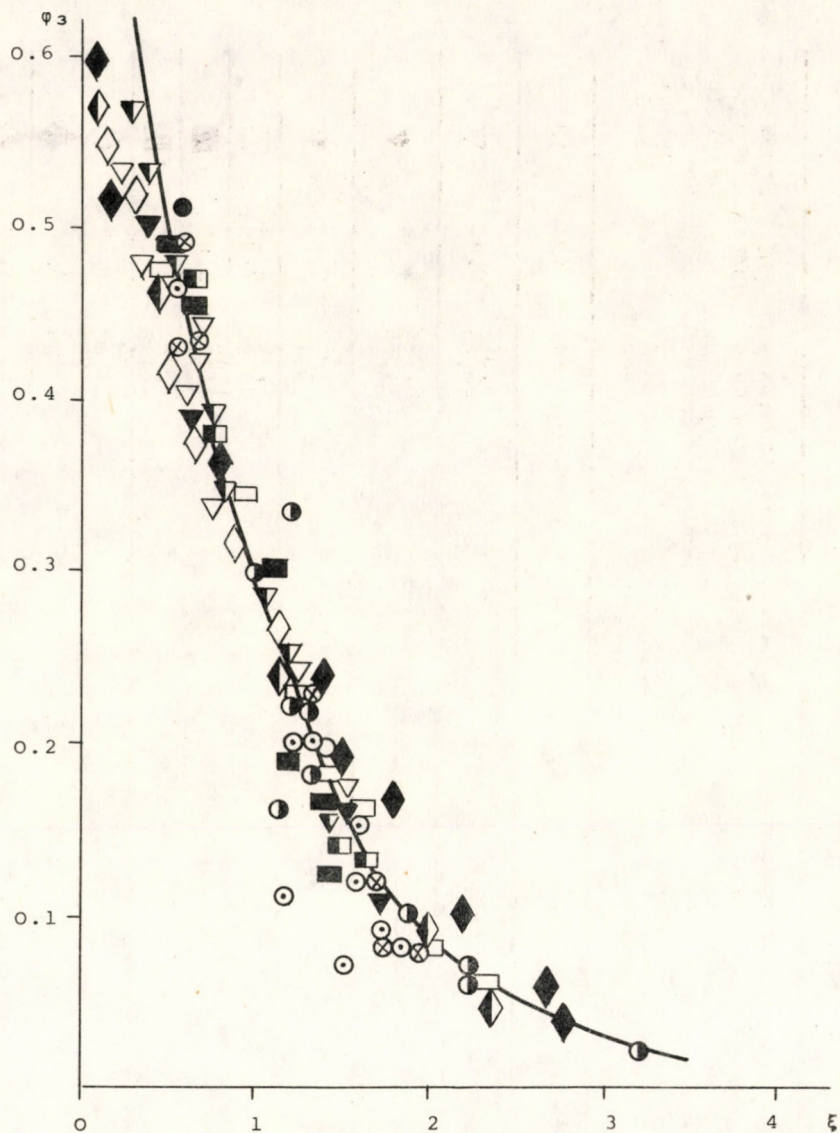


Рис.3. Зависимость объемной доли твердой фазы от безразмерной скорости жидкости. Организованный ТПС, ДПС.

Таблица 3

Условия экспериментов и значения U_2^* , использованных при построении графиков рис.2 и 3

Авторы, № лит. ссылки и тип псевдо- оживления	Высота слоя, мм	Диаметр, мм	Форма, мм	Размер, мм	Плотность, г/см ³	Вязкость, СП	Плотность, г/см ³	Фиктивные линейные скорости, см/сек	U* см/сек	Услов- ное обо- знач. то- чек на рисунках 2 и 3		
1	2	3	4	5	6	7	8	9	10	11	12	13
Lewis W.K., Gril- land E.R., Bauer W.C. [10]ДПС	1270	60,3	стекл- янные шарики	0,15	2,45			0,05- -0,57	0,45	▽		
				0,28	2,43	вода		0,24- -1,88	1,35	▼		
				0,45	2,91			0,34- -3,10	2,35	▼		
Mesure L.K., Wilhelm R.H. [11]ДПС	494- -2019	102	наф- тол-2 сфери- ческий сектор	3,19			1,01- -1,10	1,10- -8,90	5,63	□		
				4,80	1,28	вода		1,95- -11,8	8,65	■		
				6,37				2,57- -11,3	10,02	■		
Wilhelm R.H., Kwaak M. [12] ДПС		91,4	мор- ской песок стекл, шарики	0,38	2,64	вода		0,09- -2,99	1,68	◇		
				0,56				1,10- -4,67	2,44	◆		
				5,0	2,35			1,33- -24,2	14,80	◆		

Продолжение таблицы 3

Авторы, Высота лит. слоя, ссылки мм	Диа- метр но- лон- ны, мм	Форма и Раз- мер час- тиц, мм	Плот- ность, г/см ³	Жид- кость, тип	Вяз- кость, СП	Плот- ность, г/см ³	Фиктивные линейные скорости, см/сек	U [*] см/сек	Условное обознач. точек на рисунках 2 и 3							
1	2	3	4	5	6	7	8	9	10	11	12	13				
Немец Л.Л., Ра- зумов И.М., Манши- лин В.В. [13] СТПС	1500	90	песок	0,82	2,80	геп- тан	0,44	0,684	1+5	1+4	10,3	△				
						вода	1,00	1,00			5,0	▲				
						вода	8,78	1,145			1,1	▲				
						гли- церин	11,35	1,154			1,5	▲				
						16,40	1,68				0,55	△				
Наша работа СТПС	1000	100	песок	0,20					0,5- 1,7		0,75	○				
									2+7	0,3- 10,0	1,60	●				
										0,6- 8,7	3,0	●				
										0,75- 2,9	1,0	●				
Наша работа ОТПС	1000	100	песок	0,20					2+5	0,6- 3,3	2,25	○				
										1,28- 6,8	4,25	⊗				

С целью обобщения и сопоставления с литературными данными, экспериментальные данные представлены на рисунках 2 и 3 в зависимости от безразмерной скорости жидкости ξ . На этих же рисунках изображены экспериментальные данные других авторов [10-13]. Основные экспериментальные условия, при которых были получены эти результаты, показаны в таблице 3, вместе с нашими данными и указанием обозначений, принятых на рисунках.

В нашей ранней работе [14] в качестве безразмерной скорости предлагается число псевдооживления: $n = U_2/U_{20}$, где значения скорости начала псевдооживления U_{20} определялись экспериментально. Однако при обработке литературных данных, в которых значения U_{20} не измерялись (или не сообщались), надежное вычисление числа n сталкивается со значительными трудностями. Экстраполяция экспериментальных данных до значения φ_3 , соответствующее неподвижному слою, является довольно неточной, иногда приводит даже к отрицательной скорости псевдооживления [13]. Различные эмпирические или полуэмпирические формулы, предложенные в литературе [15, 16] для оценки U_{20} , дают сильное расхождение между собой. Нам кажется целесообразным в качестве масштаба скорости выбрать ту, при которой значение φ_3 находится примерно в середине диапазона своего изменения. Поэтому в настоящей работе масштабом выбрана скорость жидкости U_2^* , при которой $\varphi_3 = 0,3$. При таком выборе значение масштаба определяется в большинстве случаев интерполяцией экспериментальных данных, иногда непосредственным измерением, и только в редких случаях экстраполяцией на небольшое расстояние.

Из рисунков 2 и 3 видно, что экспериментальные точки, полученные для частиц разных размеров и различными исследователями, располагаются в двух, довольно узких полосах. В одной полосе находятся точки, соответствующие СТПС, (рис.2), а в другой изображены данные, полученные в ОТПС и в двухфазных псевдооживленных слоях жидкость-твердый материал (ДПС) (рис.3). Ход этих двух полос резко отличается друг от друга, причем в последнем случае наблюдается более резкое падение φ_3 с ростом ξ . Интересно обратить внимание на то обстоятельство, что экспериментальные данные для ОТПС находятся в той же полосе, что для ДПС. Так как структура ДПС является однородной, это подтверждает правильность визуальных наблюдений об однородности структуры организованного ТПС:

Математическая модель

Основные идеи и подходы к построению математических моделей для описания зависимости объемной доли твердой фазы от разных факторов в ДПС подробно изложены в литературе и обобщены в монографии Лева [16]. Аналогичные подходы встречаются в более новых работах [17-19]. В области ТПС можно назвать несколько работ, посвященных этому вопросу [1,2,13,21-26]. В ходе дальнейших рассуждений будем придерживаться одного из упомянутых в книге Лева [16] подходов, а именно модели Кармана, иногда называемой капиллярной моделью Кармана-Нозени [15], описывающей перепад давления при течении жидкости через неподвижный слой твердых частиц. Наша модель, описывающая зависимость объемной доли твердой фазы от истинной средней линейной скорости жидкости, строится на следующих трех основных предположениях:

1. Роль газовой фазы состоит лишь в том, что она уменьшает свободное сечение аппарата, в котором происходит псевдооживление твердых частиц одной только жидкостью. Следовательно ТПС представили как сумму двух независимых частей: пузыри газа и ДПС. Известно, что в ДПС в состоянии динамического равновесия сила гидравлического сопротивления, действующего в единице объема (ΔP), равна удельному весу твердой фазы с учетом архимедовой поправки:

$$\Delta P = \varphi_3(\rho_3 - \rho_2) \quad (3)$$

2. Стационарный ДПС рассматривается как расширенный неподвижный слой, в котором зависимость ΔP от скорости течения жидкости описывается уравнением Кармана [16]:

$$\Delta P = \lambda \cdot \frac{\mu}{d_3} \cdot \frac{U_2^2}{2g} \cdot \rho_2 \quad (4)$$

3. Имея в виду квазитурбулентность многофазных течений, коэффициент сопротивления λ напишем в следующем виде

$$\lambda = \frac{C}{Re^p}, \quad Re = \frac{U_2 d_3}{\nu_2} \quad (5)$$

и предположим, что показатель степени p постоянный во всей области существования ТПС.

Принимая во внимание, что эквивалентный диаметр канала слоя можно определить уравнением:

$$d_{\text{э}} = \frac{2}{3} \phi_3 d_3 \frac{1-\phi_3}{\phi_3} \quad (6)$$

из вышеприведенных соотношений находим вместо исходной зависимости ее обратную функцию:

$$U_2 = K(\phi_3 d_3)^{\frac{p+1}{2-p}} \frac{(1-\phi_3)^{\frac{p+1}{2-p}}}{\phi_3^{\frac{p}{2-p}}} \quad (7)$$

где

$$K = \left[2 \left(\frac{2}{3} \right)^{p+1} \cdot \frac{g}{C \cdot \mu} \cdot \frac{\rho_3 - \rho_2}{\nu_2^p \cdot \rho_2} \right]^{\frac{1}{2-p}} \quad (8)$$

после перехода к безразмерной скорости получили следующую зависимость:

$$\xi = \left(\frac{1-\phi_3}{0,7} \right)^{\frac{1+p}{2-p}} \left(\frac{0,3}{\phi_3} \right)^{\frac{p}{2-p}} \quad (9)$$

Это уравнение содержит всего один неизвестный параметр p , значение которого удалось подобрать так, чтобы рассчитанные по уравнению кривые лежали внутри полос экспериментальных точек. Таким образом получили значения $p=1,0$ для СТПС и $p=0,5$ для ОТПС. Соответствующие кривые зависимости от ϕ_3 изображены сплошными линиями на рисунках 2 и 3 соответственно. Из рисунков видно, что уравнение (9) удовлетворительно описывает наши экспериментальные данные практически во всей области существования ТПС. Систематическое отклонение влево от расчетной кривой в области $\phi_3 > 0,3$ дают экспериментальные точки, полученные в ДПС, что вероятно свидетельствует о возможно некоторой неоднородности структуры самого ДПС по сравнению с ОТПС.

Из уравнения (9) следует, что при вышеприведенных значениях p между скоростью U_2^* , плотностью твердой фазы и жидкости, вязкост-

тью жидкости и диаметром частиц должны существовать следующие зависимости:

для ОТПС:

$$U_2^* \sim \left(\frac{\rho_3 - \rho_2}{\rho_2} \right)^{2/3} \frac{d_3}{v_2^{1/3}} \quad (10)$$

для СТПС:

$$U_2^* \sim \frac{\rho_3 - \rho_2}{\rho_2 \cdot v_2} \cdot d_3^2 \quad (11)$$

Обработка соответствующих данных (таблица 3) показала, что уравнение (10) (при постоянном значении v_2 и ρ_2) справедливо в интервале $0,15 \leq d_3 \leq 0,8$ мм, $1,28 \leq \rho_2 \leq 2,64$ г/см³. Экспериментальные данные, полученные в СТПС не удовлетворяют уравнению (11). Это говорит о том, что уравнение (9) в случае СТПС можно рассматривать лишь как чисто эмпирическое соотношение, а в случае ОТПС - как приближенную математическую модель.

СПИСОК УСЛОВНЫХ ОБОЗНАЧЕНИЙ

d_3 - эквивалентный диаметр канала между частицами, м;

d_3 - диаметр твердых частиц, м;

g - ускорение силы тяжести, м/сек²;

p - константа, (-);

ΔP - перепад давления, кг/м²;

U_1, U_2 - истинные линейные скорости потоков газа и жидкости соответственно, м/сек;

U_{20} - истинная скорость начала псевдооживления, м/сек;

U_2^* - истинная скорость жидкости соответствующая значению $\Phi_3 = 0,3$, м/сек;

W_1, W_2 - фиктивные линейные скорости потоков газа и жидкости соответственно, м/сек;

λ - коэффициент трения, (-);

μ - коэффициент извилистости, (-);

ν_2 - кинематическая вязкость жидкости, $\text{м}^2/\text{сек}$;

$\varphi_1, \varphi_2, \varphi_3$ - объемные доли газа, жидкости и твердого материала в реакторе, $\text{м}^3/\text{м}^3$;

Φ_3 - фактор формы твердых частиц, (-);

ρ_2, ρ_3 - плотность жидкости и твердого материала соответственно, $\text{кг}/\text{м}^3$;

Безразмерные группы:

$$\xi = \frac{U_2}{U_2^*}, \quad n = \frac{U_2}{U_{20}}, \quad Re = \frac{U_2 d_3}{\nu_2}$$

Сокращения:

ТПС - трехфазный псевдооживленный слой

СТПС - трехфазный псевдооживленный слой без насадки

ОТПС - трехфазный псевдооживленный слой с насадкой

ДПС - двухфазный псевдооживленный слой жидкость-твердый материал

СПИСОК ЛИТЕРАТУРЫ

1. OSTERGAARD K., Chem. Eng. Sci., 20, 165, (1965).
2. OSTERGAARD K., THEISEN P. I., Chem. Eng. Sci., 21, 413, (1966).
3. OSTERGAARD K., Chem. Eng. Sci., 21, 470, (1966).
4. RIGBY G. R., VAN BLOCKLAND G. P., PARKS W. H., CAPES C. E., Chem. Eng. Sci., 25, 1729, (1970).
5. RIGBY G. R., CAPES C. E., Can. Journ. Chem. Eng., 48, 343, (1970).
6. ЕРМАКОВА А., ЗИГАНШИН Г. Н., СЛИНЬКО М. Г., ТОХТ, 4, 95, (1970).
7. БЕРБИЦКИЙ Б. Г., ВАХРУШЕВ И. А., Хим. и техн. топлив и масел, № 4, (1974).
8. ЗИГАНШИН Г. Н., ЕРМАКОВА А., ТОХТ, 4, 594, (1970).
9. ГАРЦМАН А. Н., ЕРМАКОВА А., БАХВАЛОВА В. П., РАССАДНИКОВА Н. Н., Hung. J. Ind. Chem., 3, 37, (1975).

10. LEWIS E. W., GILLILAND E. R., BAUER W. C.,
Ind. Eng. Chem., 41, 1104, (1949).
11. MECUNE L. K., WILHELM R. H.,
Ind. Eng. Chem., 41, 1124, (1949).
12. WILHELM R. H., KWAUK M., Chem. Eng. Progr., 44, 201, (1948).
13. НЕМЕЦ Л. Л., РАЗУМОВ И. М., МАНШИЛИН В. В., Хим. и техн. топлив и масел, № 2, 37, (1975).
14. СТЕФОГЛО Е. Ф., Автореферат канд. диссертации, Новосибирск, (1975).
15. ДЭВИДСОН И. Ф., ХАРРИСОН Д., "Псевдооживление", Изд. "Химия", Москва, (1974).
16. ЛЕВА М., "Псевдооживление", Гос. научно-техн. издательство нефтяной и горно-топливной литературы, Москва, (1961).
17. RUCKENSTEIN E., Ind. Eng. Chem. Fund., 3, 260, (1964).
18. HUGHMARK G. A., A. I. Ch. E. Journ. 18, 1020, (1972).
19. BLICKLE T., ORMOS Z., Hung. J. Ind. Chem., 1, 185, (1973).
20. RAMAMUSTRY K., SUBBARAJU K., Ind. Eng. Chem. Process Development, 12, № 2, 184, (1973).
21. STEWART P. S., DAVIDSON I. F., Chem. Eng. Sci., 19, 319, (1964)
22. ЕФРЕМОВ Г. И., ВАХРУШЕВ И. А., Хим. и техн. топлив и масел, № 8, 4, (1969).
23. РАЗУМОВ И. М., НЕМЕЦ Л. Л., МАНШИЛИН В. В., Хим. и техн. топлив и масел, № 12, 28, (1969).
24. РАЗУМОВ И. М., МАНШИЛИН В. В., НЕМЕЦ Л. Л., Хим. и техн. топлив и масел, № 2, 31, (1972).
25. DAHSHIRAMURTY P., RAO K. V., SUBBARAJU R. V., SUBRAHMANJAM V.,
Ind. Eng. Chem. Proc. Des. and Develop., 11, 318, (1972).
26. BRUCL, P. N., REVEL Ch., Powder Technol., 10, 243, (1974).
27. СТЕФОГЛО Е. Ф., ЕРМАНОВА А., БАХВАЛОВА В. П., Моделирование процессов в псевдооживленном слое катализатора. (Доклад на пятой Всесоюзной конференции по моделированию химических, нефтехимических и нефтеперерабатывающих процессов и реакторов - "Химреактор - 5", том. 2, стр. 116 - 119, г. Уфа, 1974 г.).

SUMMARY

The behaviour of a gas-liquid-solid three phase fluidized bed was investigated. As solid material,ribbed packing was immersed into the fluidized bed. It was shown that the presence of the packing equalizes the structure of the bed and hinders the formation of spatial inhomogenities. Experiments were carried out for the examination of the three phase fluidized bed in the presence and absence of the packing. A mathematical model is proposed for the description of the solid phase volume fraction which depends on the liquid flow rate.

МАССОПЕРЕДАЧА С ХИМИЧЕСКОЙ РЕАКЦИЕЙ НА ГРАНИЦЕ
РАЗДЕЛА ФАЗ "ГАЗ-ЖИДНОСТЬ"

А.Н.Гарцман, А.Ермакова, Н.И.Рассадникова

Институт катализа СО АН СССР
Новосибирск, 630090, СССР

Поступила в редакцию 8 декабря 1975 г.

В работе приведена иерархическая модель газожидкостного реактора и рассмотрены вопросы, связанные с решением уравнений математического описания второго уровня этой модели.

Уравнения математического описания были получены путем некоторого упрощения уравнения переноса вещества в турбулентном потоке и решены численно. При этом, в отличие от других работ, учтены явления затухания коэффициента турбулентной диффузии и изменения скорости потока в направлении перпендикулярном к поверхности раздела фаз.

Анализ результатов решения показал наличие областей т.н. "быстрых" и "медленных" реакций в зависимости от величины отношения безразмерных параметров Φ^2/Re . Область "быстрых" реакций получена при $\Phi^2/Re \geq 10$ и характеризуется нечувствительностью безразмерного межфазного диффузионного потока к микрогидродинамике в пограничном слое. Область "медленных" реакций была получена при $\Phi^2/Re \leq 0,1$ и характеризуется совпадением решения уравнений математического описания с асимптотическим решением при $\Phi = 0$.

Приведен также анализ влияния параметров, описывающих профили коэффициента диффузии и скорости потока, на величину безразмерного диффузионного потока, определены области существенного и несущественного влияния этих параметров.

Химические процессы, протекающие при взаимодействии газов и жидкостей, широко распространены в промышленности. Поскольку явления массопереноса через границу раздела фаз могут оказывать существенное влияние на скорость и направление химического превращения, протекающего в жидкой фазе, лимитировать процесс в целом, им уделяется большое внимание исследователей. Обзор работ, посвященных вышеуказанным вопросам, можно найти в монографиях [1-3].

Иерархическая модель газо-жидкостного реактора представлена на рис. 1.

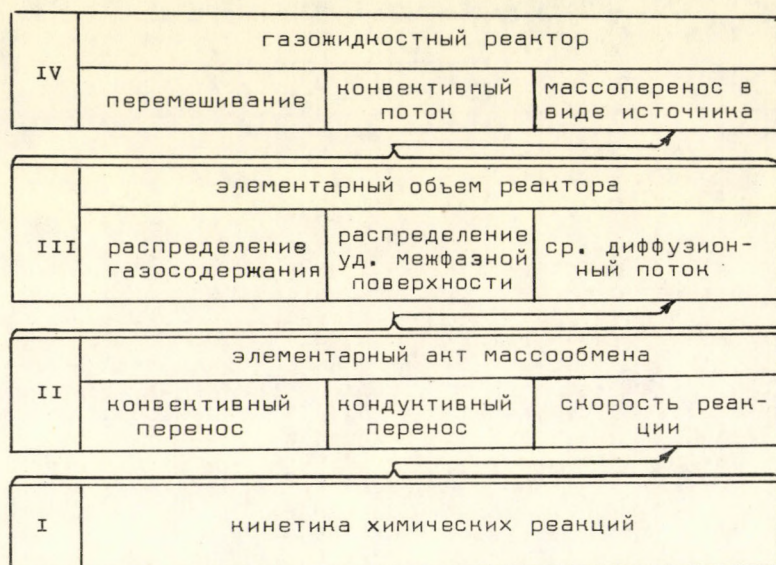


Рис. 1. Иерархическая модель газо-жидкостного реактора

Вторым уровнем этой модели является математическое описание процессов массопереноса, сопровождаемых химической реакцией и протекающих на единичной макроструктуре (пузырь, поршень, струя и т.п.) В результате анализа математической модели второго уровня определяется функциональная зависимость межфазного диффузионного потока от параметров, характеризующих локальную гидродинамическую обстановку и скорость химической реакции.

Опубликовано значительное количество работ, посвященных этому вопросу, например, работы [4-15], (более полную библиографию можно найти в книгах [1-3]). В большинстве работ авторы исходят из уравнения конвективной диффузии с теми или иными упрощениями, однако, лишь в нескольких статьях [4, 16-20] изучаются процессы переноса вещества, происходящие в турбулентных потоках. Существующие в таких потоках явления изменения скорости потока и коэффициента диффузии вещества с изменением расстояния до поверхности раздела фаз значительно усложняют рассматриваемую проблему.

Цель настоящей работы - определить какое влияние окажет учет вида профиля скорости потока и явления затухания коэффициента турбулентной диффузии на величину диффузионного потока.

Пусть уравнение переноса вещества в турбулентном пограничном слое записано следующим образом:

$$\frac{\partial c_i}{\partial \tau} + u_j \frac{\partial \bar{c}_i}{\partial x_j} - \frac{\partial}{\partial x_j} (D_{ij} \frac{\partial \bar{c}_i}{\partial x_j}) = f_i \quad (1)$$

$$i=1,2,\dots,n; \quad j=1,2,3;$$

При выводе уравнений математического описания второго уровня модели были приняты следующие допущения:

1. Химическая реакция протекает в объеме жидкой фазы.
2. Единичное образование обтекается изотропным турбулентным потоком. Поверхность единичного образования равнодоступна турбулентным пульсациям.
3. Толщина гидродинамического пограничного слоя намного меньше характерного размера единичного образования.
4. Причиной возникновения турбулентных пульсаций в основном является не относительное движение фаз, а движение двухфазного потока в реакторе с высокими линейными скоростями.
5. Осредненность турбулентного движения допускает рассмотрение процесса на данном уровне как стационарного.
6. Пренебрегаем различием коэффициентов молекулярной диффузии компонентов и перекрестными эффектами.

Принятые допущения дают возможность считать поверхность единичного образования плоской, а обтекание его потоком - плоскопараллельным. С учетом этого обстоятельства уравнение (1) можно переписать в безразмерном виде:

$$\text{Pe}W(\eta) \cdot \frac{\partial \theta_i}{\partial \xi} = \frac{\partial}{\partial \eta} \left[D(\eta) \frac{\partial \theta_i}{\partial \eta} \right] + \left(\frac{L_Y}{L_X} \right)^2 \frac{\partial}{\partial \xi} \left[D(\xi) \frac{\partial \theta_i}{\partial \xi} \right] + V_i \Phi_i^2 \quad (2)$$

В тех случаях, когда причиной возникновения турбулентных пульсаций является относительное движение фаз пренебрегают вторым членом правой части уравнения (2). Поскольку мы рассматриваем течение в системе координат, закрепленной в центре движущегося единичного образования, такое допущение является неоправданным. Суммарный коэффициент диффузии в направлении по касательной к поверхности единичного образования может оказаться большим по сравнению с коэффициентом диффузии в направлении перпендикулярном к поверхности раздела фаз. Отсюда следует, что первые два члена правой части уравнения (2) могут быть соизмеримы, несмотря на возможное выполнение общепринятого неравенства

$$\frac{\partial \theta}{\partial \eta} \gg \frac{\partial \theta}{\partial \xi}$$

Решение уравнения (2) позволяет получить зависимость осредненного диффузионного потока

$$J_i = - \int_0^1 \left[D(\eta) \frac{\partial \theta_i}{\partial \eta} \right]_{\eta=0} d\xi \quad (3)$$

от безразмерных параметров Pe_i и Φ_i , характеризующих соответственно гидродинамическое состояние системы и скорость химического превращения.

Поставленная выше задача решалась для двух вариантов модели. Модель №1 представляет собой уравнение (2) без учета второго члена

правой части и с зависимостями $D(\eta)$ и $W(\eta)$, заданными в виде алгебраических функций. Функция $D(\eta)$ во всех случаях была задана выражением

$$D(\eta) = D_0 + (1-D_0)\eta^n \quad (4)$$

отражающим явление уменьшения суммарного коэффициента диффузии по мере приближения к поверхности раздела фаз, подтверждение которого было экспериментально получено в последнее время [18-20]. Зависимость $W(\eta)$ задавалась одним из следующих соотношений:

$$W(\eta) = \begin{cases} 1 - (1-W_0)(1-\eta)^2[G+(1-G)(1-\eta)^4] & (5a) \end{cases}$$

$$W(\eta) = \begin{cases} 0,5 + 3\eta - W_0\eta^G & (5б) \end{cases}$$

$$W(\eta) = \begin{cases} W_0 + \frac{\eta}{W_0 + 10^{-3}\eta + G\eta^2} & (5в) \end{cases}$$

Описывая распределение скорости потока указанным способом, мы не ставили перед собой цель получить профиль скорости наиболее близкий к действительности. Задачей было определение чувствительности величины среднего безразмерного диффузионного потока к изменению вида профиля скорости и величин локальных значений скорости в направлении перпендикулярном к поверхности раздела. На рис. 2а,б представлен вид нескольких характерных профилей коэффициента диффузии и скорости потока, полученных из соотношений (4) и (5а) - (5в) соответственно.

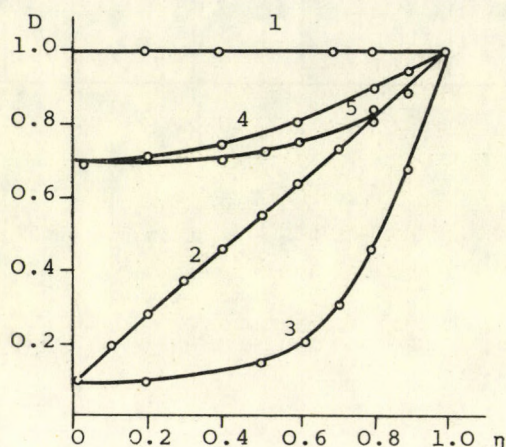


Рис. 2а Профили безразмерного коэффициента диффузии

- 1 - $Do = 1$; $n = 1$;
- 2 - $Do = 0,1$; $n = 1$;
- 3 - $Do = 0,1$; $n = 4$;
- 4 - $Do = 0,7$; $n = 2$;
- 5 - $Do = 0,7$; $n = 4$;

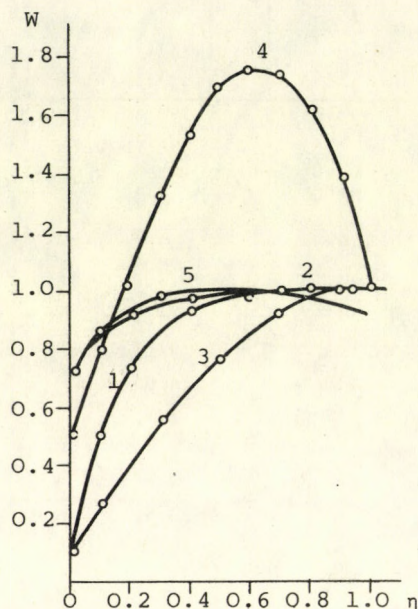
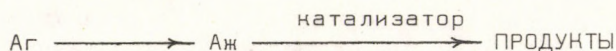


Рис. 2б Профили безразмерной скорости потока

- | | |
|--------------|--------------------------------|
| | 1 - $Wo = 0,1$; $G = 0,1$; |
| уравнение 5а | - 2 - $Wo = 0,7$; $G = 0,1$; |
| | 3 - $Wo = 0,1$; $G = 1$; |
| уравнение 5б | - 4 - $Wo = 2,5$; $G = 3$; |
| уравнение 5в | - 5 - $Wo = 0,7$; $G = 3,5$; |

Модель № 2 состоит непосредственно из уравнения (2), причем зависимости $D(\eta)$ и $W(\eta)$ задавались как описано выше, а $D(\xi)$ полагали константной и в различных вариантах варьировали от 0,1 до 1. Обе модели предполагали протекание в системе одной химической реакции первого порядка



Численное решение уравнений математического описания было получено для модели № 1 методом Кранка-Никольсона (21), а для модели № 2 - методом установления (22). При этом использовались следующие кра-

евые и начальные условия для $\theta(\eta, \xi)$:

$$\begin{aligned}\theta(\eta, 0) &= 0; \\ \theta(0, \xi \leq 1) &= 1; \\ \frac{\partial \theta}{\partial \eta}(0, \xi > 1) &= 0; \\ \frac{\partial \theta}{\partial \eta}(1, \xi) &= 0;\end{aligned}\tag{6}$$

Поставленная выше задача была решена нами ранее (4) для более простой модели, которая вытекает из уравнения (2), если в нем пренебречь вторым членом правой части и задать зависимости $D(\eta)$ и $W(\eta)$ в виде

$$D(\eta) = \text{const} = 1;$$

$$W(\eta) = \text{const} = 1;$$

т.е. предположить, что все турбулентные пульсации, действующие в направлении перпендикулярном к поверхности единичного образования, достигают последней не затухая.

В результате решения уравнений математического описания для этой модели было показано наличие областей т.н. "быстрых" и "медленных" реакций в зависимости от величины отношения ϕ^2/Re . Область "быстрых" реакций была получена при $\phi^2/Re \geq 10$ и характеризуется нечувствительностью межфазного диффузионного потока к микрогидродинамике в пограничном слое. Последнее явление объясняется тем, что "быстрые" реакции завершаются в очень тонком поверхностном слое даже при довольно больших значениях Re . Область "медленных" реакций была получена при $\phi^2/Re \leq 0,1$ и характеризуется совпадением решения уравнений математического описания модели с асимптотическим решением при $\phi=0$. Это обстоятельство дает возможность при расчете диффузионного потока свести задачу к расчету физической абсорбции, пренебрегая кинетическим членом в уравнениях математического описания.

Результаты расчетов для моделей, обсуждаемых в настоящей работе, представлены на рис. 3 и 4. Кривая 1 на рис. 3а,б соответствует асимптотическому решению при $Re=0$. Из указанных рисунков видно, что при условии $\phi^2/Re \geq 10$ решение для обеих моделей совпадает с

асимптотическим решением при $Pe=0$ (область 1). Таким образом, и для этих более сложных моделей границей области "быстрых" реакций является кривая $\phi^2/Pe=10$.

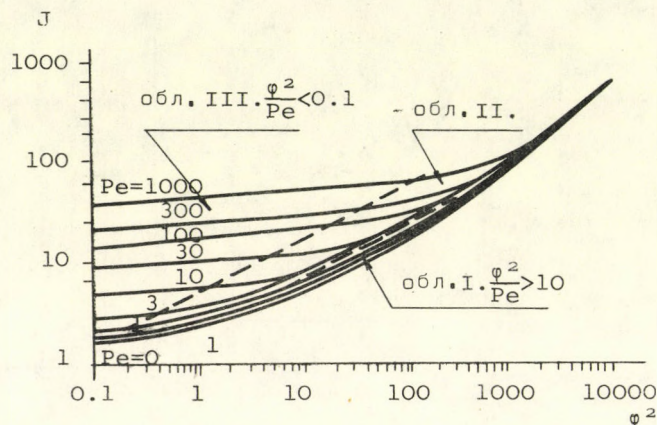


Рис. 3а. Зависимость безразмерного диффузионного потока от параметра ϕ (модель № 1, $Wo=0,5$; $Do=0,5$; $n=2$; $G=0,5$.)

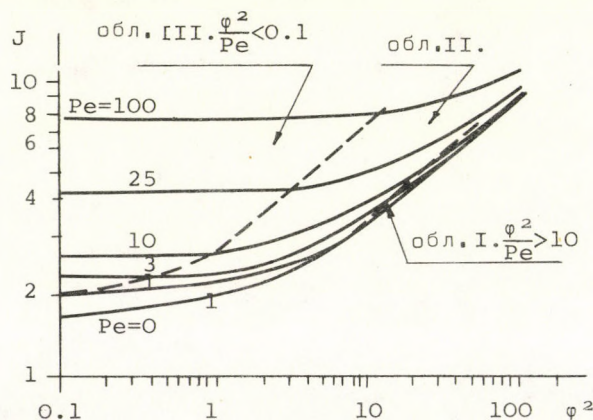


Рис. 3б. Зависимость безразмерного диффузионного потока от параметра ϕ (модель № 2, $Wo=0,5$; $Do=0,5$; $n=2$; $G=0,5$; $D(\xi)=0,7$.)

Из вышесказанного следует, что если выполняется неравенство $\phi^2/Pe \geq 10$, то скорость процесса лимитируется гидродинамикой, выбранный гидродинамический режим для такой реакции является недостаточно интенсивным и имеется возможность увеличения скорости протекания процесса в целом путем интенсификации гидродинамического режима.

Кривая 1 на рис. 4а,б соответствует асимптотическому решению при $\phi=0$. При $\phi^2/Pe \leq 0,1$ (область III) решение уравнения (2) практически совпадает с асимптотическим решением при $\phi=0$. Т.е. граница области "медленных" реакций также осталась неизменной. Скорость процесса в целом в этом случае лимитируется скоростью химического превращения и для интенсификации процесса следует искать возможность увеличить скорость собственно химической реакции.

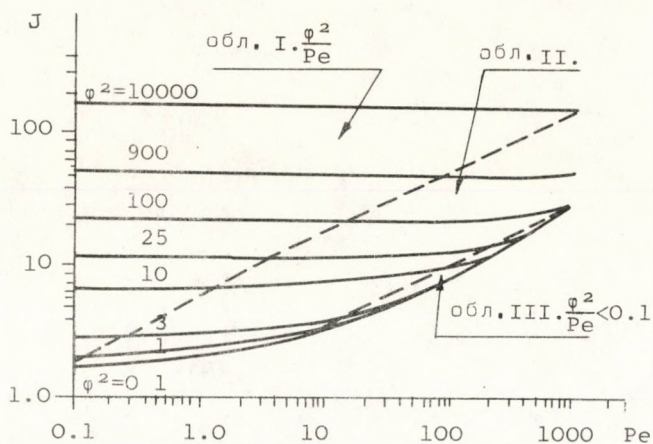


Рис. 4а. Зависимость безразмерного диффузионного потока от параметра Pe (модель № 1, $Wo=0,5$; $Do=0,5$; $n=2$; $G=0,5$.)

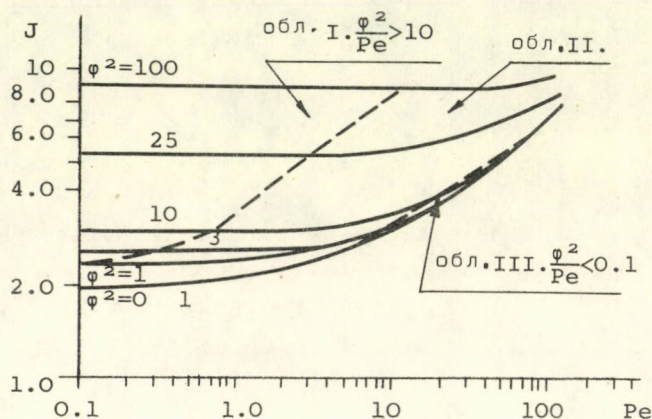


Рис. 46. Зависимость безразмерного диффузионного потока от параметра Pe (модель № 2, $Wo=0,5$; $Do=0,5$; $n=2$; $G=0,5$; $D(\xi)=0,7$.)

Определенный интерес представляет вопрос о зависимости величины среднего диффузионного потока от параметров, входящих в уравнения (4) и (5а)–(5в) и определяющих вид профилей коэффициента диффузии и скорости потока.

Как было указано выше, использованный нами вид зависимости коэффициента диффузии от расстояния до поверхности раздела фаз получил экспериментальное подтверждение, однако, до сих пор среди исследователей нет единого мнения по вопросам о величине показателя степени в уравнении (4) и о том проникают ли турбулентные пульсации к поверхности раздела, что определяет величину Do (23). Полученные в настоящей работе зависимости величины среднего диффузионного потока от параметров Do и n , представленные на рис. 5, 6 позволяют сделать вывод о том, что для любых отношений ϕ^2/Pe эти зависимости являются весьма существенными, а это диктует необходимость постановки экспериментальных работ по определению истинных

значений Do и n . В то же время, как следует из рис. 6 при значениях n от 2 до 4 наблюдается довольно слабая зависимость J от n , что возможно, и обуславливает получение различными авторами значений n от 2 до 4 при косвенном определении величины n .

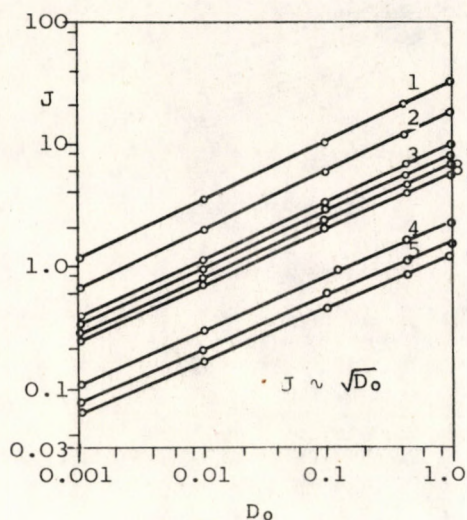


Рис. 5. Зависимость безразмерного диффузионного потока от параметра Do (модель № 1, $Wo=1$, $n=2$; $G=1$.)

- | | |
|-----------------|----------------|
| 1 - $Pe=1000$; | $\phi^2=1$; |
| 2 - $Pe=300$; | $\phi^2=1$; |
| 3 - $Pe=100$; | $\phi^2=1$; |
| 4 - $Pe=10$; | $\phi^2=1$; |
| 5 - $Pe=3$; | $\phi^2=1$; |
| 6 - $Pe=1$; | $\phi^2=1$; |
| 7 - $Pe=10$; | $\phi^2=100$; |
| 8 - $Pe=1$; | $\phi^2=100$; |
| 9 - $Pe=0,5$; | $\phi^2=100$. |

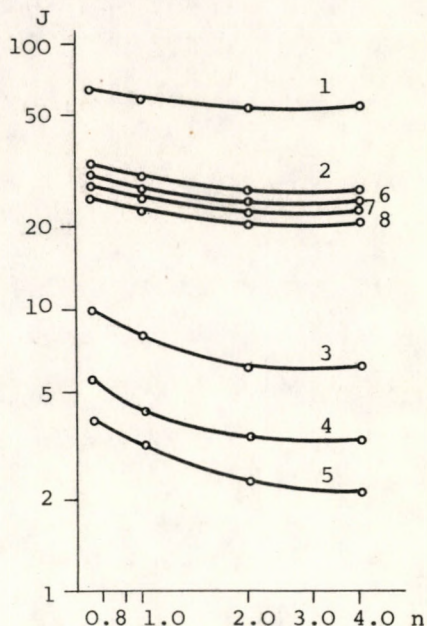


Рис. 6. Зависимость безразмерного диффузионного потока от параметра n (модель № 1, $Wo=1$, $Do=0,1$; $G=1$.)

- | | |
|----------------|----------------|
| 1 - $Pe=300$; | $\phi^2=1$; |
| 2 - $Pe=100$; | $\phi^2=1$; |
| 3 - $Pe=10$; | $\phi^2=1$; |
| 4 - $Pe=3$; | $\phi^2=1$; |
| 5 - $Pe=1$; | $\phi^2=1$; |
| 6 - $Pe=10$; | $\phi^2=100$; |
| 7 - $Pe=1$; | $\phi^2=100$; |
| 8 - $Pe=0,5$; | $\phi^2=100$. |

На рис. 7 представлена зависимость среднего безразмерного диффузионного потока от коэффициента диффузии в направлении по касательной к поверхности раздела фаз. Влияние этого параметра также является существенным при протекании процесса в любой из указанных областей.

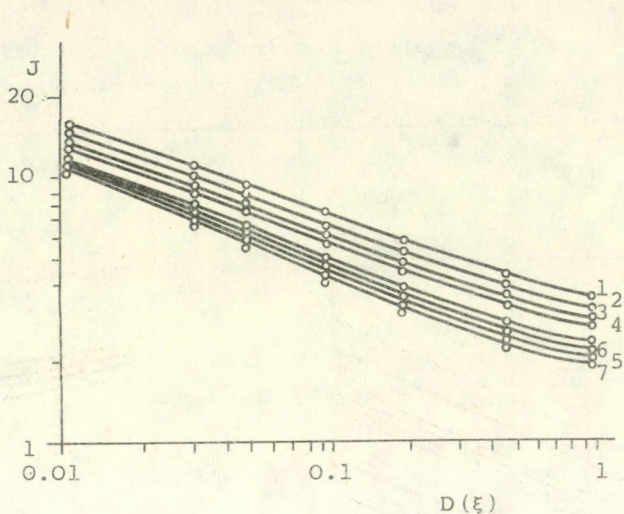


Рис. 7. Зависимость безразмерного диффузионного потока от параметра $D(\xi)$
(модель № 2, $W_0=0,1$; $D_0=0,01$;

- $n=2$; $G=2$)
- | | |
|-----------------------------|------------------------------|
| 1 - $Pe=100$; $\phi^2=1$; | 5 - $Pe=0,5$; $\phi^2=1$; |
| 2 - $Pe=30$; $\phi^2=1$; | 6 - $Pe=1$; $\phi^2=10$; |
| 3 - $Pe=10$; $\phi^2=1$; | 7 - $Pe=0,5$; $\phi^2=10$; |
| 4 - $Pe=3$; $\phi^2=1$; | |

Как следует из рис. 8,9 в области "быстрых" реакций величина среднего диффузионного потока не зависит как от параметров, определяющих вид профиля скорости, так и от того по какому из уравнений (5а)-(5в) рассчитывался этот профиль. Это объясняется тем, что, как было указано выше, при отношении $\phi^2/Pe \geq 10$ толщина концентрационного пограничного слоя значительно меньше толщины гидродинамического пограничного слоя, где существенно влияние изменения скорости потока. При $\phi^2/Pe < 10$ средний безразмерный диффузионный поток увеличивается в полтора - два раза при изменении значения W_0 от 0,1 до 1.

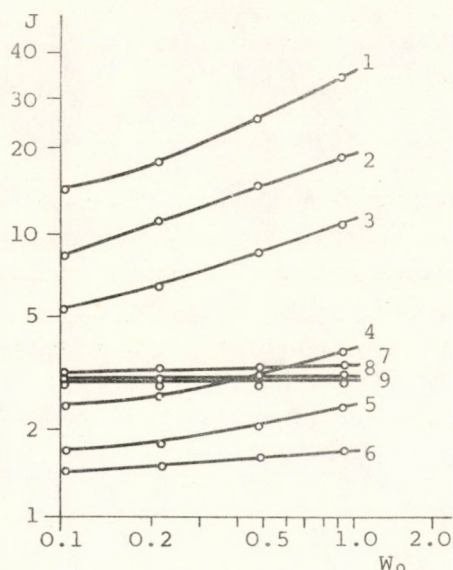


Рис. 8. Зависимость безразмерного диффузионного потока от параметра Wo (модель № 1, $Do=1$; $n=1$; $G=1$.)

- 1 - $Pe=1000$; $\phi^2=1$;
- 2 - $Pe=300$; $\phi^2=1$;
- 3 - $Pe=100$; $\phi^2=1$;
- 4 - $Pe=10$; $\phi^2=1$;
- 5 - $Pe=3$; $\phi^2=1$;
- 6 - $Pe=1$; $\phi^2=1$;
- 7 - $Pe=10$; $\phi^2=100$;
- 8 - $Pe=1$; $\phi^2=100$;
- 9 - $Pe=0,5$; $\phi^2=100$.

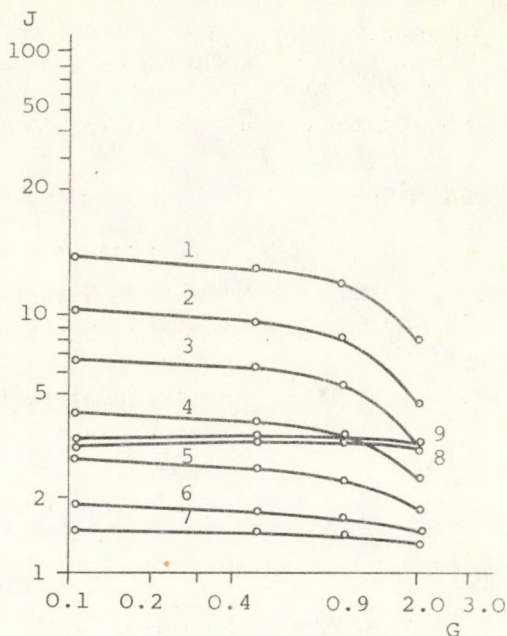


Рис. 9. Зависимость безразмерного диффузионного потока от параметра G (модель № 1, $Wo=0,1$; $Do=1$; $n=1$.)

- 1 - $Pe=1000$; $\phi^2=100$;
- 2 - $Pe=300$; $\phi^2=1$;
- 3 - $Pe=100$; $\phi^2=1$;
- 4 - $Pe=30$; $\phi^2=1$;
- 5 - $Pe=10$; $\phi^2=1$;
- 6 - $Pe=3$; $\phi^2=1$;
- 7 - $Pe=1$; $\phi^2=1$;
- 8 - $Pe=1$; $\phi^2=100$;
- 9 - $Pe=0,5$; $\phi^2=100$.

В заключение хочется отметить, что сделанные в данной работе выводы справедливы для пленочного либо поршневого режимов течения газожидкостной смеси. Применимость рассмотренных моделей для пузырькового режима течения должна быть дополнительно изучена, поскольку допущение о плоской поверхности единичного образования и плоскопараллельном обтекании в этом случае является серьезным упрощением реальной физической картины. Проверка сделанных выводов на более сложных моделях является дальнейшей задачей авторов настоящей работы.

ВЫРАЖЕНИЕ БЛАГОДАРНОСТИ

Авторы выражают благодарность доктору Йозефу Холдериту за плодотворную дискуссию при постановке задачи.

ОБОЗНАЧЕНИЯ

- C_i - концентрация реагирующего компонента в жидкой фазе, моль/м³;
- C_i^* - равновесная концентрация i -того компонента в жидкости, моль/м³;
- D_∞ - коэффициент турбулентной диффузии вдали от поверхности раздела фаз, м²/сек;
- D_{ij} - суммарный коэффициент кондуктивного переноса i -того компонента по j -той координате, м²/сек;
- $D(\eta) = \frac{D_y}{D_\infty}; \quad D(\xi) = \frac{D_x}{D_\infty};$
- $f_i(C_1, \dots, C_k)$ - скорость образования i -того компонента, моль/(м³·сек);
- $f_i^*(C_1^*, \dots, C_k^*)$ - скорость образования i -того компонента в кинетической области протекания реакции, моль/(м³·сек);
- G - параметр в уравнениях (5а) - (5в);
- i - индекс компонента;
- j - индекс координаты;
- J - осредненный безразмерный диффузионный поток;
- k - число компонентов;
- L_x - характерный линейный размер по координате x , м;
- L_y - характерный линейный размер по координате y , м;
- n - параметр в уравнении (4);
- $Pe = \frac{U_\infty L_x}{D_\infty} \left(\frac{L_y}{L_x} \right)^2;$
- U_j - j -тая составляющая скорости потока, м/сек;
- U_∞ - скорость течения потока вдали от поверхности раздела фаз, м/сек;
- wo - параметр в уравнениях (5а) - (5в);
- $w(\eta) = \frac{U_y}{U_\infty};$

- $x=x_1$ - продольная координата по течению потока, м;
 $y=x_2$ - перпендикулярная к поверхности газ-жидкость координата, м;

$$\eta = \frac{y}{L_y}; \quad \theta_i = \frac{c_i}{c_i^*}; \quad V_i = \frac{f_i}{f_i^*}; \quad \xi = \frac{x}{L_x};$$

τ - время, сек;

$$\Phi = L_y \sqrt{\frac{f_i^*}{c_i^* D_\infty}}$$

ЛИТЕРАТУРА

1. ДАНКВЕРТС, П.В.: Газо-жидкостные реакции. "Химия", М., 1973.
2. АСТАРИТА, Дж.: Массопередача с химической реакцией. "Химия", Л., 1971.
3. ЖЕЛЕЗНЯК, А.С. и ИОФФЕ, И.И.: Методы расчета многофазных жидкостных реакторов. "Химия", Л., 1974.
4. ГАРЦМАН, А.Н. и ЕРМАКОВА, А.: Труды V-ой Всесоюзной конференции по моделированию химических, нефтехимических и нефтеперерабатывающих процессов и реакторов "Химреактор-5", Уфа, 1974, т.2. 141.
5. DANCKWERTS, P.V.: Trans. Faraday Soc., 46, 300 (1950)
6. VAN DE VUSSE, J.G.: Chem. Eng. Sci., 16, 21 (1961)
7. SHERWOOD, T.K. and PIGFORD, R.L.: Absorption and Extraction. McGraw-Hill, New York, 1952.
8. VAN KREVELEN, D.W. and HOFTIJZER, P.J.: Rec. Trav. Chim., 67, 563 (1948)
9. HARDEBOL, J.: Private Communications.
10. ЛЕВИЧ, В.Г., КРЫЛОВ, В.С. и ВОРОТИЛИН, В.Г.: ДАН СССР, 161, 648 (1965)
11. НИШИНЕВСКИЙ, М.Х.: ЖПХ, №1, 25 (1951)
12. TOOR, H.L. and MARCHELLO, J.M.: AIChE Journ., 4, 98 (1958)
13. ДИЛЬМАН, В.В. и БРАНДТ, В.Б.: ТОХТ, 5, 326 (1971)
14. BENJAMIN, T.F., CHANG, R. WANG and LINDON, C. THOMAS: Can. J. Chem. Eng. 51, 755 (1973)
15. RUCKENSTEIN, ELI, VI-DUONG-DANG and GILL, WILLIAM N.: Chem. Eng. Sci., 26, 647 (1971)

16. KING, C.J.: Ind. Eng. Chem. Fundam., 5, 1 (1966)
17. SHUBERT, G. and CORCOS, G.M.: J. Fluid Mech., 29, 1 (1967)
18. LAMURELL, ALAIN P. and ORVILLE C. SANDALL: Chem. Eng. Sci., 27, 1075 (1972)
19. PRACHER, BRAHM D. and FRICKE, A.L.: Ind. Eng. Chem. Proc. Des. Develop., 13, 336 (1974)
20. MENEZ, GUY D. and ORVILLE C. SANDALL: Ind. Eng. Chem. Fundam., 13, 72 (1974)
21. САМАРСКИЙ А.А.: Введение в теорию разностных схем. "Наука", М., 1971.
22. ГОДУНОВ, С.Н. и РЯБЕНЬКИЙ, В.С.: Разностные схемы. "Наука", М., 1973.
23. РОЗЕН, А.М., НАДЕР, А.Б. и КРЫЛОВ, В.С.: Современное состояние теории массопередачи, в кн. Дж. Астарита, Массопередача с химической реакцией. стр. 169. "Химия", Л., 1971.

SUMMARY

The hierarchic model of the gas - liquid reactors was constructed and the problems are discussed which arise at the solution of the equations used for the mathematical description of the second level of the model.

Equations were derived for the mathematical description based on the simplification of the mass transfer equations. In this work the attenuation of the turbulent diffusion coefficient and the alteration of the direction of flow rate being perpendicular to the boundary surface were taken into account.

The analysis of the results showed the domain of the "fast" and "slow" reactions as the function of ϕ^2/Pe dimensionless parameter ratios.

Moreover the effect of the diffusion coefficient and the parameters describing the profiles of the flow rate were analysed.

INVESTIGATION OF FURFURAL DECARBONYLATION OVER METAL
PALLADIUM CATALYSTS

GY. GÁRDOS, L. PÉCHY, Á. RÉDEY and Mrs. E. CSÁSZÁR*

(Department of Hydrocarbon and Coal Processing Veszprém
University of Chemical Engineering and
*Petőfűrdő, Nitrogen Works)

Received: December 13, 1975.

Investigations were carried out in furan production from furfural concerning catalysts with different palladium contents. The catalysts containing 2.5 w.% palladium on alumina was found to be the most suitable from the investigated catalysts. Furfural conversion of 100 % and a furan yield of nearly 100% were measured under the given parameters. Because its major loadability and productivity it is suitable for industrial utilization in furan production.

In the previous papers [1,2] the possibilities of furan production from furfural, the oxidative decarbonylation in the presence of steam and the reductive decarbonylation in hydrogen were investigated. During the examination of the reaction, several noble metal catalysts were tested and the palladium catalysts were stated to be the most suitable ones. Catalysts containing 1.6 and 2.5w.% palladium showed good selectivity, good loadability and productivity.

The tests carried out to establish the fatigue and regenerating properties of catalysts justified the view that catalysts are adequate for the industrial realisation of furfural decarbonylation.

The present paper presents the results measured at atmospheric pressure of different palladium content catalysts supported on alumina. The technological parameters play a major role in the

heterogeneous catalytic decarbonylating reaction. The role of temperature, the furfural/hydrogen molar ratio, and the liquid load were investigated to establish the optimum parameters.

EXPERIMENTAL

The decarbonylation of furfural was investigated on five kinds of catalysts (0.65; 1.1; 1.6; 2.5; 5.0 w.% palladium content). To increase the activity of the catalysts they were treated in a special way in order to ensure that in long active periods big loadability and productivity should be reached.

The pretreatment of the catalysts involved a gradual temperature increase in a hydrogen stream. There was need for gradual temperature increase, because of the close relation between the decrease of the catalyst activity in the working period and the large scale change of the specific surface of the catalyst.

The specific surface change of the catalyst containing 2.5 w.% palladium with a specific surface of 250 m²/g is shown in Table 1, in the function of the time and treatment.

Table 1. The change of the specific surface in the function of the temperature and time

Time (h)	Temperature (°C)	Specific surface (m ² /g)
4	200	225
4	300	195
4	400	185
4	500	149

The data confirmed that the structure of the catalysts had changed considerably. To avoid a decrease of catalyst specific surface an activating method was elaborated and its application does not result in large scale change of the specific surface of the catalyst.

Both the velocity of the heating up and the temperature held in the hydrogen stream are the sensitive parameters of the gradual activation. According to these the temperature of the catalyst

was raised to 100 °C during two hours and 220°C was attained during eight hours (15 °C/h), following this 300 °C was attained by a heating velocity of 5 °C/h. After the attainment of 300 °C, the catalyst was held at this temperature for 10 hours. In such a way the decrease of the specific surface of the catalyst was below 10 %. The catalysts for the decarbonylating experiments were pretreated as mentioned earlier.

DISCUSSION

Decarbonylating Experiments on the Catalyst Containing a Lower Amount of Palladium

The experimental results derived from the lower palladium content catalysts are shown in Table 2., where the furfural conversion (%) is in the function of the temperature (°C), and the liquid load (cc furfural/cc catalyst.hour). It was justified by the measuring data that in the case of a higher palladium content the furfural conversion, the rate of decarbonylation is higher. In connection with the conversion data presented in the Table, it should be mentioned that they are equal to the furan yields as the amount of the by-product did not surpass 1 %.

The optimum temperature of the decarbonylation is 300 °C, higher or lower temperature powerfully decreases the furfural conversion. The catalyst containing 0,65 w.% palladium is not suitable for industrial utilization. In the case of a catalyst containing 1.1 w.% palladium, better furfural conversions and furan yields were achieved. A catalyst can be used as far as 320 °C with a lower liquid load, at a higher temperature the furfural conversion decreases because of the resinification of the furfural and its deposition for active sites. Its use is not appropriate because of the large residence times which are necessary for the attainment of a good conversion. Conversion of 97 % and selectivity of nearly 100 % for furan were attained by catalyst containing 1.6 w.% palladium. The catalyst retained its activity for a long time, but the tract of time of the active periods showed a decreasing trend after the regenerations.

Table 2. The change of the furfural conversion in the function of the palladium content of catalysts at different temperatures and liquid loads with a furfural/hydrogen molar ratio of 1:1

The palladium content of the catalyst (w.%)																
		0.65						1.10							1.6	
		Temperature (°C)														
	Liquid load	240	280	320	360	240	280	320	360	240	280	320	360			
	0.2	14.50	32.00	28.50	7.50	52.00	70.50	60.00	42.00	56.50	91.00	90.00	53.00			
	0.4	11.00	20.00	18.00	5.50	35.00	52.00	45.50	24.00	41.00	73.00	72.00	34.00			
	0.6	8.50	14.00	13.00	4.50	25.00	39.00	34.00	15.50	29.50	60.00	59.00	21.00			
	1.0	5.00	11.00	8.50	3.00	19.50	30.00	26.50	12.50	21.50	50.00	47.50	16.50			
	1.5	3.00	8.00	7.00	2.00	18.00	27.00	24.00	12.00	19.00	46.00	44.50	13.00			
Conversion (%)																

Decarbonylating Experiments on a Catalyst Containing 2.5 w.% Palladium

The experimental data are summarized in Table 3. The results are illustrated in Figures 1, and 2.

The effect of the liquid load and the furfural/hydrogen molar ratio on the furfural conversion can be followed in Figure 1, at the same temperature, while the effect of the temperature can be stated in Figure 2 at a constant liquid load and furfural/hydrogen molar ratio. The strong effect of the temperature on the decarbonylating reaction was confirmed in both cases. 300 °C seems to be the optimum temperature under the examined conditions.

The furfural conversion and furan yield decrease at the temperatures deviating from the optimum. The furfural/hydrogen molar ratio of 1:1 was considered to be the most suitable one at 300 °C, while the furfural/hydrogen molar ratio of 1:1.5 was stated at 340 and 270 °C, which can be explained with the furfural/hydrogen system and the order of the residence times. The furfural conversion is 100 % as far as the value of 0.75 cc furfural/cc catalyst·hour at 300 °C and beside the furfural/hydrogen molar ratio of 1:1.

The furan yield is nearly 100 % at the same parameters. Furfural conversion and furan yield of nearly 80 % were also measured beside the liquid load of 3.5 cc furfural/cc catalyst·hour. In a case of a bigger liquid load than 0.75 cc furfural/cc catalyst·hour larger scale fatigue and frequent regenerations must be taken into consideration. In a view of this a catalyst containing 2.5 w.% palladium is suitable for furan production at 300 °C furfural/hydrogen molar ratio of 1:1 and with a liquid load of 0.75 cc furfural/cc catalyst·hour.

Table 3. The change of the furfural conversion in the function of the liquid load at different temperatures and furfural/hydrogen molar ratios on a catalyst containing 2.5 w.% palladium

Liquid load	Temperature (°C)															
	300															
	340															
	Furfural/hydrogen molar ratio															
	1:0	1:0.5	1:1	1:1.5	1:2	1:0	1:0.5	1:1	1:1.5	1:2	1:0	1:0.5	1:1	1:1.5	1:2	
0.2	100.0	100.0	100.0	100.0	100.0	100.0	100.0	100.0	100.0	100.0	100.0	100.0	100.0	100.0	100.0	100.0
0.5	71.0	82.0	88.0	97.0	94.0	100.0	100.0	100.0	100.0	100.0	82.5	85.0	92.5	98.5	90.0	90.0
1.0	21.5	32.0	47.0	89.5	80.5	92.0	98.0	99.0	98.5	94.0	-	38.5	73.0	92.0	57.5	57.5
1.5	-	-	-	79.5	70.0	75.0	94.0	97.0	95.0	84.5	-	-	35.0	77.0	-	-
2.0	-	-	-	65.5	58.5	50.0	89.5	93.0	91.0	81.0	-	-	-	54.0	-	-
3.0	-	-	-	-	-	-	79.0	84.5	81.0	66.5	-	-	-	-	-	-
4.0	-	-	-	-	-	-	64.0	76.0	70.5	47.0	-	-	-	-	-	-
5.0	-	-	-	-	-	-	-	65.0	58.0	-	-	-	-	-	-	-

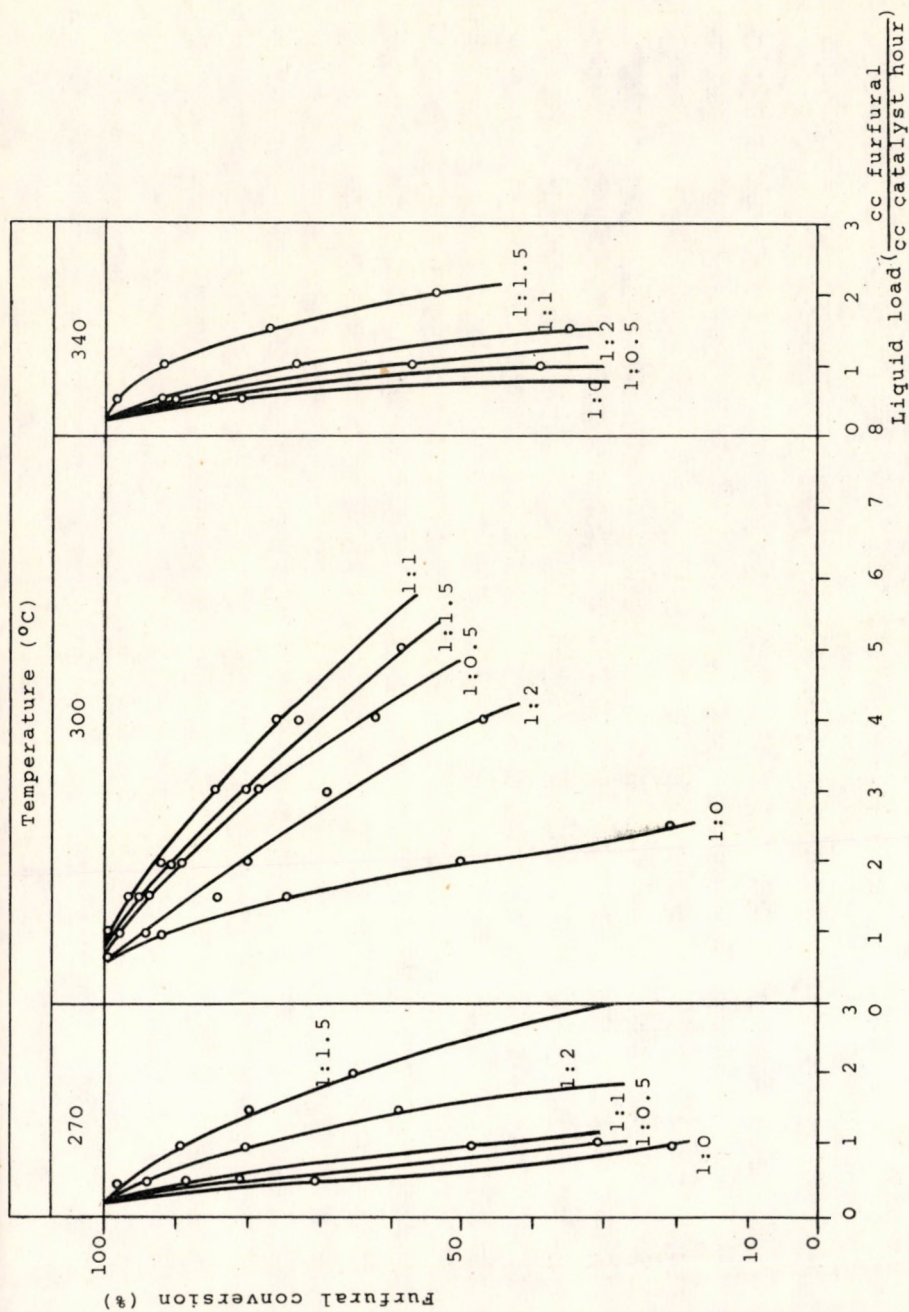


Figure 1. The furfural conversion in the function of the liquid load at different temperatures and furfural/hydrogen molar ratios

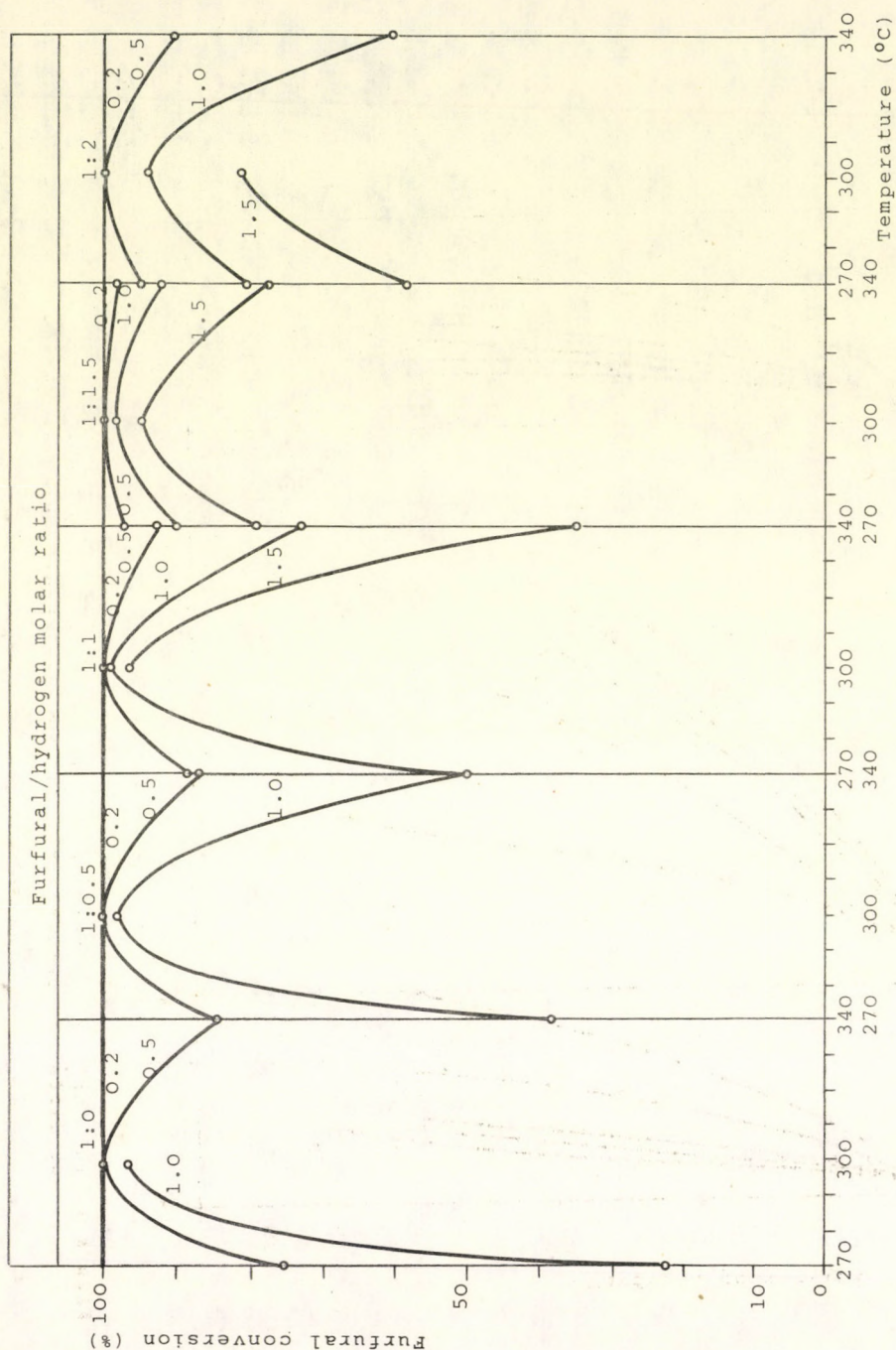


Figure 2. The furfural conversion in the function of the temperature at different furfural/hydrogen molar ratios and liquid loads

Decarbonylating Experiments on a Catalyst Containing 5.0 w.% Palladium

The measured data derived from a catalyst containing 5.0 w.% palladium are summarized in Table 4. The rate of the furfural conversion in the function of the parameter change is illustrated in Figure 3 and 4. The connections constructed in the figures unambiguously confirmed that a catalyst containing a higher amount of palladium has remarkably good decarbonylating properties.

At higher temperatures than 270 °C, the furfural conversion and furan yield are 100 %. Furfural conversion of 100 % was measured at 300 and 340 °C with a liquid load of 3.0 cc furfural/cc catalyst·hour.

The increase of the furfural/hydrogen molar ratio decreased the conversion. The furfural/hydrogen molar ratio of 1:0.5 proved to be the optimum, because of the high palladium concentration. To protect the catalyst activity it is not expedient to work at a lower molar ratio than 1:1.

The increase of the furfural/hydrogen molar ratio decreases the rate of the furfural conversion, and this effect is clearly indicated at a lower and higher temperature than 300 °C. These statements are also valid for the change of the liquid load. A catalyst containing 5.0 w.% palladium was found to have the most suitable decarbonylating properties from the examined catalysts.

A three-dimensional diagram (Figure 5) was constructed for the characterization of the reaction parameters; the furfural conversion, palladium content and temperatures were indicated on the axes. Connections were sought at a constant furfural/hydrogen molar ratio and liquid load (0.2 cc furfural/cc catalyst·hour). The conversion values belonging to the same palladium content, but to different temperatures were designated by thin continuous lines. In the case of lower palladium contents the effect of the temperature causes a maximum curve (300 °C) while in the case of higher palladium contents (2.5 and 5.0 w.%) the optimum temperature range expands (270 to 340 °C).

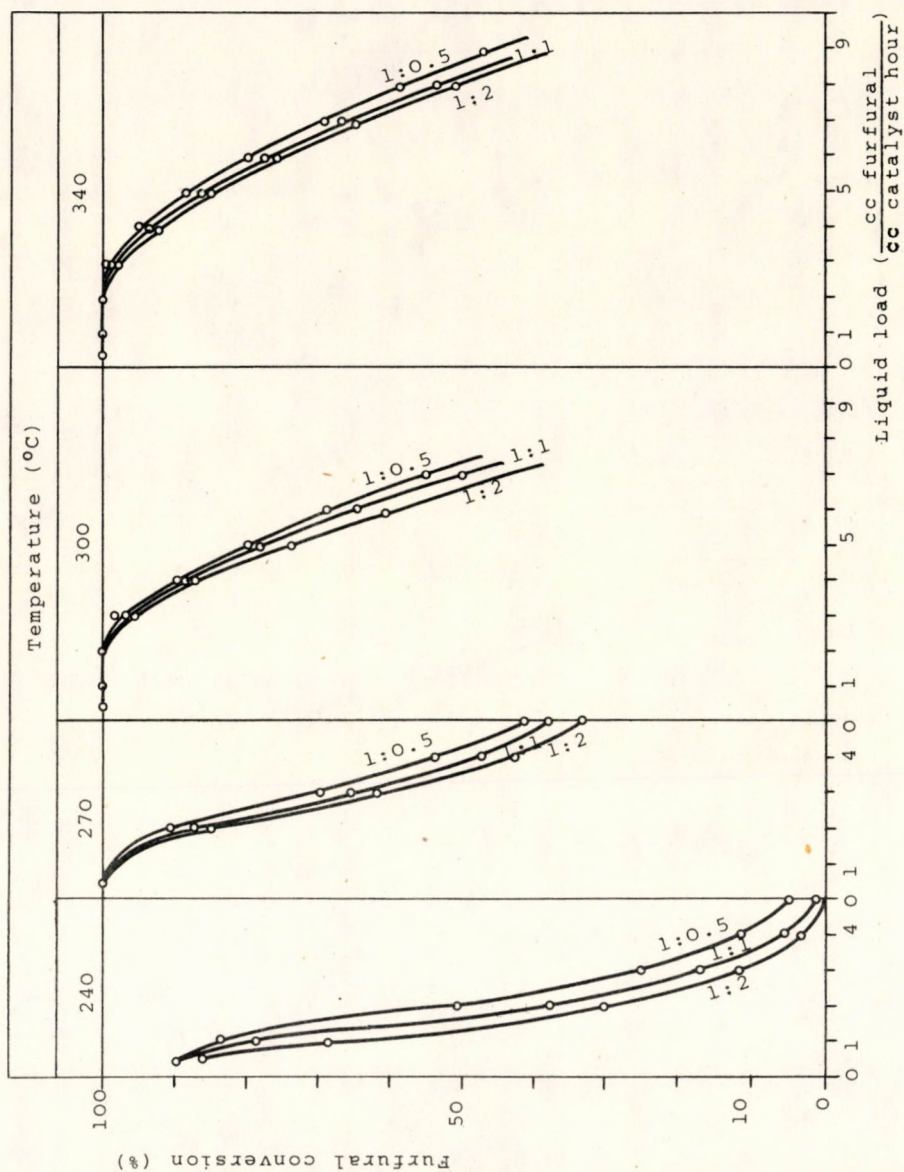


Figure 3. The furfural conversion in the function of the liquid load at different temperatures and furfural/hydrogen molar ratios

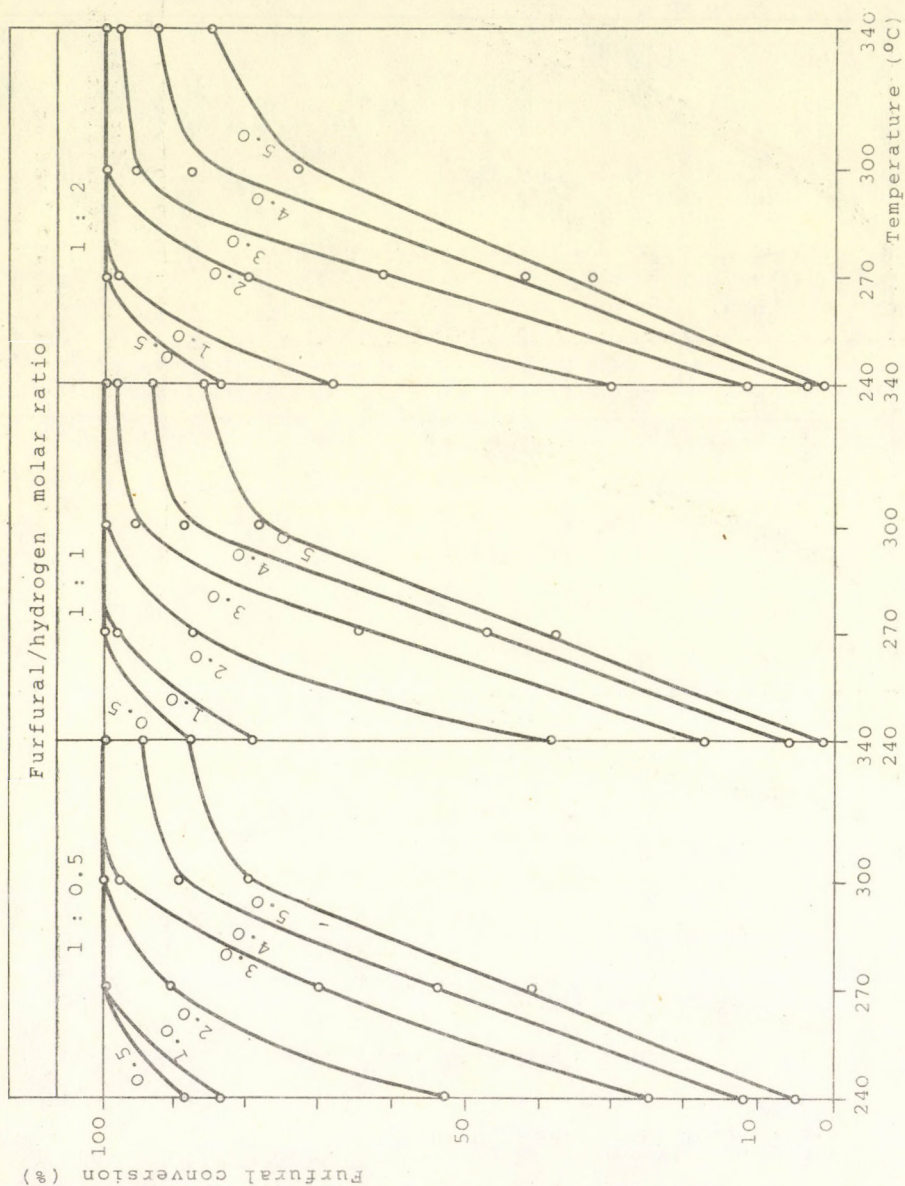


Figure 4. The furfural conversion in the function of the temperature at different furfural/hydrogen molar ratios and liquid loads

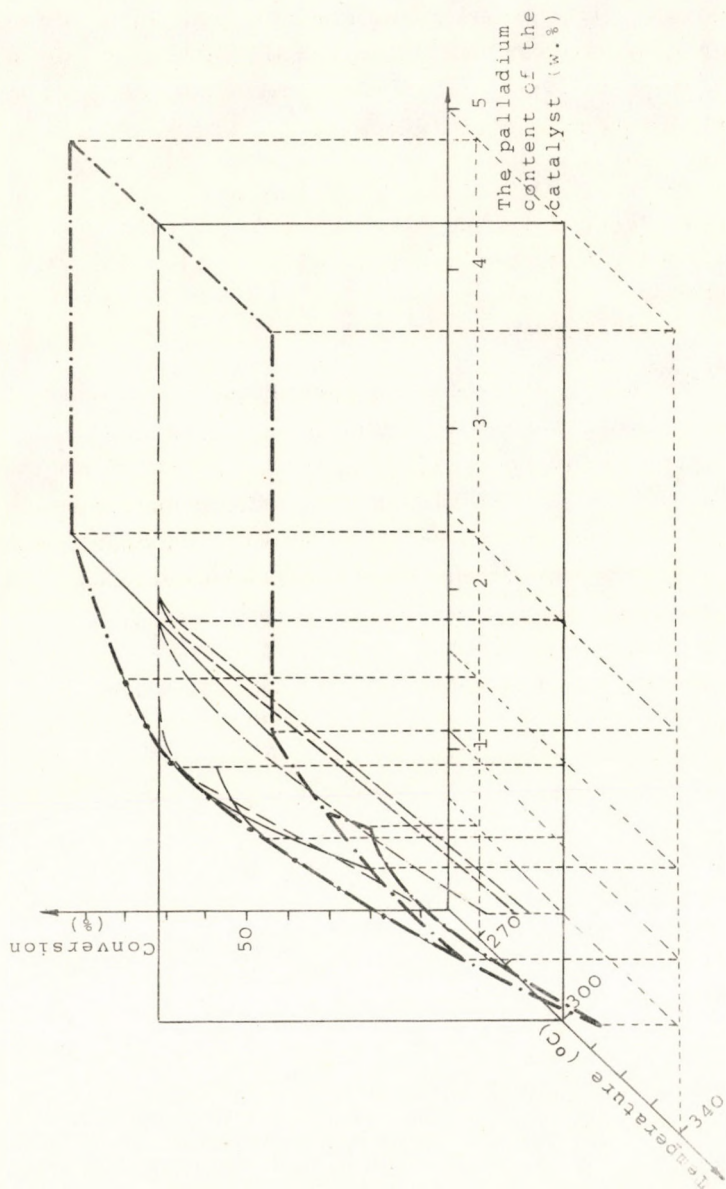


Figure 5. The furfural conversion in the function of the palladium content of the catalyst and the temperature at constant furfural/hydrogen molar ratio of 1:1 and liquid load of 0.2 cc furfural/cc catalyst hour; and the furfural conversion in the function of the palladium content of the catalyst at 300°C and 1:1=furfural/hydrogen molar ratio and liquid load of 0.2; 0.5; 1.0; 1.5 cc furfural/cc catalyst·hour

The above mentioned curve determines a plane- its outlines are designated by dotted-broken lines-which shows the furfural conversion in the function of the palladium content. A thin broken line marks the change of the furfural conversion in the function of the palladium content of the catalyst at a constant temperature (300°C) and with constant liquid loads (0.2; 0.5; 1.0; 1.5 cc furfural/cc catalyst·hour.)

The inscribing of the planes belonging to a bigger liquid load than 0.2 cc furfural/cc catalyst·hour would have disturbed the clear illustration, therefore only their isocurves are shown belonging to 300 °C (thin broken lines).

On the basis of the decarbonylating experiments the catalyst containing 2.5 w.%(possibly 1.6 w.%) palladium can be stated to be the most suitable ones among the investigated catalysts from the point of view of industrial utilization taking into consideration the production costs of the catalysts. The use of a catalyst containing 5.0 w.% palladium would increase the production cost of furan on an extreme scale.

A catalyst containing 1.6 w.% palladium has short active periods after the regenerations [2], therefore its use is inexpedient.

REFERENCES

1. GÁRDOS, Gy., PÉCHY, L., RÉDEY, Á., Mrs. CSÁSZÁR, E.: Hung.J. Ind Chem. 3, 577 (1975)
2. GÁRDOS, Gy., PÉCHY, L., Mrs. CSÁSZÁR, E., Mrs. SZIGETI, B.: Hung.J. Ind.Chem. 3, 582 (1975)

РЕЗЮМЕ

Были проведены опыты по получению фурана из фурфурола с катализаторами различного содержания палладия. Из изучаемых катализаторов самым выгодным оказался катализатор, содержащий 2,5 вес.% палладия на алюминии. Были измерены 100%-ная конверсия фурфурола и приблизительно 100%-ный выход фурана при данных параметрах. Имея в виду загрузаемость и производительность способа, он является выгодным для промышленного применения в производстве фурана.

KINETIC INVESTIGATION ON THE DECARBONYLATION
OF THE FURFURAL

GY. GÁRDOS, L. PÉCHY, Á. RÉDEY and Mrs E. CSÁSZÁR*

(Department of Hydrocarbon and Coal Processing,
Veszprém University of Chemical Engineering
and *Petfűrdő, Nitrogen Works)

Received: Januar 12, 1976.

Experiments were carried out for the kinetic investigation of the decarbonylation of the furfural using a catalyst containing 2.5 w.% palladium. The rate and kinetic equations were stated on the basis of experimental data at 300 °C at a furfural/hydrogen molar ratio of 1/1. According to the calculations, the rate determining partial process is the surface reaction.

In previous papers [1,2,3] investigations on furan production, and the parameters of the decarbonylating reaction were discussed. The effects of the temperature, the furfural/hydrogen molar ratio and the liquid load were investigated, and the most suitable catalyst - metal palladium on an alumina supporter - was selected from the catalysts for the decarbonylation of the furfural.

The kinetic investigation of the decarbonylating reaction is discussed here.

EXPERIMENTAL

The kinetic study of the decarbonylating reaction which takes place at an atmospheric pressure in the presence of hydrogen was carried out in accordance with the previously mentioned paper [3] on a catalyst containing 2.5w.% palladium on an alumina supporter. The experimental apparatus and the analytical methods are disregarded here, as they were discussed in detail earlier [1].

The experiments were carried out at 300 °C and at three different furfural/hydrogen molar ratios (1/0.5; 1/1; 1/2) with increasing feed rates (liquid loads: cc furfural/cc catalyst.hour) in order that different residence times should be attained. The decarbonylation of the furfural was also investigated without the presence of hydrogen. The results obtained under these conditions are indicated in the tables as furfural/hydrogen molar ratio of 1/0. The calculation of the kinetic study was based on the analysis of the raw material and the product, and on the method used by SZABÓ [4].

The calculating method, the rate and kinetic equations in accordance with the presumed mechanism can be found in a previous paper [5].

DISCUSSION

In the interest of the alternation of the residence time, the liquid load was varied between 0.75 and 4.00 cc furfural/cc catalyst.hour. It is to be noted that in the case of lower liquid loads than 0.75 cc furfural/cc catalyst.hour both the conversion and the furan yield were 100 %. The experimental data are summarized in Table 1, where the furfural conversion, the methyl furan, the tetrahydrofuran yields are indicated at the furfural/hydrogen molar ratios of 1/0; 1/0.5; 1/1; 1/2. On the basis of the data, it can be stated that, the increase of the liquid load decreases the rates of the furfural conversions and yields.

Table 1. The conversion and yield values in the function of different liquid loads and furfural/hydrogen molar ratios at 300°C.

Furfural/hydrogen molar ratio = 1/0						
Liquid load(cc furfural/cc catalyst·hour)						
	0.75	1.0	1.5	2.0	3.0	4.0
Conversion(%)	98.5	92.0	81.0	50.0		
Furan yield(%)	97.0	91.0	80.0	49.1		
Metil furan yield %	1.5	1.0	1.0	0.9		
THF yield(%)	0.0	0.0	0.0	0.0		
Furfural/hydrogen molar ratio = 1/0.5						
Liquid load(cc furfural/cc catalyst·hour)						
	0.75	1.0	1.5	2.0	3.0	4.0
Conversion(%)	99.0	98.1	94.0	89.6	79.0	62.0
Furan yield(%)	97.1	95.0	89.0	83.8	74.0	58.0
Metil furan yield %	1.9	2.6	3.0	3.8	3.0	2.8
THF (%)	0.0	0.5	2.0	2.0	2.0	1.2
Furfural/hydrogen molar ratio = 1/1						
Liquid load(cc furfural/cc catalyst·hour)						
	0.75	1.0	1.5	2.0	3.0	4.0
Conversion(%)	100.0	99.0	96.5	92.0	84.5	76.0
Furan yield(%)	96.3	94.6	92.2	88.0	81.1	73.8
Metil furan yield %	2.6	3.0	3.0	2.8	2.4	1.6
THF yield(%)	1.1	1.4	1.3	1.2	1.0	0.6
Furfural/hydrogen molar ratio = 1/2						
Liquid load(cc furfural/cc catalyst·hour)						
	0.75	1.0	1.5	2.0	3.0	4.0
Conversion(%)	100.0	94.0	84.5	80.0	69.3	47.0
Furan yield(%)	92.0	87.1	76.0	70.1	65.0	44.5
Metil furan yield %	3.2	3.9	5.1	5.4	2.0	1.5
THF yield(%)	2.7	3.0	3.4	4.6	1.3	1.0

The measured data were used for the illustration of the relation between the furfural concentration $(y_A)_t$ and the reciprocal space velocity $(1/S)$.

The calculated values are given in Table 2.

Table 2. Values calculated from the experimental data

		Liquid load (cc furfural/cc catalyst·hour)					
		0.75	1.0	1.5	2.0	3.0	4.0
B · 10	(g/s)	4.833	6.444	9.667	12.889	19.317	25.776
S · 10	(g/gs)	2.554	3.405	5.109	6.812	10.209	13.613
1/3 · 10	(g/s)	0.392	0.294	0.196	0.147	0.098	0.735
$(y_A)_0$	(mole/g)	1.04	1.04	1.0	1.4	1.4	1.0
	F:H ₂ =1/0	0.030	1.280	2.940	4.64	-	-
	F:H ₂ =1/0.5	0.020	0.190	0.854	1.452	2.820	4.800
$(y_A)_t$ · 10	F:H ₂ =1/1	0.0	0.145	0.503	1.131	2.129	3.198
(mole/g)	F:H ₂ =1/2	0.0	0.826	1.836	2.138	4.021	6.361

The furfural concentration in the function of the reciprocal space velocity is illustrated in Figure 1. in addition to the investigated molar ratios. The specific reaction rate of the decarbonylating reaction of the furfural can be calculated with $\Delta(y_A)_t$ values corresponding to the given values of $\Delta(1/S)$, which can be read from Figure 1.

$$w = - \frac{d(y_A)_t}{d(1/S)} \approx \frac{\Delta(y_A)_t}{\Delta(1/S)}$$

and in Table 3. according to the investigated molar ratios.

The specific reaction rate in the function of $(y_A)_t$ is demonstrated in Figure 2. The reaction rates and the mole fractions were calculated on the basis of Figure 2. and the mass of the catalyst. The calculations are summarized in Table 4. Figure 3. was constructed on the basis of Table 4. which resulted in a linearized rate equation corresponding to x/W vs. x relation according to the following rate equation:

$$W = \frac{p_A}{a^I + b^I p_A + c^I p_{B1}}$$

and to the kinetic equation

$$W = \frac{p_A}{1 + K_A p_A + K_{B1} p_{B1}}$$

respectively. The symbols are the same as used in a previous paper [5]. (Other ordinates correspond to the lines of Figure 3.)

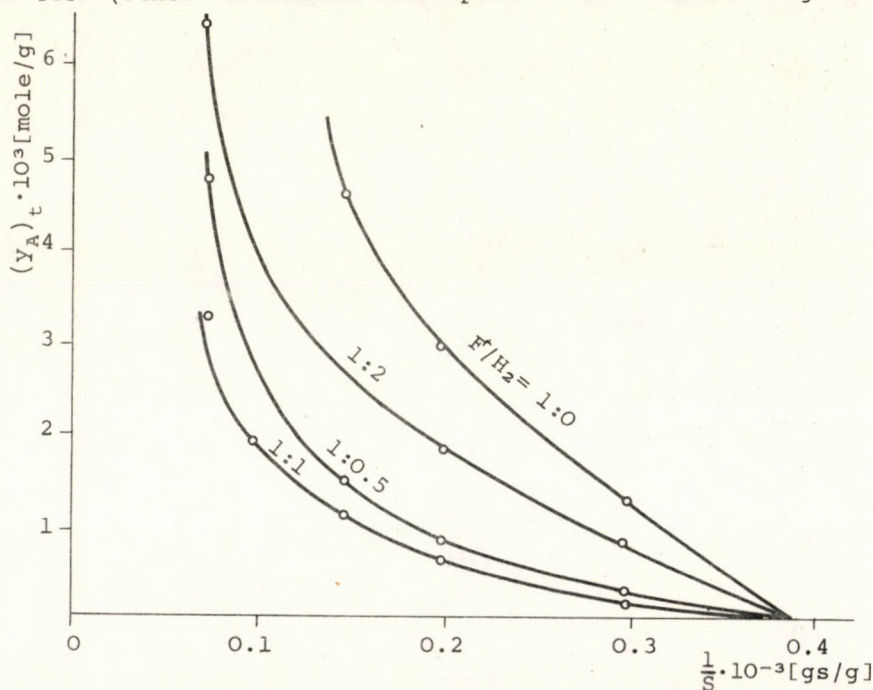


Fig.1. Furfural concentration vs. reciprocal space velocity.
T = 300 °C

Table 3. The calculation of the specific reaction rate

		$1/S \cdot 10^4$	$(y_A)_t \cdot 10^3$	$w \cdot 10^6$
		(gs/g)	(mole/g)	(mole/g s)
Furfural/hydrogen molar ratio	1/2	0.10	3.83	-
		0.15	2.60	2.02
		0.20	1.78	1.36
		0.25	1.24	0.96
		0.30	0.82	0.86
		0.35	0.38	-
	1/1	0.075	2.50	-
		0.125	1.37	1.73
		0.175	0.77	0.98
		0.225	0.39	0.50
		0.275	0.27	0.34
		0.325	0.05	0.26
	1/0.5	0.375	0.01	-
		0.10	2.62	-
		0.15	1.40	1.89
		0.20	0.73	0.99
		0.25	0.41	0.54
		0.30	0.19	0.33
	1/1	0.35	0.09	-
		0.15	4.44	-
		0.18	3.46	3.26
		0.21	2.70	2.54
		0.24	2.10	2.00
		0.27	1.63	1.58
	1/1	0.30	1.27	1.2
		0.33	0.80	1.5

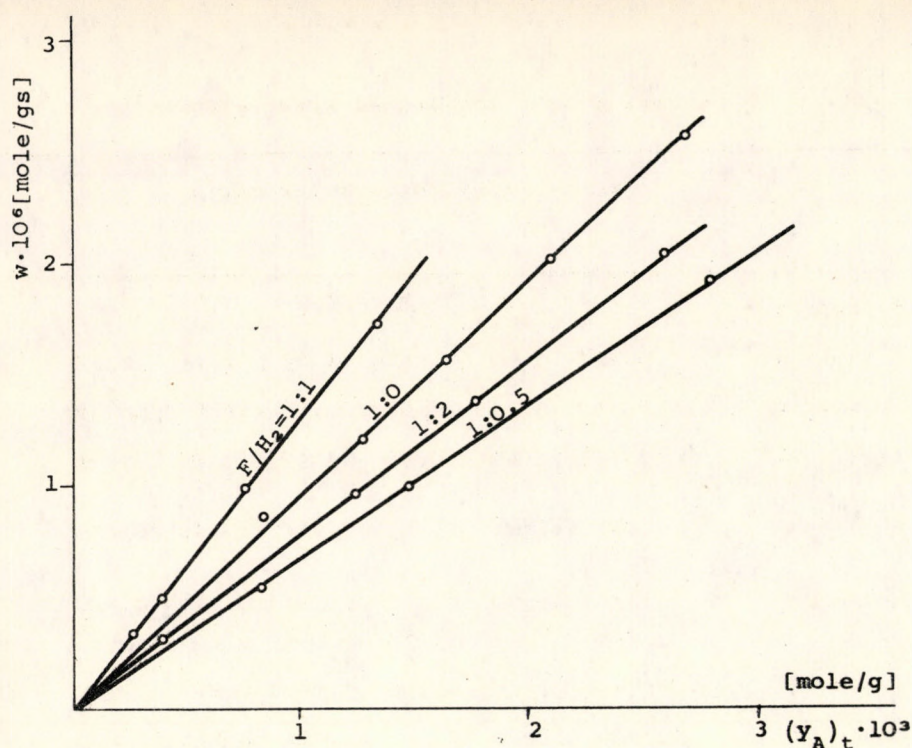


Fig. 2. The specific reaction rate vs. furfural concentration $T=300^\circ\text{C}$

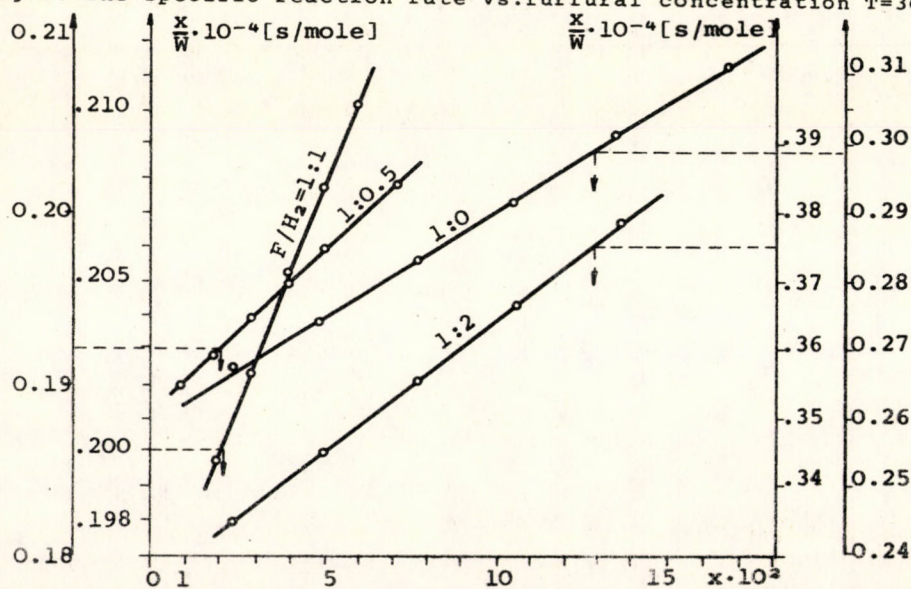


Fig. 3. The linearized rate equations based on Equation 8a. in ref. [5].

Table 4.

Data of the linearized kinetic equations

		Furfural/hydrogen molar ratio 1/0						
$(y_A)_t \cdot 10^3$ (mole/g)		0.5	1.0	1.5	2.0	2.5	3.0	
$w \cdot 10^6$ (mole/gs)		0.48	0.96	1.43	1.90	2.36	2.82	
$w \cdot 10^6$ (mole/s)		9.08	18.16	27.05	35.94	44.65	53.35	
$[2(y_A)_o - (y_A)_t] \cdot 10^2$ (mole/g)		2.03	1.98	1.93	1.88	1.83	1.76	
$x \cdot 10^2 = \frac{(y_A)_t}{2(y_A)_o - (y_A)_t} \cdot 10^2$		2.427	4.975	7.653	10.471	13.440	16.574	
$x/w \cdot 10^{-4}$ (s/mole)		0.267	0.274	0.283	0.291	0.301	0.310	
$1 - x$		0.975	0.950	0.923	0.892	0.865	0.834	
$\sqrt{1 - x}$		0.987	0.974	0.960	0.946	0.930	0.913	
$\sqrt{\frac{x}{w}}$ ($s^{1/2}/mole^{1/2}$)		51.698	52.337	53.185	53.977	54.865	55.736	
$\frac{2582 - \frac{x}{w}}{\sqrt{1 - x}}$ ($s^{1/2}/mole^{1/2}$)		2561.6	2595.0	2631.5	2671.8	2716.3	2765.9	
		1/0.5						
$(y_A)_t \cdot 10^3$ (mole/g)		0.2	0.4	0.6	0.8	1.0	1.2	1.4
$w \cdot 10^6$ (mole/gs)		0.27	0.54	0.81	1.08	1.35	1.62	1.89
$w \cdot 10^6$ (mole/s)		5.10	10.21	15.32	20.43	25.54	30.65	35.75
$[2(y_A)_o - (y_A)_t] \cdot 10^2$ (mole/g)		2.06	2.04	2.02	2.00	1.98	1.96	1.94
$x \cdot 10^2 = \frac{(y_A)_t}{2(y_A)_o - (y_A)_t} \cdot 10^2$		0.970	1.960	2.970	4.000	5.050	6.122	7.216
$x/w \cdot 10^{-4}$ (s/mole)		0.190	0.192	0.194	0.196	0.198	0.200	0.208
$1 - x$		0.990	0.980	0.970	0.960	0.949	0.938	0.927
$\sqrt{1 - x}$		0.995	0.990	0.985	0.979	0.974	0.968	0.963
$\sqrt{\frac{x}{w}}$ ($s^{1/2}/mole^{1/2}$)		43.595	43.388	44.025	44.244	44.467	44.694	44.892
$\frac{1872 - \frac{x}{w}}{\sqrt{1 - x}}$ ($s^{1/2}/mole^{1/2}$)		1844.4	1853.4	1862.8	1872.4	1882.7	1893.2	1904.1

Continued Table 4.

	Furfural/hydrogen molar ratio					
	1:1					
$(y_A)_t \cdot 10^3$ (mole/g)	0.2	0.4	0.6	0.8	1.0	1.2
$w \cdot 10^6$ (mole/gs)	0.26	0.52	0.78	1.04	1.28	1.54
$W \cdot 10^6$ (mole/s)	4.91	9.81	14.68	19.67	24.21	29.13
$[2(y_A)_0 - (y_A)_t] \cdot 10^2$ (mole/g)	2.06	2.04	2.02	2.00	1.98	1.96
$x \cdot 10^2 = \frac{(y_A)_t}{2(y_A)_0 - (y_A)_t} \cdot 10^2$	0.970	1.960	2.970	4.040	5.050	6.122
$x/W \cdot 10^{-4}$ (s/mole)	0.197	0.200	0.203	0.205	0.209	0.210
$1 - x$	0.990	0.980	0.970	0.959	0.949	0.938
$\sqrt{1 - x}$	0.995	0.990	0.985	0.979	0.974	0.968
$\sqrt{\frac{x}{W}}$ ($s^{1/2}/mole^{1/2}$)	44.426	44.699	44.978	45.312	45.667	45.840
$\frac{1948 - \frac{x}{W}}{\sqrt{1 - x}}$ ($s^{1/2}/mole^{1/2}$)	1912.9	1922.2	1931.9	1942.3	1952.3	1964.3
	1:2					
$(y_A)_t \cdot 10^3$ (mole/g)	0.5	1.0	1.5	2.0	2.5	
$w \cdot 10^6$ (mole/gs)	0.389	0.775	1.157	1.536	1.910	
$W \cdot 10^6$ (mole/s)	7.35	14.65	21.88	29.06	36.13	
$[2(y_A)_0 - (y_A)_t] \cdot 10^2$ (mole/g)	2.03	1.98	1.93	1.88	1.83	
$x \cdot 10^2 = \frac{(y_A)_t}{2(y_A)_0 - (y_A)_t} \cdot 10^2$	2.463	5.050	7.777	10.638	13.661	
$x/W \cdot 10^{-4}$ (s/mole)	0.3349	0.345	0.355	0.366	0.378	
$\sqrt{1 - x}$	0.987	0.974	0.960	0.945	0.929	
$\sqrt{\frac{x}{W}}$ ($s^{1/2}/mole^{1/2}$)	57.872	58.699	59.610	60.498	61.484	
$\frac{3250 - \frac{x}{W}}{\sqrt{1 - x}}$ ($s^{1/2}/mole^{1/2}$)	3232.2	3275.1	3322.2	3374.0	3431.5	

The illustrations of 8.b, 8.c, 8.d, 8.e. linearized rate equations discussed in a previous paper [5] have been omitted, since they do not satisfy the appropriate kinetic equations. In the above mentioned kinetic equation, the surface reaction is the rate determining step and the raw material furfural and one of the products furan adsorbed on the surface of the catalyst, according to this, the presumed mechanism is valid for the decarbonylating reaction of the furfural. The constants of the equation:

$$\frac{x}{W} = \alpha^I + \beta^I x$$

can be determined from the slope (β^I) and the axial section of the line (α^I) in Figure 5. If $K_{B_2} = 0$, that is carbon monoxide is not adsorbed on the surface of the catalyst, then the rate (k) and the equilibrium (K) constants can be calculated as follows:

$$\alpha^I = \frac{1}{k} \cdot \frac{1}{p}; \quad \beta^I = \frac{1}{k} \cdot K_A \quad \text{from:}$$

$$k = \frac{1}{p} \cdot \alpha^I; \quad K_A = \frac{\beta^I}{\alpha^I} \cdot \frac{1}{p}$$

If $K_{B_2} \neq 0$, then k and K cannot be calculated, the calculated values for the decarbonylating reaction at 300 °C according to the different furfural/hydrogen molar ratios can be seen in Table 5.

Table 5. Calculated values from Fig. 4.

		$\alpha \cdot 10^{-3}$	$\beta \cdot 10^{-3}$	$k \cdot 10^6$	$K_A \cdot 10^3$
		(s/mole)	(s/mole)	(mole/s·mm Hg)	(l/mm Hg)
Furfural/ hydrogen molar ratio	1/0	2.580	3.200	0.509	1.631
	1/0.5	1.880	3.683	1.050	3.866
	1/1	1.949	2.540	1.35	3.430
	1/2	3.250	3.909	1.21	4.747

The decarbonylation of the furfural takes place in the following stages corresponding to the calculated values:

- a.) The adsorption of the furfural on the catalyst
- b.) The decarbonylating reaction on the surface of the catalyst
- c.) The desorption of the furan from the catalyst.

The following conclusions can be drawn from the kinetic equation.

- 1.) The reaction rate is proportional to the specific surface area of the catalyst, therefore it is practical to use a catalyst with a specific surface area as high as possible.
- 2.) The application of hydrogen stream decreases the formation of the condensed products and their deposition on the surface of the catalyst, in this way the hydrogen protects the active sites from the desactivation.
- 3.) The calculated values of the equilibrium constant of the chemical reaction and the adsorption equilibrium constant of the component justify that the optimum furfural/hydrogen molar ratio is 1/1.

REFERENCES

1. GÁRDOS, Gy., PÉCHY, A., RÉDEY, A. Mrs. CSÁSZÁR E.: Hung.J. Ind. Chem. 3, 577 (1975)
2. GÁRDOS, Gy. PÉCHY, L., Mrs. CSÁSZÁR, E., SZIGETI, B.: Hung.J. Ind.Chem. 3, 4589 (1975)
3. GÁRDOS, Gy. PÉCHY, L., RÉDEY, A. Mrs. CSÁSZÁR, E.: Hung.J. Ind.Chem. 4, 13. (1975)

4. SZABÓ, Z.: Kontakt katalizis (Contact catalysis) Akadémiai Kiadó Budapest. 1966
5. GÁRDOS, Gy., KUN-SZABÓ, T., PÉCHY, L., RÉDEY, A.: Hung. J. Ind. Chem. 3, 309 (1975)

РЕЗЮМЕ

Были проведены опыты с целью испытания кинетики декарбонилирования фурфурола, применяя катализатор, содержащий 2,5 вес.% палладия. Скорость и кинетическое уравнение были установлены на основе экспериментальных данных, полученных при 300 С° и при молярном отношении фурфурол/водород 1:1. По расчетам было установлено, что лимитирующей стадией является поверхностная реакция.

EINE METHODE ZUR ANNÄHERNDEN ANALYTISCHEN LÖSUNG EINER
AUCH DAS QUELLENGLIED ENTHALTENDEN TRANSPORTGLEICHUNG

K. POLINSZKY, J. FÜLÖP, K. SEITZ, und T. VAJDA

(Forschungsinstitut für Technische Chemie
der Ungarischen Akademie der Wissenschaften,
Veszprém - Budapest)

Eingegangen am.12. Februar, 1976.

In unserer Arbeit untersuchen wir aufgrund früherer Resultate die Möglichkeiten der annähernden analytischen Lösung von Transportgleichungen, in denen das Quellenglied eine lineare Funktion des darin vorkommenden Potentials darstellt. Mit Hilfe numerischer Berechnungen wird gezeigt, daß die Annäherung in dem für die Praxis wesentlichen Bereich der unabhängigen Variablen auch in diesem Fall genügend genaue Resultate liefert.

EINLEITUNG

Die Transportprozesse der chemischen Verfahrenstechnik werden wie bekannt mit Hilfe partieller Differentialgleichungen beschrieben. Für eine exakte analytische Lösung dieser Gleichungen benötigt man einen relativ großen mathematischen Apparat, wobei die erhaltenen Resultate von komplizierter Struktur sind, so daß die für die Praxis wichtigen Berechnungen mit diesen Formeln nur in beschränktem Masse durchgeführt werden können.

Aus diesen Gründen erschien es notwendig, eine annähernde analytische Lösungsmethode auszuarbeiten, deren Aufstellung einerseits womöglich kein besonderes mathematisches Rüstzeug voraussetzt, und die erzielten Resultate gut übersichtlich und für nume-

rische Berechnungen direkt verwendbar sind. Diese Methode haben wir in einer früheren Arbeit [1] unter folgenden Anwendungsvoraussetzungen schon ausführlich beschrieben:

1. der untersuchte Prozess ist stationär, und das diesen beschreibende Gleichungssystem enthält zwei Unbekannte mit zwei unabhängigen Variablen;
2. die im Gleichungssystem figurierende partielle Differentialgleichung ist eine Fouriersche bzw. Ficksche Gleichung mit Newtonschen Randbedingungen;
3. auch die zweite Gleichung ist linear;
4. die Parameter der Differentialgleichungen sind Konstante.

In dieser Arbeit wird untersucht, auf welche Weise die obige Annäherungsmethode für den Fall erweitert werden kann, wenn in der partiellen Differentialgleichung auch ein Quellenglied vorkommt, das von dem betreffenden Potential linear abhängt. Die erweiterte Methode wird anhand eines Beispiels gezeigt, was ihre Allgemeingültigkeit nur in geringem Masse einschränkt.

BESCHREIBUNG DES PROBLEMS

Betrachten wir eine in einer unendlichen Umgebung erwärmte, sich fortbewegende, ebene Ladung, in der sich während der Wärmebehandlung auch eine exotherme oder endotherme Reaktion abspielt. Die Ladung bewegt sich im Ofen mit der Geschwindigkeit v in Richtung der x -Achse. Die Temperatur des an der Stelle $x = 0$ eintretenden Stoffes beträgt T_0 , die Temperatur des Anwärmerumes T'_0 , und es gilt notwendigerweise: $T'_0 > T_0$.

Bei der Aufstellung des mathematischen Modells von obiger Anordnung nehmen wir folgende Voraussetzungen an:

1. die Temperatur des anwärmenden Gasraums ändert sich der Ladung entlang nicht (Gas von unendlicher Wärmekapazität). Dadurch entsteht keine zweite Gleichung, das aber keine Einschränkung beinhaltet;

2. die Ladung ist hinsichtlich des Wärmetransportes anisotrop, also eine Wärmefortpflanzung tritt nur in der Querrichtung - Richtung y - auf;

3. zwischen der Ladung und dem anwärmenden Gasraum besteht eine konvektive Wärmeübertragung und in jedem beliebigen Punkt der Oberfläche der Ladung ist der Wärmestrom proportional zu dem Wärmeunterschied zwischen dem Gasraum und der Stoffoberfläche;

4. es wird angenommen, das die Stärke der in der Ladung angenommenen Wärmequelle bzw. negativen Wärmequelle proportional zur Differenz zwischen der momentanen Temperatur und der Eintrittstemperatur des Stoffes ist;

5. es handelt sich um einen stationären Prozess.

Aufgrund der obigen Annahme ergibt sich für das mathematische Modell des untersuchten Problems:

$$\lambda \frac{\partial^2 T}{\partial y^2} = \gamma v c \frac{\partial T}{\partial x} - v(T - T_0) , \quad (1)$$

mit den folgenden Anfangs- und Randbedingungen:

$$T(0, y) = T_0 , \quad (2a)$$

$$\left(\lambda \frac{\partial T}{\partial y} \right)_{y=L} = \alpha (T'_0 - T(x, L)) , \quad (2b)$$

$$\left(\lambda \frac{\partial T}{\partial y} \right)_{y=-L} = - \alpha (T'_0 - T(x, -L)) . \quad (2c)$$

In den Gleichungen bedeutet T die Temperatur der Ladung, λ stellt den Wärmeleitungskoeffizient, γ die Dichte, c die spezifische Wärme, v den Proportionalitätsfaktor der Quellenstärke und α den Wärmeübertragungsfaktor dar. Ausserdem ist zu ersehen, das die Ladung in der Querrichtung eine - symmetrisch um die Achse $y = 0$ angeordnete - Länge von $2 L$ hat.

BESCHREIBUNG DER ANNÄHERUNGSMETHODE

Führen wir nun in (1) - (2) folgende Parameterkomplexe ein:

$$a = \frac{\lambda}{\gamma v c} \quad , \quad b = \frac{v}{\gamma v c} \quad , \quad N = \frac{\alpha}{\lambda} L \quad ,$$

so ergibt sich für die zu lösende Gleichung folgende Form:

$$a \frac{\partial^2 T}{\partial y^2} = \frac{\partial T}{\partial x} - b(T - T_0) \quad ; \quad (3)$$

$$T(0, y) = T_0 \quad ; \quad (4a)$$

$$\left(\frac{\partial T}{\partial y} \right)_{y=L} = \frac{N}{L} (T'_0 - T(x, L)) \quad , \quad (4b)$$

$$\left(\frac{\partial T}{\partial y} \right)_{y=-L} = - \frac{N}{L} (T'_0 - T(x, -L)) \quad . \quad (4c)$$

Als eine annähernde analytische Lösung wollen wir den Temperaturraum nicht mit zwei Veränderlichen $T(x, y)$ bestimmen, sondern nur seinen der Variable y nach gebildeten Durchschnitt erhalten. Dieser ergibt sich laut Definition zu

$$\bar{T}(x) = \frac{1}{2L} \int_{-L}^L T(x, y) dy. \quad (5)$$

Die Gleichung für die Durchschnittstemperatur kann aus der Gleichung (3) abgeleitet werden, wenn die Durchschnittsbildung für diese laut (5) durchgeführt wird. Wir erhalten dann:

$$\frac{a}{2L} \left[\left(\frac{\partial T}{\partial y} \right)_{y=L} - \left(\frac{\partial T}{\partial y} \right)_{y=-L} \right] = \frac{d\bar{T}}{dx} - b(\bar{T} - T_0). \quad (6)$$

Durch Umformung der linken Seite von (6) mit Hilfe der Randbedingungen (4b) - (4c) ergibt sich bereits die Gleichung für die Durchschnittstemperatur:

$$\frac{Na}{L^2} (T'_0 - T(x, L)) = \frac{d\bar{T}}{dx} - b(\bar{T} - T_0) \quad . \quad (7)$$

deren Lösung infolge der darin enthaltenen unbekannten Funktion der Oberflächentemperatur nicht auf explizite Weise aufgeschrieben werden kann.

Es wird daher folgende Hilfsfunktion $z(x)$ eingeführt:

$$z(x) = \frac{T'_0 - T(x, L)}{T'_0 - \bar{T}(x)} \quad (8)$$

Mit Hilfe der Funktion (8) kann die Gleichung (7) in eine Form gebracht werden, die noch besser zu behandeln ist:

$$\frac{Na}{L^2} z(x) (T'_0 - \bar{T}) = \frac{d\bar{T}}{dx} - b(\bar{T} - T) \quad (9)$$

Falls nun die Funktion $z(x)$ entsprechend modelliert bzw. angenähert werden kann, so gilt das untersuchte Problem als lösbar.

ANNÄHERUNG DER FUNKTION $z(x)$

Führen wir die gewöhnliche Simplexform der die chemischen Transportprozesse beschreibenden Potentialfunktionen ein (wir verwenden dabei die Bezeichnungen wie für das untersuchte Problem):

$$\theta(x, y) = \frac{T'_0 - T(x, y)}{T'_0 - T_0} \quad (10)$$

dann ändert sich die Definitionsgleichung $z(x)$ aufgrund von (8) und (10) wie folgt:

$$z(x) = \frac{\theta(x, L)}{\bar{\theta}(L)} \quad (11)$$

Es kann gezeigt werden, daß diese Potentialsimplexe allgemein in folgender Form aufgeschrieben werden können:

$$\theta(x, y) = \varphi(y) + \sum_{k=0}^{\infty} A_k(y) e^{-\varphi_k x} \quad (12)$$

Hierbei sind die Koordinatenfunktionen $\phi(y)$ und $A_k(y)$ nur mehr von einer Variable abhängig, die Reihe der φ_k Werte kann mit Hilfe der Lösung der Eigenwertgleichung des Problems berechnet werden und unter ihnen besteht die Ordnungsrelation $0 < \varphi_0 < \varphi_1 < \dots < \varphi_k < \dots$ [2].

Das Simplex $\Theta(x, y)$ ist die Lösung der speziellen linearen partiellen Differentialgleichung zweiten Grades, die den Prozess beschreibt. Von den unabhängigen Variablen x und y kann x auch die Zeitkoordinate darstellen. Es ist wichtig zu beachten, dass die Funktion $\phi(y)$ in der Form laut (12) von $\Theta(x, y)$ nur dann auftritt, wenn der zu beschreibende Transportprozess nicht bloss einen Ausgleichscharakter hat. In diesen Fällen ergeben sich auch Wirkungen, welche die Entwicklung der homogenen Potentialverteilung verhindern: dem entspricht zum Beispiel der Fall einer Quelle bzw. einer negativen Quelle.

Setzt man die allgemeine Form (12) der Funktion $z(x)$ in (11) ein, so ergibt sich:

$$z(x) = \frac{\phi(L) + \sum_{k=0}^{\infty} A_k(L) e^{-\varphi_k x}}{\bar{\phi} + \sum_{k=0}^{\infty} \bar{A}_k e^{-\varphi_k x}} \quad (13)$$

Wie in [1] bereits gezeigt wurde, folgt es aufgrund von (8) aus physikalischen Überlegungen auch jetzt, dass $z(x=0)=1$, sowie daß es einen Grenzwert $\lim_{x \rightarrow \infty} z(x) = z_{\infty}$ gibt. Über den Verlauf der

Funktion $z(x)$ zwischen diesen Werten kann aber infolge der komplizierten Struktur von (13) nichts ausgesagt werden. Jedoch besteht die Möglichkeit, wie in [1], die Funktion $z(x)$ mit ihrem im Limes $x \rightarrow \infty$ angenommenen Wert z_{∞} anzunähern. Dieser Grenzwert beträgt aufgrund von (13), wie leicht einzusehen ist:

$$z(x) \approx z_{\infty} = \frac{\phi(L)}{\bar{\phi}} \quad (14)$$

Unsere Aufgabe besteht nun darin, den Grenzwert z_{∞} - ohne Verwendung der Lösung von (12), d.h. ohne die Notwendigkeit, die ursprüngliche partielle Differentialgleichung lösen zu müssen - zu bestimmen, denn unsere Annäherungsmethode ist nur in diesem Fall selbständig anzuwenden.

BESTIMMUNG DES GRENZWERTES z_∞

Schreiben wir die Laplace-Transformierte des Simplex (12) auf:

$$z(p, y) = \int_0^\infty \Theta(x, y) e^{-px} dx = \frac{\phi(y)}{p} + \sum_{k=0}^{\infty} \frac{A_k(y)}{\varphi_k + p}. \quad (15)$$

Es ist leicht einzusehen, daß die Funktion $\phi(y)$ aus der Transformierte - im Hinblick auf die zwischen den φ_k Werten bestehende Relation - durch Grenzwertbildung unmittelbar gewonnen werden kann, da nämlich

$$\lim_{p \rightarrow 0} pz(p, y) = \phi(y) + \lim_{p \rightarrow 0} p \sum_{k=0}^{\infty} \frac{A_k(y)}{\varphi_k + p} = \phi(y), \quad (16)$$

und aufgrund von (16) offenbar gilt

$$\phi(L) = \lim_{p \rightarrow 0} pz(p, L), \quad (17a)$$

$$\bar{\phi} = \lim_{p \rightarrow 0} p\bar{z}(p), \quad (17b)$$

so ergibt sich schließlich bei Verwendung von (17a)-(17b) aus (14):

$$z_\infty = \lim_{p \rightarrow 0} \frac{z(p, L)}{\bar{z}(p)}. \quad (18)$$

Es wurde also gezeigt, daß der Grenzwert z_∞ durch die obige Methode bereits aus den Laplace-Transformierten der Lösung der ursprünglichen partiellen Differentialgleichung aufgeschrieben werden kann. Dies ist von grosser Bedeutung, da die Errechnung der Laplace-Transformierten viel leichter durchzuführen ist. Wir möchten noch hinzufügen, daß dieses Verfahren offensichtlich nur in dem Fall anwendbar ist, wenn das Problem nicht nur einen reinen Ausgleichungscharakter hat, also wenn im Simplex (12) auch $\phi(y)$ vorkommt. Bei Ausgleichungsprozessen muß das unter [1] gezeigte - dieser Methode ähnliches - Verfahren angewandt werden.

Wir haben noch den Grenzwert z_{∞} im Falle des von uns untersuchten Problems zu bestimmen. Durch Vergleich von (3) und (10) ist einzusehen, daß nun für den Temperatursimplex folgende Gleichung heranzuziehen ist:

$$a \frac{\partial^2 \theta}{\partial y^2} = \frac{\partial \theta}{\partial x} + b(1 - \theta). \quad (19)$$

Die Gleichung für die Laplace-Transformierte des Simplex kann durch ähnliche Transformierung von (19) wie bei (15), und dabei unter Verwendung der auf das Simplex bezogene Bedingung (4a) aufgestellt werden:

$$a \frac{d^2 z}{dy^2} = (p - b)z + \frac{b}{p} - 1. \quad (20)$$

Die Lösung von Gleichung (20) gewinnt man auf die übliche Weise unter Berücksichtigung der Laplace-Transformierten der auf das Simplex bezogene Bedingungen (4b)-(4c):

$$z(p, y) = \frac{1}{p} - \frac{\frac{N}{pL} \operatorname{ch} \sqrt{\frac{p-b}{a}} y}{\sqrt{\frac{p-b}{a}} \operatorname{sh} \sqrt{\frac{p-b}{a}} L + \frac{N}{L} \operatorname{ch} \sqrt{\frac{p-b}{a}} L}, \quad (21)$$

und bei (21) kann die Durchschnittsbildung ähnlich wie bei (5) durchgeführt werden. Es ergibt sich dann:

$$\bar{z}(p) = \frac{1}{p} - \frac{\frac{N}{pL} \sqrt{\frac{a}{p-b}} \operatorname{sh} \sqrt{\frac{p-b}{a}} L}{\sqrt{\frac{p-b}{a}} \operatorname{sh} \sqrt{\frac{p-b}{a}} L + \frac{N}{L} \operatorname{sh} \sqrt{\frac{p-b}{a}} L}. \quad (22)$$

Mit Hilfe von (21) und (22) kann der Grenzwert (18) bereits aufgeschrieben werden:

$$z_{\infty} = \lim_{p \rightarrow 0} \frac{z(p, L)}{\bar{z}(p)} = \lim_{p \rightarrow 0} \frac{\sqrt{\frac{p-b}{a}} \operatorname{th} \sqrt{\frac{p-b}{a}} L}{\operatorname{th} \sqrt{\frac{p-b}{a}} L \left(\sqrt{\frac{p-b}{a}} - \frac{N}{L} \sqrt{\frac{a}{p-b}} \right) + \frac{N}{L}}. \quad (23)$$

Bildet man sodann bei (23) den Grenzwert, so erhält man nach Umformungen und nach Einführung des dimensionslosen Komplexes

$$\delta = \sqrt{\frac{b}{a}} L :$$

$$z_{\infty} = \frac{\delta^2 \operatorname{tg} \delta}{\operatorname{tg} \delta (\delta^2 + N) - N \delta} . \quad (24)$$

Durch das Ergebnis laut (24) haben wir das gesetzte Ziel erreicht: der als Annäherung der Hilfsfunktion $z(x)$ gewählte Wert z_{∞} wurde als Funktion der physikalischen Parameter (a , b , N und L) des untersuchten Problems aufgeschrieben. Die Genauigkeit der Annäherung wird nur mit Hilfe der numerischen Fehlerkalkulation ausgewertet, die theoretischen Überlegungen über die Art des Fehlers der Methode sind nämlich in [1] beschrieben.

BERECHNUNG DES FEHLERS DER ANNÄHERUNG

Akzeptiert man die angeführte Annäherung, so erhält die Gleichung (9) folgende Form:

$$\frac{d\bar{T}}{dx} + \left(\frac{Na}{L^2} z_{\infty} - b \right) \bar{T} = \frac{Na}{L^2} T_0' - bT_0 \quad (25)$$

Die Lösung von (25) kann unter Verwendung der auf den Durchschnitt bezogenen Anfangsbedingung (4a) durch die üblichen Methoden erhalten werden. Das Resultat ergibt nach Übergang auf den Simplex laut (10):

$$\bar{\theta}_K(x) = \frac{\exp \left[- \left(\frac{Na}{L^2} z_{\infty} - b \right) x \right] - \frac{bL^2}{Na z_{\infty}}}{1 - \frac{bL^2}{Na z_{\infty}}} , \quad (26)$$

wobei sich der Wert von z_{∞} aus (24) ergibt, und der Index K weist darauf hin, dass die Lösung eine Annäherung darstellt.

Mittels viel komplizierterer Berechnung [3] kann von den Gleichungen (3)-(4) ausgehend natürlich auch der genaue Simplex-durchschnitt θ_E bestimmt werden, den wir bei der Berechnung des Fehlers der Annäherung benötigen:

$$\bar{\theta}_E(x) = \sum_{k=0}^{\infty} \psi_k \frac{\exp \left[- \left(\frac{\beta_k^2 a}{L^2} - b \right) x \right] - \frac{bL^2}{\beta_k^2 a}}{1 - \frac{bL^2}{\beta_k^2 a}}, \quad (27)$$

hier sind

$$\psi_k = \frac{2 \sin^2 \beta_k}{\beta_k^2 + \beta_k \sin \beta_k \cos \beta_k}, \quad (28)$$

sowie die β_k Werte die Wurzeln der Eigenwertgleichung:

$$\beta_k \operatorname{tg} \beta_k = N. \quad (29)$$

Unter Verwendung von (26) und (27) können wir nun die prozentuelle Fehlerzahl aufschreiben:

$$\eta = |\bar{\theta}_E - \bar{\theta}_K| \cdot 100 \quad [\%] \quad (30)$$

durch die der Fehler unserer Annäherung charakterisiert werden kann. Mit Hilfe einer geeigneten Ähnlichkeitstransformation kann weiterhin gezeigt werden, das dieses Problem schließlich durch drei unabhängige, dimensionslose Größen: die bereits bekannten Zahlen N bzw. δ sowie $w = \frac{ax}{L^2}$ eindeutig charakterisiert wird. Unter Benützung derselben ergibt aus (26), (27) und (30) für den Fehler die folgende Form:

$$\eta(w) = \left| \sum_{k=0}^{\infty} \psi_k \frac{\exp[(\delta^2 - \beta_k^2)w] - \frac{\delta^2}{\beta_k^2}}{1 - \frac{\delta^2}{\beta_k^2}} - \frac{\exp[(\delta^2 - Nz_{\infty})w] - \frac{\delta^2}{Nz_{\infty}}}{1 - \frac{\delta^2}{Nz_{\infty}}} \right|, \quad (31)$$

wobei die darin vorkommenden Parameter durch (24), (28) und (29) angegeben sind.

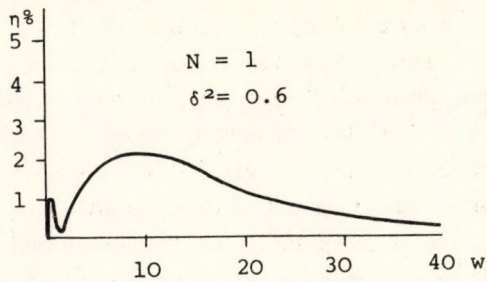


Abb. 1.

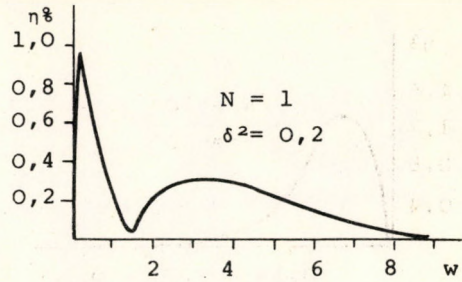


Abb. 2.

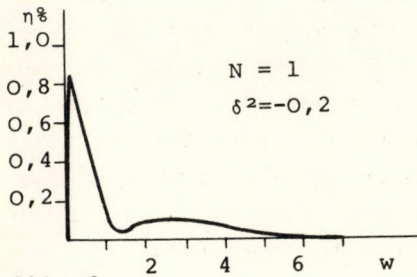


Abb. 3.

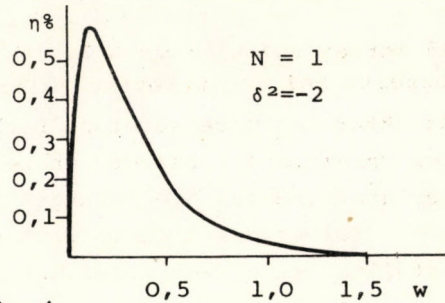


Abb. 4.

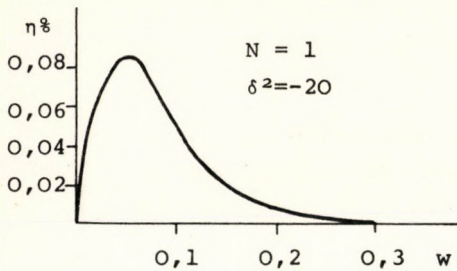


Abb. 5.

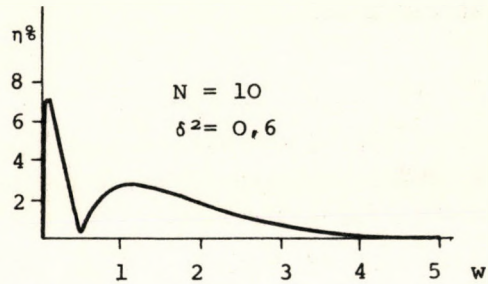


Abb. 6.

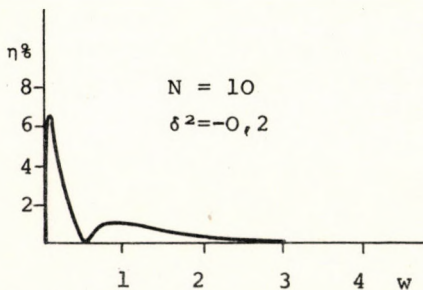


Abb. 7.

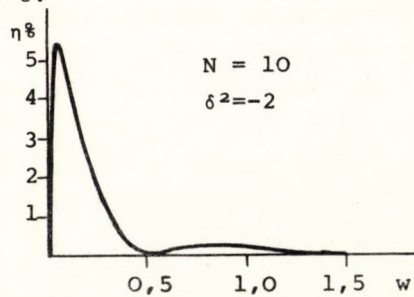


Abb. 8.

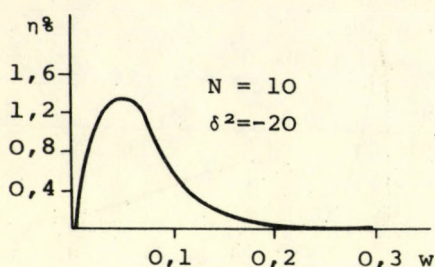


Abb. 9.

Die aufgrund der Gleichung (31) berechneten Resultate sind auf den Abbildungen 1-9. zu sehen. Wie schon auf der Grundlage von [1] zu erwarten war, beträgt der Fehler an den Stellen $x = 0$ und $x \rightarrow \infty$ Null und erreicht sein Maximum irgendwo zwischen den Grenzwerten. Es zeigt sich weiterhin, daß sich die Annäherung im allgemeinen bei großen negativen

δ^2 Werten und kleinen N -Zahlen als gut erweist, da hier der Fehler bereits bei den w Werten zwischen 0,5 - 2 verschwindet. Aus der Struktur des untersuchten Problems geht hervor, daß der Wertvorrat des Parameters δ bei dem oberen Grenzwert beschränkt ist, falls es verlangt wird, daß die Lösungen auch im Grenzfal $x \rightarrow \infty$ existieren sollen. Selbstverständlich wird - falls diese Voraussetzung nicht erfüllt ist - die Fehlerfunktion η ebenfalls divergieren.

ZEICHENERKLÄRUNG

- a Parameterkomplexe
- b A, \bar{A} Koordinatenfunktion bzw. deren Durchschnitt
- c spez. Wärmekoeffizient der Ladung [kcal/kg $^{\circ}$ K]
- k laufende Indexzahl
- 2 L Dicke der Ladung [m]
- N Nusselt-sche Zahl
- p Parameter der Laplace-Transformation
- T Wärmeverteilung der Ladung [$^{\circ}$ K]
- \bar{T} durchschnittliche Temperatur der Ladung [$^{\circ}$ K]
- T_0 Temperatur des eintretende Stoffes [$^{\circ}$ K]
- T_0' Temperatur des Wärmeraumes [$^{\circ}$ K]
- v Geschwindigkeit der Ladung [m/h]
- w Fourier-sche Zahl
- x Raumkoordinaten [m]
- y Hilfsfunktion
- z Z, \bar{Z} Laplace-Transformierte des Potentialsimplex bzw. deren Durchschnitt

- α Wärmeübertragungskoeffizient [$\text{kcal}/\text{m}^2\text{h}^\circ\text{K}$]
 β_k Eigenwert
 γ Dichte der Ladung [kg/m^3]
 δ dimensionsloser Komplex
 η Fehlerfunktion
 $\theta, \bar{\theta}$ Potentialsimplex, bzw. dessen Durchschnitt
 λ Wärmeleitungskoeffizient [$\text{kcal}/\text{m h}^\circ\text{K}$]
 $\phi, \bar{\phi}$ Koordinatenfunktion, bzw. deren Durchschnitt
 ψ_k Parameterkomplex
 ν Proportionalitätsfaktor der Quellenstärke [$\text{kcal}/\text{m}^3\text{h}^\circ\text{K}$]

LITERATUR

1. POLINSZKY, K. et al.: Acta Chimica, 85, 161 (1975)
2. CARSLAW, H. S., JAEGER, J. C.: Conduction of Heat in Solids, Clarendon Press, Oxford, 1959.
3. CRANK, J.: The Mathematics of Diffusion, Clarendon Press, Oxford, 1957.

РЕЗЮМЕ

В статье - на основе предыдущих результатов - обсуждается возможность приближенного аналитического решения транспортного уравнения, в котором источник является линейной функцией потенциала. С помощью числовых вычислений показано, что приближение является удовлетворительно точным в интервале практически важной независимой переменной.

СОДЕРЖАНИЕ

МОХИЛЛА, Р., ФЕРЕНЦ, Б., ВАРГАНЭ ИМРЕ, М. и БАКОШ, М.: Динамика системы газ-жидкость, спускающейся в прямотоке на насадке-катализаторе сферической формы	1
БЕНЦЕ, Л., МАРКО, Л., ОПИЦ, Р. и ТИЛЕ, Н.Х.: σ -органические производные вольфрама как катализаторы обменного разложения олефинов III. Изучение каталитических свойств	15
ГРЕС, И.: Рабочая область и экономичность при ротационных пленочных аппаратах	25
САБО, М. и КАЛЬДИ, П.: Непрерывный метод для получения раствора ZnS_2O_4	39
ПЛЕВА, Л. и НОВАК, Б.: Метод нахождения алгоритма для решения математической модели сложных систем	61
БЕНЕДЕН, П., ЛАСЛО, А., НЕМЕТ, А. и ВАЦИ, П.: Моделирование реакции неполного окисления в пламени метана	77
ЕРМАКОВА, А., ХОЛДЕРИТ, Й., СТЕФОГЛО, Е.Ф. и ПЬЯНОВ, В.И.: Структура организованного трехфазного неподвижного слоя. Экспериментальная зависимость содержания твердой фазы от скоростей потоков	93
ГАРЦМАН, А.Н., ЕРМАКОВА, А. и РАССАДНИКОВА, Н.И.: Массопередача с химической реакцией на границе раздела фаз газ-жидкость	109
ГАРДОШ, Дь., ПЕЧИ, Л., РЕДЕИ, А. и ЧАСАР, Е.: Изучение декарбонилирования фурфурола на катализаторе из металлического палладия с носителем	125
ГАРДОШ, Дь., ПЕЧИ, Л., РЕДЕИ, А. и ЧАСАР, Е.: Испытание кинетики декарбонилирования фурфурола	139
ПОЛИНСКИ, К., ФЮЛЕП, Я., СЕЙЦ, К. и ВАЙДА, Т.: Метод для приближенного аналитического решения транспортного уравнения, содержащего источник	151

CONTENT

MOHILLA, R., FERENCZ, B., Mrs. VARGA, M. and BAKOS, M.: Studies on the Dynamics of Downward Cocurrent Gas- -Liquid Flow in Packed-Bed Reactors	1
BENCZE, L., MARKÓ, L., OPITZ, R. and THIELE, K.-H.: σ - Organo Tungsten Derivates as Olefin Metathesis Catalyst, III. Studies on Catalytic Properties.	15
GRESZ, I.: Anwendungsbereich und Wirtschaftlichkeit der Rotationsdünnsschichtapparate (The Application Fields and Economy of Rotating Film Reactors)	25
SZABÓ, M. and KÁLDI, P.: A Continuous Method for Producing ZnS_2O_4 Solutions	39
PLEVA, L. and NOVÁK, B.: Algorithm Search Method to Solve Mathematical Models of Complex Systems	61
BENEDEK, P., LÁSZLÓ, A., NÉMETH, A. and VÁCZI, P.: Mathema- tical Model of the Partial Oxidation Flame-Reaction of Methane	77
ERMAKOWA, A., HOLDERITH, J., STEFOGLO, E.F. and PJANOW, W.I.P.: The Structure of an Organized Three-Phase Fluidized Bed. The Experimental Dependence of Hold Up of Solids Particle on the Fluid Flow Rate	93
GARCMAN, A. N., ERMAKOVA, A. and RASSADNIKOVA, N. I.: Mass Transfer with Chemical Reaction Near the Gas-Liquid Interface	109
GÁRDOS, Gy., PÉCHY, L., RÉDEY, Á. and Mrs. CSÁSZÁR, E.: Investigation of Furfural Decarbonylation over Metal Palladium Catalysts	125
GÁRDOS, Gy., PÉCHY, L., RÉDEY, Á. and Mrs. CSÁSZÁR, E.: Kinetic Investigation on the Decarbonylation of the Furfural	139
POLINSZKY, K., FÜLÖP, J., SEITZ, K. und VAJDA, T.: Eine Methode zur Annähernden analytischen Lösung einer auch das Quellenglied enthaltenden Transportglei- chung (A Method for the Approximate Analytical Solu- tion of Transport Equation Containing a Source Term). . .	151

HUNGARIAN

Journal of

INDUSTRIAL

CHEMISTRY

Edited by

the Hungarian Oil & Gas Research Institute (MÁFKI),
the Research Institute for Heavy Chemical Industries (NEVIKI),
the Research Institute for Technical Chemistry of the
Hungarian Academy of Sciences (MÜKKI),
the Veszprém University of Chemical Engineering (VVE).
Veszprém (Hungary)



Volume 4.

1976

Number 2.

CODEN: HJICAI

ISSN: 0133-0276

Editorial Board:

R. CSIKÓS and Gy. MÓZES

Hungarian Oil & Gas Research Institute
(MÁFKI Veszprém)

A. SZÁNTÓ and M. NÁDASY

Research Institute for Heavy Chemical Industries
(NEVIKI Veszprém)

T. BLICKLE and O. BORLAI

Research Institute for Technical Chemistry
of the Hungarian Academy of Sciences
(MÜKKI Veszprém)

A. LÁSZLÓ and L. PÉCHY

Veszprém University of Chemical Engineering
(VVE Veszprém)

Editor-in Chief:

Assistant Editor:

E. BODOR

J. DE JONGE

Veszprém University of Chemical Engineering
(VVE Veszprém)

The "Hungarian Journal of Industrial Chemistry" is a joint publication of the Veszprém scientific institutions of the chemical industry that deals with the results of applied and fundamental research in the field of chemical processes, unit operations and chemical engineering. The papers are published in four numbers at irregular intervals in one annual volume, in the English, Russian, French and German languages.

Editorial Office:

Veszprémi Vegyipari Egyetem
"Hungarian Journal of Industrial Chemistry"
H-8201 Veszprém, P.O.Box: 28
Hungary

Felelős szerkesztő: Dr. Bodor Endre
Kiadásért felelős: Dr. Nemezc Ernő, a VVE rektora

STUDIES ON THE ATMOSPHERIC, NON-STEADY-STATE, STRIPPING
OUT FURFURAL REACTOR, PART 1, THE MODEL OF THE PROCESS

A. LÁSZLÓ, GY. MARTON

(Department of Chemical Process Engineering, Veszprém
University of Chemical Engineering)

Received: April 22, 1976.

The main operation unit of the pentosane-containing materials or pentose solution based furfural production process is the two-stage reactor. Here, the furfural produced in the chemical reaction is extracted or stripped out. This paper presents the process-model of a laboratory scale, atmospheric, non-steady-state reactor. The model and its data set is based on experiments carried out in an isotherm (108°C) tank reactor. The formation, decomposition and stripping out steps of the furfural production were tested in 35 weight per cent sulphuric acid solution containing initially 5-28 g/l d-xylose and 4.2-75 g/l furfural, respectively. A relatively simple model structure was found adequately reflecting the chemical reaction and the coupled stripping out process.

Furfural, a potential plant component, is generally found in polysaccharide (pentosane) form. Because these polysaccharides are hydrolysed at a much faster rate than the cellulose matrix, different furfural production methods utilize that fact excluding the decomposition of cellulose itself [1].

1. FURFURAL PRODUCTION STEPS

Hydrolysing polysaccharides with strong mineral acids at elevated temperatures, simple water soluble sugars are obtained. As a following step, furfural as well as methoxy-furfural are formed from the decomposition products, pentoses, uronic acids, and hexoses, respectively. Furfural is essentially formed in two steps:

a) the first step is the water uptake, i.e. pentosane is hydrolysed to pentose

b) the second step is the water loss, i.e. releasing one mole water, pentose becomes furfural, which to prevent further decomposition, is either extracted or stripped out of the system.

In general, industry-scale furfural production methods are similar, except that the a) and b) steps are performed in one or two units and that of extraction or stripping out is used to recover the furfural produced [2, 3].

There is a considerable amount of literature on the hydrolysis process of pentosane containing materials (corn-cob, rice-straw, deciduous tree, and bagasse etc.) [5]. Similarly, there is an equally large number of publications dealing with the technological details of furfural production, for the production and decomposition reaction rates greatly depend on the quality of the pentoses hydrolysed, correspondingly, on the raw material selected. For example, the decomposition rate of d-xylose in 0.8 weight per cent sulphuric acid is about twice as high as that of d-mannose (the hexose most easily decomposed), and 1.7 times that of the d-arabinose [8]. Therefore, reagent grade d-xylose solutions were used throughout the experiments.

2. FORMATION AND DECOMPOSITION KINETICS OF FURFURAL

The reaction scheme of the homogeneous phase reaction in acidic medium can be written as follows:

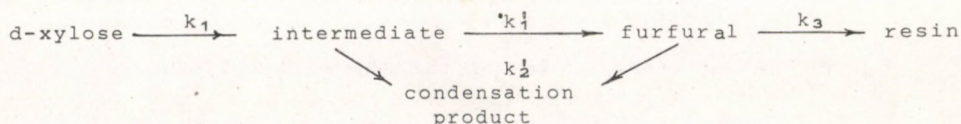


Most authors think that the elementary reactions of this consecutive scheme in dilute solutions are first-order reactions [2,3,4]. It has to be noted that the rate constants proportionally change with the acid concentration, thus the first-order kinetics hold only under strictly identical acidities or rather, pH values. MEL-NYIKOV [6] collected the decomposition rate data (k_1) of d-xylose published by several authors relating to different sulphuric acid solutions brought to the boil. This compilation is shown in Table 1, demonstrating that to achieve technologically acceptable decomposition rates (i.e. $k_1 > 0.5 \text{ h}^{-1}$) acid solutions over 25 weigh per cent concentrations have to be used at atmospheric pressures.

Table 1. Decomposition rate values of d-xylose in sulphuric acid solutions at their boiling point temperatures

Sulphuric acid concentration (weight per cent)	Boiling point ($^{\circ}\text{C}$)	Rate constant of decomposition reaction (h^{-1})
15.0	103.0	0.09
19.2	104.0	0.13
20.0	104.4	0.16
24.5	105.7	0.26
25.6	106.0	0.35
26.5	106.5	0.52
29.0	107.5	1.00
32.0	109.0	0.62
40.0	114.0	0.67
52.0	127.0	2.52

A number of explanations appeared in the literature relating to the decomposition of furfural. Omitting their analysis, the kinetic model proposed by SCHOENEMANN [7] and DUNLOP [1] was accepted and used. Its main feature is the statement that the decomposition reaction of furfural - in the presence of xylose - due to its high reactivity and polymerisation tendency, does not follow the first-order kinetics. Under given H^+ concentration and isotherm conditions the kinetics-scheme, proved by several identification tests, can be written as shown below:



Thus the kinetic equation set is written as:

$$\frac{dx}{dt} = -k_1 x \quad (1)$$

$$\frac{di}{dt} = k_1 x - k'_1 i - k'_2 f i \quad (2)$$

$$\frac{df}{dt} = k'_1 i - k'_2 f i - k_3 f \quad (3)$$

$$\frac{db}{dt} = k'_2 f i + k_3 f \quad (4)$$

However, the kinetic studies failed to identify the intermediate. It was also SCHOENEMANN, who introduced the simplifying assumption, $\frac{di}{dt} = 0$ and making use of the relations resulting from assumption, namely $k'_1 \gg k_1$ and $k'_1 \gg k'_2 f$, the intermediate i can indeed be eliminated and the necessary kinetic equations become:

$$\frac{dx}{dt} = -k x$$

$$\frac{df}{dt} = k_1 x - k_2 x f - k_3 f \quad (3.a)$$

$$\frac{db}{dt} = k_2 x f + k_3 f \quad (4.a)$$

3. THE MODEL OF THE STRIPPING PROCESS

The flowchart of the semicontinuous furfural producing stripping system is shown in Figure 1.

Assumptions:

- a) Both phases are ideally mixed,
- b) The α phase is the stagnant liquid, the β phase is the steam phase bubbling through the α liquid phase ($V^\alpha \gg V^\beta$),
- c) Only furfural takes part in the mass transfer between the phases,
- d) The α and β phases are in thermal equilibrium,

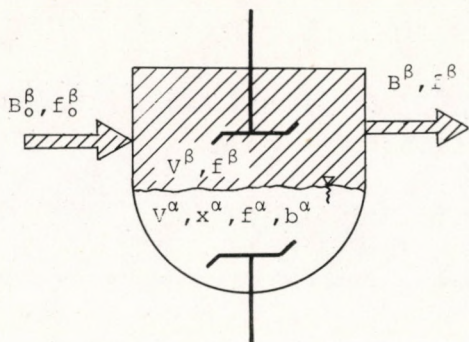


Fig.1. The flowchart of the furfural producing and stripping out system

- e) Due to the slow reaction, the quasi-equilibrium distribution of the furfural between the two phases can be accounted for with a constant K ,
- f) The transfer mechanism is adequately represented by the two-film theory, i.e. chemical reaction is assumed to take part in the bulk of the liquid phase.

Starting from Equations 1, 3.a, and 4.a changes taking part in the α -phase can be characterized by the following equations:

$$\frac{dx^\alpha}{dt} = -k_1 x^\alpha \quad (1.b)$$

$$\frac{df^\alpha}{dt} = k_1 x^\alpha - k_2 x^\alpha f^\alpha - k_D (Kf^\alpha - f^\beta) - k_3 f^\alpha \quad (3.b)$$

$$\frac{db^\alpha}{dt} = k_3 f^\alpha + k_2 x^\alpha f^\alpha \quad (4.b)$$

$$\frac{dp^\alpha}{dt} = uf^\alpha \quad (5)$$

where:

$$u = k_D \left(K - \frac{f^\beta}{f^\alpha} \right) \quad (6)$$

is the value of the transfer current relating to unit furfural mass. Thus p^α is in fact a quantity proportional to the yield of the stripped furfural. In the β phase (if $V^\beta \ll V^\alpha$)

$$B^\beta f^\beta - B_O^\beta f_O^\beta = V^\alpha k_D (Kf^\alpha - f^\beta) \quad (7)$$

or:

$$B^\beta f^\beta - B_O^\beta f_O^\beta = V^\alpha uf^\alpha \quad (8)$$

Be $f_O^\beta = 0$ for the following discussion, and let us rearrange

Equation 7, yielding the equation below:

$$\frac{f^\alpha}{f^\beta} = \frac{1}{K} + \frac{B^\beta}{V^\alpha K k_D} = \frac{1}{K} + \frac{M}{K k_D} \quad (9)$$

In technological terms M is called the stripping out module. If K and k_D do not depend on each other and on M , then Equation 9 is reduced to a linear relationship. Hence, of the K and k_D values can be kept at some constant values throughout several experiments and the corresponding f^α/f^β values are measured, then their linear correspondance indicates, on the one hand, the adequacy and the soundness of the model, and on the other hand, K can be calculated from the ordinate interscession and k_D from the slope value. In the assumption e) it was stated that K is constant, at least over the region of interest. The same, however, can only be solved, by properly modifying the experimental technique and when the compounded mass transfer coefficient k_D is concerned. Therefore, similar hydrodynamical conditions were ensured keeping the evaporation and condensation rates at constant values. (It was assumed that the chemical kinetics had no effect on the mass transfer coefficient.)

4. EXPERIMENTAL

The schematics of the experimental system is shown in Figure 2. The reactor (1) itself is made of Rasotherm glass and is a 0.5 l roundbottom flask equipped with a sampling probe. A reflux collector head (2) and a condenser (3) are attached to the reactor. Pump (4) delivers the condensed product into the receiver (5) and transfers an equal amount of distilled water back into the reactor from tank (6). Thus in the 0-190 ml/hour offtake range the predetermined fluid level and acidity could be maintained. External electric heating of the reactor was adjusted to maintain a 280 ml per hour evaporation rate throughout the experiments.

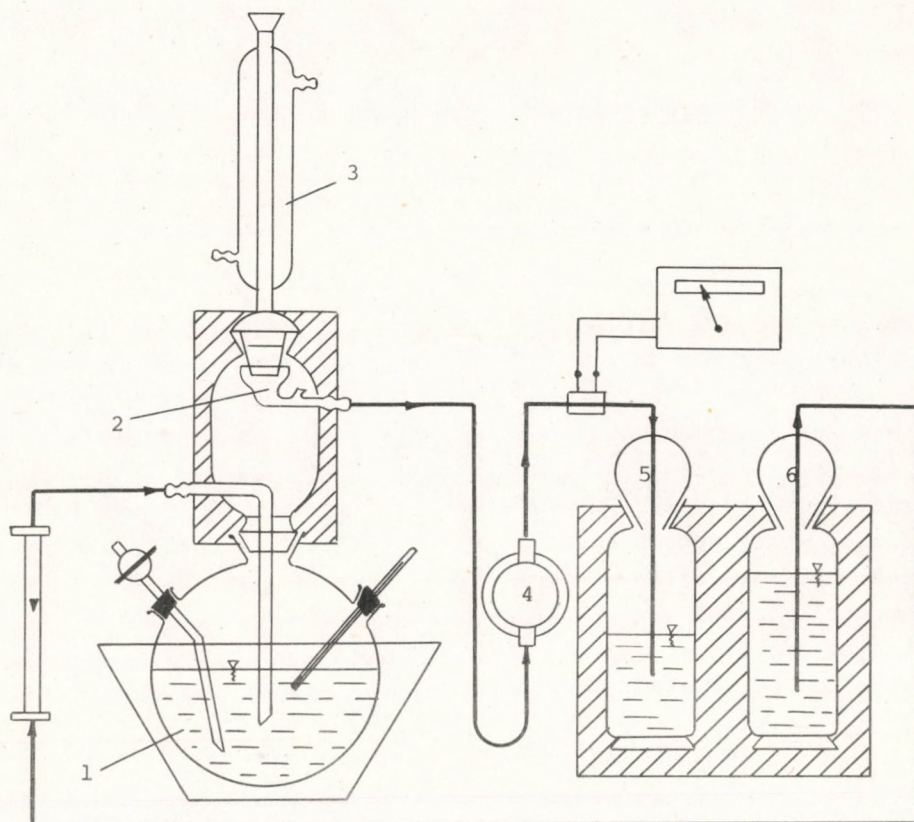


Fig.2. Schematics of the experimental set-up

4.1 Parameters of the stripping model

Stripping out experiments were carried out in 35 weight per cent sulphuric acid containing base solutions with 5-20 g/l initial d-xylose and furfural concentrations. The reactor temperature was maintained at 108°C throughout the experiments. Variables of Equation 9 and the regression line are shown in Figure 3. It can well be seen that experiments starting with either furfural or d-xylose yield the same results in the $0 < M < 2$ range.

The constants calculated from the regression line are as follows:

$$K = 12.60 \quad (\text{dimensionless})$$

$$k_D = 1.28 \quad (\text{h}^{-1})$$

4.2 Determination of the kinetic constants

The rate constant k_3 characterising the decomposition of furfural was determined from 35 weight per cent sulphuric acid solutions initially containing 4.2 g/l; 16.7 g/l and 75 g/l furfural, respectively. It was found that the decomposition kinetics do not follow the first-order mechanism. In our view the equation:

$$\frac{df}{dt} = k'_3 f^2 + k_3 f \quad (10)$$

adequately describes the kinetics of decomposition.

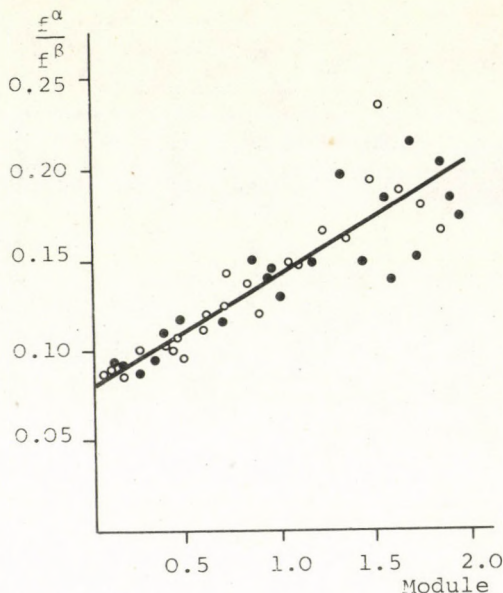
By introducing the

$$\bar{f} = \frac{f}{f_0}$$

$$\bar{k}'_3 = k'_3 f_0$$

and Fig.3. The experimentally constructed $\bar{f}^\alpha/\bar{f}^\beta$ vs M function

- Experiments starting from d-xylose
- Experiments starting from furfural



relationships the expression

$$f = \frac{k_3}{(k'_3 + k_3)e^{k_3 t} - k'_3} \quad (11)$$

is obtained.

According to the experimental results, the model is adequate if $k'_3 = 0.012 \text{ l/gh}$ and $k_3 = 0.11 \text{ h}^{-1}$. At the same time, it can be seen from Figure 4 that in the case $f_o < 5 \text{ g/l}$, the decomposition can practically be described by the first-order kinetics model. Because the highest furfural concentration in the stripping out experiment never exceeded the 5-6 g/l values, the use of this simplification is acceptable.

4.2.1 Determination of the kinetic constants k_1 and k_2 by identification method

Kinetic measurements were made in d-xylose solutions initially containing during the measurements. The equation system containing Equations 1, 3.a, and 4.a, characterizing the kinetic model was generated on a MEDA 81-T type analogue computer. By changing the parameters k_1 and k_2 , the solution, best fitting the experimental curve, was created. The adequacy of the models with the appropriate parameters proved to be excellent (see, e.g. Figure 5.)

Table 2 presents the k_1 and k_2 values derived from seven separate kinetic experiments.

Table 2. The concentration independency of the kinetic constants k_1 and k_2

$x_o \text{ (g/l)}$	$k_1 \text{ (h}^{-1}\text{)}$	$k_2 \text{ (lg}^{-1} \text{ h}^{-1}\text{)}$
3.2	1.07	0.09
5.0	0.92	0.13
8.4	0.88	0.14
11.4	0.93	0.06
15.2	1.00	0.12
22.0	0.91	0.17
28.0	0.94	0.13

Average	0.95	0.12

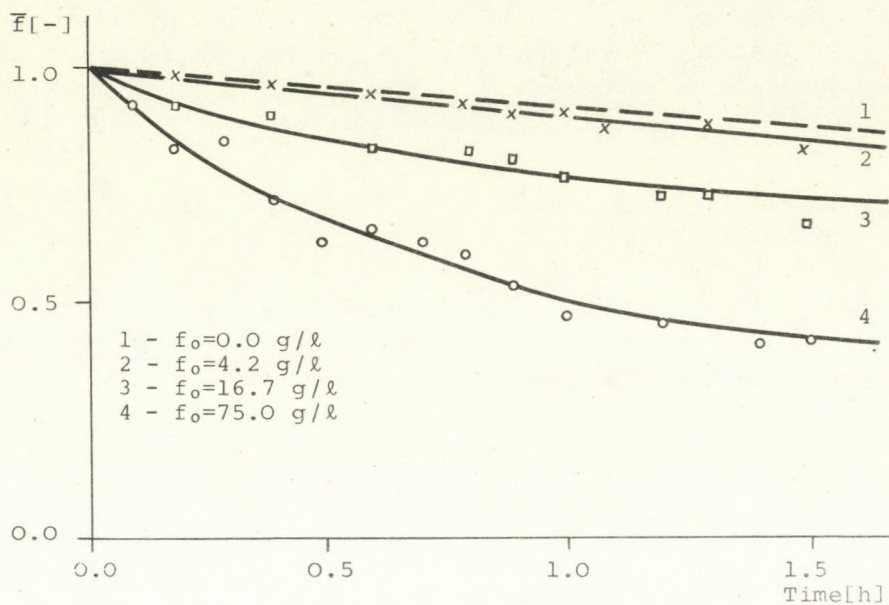


Fig.4. Decomposition of furfural in 35 weight per cent sulphuric acid solution

Table 3. Calculation of the decomposition of d-xylose and the parameter-independency test

Time (h)	Conversion, calculated with $k_1 = 0.95 \text{ h}^{-1}$	Conversion, experimental with $M = 0.60$		
		$x_0 = 5 \text{ g/l}$	$x_0 = 15 \text{ g/l}$	$x_0 = 28 \text{ g/l}$
(h)	%	%		
0.2	17.3	13.6	-	18.1
0.4	31.6	-	29.4	27.8
0.6	43.4	44.7	-	46.8
0.8	53.2	-	57.1	53.8
1.0	61.3	63.0	-	63.6
1.4	73.6	75.8	-	71.3
2.0	85.0	-	83.9	82.7
2.5	91.7	90.5	-	91.2
3.0	93.2	94.2	93.4	93.9

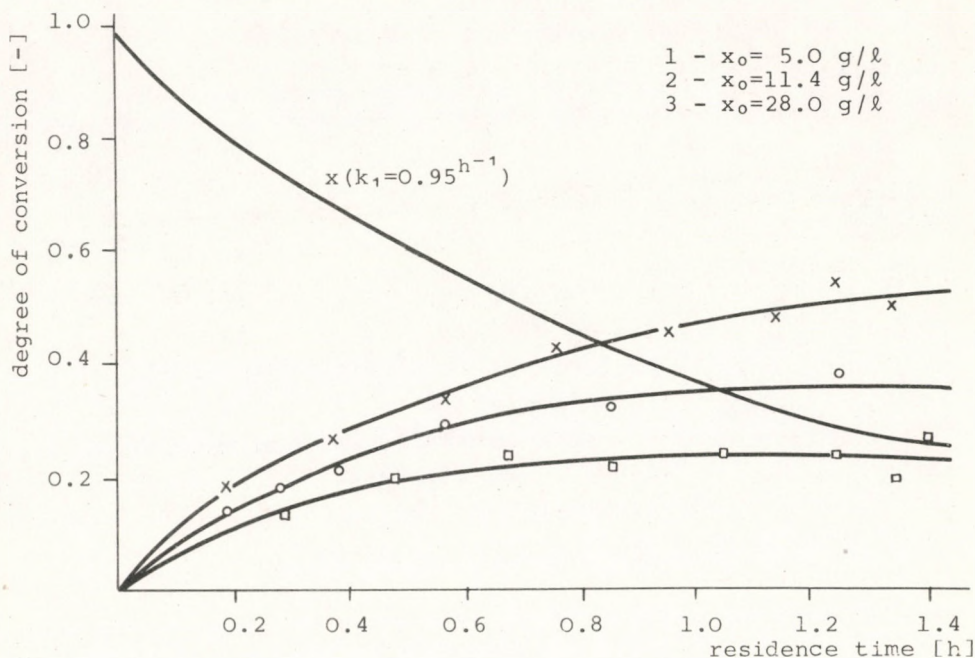


Fig.5. The computer solution of the kinetic model

The rate coefficients k_1 were also identified with the help of the stripping out model. Selecting an $M = 0.60$ steam module and employing Equations 3.b, and 9, the conversion of the decomposing d-xylose was calculated as a function of the time. Table 3 presents the conversion values measured and calculated assuming $k_1 = 0.95 \text{ h}^{-1}$. The agreement satisfies the technical needs.

The adequacy of the data base also proves the good reproducibility of the experiments. This is obviously due to the thermodynamical stability of the solution kept at its boiling point, i.e. due to the enforced isothermness of the reaction. This is further assisted by the low volatility of the sulphuric acid. It is worth while to note the salting out effect of sulphuric acid on the furfural, for the distribution ratio $K = 12.6$ is about two times that of the equilibrium vapour-liquid distribution coefficient of the

water-furfural systems.

In summary, we can conclude that the model structure presented makes use of an easily measurable or identifiable parameter set, satisfying the usual design requirements.

SYMBOLS USED

b	concentration of the byproduct in the liquid phase (g/l)
B	volumetric flow rate of the vapour phase (l/h)
f	concentration of furfural in the liquid phase (g/l)
$f = \frac{f}{x_0}$	dimensionless furfural concentration (-)
i	concentration of the intermediate in liquid phase (g/l)
$k_1, k'_1, k_2, k'_2, k_3, k'_3$	reaction rate constants
k_D	compounded mass transfer coefficient (l/h)
K	apparent equilibrium distribution coefficient (by definition $K = \frac{p}{f}^*$)
M	stripping out module (by definition $M = \frac{B}{V}$)
p	concentration of furfural in the condensate (g/l)
u	control-variable (defined in Equation 6) (l/h)
x	concentration of d-xylose in the liquid phase (g/l)
V	volume of the reaction liquid mixture (l)

Indexes

$*$	equilibrium value
α	liquid phase
β	vapour phase
o	initial value

REFERENCES

- [1] DUNLOP, A.P.: Ind. Eng. Chem., 40 (2), 204, (1948)
- [2] WILLIAMS, D.L. and DUNLOP, A.P.: Ind. Eng. Chem., 40 (2), 239, (1948)
- [3] DUNLOP, A.P.: The Furans, Reinhold Publ. Co., New York, (1953)
- [4] MOTOYOSHI OSHIMA: Chem. Proc. Monograph No. 11
- [5] MELNIKOV, N.P.: Sb. Tr. Gos. Nauk Issled. Inst. Hidroliz. Sulfitno-Spirt. Prom., 16, 160, (1967)
- [6] MELNIKOV, N.P. and ZSELTUHINA, V.A.: ibid 15, 108, (1966)
- [7] SCHOENEMANN, K.: Chem. Eng. Sci., 14, 39, (1961)
- [8] SAEMAN, J.F.: Ind. Eng. Chem., 37 (1), 43, (1945)

РЕЗЮМЕ

Основной процессионной единицей в производстве фурфурола из содержащего пентозан сырья или из раствора пентоза, является двух-фазный реактор. Образовавшийся в ходе химической реакции фурфурол здесь выпаривают или экстрагируют. В данной статье приводится модель атмосферного лабораторного реактора с нестационарным режимом. Модель и система данных опирается на эксперименты, проведенные в изотермическом (108°C) реакторе-котле. Процессы образования, разложения и выпарки фурфурола исследовались в 35 вес%-ом растворе серной кислоты, при начальном содержании д-ксилоза 5-28 г/л, и начальном содержании фурфурола 4,2-75 г/л. Химическую реакцию и связанный с ней процесс выпарки удалось выразить с помощью довольно простой модельной структуры.

STUDIES ON THE ATMOSPHERIC, NON-STEADY-STATE, STRIPPING
OUT FURFURAL REACTOR, PART 2, THE OPTIMUM TIMING OF
STRIPPING OUT

GY. MARTON, J. VASS

(Department of Chemical Process Engineering, Veszprém
University of Chemical Engineering)

Received: April 22, 1976.

The economic operation mode of a non-steady-state furfural reactor requires that a minimum amount of steam should be consumed to achieve given product qualities. As furfural is an intermediate in the chemical kinetic scheme, maintaining the reasonable optimum stripping out trajectory, simultaneously ensures the most efficient depression of the side products. The problem of optimized control was solved on the analogue computer simulation of the process model, outlined in Part 1. By introducing an analogue memory pair, applicability of the step to step solution, approximating the continuous control situation was also studied. Applying the quasi-optimised control thus obtained for the experimental reactor, satisfactory results were obtained within the usual technical accuracy limits.

The process model of the non-steady-state, stripping out furfural reactor was presented in the previous paper [1] and its applicability was proved via laboratory tests. The aim of this paper is now to formulate the conceivable variants of the control tasks relating to that system.

Three kinetic constants (k_1 , k_2 and k_3), one equilibrium coefficient (K), a compounded mass transfer coefficient (k_D), the vapour module (M) from the parameter set of the mathematical model. The experimental technique was designed to allow for limited changes of the last parameter. That means, variable M , rather, variable u , proportional to M enters the control problems as the control variable. It has to be noted that the kinetic conditions of the system studied result in a trivial solution as far as the optimum control of temperature variable concerned. This is because studying functions $k_1(T)$ and $k_2(T)$, the activation energies are found to be approximately equal [2] and by far greater than that of the function $k_3(T)$. Therefore, in order to achieve the highest furfural yield, the system should be maintained at the highest possible temperature throughout each stage of the process.

1. THEORY OF OPTIMIZED CONTROL

The model system of the non-steady-state furfural reactor is a common differential equation set, i.e. is of the following form:

$$\frac{dy}{dt} = \varphi(y, u) \quad (1)$$

The objective function functional of a control problem is written in general form as:

$$I = \int_0^{\tau_e} \varphi_0(\underline{y}, \underline{u}) dt \quad (2)$$

It is the minimum value of that functional which has to be ensured via the appropriate selection of the optimized control, $\underline{u}_{opt}(t)$. According to the general procedure of the PONTRJAGIN's maximum principle [3], the relationship:

$$H(\lambda_0, \underline{\lambda}, \underline{y}, \underline{u}) = \lambda_0 \varphi_0(\underline{y}, \underline{u}) + \underline{\lambda} \varphi(\underline{y}, \underline{u}) \quad (3)$$

has to be created, where:

$$\lambda_0 \equiv -1 \quad (4)$$

while the $\lambda(t)$ function has to satisfy the following vector equation:

$$\frac{d\lambda}{dt} = -\lambda_0 \frac{\partial \varphi_0(\underline{y}, \underline{u})}{\partial \underline{y}} - \lambda \frac{\partial \varphi(\underline{y}, \underline{u})}{\partial \underline{y}} \quad (5)$$

If the control problem is formulated as a fixed endpoint problem, then the objective function (2) can be rewritten as:

$$I = \sum_{j=1}^m c_j y_j(\tau_e) = \min! \quad (6)$$

To achieve optimized control the relationship:

$$H[\lambda(t), \underline{y}(t), \underline{u}_{opt}(t)] = \sum_{j=1}^m c_j \varphi_j[\underline{y}(t), \underline{u}_{opt}(t)] \geq 0 \quad (7)$$

and the minimum value of H according to \underline{u} , for each t also have to be expressed. Because \underline{u} is not limited and the derived function of H according to \underline{u} does exist, the relationship:

$$\frac{\partial H[\lambda(t), \underline{y}(t), \underline{u}_{opt}(t)]}{\partial \underline{u}_{opt}} \equiv 0 \quad (8)$$

Accordingly, the concrete equation system reads as follows:

$$\frac{dx}{dt} = -k_1 x \quad (9.1)$$

$$\frac{df}{dt} = k_1 x - k_2 x f - k_3 f - u f \quad (9.2)$$

where: $\frac{db}{dt} = k_2 x f + k_3 f \quad (9.3)$

$$u = \frac{M K k_D}{k_D + M} = k_D \left(K - \frac{f^\beta}{f} \right) \quad (9.4)$$

Introducing an aid variable z , defined as:

$$\frac{dz}{dt} = u \quad (9.5)$$

the objective function reads as follows:

$$I_z = (b + z) = \min! \quad (10)$$

If the aid variable is written in the form

$$\frac{dv}{dt} = M \quad (11)$$

the objective function reads as:

$$I_v = (b + M) = \min! \quad (12)$$

This latter equation is the mathematical formulation of the statement that using the optimized amount of steam in an operation lasting for a time t , the quantity of the byproducts is minimized, or expressing this in another way, the given allowed byproduct conversion is achieved with the minimum possible amount of steam. The technical economic advantage of this criterion is obvious.

However, it remains to be seen how criterion (10) is to be understood.

Discussing Equation (9.4) it can well be seen that if $M \ll k_D$, the Equation becomes:

$$u \cong KM \quad (13)$$

that is, in this case its meaning is the same as that of Equation (12). However, the fact is of greater importance that the value of k_D is not constant for industrial reactors, rather [4]

$$k_D \cong aM \quad (14)$$

and therefore:

$$u \cong KM \frac{a}{a + 1} \quad (15)$$

Thus the content of the two criteria are the same over the entire range of M considered. Therefore, the optimized control proposed automatically ensures an energetical optimum as well.

1.1 Determination of the optimized control trajectory

Let us construct function H according to Equation (7) employing the objective function (107):

$$H = \lambda_b (k_2 x f + k_3 f) + \lambda_z u = 0 \quad (16)$$

Applying Equation (5):

$$\frac{d\lambda_b}{dt} = - \frac{\partial H}{\partial b} = 0 \quad (17)$$

and

$$\frac{d\lambda_z}{dt} = - \frac{\partial H}{\partial z} = 0 \quad (18)$$

that is

$$\begin{aligned} \lambda_b &= \lambda_b(\tau_e) = c'_b \\ \lambda_z &= \lambda_z(\tau_e) = \lambda_o \equiv -1 \end{aligned}$$

respectively. Substituting into Equation (16) the following equation is obtained:

$$H = c_b (k_2 x f + k_3 f) - u = 0 \quad (19)$$

Thus the problem has to be formulated by giving the terminal b value, and duly searching for the z sets belonging to the minimums. The best solution sought can then be selected from these sets.

2. SOLUTION OF THE OPTIMIZATION PROBLEM ON ANALOGUE COMPUTERS

Equation (19) defines the control variable as proportional to the basic variable f . This explicit form permits the efficient computerized handling of the problem. Substituting Equation (19) into Equation (9.2) and using dimensionless concentrations relating to x_o , the differential equation set of the optimization problem is:

$$\frac{d\bar{x}}{dt} = -k_1 \bar{x}$$

$$\frac{d\bar{f}}{dt} = k_1 \bar{x} - k_2 x_0 \bar{x} \bar{f} - k_3 \bar{f} - c_b (k_2 x_0 \bar{x} + k_3) \bar{f}^2$$

$$\frac{d\bar{b}}{dt} = k_2 x_0 \bar{x} \bar{f} + k_3 \bar{f}$$

$$\frac{d\bar{z}}{dt} = \bar{u} = c_b (k_2 x_0 \bar{x} + k_3) \bar{f}$$

The first quadrant of Figure (I) shows the wiring schematics modelling the equation system outlined above.

2.1 Approximation of the optimized control with a step function

Let the parameters of the numeric problem have the following values:

$$k_1 = 0.95 \text{ (l/h)}$$

$$k_2 = 0.12 \text{ (l/gh)}$$

$$k_3 = 0.11 \text{ (l/h)}$$

$$x_0 = 11.00 \text{ (g/l)}$$

$$f_0 = 5.50 \text{ (g/l) in xylose equivalents}$$

$$\bar{b}_e = 0.27 \text{ (-) mass fraction}$$

Let us select the solution $\bar{z}_{1.5}=3.15$ from the solutions obtained on the analogue computer (i.e. assuming a residence time of $\tau_e=1.5$ hour, at least 3.15 z have to be consumed!)

Figure 2 presents the \bar{x} , \bar{f} and \bar{b} concentrations under optimized control and assuming a constant control parameter

$$\bar{u} = 3.15/1.5 = 2.1 \text{ h}^{-1}.$$

The concentration values at $\tau_e=1.5$ hour are tabulated in Table 1

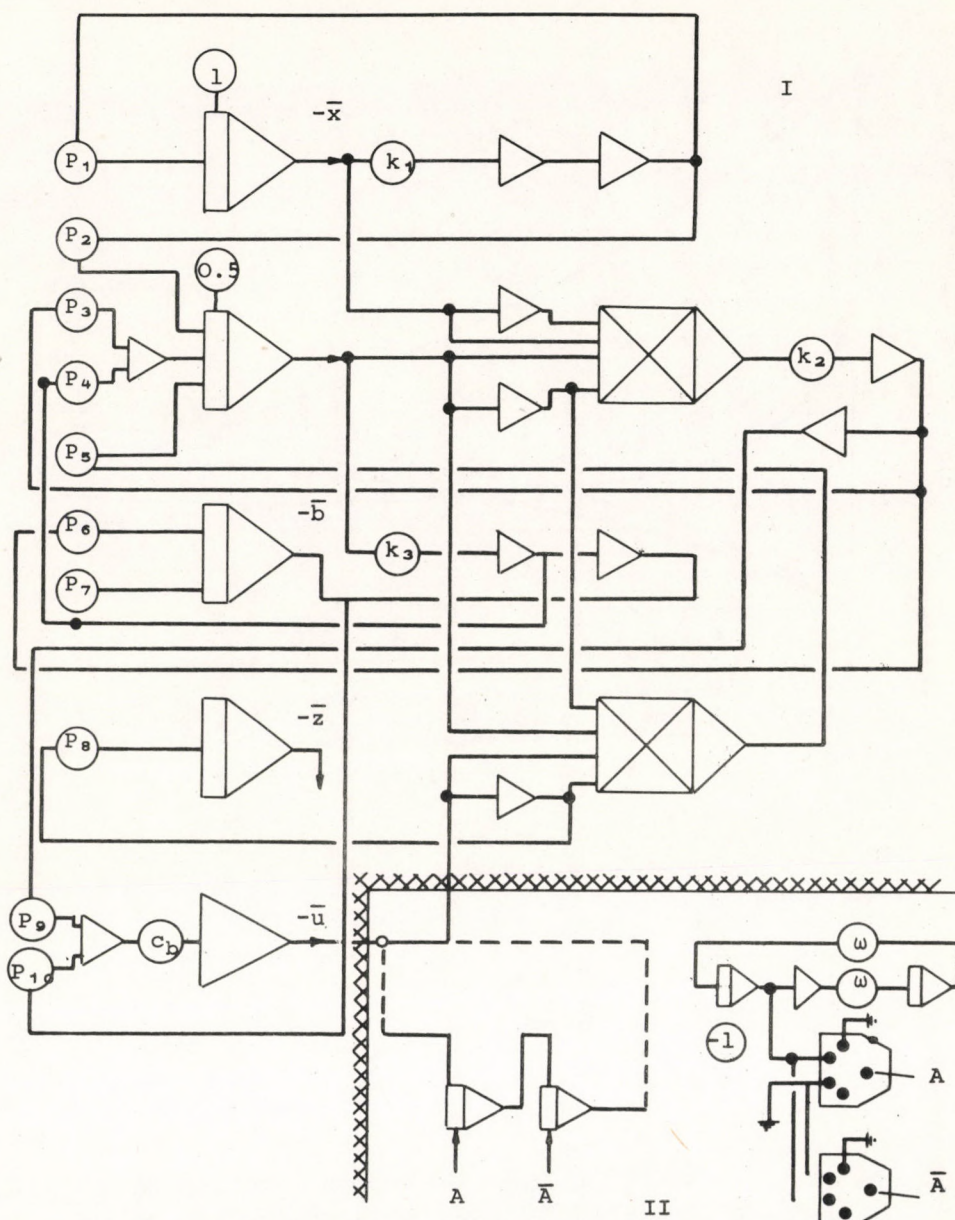


Figure 1. Wiring schematics of the optimized control problems (I) and the solution of the step-following process of control with one memory-pair (II)

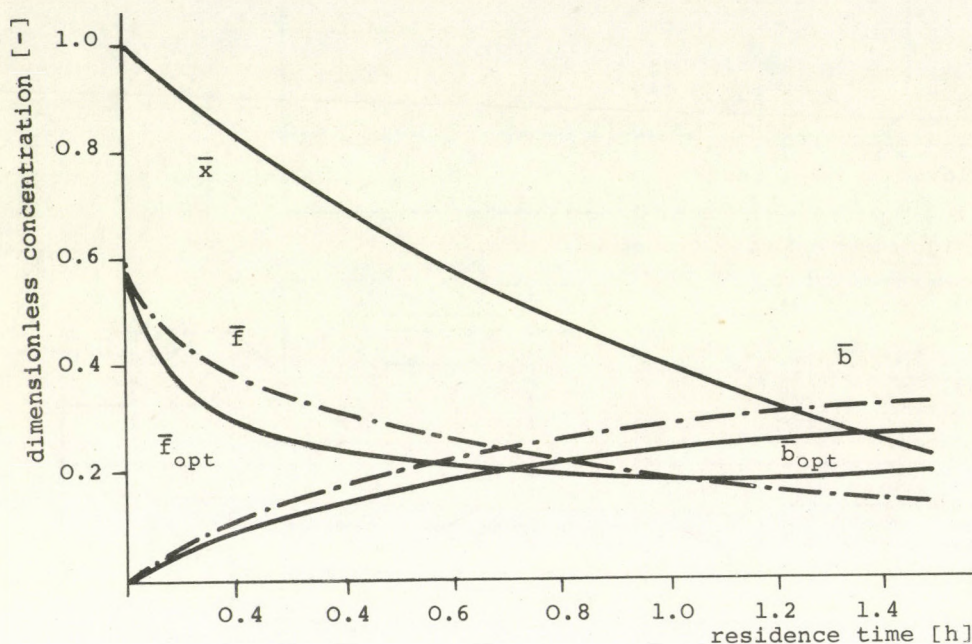


Fig.2. Transients of the state-variables in case of optimized control (full lines) and constant control (dotted line)

Table 1. Computed data by analogue computer.
at $\tau_e = 1.5$ hour

$\tau_e = 1.5$ hour	$u = 2.1 \text{ h}^{-1}$	$u = u_{\text{opt}}$
x (%)	24	24
f (%)	14	19
b (%)	33	27
p (%)	79	80

It can be seen from the data of Table 1 that the amount of byproducts is about 20 per cent less in the case of optimized stripping out than in that of the constant stripping out rate.

3. EXPERIMENTAL VERIFICATION OF THE OPTIMIZED CONDITION

As has been mentioned, the system described in Part 1, Fig-

ure 2 [1] allows for occasional changes in the condensate offtake and water input, i.e. to set constant u values over periods. Then it was aimed at following the optimized, inherently continuous control via stepped control under the condition that the inaccuracy resulting from the sampling should not exceed the 1 or 2 per cent level in the results obtained. Generally, further complications arise in calculating the length of the sampling periods of sampled signals. Taking advantage of an appropriately controlled analogue memory pair (cf. Figure 2, second quadrant) the sampled optimized control could be simulated with relative ease. Figure 3 presents

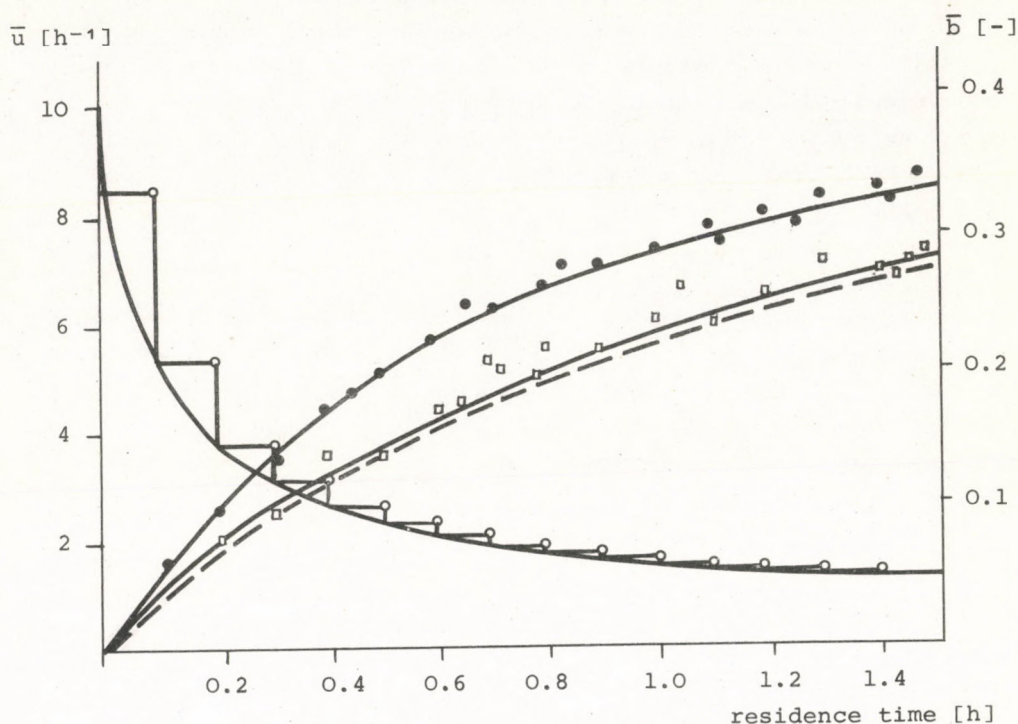


Fig.3. Plot of the optimized (—○—) and stepped (—○—) control variables comparison of the b values obtained under constant control (—○—) and the computed b values under optimized (—) and stepped (---) control with the experimental data corresponding to the stepped control.

the continuous and samples (—o—) \bar{u} values. The \bar{b} sets obtained under optimized control (full line) and stepped control (dashed line) are also shown in the diagram. Full squares represent the experimental values obtained in the latter case, while full dots correspond to the experimental \bar{b} values controlled at $u = 2.1 \text{ h}^{-1}$. Dividing the 1.5 hours long period into 15 segments, the deviation in final \bar{b} values are below 2 per cent. (Because the $\bar{z}_{1.5} = 3.26$, calculated from the approximating function is about 3 per cent greater than the original, it is obvious why the result of the quasi optimum control does appear more favourable.)

It can well be seen that though the experimental points fit closely to the computed quasi-optimum ones, their scatter is "one-sided". This is attributed to the fact that all experimental errors are accumulated in the same sense, i.e. in the phase corresponding to the deviation from the optimum, i.e. any deviation in the control programme connected in another step is accumulated as a penalty.

In summary, it can be concluded that the method shown can be used for the optimized and quasi-optimized control of the non-steady-state reactor. Time programming of the condensate offtake can be achieved in practice via a relatively simple means, thus in our opinion the economy of the process is obvious.

SYMBOLS USED

a	empirical coefficient (Equations 14 and 15) (-)
b	concentration of the byproducts (g/l)
B	volumetric flow rate of the vapour phase (l/h)
c_b	dimensionless optimizing coefficient of Equation 19 (-)
f	furfural concentration in the liquid phase (g/l)
H	Hamiltonian
j	index of the vector component
k_1, k_2, k_3	reaction rate constants
k_D	compounded mass transfer coefficient (l/h)

K	apparent equilibrium distribution coefficient (-)
M	stripping out module (by definition $M = \frac{B}{V}$) (ℓ/h)
m	number of the vector components
p	furfural concentration in the condensate (g/ℓ)
v	aid variable (defined in Equation 11)
V	volume of the reactor
z	aid variable (defined in Equation 9.5)
x	xylose concentration (g/ℓ)
<u>u</u>	vector of the control variable (ℓ/h)
<u>y</u>	vector of the state-variable
t	time

GREEK LETTERS

α	liquid phase index
β	condensed phase index
Φ	symbole of the vector-vector function
λ	aid variable of the Hamiltonian (Equation 5)
τ_e	end point of the time

REFERENCE

- [1] LA SZLO, A. and MARTON, Gy.: Hung. J. Ind. Chem., 4, 165 (1976)
- [2] SCHOENEMANN, K.: Chem. Eng. Sci., 14, 39, (1961)
- [3] BOJARINOV, A.J. and KAFAROV, V.V.: Optimalizálás a vegyiparban. (Optimalization in the Chemical Industry.) Műszaki Könyvkiadó, Budapest, 1973.
- [4] MARTON, Gy.: Hung. J. Ind. Chem., 3, 677, (1975)

РЕЗЮМЕ

В интересах экономической эксплуатации фурфуролового реактора, работающего в нестационарном режиме, для получения целевого продукта с заданным качеством, необходимо свести до минимума количество расходуемого пара. Поскольку в химико-кинетической схеме фурфурол является промежуточным продуктом, то целесообразная (оптимальная) траектория выпарки означает и как можно более действенное подавление побочных продуктов. С помощью перенесения приведенной в предыдущей статье модели процесса на аналоговую вычислительную машину, авторами была разрешена проблема оптимального управления. Подключение аналоговой пары памяти дало возможность исследовать применимость решения, наилучшим образом, шаг за шагом приближающего непрерывное уравнение. Применяя полученное таким образом квазиоптимальное управление на испытательном реакторе были получены соответствующие результаты в рамках обычной технической точности.

AGITATORS BUILT UP OF NEW ELEMENTS AND THE
APPLICATION THEREOF, PART 2

L. MÉSZÁROS*, M. SZABÓ*, J. GREGA** and L. TASI**

(*Institute of Applied Chemistry, Attila József University
of Sciences, Szeged

**Northern Hungarian Chemical Works, Sajóbábony)

Received: November 10, 1975

The previous paper presented a short account of the new-type agitators built up of point-like and line-like elements.

These new elements and their properties were presented with reference to the results of those experiments carried out with their most evident form of realization, with the rotation-type linear agitator.

This paper presents the results of further experiments carried out with rotation-type linear agitators. The effect of the geometrical properties of the line elements upon the efficiency of the agitator is shown.

The results of the dispersion experiments carried out with the rotation-type line agitators are presented.

It is concluded that the rotation-type line agitator can advantageously be applied to carry out emulsification, suspension operations; and in general, to carry out intensified heterogeneous-phase operation in such systems where one of the phases involved is a liquid phase.

Preliminaries

The previous paper presented the description of new-type agitators composed of new elements of point-like (therefore zero-dimensional) and line-like (one-dimensional) elements. This agitator series is the result of the joint research project of the Institute of Applied Chemistry, Attila József University of Sciences, Szeged and the Northern Hungarian Chemical Works [1, 2].

The characteristics of these elements were described and the decisive role of their geometry was pointed out.

The results of the emulgeation experiments carried out with the rotation-type linear agitator, one of their most evident forms of realization, were presented.

This paper presents the results obtained in further tests of rotation-type linear agitator.

As mentioned, the rotation-type linear agitator is a rotary stirrer built up of resilient linear elements whose number is (s) and are coupled at one point to the shaft, their (q) thickness is in the 10 to 5000 μ range, their (ℓ) length is at least fifty times that of their thickness; and the elements can freely be deflected along their (ℓ) length while the frequency of this vibration experienced during this deflection depends on their (ρ) elasticity and the η viscosity of the solvent and the n number of revolutions per minute of the rotating shaft.

The most important characteristic of linear elements is that the ratio of their length to their thickness is considerable, i.e. $l > 50 q$. Their total volume is insignificant compared to that of the liquid to be agitated, therefore, they are justly considered to be one-dimensional elements. It was found that the decreased geometrical dimensions of these elements with reference to those of the conventional agitators is an advantage in carrying out dispersion operations, i.e. the efficiency of the rotation-type linear agitators is influenced by the (q) thickness, (ℓ) length of the elements, the $\Sigma \ell$ total length of the elements which the agitators is composed of and the n number of those elements and their $\Sigma \ell/V$ longitudinal density.

The effect of a change in the thickness of the linear elements upon the dispersing ability

It was shown that increased efficiency is achieved by the appropriate selection the geometrical dimensions of the elements and this factor is of critical, decisive importance. This statement is well documented by those experiments in which except (q), all the other parameters (l , s , η , ρ) were kept constant.

Liquid paraffin, heated to 100°C was dispersed in water throughout these experiments, and sudden cooling was used to freeze the droplets formed. The droplets were separated and their size-distribution curve was determined from a sieve analysis test.

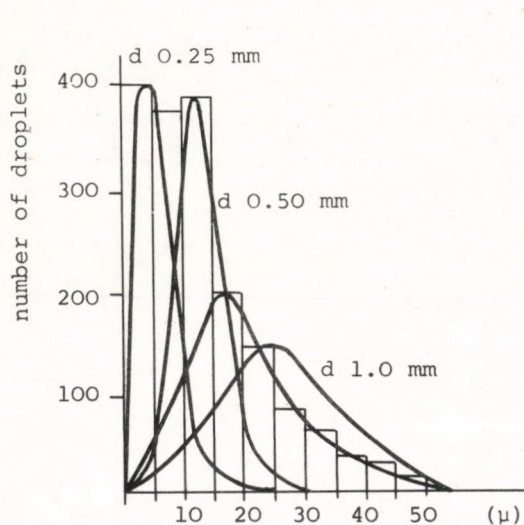


Figure 1.

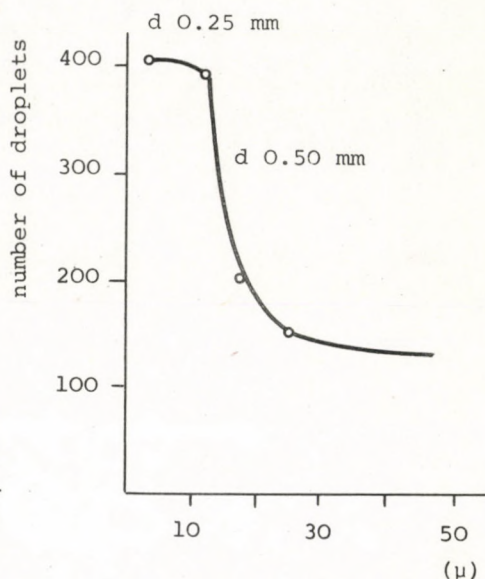


Figure 2.

The results obtained are shown in Figures 1 and 2. It can be seen that if (q) is decreased from $1000\ \mu$ to $250\ \mu$, the size of the paraffin particles formed is also decreased from $25\ \mu$ to $5\ \mu$. It

can also be noted that the shape of the particle size distribution curve is also altered. Decreasing (q) results in steeper distribution curves with higher maximum values, while the heterodispersity of the system is decreased, the particle size range of the dispersion formed becomes narrower and homodispersity begins to prevail in the system.

There is no doubt that having changed the values of s , l , and n , the q -dependency of the degree of dispersity is also changed and that the optimum point is shifted. Nevertheless, it can be concluded that in general, (d), the average particle size decreases linearly with decreasing (q).

The effect of the rotation speed of the agitator on the dispersion operation

An experiment, similar to that described previously was carried out keeping all the parameters constant (q , l , s , ρ) except the rotation speed (rpm) of the agitator.

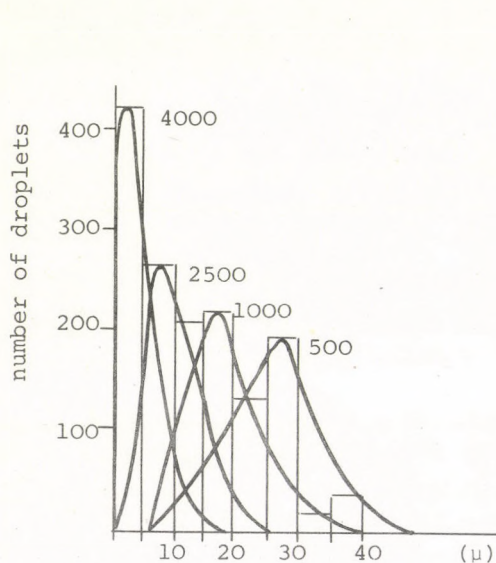


Figure 3.



Figure 4.

Figure 3 and 4 present the particle size distribution obtained at four different (rpm) values.

It can be concluded that at the beginning (d), the average particle size, linearly decreases with increasing rotation speed, then having passed a certain (rpm) value it levels off. This optimum value of the degree of dispersity depends on the (q) thickness of the linear element and at different (rpm) figures it yields different (d) average particle size values.

Suspension-polymerization bead-polymer production experiments carried out by the rotation-type linear agitator

The reason for selecting the suspension polymerization of styrene as the model reaction of the experiment was that the particle size distribution of the beads - assuming otherwise constant experimental parameters - considerably depends on the stirring, i.e. the efficiency of the dispersing operation.

At the same time, the particle size distribution of the beads formed and cured can easily be determined.

The chemical parameters of the suspension-polymerization operation was selected according to literature recommendations, e.g. styrene feed-in, temperature, catalyst feed-in, time of the polymerization reaction, and stabilizer feed-in, etc. Meticulous care was exercised in keeping these parameters constant throughout the entire experiment-series. Agitators of two types, the conventional turbine-type agitator and the rotation-type linear agitator, were employed and, in both cases, two rotation speed settings, 240 rpm and 420 rpm were tested.

The particle size distribution curves determined from the sieve analysis tests are presented in Figures 5, 6, 7 and 8.

Comparing the particle size distribution curves obtained in the experiments carried out with the turbine-type agitator (Figures 5 and 6) to those of the rotation-type linear agitator (Figures 7 and 8), it is immediately apparent that the average particle size of the beads produced with the rotation-type linear agitator is

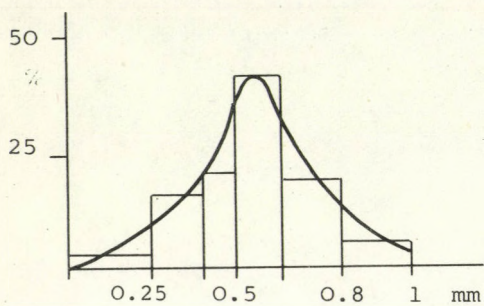


Figure 5.

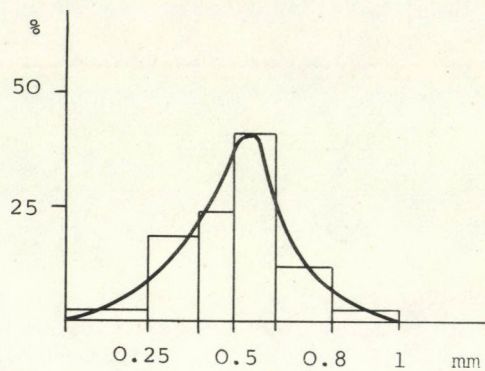


Figure 6.

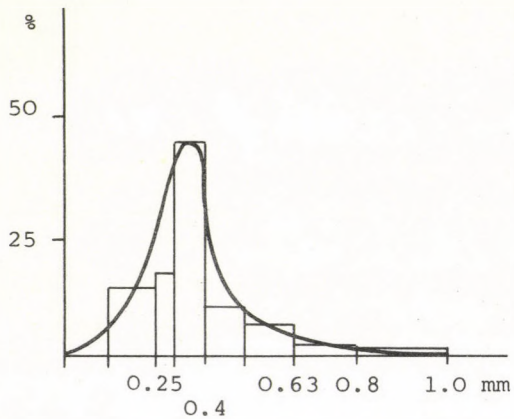


Figure 7.

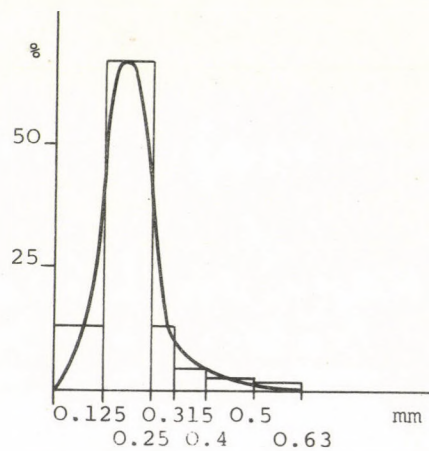


Figure 8.

shifted towards the lower micron figures and, at the same time, the span of the distribution curve is also narrower. The degree of heterogeneity of the beads produced by the rotation-type linear agitator is so much reduced that it is apparent even on visual inspection that the size of the product is much more homogeneous. This observation is also duly supported by the sieve analysis data as the quantity of the most abundant particle size fraction amounted only to 26 % by weight of the total quantity of the beads produced with the conventional, turbine-type agitator, while the same parameter with the rotation-type linear agitator was as high as 65 % by weight.

The results outlined above suggest that the rotation-type linear agitator provides an effective means to control the average particle size produced in similar suspension-type polymerization operations.

If a sufficiently large number of experiments are carried out, changing the geometrical dimensions of the linear elements and monitoring the particle size distribution of the bead polymers produced, a correlation plot can be obtained enabling the optimum dimensions of the linear elements to be selected, leading to the desired bead size.

The logic employed in selecting the parameter ranges to be tested in future

It is obvious from the experiments outlined earliner that in the very same material system, changing the geometrical dimensions of the linear elements brings about a shift in the optimum points of the degree of dispersity and these points can only be experimentally determined.

Considering that all five of the q , l , s , ρ and η parameters can be changed, the number of the experiments to be carried out is fairly high. Therefore, it seems plausible to try to determine what limits could be drawn to narrow down the range of the parameters to be tested without jeopardizing the validity and universality of the conclusions.

Obviously, there is no need to test several types of materials of construction, covering a wide span of q , because neither the very stiff nor the very soft brands of the materials are suitable. Therefore a test series carried out with three or four materials of construction of different modules of elasticity seem to provide a clear picture of the effect of this parameter.

It is also straightforward that the dispersing effect of the line agitator is shown at its optimum at high rotation speed values. Therefore, the 4,000 - 15,000 rpm range seems to warrant a test series.

There is no discussion about the importance of the viscosity of the medium to be dispersed as it alters the efficiency of the dispersion operation. But to test that effect, three systems of considerably different viscosity seem sufficient.

The number of the experiments primarily depends on the extent that the geometrical parameters, q , ℓ and s , are varied. This number, no doubt, is high. But even so, limiting assumptions can be made for the ranges of the possible geometrical parameters, thereby the number of experiments can well be kept within reasonable limits.

It is evident that the q and ℓ parameters of a linear element made of a material, characterized by the appropriate value, cannot be selected at will, rather, each q thickness has a corresponding minimal ($\ell = 50 q$) and maximal length limit beyond that limit the elements become deformed and form a "tangle".

Furthermore, it is conceivable that the length-maximum of the linear elements practically determines the upper s number of elements that can be applied so that they can still deflect and freely vibrate as demanded by the medium to be agitated. Consequently, there more linear elements cannot be employed than this upper number, otherwise they mutually interfere with each other's movement.

The third most important parameter of the elements, (q) , is limited at the lower sizes by the characteristics of the material of construction. The most significant and decisive of them are the fatigue stress limit and elasticity. The upper value of (q) should not possibly exceed the 2 mm figure, making the testing of this

parameter meaningful only in the range below that limit.

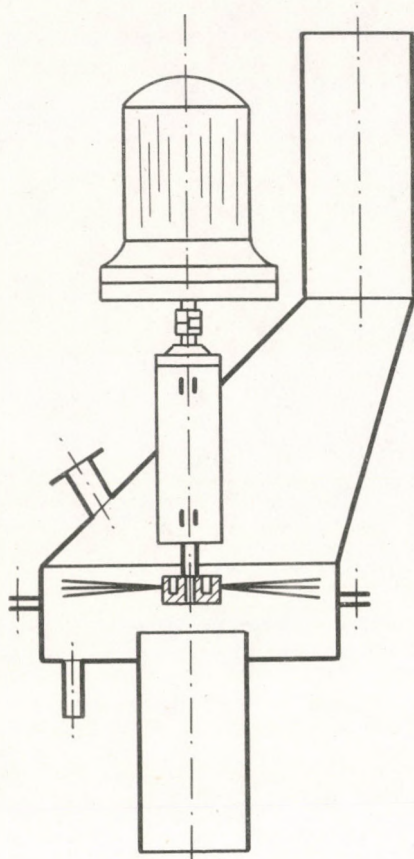


Figure 9.

The aim of the papers was to give an account of the new-type agitators we have developed, basically differing, both in the construction and method of operation, from the conventional agitators widely employed in the chemical industry.

As it can be seen from the last section projecting the fields of the future experiments, considerable research is still needed before all the parameters essential for construction design and all the phenomena essential for the understanding of their effect and method of working are understood and explained.

Having covered a significant part of that field, we intend to report once again on the results obtained.

It should be mentioned that several chemical reactions were of basic importance: saponification, sulphonation, and nitration, etc.,

were carried out in the existing five, large laboratory-scale model systems now in operation (stirrer, film-reactor, spray-drier, melt-reactor, and dust-precipitator; their schematics are shown in Figure 9). Basically physical operations suspending, emulgeation, gas absorption, and drying, etc. also proved that the time necessary to complete these operations is reduced to one fourth - one tenth of the original time, if, the operation is carried out with the new-type linear agitator.

REFERENCES

1. MÉSZÁROS, L., GREGA, J., LAKÓ, L., MARKÓ, L., SALAMON, Z., SZATMÁRY, I., TASI, L.:

Hung. Patent appl. No. EA-116 (166.693),
British Patent appl. No. 45 553,
Austrian Patent appl. A - 4188,
Bulgarian Patent appl. No. 26 913,
Czechoslovak Patent appl. No. PV-3691,
Danish Patent appl. No. 2817,
French Patent appl. No. 74 , 22 469,
Japanese Patent appl. No. 49-124 556,
Yugoslav Patent appl. No. P-1680,
Polish Patent appl. No. P-173 895,
German (FRG) Patent appl. No. P-24 29 255,5,
Norwegian Patent appl. No. 743 713,
Romanian Patent appl. No. 79 082,
Swedish Patent appl. No. 74 06754-7,
Soviet Patent appl. No. 2 038 429, and
GDR, Canadian, Italian, Swiss and U.S. patent applications
are pending.

2. MÉSZÁROS, L., GREGA, J., LAKÓ, L., SALAMON, Z., SZATMÁRY, I.,
TASI, L.:

Stirrers Built Up of New Elements. (Lecture presented at the
1974 Chemists' Congress, Miskolc. Organized by the Hung.Chem.
Soc.)

РЕЗЮМЕ

В предыдущей статье цикла речь шла об агитаторах, построенных из разработанных авторами точечных и линейнообразных элементов нового типа. Эти новые элементы и их качества были показаны с помощью результатов опытов, проведенных на ротационном линейном агитаторе, являющимся наиболее простой формой их исполнения.

В данной статье будет показано влияние геометрических свойств линейных элементов на эффективность агитатора. Здесь приводятся результаты опытов по диспергированию, проведенных на ротационных линейных агитаторах.

На основе этих результатов можно установить, что они могут быть с успехом применены при эмульсации, суспендировании и вообще при интенсивном проведении таких гетерогенных процессов, где одна из фаз является жидкостью.

INFLUENCE OF SUBSTRATES ON THE CATALYTIC
ACTIVITY OF FERRIC OXIDE

S.S. JEWUR, J.C. KURIACOSE

(Department of Chemistry, Indian Institute of
Technology, Madras, India)

Received: May 19, 1976

Ferric oxide catalyses ketonisation of acetic acid and dehydrogenation, dehydration as well as hydrogenolysis of alcohols. The ketonisation of acetic acid has been studied in the presence of isopropyl alcohol, benzyl alcohol and tertiary butyl alcohol at 375 and 440°C in a flow reactor. On the basis of the mutual influence of the acid and alcohols on each others' reaction and the temperature coefficient of the ketonisation reaction, it is suggested that the mechanism of the ketonisation reaction is temperature dependent.

INTRODUCTION

Ferric oxide is one of the multifunctional catalysts that promotes dehydrogenation, dehydration and hydrogenolysis of alcohols which is also found to catalyse the ketonisation of fatty acids. While there is much information available on the studies of various decomposition reactions of alcohols on semiconductor oxides little is known about the ketonisation reactions of acids. This investigation has been undertaken with a view to understand the primary nature of the catalytic activity exhibited by ferric oxide in the

ketonisation of acids. The present paper deals with the study of the nature of the catalytic activity of ferric oxide and the modification of the activity brought about by co-substances.

EXPERIMENTAL

The reactions were studied at atmospheric pressure using a flow type reactor, mercury being used to displace the reactant into the reactor [1]. α -Fe₂O₃ was prepared starting from FeCl₃.6H₂O (SM LR, purity 99.3 %) [2] and characterised by X-ray analysis. The oxide was heated at 500°C for 5 hours and crushed into a uniform granular form and used. Acetic acid (BDH, LR) used in the reaction was purified by distillation after refluxing it with potassium permanganate and acetic anhydride according to the procedure suggested by Orton and Bradfield [3]. Isopropyl alcohol (BDH, AR) was used without further purification. Benzyl alcohol (BDH, LR) was purified by distillation after refluxing it over pellets of pure sodium hydroxide.

Preliminary experiments were performed to fix the proper grain size and the volume of the catalyst. From the plot of percentage conversion of acetic acid as a function of the size of the crystallite, an optimum grain dimension of 1.4 mm (mesh size 8) was fixed for further experiments. The volume of 1.25 ml of the catalyst was chosen at which there was a linear increase in conversion with volume of the catalyst. The conversion of acetic acid was followed by titrating the unreacted acid against standard alkali. The quantity of acid reacted was also computed on the basis of the carbon dioxide evolved. Liquid products were condensed in a cold trap and analysed by vapour phase chromatography using a carbowax column. Hydrogen gas was used as a carrier maintaining the column temperature at 10-15°C above the highest boiling in the mixture to be analysed.

RESULTS AND DISCUSSION

Studies using mixtures of acetic acid and alcohols were car-

ried out with a view to understand the nature of primary activities of ferric oxide which may be responsible for the ketonisation reaction. Ferric oxide promotes both dehydration and dehydrogenation would compete for only the type of activity it needs for its reaction, leaving the other free for acetic acid adsorption. If this "other" activity is the one that promotes ketonisation, acetic acid would undergo uninhibited ketonisation in the presence of such an alcohol. It was considered that thus one can make available to the acid, only one type of activity.

The predominant reaction of isopropyl alcohol was dehydrogenation giving acetone with dehydration to propylene taking place to a very small extent. Benzyl alcohol underwent both dehydrogenation and hydrogenolysis reactions giving benzaldehyde and toluene respectively. Tertiary butyl alcohol gave only isobutene and water by dehydration. Small amounts of ester were noticed in the case of mixtures of isopropyl alcohol and benzyl alcohol with acetic acid.

Mutual influence of acetic acid and alcohols at 375°C

Fig. 1 represents the influence of isopropyl alcohol, benzyl alcohol and tertiary butyl alcohol on the ketonisation of acetic acid at 375°C. The partial pressure studies on the reactions of pure substances in presence of nitrogen as the diluent were undertaken for purpose of comparison. All these alcohols were found to suppress the ketonisation reaction and the amount of inhibition follows the order; tertiary butyl alcohol > benzyl alcohol > isopropyl alcohol, at all partial pressures. The ketonisation of acetic acid falls sharply as the partial pressure of the acid is decreased from one atmosphere in presence of alcohols as compared to the rate of ketonisation in nitrogen. Hence the decrease in ketonisation is not due to want of acetic acid in the gas phase but because the acetic acid cannot get adsorbed on the catalyst utilising the proper active sites in a manner conducive to ketonisation.

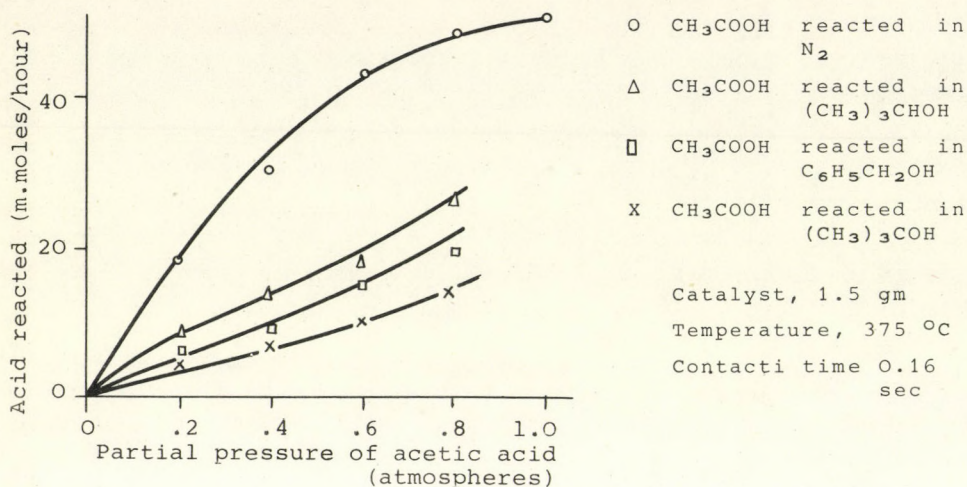


Fig. 1. Effect of various alcohols on the ketonisation of acetic acid

- O H_2 in presence of N_2
 ■ H_2 in presence of CH_3COOH
 Δ $\text{CH}_3\text{CH} = \text{CH}_3$ in presence of N_2
 \blacktriangle $\text{CH}_3\text{CH} = \text{CH}_2$ in presence of CH_3COOH

Catalyst, 1.5 gm
 Temperature, 375°C
 Contact time 0.16 sec

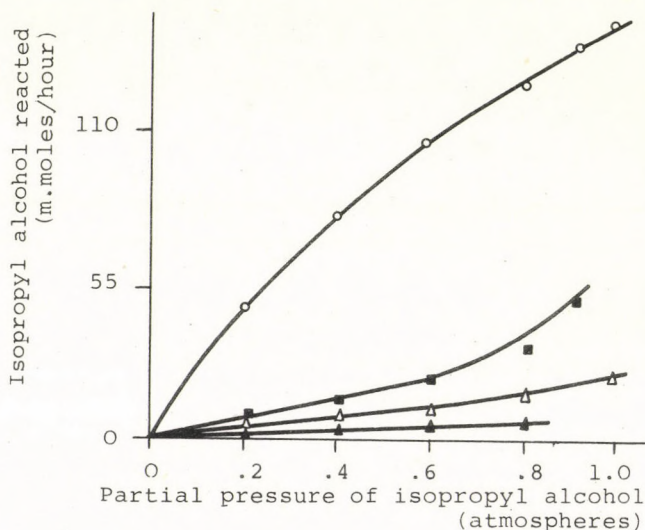


Fig. 2. Effect of acetic acid on the dehydrogenation and dehydration of isopropyl alcohol

In the experiments at 375°C carried out with the mixtures of acetic acid and isopropyl alcohol, the dehydrogenation reaction of isopropyl alcohol was found to be severely hindered as shown in Fig.2. Similarly the dehydrogenation as well as the hydrogenolysis reactions of benzyl alcohol were affected by acetic acid as represented in Fig.3. The decrease in the hydrogenolysis reaction may be due to the unavailability of adsorbed hydrogen as a result of the suppressed dehydrogenation of benzyl alcohol. The experimental runs carried out with the type of activity needed for ketonisation is competed for by the alcohols that undergo dehydrogenation. The observations that the dehydration of tertiary butyl alcohol and ketonisation of acetic acid are mutually inhibited in the presence of each other (Fig.4 and 1), bring about the importance of the dehydration activity for the ketonisation reaction. The results of the study of the dehydration reaction of isopropyl alcohol in the presence of acetic acid also indicates inhibition lending further support to the suggestion that the dehydration activity of the catalyst is also necessary for the ketonisation of acetic acid.

O $\text{C}_6\text{H}_5\text{CHO}$ in presence of N_2

● $\text{C}_6\text{H}_5\text{CHO}$ in presence of CH_3COOH

Δ $\text{C}_6\text{H}_5\text{CH}_3$ in presence of N_2

\blacktriangle $\text{C}_6\text{H}_5\text{CH}_3$ in presence of CH_3COOH

Catalyst, 1.5 gm

Temperature, 375°C

Contact time 0.16 sec

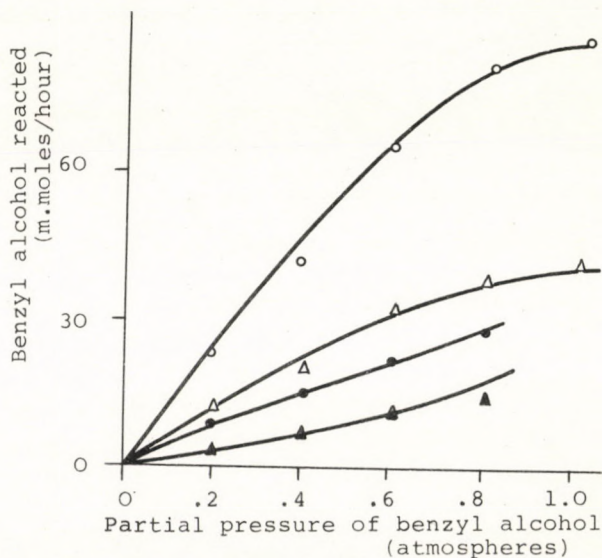


Fig. 3. Effect of acetic acid on the dehydrogenation and hydrogenolysis of benzyl alcohol

Mutual influence of acetic acid and alcohols at 440°C

Experiments with the mixtures of acid and alcohols were conducted at 440°C. Figs. 4 to 7, represent the mutual influence of alcohols and acetic acid on each other's reaction.

The presence of alcohols that undergo dehydrogenation (isopropyl alcohol and benzyl alcohol) was found to enhance the rate of ketonisation of acetic acid as shown in Fig. 5. But the dehydrogenation reactions of these alcohols was severely inhibited by acetic acid as shown in Figs. 6 and 7. Tertiary butyl alcohol does not have any effect on the rate of ketonisation of acetic acid, Fig. 5. But the dehydration of tertiary butyl alcohol was suppressed by acetic acid as shown in Fig. 4.

As far as the influence of alcohols on the rate of ketonisation at 440°C is concerned one can easily conclude that the catalytic behaviour of ferric oxide toward ketonisation at elevated temperatures is altogether different from that at temperatures less than 400°C. The fact that both dehydration and dehydrogenation reactions of alcohols are severely hindered by acetic acid at 440 °C indicates the preferential adsorption of acetic acid on the catalyst. The observed increase in the rate of ketonisation in the presence of isopropyl alcohol and benzyl alcohol might have been brought about by the adsorbed hydrogen which may be responsible for the modification of the catalytic activity of ferric oxide facilitating the ketonisation reaction. The alcohols which produce hydrogen over the catalyst have two opposite effects: one a competition for the surface and the other a modification of the catalytic activity. In the present case the latter effect exceeds the former so as to give an overall increase in the rate of ketonisation. The presence of tertiary butyl alcohol which can undergo only dehydration does not affect the ketonisation reaction at 440°C, while its dehydration rate has fallen considerably. This observation points to the fact that the catalyst exhibits different types of activity towards the ketonisation reaction in two temperature ranges. Moreover this observation is supported by the difference in the activation energy in the two temperature ranges [3] below and above 400°C. Since the reaction is not altered, the discontinuity observed in the Arrhenius

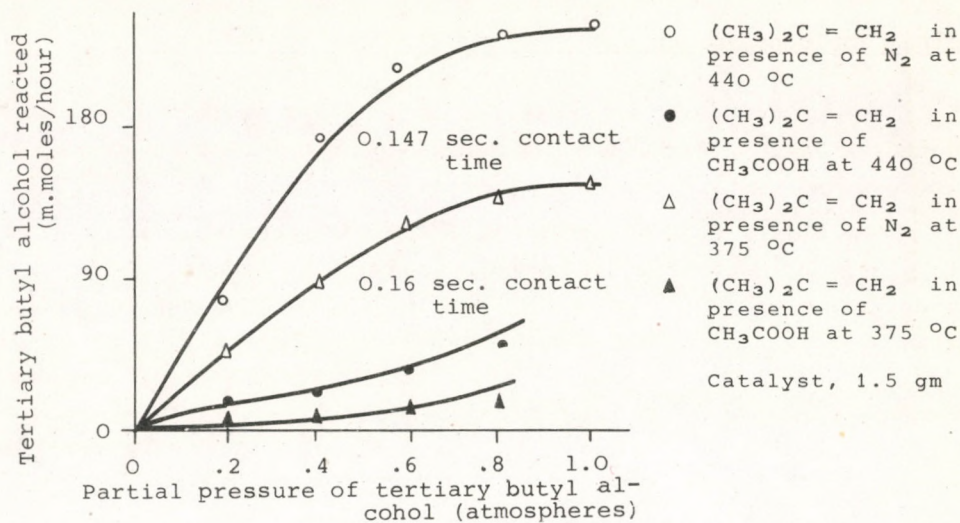


Fig. 4. Effect of acetic acid on dehydration of tertiary butyl alcohol

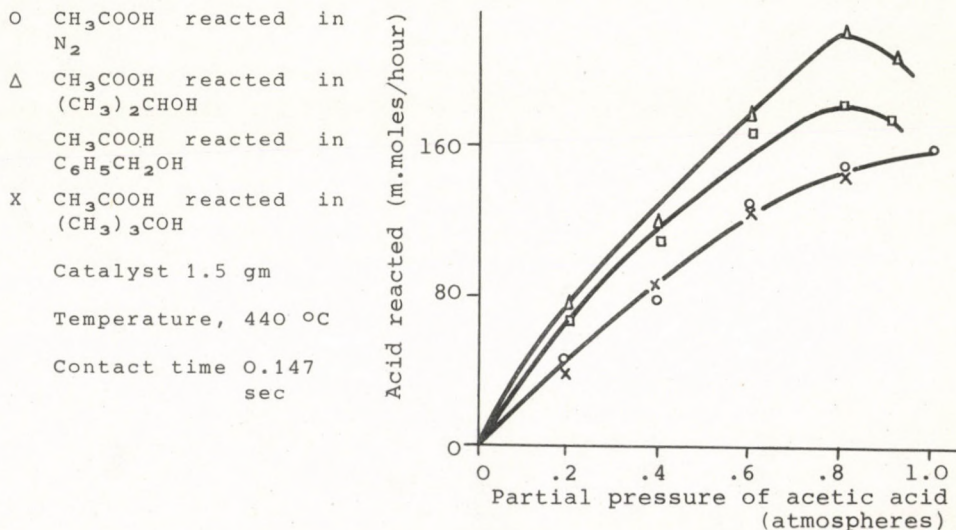


Fig. 5. Effect of various alcohols of the ketonisation of acetic acid

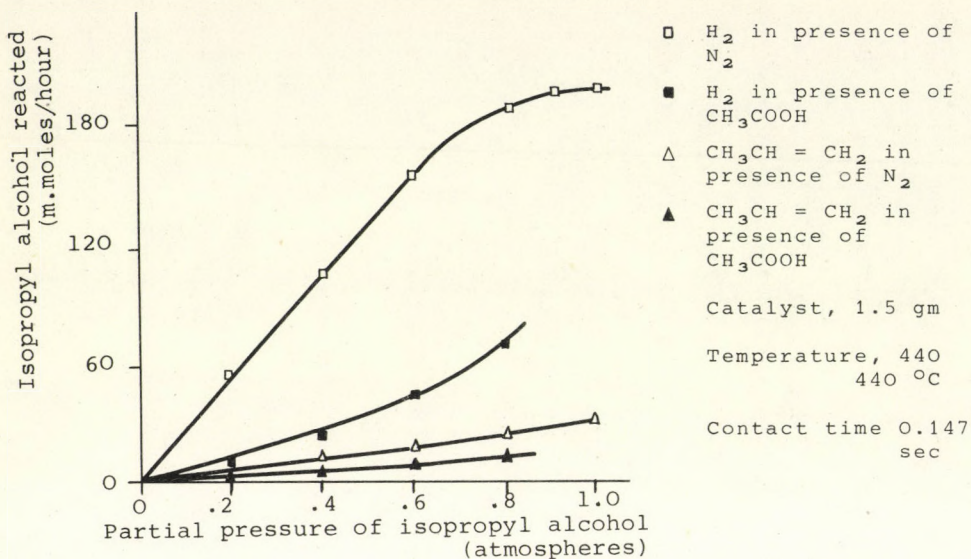


Fig. 6. Effect of acetic acid on dehydrogenation and dehydration of isopropyl alcohol

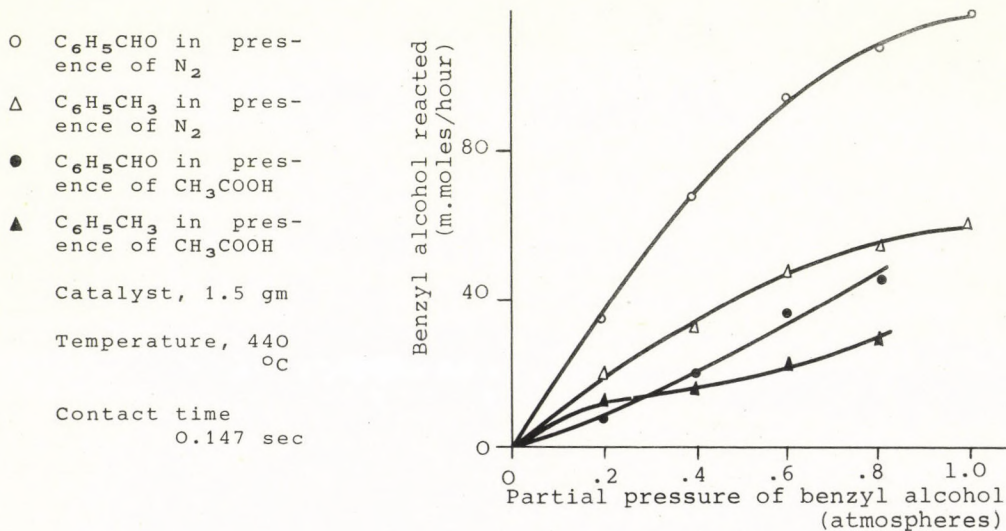


Fig. 7. Effect of acetic acid on dehydrogenation and hydrogenolysis of benzyl alcohol

plot is attributed to a change in the rate determining step in the mechanism [4-6].

The same mixtures of reactions can exert different influences on each others reactions at different temperatures. This appears to be a consequence of the difference in the temperature coefficients of the adsorption coefficients, the nature of the interaction between the various constituents in the vapour phase and the catalyst surface, and the changes in the intrinsic behaviour of the catalyst itself with temperature.

REFERENCES

1. PANDAO, S.N., KURIACOSE, J.C., SASTRI, M.V.C: J.Sci.Ind.Res. (India), 21D, 180 (1962),
2. SKARCHENKO, V.K., FROLOVA, V.S., GOLUBCHENKO, I.T., MOSSIENKO, V.P., GALICH, P.N.: Kinetics and Catalysis, 5, 818 (1964),
3. JEWUR, S.S., Ph.D. Thesis, I.I.T., Madras, India, 1976, p. 38,
4. MARS, P., MAESSEN, J.G.H.: Proceedings of the Third International Congress on Catalysis, North Holland, Amsterdam, 1965, Vol. I, p. 266,
5. JIRU, P., TOMKOVA, D., JARA, V., WANKOVA, J.: Proceedings of the Second International Congress on Catalysis, Technip, Paris, 1961, Vol. II, p.2113,
6. HERTL, W.H., FARRAUTO, R.J.: J. Catalysis, 29, 352 (1973).

РЕЗЮМЕ

Оксид железа обладает каталитической активностью при кетонизации уксусной кислоты, при ее дегидрогенизации, дегидратации, и гидрогенировании. Кетонизация уксусной кислоты исследовалась при 375°C и 400°C в присутствии изопропилового бензилового и терц.бутилового спиртов, в проточном реакторе. Поскольку кислота и спирты взаимно воздействуют на реакции друг друга, а температурный коэффициент реакции кетонизации обладает характерной величиной, то был сделан вывод о том, что механизм реакции кетонизации зависит от температуры.

A TWO-STAGE COMPUTATION METHOD FOR
TECHNOLOGICAL SYSTEMS

L. TIMÁR, Z. CSERMELY

(Hungarian Oil and Gas Research Institute, Veszprém)

Received: March 9, 1976

A computerized method is presented that was designed for the calculation of mass and heat balances of technological processes.

The method presented groups the linear and nonlinear relationships of the model according to their types. The two, alternately applied stages of the computation are: first, the simultaneous solution of the linear equations for the whole technological system; secondly, the correction of the coefficients of the linear equation systems by solving the nonlinear models. The procedure outlined must be repeated until the required accuracy is obtained.

The advantages of the method are that its convergence is reliable and no separate iteration is required for the computation of the recirculations.

INTRODUCTION

The computation of the mass and heat balances of complex technological system is, from the mathematical point of view, the solution of a multivariable equation system consisting of linear and nonlinear relationships. The difficulty in-

volved in the practical solution process exponentially increases with increasing technological system complexity and soon necessitates the use of computers. The realisation of this point resulted in several computer programmes or programme systems published over the past decade (e.g. Ref. 1 to 7).

Basically there are two strategies available to choose from when carrying out computerized calculations of multielement, complex technological schemes:

a) The essence of the generally used sequencing method is that the equation set characterizing the complete system is grouped according to operation units, and starting from a certain point of the scheme and following the direction of the information flow, the given equation systems are solved. The computation has to be organized in such a manner that the data required for the next unit becomes available in due course. The recirculation establishes an information feed-back, mathematically this results in nonlinear equation systems which might present some convergency problem.

The sequencing method described is used, among others, in the SIMUL system developed in Hungary [3].

b) The other, essentially different strategy is the simultaneous solution of all of the equations of the system. Due to computation technological difficulties resulting from the size of the problem, this method is restricted in practice to linear equation systems. The essence of the method is that the relationships of the input and output streams of the separation units and those of the "branchings" are defined by ratio equations in which the coefficients represent the ratio of a given input material in the output streams. These values have to be known prior to the initiation of the computation. The system of the heat and component balance equations is automatically generated on the basis of the schematics and thus the problem is reduced to the solution of a linear equation system.

Obviously, the method outlined can only be applied if the ratio coefficients and the operation parameters are preset or known from actual measurements [4, 7].

THE TWO-STAGE PROCESS

Based on experience in the field of the computation of complex systems, and especially on the solutions of recirculations [5] it seemed straightforward to try to exploit the advantages of both of the strategies, possibly without their drawbacks. Starting from this point, the basic principles of a two-stage simulation process were developed.

The equation system describing the technological scheme is decomposed to allow the simultaneous solution of the linear and the consecutive solution of the nonlinear equations. To do so, similarly to the sequencing method, the nonlinear equations are grouped according to the operation units, while the linear equations are generated according to the simultaneous method, based on information concerning the schematics and separation, as well as the branching ratios defined above (in the following, for the sake of simplicity the term separation ratios is used).

The main steps of the computation process are as follows (Fig.1):

The 1st step is the generation and simultaneous solution of the linear equation system on the basis of information concerning the schematics, the known component flow data and estimated separation ratios.

The 2nd step is the solution of the nonlinear equation sets in any convenient order for the unknown component flows, based on the component flows and composition data obtained in the 1st step, as well as the estimated temperature and given pressure data. As a result, new data are obtained for the separation ratio and temperature values.

The 1st and 2nd steps are repeated one after the other as many times as necessary to obtain unchanged separation ratios within prespecified limits. Thus, the method is based in a series of corrections, carried out on the coefficients of the linear equation system, obtained through the solutions of the nonlinear equations systems.

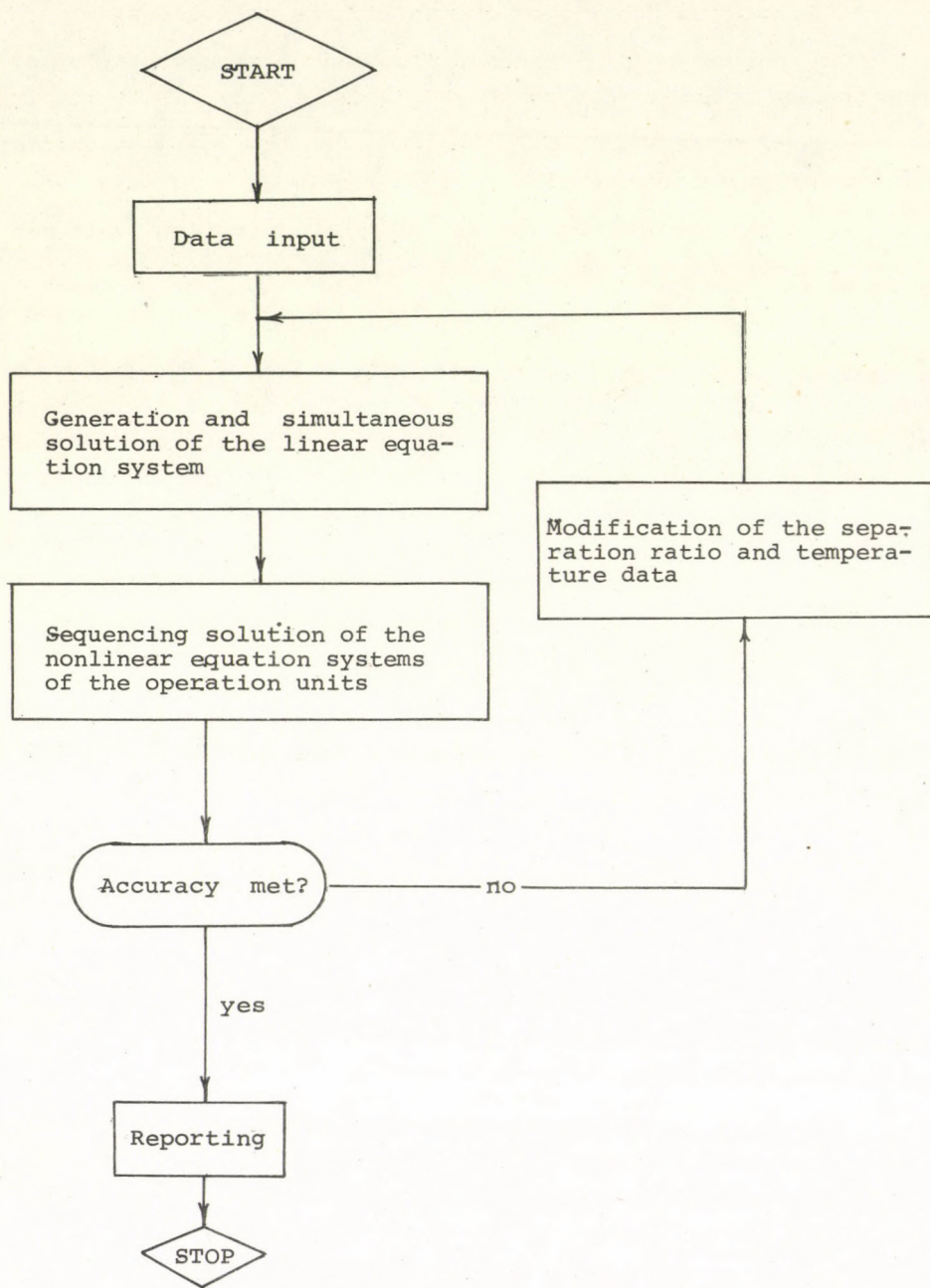


Fig. 1.

Logical schematics of the computation

The main advantages of the method are as follows:

a) The method can be used independently from the types of the operation units, the components and the flow scheme involved.

b) No extra iteration is needed for the computation of the recirculations and controls.

c) The computation order of the operation unit can be freely chosen.

d) The method is equally useful for design or modelling purposes.

Claim a). ensures the universal applicability of the program, claims b). to d). are the result of the combined nature of the solution method selected.

COMPUTATION FLOWCHART

Using an appropriate sign system, the computation flowchart provides an easily visualizable picture of the logics of the simulation, and contains the important information relevant to the computation. To obtain this flowchart a simplified technological flowchart is taken showing only those parts of the whole system at an adequately detailed level, which are to be modelled. This simplification results in the omission of certain units, conduits control or recording instruments. A possible and adequate symbol system of the operation units is shown in Figure 2. A rectangle is assigned to each unit containing the serial number of the computation and the typifying, encircled code number. The connection indices, identifying the component flows are written in parenthesis at the appropriate junction points of the flows concerned.

The input and output component flows are shown as straight line arrows, the energy flows as curvilinear arrows. A serial number is assigned to the component flows in a similar manner to the operation units.

Type	Dividing	Mixing	Throttling	Pump
Code number	1	2	3	4
Symbol				

Type	Separator	Plate absorber	Cooler	Rectification column with plates
Code number	5	6	7	8
Symbol				

Figure 2. Symbol System of the Operation Units

THE PROCESS MATRIX

The information pertaining to the computation flowchart has to be entered in numerical form. The information relating to the coupling and type of the operation units is given in the process matrix (Figure 3.). The element $P_{i,j}$ of the matrix is the serial number of that component flow which is the j^{th} (coupling index) flow of the i^{th} operation unit of code number $P_{i,0}$. If the sign of $P_{i,j}$ is positive, then the flow is an input flow; if it is negative, then it is an output flow. If that value is zero then there is not such a connection point in the system.

Ser. number	Code number	Connection points			
	0	1	2j.....	N
1	$P_{1,0}$	$P_{1,1}$	$P_{1,2}$ $P_{1,j}$	$P_{1,N}$
2	$P_{2,0}$	$P_{2,1}$	$P_{2,2}$ $P_{2,j}$	$P_{2,N}$
.				.	
.				.	
i	$P_{i,0}$	$P_{i,1}$	$P_{i,2}$ $P_{i,j}$	$P_{i,N}$
.				.	
.				.	
L	$P_{L,0}$	$P_{L,1}$	$P_{L,2}$	$P_{L,j}$	$P_{L,N}$

Fig. 3.

The structure of the process matrix

GENERATION AND SOLUTION OF THE LINEAR EQUATION SYSTEM

The linear equation system of the process consists of the statements relating to the component flows, the component balance equations written for the appropriate connection points, and the ratio equations representing the relationship between the input and output component flows at the branchings and separation units. The equation system written for a single component reads as

follows:

$$\underline{\underline{A}} \underline{\underline{m}} = \underline{\underline{b}} \quad (1)$$

where:

$$\underline{\underline{A}} = [a_{r,s}]$$

$$\underline{\underline{m}} = [m_m]$$

$$\underline{\underline{b}} = [b_r]$$

$$r = 1, 2, \dots, n$$

$$s = 1, 2, \dots, n$$

The determination of elements a_{rs} and b_r is carried out for each equation type according to Table 1.

The equation system (1) is solved for each component, using e.g. the Gauss elimination method. The component flows obtained are used to calculate the overall mass flows and concentrations.

Table 1. The types of the equations

Type	Equation	a	b
Stated component flow	$m_{in} = M_{in} \cdot z_{in}$ or $m_{out} = M_{out} \cdot z_{out}$	$a_{in} = 1$ or $a_{out} = 1$	$M_{in} \cdot z_{in}$ or $M_{out} \cdot z_{out}$
Component balance equation	$m_{in} - m_{out} = 0$	$a_{in} = 1$ or $a_{out} = -1$	0
Ratio equation	$\alpha \cdot m_{in} - m_{out} = 0$	$a_{in} = \alpha$ and $a_{out} = -1$	0

NONLINEAR EQUATION SYSTEMS

The models of the separation operation units can consist of the component balance equations, temperature balance equations

and equilibrium relationships. It is not practical to use some general method to solve them and it is always up to the developer of the model decide - considering the stability, space and time requirements - which of the available numeric methods (direct iteration, Newton-Raphson method or its variants, etc.) is to be applied to the best advantage.

The solution of the nonlinear equation systems yields the new temperature and corrected ratio-coefficient data. The ratio coefficients are defined for each type of the units. The relationships of the units shown in Figure 2 are summarized in Table 2.

Table 2. Definition of the separation ratios

Code number of the operation unit	$\alpha_{i,c} \quad c=1,2,\dots,k$
1	$\alpha_{i,c} = \frac{M P_{i,2} }{M P_{i,1} }$
5	$\alpha_{i,c} = \frac{m P_{i,3} ,c}{m P_{i,1} ,c}$
6	$\alpha_{i,c} = \frac{m P_{i,4} ,c}{m P_{i,1} ,c + m P_{i,2} ,c}$
8	$\alpha_{i,c} = \frac{m P_{i,4} ,c}{m P_{i,1} ,c}$
2,3,4,7	α is nonrelevant

CONVERGENCY METHOD

It follows from the simultaneous solution method of the component balance equations that no extra iteration is required for the computation of the mass flow recirculations. Instead, the coefficients of the appropriate ratio equations have to be corrected by some nonlinear equation solving method. In general, a better estimate can be obtained for the separation ratios than for the absolute quantities of the recirculated component flows (e.g. for the components not subject to partition $\alpha = 0$ or $\alpha = 1$, and for the key components $\alpha = \text{estimated, measured or 'reset yield values}$).

The nonlinear equation set relating to the unknown ratios is as follows (for the sake of clarity, the component index is omitted).

$$\begin{aligned}
 f_1(\alpha_1, \alpha_2 \dots \alpha_i, \dots \alpha_s) - \alpha_1 &= 0 \\
 f_2(\alpha_1, \alpha_2 \dots \alpha_i, \dots \alpha_s) - \alpha_2 &= 0 \\
 &\cdot \\
 &\cdot \\
 &\cdot \\
 f_i(\alpha_1, \alpha_2 \dots \alpha_i, \dots \alpha_s) - \alpha_i &= 0 \\
 &\cdot \\
 &\cdot \\
 &\cdot \\
 f_s(\alpha_1, \alpha_2 \dots \alpha_i, \dots \alpha_s) - \alpha_s &= 0
 \end{aligned} \tag{2}$$

Here f_1, f_2, \dots, f_s represent the appropriate forms of the mathematical models of the given separating operation units. To calculate the function values, the equation set of the operation unit has to be solved. Experience justifies the assumption that the separation ratio of the i^{th} unit, i.e.:

$$\left| \frac{\partial f_i}{\partial \alpha_i} \right| > \sum_{\substack{j=1 \\ j \neq i}}^s \left| \frac{\partial f_i}{\partial \alpha_j} \right|, \quad i = 1, 2, \dots, s \quad (3)$$

Substituting (3) into Equation (2), it reads much simpler:

$$\begin{aligned} f_1(\alpha_1) - \alpha_1 &= 0 \\ f_2(\alpha_2) - \alpha_2 &= 0 \\ &\cdot \\ &\cdot \\ &\cdot \\ f_i(\alpha_i) - \alpha_i &= 0 \\ &\cdot \\ &\cdot \\ &\cdot \\ f_s(\alpha_s) - \alpha_s &= 0 \quad i = 1, 2, \dots, s \end{aligned} \quad (4)$$

Equation set (4) suggests the following direct-iteration method:

$$\alpha_i^{(t+1)} = f_i(\alpha_i^{(t)}) \quad i = 1, 2, \dots, s \quad (5)$$

If the initial values are too bad then certain damping might be required in changing α .

Thus one arrives at the weighted direct iteration:

$$\alpha_i^{(t+1)} = (1 - \delta) \cdot \alpha_i^{(t)} + \delta \cdot f_i(\alpha_i^{(t)}) \quad i = 1, 2, \dots, s \quad (6)$$

where the following relationship holds for the weighting factor, δ :

$$0 \leq \delta < 1$$

COMPUTER PROGRAMME

A computer programme called MASTEP was compiled in ALGOL language for this method, the programme contains the equation systems of the mathematical models of the operation units in programme-blocks. Its present set is shown in Figure 2.

In the programme-block designs, in recommendations literature and our own experience were considered in selecting the algorithm of the appropriate units (8) and the main criterion governing our choice was numeric stability.

APPLICATION OF THE MODEL

The technological problem

The use of the computation method is demonstrated via an example. The problem chosen involves a certain multistage distillation unit with product reflux. This connection scheme is frequently used, e.g. in natural gas processing plants. The aim of the two stage separation is to produce light petroleum fractions from the condensate obtained from natural gas. The product reflux flows serve to increase the inner material throughput of the rectification columns. This is essentially necessary if the quantity of the processable raw material remains below the minimum level required to ensure stable column operation. Such a material shortage can be caused by an output drop on the fields and/or change in the quality of the gas produced or partial shut-down of the connected plants (e.g. gas storage facilities). The simplified schematics of the technological process are shown in Figure 4.

The problem to be solved is the determination of the magnitude of the reflux flows to ensure the given loading.

The calculation

No explicit relationship can be formulated between the loading and reflux, therefore a reiteration, i.e. repeated recalculation

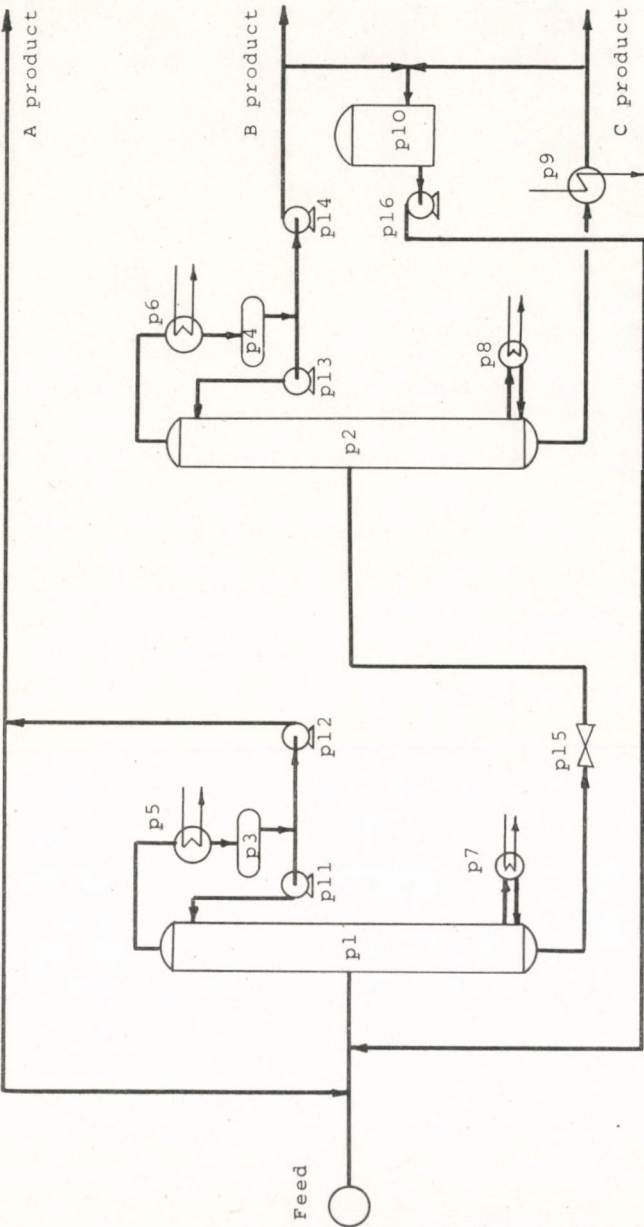


Figure 4. The Simplified Technological Flow Sheet

tion of the whole system is required. One step of this process is the solution of the component and heat balance equations belonging to a given component reflux.

Based on the technological flowsheet and the problem to be solved, the computation flowsheet is prepared (Figure 5) containing only those units which are indispensable for the solution.

The process matrix can be formulated which represents the numerical mapping of the computation flowchart, once the serial numbers of the operation units and the component flows, as well as the coupling indices are known. The process matrix is given in Table 3.

Table 3. The process matrix of the problem

Code number	Connection points				
2	1	6	- 2	0	
2	2	17	- 3	0	
8	3	0	- 4	- 7	
3	7	0	- 8	0	
8	8	0	- 9	-12	
1	12	-14	-13	0	
1	9	-11	-10	0	
7	14	-15	0	0	
2	11	15	-16	0	
4	16	0	-17	0	
1	4	- 6	- 5	0	

The initial values of the calculation are the present values of the component flows and the operation parameters of the units, the process matrix determining the connection and type of units involved, and the estimates given for the ratio coefficients and temperature data.

Estimates are based on actual measured data obtained on a variant without product reflux.

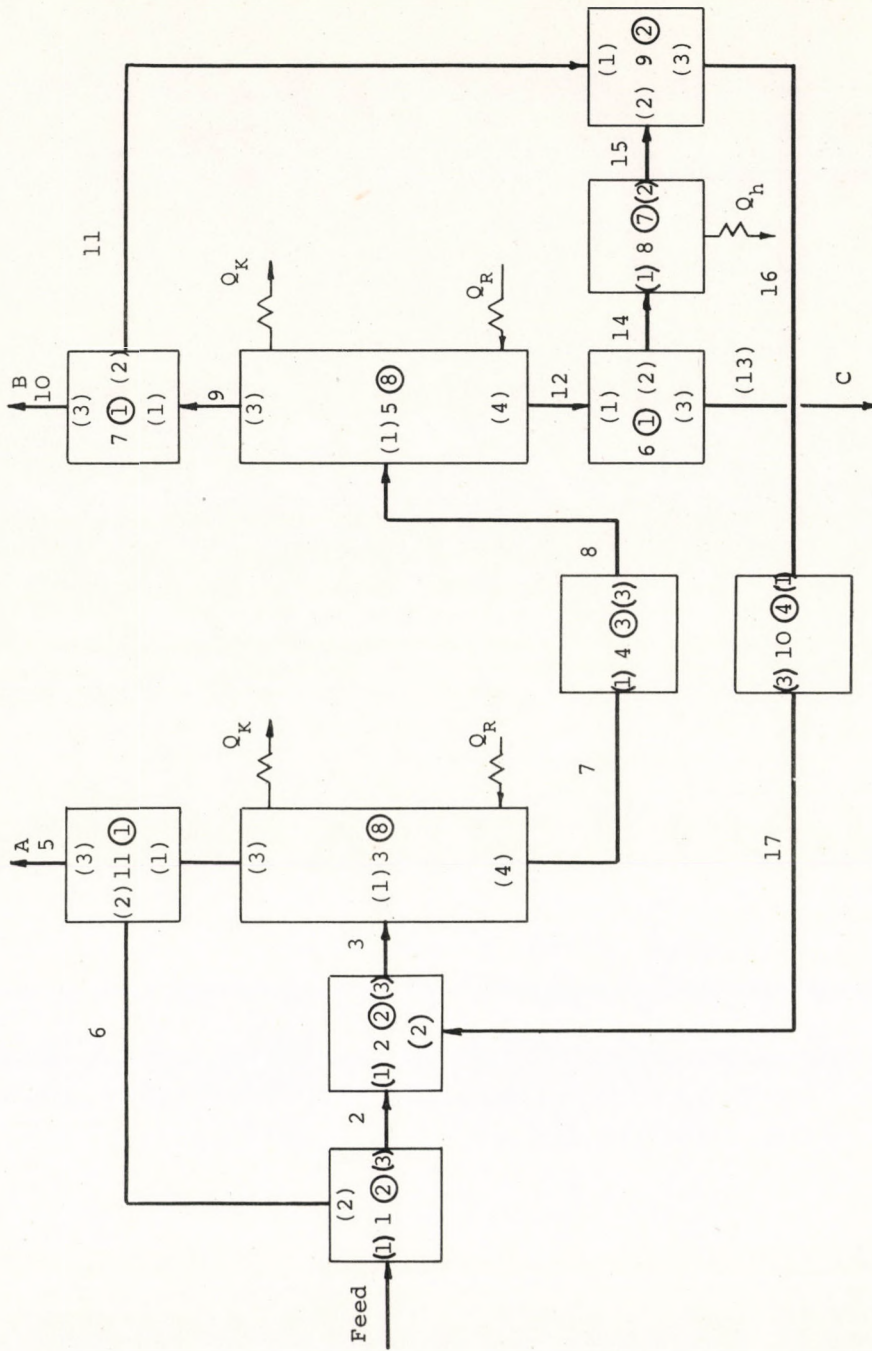


Figure 5. The Computation Flow Sheet

Table 4. Parameters of the component flows

Serial number of the flow	Component flow, kmole/h	Temperature, K	Pressure, N/m ² ×10 ⁻⁵	Composition, kmole/kmole	
1	76.00	345.00	19	0.0140	0.4717
2	113.67	339.38	19	0.0188	0.6316
3	152.00	338.05	19	0.0141	0.4740
4	74.89	327.71	19	0.0286	0.9541
5	37.21	327.71	19	0.0286	0.9541
6	37.67	327.71	19	0.0286	0.9541
7	77.11	406.00	19	0.0000	0.0090
8	77.11	368.75	7	0.0000	0.0090
9	39.79	327.25	7	0.0000	0.0174
10	19.76	327.25	7	0.0000	0.0174
11	20.03	327.25	7	0.0000	0.0174
12	37.32	401.00	7	0.0000	0.0000
13	19.03	401.00	7	0.0000	0.0000
14	18.30	401.00	7	0.0000	0.0000
15	18.30	340.00	7	0.0000	0.0000
16	38.33	334.24	7	0.0000	0.0091
17	38.33	334.24	19	0.0000	0.0091

Table 4. (continued)

C o m p o s i t i o n							Serial num- ber of the flow
kmole/kmole							
0.2600	0.1447	0.0628	0.0339	0.0109	0.0019	0.0001	1
0.1796	0.0967	0.0420	0.0227	0.0073	0.0013	0.0001	2
0.2618	0.1420	0.0616	0.0333	0.0107	0.0019	0.0001	3
0.0173	0.0000	0.0000	0.0000	0.0000	0.0000	0.0000	4
0.0173	0.0000	0.0000	0.0000	0.0000	0.0000	0.0000	5
0.0173	0.0000	0.0000	0.0000	0.0000	0.0000	0.0000	6
0.4992	0.2800	0.1214	0.0655	0.0211	0.0037	0.0002	7
0.4992	0.2800	0.1214	0.0655	0.0211	0.0037	0.0002	8
0.9663	0.0163	0.0000	0.0000	0.0000	0.0000	0.0000	9
0.9663	0.0163	0.0000	0.0000	0.0000	0.0000	0.0000	10
0.9663	0.0163	0.0000	0.0000	0.0000	0.0000	0.0000	11
0.0012	0.5611	0.2508	0.1354	0.0435	0.0076	0.0004	12
0.0012	0.5611	0.2508	0.1354	0.0435	0.0076	0.0004	13
0.0012	0.5611	0.2508	0.1354	0.0435	0.0076	0.0004	14
0.0012	0.5611	0.2508	0.1354	0.0435	0.0076	0.0004	15
0.5056	0.2764	0.1197	0.0646	0.0208	0.0036	0.0002	16
0.5056	0.2764	0.1197	0.0646	0.0208	0.0036	0.0002	17

The computation process is an automatic one, but there is also a provision for external manipulation (e.g. to change some of the preset values).

The computed component flow values are presented in Table 4. The energy flow values are printed when the operation unit proper is calculated (e.g. the heat of condensation, and heat of evaporation, etc.).

Convergency test

The numerical stability of the method in the case of the problem presented is well represented in Figure 6. The average relative deviation describing the extent of the convergency is calculated as follows [9]:

$$E = \sqrt{\frac{\sum_{i=1}^s \sum_{c=1}^k \left(\frac{\alpha_{i,c}^{(t+1)} - \alpha_{i,c}^{(t)}}{\alpha_{i,c}^{(t)}} \right)^2}{k \times s}} \times 100$$

The convergency achieved in the given problem corresponds to an accuracy of 0.1 per cent the practical product yields.

Experience gained through the simulation of natural gas processing plants shows that the convergency of the method is reliable regardless of whether the number of recycles is increased (to 3 or more). In the case of well-estimated separation ratios (e.g. based on actual measured values) no weighting is necessary.

In the future, the programme will be further developed

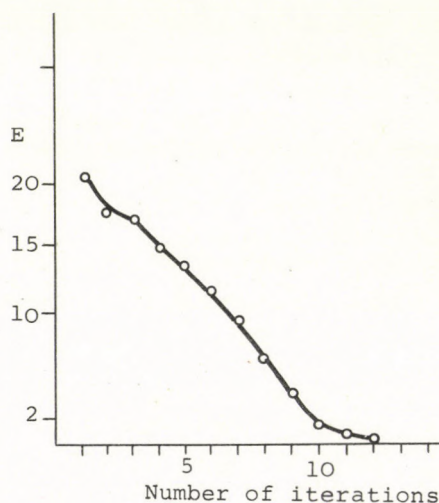


Figure 6. The Convergency Curve

due to the improvement of the convergency method (determination of the optimized value, e.g.[10]) and the extension of the programme-block set of the operation units (e.g. units including chemical reaction).

SYMBOLS USED

A	coefficient matrix of the component balance equations
b	constant vector of the component balance equation
c	component index
i	serial number of the operation unit
j	coupling index
k	number of components
L	number of the operation units
m	component flow, (kmole/sec)
M	mass flow, (kmole/sec)
n	number of material flows
N	maximum number of the connection point for a given unit
p	pressure, (N/m ²)
P	process matrix
r	changing index
s	number of the branchings and separation units
t	number of the iterative steps
T	temperature, (K)
z	composition, (kmole/kmole)

REFERENCES

- [1] SHANNON, P.T.: Chem. Eng. Progr., 62 (6) 49, (1964)
- [2] HARRIS, R.E.: Chem. Eng. Progr., 68 (10) 58, (1972)
- [3] BENEDEK, P. et al.: Bonyolult műveleti egységek szimulációja (Simulation of Complex Operation Units), Akadémiai Kiadó, Budapest, 1973.
- [4] HEUCKE, Ch.: Chemie-Ing.-Techn., 42, 502, (1970)

- [5] TIMÁR, L., PILHOFFER, Th.: Verfahrenstechnik, 7 (2) 53, (1973)
- [6] RAVITZ, A.E., NORMAN, R.L.: Chem. Eng. Progr., 60 (5) 71, (1964)
- [7] NICHOLS, Ch.R.: Oil and Gas J., 57 (7) 101, (1959)
- [8] CSERMELY, Z., TIMÁR, L.: Tridiagonal Matrix Method for Modelling of Distillation Column. Lecture presented at the "Műszaki Kémiai Napok", Keszthely, April 11-13, 1974. No. 16/27.
- [9] BATUNER, L.M., POZIN, M.E.: Matematikai módszerek a kémiai gyakorlatban (Mathematical Methods in Chemical Practice), Műszaki Könyvkiadó, Budapest, 1963. p. 532
- [10] LAPIDUS, L.: Digital Computation for Chemical-Engineers, McGraw-Hill, New York, 1962. p. 175.

РЕЗЮМЕ

Статья знакомит с методом, применимым для расчета на ЭВМ баланса массы и тепла технологических процессов.

При данном методе линейные и нелинейные зависимости, составляющие модель процессионных единиц, группируются по типам. Двумя ступенями, поочередно применяемыми в расчете, является одновременное решение линейных уравнений для всей технологической системы а затем корректирование коэффициентов системы линейных уравнений путем решения нелинейных моделей. Это повторяется вплоть до достижения желаемой точности.

Преимущество метода заключается в надежности сходимости, а также в том, что для расчета рециркуляций не требуется особой итерации.

PLATE ABSORBER MODELLING BY MATRIX METHOD*

Z. CSERMELY, L. TIMÁR

(Hungarian Oil and Gas Research Institute)

Received: March 9, 1976.

The mathematical models of plate separators consist of multivariable, nonlinear equation sets. Several algorithms can be deduced to carry out grouping of these equations by types, to choose the convergency method applicable or to execute the simultaneous or consecutive solution of the equation subsets obtained.

The results of a study are presented that were aimed at finding the possibilities of exact means to select the most efficient computation methods, depending on the characteristics of the mixture to be separated and the type of the column (simple adsorber, and desorber, etc.).

The performance of an operation unit consisting of a given number of theoretical plates can be described - for the purpose of mathematical modelling - by similar equation sets which are independent from the particular technological purpose or properties of the mixture to be separated. In a mathematical sense, the task is to solve this equation system consisting of multivariable, linear and nonlinear relationships. By decomposition, i.e. by separating the equation set into groups, several possible variants of the solutions, i.e. several algorithms can be obtained, depending on the number of the theoretically possible decomposition schemes and

Lecture presented at the Műszaki Kémiai Napok '75 (Technical Chemistry Days '75), Keszthely.

solution orders.

Based on that principle several algorithms were constructed and successfully identified with existing, practically used solution methods [1]. Two of the possibilities were discussed in detail and shown to be applicable for the modelling of complex rectification columns used for diverse applications [1, 2].

Research was carried out along two lines. Apart from the depth of the decomposition, a new governing principle was introduced to work out the theoretically possible methods, and by modelling plate absorbers the range of the application possibilities studied was extended.

1. BASIC VARIANTS OF THE MATRIX METHODS

Under isobar conditions, generally prevalent in separation methods, the equations describing the operation are the mass, the component and the heat balance equations together with the equilibrium relationships applied for each of the theoretical plates. Executing all the possible substitutions, e.g. expressing the mass flow of the liquid leaving a plate by that of the rising vapour and the mass balance equation, the vapour concentration by the mole fraction of the liquid phase and the component equilibrium, an equation set, containing three types of relationships was obtained. In matrix representation the relationships are as follows (for n theoretical plates and k components):

Component balance equations:

$$\underline{M}(\underline{x}, \underline{T}, \underline{V}) = \underline{0}$$

(m.k)

Mole fraction definition (sum) equations:

$$\underline{S}(\underline{x}, \underline{T}, \underline{V}) = \underline{0}$$

(n)

Heat balance equations:

$$\underline{H}(\underline{x}, \underline{T}, \underline{V}) = \underline{0}$$

(n)

The equation set is solved by an advantageously selected iterative process, e.g. by the Newtonian method or a variant

of it, applying estimated initial values. The solution yields the liquid concentration \underline{x} ; the plate temperature \underline{T} , and the vapour flow \underline{V} , values which satisfy the equation system within specified limits.

1.1 Variants without decomposition

It is the most general method when the equation set is simultaneously solved for each of the variables with no decomposition at all [3].

The drawbacks of this approach are that the time and the storage capacity required for the solution are of considerable magnitude and the convergency is trustable, but with fairly good initial values. This brings about significant difficulties, especially when the initial concentration values are to be estimated. A possible alternative to solve this problem is to determine the initial concentrations from the component balance equations along with the initial \underline{T} as well as \underline{V} values, which can be fairly well estimated [4].

However, the drawbacks of the general solution are best eliminated by the decomposition methods.

1.2 Variants with decompositions

Two governing principles were used work out the variants. One of them is the depth of the decomposition, i.e. how many subsets are used when the equations are classified (three separate groups for each three of the types; two groups, one group for the one type, the other for the other two types of equation. Further variants can be deduced in each case according to which variable is calculated by which group.

The number of the variants is smaller than that if the combinatorical possibilities, for the compositions can be calculated only from the component balance equations.

1.2.1 Variants with complete decomposition

According to the types of the equations, three subsets are formed. Liquid concentrations are calculated from the component balance equations using the estimated temperature profile as well as the vapour flow profile. From here on there are two basic variants.

The bubble point method (BP) is obtained if the temperature is calculated from the sum equations while the vapour flows are obtained from the heat balance equations. This variant is the same as that of the Wang-Henke method, described in the literature [5].

The sum rate method is obtained if the vapour flows are calculated from the sum equations and the temperature values are obtained from the heat balance equations [6].

The computation schematics of the method based on the complete decomposition method are shown in Figure 1.

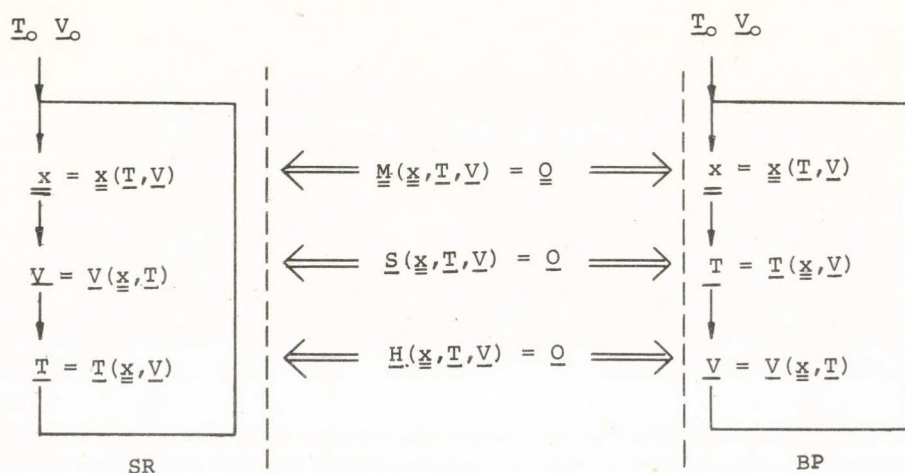


Fig. 1. Computation schematics of the basic variants obtained with complete decomposition.

1.2.2 Variants with partial decomposition

Two of the three equation subsets are compounded and simultaneously solved (e.g. by the Newtonian method), followed by the consecutive - but in itself simultaneous - solution of the third subset left over.

Any of the three types can be handled in itself, but not each of them can be used to compute each of the variables, for the concentrations can only be determined from the component balance equations. Thus the number of the basic variants is five.

Estimated initial temperature and vapour flow values have to be secured for each variant. Starting from these values, the iterative cycle results in the concentrations and new profiles. Then, the calculation is once again repeated with those new data. The calculation cycle is repeated until the desired accuracy figures of the selected variables are met.

To facilitate an easier grasp, characteristics of the variants are shown in Table 1.

It can be seen that three of the theoretically deduced variants have no practical counterpart known from the literature. Thus, these methods represent the unresearched means of the solution technique and further studies are required to find out if any such practical problem exists where they can be applied to advantage over the known methods.

2. APPLICATION OF THE BASIC VARIANTS FOR ABSORBER MODELLING

According to the literature and our experience in the field of modelling rectification columns, the applicability of the algorithms constructed from the very same basic relationships, but having different structures, depend on the type of the column and the characteristics of the mixture to be separated. The aim of the present studies is to work out a quantitative method to select the appropriate basic variant used to model plate absorbers.

From the basic variant of the matrix methods the BP and BPT methods applied for rectification columns, and the SR (sum rate)

Table 1. Basic variant formed with partial decomposition

1 st step of the reiterative cycle	2 nd step of the variant	Name of the variant	Corresponding known method
Calculation of \bar{x}, \bar{T} from the equation \bar{M}, \bar{S}	Calculation of \bar{V} from the equation subset \bar{H}	T-correction variant of the bubble-point method (BPT)	[7]
Calculation of \bar{x}, \bar{V} from the equation subset \bar{M}, \bar{S}	Calculation of \bar{T} from the equation subset \bar{H}	V-correction variant of the sum rate method	
Calculation of \bar{x} from the equation subset \bar{M}	Calculation of \bar{T}, \bar{V} from the equation \bar{S}, \bar{H}	Simultaneous T-V correction	[8]
Calculation of \bar{x}, \bar{T} from the equation \bar{M}, \bar{H}	Calculation of \bar{V} from the equation subset \bar{S}	T-correction variant of the sum rate method	
Calculation of \bar{x}, \bar{V} from the equation subset \bar{M}, \bar{H}	Calculation of \bar{T} from the equation subset \bar{S}	V-correction variant of the bubble-point method	

method proposed for the calculation of plate absorbers were used along with their appropriate computer programmes.

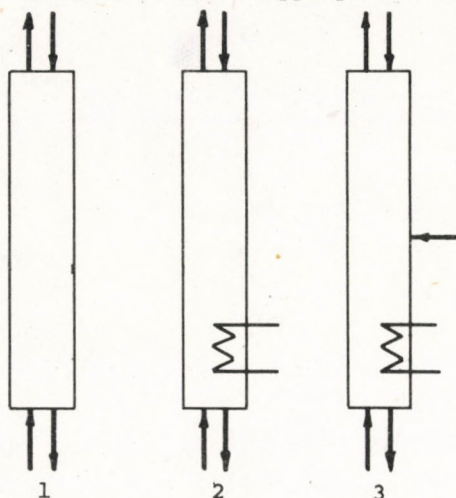


Fig. 2. The adsorber types studied

- 1 simple absorber
- 2 stripper
- 3 absorber with reboiler

The absorbers studied are shown in Figure 2.

Four data sets, obtained from the literature and actual natural gas processing plants on three typical industrial systems were used as test data.

The materials of the test examples are light hydrocarbons. In two examples the technological aim is dry gas production. The "dry gas" consists mostly of methane from natural gas in a simple absorber, under different operation conditions [10, 6]. The third example relates to the de-ethanization of gasoline [11], while the fourth example makes use of the data set

of an absorber equipped with a reboiler, used for the separation of the light components (lighter than propane) of raw gasoline [10].

The linear temperature profiles computed from the product temperatures corresponding to sharp separations and from the vapour flow values assuming constant molar flow were taken as initial values in each of the examples.

The convergency rate data obtained with the three different algorithms are shown. The measure of the convergency is the square sum of the differences between unity and the sum of the mole fractions for each of the plates (E). For the sake of simplicity, logarithmic scale is used in the figures ($\ln E$ versus the number of the iterative cycles).

Figures 3 and 4 present the convergency of the computation for two simple absorbers, while Figures 5 and 6 show those if the stripping column and the absorber with reboiler.

It can be seen that in the case of simple absorbers the convergency of the SR method is trustable, the BP and the BPT methods

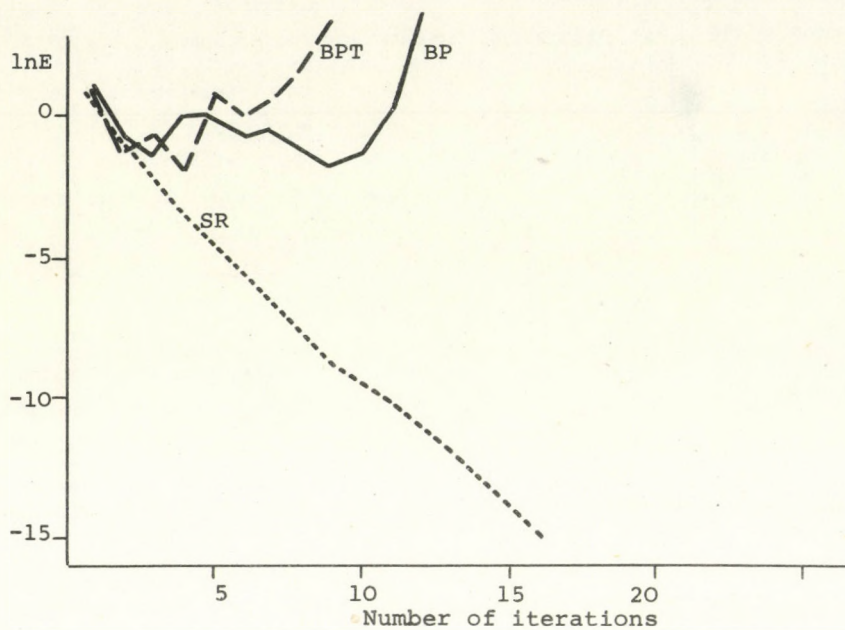


Fig. 3. Convergence of the Computation of a Simple Absorber [10]

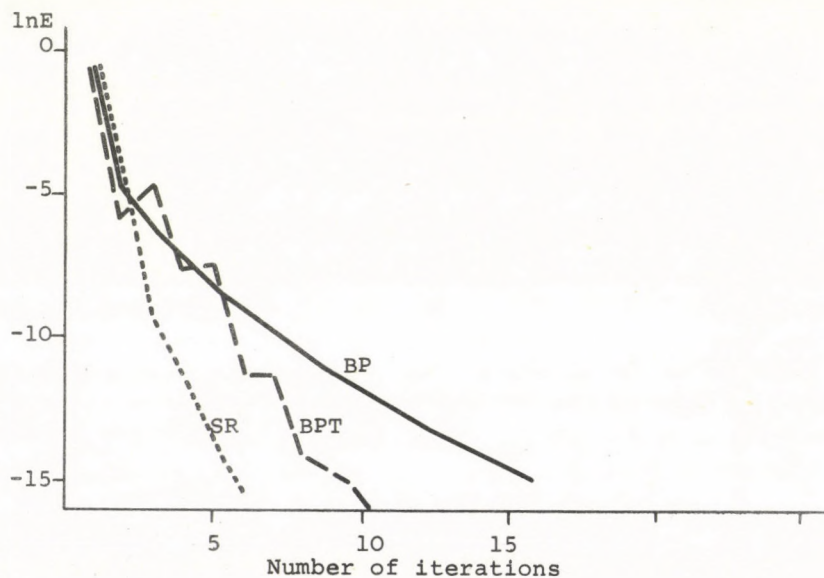


Fig. 4. Convergence of the Computation of a Simple Absorber [6]

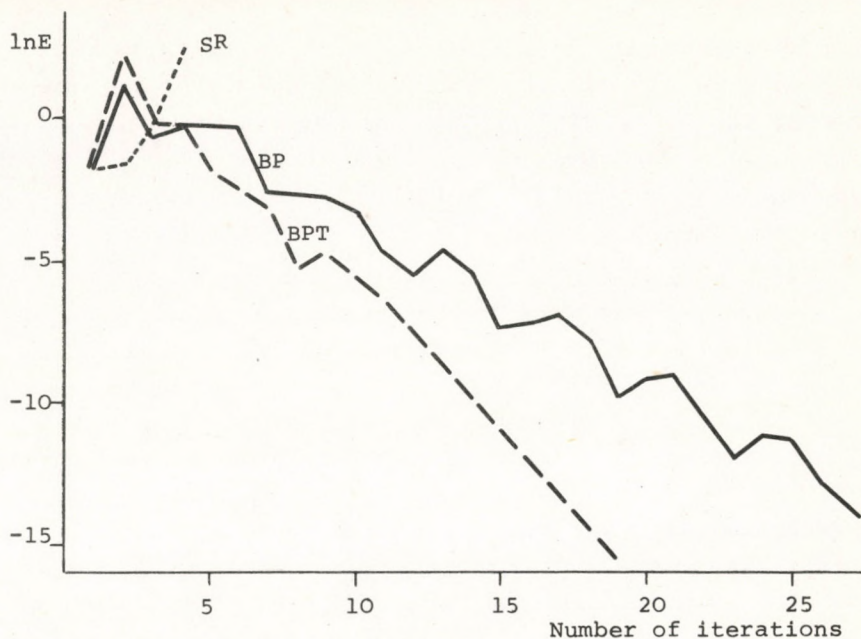


Fig. 5. Convergency of the Computation of the Stripper [11]

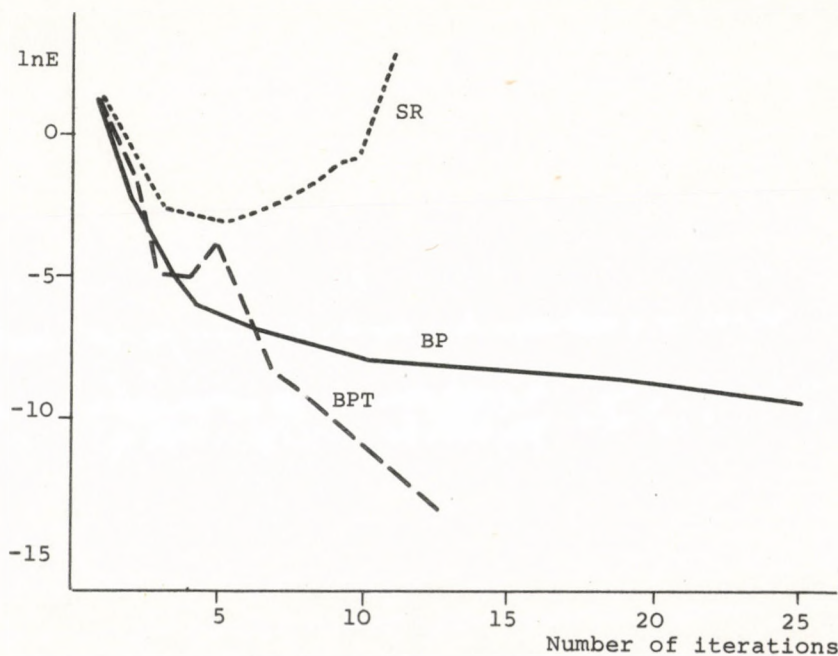


Fig. 6. Convergency of the Computation of the Absorber with Reboiler [10]

are divergent in the first example and though in the second example they were convergent, the convergency rate was inferior to that of the SR method. In the case of the stripping column and absorber with reboiler, the SR method became divergent after the first few iterative cycles, the BP and BPT methods were convergent, the convergency-rate of the former was smaller.

Analysing the figures it can thus be concluded that different behaviours depend on the type of the system (with or without reboiler), but this information is insufficient for an unambiguous decision. Several indicators were proposed in the literature to solve this problem. The SR method is to be applied in those cases where the theoretical plate number is low [9], and for such mixtures where the boiling point ranges are wide [9]; for lower pressures [6] and where the difference between the temperatures of the head and bottom products is smaller than 100°C [6]. Table 2 summarizes these values in the case of the examples given. Two new variables were added because they were technologically important. The BP method is appropriate for the maximum vapour-liquid ratio and low light component fractions in the feed, while for high light component fractions the SR method is appropriate.

Studying the table it can be seen that the choice is not always unambiguous and there is also no information as to what the limits of applicability are in the case of both the methods. From the examples shown it can be concluded that up to eight theoretical plates the SR method should be used, and above it the BP method should be used; a conclusion obviously not soundly founded. If the choice is based on the boiling point range of the feed, the opposite conclusion is reached.

According to the studies carried out so far, the task cannot be solved by picking a single, fortunately chosen parameter.

The equation set itself is studied in the following section, because though implicitly it contains quantitatively the effects of both the type of unit and that of the characteristics of the mixture encountered in the given problem.

Therefore, the BP and SR methods were studied in detail. In both methods the first step is the calculation of the composition from the material balance; although the method differs in the way

Table 2. Comparison of the parameters suggested

Example	Applicable method	t_{\max}	t_{bp}	p	n	V/L	z_{kk}
Absorber	SR	12	71	90	6	10	0,82
Absorber	SR, BPT, BP	16	106	14	8	3	0,85
De-ethanizer (stripper)	BPT, BP	111	243	20	11	0,5	0,20
Absorber with reboiler	BPT, (BP)	114	264	18	16	1,6	0,38

t_{\max} maximal temperature difference, ($^{\circ}\text{C}$)
 t_{bp} boiling point range of the feed, ($^{\circ}\text{C}$)
 p pressure, (atm)
 n number of theoretical plates,
 V/L maximal vapour-liquid ratio, (kmole/kmole)
 z_{kk} fraction of the light components in the feed,
 (kmole/kmole)

the sum and the heat balance equations are used (Figure 1).

In this step the task is the determination of the temperature and the vapour flow values from the equation set:

$$\left. \begin{aligned} S(T, V) &= 0 \\ H(T, V) &= 0 \end{aligned} \right\}$$

written here only for a single plate for the sake of clarity.

Applying the Newtonian method, the following linearized relationships are obtained from the initial T and V values:

$$S(T_0, V_0) + \frac{\partial S}{\partial T} (T - T_0) + \frac{\partial S}{\partial V} (V - V_0) = 0$$

$$H(T_0, V_0) + \frac{\partial H}{\partial T} (T - T_0) + \frac{\partial H}{\partial V} (V - V_0) = 0.$$

Both the BP and the SR methods determine the new T and V values from the equations by the method of continuous approximation. This is also the principle of the Gauss-Seidel iterative method used to solve the linear equation set. The sufficient condition of convergency is that each successive equation of the set should be dominated by a new variable. Applying the analogy onto the coefficients of the variables of the problem studied, i.e. onto the derivatives, the condition of convergency is that a given relationship should be used for the computation of that very variable towards which it is most sensitive, i.e. the partial derivative of which has the highest absolute value. The method can only be used for the solution of the problem if it is assumed that the magnitude of the derivatives do not change during the iterative process.

In the complete equation set T and V are the vectors according to plates, thus instead of the derivatives the matrices of the derivatives should be compared. According to previous experience it is generally sufficient to compare a characteristic parameter, e.g. the Euclidian norms of the matrices when the magnitude relationship of the matrices is sought.

According to our process, the BP method is to be used if the relationship:

$$\left\| \frac{\partial S}{\partial T} \right\| > \left\| \frac{\partial S}{\partial V} \right\| \wedge \left\| \frac{\partial H}{\partial T} \right\| < \left\| \frac{\partial H}{\partial V} \right\|$$

holds and the SR method is to be used if the relationship:

$$\left\| \frac{\partial S}{\partial T} \right\| < \left\| \frac{\partial S}{\partial V} \right\| \wedge \left\| \frac{\partial H}{\partial T} \right\| > \left\| \frac{\partial H}{\partial V} \right\|$$

holds.

Having studied the examples it was concluded that in the case of a system performing multiple tasks, e.g. the absorber with reboiler, there is a difference of a magnitude between the Euclidian norms belonging to the two sections of the column. The value obtained for the upper section approaches that of the simple absorber while the value of the lower is close to that of a stripper or a rectification column. This fact suggests a new version of the solution method where within the model of the system, different basic variants are used for the different sections.

This work will be continued in the future to obtain a method which can be used to generate the model automatically from the basic equations, knowing the characteristics of the mixture to be separated and those the column.

SYMBOLS USED

E	measure of the convergency
H	function symbol of the heat balance
k	number of the components
M	function symbol of the component balance
n	number of the theoretical plates
p	pressure, (atm)
S	function symbol of the mole fraction definition equation
T	temperature, (K)
t_{bp}	boiling point range of the feed, ($^{\circ}\text{C}$)
t_{max}	maximal temperature difference, ($^{\circ}\text{C}$)
V	mass flow of the vapour phase, (kmole/sec)
V/L	maximal vapour-liquid ratio, (kmole/kmole)
X	liquid phase mole fraction, (kmole/kmole)

REFERENCES

- [1] CSERMELY, Z., TIMÁR, L.: Tridiagonal Matric Method for Modelling of Distillation Column. Lecture presented at the "Műszaki Kémiai Napok", Keszthely, April 11-13, 1974. No. 16/27.
- [2] CSERMELY, Z., TIMÁR, L.: Experiences in Modelling of Complex Distillations Columns with Matrix Method, Paper presented at the "MKE Chemists' Conference", Miskolc, Sept. 3-5, 1974.
- [3] NAPHTALI, L.M., SANDHOLM, D.P.: A.I.Ch.E.J., 17 148, (1971)
- [4] ISHII, Y., OTTO, F.D.: Can.J.Chem.Eng., 51 601, (1973)
- [5] WANG, J.C., HENKE, G.E.: Hydr.Proc., 45 (8) 155, (1966)
- [6] SUJATA, A.D.: Hydr.Proc., 40 (12) 137, (1961)
- [7] JEDLOVSKY, P.: Studies of Computer and Automatic Institute, Hungarian Academy of Sciences, 13, Budapest, (1973)
- [8] TOMICH, J.F.: A.I.Ch.E.J., 16 229, (1970)
- [9] FRIDAY, J.R., SMITH, B.D.: A.I.Ch.E.J., 10 698, (1964)
- [10] BURMINGHAM, D.W., OTTO, F.D.: Hydr.Proc., 46 (10) 163, (1967)
- [11] CSERMELY, Z., SIKLÓS, J., and SIMON, F.: Analysis of Behaviour of Stabilizer Column by Computer Simulation. Paper presented at 13th Hungarian Mining and Metallurgical Society Congress, Hajduszoboszló, Oct. 3-6, 1972.

РЕЗЮМЕ

Зависимости, из которых строится модель тарельчатых разделяющих установок, составляет нелинейную систему уравнений. Группировка уравнений по типам, одновременное или последовательное решение полученных частичных систем уравнений и выбор метода сходимости может привести к большому числу алгоритмов.

В статье приводятся полученные до настоящего времени результаты исследований, целью которых является то, чтобы для различных задач была найдена точная возможность для выбора наиболее эффективного расчетного метода, в зависимости от свойств разделяемой материальной системы и от типа установки / простой абсорбер, десорбер и т.д./

EVAPORATOR SYSTEM STUDIES

L. PLEVA, B. NOVÁK

(Department of Mechanics,
Veszprém University of Chemical Engineering,
Veszprém)

Received: March 9, 1976

The construction of a practice-oriented general model applicable to evaporator systems is presented. The evaporators proper are considered as systems and complex operation units. Multistage evaporators with vapour offtake provisions are constructed from these units. The results are obtained by solving multivariable nonlinear equations. An algorithm-searching method is used for the solution.

For the sake of clarity, the relationships existing among the parameters of major importance are shown graphically.

CONSTRUCTION OF THE SYSTEM-MODEL OF EVAPORATORS

Evaporation is a complex phenomenon exhibiting both thermic and hydrodynamic properties. In addition, it is also accompanied by certain physical-chemical aspects. In therefore follows that the description of a single stage evaporator, even under steady state conditions, is a rather complicated task [1].

Evaporation of aqueous solutions is an especially frequent task. In this case the heating-steam consumption is considerable.

Significant reduction of the specific steam consumption (ϕ) was achieved in the case of multistage systems, known over a hundred years. Correspondingly, the thermic problems were dealt with by energy economics. Though the heat pump evaporation has not become a widespread method in Hungary the energeticians produced significant results with the evaporator systems applying vapour offtake.

Evaporator system studies can have different goals. Correspondingly, models with different description depths can be applied, i.e. the performance of the physical model under different operating conditions should be tested on mathematical models constructed from simpler or more complex equation sets. Thus, e.g. the single-stage evaporator can be modelled by a system consisting of the following operation units, coupled into a loop with or without circulation:

- a mixing head at the junction point of the feed and the back-fed circulation,
- a heater used to bring the solution to the boil, such as a steam heated heat exchanger,
- a boiler section, a heat exchanger keeping the hot solution at the boil,
- a separator, to separate vapour and the thick solution arriving from the boiler,
- a branching to separate the offtake of the thick solution from the circulation,
- a pump to circulate and feed in the solution.

The physical models of more complex evaporators, e.g. that of a Kestner-type caustic evaporator can be generated from the above mentioned operation units. Studying any of the evaporator units (stages), some arrangement of the above basic components is generally encountered. This means that the evaporator units proper can also be treated as systems. However, in technological practice the multistage batteries composed of several evaporator units are called evaporator systems. Here it is permissible for the evaporator units proper to be treated as separate operation units [2]. Eventually, it is only the computer capacity available and the

economics of the engineering efforts invested that determine whether the evaporator system is treated as a complex system constructed from subsystems of the stages or not.

The following points are to be noted in constructing the mathematical model of a stage. It is not always advisable to seek a maximally detailed description, however, care should be taken to ensure that the model is a trustworthy and adequately accurate representation of reality. It is advisable to use models that are valid over a wide parameter range.

The level of details is, first of all, determined by the expectations the model is to meet. After that point, models can arbitrarily be classified as simple, medium and complicated models. Figure 1. presents a four-stage co-current evaporator system with no vapour offtake, constructed from models characterized by a minimal number of variables.

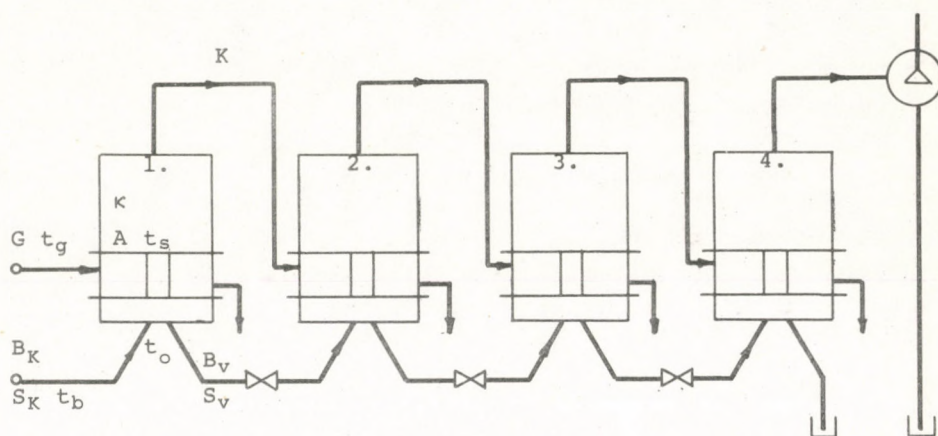


Fig. 1. Four-stage evaporator system with no offtake

Applying a description of similar depth for a three-stage system and stating, e.g. that the heater surfaces are equal, $A_1 = A_2 = A_3$, specifying the heat transfer coefficients κ_1 , κ_2 and κ_3 , as well as the prescribed concentrations, an equation set consisting of twenty two nonlinear equations yielded the required solution [3].

If the evaporator is considered as a separate operation unit then it can be connected to several other systems, the connections varying according to the type of the latter ones [7]. Branching is found in the vapour line, i.e. the unity of the model is composed from the operation units of the evaporator proper and that of the branching.

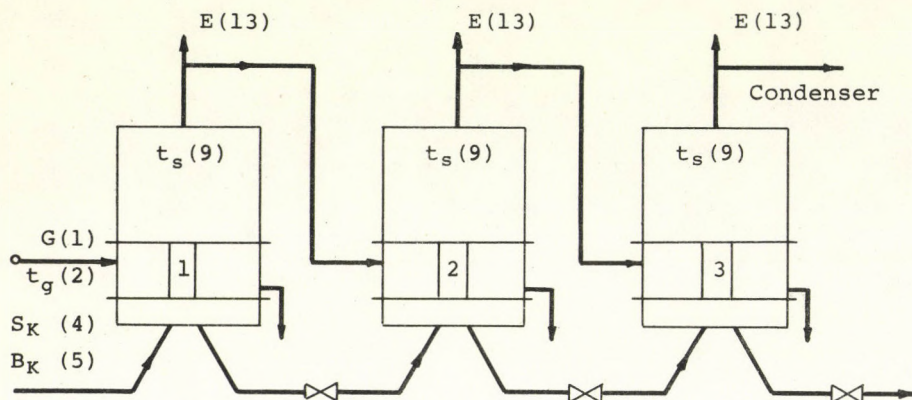


Fig. 2. Three-stage evaporator system with offtake

This approach is mandatory because vapour offtake is very frequently encountered in real industrial systems. No vapour offtake or extra vapour input (negative offtake) is introduced into the mathematical model by stating $E = 0$ and $E < 0$, respectively. To facilitate an easier treatment in the later stages of the computation, the seventeen variables (L) used to describe the evaporator were designated by code numbers. In addition, the mathematical model contains the equation set consisting of ten nonlinear, independent equations (M) yielding in a degree of freedom, $DF = L - M = 17 - 10 = 7$.

The implicit forms of the independent equations are as follows:

$$f_1(V, K, E) = 0$$

the mass flow balance equation relating to the branching

- $f_2 (\varphi, G, V) = 0$ the specific heating-steam consumption
 $f_3 (\Delta t_a, B_v, t_o) = 0$ the boiling point temperature rise, (Δt_a)
 $f_4 (V, G, r_g, r, S_k, t_o, t_b) = 0$ the heat balance equation of the evaporator proper
 $f_5 (B_v, S_v, B_k, S_k) = 0$ the dissolved material or dry material balance equation of the solution
 $f_6 (r_g, t_g) = 0$ the latent heat of vapour at the temperature of the heating steam
 $f_7 (r, t_o) = 0$ the latent heat of vapour at the temperature of the solution
 $f_8 (t_o, \Delta t_a, t_s) = 0$ the relationship between the saturation temperature t_s , the boiling point rise Δt_a , and the solution temperature t_o
 $f_9 (S_v, S_k, V) = 0$ the mass balance equation of the evaporation
 $f_{10} (kA, t_g, t_o, S_k, t_b, V, r) = 0$ the heat transfer equation.

Conditions:

$Q_{\text{loss}} = 0 \frac{\text{kcal}}{\text{h}}$ there is no heat loss

$c = 1 \frac{\text{kcal}}{\text{kg}^\circ\text{C}}$ specific heat of water

Vapour is assumed to be pure steam

Solution is thoroughly mixed.

The code of numbers corresponding to the variables are shown under the heading SYMBOLS USED.

The depth of the description is limited because the impulse flows are ignored. Thus, the pressure existing in the evaporator (and the same statement holds for the systems built from them as well) can only be calculated by indirect methods, via the boiling temperature value.

The term "complicated model" is restricted to those cases where the mathematical model consists of more than twenty independent equations and computerized algorithm searching is indispensable.

able. Generally, the number of degrees of freedom, (DF) and thus number of the input parameters, is between 8 and 15, while the number of variables is between 30 and 40 [4]. Such descriptions are obtained if the impulse flows are noted along with the heat transfer coefficient functions are entered into the model. In such cases, even with a single stage evaporator, one is frequently forced to solve complicated multivariable differential equation sets, especially if the evaporator is considered to be a system of differential operation units.

The determination of the appropriate algorithm (computation order) [5, 6] is of considerable assistance in solving such problems. Earlier the authors of this paper reported one such system showing its productivity enhancing effect in everyday engineering practice [7].

STUDIES ON THE THREE STAGE EVAPORATOR SYSTEM

The occurrence matrix shown in Figure 3 summarizes the solution of the three stage evaporator with vapour offtake shown in Figure 2, under the given input system. Here the rows contain the equations arranged already according to the computation order and the variable occurring in the equations are denoted with x . In the column in front of the rows, the equations, designated by a number, belonging to the three stages, are referred to (e.g. 6 is identical to f_6).

The first column in front of the matrix contains the number of the equations of the first system, the second those of the second, etc. In the heading, the upper line contains the code numbers of variables belonging to the first unit, and the second line those of the second unit, etc.

Thus, e.g., the lowermost line means that from the sixth equation of the third stage, the third variable of that stage, the latent heat of the heating steam (r_g) is obtained. In the heading the input system, the coded variables were arranged into lines corresponding to the three stages.

Thus the 2nd variable of the third stage, (t_g) is identical

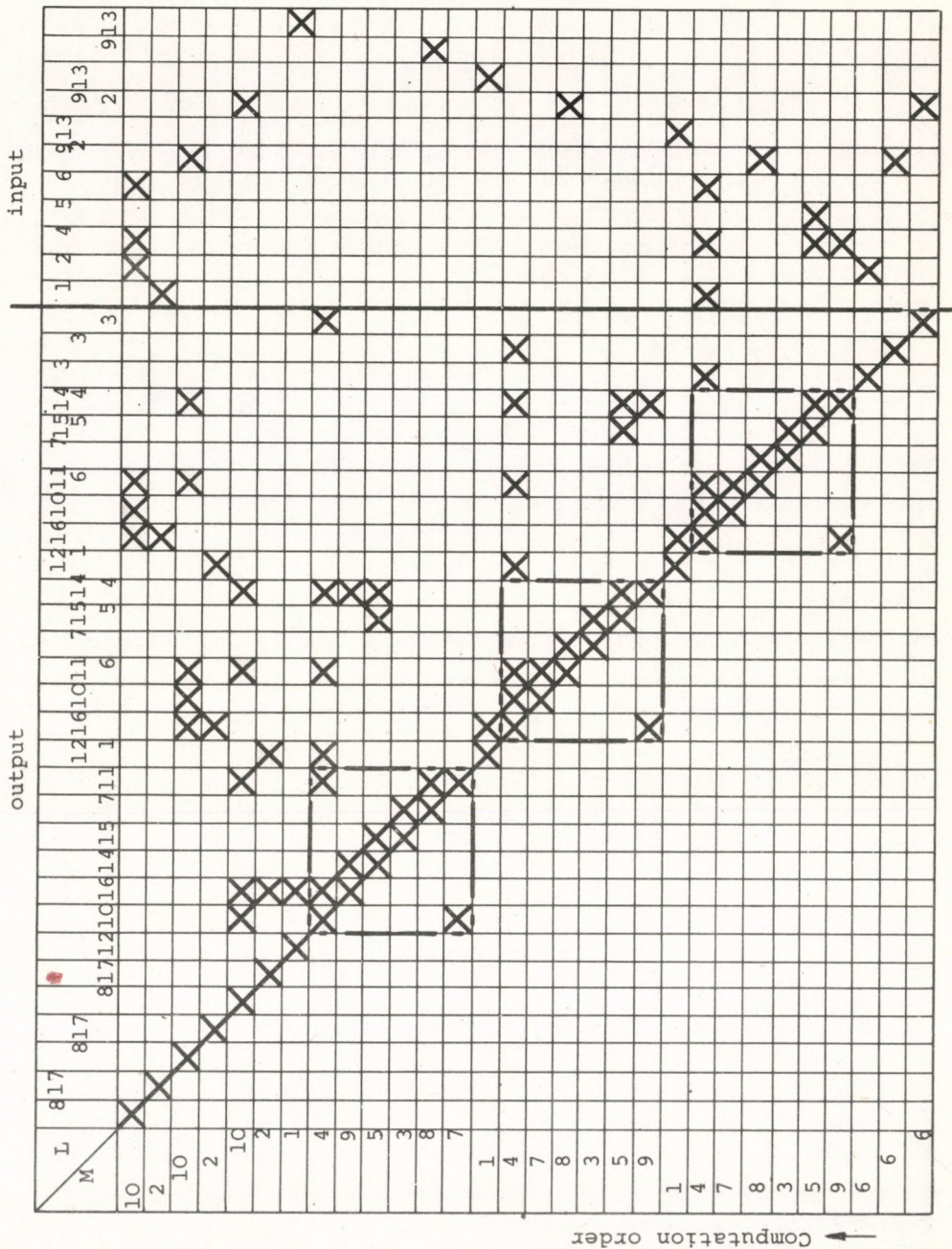


Fig. 3. The Occurrence Matrix

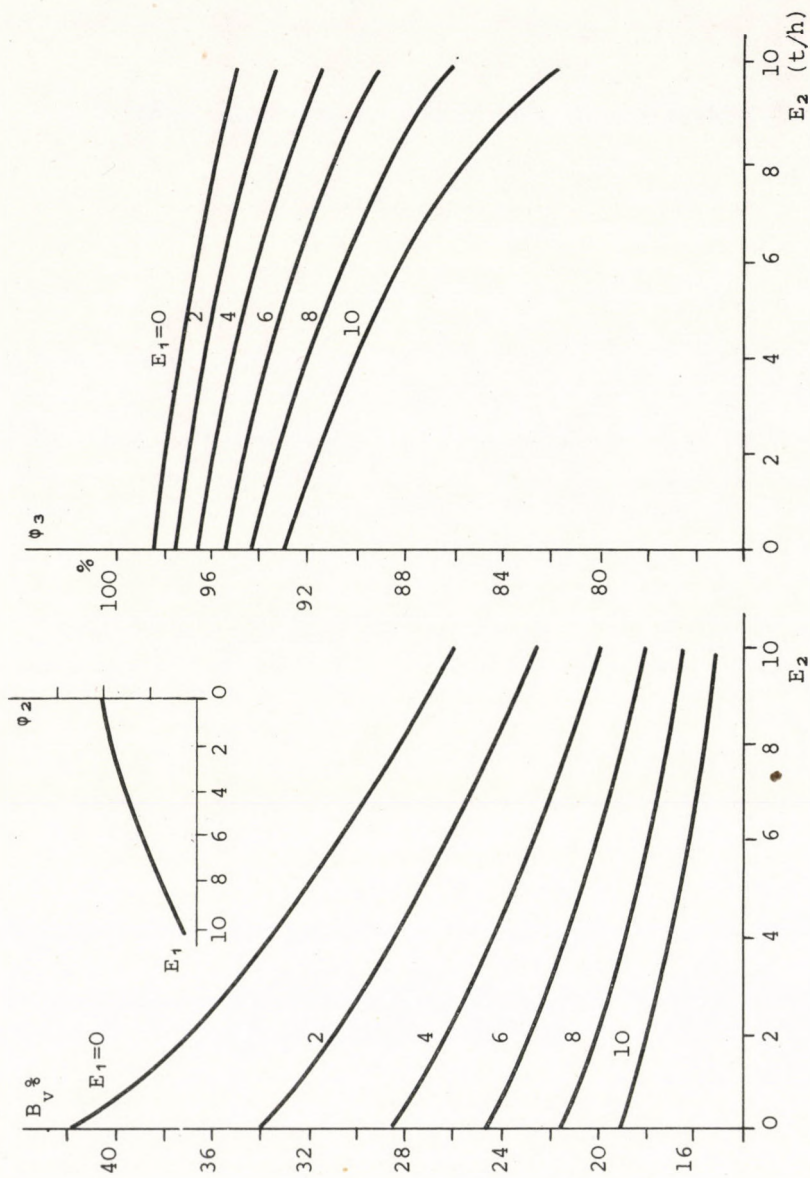
to the 9th variable of the second stage, the temperature of the vapour, (t_s). The identity refers to the connections of the particular stages. This is indicated by numbers (referring to variables) written above each other in the heading.

Three squares, indicating interactions, are found in the matrix; here, besides the unknown, located in the main diagonal, there is yet another unknown variable. The iterative cycles appear, in this connection, within the appropriate units, because there is no feed-back in selected for the example shown, the output data of any stage become the input data of any successive stage at the junction point.

The example was solved under different values of the input system shown and the relationships existing between the parameters of major practical importance: specific steam consumption (φ), heat transferring ability (κA) and offtakes (E), were obtained.

RELATIONSHIPS BETWEEN THE MAJOR PARAMETERS

The three stage sodium hydroxide evaporator is examined below as a function of the changing vapour offtake values of the particular units. Offtakes influence only stages placed behind the offtake points. Changing the offtake in the third stage influences neither the concentration nor the (κA), but only the φ_0 values. Therefore, throughout these studies, only the effects of changing the offtakes of the 1st and 2nd stages were recorded. Increasing offtake brings about a decrease in φ_2 , φ_3 , φ_0 (Figures 4 and 6), in the required transferring abilities, (κA)₂, (κA)₃ (Figure 5) and significantly, also in the final concentration value (B_v) (Figure 4). Thus, if a more concentrated solution is sought, it can only be achieved via poorer specific vapour consumption (φ_2 , φ_3 and φ_0) and smaller offtake values. During the calculations, only the first and second stage offtakes were varied, the remainder of the initial values are kept constant. The constant initial values were as follows:

Fig. 4. The B_v vs E_2 and ϕ_3 vs E_2 diagrams

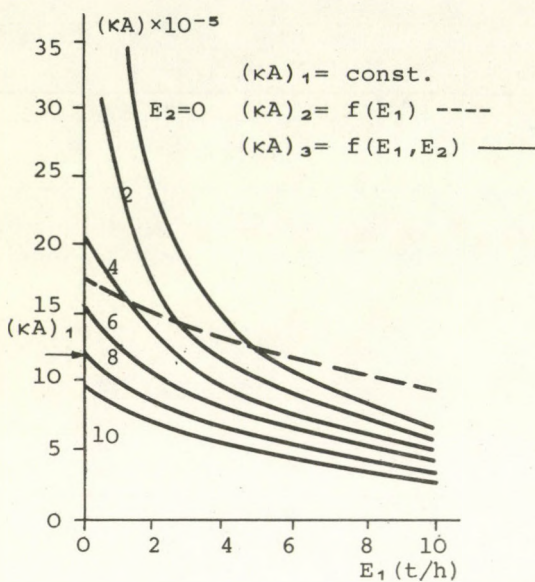
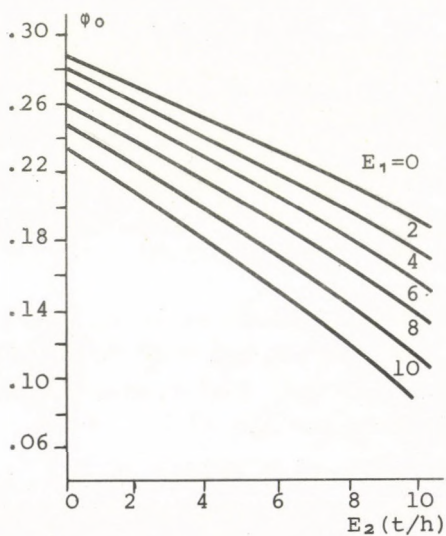


Fig. 5.

The (κA) vs E_1 diagram

Fig. 6.

 φ_0 vs E_2 diagram

1st stage:

$$G (1) = 2.65 \times 10^4 \text{ (kg/h)}$$

$$B_k (5) = 6.9 \text{ (\%)}$$

$$t_g (2) = 131 \text{ (}^\circ\text{C)}$$

$$t_b (6) = 117 \text{ (}^\circ\text{C)}$$

$$S_k (4) = 9.57 \times 10^4 \text{ (kg/h)}$$

$$t_s (9) = 117 \text{ (}^\circ\text{C)}$$

2nd stage:

3rd stage:

$$t_s (9) = 105 \text{ (}^\circ\text{C)}$$

$$t_s (9) = 86.5 \text{ (}^\circ\text{C)}$$

The offtakes from the 1st and 2nd stage were varied between 0 and 10 (t/h).

The effects of offtake on certain parameters are shown graphically. Based on the diagrams shown, the effects of changing some of the parameters upon each other can easily be followed. Thus, the changes to be implemented, to reach a given condition, can be determined.

From the diagrams it is readily apparent that the theoretical maximal concentration is 41.5 % under the conditions:

$$(\kappa A_1) : (\kappa A_2) : (\kappa A_3) = 11.5 : 16.7 : 107$$

Due to economical factors, such a ratio must not be created, because then the surfaces of the particular stages become too widely different. Surfaces of roughly equal magnitude would be desirable.

In general, the ratios $\kappa_1 : \kappa_2 : \kappa_3 = 2 : 1.6 : 1$ are acceptable for three stage evaporator systems. Assuming equal surfaces, the (κA) ratios become equal to the κ ratios. Since the offtake from the 1st stage does not effect the operation of the first stage, $(\kappa A)_1$ is always constant. Taking it as the basic value, $(\kappa A)_2$ and $(\kappa A)_3$ become:

$$(\kappa A)_1 = 1.14 \times 10^6$$

$$(\kappa A)_2 = 9.2 \times 10^5$$

$$(\kappa A)_3 = 5.75 \times 10^5$$

Based on these data offtake values, corresponding to maximal

utilization of the surfaces of all three of the stages, can be calculated.

$$\text{From } (\kappa A)_2 : E_1 = 10 \text{ (t/h)} \quad (\text{Figure 5})$$

$$\text{From } (\kappa A)_1 \text{ and } E_1 : E_2 = 2.25 \text{ (t/h)} \quad (\text{Figure 5})$$

Then the achievable concentration B_v can be calculated: $B_v = 17.8\%$ (Figure 4). The value φ_0 becomes: $\varphi_0 = 0.21$ (Figure 6).

If no offtake is allowed, but the surfaces are nevertheless kept constant, then the third stage becomes the "tight bottleneck" limiting the productivity of the two previous stages; thus, with no offtake whatsoever, lower final concentration is obtained. If the offtake is increased to, e.g. $E_2 = 6$, then the transferring ability of the third stage becomes: $(\kappa A)_3 = 4.01 \times 10^5$ (that is only 69.7 per cent of the total capacity of the 3rd stage). The final concentration becomes: $B = 16.2\%$ but the value of φ_0 is improved $\varphi_0 = 0.155$. If offtake is increased (from $E_1 = 10$ (t/h) and $E_2 = 2.25$ (t/h)), then the last elements of the system are not loaded entirely; if offtake is lowered, then the first elements work away from the optimum point.

As in this case (κA) values were permitted to change, the diagrams obtained are most useful for design purposes, because the surfaces (with known κ values) can be calculated. Obviously, dealing with existing systems, the surfaces are given. Therefore, using these input data, other calculations have to be performed and diagrams constructed.

SYMBOLS USED

		Code number
G	mass flow of the heating steam fed-in, (kg/h)	1
t_g	temperature of the heating steam, ($^{\circ}\text{C}$)	2
r_g	latent heat of the heating vapour (kcal/kg)	3
S_k	overall mass flow of the solution entering the system, (kg/kg)	4
B_k	concentration of the solution entering the system, (w%)	5

		Code number
t_b	temperature of the solution entering the system, (°C)	6
Δt_a	boiling point temperature rise of the solution, (°C)	7
κA	heat transferring ability, (kcal/h °C)	8
t_s	temperature of the vapour formed, (°C)	9
r	latent heat of the vapour, (kcal/kg)	10
t_o	temperature of the solution in the evaporator, (°C)	11
K	mass flow of vapour after offtake, (kg/h)	12
E	mass flow of steam offtake, (kg/h), (t/h)	13
S_v	overall mass flow of the solution leaving the system, (kg/h)	14
B_v	concentration of the solution leaving the system, (w %)	15
V	mass flow rate of the overall vapour formed, (kg/h)	16
φ	specific steam consumption, (kg/kg)	17

SUBSCRIPTS

1, 2, 3 denoting the stages

o overall

REFERENCES

- [1] SZOLCSÁNYI, P.: Vegyész mérnoki számítások termodinamikai alapjai. (Thermodynamical Basis of Chemical Engineering Calculations.) Műszaki Kiadó, Budapest, 1975. p.325
- [2] BENEDEK, P.: Bonyolult műveleti egységek matematikai szimulációja. - A kémia újabb eredményei 15. (In "Latest Results in Chemistry" series.) Akadémiai Kiadó, Budapest, 1973. p.29.
- [3] LEDET, W.P., HIMMELBLAU, D.M.: Advan. Chem. Eng., No.8. 229, (1970)
- [4] BENEDEK, P., LÁSZLÓ, A.: A vegyész mérnoki tudomány alapjai. (Fundamentals of Chemical Engineering.) Műszaki Kiadó, Budapest, 1964.
- [5] LEDET, W.P., HIMMELBLAU, D.M.: Advan. Chem. Eng., No.8. 233, (1970)
- [6] PLEVA, L.: in Ref. 1, p.330.
- [7] PLEVA, L., NOVÁK, B.: Hung. J. Ind. Chem., 4, 61 (1976)

РЕЗЮМЕ

Авторами показано построение модели обычной системы эвапораторов, которая может применена и на практике. Отдельно взятые эвапораторы рассматриваются как система и как составная процессионная единица. Из них строятся системы эвапораторов, пригодные для сложного многоступенчатого отъема пара. Результаты получены через решение нелинейных систем уравнений со многими неизвестными. Для этого применяется метод поиска алгоритма. Для наглядности графически представлены зависимости между наиболее важными параметрами в рабочей области моделей.

APPROACHING ANALYSIS FOR DISTRIBUTED
SYSTEMS

B. Paláncz

(Organizing and Computing Centre of the
Metallurgical and Machine Industry)

Received: March 9, 1976.

Approximation of distributed models by ordinary differential equations is one of the methods for solving optimal control, stability and identification problems concerning those models described by partial differential equations.

A method is presented for determining those approximating equations, based on a modified form of finite-elements.

INTRODUCTION

Although the improvement of the theoretical investigations of the optimal control, stability and identification problems of distributed systems described by partial differential equations is very progressive [1, 2], the approaching methods still have significant importance from the viewpoint of applications and numerical realizations.

A method based on a modified form of finite-elements [3] is presented for solving the problem of approximation of partial differential equations by ordinary ones.

The structure of these approaching equations is the same as the structure of equations well known from the literature of system theory [4]. In this way, every result formerly attained for optimal control, stability and identification problems of lumped systems can also be applied to distributed ones.

SOLVING A HEAT CONDUCTION PROBLEM TO ILLUSTRATE THE METHOD

Let us consider a simple heat conduction problem that can be described by the following equations (see Fig.1):

$$\frac{\partial T}{\partial \tau} = a \frac{\partial^2 T}{\partial x^2}, \quad 0 < x < L \quad (1)$$

Boundary conditions:

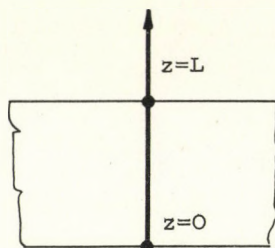


Fig.1.

$$\left. \frac{\partial T}{\partial x} \right|_{x=0} = 0; \quad \left. \frac{\partial T}{\partial x} \right|_{x=L} = U(\tau) \quad (2)$$

Initial condition:

$$T(x, 0) = T_0(x) \quad (3)$$

In addition, let us specify a functional as:

$$I = \int_0^\theta \int_0^L [T(x, \tau) - T_e(x, \tau)]^2 dx d\tau \quad (4)$$

where T_e is a predefined function.

The problem is how to change the heat flux differing from $U(\tau)$ only in a constant (k) in order to minimize the function (4). E.g. to achieve a process in the best way a specified temperature field $T_e(x, \tau)$ is required and the task is to determine the function $U(\tau)$ which gives $T(x, \tau)$ being very close to $T_e(x, \tau)$.

Transform this model into the well known form of lumped system, so the approximate form is:

$$\frac{d\underline{t}}{d\tau} = \underline{A}\underline{t}(\tau) + \underline{B}\underline{u}(\tau) \quad (5)$$

$$\underline{t}(0) = t_0 \quad (6)$$

$$\bar{\gamma} = \int_0^{\theta} f[\underline{t}(\tau), \tau] d\tau \quad (7)$$

Let us search the solution in the following form:

$$T(x, \tau) = \varphi(x)\psi(\tau), \quad (8)$$

Variation of T with respect to τ is:

$$\delta_{\tau} T(x, \tau) = \varphi(x) \delta\psi(\tau), \quad (9)$$

Using Equ. (9) and (1), one obtains:

$$(\delta_{\tau} T) \frac{\partial T}{\partial \tau} = a \frac{\partial}{\partial x} \left(\frac{\partial}{\partial x} \delta_{\tau} T \right) - a \frac{\partial T}{\partial x} \frac{\partial}{\partial x} \delta_{\tau} T \quad (10)$$

Integrating both sides of equation (10) with respect to x , we obtain:

$$\int_0^L (\delta_{\tau} T) \frac{\partial T}{\partial \tau} dx = a \left[\frac{\partial T}{\partial x} \delta_{\tau} T \right]_0^L - a \int_0^L \frac{\partial T}{\partial x} \frac{\partial}{\partial x} \delta_{\tau} T dx, \quad (11)$$

Considering (2), it is easy to show that:

$$\int_0^L \left[(\delta_{\tau} T) \frac{\partial T}{\partial \tau} + a \frac{\partial T}{\partial x} \frac{\partial}{\partial x} \delta_{\tau} T \right] dx - aU(\tau) \delta_{\tau} T(L, \tau) = 0 \quad (12)$$

Formula (12) with the initial condition is the integral form of the problem described in Equ. (1)-(3).

Let us approach the temperature distribution in the following form:

$$\tilde{T}(x, \tau) = \sum_{i=1}^3 \beta_i(x) t_i(\tau), \quad (13)$$

Let $\beta_i(x)$ functions be polynomial of second degree. In this case they are (see Fig.2):

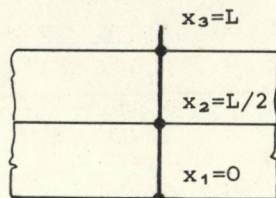


Fig.2.

$$\beta_1(x) = \frac{4}{L^3} \left[\frac{L^2}{2} \frac{L}{2} + \left(\frac{L^2}{4} - L^2 \right) x + \frac{L}{2} x^2 \right], \quad (14)$$

$$\beta_2(x) = \frac{4}{L^3} [L^2 x - L x^2],$$

$$\beta_3(x) = \frac{4}{L^3} \left[\frac{L}{2} x^2 - \frac{L^2}{4} x \right],$$

so

$$\beta_i(x_j) = \begin{cases} 1 & \text{if } i=j \\ 0 & \text{if } i \neq j \end{cases} \quad i, j = 1, 2, 3 \quad (15)$$

Since

$$\begin{aligned} \delta_\tau \tilde{T} &= \sum_{i=1}^3 \beta_i(x) \delta_\tau t_i(\tau), \\ \frac{\partial \tilde{T}}{\partial \tau} &= \sum_{i=1}^3 \beta_i(x) \frac{dt_i}{d\tau}(\tau), \\ \frac{\partial \tilde{T}}{\partial x} &= \sum_{i=1}^3 \frac{d\beta_i}{dx}(x) t_i(\tau), \\ \frac{\partial}{\partial x} \delta_\tau \tilde{T} &= \sum_{i=1}^3 \frac{d\beta_i}{dx}(x) \delta_\tau t_i(\tau), \end{aligned} \quad (16)$$

Using Equ. (12), one obtains:

$$\Omega_1 \delta_\tau t_1(\tau) + \Omega_2 \delta_\tau t_2(\tau) + \Omega_3 \delta_\tau t_3(\tau) = 0 \quad (17)$$

where:

$$\begin{aligned}\Omega_1 &= \left\{ \sum_{j=1}^3 \frac{dt_j}{d\tau} \int_0^L \beta_1 \beta_j dx + a \sum_{j=1}^3 t_j \int_0^L \frac{d\beta_1}{dx} \frac{d\beta_j}{dx} dx \right\}, \\ \Omega_2 &= \left\{ \sum_{j=1}^3 \frac{dt_j}{d\tau} \int_0^L \beta_2 \beta_j dx + a \sum_{j=1}^3 t_j \int_0^L \frac{d\beta_2}{dx} \frac{d\beta_j}{dx} dx \right\}, \\ \Omega_3 &= \left\{ \sum_{j=1}^3 \frac{dt_j}{d\tau} \int_0^L \beta_3 \beta_j dx - aU(\tau) + a \sum_{j=1}^3 \frac{d\beta_3}{dx} \frac{d\beta_j}{dx} dx \right\},\end{aligned}\quad (18)$$

Since variations $\delta_\tau t_i(\tau)$ are independent:

$$\Omega_1 = \Omega_2 = \Omega_3 = 0 \quad (19)$$

so

$$\underbrace{\begin{bmatrix} \alpha_{11} & \alpha_{12} & \alpha_{13} \\ \alpha_{31} & \cdot & \alpha_{33} \end{bmatrix}}_{\underline{A}} \frac{d}{d\tau} \begin{bmatrix} t_1 \\ t_2 \\ t_3 \end{bmatrix} - \underbrace{\begin{bmatrix} 1 & & \\ & 1 & \\ & & a \end{bmatrix}}_{\underline{\Phi}} \begin{bmatrix} 0 \\ 0 \\ U \end{bmatrix} + \underbrace{\begin{bmatrix} \tilde{\beta}_{11} & \tilde{\beta}_{12} & \tilde{\beta}_{13} \\ \cdot & & \\ \tilde{\beta}_{31} & \cdot & \tilde{\beta}_{33} \end{bmatrix}}_{\underline{\beta}} \begin{bmatrix} t_1 \\ t_2 \\ t_3 \end{bmatrix} = \underline{0} \quad (20)$$

where:

$$\begin{aligned}\alpha_{ij} &= \int_0^L \beta_i(x) \beta_j(x) dx, \\ \beta_{ij} &= a \int_0^L \frac{d\beta_i}{dx} \frac{d\beta_j}{dx} dx \\ i, j &= 1, 2, 3\end{aligned}\quad (21)$$

In this way:

$$\underline{\underline{A}} = -\underline{\underline{A}}^{-1}\underline{\underline{B}}, \quad (22)$$

$$\underline{\underline{B}} = \underline{\underline{A}}^{-1}\underline{\underline{D}}, \quad (23)$$

Initial condition:

$$t_i(0) = T_o(x_i), \quad i=1,2,3 \quad (24)$$

In order to change the form of the functional (4) one can use Equ. (13) and (21), so:

$$f[\underline{\underline{t}}(\tau)\tau] = \lambda(\tau) - \sum_{i=1}^3 (2\gamma_i - \sum_{j=1}^3 \alpha_{ij} t_j(\tau)) t_i(\tau), \quad (25)$$

where:

$$\gamma_i(\tau) = \int_0^L \beta_i(x) T_e(x, \tau) dx, \quad (26)$$

$$\lambda(\tau) = \int_0^L T_e^2(x, \tau) dx, \quad (27)$$

So, we could transform the original problem (1)-(4) into (5)-(7).

GENERALIZATION OF THE METHOD

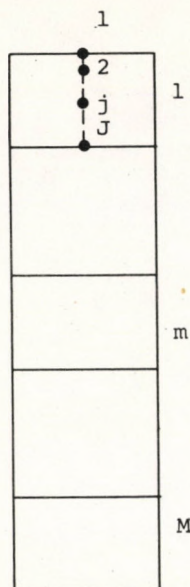
The method mentioned above can also be applied in more complicated cases. Let the equations to be investigated be:

$$\frac{\partial u}{\partial \tau}(x_i, \tau) + \frac{\partial}{\partial x_i} \left[a(x_i, \tau) \frac{\partial u}{\partial x_i} \right] + b_1(x_i, \tau) = 0, \quad (28)$$

$$x_i \in V$$

Boundary condition is:

$$\frac{\partial u}{\partial x_i} + b_2(\tau) = 0, \quad x_i \in S \quad (29)$$



Initial condition is:

$$U(x_i, t_0) = S(x_i), \quad (30)$$

One can improve the approximation by increasing the number of the intervals dividing the region of x and using polynomial of second degree in every interval (see Fig.3).

Then the approaching function is:

$$T_m(x, \tau) = \sum_{j=1}^{j=3} \beta_j(x) t_j(\tau), \quad (31)$$

$$m = 1, 2, \dots, M$$

Fig.3.

where

$$\begin{aligned} \beta_1(x) &= \frac{1}{\Delta} \left[x_2 x_3 (x_3 - x_2) + (x_2^2 - x_3^2)x + (x_3 - x_2)x^2 \right], \\ \beta_2(x) &= \frac{1}{\Delta} \left[x_1 x_3 (x_1 - x_3) + (x_3^2 - x_1^2)x + (x_1 - x_3)x^2 \right], \\ \beta_3(x) &= \frac{1}{\Delta} \left[x_1 x_2 (x_2 - x_1) + (x_1^2 - x_2^2)x + (x_2 - x_1)x^2 \right], \end{aligned} \quad (32)$$

$$\Delta = (x_2 - x_1)(x_3 - x_2)(x_3 - x_1)$$

The approaching differential equations are:

$$\alpha_{ij} \frac{dt_j}{d\tau} + \beta_{ij} t_j + \gamma_i = 0 \quad \begin{matrix} m = 1, 2, \dots, M \\ i, j = 1, 2, \dots, j = 3 \end{matrix} \quad (33)$$

where:

$$\begin{aligned}
 \alpha_{mij} &= \beta_{mi} \beta_{mj} dV_m \\
 \tilde{\beta}_{mij} &= - \int_{V_m} a_m (\nabla \cdot \beta(x))_i (\nabla \cdot \beta(x))_j dV_m \\
 \gamma_{mi} &= \int_{V_m} \beta_{mi}(x) b_1 dV_m - \int_{S_m} \beta_{mi}(x) b_2(\tau) n_m dS_m
 \end{aligned} \tag{34}$$

CONCLUSIONS

A method is presented for approaching analysis for distributed systems, which provides a possibility to transform the model equations into ordinary differential equations.

The advantages of this model appearing clearly from the example given as an illustration are: simplicity, good approximation and suitable structure for investigating optimal control as well as identification problems.

SYMBOLS USED

- a - thermal diffusivity, (m^2/h)
- k - thermal conductivity, ($kcal/mh^\circ C$)
- q - heat flux, ($kcal/m^2h$)
- u - variable,
- x - co-ordinate, (m)

- L - thickness of slab, (m)
- $U=q(\tau)/k$ - decision function, ($^\circ C/m$)
- T - temperature, ($^\circ C$)
- \tilde{T} - approaching function of temperature, ($^\circ C$)
- V - volume, (m^3)
- S - surface, (m^2)

Greek letters

$\beta_i(x)$, $\varphi(x)$, $\psi(\tau)$, $t_i(\tau)$ - functions, def. Equ. (8) and (13)

τ - time, h

$\delta_\tau(')$ - variation with respect to τ

θ - total time of the process, h

Γ - functional, def. Equ. (4)

Index

o - initial value

e - prescribed value

m,j,i - index of the sections

REFERENCES

- [1] FATTORINI, H.O.: SIAM J. Control, 1975, 1
- [2] COWLES, D.E.: Optimization Theory and Applications, 5, 300 (1972)
- [3] ZADEH, L.A., POLAK, E.: Rendszerelmélet. (System Theory) Budapest, Műszaki Könyvkiadó, 1972
- [4] HIH, S., HHU, C. and LEECH, W.J.: A Discrete Method to Heat Conduction Problems. 5th International Heat Transfer Conference, Tokyo, 1975. Cu.2.4.

РЕЗЮМЕ

Одной из возможностей приближенного решения моделей с распределенными параметрами, т.е. описанных парциальными дифференциальными уравнениями, а также проблем их управления, устойчивости и идентичности, является приближение модели с помощью системы обычных дифференциальных уравнений. Приведен метод определения такой приближенной системы уравнений, который по существу основан на видоизмененной форме конечных элементов.

SOLUBILITY OF GASES IN NORMAL-ALKANES

J. MAKRANCZY, Mrs. K. MEGYERY-BALOG, L. RUSZ and L. PATYI

(Institute of General and Inorganic Chemistry,
University of Chemical Engineering, Veszprém, Hungary)

Received: September 14, 1976

Solubilities of a number of gases were determined in members of the n-pentane — n-hexadecane series. Relationships between gas solubilities and physico-chemical properties of members of the series were studied.

It was found that gas solubilities varied linearly in the function of reciprocal parachor values of the solvents, and the slopes of the lines were proportional to the sizes and mean polarizabilities of the gases dissolved.

An equation was derived to calculate solubilities of apolar and moderately polar gases in n-alkanes. The equation is not applicable for polar gases, because the interactions between the gas and liquid molecules cannot be neglected in such cases.

It is well known that members of homologous series in organic chemistry display certain regularities - frequently characterized by mathematical relationships - as far as some of their physico-chemical properties are concerned. The relationship describing the change of a certain property of the homologous series is generally not a simple, linear, but more complicated - though formulatable - relationship. Because the solubility of a given gas

depends on both the gas and the solvent, the hypothesis stating the existence of a relationship between the solubility values obtained in a homologous series and the carbon number of the members of the series seemed reasonable. This hypothesis is supported by the work of SEYMOUR and SOSA [1], who stated that the solubility parameters defined by HILDEBRAND and SCOTT [2, 3], known in the literature as cohesive energy density (CED), are linear functions of the logarithms of the carbon numbers.

Some of the regularities found in the course of studies on the solubility of gases in members of the normal-alkane homologous series are presented here.

1. EXPERIMENTAL

There are only a very limited number of gas solubility data measured in normal-alkanes available in literature. Therefore, solubilities of 15 gases in 12 members of the normal-alkane series were determined. The first member of the series was n-pentane, the last one n-hexadecane (C_5 through C_{16}). Measurements were carried out at a constant 25 °C temperature. (Later on, solubility values were also obtained at 40 °C to check the validity of the relationships derived at 25 °C.)

Gas solubility measurements were carried out - as usual - in the saturation apparatuses [4]. Partial pressure of the component to be dissolved was always kept at 760 torr in the equilibrium mixture, so the gas solubility values are reported as Ostwald coefficients. Analytical grade reagents of Hungarian and foreign origin were used (both liquids and gases). In those few cases where literature data were available, the measured values agreed to them within $\pm 4\%$. An absolute error of $\pm 3\%$ was calculated for the measurements made.

2. DISCUSSION

Studying the solubility data two general conclusions can be made:

- solubility of a given gas (expressed either as Ostwald or Bunsen coefficient) decreases with the increasing carbon number
- solubility of apolar gases in a given n-hydrocarbon increases with increasing molecular size of the gas (a similar tendency can also be noted with polar gases).

Parachors of the members were used to take into consideration the properties of the homologous series. There are a number of factors compounded in the parachor value, each of which are significantly influence solubility; it can be used over a wide temperature range, its values are sums of increments and so the value is easily calculated.

Solubilities of the gases studied were plotted as functions of the reciprocal parachors of the n-alkanes (Figure 1a and 1b). The following conclusions were drawn:

- There is a linear relationship between the gas solubilities and the reciprocal parachors of the members of the n-alkane series - except for the value of ammonia. Extrapolated lines of the apolar gases meet in the origin. Lines of the moderately polar gases also tend to here, at least within the limits of experimental error. Lines of the strongly polar gases have positive interception values. (It follows that in the case if apolar and moderately polar gases, zero gas solubility would be found in n-hydrocarbons containing an infinitely large number of carbon atoms, while even in this case there would be some solubility for the strongly polar gases, such as SO_2 and H_2S .)
- Slopes of the gas solubility lines are different for each gas, the bigger or more polarizable the gas molecules, the bigger the slope values.

There are two significant consequences of the above two observations:

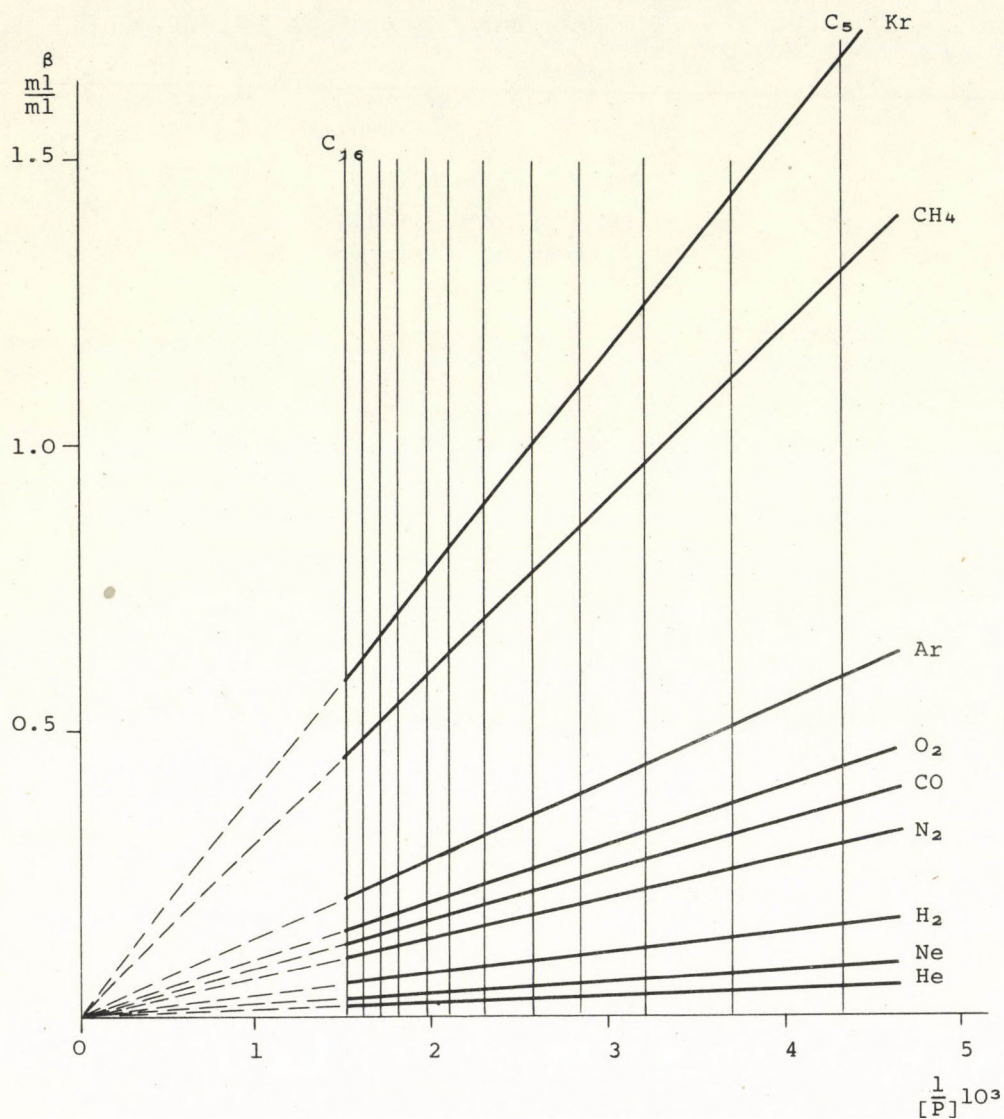


Fig. 1a. Relationship of Gas Solubility and Parachors of n-Alkanes

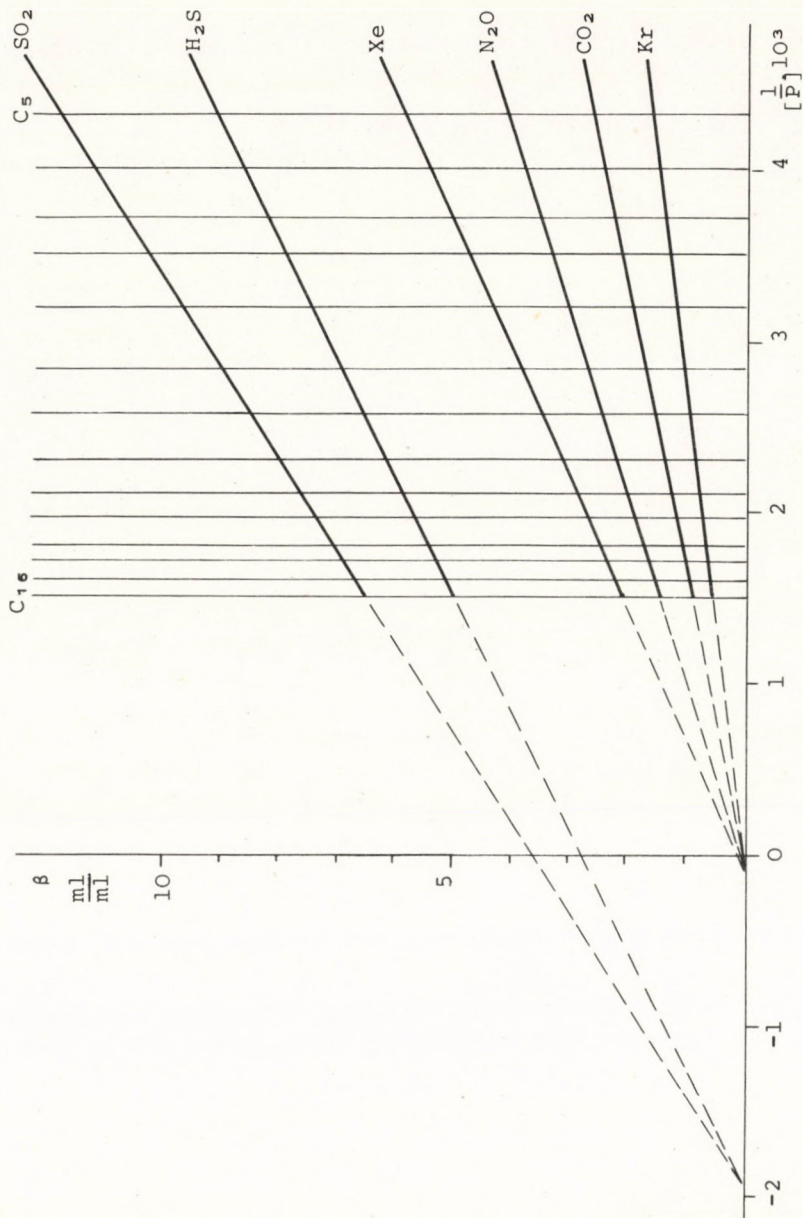


Fig. 1b. Relationship of Gas Solubility and Parachors of n-Alkanes

- a) The following relationship holds for the solubility of apolar gases measured in the n-alkane series:

$$\beta_n [P]_n = \text{constant}$$

where:

β_n is the solubility of the apolar or moderately polar gas in the n^{th} member of the series,
 $[P]_n$ is the parachor value of the n-alkane proper.

The relationship for the more polar gases can only be formulated if the intercepts are known:

$$(\beta-b)[P] = \text{constant}$$

where:

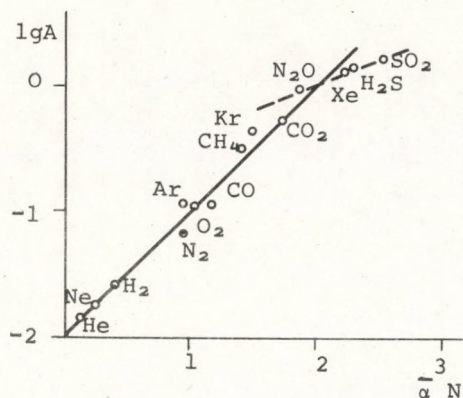
b is the intercept of the line.

- b) The practical value of the relationship mentioned in a), is that once the solubility of an apolar or moderately polar gas is known in any member of the series, the solubility found in the remainder can be calculated. (The same value for polar gases can only be calculated from two known data.)

As it was previously mentioned, slopes of the lines increase with increasing polarizability, therefore the relationship between the mean polarizability and the slope value was studied. (Because parachors are expressed as functions of the solvent molar volumes, $[P] = V\sigma^{1/4}$, the mean polarizability referring to one mole gas was used. The following simple relationship was graphically obtained between the slope (A) and mean polarizability data ($\bar{\alpha}$):

$$\lg A = k\bar{\alpha}N - 2$$

(where N is the Avogadro number, k is a proportionality constant). This is graphically shown in Figure 2.



Using the co-ordinates given in Figure 1, solubilities of apolar and moderately polar gases are given by the following equation:

$$\beta = \frac{A}{[P]} 10^3$$

As $\lg A = k\bar{\alpha}N - 2$, the above equation can be rearranged:

$$\lg \beta = 1 + k\bar{\alpha}N - \lg[P]$$

Fig. 2. Relationship of slopes and mean gas polarizabilities

Dimensional analysis was used to show that k was no dimensionless, but had the dimension of $(\text{dyn/cm})^{\frac{1}{4}}$, i.e. it could be derived from interfacial tension. Thus the interfacial tension measured between the gas and its liquid form was taken at the 1/4-th power and substituted into the equation, which took the following final form:

$$\lg \beta = 1 + \sigma_g^{\frac{1}{4}} \bar{\alpha}_g N - \lg[P]_1$$

Using the above equation the Ostwald coefficients were calculated and compared to the ones measured. Deviation was expressed as a relative error in the usual manner:

$$\% \text{ Rel. error} = \frac{\beta_{\text{measured}} - \beta_{\text{computed}}}{\beta_{\text{measured}}} \times 100$$

(Parachor values were taken from ALTENBURG's paper [6], while the mean polarizability values were obtained from the book of HIRSCHFELDER et al [5]. Interfacial tension values for gases were obtained from handbooks or if not available, they were calculated by an approximative method [9].

Data measured and obtained by the derived equation are shown in Table 1. Relative deviations are also shown.

Table 1. Solubility of gases in n-alkanes at 25 °C

Gas sol- vent	He			Ne			Ar			Kr		
	β meas.	β calc.	Rel. de- viation	β meas.	β calc.	Rel. de- viation	β meas.	β calc.	Rel. de- viation	β meas.	β calc.	Rel. de- viation
C5	0,055	0,0498	9,38	0,087	0,0853	1,95	0,600	0,5814	3,10	1,668	1,670	0,13
C6	0,044	0,0425	3,29	0,076	0,0728	4,21	0,477	0,4964	-4,07	1,411	1,425	-0,97
C7	0,044	0,0362	17,72	0,069	0,0634	8,11	0,418	0,4322	-3,35	1,229	1,241	-0,98
C8	0,037	0,0328	11,32	0,057	0,0562	1,40	0,373	0,3827	-2,60	1,095	1,099	-0,42
C9	0,028	0,0295	-5,50	0,047	0,0506	-7,65	0,338	0,3446	-1,95	0,988	0,990	-0,11
C10	0,025	0,0268	-7,16	0,045	0,0458	-1,77	0,305	0,3126	-2,49	0,886	0,898	-1,32
C11	0,022	0,0245	-11,27	0,043	0,0419	2,55	0,296	0,2856	3,51	0,825	0,821	0,57
C12	0,022	0,0226	-2,64	0,040	0,0386	3,50	0,263	0,2635	-0,19	0,756	0,757	-0,07
C13	0,019	0,0209	-10,11	0,036	0,0358	0,55	0,247	0,2440	1,21	0,700	0,701	-0,20
C14	0,017	0,0195	-14,59	0,033	0,0330	0,00	0,230	0,2273	1,17	0,657	0,653	0,62
C15	0,016	0,0182	-14,06	0,031	0,0312	0,64	0,218	0,2130	2,29	0,625	0,612	0,99
C16	0,015	0,0172	-14,53	0,027	0,0291	7,77	0,206	0,2004	2,81	0,583	0,576	1,22
<hr/>												
	Xe			H2			N2			O2		
	β meas.	β calc.	Rel. de- viation	β meas.	β calc.	Rel. de- viation	β meas.	β calc.	Rel. de- viation	β meas.	β calc.	Rel. de- viation
C5	5,916	5,906	0,16	0,142	0,156	-9,85	0,306	0,299	2,25	0,432	0,428	0,97
C6	5,065	5,042	0,45	0,120	0,134	-11,66	0,262	0,255	2,56	0,368	0,365	0,76
C7	4,432	4,390	0,94	0,109	0,116	-6,42	0,229	0,222	2,93	0,322	0,318	1,21
C8	3,897	3,888	0,22	0,096	0,103	-7,29	0,199	0,197	1,06	0,284	0,282	0,85
C9	3,493	3,501	-0,23	0,088	0,093	-5,68	0,178	0,177	0,39	0,258	0,254	1,71
C10	3,165	3,175	-0,30	0,081	0,084	-3,70	0,156	0,161	-3,08	0,231	0,230	0,43
C11	2,914	2,901	0,46	0,079	0,077	2,53	0,146	0,147	-0,62	0,211	0,210	0,38
C12	2,685	2,676	0,34	0,078	0,071	8,84	0,132	0,136	-2,65	0,199	0,194	2,56
C13	2,478	2,479	-0,05	0,074	0,065	12,16	0,124	0,126	-0,81	0,179	0,180	-0,39
C14	2,314	2,310	0,17	0,064	0,061	4,68	0,116	0,117	-0,88	0,170	0,167	1,67
C15	2,150	2,265	-5,33	0,062	0,067	8,06	0,111	0,109	1,35	0,152	0,157	-3,09
C16	2,019	2,036	-0,83	0,060	0,054	10,00	0,102	0,103	-1,08	0,145	0,148	-1,72

Table 1. (continued)

Gas sol- vent	CH ₄			CO ₂			H ₂ S
	β meas.	β calc.	Rel. de- viation	β meas.	β calc.	Rel. de- viation	β meas.
C ₅	1,279	1,282	-0,24	2,685	2,599	3,20	9,147
C ₆	1,146	1,095	4,46	2,270	2,236	1,50	8,230
C ₇	0,956	0,953	0,28	1,976	1,947	1,47	7,520
C ₈	0,849	0,844	0,58	1,746	1,724	1,26	6,986
C ₉	0,762	0,760	0,20	1,550	1,552	-0,01	6,560
C ₁₀	0,693	0,690	0,52	1,397	1,408	-0,79	6,232
C ₁₁	0,633	0,630	0,47	1,227	1,287	-0,78	5,949
C ₁₂	0,586	0,581	0,84	1,179	1,188	-0,76	5,698
C ₁₃	0,541	0,538	0,55	1,091	1,099	-0,73	5,501
C ₁₄	0,508	0,502	1,18	1,015	1,024	-0,90	5,305
C ₁₅	0,474	0,470	0,82	0,950	0,959	-0,95	5,152
C ₁₆	0,448	0,442	1,18	0,895	0,903	-0,89	4,999

	CO			N ₂ O			SO ₂
	β meas.	β calc.	Rel. de- viation	β meas.	β calc.	Rel. de- viation	β meas.
C ₅	0,395	0,354	10,51	4,093	4,582	-11,94	11,876
C ₆	0,329	0,302	8,27	3,471	3,568	-2,79	10,876
C ₇	0,282	0,263	6,81	3,034	3,106	-7,20	9,790
C ₈	0,234	0,233	0,56	2,729	2,751	-0,81	9,092
C ₉	0,217	0,210	3,41	2,478	2,477	-0,01	8,558
C ₁₀	0,191	0,190	0,47	2,270	2,247	1,01	8,110
C ₁₁	0,177	0,174	1,86	2,063	2,053	0,48	7,826
C ₁₂	0,166	0,160	3,49	1,877	1,894	-0,91	7,444
C ₁₃	0,151	0,148	1,72	1,779	1,754	1,41	7,182
C ₁₄	0,136	0,138	-1,62	1,637	1,634	0,18	6,942
C ₁₅	0,128	0,129	-1,17	1,550	1,530	1,29	6,735
C ₁₆	0,120	0,122	-1,50	1,484	1,440	2,96	6,571

Table 2. Solubility of gases in n-alkanes at 40 °C

Gas sol-vent	Ar			N ₂			O ₂		
	$\beta_{\text{meas.}}$	$\beta_{\text{calc.}}$	Rel.de- viation	$\beta_{\text{meas.}}$	$\beta_{\text{calc.}}$	Rel.de- viation	$\beta_{\text{meas.}}$	$\beta_{\text{calc.}}$	Rel.de- viation
C ₅	0.462	0.433	1.34	0.266	0.241	9.40	0.362	0.339	6.35
C ₆	0.390	0.370	5.13	0.223	0.206	7.62	0.291	0.289	0.69
C ₇	0.333	0.322	3.30	0.180	0.179	0.55	0.264	0.251	4.92
C ₈	0.292	0.285	2.40	0.161	0.159	1.24	0.229	0.223	2.62
C ₉	0.265	0.257	3.02	0.145	0.143	1.38	0.200	0.201	-0.5
C ₁₀	0.231	0.233	-0.87	0.131	0.130	0.76	0.183	0.182	0.55
C ₁₁	0.214	0.213	0.47	0.122	0.119	2.46	0.165	0.163	1.21
C ₁₂	0.196	0.196	-	0.105	0.109	-3.81	0.153	0.153	-
C ₁₃	0.181	0.182	-0.55	0.100	0.101	-1.00	0.144	0.142	1.39
C ₁₄	0.169	0.169	-	0.092	0.092	-	0.131	0.132	-0.76
C ₁₅	0.160	0.158	1.25	0.085	0.088	3.53	0.126	0.124	1.59
C ₁₆	0.143	0.149	-4.20	0.081	0.082	1.23	0.119	0.116	2.52
<hr/>									
	CO ₂			N ₂ O			$\beta_{\text{meas.}}$		
	$\beta_{\text{meas.}}$	$\beta_{\text{calc.}}$	Rel.de- viation	$\beta_{\text{meas.}}$	$\beta_{\text{calc.}}$	Rel.de- viation	$\beta_{\text{meas.}}$	$\beta_{\text{calc.}}$	Rel.de- viation
C ₅	2.175	2.140	1.61	3.688	3.642	1.24	6.93	8.90	
C ₆	1.858	1.827	1.67	3.146	3.109	1.18	6.23	8.02	
C ₇	1.602	1.555	2.98	2.712	2.707	0.18	5.69	7.34	
C ₈	1.420	1.409	0.77	2.415	2.398	0.73	5.28	6.82	
C ₉	1.275	1.266	0.71	2.153	2.159	-0.28	4.96	6.40	
C ₁₀	1.151	1.150	0.09	1.952	1.958	-0.31	4.71	6.08	
C ₁₁	1.051	1.051	-	1.803	1.789	0.77	4.50	5.81	
C ₁₂	0.969	0.970	-0.1	1.655	1.651	0.24	4.31	5.56	
C ₁₃	0.892	0.899	-0.78	1.528	1.529	0.07	4.15	5.36	
C ₁₄	0.835	0.837	0.24	1.421	1.391	2.11	4.02	5.18	
C ₁₅	0.782	0.784	0.26	1.323	1.334	-0.83	3.89	5.04	
C ₁₆	0.733	0.738	0.68	1.255	1.255	-	3.80	4.90	

It can be seen that there is a rather good agreement between the measured and calculated values in the case of apolar and moderately polar gases. This is especially true for the gases with accurately known parameters, such as CO_2 , CH_4 , Xe, Kr and O_2 . The greatest deviation occurs in the cases where the interfacial tension was obtained from approximations and where the other constants required for the calculation were rather uncertain. Such gases were helium and neon. Solubilities of two polar gases were not calculated (H_2S and SO_2), because these gases had positive interceptions and further research is needed to determine their meaning and true numerical values. It is worth noting that other gas solubility measurements of the authors - such as those obtained with n-alcohols - proved that the interactions must not be neglected in the case of apolar - polar and polar -polar gas -liquid systems.

As mentioned earlier, further measurements were made at 40°C to check the validity of the relationships obtained. Calculated values were compared to those measured. It was found that the appropriately derived equation also described the solubilities at 40°C . There was only a slight deviation between the calculated and measured data, shown in Table 2. Again no calculations were made in the case of H_2S and SO_2 because to do so would involve the interception values. This problem will be reviewed in a later paper.

REFERENCES

- [1] SEYMOUR, R.B., SOSA, J.M.: Nature (London), 248 759 (1974)
- [2] HILDEBRAND, J., SCOTT, R.: Solubility of Nonelectrolytes. 3rd ed., Reinhold, New York, 1949.
- [3] HILDEBRAND, J., SCOTT, R.: Regular Solutions. Prentice Hall, Englewood Cliffs, New Jersey, 1962.
- [4] BODOR, E., BOR, Gy., MOHAI, B. and SIPOS, G.: Veszprémi Vegyipari Egyetem Közleményei, 1 55 (1957)
- [5] HIRSCHFELDER, J.O., CURTISS, C.F. and BIRD, R.B.: Molecular Theory of Gases and Liquids. J.Wiley and Sons, New York, 1954.
- [6] ALTENBURG, K.: J. Chem., 2 328 (1962)
- [7] D'ANS, J., LAX, E.: Taschenbuch für Chemiker und Physiker, Springer Verlag, Berlin-Göttingen-Heidelberg, 1949.
- [8] NIKOLSKI, B.P.: Handbuch des Chemikers, VEB Verlag Technik, Berlin, 1956.
- [9] HECHT, G.: Gázok, folyadékok termodinamikai anyagi jellemzőinek számítása. (The Calculation of Thermodynamic Characteristics of Gases and Liquids.). Műszaki Könyvkiadó, Budapest, 1972.

РЕЗЮМЕ

Экспериментальным путем определялась растворимость многих газов в членах гомологического ряда нормальный пентан - нормальный гексан, исследовалось, какая зависимость имеется между растворимостью и химическими свойствами жидкостей данного гомологического ряда.

Установлено, что в зависимости от обратного числа паракорных значений растворителей растворимость газов изменяется линейно и тангенс таких полученных прямых пропорционален размеру растворимой молекулы и ее средней поляризуемости.

Из рассмотренных систем газ - жидкость для типа неполярных - полярных и слабо полярных - неполярных выведено уравнение, с помощью которого может быть рассчитана растворимость газов в нормальных алканах. Это уравнение для полярных газов неприменимо поскольку в таком случае взаимодействие между молекулами газа и жидкости уже нельзя отбросить.

Авторы приводят в виде таблиц результаты, полученные экспериментальным и расчетным путем.

CLASSIFICATION OF NON-CATALYTIC HETEROGENEOUS
GAS-LIQUID AND LIQUID-LIQUID REACTIONS

T. BLICKLE and E. NAGY

(Research Institute for Technical Chemistry of
the Hungarian Academy of Sciences, Veszprém)

Received: September 30, 1976.

Heterogeneous chemical reactions occurring in gas-liquid and liquid-liquid systems are treated according to the principles of system-theory developed in the Research Institute for Technical Chemistry of the Hungarian Academy of Sciences. Classification of the reactions mentioned and the number of their possible variants are given by six property-classes. The extended Damköhler equations are presented using the system of component balance equations of the heterogeneous reactions. The transfer terms in these equations are presented by separate balance equations.

The diffusion expression relating to the laminar film formed between the phases is solved in the case of first order reactions; balance equations relating to the bulk phases and the transfer terms of these equations are presented using reaction kinetical and transfer kinetical parameters.

A number of non-catalytical reactions occur in more than one phase. The extension of intensive technologies over the past decades emphasized the significance of industrial processes occurring in more than one phase. This and their varied nature necessitate their classification. Heterogeneous chemical reaction occurring in gas-liquid and liquid-liquid systems were treated using the system

theory developed in the Research Institute for Technical Chemistry of the Hungarian Academy of Sciences [1]. The system of balance equations describing the systems mentioned in presented [2].

Mass transfer coupled to chemical reaction is one of the phases of gas-liquid and liquid-liquid systems dealt with here. According to the criteria of heterogeneous reactions, one or more of the reacting components are to be found simultaneously in two phases, and one or more of the reacting components are subject to mass transfer, eventually arriving into the very phase where chemical reaction takes place.

Consider a classification of the heterogeneous reactions based on property-classes formed from different properties [1], where an "element-group" structure-element [1], formed from one respective element of each of the property-classes is used to denote a heterogeneous reaction determined by the property elements. Compositions of respective elements of property-classes from a possible classification of the heterogeneous reactions. Subjectivity of this classification is the result of the multitude of ways used to determine element classes.

Before carrying out this classification let us define the terms external and internal components, used there. Components are termed external components if, on the one hand, they do not participate in the mass transfer process (or rather, even if they participate, it is not taken into consideration because due to the definition of equilibrium, each component is subject more or less to phase changes), i.e. they are genuine inert components; and on the other hand, if their concentrations (or in the case of pure phases, their quantities) are so vast that any changes caused by chemical reactions have a negligible effect on mass transfer. No balance equation has to be formulated for such compounds, because their concentrations or mass rates are constant. Their effects - if acting as one of the parties in the chemical reaction - can be taken into consideration via the rate constants (e.g. pseudo n^{th} -order kinetics). Obviously, if an external component is subjected to phase change it becomes an internal component in the other phase.

Components with changing concentrations or quantities are

called internal quantities. Balance equations have to be formulated for each of them. According to the previous discussion, the following six property-classes are defined: the chronology of the "life" of the component is followed in the classification, i.e. components are followed from the formation of phases to the reaction.

a). Construction of phases: Constructing phases from the two types of components, namely external and internal, the following property-class elements are identified:

1. $K_f B_{sz}$ - solution
2. $K_f B_f$ - mixture
3. $K_f B_g$ - solution
4. K_f - liquid of one component
5. B_f - liquid of one component
6. $K_g B_g$ - mixture
7. K_g - gas of one component
8. B_g - gas of one component

No distinction is made between gas and vapour. The number of components is not limited, i.e. phases with one and/or more external components were not distinguished (e.g. classification of a homogeneous phase consisting of 3 components and considering the ratios of the components as well, is presented in [1]. Ratio of the components is taken care of, in this case, in the distinction made between external and internal quantities).

b). Contact mode of the phases.

This point is not treated here, a detailed discussion can be found in the reference [1]. This classification presents the possible constructions of operation units and apparatuses determining the contact modes of the phases.

c). Direction of mass flow between phases.

1. Liquid → gas
2. Gas ← liquid
3. Liquid - gas

As mentioned before, any of the components of the phases can enter the mass-transfer process, so optionally several simultaneous component transfers have to be considered. Components subject to a phase change must enter chemical reactions in the receiving phase, or if component transfer is bidirectional, chemical reactions can occur in both phases.

d). Classification of chemical reactions according to the number of reactions and their time-dependence:

Overall equations of the reactions taking place are considered in the classification process. Thus elementary reaction partners, radicals, and immediately decomposing intermediates occurring in the elementary steps of the reaction mechanisms are not taken into consideration.

Reactions are distinguished as follows:

1. Parallel reactions
2. Consecutive reactions
3. Single reaction.
4. Parallel and consecutive reactions.

The number of elements in this property class is $2 + (p + q) + pq$ where: pq is the possibility of the co-existing occurrences of the parallel and consecutive reactions, also taking into consideration the number of reactions. 2 stands for the heterogeneous chemical reaction consisting of one reaction consisting of one reaction proper ($p > 1$ and $k > 1$).

e). Thermostatic classification of chemical reactions

1. Non-equilibrium reactions
2. Equilibrium reactions.

f). Classification of chemical reactions according to the number of reactants and components formed.

This property-class classifies chemical reactions according to the number of reactants formed in the reactions proper. Considering that one or more reactants resident in the absorbent phase can enter a reaction, with one or more components taking part in phase changes and the number of products can change as well, the total number of reactions is $f_{k=1}$ [1]. In addition, considering that the stoichiometric coefficient of a component can also assume

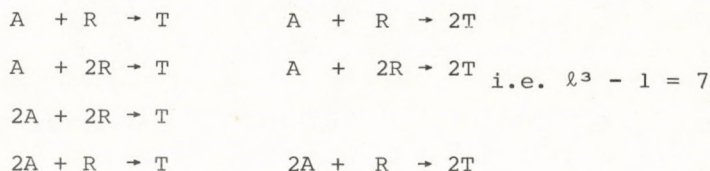
values greater than 1 (any integer up to the maximal value of ℓ), the number of the reaction is significantly increased:

$$f_{\ell=1} = (2+3+\dots+(m+n+t))(m+n+t) - (1^2+2^2+\dots+(m+n+t-1)^2) \quad (1)$$

With given m , n and t values changing the stoichiometric coefficient between 1 and ℓ , the number of possible reactions is as follows:

$$\begin{aligned} f &= \ell^{m+n+t} - z \\ z &= \ell - 1, \quad \ell < 4 \\ z &= 2^{m+n+t} \quad 4 \leq \ell < 8 \end{aligned} \quad (2)$$

E.g., if $m = 1$, $n = 1$, $t = 1$ and $\ell = 2$, the possible reactions:



If values of m , n and t can change between 1 and the given figures, the number of the totally possible reactions is obtained by summing f values:

$$f_{\ell} = \sum_{m+n+t=2}^{m+n+t} (f_{\ell=1}) \ell^{m+n+t} - z \quad \begin{matrix} m \neq 0 \\ t \neq 0 \end{matrix} \quad (3)$$

The number of reversible reactions is equal. If consecutive reactions can also take place, their intermediates increase the value of m while effecting t as well.

The reaction-order as a property class is not treated in detail, because the number of components and the kinetics are rarely independent; thus in general, the number of components also determines the reaction-order. Consequently no finer classification of the reactions could be obtained according to the reaction-order.

Eventually, six property-classes were used to classify the heterogeneous reactions. The Descartes-multiples of the elements of each of the property classes of a chemical reaction defined the chemical reaction considered, (only one, but at least one element of each of the property-classes belong to the heterogeneous reactions).

Thus, the total number of heterogeneous reactions obtainable from this classification scheme is:

$$4 \times 4 \times 3 \times (2 + p + q + p \times q) \times f_{\ell}.$$

BALANCE EQUATIONS OF THE HETEROGENEOUS REACTIONS

Although a classification of the operation units - unambiguously influencing the mathematical relationships used in the description - was omitted, nevertheless, the balance equation system of heterogeneous reactions is given as one deduced from general principles, and from this system the mathematical models best fitting certain discrete variants, are obtained. The mathematical description starts from the extended Damköhler equation describing the component flow. No heat equation is formulated, because the system is thought to be isotherm, and no impulse equations are obtained.

Two of the terms of the extended component Damköhler equation were modified to facilitate a more convenient description of the balance equations of heterogeneous chemical reactions. Turbulence of the phases is taken care of via the mixing coefficient of the conductive term - it is widely applied in the literature mentioned [4, 5]; the transfer term of the Damköhler equation - the transfer coefficient and the driving force - is given by physico-chemical and reaction kinetical characteristics using the two-film theory. It is assumed that there is merely a diffusion flow through the films formed at the contact surfaces of the phases, and the convection and local changes, dependent in the direction of flows of the phases, are neglected. Accordingly, separate balance equations are constructed for the films and by solving them, the relationships giving the transfer coefficient and the driving force are obtained.

Transfer coefficients are considerably influenced by the chemical reactions, and in general the driving forces also change and are not equal to the differences of bulk phase concentrations.

In principle, a balance equation has to be obtained for each of the components influencing the heterogeneous reaction. No balance equation is written for the external components or for the products formed, because their quantities are given by the concentration changes of the reactants. Reaction products that also act as reactants are considered internal components, while products participating in phase changes are considered absorbing components.

The balance equations relating to laminar films are:

a) For components subject to phase changes:

$$\operatorname{div} (D_i^A \operatorname{grad} C_i^A) - \sum_{j=1}^j \ell_{ij}^A G_{ij}^A = 0 \quad (4)$$

b) For reactants:

$$\operatorname{div} (D_i^R \operatorname{grad} C_i^R) - \sum_{j=1}^j \ell_{ij}^R G_{ij}^R = 0 \quad (5)$$

where: $G_{i,j}^A = r_j^A (C_a^A C_r^R)$ $a = 1, 2, \dots, m$
 $r = 1, 2, \dots, n$

Similarly, $G_{i,j}^R$ values can be expressed. If j denotes the same reaction and $\ell_{ij}^A = \ell_{ij}^R$ then obviously $G_{ij}^A = G_{ij}^R$. The G value that also contains the reaction kinetics, shows which reactions are independent and which are dependent, at the same time, also determining the interdependence of the balance equations. Flow densities in a given point of the contacting surfaces can be obtained from Equation (4) (see Equation), along with the transfer flow densities entering the bulk phases through the film of δ thickness (see Equation 7). These equations can be applied for both phases. If no chemical reaction takes place, the two flows are equal.

$$J_i^{oA} = -D^A \frac{\partial C_i^A}{\partial \bar{r}} \bigg|_{\bar{r}=\bar{r}_0} \quad (6)$$

$$J_i^{\delta A} = -D^A \frac{\partial C_i^A}{\partial \bar{r}} \bigg|_{\bar{r}=\bar{r}_O+\delta} \quad (7)$$

Integrating the above equations, the total quantity transferred can be obtained.

Balance equations relating to the bulk phase are as follows:

a). Absorbent phase:

$$\begin{aligned} -\operatorname{div} K_1 \operatorname{grad} C_{oi}^A \pm \operatorname{div} C_{oi}^A \times v + J_i^{\delta A} \omega - \sum_{j=1}^j \ell_{ij}^A G_{ij}^A &= \\ &= \frac{\partial C_{oi}^A}{\partial t} \end{aligned} \quad (8a)$$

$$-\operatorname{div} K_1 \operatorname{grad} C_{oi}^R \pm \operatorname{div} C_{oi}^R \times v - \sum_{j=1}^j \ell_{ij}^R G_{ij}^R = -\frac{\partial C_{oi}^R}{\partial t} \quad (8b)$$

b). Component donor phase:

$$-\operatorname{div} K_2 \operatorname{grad} C_{oi}^A \pm \operatorname{div} C_{oi}^A \times v - J_i^{\delta A} \omega = -\frac{\partial C_{oi}^A}{\partial t} \quad (9)$$

The above equations are obtained for each of the internal components. Solving the independent relationships thus obtained, the concentration relationships describing the components proper are obtained.

Equations (4) and (5) are solved under the boundary conditions

$$\bar{r} = \bar{r}_O \quad C_i^A = C_i^{xA} \quad \frac{\partial C_i^R}{\partial \bar{r}} = 0 \quad (10a)$$

$$\bar{r} = \bar{r}+ \quad C_i^A = C_{oi}^A \quad C_i^R = C_{oi}^R \quad (10b)$$

Boundary and initial conditions can similarly be given for the bulk phase as well [3].

The balance equations obtained are shown below in connection with two examples, by solving the balance equations of the film [Equations (4) and (5)] and giving the transfer flow densities [Equations (6) and (7)] in the case of a one-dimensional model.

The direction of the diffusional mass transfer in the film is thought to be perpendicular to the direction of convection and concentration changes in the bulk phases.

Consider the $A \rightarrow T$ first-order reactions:

Balance equations relating to the film areas follows:

a). Component donor phase:

$$D_2^A \frac{d^2 C_2^A}{dz^2} = 0 \quad (11)$$

b). Absorbent phase:

$$D_1^A \frac{d^2 C_1^A}{dz^2} - k_1 C_1^A = 0 \quad (12)$$

Balance equations relating to the bulk phase:

$$-K_2 \frac{\partial C_{o2}^A}{\partial x^2} \pm v \frac{\partial C_{o2}^A}{\partial x} - J_1^{oA} \omega = -\frac{\partial C_{o2}^A}{\partial t} \quad (13)$$

$$-K_1 \frac{\partial C_{o1}^A}{\partial x^2} \pm \frac{\partial C_{o1}^A}{\partial x} + J_1^{\delta 1A} \omega - k_1^A C_{o1}^A = \frac{\partial C_{o1}^A}{\partial t} \quad (14)$$

where:

$$J_1^{oA} = -D_1^A \left. \frac{dC_1^A}{dz} \right|_{z=0} \quad (15)$$

$$J_1^{\delta 1A} = -D_1^A \left. \frac{dC_1^A}{dz} \right|_{z=\delta_1} \quad (16)$$

Solving Equation (11) the physical transfer flow density obtained:

$$J_2^{oA} = \frac{D_2^A}{\delta_2} C_{o2}^A - C_2^{*A} \quad (17)$$

From Equation (12):

$$C_1^A = \frac{C_{o1}^A \operatorname{sh} \rho z + C_1^{*A} \rho \delta_1 - z}{\operatorname{sh} \rho \delta_1} \quad (18)$$

from here:

$$J_1^{oA} = \frac{D_1^A \rho}{\operatorname{sh} \rho \delta_1} C_1^{*A} \operatorname{ch} \rho \delta_1 - C_{o1}^A \quad (19)$$

$$J_1^{\delta 1A} = \frac{D_1^A \rho}{\operatorname{tgh}(\rho \delta_1)} C_1^{*A} \operatorname{ch}(\rho \delta_1) - C_{o1}^A \quad (20)$$

where:

$$\rho = \frac{k_1}{D_1^A}$$

Analysing Equations (19) and (20) the role of the rate coefficient is obtained. It follows from Equation (19):

$$J_1^{oA} = k_1 D_1^A C_1^{*A} \quad \text{if } k_1 \rightarrow \infty \quad (19a)$$

$$J_1^{\delta 1A} \rightarrow 0 \quad C_{o1}^A \rightarrow 0 \quad (20a)$$

that the amount components transferred through the surface is proportional to the square root of the rate coefficient Equation (19a), and the increase of J_1^{DA} is limited by the gas-side resistance if k_1 is further increased [Equation (22)]. Simultaneously, increasing k_1 makes J_1^{1A} approach zero [Equation (20a)].

Transfer flow density into the bulk of the adsorbent phase, expressed by the overall transfer coefficient between the two phases and the driving force [using the gas-side concentrations to express the latter (Equation 21)] is obtained from Equations (17) and (20).

$$J_1^{\delta 1A} = \beta_1 \gamma \frac{\beta \gamma_{He}}{\beta_1 + \beta \gamma_{He}} C_{o2}^A - \gamma \cdot 1 + \frac{\beta_1}{\beta \gamma_{He}} \cdot 1 + \frac{k_1 D_1^A}{\beta_1 \beta \gamma_{He}} C_{o1}^{*A} \quad (21)$$

and:

$$J_1^{oA} = \frac{1}{\frac{1}{\beta_2^o} + \frac{\gamma_{He}}{\beta_1}} (C_{o2}^A - C_{o1}^{*A} / \gamma) \quad (22)$$

respectively, where:

$$\gamma = \operatorname{ch}(k_1 D_1^A / \beta_1^o) \quad \beta_1 = \frac{k_1 D_1^A}{\operatorname{tgh}(k_1 D_1^A / \beta_1^o)}$$

Substituting Equations (21) and (22) into Equations (7) and (8), balance equations relating to the bulk phases are obtained [Equations (23)-(25)] and by solving them the component concentra-

tion distributions are obtained:

a). For the adsorbent phase:

$$\begin{aligned}
 -\operatorname{div} (K_1 \operatorname{grad} C_{01}^A) \pm \operatorname{div} (C_{01}^A v) + \beta_1 \gamma \frac{\beta_1 \gamma_{\text{He}}}{\beta_1 + \beta_1 \gamma_{\text{He}}} (C_{02}^A - \alpha_6 C_{01}^{xA}) \omega - \\
 - k_1 C_{01}^A = - \frac{\partial C_{01}^A}{\partial t}
 \end{aligned} \quad (23)$$

where:

$$\alpha_6 = \gamma + \frac{\beta_1}{\beta_1 \gamma_{\text{He}}} + \frac{k_1 D_1^A}{\beta_1 \beta_1 \gamma_{\text{He}}} \quad (24)$$

b). For the component donor phase:

$$\begin{aligned}
 -\operatorname{div} (K_2 \operatorname{grad} C_{02}^A) \pm \operatorname{div} (C_{02}^A v) - \beta_0^O (C_{02}^A - C_{01}^{xA} / \gamma) = \\
 = - \frac{\partial C_{01}^A}{\partial t}
 \end{aligned} \quad (25)$$

where:

$$\beta_0^O = 1 / (1 / \beta_2^O + \text{He} / \beta_1)$$

From the values of J_1^{OA} and $J_1^{\delta 1A}$ a fraction of the transferred material reacting in the film is obtained. If the total amount of the transferred material reacts in the film, the concentration value is Equation (14) becomes zero and this relationship is omitted from the description of the systems. Considering this, two characteristic ranges of chemical reaction rate can be identified:

$$\text{a). } \Omega = J_1^{OA} / J_1^{\delta 1A} \leq 35$$

$$\text{b). } \Omega > 35$$

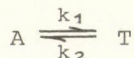
In the case b). less than 3 % of the material adsorbed enters the bulk of the adsorbent phase. If $k_1 D_1^A / (\beta_1^O)^2 > 12$ then

$\Omega > 35$ is obtained.

In the case a). the system is described by Equations (1-3), (14) and (21-22). They include the physical transfer ($\Omega = 1$), while Equations (21-22) give the multiple of the convection transfer coefficient and the driving force [6].

In the case of second - and higher - order reactions the balance equations relating to the film and expressed for one component require the solution of sixth or even higher-order differential equations, which lacking the roots of the characteristic equation, can only be treated by approximative methods. Similarly, no analytical solution of the value equations relating to the bulk phases is known for reactions like this.

Consider now the balance equations of the reversible reaction:



Consider the general case with no established equilibrium between the components in the film and an established equilibrium between the bulk phase concentrations. The balance equations relating to the film formed in the absorbent phase:

$$D_1^A \frac{d^2 C_1^A}{dz^2} = k_1 C_1^A - k_2 C_1^T = k_1 (C_1^A - C_1^T/K) \quad (26)$$

$$D_1^T \frac{d^2 C_1^T}{dz^2} = -k_1 (C_1^A - C_1^T/K) \quad (27)$$

where:

$$K = k_1/k_2$$

Compounding Equations (26) and (27) in incomplete fourth order common differential equation is obtained describing changes of both A and T.

The concentration distribution of component A:

$$C_1^A = \alpha_2 \exp(\alpha_1 z) + \alpha_3 \exp(-\alpha_1 z) + \alpha_4 z + \alpha_5 \quad (28)$$

where:

$$\alpha_1 = \left((KD_1^T + D_1^A) k_1 / D_1^T D_1^A K \right)^{1/2}$$

$$\alpha_2 = K^2 (1 + D_1^A / D_1^T K) \exp(-\alpha_1 \delta_1) (C_1^{*A} - C_{o1}^A) / p$$

$$\alpha_3 = K^2 (1 + D_1^A / D_1^T K) \exp(\alpha_1 \delta_1) (C_{o1}^A - C_1^{*A}) / p$$

$$\alpha_4 = 2K (1 + D_1^A / D_1^T K) D_1^A / D_1^T \alpha_1 \operatorname{ch}(\alpha_1 \delta_1) (C_1^{*A} - C_{o1}^A) / p$$

$$\alpha_5 = -2 (D_1^A / D_1^T \alpha_1 \delta_1 \operatorname{ch}(\alpha_1 \delta_1) (K + D_1^A / D_1^T) C_1^{*A} + 2 \operatorname{sh}(\alpha_1 \delta_1) (K + D_1^A / D_1^T) C_{o1}^A) / p$$

$$p = -2 (K + D_1^A / D_1^T) (K \operatorname{sh}(\alpha_1 \delta_1) + D_1^A / D_1^T \operatorname{ch}(\alpha_1 \delta_1))$$

Considering Equations (15) and (16), the component flows in the points $z = 0$ and $z = \delta_1$ are obtained from Equation (28) shown above:

$$J_1^{oA} = \left(\beta_1^o + \frac{KD_1^T}{\delta_1} \right) \frac{D_1^A \alpha_1 \delta_1}{D_1^A \alpha_1 \delta_1 + D_1^T K \operatorname{tgh}(\alpha_1 \delta_1)} (C_1^{*A} - C_{o1}^A) \quad (29)$$

$$J_1^{\delta_1 A} = \beta_1^o \frac{K \alpha_1 \delta_1 D_1^T + D_1^A \operatorname{ch}(\alpha_1 \delta_1)}{D_1^A \alpha_1 \delta_1 \operatorname{ch}(\alpha_1 \delta_1) + KD_1^T \operatorname{sh}(\alpha_1 \delta_1)} (C_1^{*A} - C_{o1}^A) \quad (30)$$

Values of the component transfer flow densities relating to the irreversible first order reaction with increasing k_1 [Equations (19 and 20)] are obtained from Equations (29) and (30).

The gas side resistance can be defined by Equations (29) and (30), similarly to Equations (21) and (22).

A third area of the chemical reaction rate, that of the instantaneous reactions should also be mentioned. This area bears significance in the case of reactions involving at least two or more components. Then, due to the high reaction rate, the concentration of both the components drops to zero in the film. Thus, reaction takes place only in the plane where components arrive at via diffusion.

Therefore, e.g. in the case of the reaction $A + R \rightarrow T$ the relationship giving the absorption rate [7, 8] is:

$$J_1^{oA} = \beta_1^o C_1^{*A} + \frac{D_1^R C_{o1}^R}{D_1^A} \quad (31)$$

The balance equations shown are generally valid equations and depending on the given case, and operation unit, the actual technology can become considerably simpler and some of their terms can easily be neglected.

SYMBOLS USED

- A - component subject to phase change
- C - concentration, (kmole/m^3)
- D - diffusion coefficient, (m^2/h)
- G - reaction rate, ($\text{kmole/m}^3\text{h}$)
- He - Henry's coefficient,
- J - component transfer flow density, ($\text{kmole/m}^2\text{h}$)
- j_a - number of reactions involving component A
- j_r - number of reactions involving R
- K - equilibrium coefficient
- k_1 and k_2 - mixing coefficient, (m^2/h)
- k - rate coefficient (its dimension depend on the reaction order)
- l - stoichiometric coefficient
- m - number of absorbing reactants
- n - number of reactants in the absorbent phase
- p - number of parallel reactions
- q - number of consecutive reactions
- R - reactant
- \bar{r} - space co-ordinate of a given point of the contacting surface, (m)
- \bar{r}_0 - space co-ordinate of a given point of the contacting surface
- $\bar{r}+\delta$ - co-ordinate of a point of the surface of the laminar film at the side of the main phase
- t - number of products
- t - time, (h)
- v - convective flow rate, (m/h)
- z - co-ordinate, (m)
- x - Co-ordinate, (m)
- δ - thickness of the laminar film, (m)

β^0 - physical transfer coefficient, (m/h)

ω - specific contact area, (m^2/m^3)

$\rho = k_1 D_1^A$

Subscripts

- f - liquid
- g - gas
- i - serial index
- j - serial number of the reaction
- sz - solid
- o - bulk phase property
- ö - overall
- 1 - absorbing phase
- 2 - component phase

Upper indices

- x - equilibrium
- A, R, T - components respectively
- o - contacting surface of the phases
- ö - surface of the laminar films of thickness at the main - phase side

REFERENCE

- [1] BLICKLE, T., SEITZ, K.: A modern algebrai módszerek felhasználása a műszaki kémiában. (Use of Modern Algebraic Methods in Technical Chemistry) Budapest Műszaki könyvkiadó, 1975.
- [2] CSUKÁS, B.: Műszaki kémia mérlegegyenleteiről. (Balance Equations of Technical Chemistry in Scientific Results of the MTA MÜKKI.) Vol.4. p.7. (1976).

- [3] MOHILLA, R., FERENCZ, B.: Vegyipari folyamatok dinamikája. (Dynamics of Chemical Industrial Processes.) Budapest, Műszaki Könyvkiadó, 1972.
- [4] MIYANCHI, F., VERMEULEN, T.: Ind. Engng. Chem., Fundamentals, 2, 113. (1963)
- [5] BORLAI, O., NAGY, E., SZÉPVÖLGYI, J., and UJHIDY, A.: Hung. J. Ind. Chem. (in press).
- [6] BENEDEK, P., LÁSZLÓ, A.: A vegyészmérnöki tudomány alapjai. (Fundamentals of Chemical Engineering.) Budapest, Műszaki Könyvkiadó, 1964. p. 91.
- [7] DANCKWERTS, F.: Gas-Liquid Reactions. New York, McGraw-Hill, 1970.
- [8] ASTARITA, G.G.: Massoperedacha s khimicheskoi reaktsiei. Leningrad, Khimiya, 1971.

РЕЗЮМЕ

В соответствии с принципами теории систем, разработанной в Технико-химическом институте Венгерской Академии Наук, рассматриваются гетерогенные химические реакции между фазами жидкость-газ, и жидкость-жидкость. Шестью классами свойств задаются разделение вышеупомянутых гетерогенных химических реакций и число возможных вариаций реакций. Применяя расширенное уравнение Дамкелера, дается система уравнений компонентного балланса для гетерогенных реакций, где члены передачи выражены через отдельные уравнения балланса.

В случае реакций первого порядка для образующейся между фазами ламинарной пленки найдено решение диффузионной зависимости и выразив с помощью кинетических параметров реакции и передачи, дается уравнение балланса для основной массы фаз и члены передачи.

PRACTICAL EXPERIENCES IN THE SIMULATION AND OPTIMIZATION
OF COMPLEX CHEMICAL PROCESSES

K. HARTMANN^x, R. DITTMAR^x and K. DAMERT^{xx}

(^xTechnical University "Carl Schorlemmer" Leuna-Merseburg, GDR

^{xx}Petrolchemisches Kombinat, Schwendt, GDR)

Received: June 3, 1976.

The problem of the simulation and optimization of complex chemical systems is considered. Different methods for simulation and optimization are considered especially from the point of view of numerical computation on digital computers. The concept of flowsheet simulation is critically confronted with the equation oriented approach. On two examples several algorithms are compared. The adjoint process is used for the computation of first derivatives of complex systems. The calculation of first order static sensitivity coefficients is also considered. It is concluded that the flowsheet simulation concept is only in the design stage as an effective tool. In optimization, this method lead to nested iterations of high dimensionality. However, a minimal number of iteration variables is obtained with the equation oriented approach.

1. INTRODUCTION

In recent years, calculation and optimization methods involving complex chemical processes have received considerable attention in literature. In the calculation of chemical processes, flow-

sheet simulation was extensively studied because the simplification of the design procedures connected therewith promised to be of considerable use [1, 2]. Moreover, emphasis was placed on the equation oriented calculation of systems which enable problems to be solved with a saving in computer time [3-5]. The investigations of optimization were concentrated on the development of search strategies for different types of problems, and the direct strategies that were gaining special importance.

On the other hand, methods such as dynamic programming, the maximum principle, or the multilevel technique, did not play such a major role in the practical application to the chemical industry. This was primarily due to the following facts: These methods proved to be superior to the search strategies only in large problems (number of variables, number of process units with nonlinear models, and of couplings). However, the treatment of such "large problems" is not only problematical because of the expense of computer time, what is more important is that due to the inaccuracy of the models and the multiplicity of solutions, the results computed at considerable expense do not attain the real optimal conditions.

In the treatment of problems, which at present can be solved at a reasonable expense, the search strategies proved to be easily manageable and reliable, and in most cases led to a reasonable result. The application of such methods is described here. At present, relatively few results are available for the simultaneous consideration of system calculation and optimization. It is the aim of this paper to discuss the effective solution of simulation and optimization problems.

In chapter 2, the algorithms used for this purpose are given. A procedure for the calculation of derivatives in complex systems is presented. In chapter 3, two model systems are treated in which the calculations were carried out. In chapter 4, the essential results of the investigations are summarized. The following problems are discussed:

- a). Comparison of iteration methods for the solution of simulation problems;

- b). Comparison of optimization procedures;
- c). Application of the method of adjoint process to the calculation of derivatives in optimization and sensitivity analysis;
- d). Comparison of flowsheet simulation and equation oriented calculation of systems.

2. BASIC ALGORITHMS FOR THE CALCULATION AND OPTIMIZATION OF SYSTEMS

Fig. 1. presents the scheme of a complex chemical process. It consists of units or element which are represented by small boxes. The input variables of the k-th element are:

$$\underline{x}^{(k)} = (x_1^{(k)} \dots x_{mk}^{(k)})^T,$$

the output variables:

$$\underline{y}^{(k)} = (y_1^{(k)} \dots y_{nk}^{(k)})^T.$$

For each element, the equations of a mathematical model:

$$f_i(\underline{y}^{(k)}, \underline{x}^{(k)}, \underline{u}^{(k)}) = 0 \quad i = 1 \dots n_k \quad (1)$$

are given. As to the form of this connection, it is assumed that the \underline{y} can be calculated as being unique from the given \underline{x} and \underline{u} . The variables

$$\underline{u}^{(k)} = (u_1^{(k)} \dots u_{rk}^{(k)})^T$$

designate the design and control variables of the k-th element. A system is determined by (1) and the structural relations between the input and output variables of different elements:

$$y_{g(k,i)}^{h(k,i)} = x_i^{(k)} \quad (2)$$

The task of the flowsheet simulation is to calculate the values of output variables of the whole system

$$\underline{y}^o(k) = (y_1^o(k) \dots y_{nk}^o(k))^T$$

from the given system input variables

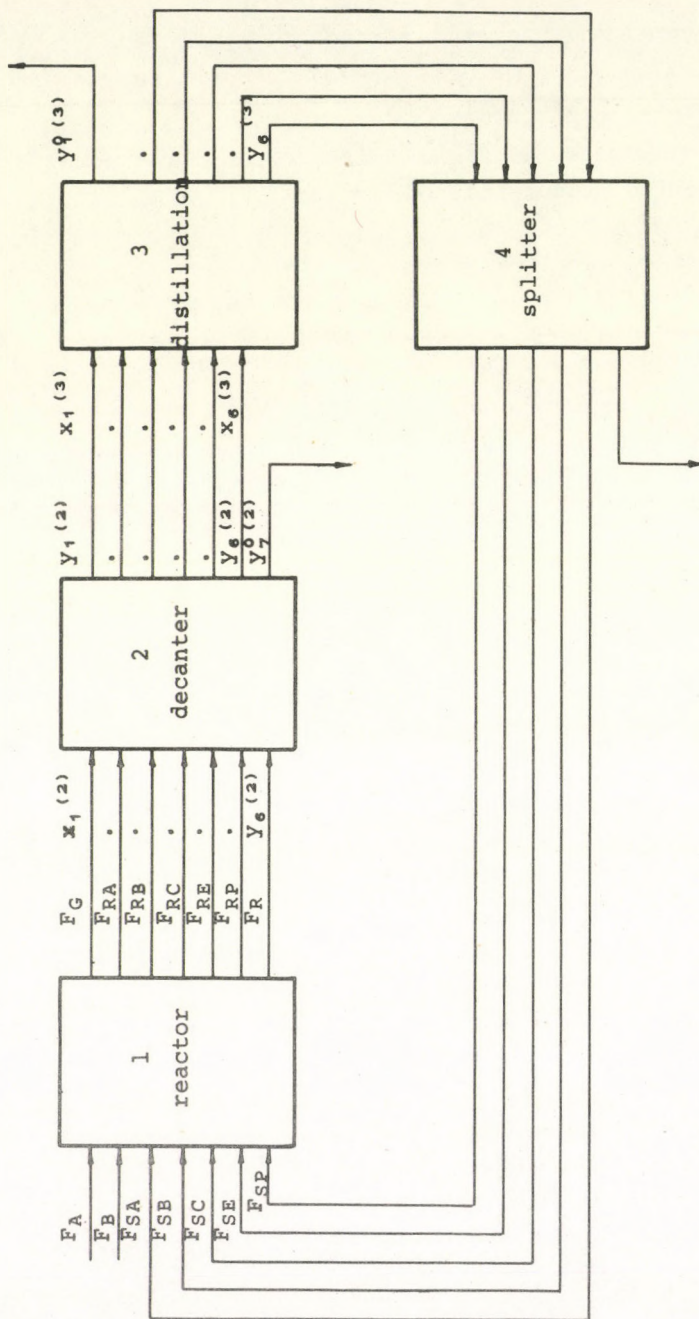


Figure 1. Williams-Otto Plant as an Example of a Complex Chemical System

$$\underline{x}^o(k) = (x_1^o(k) \dots x_{P_k}^o(k))^T$$

and the given design and control variables

$$\underline{u}^T(k) = (u_1^T(k) \dots u_{T_k}^T(k))^T$$

This problem can be solved directly only in very simple cases. When there are no recycles in the systems, the output variables can be calculated stepwise from the input variables.

2.1 Approaches to the Calculations of Complex Systems

Systems with recycles require iterative calculation. For this purpose, the system must be torn. In simple systems, the position of the most favourable variables to be torn can be determined visually. For larger systems, efficient algorithms were developed which automatically determine the position of the optimal tear variables. In flowsheet simulation, the following points are of special importance:

- a). The task of flowsheet simulation is to organize the solution of systems of equations which in general are nonlinear by balancing the recycles;
- b). The basic point is the topology of the system only the form of the model equations being of no importance;
- c). When type models for the elements exist, various structure variants can be calculated without difficulty.

The essential disadvantage of the flowsheet simulation concept is the following. If within a recycle there is an element whose output variables can be calculated only by iterative methods, the system calculation always leads to nested iterations. However, to solve this problem it would be completely sufficient to choose the iterations of the implicit element as iteration variables of the whole recycle.

Therefore, it appears to be advantageous to not only consider the topological system calculation, but also a method of calcula-

tion for complex systems based on the concrete form of the system equations. In this case, the system of model and structure equations(1)-(2) is considered as simultaneous, i.e. a nonlinear system of equations, disregarding the question as to which element belongs to each equation. Using the various algorithms (3-5), a favourable order of solution of the equations and a favourable choice of the iteration variables can be determined. However, there is the disadvantage that standard models in the usual form

$$y_i^{(k)} = f_i(\underline{x}^{(k)}, \underline{u}^{(k)})$$

cannot be used directly, because it may occur that the equations must be transformed according to the structure of the general system.

2.2 Simulation and Optimization Procedures Used

The optimization of chemical processes calculated by use of flowsheet simulation is carried out as follows: The values of the parameters to be varied (which may be system input and design control variables) are determined by an optimization procedure. The objective function is calculated at these values. For the choice of optimization variables, the equation oriented calculation of the system yields more possibilities. This choice is not restricted to the system inputs and design/control variables. Therefore, it is often possible to find much more effective methods of calculation. In chapter 4 an example is shown in which the flowsheet simulation leads to nested iterations, but the equation oriented simulation can be carried out without any iterations.

Literature offers a series of different methods for the optimization. Our investigation was restricted to:

- a). Powell's direct method [7];
- b). The method of Rosenbrock [8];
- c). The method of Fletcher and Powell [9];
- d). The complex method of Box [10];
- e). The non-local "graben" method [11].

The solution of iteration problems could be carried out by using one of the optimization methods mentioned. However, as was

shown by experience, this is ineffective. It is more useful to apply algorithms adopted to the special problem. We examined:

- a). The method of successive substitution;
- b). Broyden's method [12];
- c). Jones' spiral algorithm [13];
- d). The Chabyshev approximation [14].

Since the first three methods are well known, a short description of the fourth is given. The system of nonlinear equations is written as:

$$W_i f_i(p) = 0 \quad (3)$$

The values W_i designate constant weights enabling the equations to be uniformly satisfied. $f_i(p)$ is expanded about the point p_0 in a Taylor series up to the first order:

$$W_i \left[f_i(p_0) + \sum_j \frac{\partial f_i}{\partial p_j} \delta p_j \right] = 0 \quad i = 1, \dots, n \quad (4)$$

The Chebyshev approximation aims at minimizing the maximum deviation:

$$\min_{\delta p} \max_{1 \leq i \leq n} \left| W_i \left[f_i(p) + \sum_j \frac{\partial f_i}{\partial p_j} \delta p_j \right] \right| \quad (5)$$

This problem can be solved as a linear optimization problem. Suppose λ to be the maximal deviation in the linear approximation. Then we have:

$$\begin{aligned} \lambda &= \min ! \\ W_i \left[f_i(p_0) + \sum_j \frac{\partial f_i}{\partial p_j} \delta p_j \right] &\leq \lambda \\ -W_i \left[f_i(p_0) + \sum_j \frac{\partial f_i}{\partial p_j} \delta p_j \right] &\leq \lambda \end{aligned} \quad (6)$$

In order to avoid a violation of the range of validity of the linear approximation, limits are given for δp . For details see ref. [14]. An iteration is finished when the actual nonlinear deviation is decreased:

$$\max_{1 \leq i \leq n} \left| w_i \left[f_i(\underline{p}_0 + \delta \underline{p}) \right] \right| \leq \max_{1 \leq i \leq n} \left| w_i \left[f_i(\underline{p}_0) \right] \right| \quad (7)$$

The $\delta \underline{p}$ are the results of linear optimization. If the condition is not satisfied, the variation of parameters is further restricted, and the linear optimization is repeated. In many cases, the use of the Chebyshev approximation is unavoidable, although its computer programme is used much core. After a large number of numerical experiments, the conclusion was reached that the convergence of the Chebyshev approximation is more reliable than that of all other methods.

2.3 The Calculation of Derivatives in Complex Systems

Using modified gradient methods for nonlinear optimization of chemical processes, the derivatives of the objective function ϕ to the optimization variables \underline{x}_0 and \underline{u} must be determined. For complicated systems these derivatives cannot be calculated analytically. For n derivatives, however, the numerical calculation of derivatives with the aid of differences requires $(n+1)$ iterative system calculations. If the increments are chosen to be small in order to maintain the local property of the derivative, the iterations for the solution of the system of nonlinear equations must be of adequate accuracy. Due to these problems, it is interesting to examine other methods for the calculation of gradients. Ostrovskij and Volin [15] reported a procedure which reduces the calculation of the derivatives of the general system $\partial \phi / \partial \underline{x}^0$ and $\partial \phi / \partial \underline{u}$ to the calculation of the derivatives $\partial \underline{y} / \partial \underline{x}$ of the single elements and the solution of a system of linear equations. A short explanation will be given of this procedure. The starting point is formed by equations (1)-(2) of the model. The objective function of the process must be written as $\phi = \phi(\underline{x}^0, \underline{y}^0, \underline{u})$. Eliminating the dependent variables \underline{y}^0 we obtain $\phi^* = \phi^*(\underline{x}^0, \underline{u})$. Then the derivatives $\partial \phi^* / \partial \underline{x}^0$ and $\partial \phi^* / \partial \underline{u}$ have to be found. The elimination of the dependent variables \underline{y}^0 from ϕ can be carried out as follows. First, an auxiliary function L is evaluated:

$$\begin{aligned}
 L = & \phi + \sum_{k=1}^N \sum_{i=1}^{n_k} \left[-y_i^{(k)} + f_i^{(k)}(\underline{x}^{(k)}, \underline{u}^{(k)}) \right] \lambda_i^{(k)} \\
 & + \sum_{k=1}^{N_1} \sum_{i=p_k+1}^{m_k} \left[-x_i^{(k)} + y_{g(k,i)}^{h(k,i)} \right] \mu_i^{(k)} \\
 & + \sum_{k=N_2+1}^N \sum_{i=1}^{m_k} \left[-x_i^{(k)} + y_{g(k,i)}^{h(k,i)} \right] \mu_i^{(k)}
 \end{aligned} \quad (8)$$

By setting to zero the derivatives of L by the dependent variables, the following system of linear equations is obtained:

$$\mu_j^{(k)} = \sum_{i=1}^{n_k} \lambda_i^{(k)} \frac{\partial f_i^{(k)}}{\partial x_j^{(k)}} \quad k = \begin{cases} 1 \dots N_1 ; j = p_k+1 \dots m_k \\ N_1+1 \dots ; j = 1 \dots m_k \end{cases} \quad (9)$$

$$\mu_j^{o(k)} = \sum_{i=1}^{n_k} \lambda_i^{(k)} \frac{\partial f_i^{(k)}}{\partial x_{j_o}^{o(k)}} \quad k = 1 \dots N ; j = 1 \dots p_k \quad (10)$$

$$\mu_i^{(k)} = \lambda_{g(k,i)}^{h(k,i)} \quad k = \begin{cases} 1 \dots N_1 ; i = p_k+1 \dots m_k \\ N_1+1 \dots N ; i = 1 \dots m_k \end{cases} \quad (11)$$

$$\lambda_i^{o(k)} = \frac{\partial \phi}{\partial y_i^{o(k)}} \quad k = N+1 \dots N ; i = 1 \dots g_k^L \quad (12)$$

The derivatives $\partial \phi^*/\partial \underline{x}^o$ and $\partial \phi^*/\partial \underline{u}$ are obtained by differentiation of L by the independent variables:

$$\frac{\partial \phi^*}{\partial \mu_s^{(k)}} = \frac{\partial \phi}{\partial \mu_s^{(k)}} + \sum_{i=1}^{n_k} \lambda_i^{(k)} \frac{\partial f_i^{(k)}}{\partial \mu_s^{(k)}} \quad k = 1 \dots N ; s = 1 \dots r_k \quad (13)$$

$$\frac{\partial \phi^*}{\partial x_{s_o}^{o(k)}} = \frac{\partial \phi}{\partial x_{s_o}^{o(k)}} + \mu_s^{(k)} \quad k = 1 \dots N ; s = 1 \dots p_k \quad (14)$$

The calculation of these derivatives can then be carried out in the following steps:

1. Iterative calculation of the system for given values of the optimization variables \underline{x}^0 and \underline{u} .
2. Calculation of the derivatives $\partial \underline{y} / \partial \underline{x}$ of the elements. In linear and simple explicit nonlinear models, these derivatives can be evaluated analytically. If the elements are described by implicit systems of nonlinear equations, a numerical differentiation is required. However, the results of this differentiation is in general more exact than the numerical determination of the derivatives of the whole systems.
3. Analytical and numerical determination, **respectively**, of the derivatives of the original objective function ϕ by \underline{x}^0 and \underline{u} and of the boundary conditions (12).
4. Calculation of the adjoint process (1-12). In order to solve some equations, only the relation (9) are used for the $\lambda_i^{(k)}$, and the structural relations (11) are substituted directly. The remaining variables are then obtained from (10).

If the system of equations for the adjoint process is of great dimension, special algorithms can be used for the solution of sparsely structured linear equations.

Here it should be pointed out that the algorithm presented is also suitable for the calculation of static first order sensitivity coefficients. This term denotes the normalized first derivatives of any intermediate system variable \underline{y} or system output variable \underline{y}^0 by model parameters \underline{p} , system input variables \underline{x}^0 , and design/control variables \underline{u} . The sensitivity coefficient of the output variable $y_i^{(k)}$ of the element k relative to the model parameter $p_j^{(l)}$ of the element l is obtained as:

$$S_{ij}^{kl} = \frac{\partial y_i^{(k)} \times \partial p_j^{(l)}}{\partial p_j^{(l)} \times \partial y_i^{(l)}} \quad (15)$$

The calculation of S can be reduced to the calculation of $\partial \phi^* / \partial \underline{u}^*$ in a simple manner. This merely requires acceptance of \underline{p} as the additional control variables and \underline{y} as the additional function. From the mathematical point of view, this is the same prob-

lem. The adjoint process then has to be calculated anew for each component of y .

3. MODEL SYSTEMS

Due to their extension, complex chemical processes as they exist in practice are not suitable for treatment within the scope of an article. For this reason, the methods for calculation and optimization of such systems will be demonstrated by two relatively small problems: the Williams-Otto-plant, and the part of an ACN plant. Although the systems treated consist of only a few units, they include nearly all characteristic difficulties which have to be solved in large systems. The Williams-Otto-plant (16) consist of four elements, a reactor, a decanter, a distillation, and a splitter (Fig. 1.). In the reactor, three reactions occur between the components A,B,C,E,G and P:



The equations are represented in (18) and completely given in part 4.2. Only the set of constants for the reactions are given here:

$$\begin{aligned} k_i &= A_i \exp(-B_i/T) \\ A_1 &= 5.9755 \text{ E} + 9 & A_2 &= 2.5963 \text{ E} + 12 & A_3 &= 9.628 \text{ E} + 15 \\ B_1 &= 12000. & B_2 &= 15000. & B_3 &= 20000. \\ M_A &= M_B = M_P = 100. & M_C &= M_E = 200. & M_G &= 300. & \rho &= 50. \end{aligned}$$

Here M designate the molecular weights, ρ the density. In the decanter the component G is removed (F_G), while a part of P is removed by distillation:

$$F_P = F_{RP} - 0.1 F_{RE} \quad (17)$$

The part F_D of the flow is separated from the process by the splitter, the remainder is recycled. Input variables of the system are F_A and F_B , output variables are F_G , F_P and F_D . As control vari-

ables, T and V (temperature and volume of the reactor) and the value α indicating the part of F_D in the flow are chosen:

$$F_D = \alpha (F_R - F_G - F_P) \quad (18)$$

The input and control variables should be chosen in such a way that the objective function F (%-return) is maximized:

$$F = \frac{1}{6V\rho} (84 F_A - 201.96 F_D - 336 F_G + 1955.52 F_P - 2.22 F_R - 60 \times V \times \rho) \quad (19)$$

The simplified part of an acryl nitrile plant is shown in Fig. 2. In the reactor, propylene and ammonia are catalytically oxidized to yield acryl nitrile. The amount of heat produced is removed by an evaporator on the lower part (WD-WD') and a heat exchanger in the upper part (D1-D4) of the reactor. The system is completed by the separator, the mixer, and two other heat exchangers. Due to limitation of space, the model of the reactor and one heat exchanger only are represented (the indices are the same as those in the designation of streams in Fig. 2.).

$$F_{WD'} = F_{WD}; \quad F_{D4} = F_{D1}; \quad F_P = F_{L4} F_{NH} F_{PR}; \quad (20)$$

$$T_G = \frac{F_{NH} C_{NH} T_{NH} + F_{PR} C_{PR} T_{PR} + F_{L4} C_{L4} T_{L4}}{C_P (F_{L4} + F_{NH} + F_{PR})} \quad (21)$$

$$\frac{\Delta H_R}{R} \frac{k_P P_{PR}}{T_P} V = F_P C_P (T_P - T_G) + k_v A_v \frac{(T_P - T_{WD}) - (T_P - T_{WD'})}{\ln \frac{T_P - T_{WD}}{T_P - T_{WD'}}} + k_u A_u \frac{(T_P - T_{D1}) - (T_P - T_{D4})}{\ln \frac{T_P - T_{D1}}{T_P - T_{D4}}} \quad (22)$$

$$k_v A_v \frac{(T_P - T_{WD}) - (T_P - T_{WD'})}{\ln \frac{T_P - T_{WD}}{T_P - T_{WD'}}} = F_{WD} r_W x_a + F_{WD} C_W (T_{WD} - T_{WD'}) \quad (23)$$

$$k_u A_u \frac{(T_P - T_{D1}) - (T_P - T_{D4})}{\ln \frac{T_P - T_{D1}}{T_P - T_{D4}}} = F_{D1} C_{D1} (T_{D4} - T_{D1}) \quad (24)$$

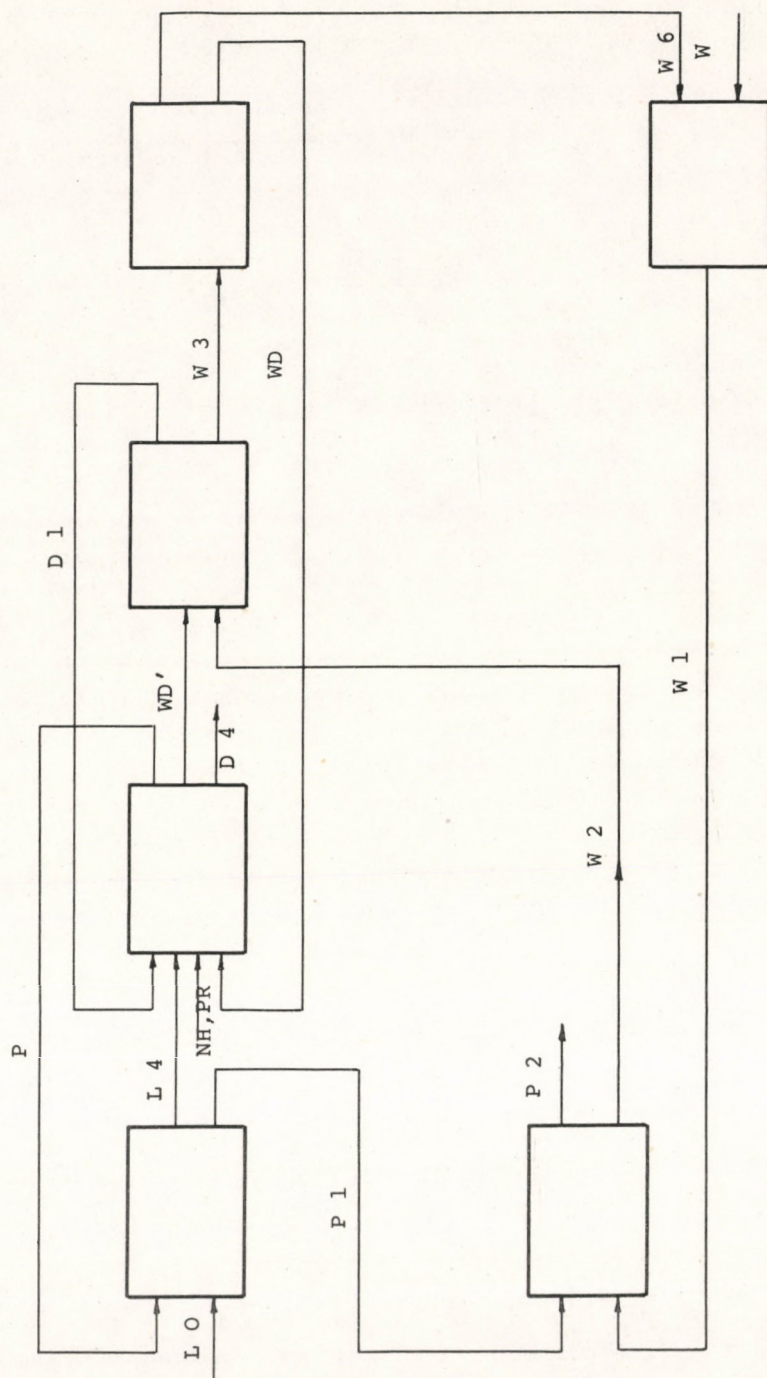


Figure 2. Simplified Part of an ACN Plant

$$F_{L4} = F_{Lo} ; \quad F_{P1} = F_P ; \quad h = 1 - \frac{F_P c_P}{F_{Lo} c_{Lo}} ; \quad (25)$$

$$T_{P1} = T_{Lo} - (T_P - T_{Lo}) \frac{F_{Lo} c_{Lo}}{F_P c_P} \left[1 - \frac{h}{1 - \frac{F_P c_P}{F_{Lo} c_{Lo}} \exp\left(-\frac{k_1 A_1}{c_P F_P} h\right)} \right] \quad (26)$$

$$T_{L4} = T_{Lo} + \frac{F_P c_P}{F_{Lo} c_{Lo}} (T_P - T_{P1}) \quad (27)$$

The other models were formed from the material and energy balances of the elements. Details can be taken from [17].

4. CALCULATION AND OPTIMIZATION OF TWO MODEL SYSTEMS

4.1 Williams-Otto-Plant

For the calculation of the Williams-Otto-plant, we first started from the balance equations given in (18). (Equ. 15-23 of Adelman and Stevens). F_A , F_B , T , and V were given, and the remaining system of nonlinear equations was solved by using the spiral procedure. No unique solution was found to exist (see different solutions in Table 1.). In the first column, the value of the objective function is listed. In the last one, the absolute accuracy of the solution is presented. The fact that the solution is not unique is due to the dependence of Adelmans equations.

Table 1. Three different solutions of equations (15)-(23) in (18)

F	F _{RA}	F _{RB}	F _{RC}	F _{RG}	F _{RP}	F _G	diff.
72.49	18.185	60310.	3330.	60546.	10815.	3609.	1.E-7
169.83	16594.	64684.	3579.	58685.	11752.	1572.	7.E-8
272.55	29659.	70688.	8277.	46376.	10384.	-3019.	2.E-10

In order to obtain a unique problem, the variable α (see Equ. 18) was introduced. Thus, the correct set of balance equations has the

form:

$$-k_1 F_{RA} F_{RB} \rho V / F_R^2 - \alpha F_{RA} + F_A = 0 \quad (28)$$

$$(-k_1 F_{RA} F_{RB} - k_2 F_{RB} F_{RC}) \rho V / F_R^2 - \alpha F_{RB} + F_B = 0 \quad (29)$$

$$(M_C / M_B k_1 F_{RA} F_{RB} - M_E / M_B k_2 F_{RB} F_{RC} - k_3 F_{RP} F_{RC}) \rho V / F_R^2 - \alpha F_{RC} = 0 \quad (30)$$

$$k_2 M_E / M_B F_{RB} F_{RC} \rho V / F_R^2 - \alpha F_{RE} = 0 \quad (31)$$

$$(k_2 F_{RB} F_{RC} - M_P / M_C k_3 F_{RC} F_{RP}) \rho V / F_R^2 - \alpha (F_{RP} - F_P) - F_P = 0 \quad (32)$$

$$M_G / M_C k_3 F_{RC} F_{RP} \rho V / F_R^2 - F_G = 0 \quad (33)$$

$$F_{RP} - .1 F_{RE} - F_P = 0 \quad (34)$$

$$R_{RA} + F_{RB} + F_{RC} + F_{RE} + F_{RP} + F_G - F_R = 0 \quad (35)$$

F_A , F_B , T , V , and α can be chosen arbitrarily. The eight variables F_{RA} , F_{RB} , F_{RC} , F_{RE} , F_{RP} and F_G , F_P , F_R can be calculated from the equations given above. The first method of calculation is the application of flowsheet simulation. For this purpose, the system shown in Fig. 1. would serve as a basis. Since there is a recycle, iteration is required. It is reasonable to tear the stream between distillation and splitter or between splitter and reactor. In both cases one would obtain 5 iteration variables. It is very important that the calculation of the output variables of the reactor can be carried out only by iteration. This means that there is nested iteration required for the calculation of the Williams-Otto-plant, internally six dimensional, externally five dimensional.

Obviously, such a nested iteration is not necessary. It would be quite sufficient to use the iteration variables of the reactor as iteration variables of the whole recycle. This means, however, that the reactor cannot be used as a usual element model. Another possibility of calculation is to start from the structure of the equations. In this case, several methods are possible.

The primary aim was to make use of the knowledge of reaction kinetics. There are only three linear independent reactions. If

three key components are chosen, the remaining components can be calculated as linear combinations. Thereby the dimension of the system of the equations to be solved can be reduced to three. Substituting one equation directly and choosing F_{RA} and F_{RB} as iteration variables, the system of equations:

$$M_E/M_B k_2 F_{RB} F_{RC} VR2 - F_{RE} = 0 \quad (36)$$

$$M_G/M_C k_3 F_{RC} F_{RP} VR2 - F_G = 0 \quad (37)$$

with $ANE = F_A - \alpha F_{RA}$ and $VR2 = ANE/(k_1 F_{RA} F_{RB})$ is obtained. Details are given in [14].

The spiral procedure and the Chebyshev approximation were used for the solution. In this case, there are some characteristic problems which also occur in the calculation of larger systems. The first equation is given the weight 1, the other the weight 40 in order that both may be satisfied equally within the scope of the accuracy.

Borth the iteration procedures used require the derivatives of the left-hand sides of the equations by the iteration variables. The derivatives were formed numerically. A relative change of the variables of 10^{-3} (i.e. 0.1 %) results in changes in the first position of the left-hand sides. An approximation of the derivatives cannot be obtained. Therefore, the relative change was chosen to be 10^{-6} which results in changes of the left-hand sides in the fourth position. It was found by test calculations that the system of equations is not solved with sufficient accuracy when the increments of the derivatives are too big. However, with the chosen increment of 10^{-6} the results were exact for more than nine digits (the ICL 4130 computer used has 11 significant positions with single precision). As an additional problem, it was found that some variables, especially F_{RC} and F_G , could become negative. Moreover, F_R was not always calculable (negative radicand). This problem was solved by penalty functions.

Basing upon the system of equations (36)-(37), the Williams-Otto-plant was optimized by various procedures. Because of the special form of the objective function, only the ratio of F_A to F_B is essential, but not the absolute values of both variables. There-

fore, it was set $F_B = \text{const.}$ F_A , T , V , and α remain as variables for the optimization. The optimization was carried out in the basis of two different starting points, the DiBella solution [19]:

$$F_A = 13546.24; \quad T = 656.1; \quad V = 59.56; \quad \alpha = .247; \quad (F_B = 31522.56),$$

and the Williams solution [16]:

$$F_A = 14500.; \quad T = 640.; \quad V = 92.8; \quad \alpha = .447; \quad (F_B = 33350.).$$

The calculation was carried out with $F_A/1000.$, T , V , and 100α in order to be able to compare all optimization procedures (see the discussion below for the application of the Fletscher-Powell procedure). First, the three direct procedures and the non-local "graben" method were used. The restriction of temperature $580 < T < 680$ was covered by a penalty function which, however, was not reached. The starting complex for the complex method was built up by random numbers.

Due to different magnitudes of the parameters, a transformation for the non-local "graben" method is needed. Instead of T , V , and F_A :

$$(T - 580)/100, \quad (V - 20)/80 \text{ and } (F_A - 13000)/1000 \text{ were used.}$$

The step length was 0.02.

An optimal value of the objective function of 121.534 was obtained uniformly by all optimization procedures. The optimal values of the parameters are:

$$T = 674.43; \quad F_A = 13831.; \quad V = 31.48; \quad \alpha = .1002 \text{ for } F_B = 3152.56$$

and

$$T = 674.43; \quad F_A = 14633.; \quad V = 33.31; \quad \alpha = .1002 \text{ for } F_B = 33350.00.$$

Table 2 shows how many iterations and objective functions had to be evaluated. According to this Table, the best results were obtained by Powell's procedure. Rosenbrock's procedure is disadvantageous in the vicinity of the optimum (slow convergence). Quick results can be obtained by the non-local method if it is sufficient to obtain an approximation of the optimum. The complex procedure of Box, however, should be applied only to truly restricted problems.

Apart from the optimization procedures already examined, the method of Fletscher and Powell is often used successfully. It requires the first derivatives of the objective function to be calculated with great accuracy. The method of the adjoint process was found to be applicable to the exact calculation of the derivatives of complex systems. In the following, it is applied to the Williams-Otto-plant.

Table 2. Optimization of the Williams-Otto-plant by different procedures

method	start	F	iterations	function evaluation
Rosenbrock	DB	121.53419	16	310
	W	121.53422	13	300

Powell	DB	121.53423	6	132
	W	121.53423	10	205

Box	DB	121.53277		340
	W	121.53372		307

non-local "grabe"	DB	121.40125	18	174
	W	121.49569	33	274

We did not start from the system of Fig. 1, but included the decanter, distillation and splitter in one element, considering only six inputs at the reactor (F_R is the sum) in order to prevent the system of equations from becoming too large. Moreover, this selection of the system is advantageous in that the derivatives of the output variables of each element can be calculated uniformly.

The derivative of the i -th output variable by the j -th input variable of element 1 is designated by Pl_{ij} (in the same manner $P2_{ij}$ for element 2). Thus, the equations of the adjoint process are:

$$\mu_j^{(1)} = \sum_{i=1}^6 \lambda_i^{(1)} Pl_{ij} \quad j = 1, 2 \quad (38)$$

$$\mu_j^{(1)} = \sum_{i=1}^6 \lambda_i^{(1)} Pl_{ij} \quad j = 3, 4 \quad (39)$$

$$\mu_j^{(2)} = \sum_{i=1}^3 \lambda_i^{(2)} P_{2ij} - \sum_{i=4}^8 \lambda_i^{(2)} P_{2ij} \quad j = 1,6 \quad (40)$$

$$\lambda_i^{(1)} = \mu_i^{(2)} \quad i = 1,6 \quad (41)$$

$$\mu_i^{(1)} = \lambda_{i+2}^{(2)} \quad i = 3,7 \quad (42)$$

$$-\lambda_1^{(2)} = \frac{\partial \phi}{\partial F_G}; \quad \lambda_2^{(2)} = \frac{\partial \phi}{\partial F_P}; \quad \lambda_3^{(2)} = \frac{\partial \phi}{\partial F_D} \quad (43)$$

The original objective function has to be transformed since it must depend only on system input, output and design control variables:

$$\phi = \frac{1}{6V\rho} (84 F_A - F_D (201.96 - 2.22/\alpha) - 338.22 F_G - 1953.3 F_P - 60 V \rho) \quad (44)$$

For the derivative of the objective function ϕ^* by the variables which are of interest, we used equations (13)-(14). In the reduced form (substitution of the structural relations), the coefficient matrix and the right-hand side of the adjoint process have the form:

$\lambda_1^{(1)}$...	$\lambda_6^{(1)}$	$\lambda_4^{(2)}$...	$\lambda_8^{(2)}$	RHS
-1	...	0	P_{241}	...	$P_{281} - \sum_{i=1}^3 \lambda_i^{(2)} P_{2i1}$	
.						
.						
0		-1	P_{246}	...	$P_{286} - \sum_{i=1}^3 \lambda_i^{(2)} P_{2i6}$	
P_{113}		P_{163}	-1		0	0
.						
.						
P_{117}		P_{167}	0		-1	0

Thus, the dimension of the system of equations to be solved

equals the number of internal couplings of the system. The values of P2 can be easily calculated, P1, however, cannot be calculated analytically since the equations of the first element do not exist in the form $y_i^{(1)} = f_i^{(1)}(\underline{x}^{(1)}, \underline{u}^{(1)})$, but in the form $x_j^{(1)} = g_j^{(1)}(\underline{y}^{(1)}, \underline{u}^{(1)})$. However, since the derivatives $\partial x_j^{(1)} / \partial y_j^{(1)}$ can be calculated analytically, Pl_{kj} is calculated from:

$$\delta_{ij} = \sum_{k=1}^6 \frac{\partial g_j^{(1)}}{\partial y_k^{(1)}} Pl_{ki} \quad (45)$$

In Table 3, the derivatives calculated by the adjoint process are compared with those calculated numerically with various increments. In order to examine the sensitivity of the Fletscher-Powell procedure compared with an inaccurate derivative, the optimization was carried out for three cases:

- Calculation of derivatives by the adjoint process;
- Calculation of derivatives by differences (increment 10^{-5});
- Calculation of derivatives by the adjoint process with simulation of errors in the derivatives of elements by addition of small random numbers.

Table 3. Derivatives calculated for Williams (diBella)-solution

ZUW	$\partial \phi / \partial T$	$\partial \phi / \partial V$	$\partial \phi / \partial F_A \times 10^3$	$\partial \phi / \partial \alpha \times 10^{-2}$
1.E-7	.14733(.52433)	.00002(.49318)	.3520(.6050)	1.5491(2.7823)
1.E-6	.14734(.52379)	-.00178(.47609)	.3770(.5552)	1.5304(2.7359)
1.E-5	.14770(.52430)	-.00151(.47529)	.3782(.5542)	1.5304(2.7336)
1.E-4	.15138(.52954)	-.00143(.47534)	.3793(.5556)	1.5304(2.7334)
1.E-3	.18782(.58174)	-.00087(.47616)	.3885(.5733)	1.5301(2.7334)
adj. proc.	.14731(.52371)	-.00149(.47523)	.3783(.5537)	1.5304(2.7333)

If the Williams-Otto solution is chosen as a starting point, the optimization breaks off after iterations without an essential improvement of the objective function value. This is due to the fact that within the first iteration a one-dimensional minimum is searched in the direction of the gradient:

$$\max_{\lambda} \phi (656.1 + .524 \lambda, 59.56 + .457 \lambda, 13546. + .000554 \lambda, \\ .247 + 273.33 \lambda)$$

Thus, F_A is changed very little, α , however, undergoes an extremely strong change. Therefore, $F_A/1000$ and 100α were used in the calculations in order to obtain comparable magnitudes. The results of the optimization are listed in Table 4.

Table 4. Results of optimization by Fletscher-Powell method

start	uncertainties of element derivatives	ZUW	F	I ₁	I ₂	I ₃
DB		1.E-5	121.5342227	13	72	124
DB			121.5342261	12	82	
DB	1.E-4		121.5340869	14	74	
DB	1.E-5		121.5342238	14	77	
DB	1.E-6		121.5342260	12	67	
W			121.5342260	18	102	
W		1.E-5	121.5342202	18	100	172

I₁ - Iterations, I₂ - Objective function evaluations (except derivatives), I₃ - Objective function evaluations (total)

In the concrete case, the course of the optimization is relatively insensitive against inaccuracies in the derivatives of the elements. The use of the adjoint process hardly yields any advantage (in spite of a considerably higher additional expense). Only the accuracy of the optimal values is slightly improved.

Thus far two methods of calculation and optimization of complex system have been discussed. A third method is the simplification of the calculation by examination of the model equations. In this case, we start from the complete set of equations describing the general system. These are equations (28)-(35) and:

$$\alpha (F_{RA} + F_{RB} + F_{RC} + 1.1 F_{RE}) - F_D = 0 \quad (46)$$

$$(1 - \alpha) F_{RA} - F_{SA} = 0 \quad (47)$$

$$(1 - \alpha) F_{RB} - F_{SB} = 0 \quad (48)$$

$$(1 - \alpha) F_{RC} - F_{SC} = 0 \quad (49)$$

$$(1 - \alpha) F_{RE} - F_{SE} = 0 \quad (50)$$

$$.1 (1 - \alpha) F_{RP} - F_{SP} = 0 \quad (51)$$

The 14 equations contain 19 variables. Five of these can be chosen arbitrarily. The task is to find the independent variables and the order of solution in such a way that the amount of calculation is minimized (as few iteration variables as possible). The occurrence matrix, which in the concrete case has the structure represented in Table 5, is taken as a basis. There is no universal algorithm to solve this problem. In many cases, however, satisfactory results are obtained by the method of Ledet and Himmelblau [3], Ramirez and Vestal [4], and Soylemez and Seider [5]. The last algorithm also permits the automatic rearrangement of equations.

Table 5. Occurrence matrix

F _A	F _B	T	V	F _{RA}	F _{RB}	F _{RC}	F _{RE}	F _{RP}	F _G	F _R	F _P	F _D	F _{SA}	F _{SB}	F _{SC}	F _{SE}	F _{SP}
		1	1			1		1	1	1							
1		1	1	1	1					1			1				
	1	1	1	1	1	1				1				1			
		1	1	1	1	1		1		1					1		
		1	1		1	1	1			1						1	
		1	1		1	1		1		1							1
				1	1	1	1	1	1	1							
				1	1	1	1	1			1						
				1	1	1	1	1				1					
				1									1				
				1										1			
				1											1		
				1		1										1	
				1		1											1

The following problems will now be examined. The first task is to calculate the Williams-Otto plant choosing the independent variables arbitrarily. In the second task, T , V , F_A , and F_B , α , are chosen previously as independent variables (this corresponds to the flowsheet simulation discussed above). It can be shown that the expense of calculation is essentially dependent in the formulation of the equations. A system of equations written in the sense of optimal programming will prove to be most effectively capable

of solution. For this purpose, three variants are examined. In the first, equations (28)-(35) and (46)-(51) are directly used. In the second equations (35) is deleted, and into the other equations we introduce the sum $F_{RA} + \dots + F_G$ explicitly for F_R . The third variant corresponds R_1 , R_2 , and R_3 are introduced, and equations (28)-(33) are formulated with these variables:

$$\beta - V\rho/F_R^2 = 0 \quad (52)$$

$$R_1 - \beta k_1 F_{RA} F_{RB} = 0 \quad (53)$$

$$R_2 - \beta k_2 F_{RB} F_{RC} = 0 \quad (54)$$

$$R_3 - \beta k_3 F_{RC} F_{RP} = 0 \quad (55)$$

The best ways of calculation were determined for each task and for each variant. It was found that the algorithm of Ramirez and Vestal does not always yield optimal results. Table 6 shows how many iteration variables must be chosen in each case. According to this Table, it is more favourable to have the independent variables determined by the procedure, if possible. Moreover, the expenses of iteration are a minimum when the equations are written optimally from the beginning. (For nonlinear expressions occurring in at least two equations, new variables must be introduced).

Table 6. Number of iteration variables for Williams-Otto-plant

	task 1	task 2
variant 1	1	3
variant 2	2	5
variant 3	0	2

In task 1 (variant 3), T , R_2 , F_{RE} , F_{RP} , and β were obtained as independent variables. No iterations are required. β was set at constant in order to obtain a unique problem.

In optimization by Powell's procedure, the computing times are one magnitude lower compared with the calculation with iterations. The results for the Williams start ($\beta = 5.05 \text{ E-7}$) and the DiBella start ($\beta = 1.12 \text{ E-7}$) are:

$$\begin{aligned}
 \phi &= 121.534266 & T &= 674.43 & R_2 &= 3.0219 \text{ E} + 8 & F_{RE} &= 3228.58 \\
 & & F_{RP} &= 428.47 & & & & \text{(Williams start) and} \\
 \phi &= 121.534266 & T &= 674.43 & R_2 &= 5.5779 \text{ E} + 9 & F_{RE} &= 13475.38 \\
 & & F_{RP} &= 1788.35 & & & & \text{(DiBella start).}
 \end{aligned}$$

4.2 Part of the Acryl Nitrile Plant

By analysis of the ACN plant, four recycles (reactor-heat exchanger 1, separator-reactor, splitter-reactor, splitter-mixer-heat exchanger 2-separator) can be recognized. The last two recycles have section W3 in common, therefore, only three loops are independent. Since all streams have two dimension (T , F), and iteration problem with five variables T_P , F_P , F_{D1} , T_{W3} , F_{W3} is obtained for the calculation of the recycles (T was assumed to be constant). Since the reaction model itself can be solved only by iteration, a nested iteration problem is obtained, i.e. the internal iteration (calculation of the reactor) must be carried out completely at each step of the external iteration (calculation of the recycles). The number of the iteration variables can be decreased and the coupling of iterations can be removed in the following manner:

- a). Detailed examination of the material balances of the general system and of single partial systems. Thus, for example it can easily be found that the variables F_P and F_{D1} can always be calculated directly from input variables of the system:

$$F_P = F_{LO} + F_{NH} + F_{PR} \quad (56)$$

$$F_{D1} = F_W \quad (57)$$

Moreover, we always obtain $F_{W3calc.} = F_{W3estim.}$ Thereby a reduction to two external (T_{W3} , T_P) and two internal (T_{D4} , T_P) iteration variables was achieved.

- b). Tearing the system after elements with implicit non-linear model equations (in this case, after the reactor). Thereby iteration variables which would pertain to the external as well as to the internal iteration

problem are deleted (in this case, T_p). Now there is only one iteration problem with three variables (T_p , T_{D4} , T_{W3}) to be solved.

The same result is obtained by the application of the algorithm of Ramirez and Vestal to the original system of model equations. Here, the calculation cannot be carried out without iteration. In the following, however, the nested iteration (two internal and two external iteration variables) was retained in the calculation of this example in order to test the effectiveness of different combinations of iteration procedures. Table 7 shows the results of the convergence test by different variants of calculation. The procedure of successive substitution did not yield any convergence for both the internal and external problem even if well-chosen starting values were used. Broyden's method was strongly dependent on the starting values, but with good starting values it worked with a high speed of convergence. The procedures of nonlinear regression (spiral algorithm and Chebyshev approximation) were reliable and stable even with bad starting values, the speed of convergence of the spiral procedure being greater than that of the Chebyshev approximation. On the other hand, the range of convergence of the latter was greater.

Table 7. Convergence properties of several iteration algorithms

	s.s.		Broyden		Jones		Tscheby.	
	outs.	ins.	outs.	ins.	outs.	ins.	outs.	ins.
s.s. outs.	-		-		-		-	

Jones outs			-		+		+	

Tscheby. outs.								+

An essential fact should be pointed out. From the experiments the property of convergence were shown to be dependent not only on the iteration procedure used and the starting values, but also on the accuracy of the model. In this example, an arithmetic mean temperature was at first used in the calculation of the heat-ex-

changer, and the separator was calculated on the basis of a simplified enthalpy balance. All iteration procedures used did not yield any convergence, or the results were physically meaningless. It can be expected that this problem frequently occurs in more complicated systems.

The ACN plant also served as a basis for the calculation of static sensitivity coefficients according to equation (15). The first order sensitivity coefficients of the intermediate and output variables of the system \underline{y} and \underline{y}^o were calculated by using the adjoint process as well as by the formation of differences:

$$s_{ij}^{kl} = \frac{y_i^{(k)}(p_j^{(1)} + \Delta p_j^{(1)}) - y_i^{(k)}(p_j^{(1)})}{\Delta p_j^{(1)}} \quad (58)$$

$$\Delta p = \delta \times p \quad 10^{-6} \leq \delta \leq 10^{-3}$$

The establishing of the adjoint system was carried out in a similar manner to the basic system. According to the procedure depicted in chapter 2, a linear system of equations of the dimension 21×21 was obtained. The necessary derivatives of the elements were calculated numerically (reactor) and analytically (other elements), respectively. Table 8 represents selected derivatives of the output variables calculated numerically with different increments and by the method of the adjoint process. As can be seen from the Table, the numerical derivatives in the range $10^{-5}p \leq p \leq 10^{-3}p$ of the increments are stable and in general very well agree with the derivatives determined by the method of the adjoint process.

Table 8. Selected sensitivity coefficients of system output T_p 2

	ZUW	1.E-3	1.E-4	1.E-5	1.E-6	adj.process
p_j						
F_{Lo}		1.0153E-3	1.0156E-3	1.0173E-3	1.0333E-3	1.0464E-3
T_{Lo}		1.5814E-1	1.5814E-1	1.5822E-1	1.5894E-1	1.5813E-1
k_1		-2.3442E-1	-2.3448E-1	-2.3367E-1	-2.2617E-1	-2.3459E-1
F_1		-3.7541E-2	-3.7551E-2	-3.7420E-2	-3.6219E-2	-3.7567E-2
k_1^y		-1.0304E-1	-1.0309E-1	-1.0297E-1	-3.5517E-1	-1.0309E-1
F_v^y		-4.4019E-1	-4.4044E-1	-4.3990E-1	-1.5174E+0	-4.4043E-1
H^v		5.3766E-4	5.3778E-4	5.3827E-4	5.4285E-4	5.3767E-4
a		7.8736E+2	7.8501E+2	7.8482E+2	7.8523E+2	7.5738E+2
T_w		3.8739E-1	3.8739E-1	3.8744E-1	3.8796E-1	3.8756E-1

In order to recognize possible errors, the behaviour of the sensitivity coefficients calculated by the adjoint process towards the accuracy of the derivatives of the elements $\partial y/\partial x$ was examined. For this purpose, the $\partial y/\partial x$ were dispersed with the aid of random numbers, and the effect on the results was examined.

$$\left(\frac{\partial y}{\partial x}\right)^* = \left(\frac{\partial y}{\partial x}\right)(1+z) \quad -0.5 \varepsilon \leq z \leq 0.5 \varepsilon \quad (59)$$

(ε uniform distributed random number 0.1)

Selected results are represented in Table 9. Since the error in the calculation of the derivatives of elements in practice do not exceed the third position ($\varepsilon = 10^{-1}$ can practically be excluded), the conclusion can be drawn that the adjoint process is relatively stable against normal inaccuracies of the derivatives of elements. However, major deviations were found to exist in certain sensitivity coefficients between numerical results and those obtained by the method of adjoint process. Here, the values of the whole system derivatives were also considerable influenced by the dispersion of the element derivatives.

Table 9. Influence of derivations of element derivatives on system output sensitivity coefficients

p_j	E	0	1.E-4	1.E-3	1.E-1
F_{LO}		1.0464E-3	1.0470E-3	1.0480E-3	1.1960E-3
T_{LO}		1.5813E-3	1.5812E-3	1.5830E-3	1.7270E-3
k_1		-2.3459E-1	-2.3459E-1	-2.3480E-1	-2.5701E-1
F_1		-3.3459E-1	-3.7568E-1	-3.7604E-1	-4.1152E-1
k_v		-1.0309E-1	-1.0308E-1	-1.0322E-1	-1.1731E-1
F_v		-4.4043E-1	-4.4046E-1	-4.4104E-1	-5.0134E-1
H_v		5.3767E-4	5.3767E-4	5.3842E-4	6.1201E-3
a		7.5738E+2	7.1412E+2	7.0554E+2	-3.1620E+2
T_w		3.8756E-1	3.8744E-1	3.8781E-1	4.3080E-1

In Table 10, the sensitivity coefficients $\partial F_{WD}/\partial a$ and $\partial F_{WD}/\partial F_W$ for the numerical calculation are compared with those computed by the method of adjoint process. It was proved that the error of the derivatives calculated by the method of adjoint

process resulted from the loss of positions in the solution of the system of linear equations and that it can be removed by calculation with double precision. The conclusion must be drawn from the investigations that a comparison with the numerically computed derivatives should be carried out at least in the first application of the method of adjoint process.

Table 10. Great deviations in sensitivity coefficients

	numerical	adjoint process
a	-1.0000E+5	-1.0154E+5
m _w	.0000	-9.2653E-2

In the computation of sensitivity coefficients, the comparison of computing times between the numerical calculation of differences and the method of adjoint process is determined by the ratio of the number of independent variables ($p, \underline{x}^0, \underline{u}$) to the number of the dependent variables considered ($\phi, \underline{y}, \underline{y}^0$). The number of the dependent variables equals the number of right-hand side of the system of linear equations. The number of independent variables determines the number of necessary system calculations in the numerical differentiation, the number of dependent variables being insignificant here since they are all determined simultaneously. Thus, the effectiveness of the application of the adjoint process increases with the increasing number of independent variables. However, for the purpose of sensitivity analysis, the accuracy of the derivatives cannot be increased essentially.

5. CONCLUSIONS

Method of calculation and optimization were examined and discussed with two model systems. The most important results can be summarized as follows

1. The application of general flowsheet simulation programmes offers the following advantages: Applicability without prior special

knowledge, applicability of standardized models of elements, simple generation of structure variants; whereas unnecessarily large and nested iteration problems proved to be disadvantageous. Therefore, the computation of numerically difficult system becomes problematical, and the optimization using the flowsheet simulation is often impossible due to the high demand of time. Therefore, the application of the flowsheet simulation is most reasonable in the stage of design.

2. The equation oriented computation of the system offers major advantages with respect to accuracy and computation speed. The iteration time required can be essentially decreased. A disadvantage is the fact that element models cannot be used in the common form, and a new analysis of the model may become necessary when the general structure is changed. In practice, this method will succeed only if programmes are available which allow their rearrangement. A first step in this direction was achieved by Soylemez and Seider [5].

3. In the solution of the iteration problems, the Chebyshev approximation is distinguished by a high security of convergence, however, in easy problems, it is slightly inferior to other procedures with respect to speed.

4. The application of the method of adjoint process can improve the accuracy of the first derivatives of the objective function. The disadvantages are the increased expense due to the formation of derivatives of elements, the organization of the computation of the system of linear equations, and the possibility that due to numerical effects which are difficult to control, major errors occur in the derivatives. Therefore, the application of the adjoint process for optimization by use of gradient procedures cannot be universally recommended. In the case of sensitivity analysis, its application is advantageous if the number of independent variables is relatively big.

5. At present, the major difficulty in the calculation and optimization of large systems is not due to the lack of effective methods, but to the inaccuracy of the many models of the elements used.

NOMENCLATURE

$\underline{x}^{(k)} = (x_1^{(k)} \dots x_{mk}^{(k)})^T$	input variables of element k
$\underline{y}^{(k)} = (y_1^{(k)} \dots y_{nk}^{(k)})^T$	output variables of element k
$\underline{u}^{(k)} = (u_1^{(k)} \dots u_{rk}^{(k)})^T$	designs and controls of element k
$\underline{x}^o(k) = (x_1^o(k) \dots x_{pk}^o(k))^T$	system input variables
$\underline{y}^o(k) = (y_1^o(k) \dots y_{qk}^o(k))^T$	system output variable
N	total number of elements
N_1	number of system input elements
N_2	number of system output elements
S	sensitivity coefficient t
F_i	flow rated
V	reactor volume
T_i	temperatures
C_i	heat capacities
k_i	heat transfer coefficients
A_i	heat transfer areas

Greek Letters

$\underline{\lambda}^{(k)} = (\lambda_1^{(k)} \dots \lambda_{nk}^{(k)})^T$	adjoint input variables, element k
$\underline{\mu}^{(k)} = (\mu_1^{(k)} \dots \mu_{mk}^{(k)})^T$	adjoint output variables, element k
$\underline{\lambda}^o(k) = (\lambda_1^o(k) \dots \lambda_{gk}^o(k))^T$	adjoint system input variables
$\underline{\mu}^o(k) = (\mu_1^o(k) \dots \mu_{pk}^o(k))^T$	adjoint system output variables
ϕ, ϕ^*	objective functions

REFERENCES

- [1] SHANNON, P.T. et al.: Chem.Eng.Prog., 62, 381, (1966)
- [2] WINTER, F. et al.: The Concept Method of Complex Plant Simulation. 7. Symp. der Europ. Föderation für Chemieingenieurwesen, Erlangen, 1974.
- [3] LEDET, W.P., HIMMELBLAU, D.M.: Decomposition Procedures for Large Scale Systems. Adv.Chem.Eng., 8, 185, (1970)
- [4] RAMIREZ, W.F., VESTAL, Ch.R.: Algorithms for Structuring Design Calculations. Chem.Eng.Sci., 27, 2243 (1972)
- [5] SOYLEMEZ, S., SEIDER, W.D.: A new Technique for Precedence Ordering Chemical Process Equation Sets. A.I.Ch.E.J., 19, 934, (1973)
- [6] BEVERIDGE, G.S.G., SCHECHTER, R.S.: Optimization: Theory and Practice. McGraw-Hill, New York, 1970.
- [7] POWELL, M.J.D.: An Efficient Method for Finding the Minimum of a Function of Several Variables Without Calculating Derivatives. Comp.J., 7, 155, (1964)
- [8] ROSENBROCK, H.H.: An Automatic Method for Finding the Greatest or Least Value of a Function. Comp.J., 3, 175, (1960)
- [9] FLETCHER, R., POWELL, M.J.D.: A Rapidly Convergent Descent Method for Minimization. Comp.J., 6, 163, (1963)
- [10] BOX, M.J.: Comp.J., 9, 67, (1966)
- [11] GELFAND, I.M., ZEJTLIN, M.L.: Advances of Mathematics, 17, 3, (1962) (in Russ.)
- [12] BROYDEN, G.G.: Quasi-Newton Methods and their Application to Function Minimization. Maths.Comput., 21, 368, (1967)
- [13] JONES, A.: Comp.J., 13, 301, (1970)
- [14] PAMERT, K., REINIG, G., and BALZER, D.: Nichtlineare Optimierung für Modellierung und Prozess-steuerung-Algorithmen, FORTRAN-Programme, Anwendungen. Akademie-Verl., Berlin, 1976. (in press)
- [15] OSTROWSKIJ, G.M., WOLIN, Ju.: Methoden der Optimierung komplexer verfahrenstechnischer Systeme. Akademie-Verl., Berlin, 1973.
- [16] WILLIAMS, T.J., OTTO, R.E.: A.I.Ch.E.Trans., 79, 458, (1960)
- [17] MÖLLMANN, I.; Dissertation A., TH Leuna-Merseburg, 1975.
- [18] ADELMAN, A.W., STEVENS, F.: Process Optimization by the Complex Method. A.I.Ch.E.J., 18, 20, (1972)
- [19] DiBELLA, C.W., STEVENS, W.F.: Ind.Eng.Chem. Process Design Development, 4, 16, (1965)

РЕЗЮМЕ

Статья касается приближения и оптимизации комплексных химических систем. Авторы приводят различные методы приближения и оптимизации, и проделывают это принимая во внимание аспекты численных расчетов, произведенных на цифровых ЭВМ. Приближение, построенное для части процесса, критически сравнивается с решениями, основанными на уравнениях. Многочисленные вспомогательные методы применяются для расчета первой переменной комплексной системы.

Рассмотрен также и расчет статического коэффициента чувствительности первой степени. Может быть сделан вывод, что приближение части процесса может быть применено, как эффективный метод, пока что только в стадии проектирования. При оптимизации этот метод приводит к целому ряду многомерных итераций. В то время как при решении с помощью уравнений можно рассчитывать на минимальное количество итерационных переменных.

CONTENTS

LÁSZLÓ, A. and MARTON, Gy.: Studies on the Atmospheric, Non-Steady-State, Stripping Out Furfural Reactor, Part 1. The Model of the Process	165
MARTON, Gy. and VASS, J.: Studies on the Atmospheric, Non-Steady-State, Stripping Out Furfural Reactor, Part 2. The Optimum Timing of Stripping Out	179
MÉSZÁROS, L., SZABÓ, M., GREGA, J. and TASI, L.: Agitators Built Up of New Elements and the Application Thereof, Part 2.	191
JEWUR, S.S. and KURIACOSE, J.C.: Influence of Substrates on the Catalytic Activity of Ferric Oxide	201
TIMÁR, L. and CSERMELY, Z.: A Two-Stage Computation Method for Technological Systems	211
CSERMELY, Z. and TIMÁR, L.: Plate Absorber Modelling by Matrix Method	231
PLEVA, L. and NOVÁK, B.: Evaporator System Studies	245
PALÁNCZ, B.: Approaching Analysis for Distributed Systems	259
MAKRANCZY, J., Mrs. MEGYERY-BALOG, K., RUSZ, L. and PATYI, L.: Solubility of Gases in Normal-Alkanes	269
BLICKLE, T. and NAGY, E.: Classification of Non - Catalytic Heterogeneous Gas-Liquid and Liquid-Liquid Reactions	281
HARTMANN, K., DITTMAR, R. and DAMERT, K.: Practical Experiences in the Simulation and Optimization of Complex Chemical Processes	297

СОДЕРЖАНИЕ

ЛАСЛО, А., МАРТОН, ДЬ.: Исследование выпарного фурфуролового реактора с нестационарным режимом, работающего при атмосферном давлении I. Процесссионная модель.....	165
МАРТОН, ДЬ., ВАШШ, Й.: Исследование выпарного фурфуролового реактора с нестационарным режимом, работающего при атмосферном давлении II. Оптимальная трактовка выпарки.....	179
МЕСАРОШ, Л., САБО, М., ГРЕГА, Й., ТАШИ, Л.: Агитаторы, построенные из новых элементов, и их применение. II.....	191
ДЖЕВЬЮ, С., КУРЬЯКОЗ, Д.Ц.: Влияние субстратов на каталитическую активность окисла железа (III).....	201
ТИМАР, Л., ЧЕРМЕЙ, З.: Расчет технологических систем двухступенчатым методом.....	211
ЧЕРМЕЙ, З., ТИМАР, Л.: Моделирование тарельчатого абсорбера матричным методом.....	231
ПЛЕВА, Л., НОВАН, Б.: Исследование системы эвапораторов.....	245
ПАЛАНЦ, Б.: Приближенный анализ дистрибутивных систем.....	259
МАНРАНЦИ, Й., БАЛОГНЕ, К., РУС, Л., ПАТЬИ, Л.: Растворимость газов в нормальных алканах.....	269
БЛИКЛЕ, Т., НАДЬ, Э.: Систематизация гетерогенных некаталитических реакций типа газ-жидкость, жидкость-жидкость.....	281
ХАРТМАН, К., ДИТТМАР, Р., ДАМЕРТ, К.: Практические выводы о приближении и оптимизации комплексных химических систем.....	297

HUNGARIAN

Journal of

INDUSTRIAL

CHEMISTRY

Edited by

the Hungarian Oil & Gas Research Institute (MÁFKI),
the Research Institute for Heavy Chemical Industries (NEVIKI),
the Research Institute for Technical Chemistry of the
Hungarian Academy of Sciences (MÜKKI),
the Veszprém University of Chemical Engineering (VVE).
Veszprém (Hungary)



Volume 4.

1976

Supplement 1-2.

HU ISSN: 0133-0276
CODEN: HJICAI

Editorial Board:

R. CSIKÓS and Gy. MÓZES

Hungarian Oil & Gas Research Institute
(MÁFKI Veszprém)

A. SZÁNTÓ and M. NÁDASY

Research Institute for Heavy Chemical Industries
(NEVIKI Veszprém)

T. BLICKLE and O. BORLAI

Research Institute for Technical Chemistry
of the Hungarian Academy of Sciences
(MÜKKI Veszprém)

A. LÁSZLÓ and L. PÉCHY

Veszprém University of Chemical Engineering
(VVE Veszprém)

The "Hungarian Journal of Industrial Chemistry" is a joint publication of the Veszprém scientific institutions of the chemical industry that deals with the results of applied and fundamental research in the field of chemical processes, unit operations and chemical engineering. The papers are published in four numbers at irregular intervals in one annual volume, in the English, Russian, French and German languages.

Editorial Office:

Veszprémi Vegyipari Egyetem
"Hungarian Journal of Industrial Chemistry"
H-8201 Veszprém, P.O. Box: 28.
Hungary

Felelős szerkesztő: Dr. Bodor Endre
Kiadásért felelős: Dr. Nemezc Ernő, a VVE rektora
Készült a Váci ÁFESZ nyomdában. Felelős vezető: Kiss János

P r e f a c e

The rapid extension of automation was made necessary by the growing demands of mankind and was made possible by the quick development of science and technology. Among the various assignments of automation increased attention has to be paid to the modelling of human thinking, to the automation of mental work or, as it is said, to the research carried out to evaluate artificial intelligence.

The structure theory seems to be applicable for the description of matters and phenomena of the concrete world. Assuming that the matters and phenomena can be characterized by their natures, using the structure theory, primarily the natures are described by an abstract quality set. It is also assumed that certain relations exist between the natures, i.e. there are natures which can exist only at given values of the other natures, in the algebraic description of this assumption the permitted subset of the property power set is valid. These allowed nature value combinations define matters and phenomena of the real world and the algebraic model is equivalent with them.

The structure theory which can advantageously be used for the description of phenomena is a suitable tool in the research of artificial intelligence.

The Special Committee for Computation Technique and System Theory, connected to the Veszprém Division of the Hungarian Academy of Sciences, set up the Committee of System Structure in 1974. This latter Committee, collaborating with the Research Institute for Technical Chemistry of the Hungarian Academy of Sciences carries out joint research work on the field of system theory and uses the results in technical chemistry.

The system theory was first interpreted at the 1975 Technical Chemistry Days at Keszthely (Hungary). This volume presents the delivered lectures.

Dr. T. Blicke
Director of the Research Institute for
Technical Chemistry of the HAS.
Chairman of the Special Committee for
Computation Technique and System Theory
of the VDHAS.

ALGEBRAIC STUDY OF STRUCTURES

T. BLICKLE*, K. SEITZ**, C. JUHÁSZ* and Mrs. A. FONÓD-LAKOS*

(*Research Institute for Technical Chemistry of the
Hungarian Academy of Sciences, Veszprém

**Budapest Technical University)

The algebraic properties of structures defined by (T, H) matrixes are shown and a method for the generation of the structures is given. It is proved that an equivalent method, i.e. with the aid of the (H, H) matrix, exists for the determination of the structures.

Properties of special semi-lattice applicable for the investigation of systems structures are shown by different examples. A method is given for the determination of the minimum defining relation system of the above mentioned special semi-lattice and the primary equivalency classes according to K. Some examples of suitable transformations of the semi-lattice are also shown.

1. Structure

Let H be an arbitrary finite set. Let T be a set of properties of the elements in H . Let $[T, H]$ be a $0, 1$ matrix containing 1 in the $t \in T$ line of the $h \in H$ column if the h element is of t property, otherwise 0. .

Let F be a function corresponding set of those elements in H which have t property to every $t \in T$ property.

The $[T, H]$ matrix is called a structure if:

- (TH 1) In any line of the $[T, H]$ matrix both 0 and 1 occur.
- (TH 2) Any two columns of the $[T, H]$ matrix differ from each other.
- (TH 3) The T set has a $\tau = \{T_i\}_{i=1}^n$ equivalency classification for which:
- (TH 3)/(1) if $T_i \in \tau$ then $\bigcup_{t \in T_i} F(t) = H$
- (TH 3)/(2) if $T_i \in \tau$, $t \in T_i$, $t' \in T_i$ and $t \neq t'$ then $F(t) \cap F(t') = \phi$

conditions are fulfilled. The number n is termed the order of the structure.

It can be proved that every column of the $[T, H]$ matrix contains 1 of exactly n number.

Let $(T, 0)$ be the following algebraic structure above the T set:

(T 1) If $t \in T$ and $t' \in T$ then

$$(T 1)/(1) \quad t \circ t' = \begin{cases} t & \text{if } t = t' \\ \mathbb{0} & \text{if } F(t) \cap F(t') = \phi \\ \widetilde{tt} & \text{if } F(t) \cap F(t') \neq \phi \end{cases}$$

$$(T 1)/(2) \quad F(\mathbb{0}) = \phi; \quad F(tt') = F(t) \cap F(t')$$

(T 2) If $t \in T$ and $t' \in T$ then $t \circ t' = t' \circ t$

(T 3) If $t \in T$, $t' \in T$ and $t'' \in T$ then $t \circ (t' \circ t'') = (t \circ t') \circ t''$.

This algebraic structure is termed structure algebra.

The (T, \circ) structure algebra has the following properties that can be proved:

- (α) (T, \circ) is a semi-lattice of zero element in that the $x = \mathbb{0}$ equation for any a has a solution differing from $\mathbb{0}$.
- (β) In the (T, \circ) the primary element has a $\phi \neq P$ set for which:

- (i) the decomposition by the primary element is unambiguous
- (ii) the P set has a $\mathcal{P} = \{p_i\}_{i=1}^n$ equivalency classification for which;
 - (1) if $P_i \in \mathcal{P}$ then P_i has at least two elements.
 - (2) If $P_i \in \mathcal{P}$, $p \in P_i$, $p' \in P_i$ and $p \neq p'$ then $p \circ p' = \emptyset$.
 - (3) If S_i denotes all none \emptyset products consisting of i primary coefficients then $S_i \neq \emptyset$ and $\{\emptyset\} \cup \{S_i\}_{i=1}^n$ set system gives an equivalency classification of (T, \circ) .

One to one accordance can be set up between the S_n and H sets.

It is provable that for any (A, \circ) algebraic structure of α and β property, a structure having (T, \circ) structure algebra that is isomorphous with (A, \circ) can be found.

It is provable that for any (A, \circ) α , β structure an (A', \circ) α , β structure can be given in which the following conditions are fulfilled:

- (DR 1) The (A', \circ) structure unequivocally can be given by defining relations of two parameters described between the $P' = \{p'_i\}_{i=1}^n$ primary equivalency classes.
- (DR 2) (A', \circ) is the epimorphous successor of the (A, \circ) structure.
- (DR 3) One to one accordance can be set up between S_n and S'_n .

It is provable that if in the $\{S_i\}_{i=1}^n$ set there is an S_j $j < n$ class that one to one can be mapped to S_n the (A, \circ) α , β structure has an φ endomorphism mapping S_n to S_j . In this case the $\varphi(A, \circ)$ structure is termed the core of (A, \circ) α , β structure.

If $S_n = K_1 \circ K_2$ where $K_1 \neq \emptyset \neq K_2$ and the K_1 and K_2 complexes have not common primary coefficients, the structure in first order is not coherent.

If $S_n = K_1 \cup K_2$ where $K_1 \neq \emptyset \neq K_2$ and the K_1 and K_2 complexes have not common primary coefficients, the structure in second order is not coherent.

Let (A, o) be an α, β structure given in accordance with DR 1 and all unnecessary defining relations are omitted. Let G be a graph, the points of which can be one to one according to the primary equivalency classes of P and the p_i point is connected by an edge with the p_j point, only if the defining relation between the corresponding p_i and p_j equivalency classes is given. This graph is termed structure graph belonging to the defining relation system.

It is provable that the G graph is coherent if the structure is coherent in the first and the second orders.

Let us assume that $\mathcal{P}_a = \mathcal{P}_1 \cup \{p_i\}$ and $\mathcal{P}_b = \mathcal{P}_2 \cup \{p_i\}$ primary equivalency classes determine by the defining relations two, (A_a, o) and (A_b, o) substructures of (A, o) α, β structure and for the above substructures: $(A_a, o) \circ (A_b, o) = (A, o)$. This $((A_a, o), (A_b, o))$ structure pair is termed the secondary structure being supported by the p_i point.

The secondary structure being supported by the articular point of a higher order or more articular points, can be similarly interpreted.

2. Structure generation

Let the $[T, H]$ 0,1 matrix be given.

Problem: Does this $[T, H]$ 0,1 matrix describe a structure?

The answer is given by the transformation of the matrix:

- (i) lines containing only 0 or only 1 are omitted.
- (ii) only one of similar columns is regarded, the others are omitted.

- (iii) the column containing 1 in the least number is placed to $[T, H_1]$ matrix, the others to the $[T, H_2]$ matrix.
- (iv) elements of the T set are grouped into equivalency classes: properties from which a $[T_i, H_1]$ matrix containing exactly one 1 can be constructed belong to an equivalency class.

If the $[T, H_1]$ matrix cannot be given as a union of such $[T_i, H_1]$ matrices, the $[T, H]$ matrix is not a structure.

The equivalency classification gained above is also transmitted to the $[T, H_2]$ and $[T, H]$ matrices.

- (v) Only one of similar equivalency classes of $[T, H]$ is regarded and adequate lines of $[T, H_1]$ and $[T, H_2]$ are also omitted.
- (vi) If the $[T, H_2]$ matrix has a column which does not contain 1 in any equivalency class only 0, the $[T, H]$ matrix is not a structure.
- (vii) The $[T, H_1]$ and $[T, H_2]$ matrices are interwoven: let us suppose that the h column of $[T, H_2]$ matrix in the T_j equivalency class contains i times 1, namely the $j^{t_1}, j^{t_2}, \dots, j^{t_i}$ properties. Let us add a new j^{t^*} element to the T_j class.

Let the $[T, H_2]$ matrix be completed with the j^{t^*} line containing only 0. Let us write 0 to the $j^{t_1}, j^{t_2}, \dots, j^{t_i}$ places and 1 to the j^{t^*} place in the h column of the $[T, H_2]$ matrix. If this combination occurs even in other columns of the $[T, H_2]$ matrix, in the T_j equivalency class, this modification must also be carried out there. To the remaining places of the j^{t^*} line let us write 0.

By the continuation of this procedure it can be attained that in every column of the $[T, H_2]$ matrix, exactly one 1 occurs in every equivalency class. The union of $[T, H_1]$ and $[T, H_2]$ gives the new $[T, H]$ matrix.

- (viii) Lines consisting of only 0 or 1 are omitted. Only one of similar columns is regarded. Only one of similar equivalency classes is regarded.

If the $[T, H]$ matrix does not fulfil the $[TH\ 3]$ condition a structure cannot be constructed.

- (ix) The structure algebra is constructed. The core of the structure is selected.
- (x) The structure is cut into a maximum number of pieces, being coherent in the first and second order.
- (xi) The structure is transformed according to the (DR 1)-(DR 3) properties: if the order of the $[T, H]$ structure is n , unequivocal definition of S_n by S_{n-1} , then that of S_{n-1} by S_{n-2} etc., will be discussed.

Let us suppose that S_{i+2} is still unequivocally defined by S_{i+1} however S_{i+1} is not defined by S_i . It means that:

$$(a) \quad {}_1t_1 = {}_1t_1 \circ \dots \circ {}_1t_{i-1} \quad {}_1t_i \in S_i \text{ and}$$

$${}_2t_2 = {}_1t_1 \circ \dots \circ {}_1t_{i-1} \quad {}_2t_i \in S_i$$

$${}_1t_i \circ {}_2t_i \neq \emptyset \text{ however}$$

$$(b) \quad ({}_1t_1 \circ \dots \circ {}_1t_{i-1} \circ {}_1t_i) \circ {}_2t_i = \emptyset$$

If ${}_1t_i \in {}_1t_j$ ($1 \leq j \leq i$) let the $\{{}_1t_j\}_{j=1}^i$

classes be reduced to a new

$$T_i^* = \bigcap_{j=1}^i T_j \setminus \left(\{\emptyset\} \cup \bigcup_{i=1}^{i-1} S_i \right) \text{ class.}$$

Let this procedure be repeated up to $i=2$. It is provable that a structure algebra fulfilling (DR 1)-(DR 3) can be gained in this manner

- (xii) If an easier survey is necessary, let the structure be decomposed to a secondary structure.

3. Giving the Structure by $[H, H]$ matrices

Let H be an arbitrary set. Let us construct the $[H, H]$ symmetrical $0,1$ matrix containing 1 in the $h' \in H$ line of the $h \in H$ column if h is similar to h' (i.e. they have at least one common property) otherwise 0.

Let R be a relationship of two variables on the H set for which hRh' is valid exactly if the h element is similar to h' . This relationship is reflexive, and symmetrical, but not transitive.

Let $\overset{O}{H}$ be the family of subsets of H for which any two elements are in R relation.

Let \tilde{H} be family of those subsets of $\overset{O}{H}$ that give the equivalency classification of H .

If a T property system exists for which $[T, H]$ is a structure, then the power set of H provably has a subset above which the α, β structure, being isomorphous with the algebra of $[T, H]$ structure, can be interpreted by the \cap operation.

The method has the advantage of not forcing a property system defined by us upon the H set, but its drawback is the complicated algorithm. For this reason, its application is verified only by the impossibility of the structure generation by more T property systems.

4. System Construction

(A) Let H be an arbitrary set. Let T_a and T_b be two property systems belonging to H set. Let $[T_a, H_a]$ and $[T_b, H_b]$ be the adequate structures.

Let $T_c = T_a \cup T_b$. $[T_c, H_c]$ can also be proved to be a structure even more detailed than $[T_a, H_a]$ and $[T_b, H_b]$ respectively.

- If the $[T_c, H_c]$ structure is transformed according to (DR 1)-
 • - (DR 3) properties, the defining relations of $[T_a, H_a]$ and $[T_b, H_b]$ do not change, but new relations are also connected to them.

If the algebras of $[T_a, H_a]$ and $[T_b, H_b]$ structures are isomorphic, the defining relation system of $[T_c, H_c]$ may be simplified to a large extent.

ⓑ Let H be an arbitrary set. Let $[T_1, H_1]$ be a structure constructed by elements of H . Let $T_i \in \tau_1$ be a property class.

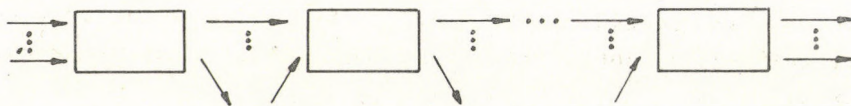
Evidently by increased the fineness of the T_i class, the $[T_1, H_1]$ structure also becomes increasingly finer.

ⓒ Let $[T_1, H_1], [T_2, H_2], \dots, [T_n, H_n]$ be structures for which $H_i \in \tau_{i+1}$. In this case a series of structures constructed on each other is gained that can be applied for the study of the "evolutive" properties.

5. Structure of Technical Chemical Systems

A technical chemical system consists of input and output materials, apparatuses realizing physical and chemical changes on the materials and series constructable from them, respectively. (Apparatuses of similar function connected parallel for simplicity are regarded as single ones.)

The technical chemical systems can thus be given by the following scheme:



where fingers symbolize material flows, and the rectangles symbolize the apparatuses.

The technical chemical systems are thus described by the following properties:

- (i) classes of input materials.
- (ii) Classes of output materials.
- (iii) Classes of changes occurring in the apparatuses.
- (iv) Classes describing phases in the apparatuses.
- (v) Classes of existing properties of apparatuses.

The structure of input and output materials can be constructed putting together the structure of the materials. It becomes quite simple to utilize the isomorphism structures put together. However, input and 'output' materials of different apparatuses, changes, phases and existing properties belonging to the apparatuses are also isomorphous. So the system can be relatively simplified.

The condition for the connection of the apparatuses is the appearance of at least one output material of the preceding apparatus among the input materials of the following one. Chemical mappings of the apparatuses are described by defining the relations connecting the input and output materials.

The substructure - consisting of classes of input and output materials and changes - is provably an abstract automaton having the input material as input and the output material as output signs.

РЕЗЮМЕ

Авторами показаны алгебраические свойства структуры заданной матрицей (T, H) , и приводят также метод для обобщения структуры. Ими доказано, что матрица (H, H) адекватна с предыдущим методом описания структур.

Свойства специальной полусети, пригодной для исследования структуры систем показаны на различных примерах. Дается метод для определения - минимальной определяющей системы реляций упомянутой специальной полусети и классов эквивалентности по H . На примерах исследуются несколько целесообразных преобразований полусети.

RECENT RESULTS IN THE THEORY OF SEMIGROUPS OF TYPE α

K. SEITZ and B. GREGA

(Technical University, Budapest)

Following interpretation of the semi-group of α -type the ideal of these semi-groups were determined.

As the next stage structure of automorphism group of semi-group of α -type is discussed.

Finally practical application of the gained results is shown.

INTRODUCTION

In the abstract algebraic study of the structure of systems in chemical engineering, semigroups of type α play a fundamental role [1, 2].

This paper primarily deals with the generating of semigroups of type α . The results obtained are very useful in the investigation of the structure of semigroups of type α which are of fundamental importance in the structure theory of chemical engineering.

1. The Concept and Basic Properties of Semigroups of Type α

A semigroup F is said to be of type α if and only if the following conditions hold:

1°. For arbitrary elements a, b in F

$$ab = ba$$

2°. For every element a in F

$$a^2 = a$$

3°. There exists a zero element 0 in F .

4°. For every element a in F there is at least one non-zero element x in F such that

$$ax = 0$$

It is well-known that - following KLEIN—BARMEN [3] - a commutative idempotent semigroup is also called a semilattice. Thus every semigroup of type α is a semilattice.

An interesting property of the semigroups of type α is that they have no identity element.

For, if e were an identity element of F , then there would be a non-zero element x in F such as $ax = 0$, that is:

$$ex = \begin{cases} 0 \\ x \end{cases}$$

which is a contradiction because $x \neq 0$.

Denote $Z(a)$ the set of all elements x of F for which the product $xa = 0$.

The following lemmas can be proved:

Lemma 1.1. $Z(a)$ is a subsemigroup of F .

Lemma 1.2. If $p, q \in F$, then $Z(p)Z(q) \leq Z(pq)$.

Lemma 1.3. In the case $a \in F$ the subsemigroup $Z(a)$ is an ideal of the semigroup F of type α .

A subset K of the semigroup F of type α is called quasi-idempotent if and only if $K \cdot K = K \cup 0$.

Denote F the set of all quasi-idempotent subsets of the semigroup F .

Lemma 1.4. The set F is a commutative semigroup with respect to the set product in F .

2. Special semigroups of type α

The following two theorems are true:

Theorem 2.1. If $a \in F$, then the set $a \cup Z(a)$ is a subsemigroup of type α of F .

Theorem 2.2. Suppose that F_1, F_2 are subsemigroups of type α of F , and for every element $c_i \in F_i$ ($i = 1, 2$) the inclusion holds: $Z(c_i) \leq F_i$, moreover $F_1 \cap F_2 = O$. Then the product $F_1 \cdot F_2$ is again a semigroup of type α .

Let us denote by $F(a)$ the set of all elements x of the semigroup F of type α for which $ax = a$. The set $F(a)$ is not empty because of $a \in F(a)$.

Theorem 2.3. In the case $a \in F$ the set $F(a) \cup Z(a)$ is a subsemigroup of type α of the semigroup F .

3. Generating of Finite Semigroups of Type α

Let g_1, g_2, \dots, g_n be a minimal generating system of the semigroup F of type α .

Denote T the set of all relations of the form

$$g_{i_1} g_{i_2} \dots g_{i_s} = O \quad (n \geq s \geq 2),$$

where the left hand side does not contain unnecessary factors, that is, the cancellation of any factor makes the relation false.

It is easy to see that to every element of the minimal generating system g_1, g_2, \dots, g_n there is at least one relation containing it as a factor.

Let us denote by π the set of all elements in F which are obtained from the left hand side of the relations in T omitting at least one factor.

Thus the set of all non-zero elements of F coincides with π because if $g_{j_1} g_{j_2} \dots g_{j_r} = 0$, ($n \geq r \geq 2$), then the relation in question either belongs to T , or there is a factor of $g_{j_1} g_{j_2} \dots g_{j_r}$ which is the left hand side of a relation in π .

If $g_{j_1} g_{j_2} \dots g_{j_r} \neq 0$, then there exists an element $g_{j_{r+1}} g_{j_{r+2}} \dots g_{j_{r+1}}$ for which we have:

$$g_{j_1} g_{j_2} \dots g_{j_r} \cdot g_{j_{r+1}} \dots g_{j_{r+1}} = 0,$$

and the cancellation of any factor of the product in the left hand side make this relation false.

Thus if g_1, g_2, \dots, g_n is a minimal generating system of a semigroup F of type α , then the set T determines the representation of any element in F .

REFERENCES

1. SEITZ, K., BLICKLE, T.: The structure of systems. Department of Mathematics, Karl Marx University of Economics, Budapest, 1974.
2. SEITZ, K.: Műszaki kémiai rendszerek szerkezete. (The structure of technical chemistry systems). MTA Műszaki Kémiai Kutató Intézet Tudományos Eredményei II. 1974.
3. Mrs. KLEIN-BARMEN: Math Zeitsch. 39, 227 (1935).

РЕЗЮМЕ

После истолкования полугрупп типа α проводится определение их идеалов.

Далее разбирается структура автоморфизма полугрупп типа α . И наконец авторы указывают на практическое применение полученных результатов.

APPLICATION OF OUTER DIRECT PRODUCTS OF SEMIGROUPS
IN THE STUDY OF STRUCTURES

K. SEITZ* and T. BLICKLE**

(*Technical University, Budapest and

**Research Institute for Technical Chemistry of the
Hungarian Academy of Sciences, Veszprém)

Activity of authors aimed at development of method applicable for determination of function relations of structure elements, and so change between the structure elements on the basis of their costs becomes possible.

The outer direct product of semi-groups of α and β type with special semi-lattices is applied for solution of the problem.

Let S be a given α, β structure. Let F be a given set of relations defined on the set-theoretical union of two given sets: A, B .

Let

$$S = K_1 \cup K_2 \cup \dots \cup K_n$$

be a decomposition of type x of S . Then there is an ideal \mathcal{C} of type x which is uniquely determined by this decomposition. Let:

$$\tilde{S} = \{K_{i_1}, K_{i_2}, \dots, K_{i_r}\} \leq S \quad (r \leq n)$$

where the equivalence classes $K_{i_1}, K_{i_2}, \dots, K_{i_r}$ are chosen so that the ideal of type x of S is equal to \mathcal{C} .

Then we correspond to every element of the equivalence classes $K_{i_1}, K_{i_2}, \dots, K_{i_r}$ an element of F^* (where F^* is the power set of F) so that

$$a, b \in K_{i_j} \quad (i \leq j \leq r)$$

$$a \rightarrow f_a^* \in F^*$$

$$b \rightarrow f_b^* \in F^*$$

imply

$$a \cdot b \rightarrow f_a^* \cup f_b^*$$

Denote \hat{F} the set of all elements f_a^* , when it runs over the elements of \tilde{S} .

It is evident that $F^* \supseteq \hat{F}$ and \hat{F} is a semilattice with respect to set-theoretical union.

Let us now consider the following outer direct product:

$$\tilde{S} \times \hat{F}$$

Let C be a given set of parameters.

Let ϕ be a set of real valued functions of the form $\phi(\underline{b}, \underline{c})$ where \underline{b} is a column vector of some elements of B , and \underline{c} is a column vector of some elements of C .

Denote ϕ^* the set of all possible functions of the form:

$$\phi_{i_1} + \phi_{i_2} + \dots + \phi_{i_s} \quad (i_p \neq i_q, \text{ if } p \neq q).$$

Next we define an operation \oplus on the set ϕ^* as follows:

if $u, v \in \phi^*$, then:

$$u \oplus v = w,$$

where w is the sum of all elements from ϕ , which are the addable sums in at least one of u and v . Thus evidently $w \in \phi^*$.

It is easy to see that for any triplet a, b, c in the case of ϕ^* we have:

$$(a \oplus b) \oplus c = a \oplus (b \oplus c),$$

$$a \oplus a = a,$$

$$a \oplus b = b \oplus a$$

This means that the set ϕ^* is a semilattice with respect to the operation \oplus .

Let us denote \hat{S} the α, β structure generated by the following equivalence classes of type x :

$$K_{j_1}, K_{j_2}, \dots, K_{j_s} \subseteq S$$

Suppose that the ideal of type x of \hat{S} coincides with that of S .

Then it corresponds to every element of the equivalence classes:

$$K_{j_1}, K_{j_2}, \dots, K_{j_s}$$

an element from ϕ^* so that:

$$g, h \in K_{j_p} \quad (1 \leq p \leq s)$$

$$g \rightarrow \varphi_g^* \in \phi^*$$

$$h \rightarrow \varphi_h^* \in \phi^*$$

imply

$$g \cdot h \rightarrow \varphi_g^* \oplus \varphi_h^*$$

Let us now consider the following outer direct product:

$$\tilde{S} \times \hat{F} \times \phi^*$$

each of whose factors is of the form $(\hat{S}, f^*, \varphi^*)$, where $\tilde{S} \in S$, $f^* \in F$, $\varphi^* \in \phi^*$.

Denote $\mu(f^*)$ the number of elements of the set f^* . Consider now the elements of the set f^* - which are relations between subsets of A and B - from the standpoint of how many elements are contained by them from A, B respectively.

The number of the elements from B in elements of the set f^* will be denoted by $\mu_B(f^*)$.

Then we choose $\mu_B(f^*) - \mu(f^*)$ elements from the set B and give values for them so that the value of φ^* should be minimal.

If S has such parameters from B , we say that it is an optimized structure-element and the value of the corresponding φ^* is said to be the minimal cost.

Let us consider now an arbitrary element s of the structure S . Let us take that subset of the ideal \mathcal{E} whose elements are non-zero and of the form $s \cdot s'$, where $s' \in S$. We optimize these elements in the above mentioned fashion, and we select those, whose minimal cost is the smallest. This is called a practical ideal-element corresponding to the element s .

РЕЗЮМЕ

Целью авторов является выработка такого метода, с помощью которого можно определить систему функциональных зависимостей структурных элементов, величину затрат, связанных со структурными элементами, оптимальные параметры, а также выбирать среди затрат отдельных структурных элементов.

Для решения задачи применяется внешнее прямое произведение полугрупп типа α и β со специальными полусетями.

INVESTIGATION OF THE STRUCTURE OF THE SEMIGROUP $(\hat{F}^+ \times \hat{F}^+, \odot)$
AND OF THE PARTIAL SEMIGROUP $(F^+ \times F^+, \otimes)$ OF THE PARTIAL
ALGEBRAIC STRUCTURE $S(\hat{F}^+ \times \hat{F}^+, \odot, \otimes)$

K. SEITZ* and J. BALÁZS**

(*Technical University, Budapest and

**L. Eötvös University, Budapest)

Structure of the $(\hat{F}^+ \times \hat{F}^+, \odot)$ semi-group and the
 $(\hat{F}^+ \times \hat{F}^+, \otimes)$ partial semi-group is studied.

Following verification of the above structure
thesis different possibilities of generalization and
practical application of results are shown.

INTRODUCTION

In the abstract algebraic study of the structure of chemical
engineering systems the partial algebraic structures $S(F^+ \times F^+, \odot, \otimes)$
play a fundamental role.

In this paper, the structure of the semigroup $S(\hat{F}^+ \times \hat{F}^+, \odot)$
and the structure of the partial semigroup $S(\hat{F}^+ \times \hat{F}^+, \otimes)$ will be
generally examined.

The results obtained provide significant assistance in ela-
borating principles of the optimal connection of subsystems in
chemical engineering.

For the definitions of most of the notions used in the semi-
group-theoretical part reference is made to published works [2, 3].

1. The Study of Ideals in the Commutative Semigroup $(S(\hat{F}^+ \times \hat{F}^+, \odot))$

First the following result is proved

Theorem 1.1. The group $G(\hat{F}^+ \times \hat{F}^+)$ is the universally minimal ideal of $S(\hat{F}^+ \times \hat{F}^+, \odot)$.

Proof. Let $(x, y) \in S(\hat{F}^+ \times \hat{F}^+, \odot)$ and $(a, b) \in G(\hat{F}^+ \times \hat{F}^+)$. Since $(x, y) \odot (a, b) = \uparrow\uparrow (ax, by)$ and $\uparrow\uparrow (ax, by) \in G(\hat{F}^+ \times \hat{F}^+)$, the group $G(\hat{F}^+ \times \hat{F}^+)$ is an ideal of $S(\hat{F}^+ \times \hat{F}^+, \odot)$.

If \mathfrak{J} is an ideal of $S(\hat{F}^+ \times \hat{F}^+, \odot)$, then $(x, y) \in S(\hat{F}^+ \times \hat{F}^+, \odot)$ and $(u, v) \in \mathfrak{J}$ imply

$$(\varepsilon, \varepsilon) = (v, u) \odot (u, v) \in \mathfrak{J}$$

and thus $\uparrow\uparrow (x, y) \in \mathfrak{J}$ is gained because of $(x, y) \odot (\varepsilon, \varepsilon) \in \mathfrak{J}$ hence the inclusion:

$$G(\hat{F}^+ \times \hat{F}^+) \subseteq \mathfrak{J}$$

follows.

Therefore $G(\hat{F}^+ \times \hat{F}^+)$ is a minimal ideal of $S(\hat{F}^+ \times \hat{F}^+, \odot)$.

Let K be an arbitrary subset of $S(\hat{F}^+ \times \hat{F}^+, \odot)$. It is shown that $G(\hat{F}^+ \times \hat{F}^+) \cup K$ is an ideal of $S(\hat{F}^+ \times \hat{F}^+, \odot)$.

For, if $(x, y) \in S(\hat{F}^+ \times \hat{F}^+, \odot)$ and $(a, b) \in G(\hat{F}^+ \times \hat{F}^+)$, moreover $(p, q) \in K$, then:

$$(x, y) \odot (a, b) = \uparrow\uparrow (ax, by)$$

and

$$(x, y) \odot (p, q) = \uparrow\uparrow (px, qy)$$

Thus $(x, y) \odot (a, b)$ and $(x, y) \odot (p, q)$ belong to $G(\hat{F}^+ \times \hat{F}^+)$.

2. The Study of Subsemigroups and Decomposition of the Semigroup $(S(\hat{F}^+ \times \hat{F}^+, \odot))$

To every element p of \hat{F} we define a unary operation on the set $\hat{F}^+ \times \hat{F}^+$ as follows:

for

$$(a, b) \in \hat{F}^+ \times \hat{F}^+ \text{ let } \Downarrow^P(a, b) = (pa, pb)$$

It can be seen immediately that

$$\Uparrow(\Downarrow(a, b)) = \Uparrow(a, b)$$

By making use the operations \Uparrow^P the semigroup $S(\hat{F}^+ \times \hat{F}^+, \odot)$ can be represented in the following form:

$$S(\hat{F}^+ \times \hat{F}^+, \odot) = \bigcup_{p \in \hat{F}^+} [\Uparrow^P G(\hat{F}^+ \times \hat{F}^+)],$$

where $\Uparrow^P G$ is the set of all elements of the form $\Downarrow^P(a, b)$ with $(a, b) \in G(\hat{F}^+ \times \hat{F}^+)$.

Let G^* be a subgroup of the group $G(\hat{F}^+ \times \hat{F}^+)$. It is easy to show that $\bigcup_{p \in \hat{F}^+} (\Downarrow^P G)$ is a subsemigroup of $S(\hat{F}^+ \times \hat{F}^+, \odot)$.

Denote $S_1(\hat{F}^+ \times \varepsilon, \odot)$ and $S_2(\varepsilon \times \hat{F}^+, \odot)$ the set of all elements of the form (a, ε) and (ε, a) , $(a, \varepsilon \in \hat{F}^+)$.

It can be to proved that $S_1(\hat{F}^+ \times \varepsilon, \odot)$ and $S_2(\varepsilon \times \hat{F}^+, \odot)$ are subsemigroups with an identity element of $S(\hat{F}^+ \times \hat{F}^+, \odot)$ and

$$S(\hat{F}^+ \times \hat{F}^+, \odot) = S_1(\hat{F}^+ \times \varepsilon, \odot) \cup S_2(\varepsilon \times \hat{F}^+, \odot)$$

If R is a subsemigroup with an identity element of the semigroup $S(\hat{F}^+ \times \hat{F}^+, \odot)$ then for any $(a, b) \in R$ we have $(a, b) \odot (\varepsilon, \varepsilon) \odot \Uparrow R \subseteq R$. Hence if $R \supseteq \Uparrow R$, then any element of $R \setminus \Uparrow R$ can be written in the form:

$$\Downarrow^P(u, v) = (pu, pv)$$

where $\varepsilon \neq p \in \hat{F}^+$ and $(u, v) \in \Uparrow R$.

If L is an arbitrary subset of R , it is easy to see that $(\Uparrow R) \cap L$ is an ideal of R .

If $(\varepsilon, \varepsilon) \notin R$, then generally $R \not\supseteq \Uparrow R$, but in the case of $R \not\supseteq \Uparrow R$ any element of R not belonging to $\Uparrow R$ can be written in the form (pu, pv) , where $\varepsilon \neq p \in \hat{F}^+$ and $(u, v) \in \Uparrow R$.

A semigroup P , following THIERRIN [2], is said to be a homomorphism if it has an idempotent element i which is commutable with every element of P and to any element a in P there is an $a' \in P$ such that $aa' = 1$.

It can be shown that $S(\hat{F}^+ \times \hat{F}^+, \odot)$ is a homomorphism.

3. The Study of the Partial Semigroup $S(\hat{F}^+ \times \hat{F}^+, \otimes)$

Denote $L(a,b)$ and $R(a,b)$ the set of all elements $(x,y) \in \hat{F}^+ \times \hat{F}^+$ for which the product $(x,y) \otimes (a,b)$ does exist.

Denote $H(a)$ the set of all elements of \hat{F}^+ for which $a \Delta z \neq \varepsilon$.

It can be seen at once that the structure of $L(a,b)$ and $R(a,b)$ is essentially determined by the structure of $H(a)$ and $H(b)$ in view of the relations:

$$L(a,b) = \bigcup_{x \in \hat{F}^+} \bigcup_{y \in H(a)} (x,y)$$

and

$$R(a,b) = \bigcup_{y \in \hat{F}^+} \bigcup_{x \in H(b)} (x,y)$$

In the case of $a \in \hat{F}^+$, $x,y,z \in H(a)$ one has $a \Delta (xy) \neq \varepsilon$ and $(xy)z = x(yz)$, hence it follows that $H(a)$ is a subsemigroup of \hat{F}^+ , moreover $\varepsilon \notin H(a)$ because $a \Delta \varepsilon = \varepsilon$.

It can be shown that $\bar{H}(a) = \hat{F}^+ \setminus H(a)$ is a submonoid of \hat{F}^+ .

The following two theorems are true:

Theorem 3.1. If $a,b \in \hat{F}^+$, then

$$\bar{H}(a) \cap \bar{H}(b) = \bar{H}(ab)$$

Theorem 3.2. If $a,b \in \hat{F}^+$, then

$$H(a) \cup H(b) = H(ab)$$

Denote T and \bar{T} the set of all sets $H(z)$ and $\bar{H}(z)$ where $z \in \hat{F}^+$.

The above results imply that (T, \cup) and (T, \cap) are semilattices.

Denote S_p the set of all elements (pa, pb) in $\hat{F}^+ \times \hat{F}^+$ where $a \neq p \in \hat{F}^+$.

The following theorem is true:

Theorem 3.3. S_p is a subsemigroup of the partial semigroup $S(\hat{F}^+ \times \hat{F}^+, \otimes)$.

If, for elements p, q in F we have $q = pz$, $z \in \hat{F}^+$, then it is easy to see that $S_q \subseteq S_p$.

Also, it can be shown that S_q is an ideal of S_p .

REFERENCES

1. SEITZ, K., BLICKLE, T.: The structure of systems, K. Marx University for Economics, Dept. of Math., Budapest, 1974.
2. THIERRIN, G.: Comptes Rendus Acad. Sci. Paris 234, 1519 (1952).
3. CLIFFORD, A.H., PRESTON, G.B.: The algebraic theory of semigroups I-II. Amer. Maths. Soc., Math. Surveys, Providence, R.I., 1961, 1967.

РЕЗЮМЕ

Авторами была изучена структура полугруппы $(\hat{F}^+ \times \hat{F}^+, \odot)$ и частичной полугруппы $(F^+ \times F^+, \otimes)$.

После доказательства вышеуказанных структурных теорем показаны отдельные возможности для обобщения и практического применения достигнутых результатов.

RECENT RESULTS IN THE THEORY OF PARTIAL SEMIGROUPS

J. SZÉP* and K. SEITZ**

(*Karl Marx University of Economics, Budapest and

**Technical University, Budapest)

Activity of authors aimed at study of structure of partial semi-groups having basic importance in construction of complex automaton structures.

More structure theses are proved and their practical applications are shown too.

Let us consider the commutative semigroups \hat{F}^+ and \hat{F}^- defined in the reference [1]. Suppose that $\hat{F} = \hat{F}^+ \cup \hat{F}^-$ and ε is the identity element. Consider the Cartesian product $\hat{F}^+ \times \hat{F}^+$ on which we define the operation " \otimes " as follows:

For the arbitrary elements $(a,b), (c,d) \in \hat{F}^+ \times \hat{F}^+ (a,b,c,d \in \hat{F}^+)$ let:

$$(a,b) \otimes (c,d) = [ac \varphi(a,b,c,d), bd \varphi(a,b,c,d)]$$

where the function $\varphi(a,b,c,d)$ has the following properties:

1. $\varphi(a,b,c,d) \in \hat{F}$
2. $\varphi(aa', ba', cd) = \alpha(a') \cdot \varphi(a,b,c,d)$
 $\varphi(a,b,cc', dc') = \beta(c') \cdot \varphi(a,b,c,d)$
 $a', c' \in \hat{F}^+; \alpha(a') \in \hat{F}; \beta(c') \in \hat{F};$
3. $\varphi(a,b,c,d) = \varphi(c,d,a,b)$

The algebraic system defined above will be denoted by:

$$S(\hat{F}^+ \times \hat{F}^+, \circ)$$

In the first place we want to know under what conditions this system will be a semigroup with respect to the operation \circ .

It is evident that it is sufficient to make the associativity certain.

First, the property 2) of the function φ implies

$$4. \quad \alpha(a'a'') = \alpha(a') \alpha(a'')$$

furthermore, 3) implies that

$$\alpha \equiv \beta$$

that is, α is a homomorphic mapping of \hat{F}^+ into \hat{F} .

Using the notation $\alpha(a) = x$ it can be shown that

$$\alpha(x) = x^{-1}$$

i.e., the function α is uniquely determined. If, especially, x runs over all the elements of \hat{F}^+ , then the mapping $\alpha(x): \hat{F}^+ \leftrightarrow \hat{F}^-$ is an isomorphism.

T h e o r e m 1. The system $S(\hat{F}^+ \times \hat{F}^+, \circ)$ is a semigroup if the function φ has the properties, 1., 2., 3., the function $\alpha(a)$ is an isomorphism between \hat{F}^+ and \hat{F}^- , finally the equality:

$$\varphi(ac, bd, e, f) = \varphi(a, b, ce, df)$$

holds for every six elements a, b, c, d, e, f of \hat{F}^+ .

We shall now define a second operation denoted by \otimes as follows:

$$(a, b) \otimes (c, d) = [(ac \psi(b, c)), (bd \psi(b, c))]$$

where $(a, b), (c, d) \in \hat{F}^+ \times \hat{F}^+$ and the function ψ satisfies the following conditions:

- (i) $\psi(b, c) \in \hat{F}$;
- (ii) $\psi(b, c) = \psi(c, b)$;
- (iii) $\psi(bb', cb') = \gamma(b') \psi(b, c)$;
- (iv) $\psi(a, \varepsilon) = \varepsilon, a \in \hat{F}^+$

An easy calculation shows that the structure $(\hat{F}^+ \times \hat{F}^+, \otimes)$ is a semigroup, if, for arbitrary elements $(a, b), (c, d), (e, f)$ we have:

$$\psi(b, c) \psi[b, d \psi(b, c), e] = \psi(d, e) \psi[b, c, e. \psi(d, e)]$$

It can be proved that for the function $\gamma(a)$ we have either:

$$1. \quad \gamma(a) = \varepsilon a \quad (a \in \hat{F}^+)$$

or:

$$2. \quad \gamma(a) = a^{-1}$$

With the operation \otimes we can define a partial semigroup if the operation is defined if and only if:

$$\psi(b, c) \neq \varepsilon$$

In the case of this partial semigroup the function:

$$\gamma(a) = a^{-1}$$

is determined uniquely. .

REFERENCES.

1. SEITZ, K., BLICKLE, T.: The structure of systems, Department of Mathematics, Karl Marx University of Economics, Budapest, 1974-2.

РЕЗЮМЕ

Целью авторов является изучение структуры перциальных полугрупп, играющих основную роль в строении сложных автоматных структур.

Доказывается несколько структурных теорем и показано их практические применения.

CONTINUOUS STRUCTURES

C. JUHÁSZ

(Research Institute for Technical Chemistry of the
Hungarian Academy of Sciences, Veszprém)

Topological interpretation of structures is discussed. Widening of idea of structure by continuous functions interpreted above the continuous object classes is shown. Equivalency between the former and newer interpretations is studied too.

Notations

Let H be an arbitrary set. Denote $P(H)$ the power set of H , that is, $P(H) = \{A : A \subset H\}$.

Let $\tau = \{T_i\}_{i \in I}$ be an arbitrary series of sets. Denote $X\tau$ the Cartesian product $\prod_{i \in I} T_i$. Let $\tau' \subset \tau$. Let $x \in X\tau$ be an arbitrary point. Denote by $x \downarrow X\tau'$ the projected image of the point x into the space $X\tau'$.

Let T be an arbitrary set. Let σ be a topology over the set T . Let $H \subset T$ be an arbitrary subset. Denote $(H, \sigma/H)$ the subspace of the topological space (T, σ) , where σ/H is the corresponding subspace topology.

Let $\{(T_i, \sigma_i)\}_{i \in I}$ be a series of topological spaces. Denote $(X\tau, X\sigma)$ the Tychonoff product of these spaces.

Let H be an arbitrary set. Denote $|H|$ the cardinality of H .

STRUCTURE

Let H be an arbitrary set having at least two elements. Let T be a set of properties of elements in H . Denote $F(t)$ the set of all elements $h \in H$ which have the property $t \in T$. It can be said that the couple (H, T) is a structure with respect to the mapping F , if the following conditions hold:

(HT1) If $t \in T$, then $\emptyset \neq F(t) \neq H$.

(HT2) If $h \in H$, $h' \in H$ and $h \neq h'$, then there exists an element $t \in T$ so that either $h \in F(t)$ and $h' \notin F(t)$ or $h \notin F(t)$ and $h' \in F(t)$.

(HT3) There exists an equivalence classification: $\tau = \{T_i\}_{i \in I}$ for which:

(HT3)/(1) If $T_i \in \tau$, then $\bigcup_{t \in T_i} F(t) = H$.

(HT3)/(2) If $T_i \in \tau$, $t \in T_i$, $t' \in T_i$ and $t \neq t'$, then

$$F(t) \cap F(t') = \emptyset.$$

It can be proved that the set H can be mapped to the set $E(H) = H' \subset X_\tau$ by a one-to-one function.

Free structure

Let $\tau = \{T_i\}_{i \in I}$ be a series of arbitrary, non-empty, pairwise disjoint sets. Let $T = \bigcup_{i \in I} T_i$. Let F' be a function defined on the set T , whose range is contained by the set $P(X_\tau)$. Let $H' = \bigcup_{t \in T} F'(t)$. It can be said that the pair (F', T) is a free structure over the set H' , if the following conditions hold:

(FT1) If $T_i \in \tau$, then $|T_i| \geq 2$.

(FT2) If $T_i \in \tau$, then $\bigcup_{t \in T_i} F'(t) = H'$.

(FT3) If $t \in T_i \in \tau$, then $F'(t) \cap T_i = \{t\}$.

It can be shown that if (H, T) is a structure with respect to the mapping F , then $(E \circ F, T)$ is a free structure over the set $E(H) = H'$ and if (F', T) is a free structure over the set H' , then (H', T) is a structure with respect to the mapping F' .

Continuous Structure

Suppose that the $T_i \in \tau$ classes of properties have the topologies $\sigma_i \in \sigma$. Denote $(X\tau, X\sigma)$ the product space of Tychonoff.

It can be said that the free structure (F', T) is continuous in the point $h \in H'$, if, for every $i \in I$, to the neighbourhood $h \in G \in X\sigma/H'$ of the object h there exists a neighbourhood $h \downarrow T_i \in U_i \in \sigma_i$ of the property $h \downarrow T_i$ so that $U_i \subset G \downarrow T_i$.

It can be shown that a free structure is continuous in every interior point of the set H' , but the continuity of a free structure in a point $h \in H'$ does not imply that h is an interior point of H' .

Sub-structure

Let (F', T) be an arbitrary free structure over the set H' . Let $\emptyset \neq \tau' \subset \tau$ be an arbitrary subset. Let:

$$T' = \bigcup_{T_i \in \tau'} T_i$$

and F'' be a function defined as follows:

$$\text{if } t \in T', \text{ then } F''(t) = F'(t) \downarrow X\tau'.$$

Let $H'' = H' \downarrow X\tau$.

It can be shown that (F'', T) is a free structure over the set H'' . This free structure will be called the substructure of the free structure (F', T) over the set τ' .

It can be shown that if the free structure (F', T) is continuous in the point $h \in H'$, then its sub-structure over the set τ' is continuous in the point $h \downarrow X\tau'$.

Secondary structure

It can be said that the free structure (F', T) is symmetric with respect to a property class $T_j \in \tau$ if the set τ has a disjoint decomposition:

$$\tau = \tau_1 \cup \{T_j\} \cup \tau_2; \quad \tau_1 \neq \emptyset \neq \tau_2$$

so that the sub-structures (F_a, T_a) and (F_b, T_b) corresponding to the sets $\tau_a = \tau \setminus \tau_2$, and $\tau_b = \tau \setminus \tau_1$ satisfy the following condition:

$$(MSZ) \quad \text{If } x \in X\tau, x \downarrow X\tau_a \in H_a \text{ and } x \downarrow X\tau_b \in H_b$$

then $x \in H'$.

Suppose that the free structure (F', T) over the set H' is symmetric with respect to the property class T_j . Let (F_1, T_1) and (F_2, T_2) sub-structures over the sets $H_1 \in \tau_1$ and $H_2 \in \tau_2$. Let:

$$\tau_n = \{H_1, T_j, H_2\} \quad \text{and} \quad T_m = H_1 \cup T_j \cup H_2$$

A function F_M can be defined as follows:

if $h_i \in M_i$ ($i = 1, 2$), then:

$$F_M(h_i) = \{x \in X\tau_n : x \downarrow X\tau_i = h_i, x \downarrow X\tau_a \in H_a, x \downarrow X\tau_b \in H_b\}$$

if $t \in T_j$, then:

$$F_m(t) = \{x \in X\tau_n : x \downarrow T_j = t, x \downarrow X\tau_a \in H_a, x \downarrow X\tau_b \in H_b\}$$

It can be shown that (F_M, T_M) is a free structure over the set H' . This free structure is said to be the secondary structure corresponding to the property class T_j .

It can be proved that the topology $X\mathcal{G}/H'$ is equivalent to the corresponding topology $(X\mathcal{G}_1/H_1 \times \mathcal{G}_j \times X\mathcal{G}_2/H_2)/H'$.

It can be shown that the continuity of (F', T) in a point $h \in H'$ does not imply the continuity of (F_M, T_M) in the point $h \in H'$, but if (F_M, T_M) is continuous in the point $h \in H'$, and the corresponding (F_1, T_1) and (F_2, T_2) is continuous in the points $h \downarrow X\tau_1$ and $h \downarrow X\tau_2$, then (F', T) is continuous in the point $h \in H'$.

The concept of a secondary structure consisting of more classes can be similarly defined.

Composition

Let (F_a, T_a) and (F_b, T_b) be two free structures over the sets H_a and H_b . Suppose that the condition:

$$(KSZ) \quad \tau_a \cap \tau_b = \{T_j\}$$

holds. In this case the structures are called composable.

Let $\tau_1 = \tau_a \setminus \tau_b$, $\tau_2 = \tau_b \setminus \tau_a$. Let (F_1, T_1) and (F_2, T_2)

be sub-structures over the sets $H_1 \in \tau_1$ and $H_2 \in \tau_2$.

Let $\tau_M = \{H_1, T_j, H_2\}$, $T_M = H_1 \cup T_j \cup H_2$ and F_M be the function defined above.

It can be shown that (F_M, T_M) is a free structure over the set

$$H' = \bigcup_{t \in T_j} F_M(t)$$

This free structure is said to be the composition kernel of the free structures (F_a, T_a) and (F_b, T_b) .

Let $T = T_a \cup T_b$ and F' be defined as follows:

if $t \in T_i \in \tau_k$ ($k = 1, 2$), then $F'(t) = \{F_M(h) : h \in H_k, h \downarrow T_i = t\}$
and

if $t \in T_j$, then $F'(t) = F_M(t)$.

It can be shown that (F', T) is a free structure which is symmetric with respect to the property T_j over the set H' . The composition kernel (F_M, T_M) is the secondary structure corresponding to T_j . This free structure is said to be the composition of the free structures (F_a, T_a) and (F_b, T_b) .

Concerning the continuity of the composition, the statements of the preceding part of the paper remain true.

The composition of more structures can similarly be defined.

РЕЗЮМЕ

Автор излагает топологическое толкование структур. Он показывает, каким образом удалось расширить понятие структуры с помощью непрерывных функций над классами непрерывных объектов. Затрагивается и вопрос эквивалентности прежнего и нового истолкований.

DESCRIPTION OF MATERIAL SYSTEMS BY CONTINUOUS STRUCTURE

T. BLICKLE and Mrs. E. BÁTOR

(Research Institute for Technical Chemistry of the
Hungarian Academy of Sciences, Veszprém)

The structure of materials is build up by the aid of discrete and continuous classes of properties. The properties are selected so that a change in any of them characterizes a technical chemical process, for a technical chemical process has at least one changing property. Numericality, the mean surface and diameter of dispersed particles as well the inhomogeneity moments of continuous properties are regarded as continuous properties constructing the structure of materials.

A description of the structure of material systems based on the material properties and relations between them, was published earlier. The following properties were taken into consideration during the qualitative description:

$$[x, c, b, k, \beta, \varphi, T, P] \quad (1)$$

The above properties can be divided into two groups depending on whether they can have discontinuous values or can change continuously. So discontinuous:

$$[c, b, k, \beta, \varphi] \quad (2)$$

and continuous:

$$[x, T, P] \quad (3)$$

classes of objects can be distinguished.

In order to form a uniform method for quantitative treatment of technical chemical changes, a study of upper and lower limits of properties became necessary.

Properties having the following characteristics have to be taken into consideration:

1. any of these properties changes in, at least one, technical chemical process,

2. in any technical chemical transformation, there is at least one property among the properties taken up which changes.

Properties in the (1-3) line vectors correspond to the 1. condition, however, they do not satisfy the second one, because e.g. during processes of changes in size or homogenization the above properties do not necessarily change.

In the case of material consisting of dispergated particles, if $F'(r)$ is the whole surface of the particles of r characteristic size and f is the surface of a single particle, then the:

$$\phi(r) = \frac{F'(r)}{f} \quad (4)$$

function gives the number of particles of studied size. The whole surface of the set consisting of dispergated particles is as follows:

$$F = \int_{f_0}^{\infty} \frac{F'(r)}{f} df \quad (5)$$

If particles are spheres and r is their radius, then:

$$F = \int_{r_0}^{\infty} \phi(r) 8\pi r dr = 8\pi \phi_1 \quad (6)$$

The mean surface of particles is

$$\bar{f} = \frac{1}{F} \int_{f_0}^{\infty} F'(r) df \quad (7)$$

which for spherical particles has the following form:

$$\bar{f} = \frac{\int_{r_0}^{\infty} \phi(r) 4r^2 \pi dr}{8\pi\phi_1} = 4\pi \frac{\phi_2}{\phi_1} \quad (8)$$

The numericality of the investigated set can be expressed as follows:

$$N = \frac{F}{\bar{f}} = 2 \frac{\phi_1^2}{\phi_2} \quad (9)$$

The volume of set is:

$$V = \int_{r_0}^{\infty} \frac{F'(r)}{f} dv \quad (10)$$

In the case of spherical particles it has the following form:

$$V = \int_{r_0}^{\infty} \phi(r) 4r^2 \pi dr = 4\pi\phi_3 \quad (11)$$

The diameter:

$$D = 2 \int_{r_0}^{\infty} \phi(r) dr = 2\phi_0 \quad (12)$$

The mean diameter of the particles:

$$\bar{d} = \frac{D}{N} = \frac{\phi_0\phi_2}{\phi_1^2} \quad (13)$$

Let us define the specific numericality, relating to the unit of volume, as follows:

$$\bar{n} = \frac{N}{V} = \frac{\phi_1^2}{2\pi\phi_2\phi_3} \quad (14)$$

The specific numericality (\bar{n}) the mean diameter (\bar{d}) and the mean surface (\bar{f}) will be regarded as continuous characteristics of material systems:

$$[x, T, P, \bar{n}, \bar{d}, \bar{f}] \quad (15)$$

so the systems theoretical method can be applied for the quantitative description of processes accompanied by a change in size.

However, the properties given above still do not make an investigation of homogenization processes possible. An optional θ continuous property can usually be given not by a constant value, but by $\theta(y)$ function according to y space or time co-ordinates, and the value of this function can change during technical chemical processes. For this reason, the moments of inhomogeneity were interpreted so that the k -th moment was the following:

$$\theta I_k = \frac{1}{Y} \int_0^Y (\bar{\theta} - \theta)^k dy \quad (16)$$

where:

$$k \geq 2$$

$$\bar{\theta} = \frac{1}{Y} \int_0^Y \theta dy \quad (17)$$

A k value can always be given so that the $\theta(y)$ function can be approximated optionally by inhomogeneity moments of k number. The inhomogeneity moments - in the case of all continuous properties - will be regarded as those belonging to properties describing material systems:

$$[x, T, P, \bar{n}, \bar{d}, \bar{f}, x^{I_2} \dots x^{I_k}, T^{I_2}, \dots T^{I_k}, P^{I_2}, \dots, P^{I_k}, \\ n^{I_2}, \dots n^{I_k}, d^{I_2}, \dots d^{I_k}, f^{I_2}, \dots f^{I_k}] \quad (18)$$

Properties given in (2) and (18) line vectors make a uniform qualitative and quantitative description of any technical chemical change possible.

Structure constructed on (2) and (18) properties are regarded as the main point of material systems. This does not change even if the line is completed by further derived properties, e.g. heat conductivity, specific heat, and dielectric constant, etc. These latter characteristics are unambiguous consequences of (2) and (18) properties and only one value from these can belong to an element

of structure. This means that the derived properties do not give further information on the separation of the elements of structure, however, they make it possible to apply the method to those cases when relations between the basic properties are still not known and these properties can also be favourably used for the connection of structures. Generally it cannot be stated in advance which derived properties should be taken into consideration, it always depends on the given task.

SYMBOLS USED

b	biological structure
c	chemical structure
d	diameter
f	surface of particle
F	total surface of dispergated particles
I	inhomogeneity moments
k	crystal structure
N	numericality
P	pressure
T	temperature
r	characteristic measure or radius
V	volume
x	concentration
Y	time or space co-ordinate
β	state
φ	form
θ	any continuous property

REFERENCE

1. MTA Műszaki Kémiai Kutató Intézet Tudományos Eredményei II. A Műszaki kémiai rendszerek szerkezete (The Structure of Systems in Technical Chemistry). Veszprém, 1974.

РЕЗЮМЕ

Структура материальных систем основывается на классах объектов различного типа.

В случае непрерывных классов объектов реляции задаются в виде непрерывной функции.

При описании материальных систем значительную роль отводится производным свойствам, не несущим новой информации к разделению элементов структуры. Но они дают возможность для применения алгебраических методов в случаях, когда зависимости между основными свойствами неизвестны, они применимы также при соединении структур.

COMPUTER ALGORITHMS FOR THE INVESTIGATION OF
STRUCTURES OF SYSTEMS IN CHEMICAL ENGINEERING

G. VERESS*, T. BLICKLE** and M. GALBAVY***

(*Technical University, Budapest

**Research Institute for Technical Chemistry of the
Hungarian Academy of Sciences, Veszprém

***Research Institute for Automation and Computer Technology,
Hungarian Academy of Sciences, Budapest)

In order to apply broadly in the practice results obtained in the field of systems theoretical research of technical chemical systems construction of computer algorithms for carrying out algebraic operations used often in the systems researches is necessary.

The computer programs for calculation of

1. reducing to prime factors
2. common multiple and divisor
3. complex operation

are shown which were developed in the first stage of the authors' activity.

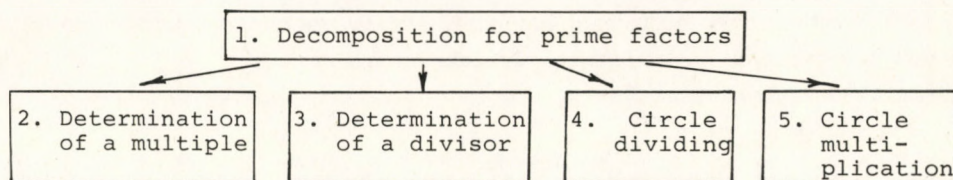
In order to practically apply the theoretical results obtained in the field of the structure of systems in the chemical engineering it is necessary to prepare certain computer algorithms for making the algebraic operations.

Such fundamental algebraic operations are, for example:

- a) decomposition for prime factors
- b) determination of a multiple

In the following the above operations concerning the algebraic system E are demonstrated.

The construction of the algorithm



1. Decomposition for prime factors

With regard to the system E the prime elements (e_1, \dots, e_6) are known. In the row of the first non-prime element, in the column of a prime element there is an e_i whose index is equal to the row index.

These will be the prime factors of the element e_i . For example: the 7th row contains: $e_7, 0, e_7, 0, e_{11}, 0$ and e_7 is in the first and third column of the prime element, thus the decomposition of e_7 is $(1, 0, 1, 0, 0, 0)$. Carrying out this procedure for each non-prime row of E , we obtain the complete prime decomposition.

P =

	e_1	e_2	e_3	e_4	e_5	e_6
e_7	1	0	1	0	0	0
e_8	0	1	0	1	0	0
e_9	0	0	1	0	1	0
e_{10}	0	0	0	1	0	1
e_{11}	1	0	1	0	1	0
e_{12}	0	1	0	1	0	1
e_{13}	1	0	0	0	1	0
e_{14}	0	1	0	0	0	1

2. Determination of a multiple

Definition: e_a is a multiple of e_b if every prime factor of e_b is a prime factor of e_a .

If the above matrix \underline{P} is given, then we can determine by logical operations, every multiple of any element e_i .

	e_7	e_8	e_9	e_{10}	e_{11}	e_{12}	e_{13}	e_{14}
e_7	1	0	0	0	1	0	0	0
e_8	0	1	0	0	0	1	0	0
e_9	0	0	1	0	1	0	0	1
$\underline{T} = e_{10}$	0	0	0	1	0	1	0	0
e_{11}	0	0	0	0	1	0	0	0
e_{12}	0	0	0	0	0	1	0	0
e_{13}	0	0	0	0	1	0	1	0
e_{14}	0	0	0	0	0	1	0	1

The matrix \underline{T} shows that e_7 has the multiples e_7 and e_{11} ,
 e_8 has the multiples e_8 and e_{12} ,
 e_{12} has the multiples e_{12} , etc.

3. Determination of a divisor

Definition: e_a is a divisor of e_b , if every prime factor of e_a is also a prime factor of e_b .

Thus, if we exchange the role of rows and columns in the matrix \underline{T} , then we obtain the matrix of a divisor \underline{O} .

4. Circle dividing; a complex operation

Definition:

$$e_i \circ e_j = \begin{cases} e_k & \text{if } e_j \text{ is a divisor of } e_i; e_k \text{ is the element} \\ & \text{without common prime factors} \\ e_i & \text{if } e_i = e_j \\ 0 & \text{if } e_j \text{ is not a divisor of } e_i \\ 0 & \text{if } e_i = 0 \text{ or } e_j = 0. \end{cases}$$

The operation can be made by logical comparison. It follows from the definition that it is necessary to have the matrices P and O, for the circle dividing.

5. Circle multiplication; a complex operation

Definition: $e_i \circ e_j = e_k$ where e_k contains all the prime factors of both e_i and e_j with multiplicity one.

The operation can be settled by logical comparison, for which the matrix P is necessary. — . —

With the aid of the above complex operations we have solved the following set-determination problem.

Given: K_a , \hat{K}_a , K_b .

To find: \hat{K}_b

We know that $\hat{K}_a \subseteq K_a$, $\hat{K}_b \subseteq K_b$

$$\hat{K}_b \cup \emptyset = (\hat{K}_a \circ K_b) \circ \hat{K}_a$$

		1	2	3	4	5	6	7	8	9	10	11	12	13	14
K_a	1	1	0	0	0	0	0	1	0	0	0	1	0	1	0
	2	0	1	0	0	0	0	0	1	0	0	0	1	0	1
	3	0	0	1	0	0	0	1	0	1	0	1	0	0	0
	4	0	0	0	1	0	0	0	1	0	1	0	1	0	0
R_a	5	0	0	0	0	1	0	0	0	1	0	1	0	1	0
	6	0	0	0	0	0	1	0	0	0	1	0	1	0	1
	7	1	0	1	0	0	0	1	0	0	0	1	0	0	0
	8	0	1	0	1	0	0	0	1	0	0	0	1	0	0
K_b	9	0	0	1	0	1	0	0	0	0	0	1	0	0	0
	10	0	0	0	1	0	1	0	0	0	1	0	1	0	0
	11	1	0	1	0	1	0	0	0	0	0	1	0	0	0
	12	0	1	0	1	0	1	0	0	0	0	0	1	0	0
	13	1	0	0	0	1	0	0	0	0	0	0	0	1	0
	14	0	1	0	0	0	1	0	0	0	0	0	1	0	1

If \hat{K}_a has 2 elements and

K_b has 6 elements

then $\hat{K}_a \circ K_b = K_c$ has 12 elements.

If K_c has 12 elements and

\hat{K}_a has 2 elements

then $K_c \circ \hat{K}_a = \hat{K}_b \cup \emptyset$ has 24 elements.

This problem was solved on a CDC-3300 computer by algorithms written for the complex operations. The running time was only 43 seconds.

Each algorithm is also very appropriate for solving large scale problems. All the algorithms except the prime decomposition, require only a little memory in the computer because we have 0-1 variables, and the information can be stored in bits.

РЕЗЮМЕ

Для того, чтобы полученные в области исследования структуры систем технической химии теоретические результаты нашли широкое практическое применение, оказалось необходимым составление вычислительных алгоритмов, которые нужны для выполнения алгебраических операций, часто встречающихся в исследовании структур.

Авторами излагаются системы программ для расчета на вычислительной машине.

- 1) общего кратного и делителя,
- 2) комплексной операции

которые были разработаны авторами в первом периоде их работы, как наиболее часто встречающиеся алгебраические операции.

ALGEBRAIC AUTOMATON OF CONSTRUCTIONS

T. BLICKLE* and A. BEZEGH**

(*Research Institute for Technical Chemistry of the
Hungarian Academy of Sciences, Veszprém and

**EGYT Pharmacochemical Works, Budapest)

The algebraic investigation of different operations realizable in similar operation units and system of operational units is discussed. An $A(S_b, S_k, S_v, \dots)$ algebraic automaton is interpreted, where S_b inlet, S_k outlet, and S_v state sets have properties being characteristic for structure and $\lambda: S_b \times S_v \rightarrow S_k$ and μ are metrics interpreted on the structure S_v .

The $S_b \times S_v \rightarrow S_v$ function describing the change in the state of the algebraic automaton becomes well defined by μ .

The $\alpha\beta$ structure of the defined automaton serve for analysis and synthesis of the systems.

The free semigroup of maps were recently studied [1], with the aim of elaborating an algebraic structure from a rather constrained set-system, which would fulfil the aims of chemical engineering, and being simple could easily be used in practice.

Some conceptions of algebraic automaton will be applied, hence these will be discussed first.

An automaton or sequential machine is the $A = (X, Y, Z, f, g)$ quintuple, where X is a finite set - the generating set of the input free semigroup, Y is a finite set the generating set of the output free semigroup, and Z is the set of states of the automaton.

If Z is a finite set, A is termed a finite-state machine or finite automaton. The f and the g are functions having the following maps:

$$f: X \times Z \rightarrow Z$$

$$g \begin{cases} g_1: X \times Z \rightarrow Y, \text{ or} \\ g_2: Z' \rightarrow Y, \text{ where } Z' = Z \times Y \end{cases}$$

The output in the case of g_1 appears with a transition from one state to the other, while in the case of g_2 with one of the Z' states. Hence, different g 's define different automaton. The latter is the so-called state-output machine. An arbitrary transition-output machine can be replaced by an equivalent state-output machine [2]. In the following the state-output machines are reviewed.

In the discussed case, the generating set of the input and the output free semigroup, respectively, are constructions with $\alpha\beta$ properties which are the following:

$$\alpha_1 : \text{associative, } (s_i \cdot s_j) \cdot s_k = s_i (s_j \cdot s_k)$$

$$\alpha_2 : \text{commutative, } s_i \cdot s_j = s_j \cdot s_i$$

$$\alpha_3 : \text{idempotent, } s_i \cdot s_i = s_i$$

$$\alpha_4 : \text{zero element exists, } s_i \cdot 0 = 0$$

$$\alpha_5 : \forall s_i, \exists s_j \neq 0 : s_i \cdot s_j = 0$$

$$\beta_1 : \text{definable by product of prime elements only,}$$

$$\beta_2 : \text{an equivalence classification exists, where the product of each of the different elements in one and the same class is zero.}$$

The transformation described by the automaton is a unary operation on an irreducible equivalence class of construction. This operation is a permutation of the given class. The result of the operation is that the index of an element of the equivalence class is incremented by 1. If the argumentum is the element with the maximal index, then the result is the element with index 1.

$$(\hat{K}_a, v_a)$$

n = number of the elements of \hat{K}_a

$$v_a(\hat{k}_a) = \hat{k}_{a+1}, \quad (i < n)$$

$$v_a(\hat{k}_a) = \hat{k}_1$$

If the repeated application of this function is denoted by an exponent, then the highest exponent is equal to the number of elements of the irreducible equivalence class. This is a finite cyclic group generated by v_a , which is a subgroup of the permutation group, and is isomorphic to the group of integers under addition modulo n .

$$v_a(v_a(\hat{k}_a)) = v_a^2(\hat{k}_a) = \hat{k}_{a+2}, \quad (i < n-1)$$

$$v_a^n(\hat{k}_a) = \hat{k}_a, \text{ so } v_a^n = \epsilon \text{ the identity.}$$

Considering the set of functions with different exponents and its compositions it is obviously a structure with an associative, commutative binary operation, with identity and inverse, thus it is an abelian group.

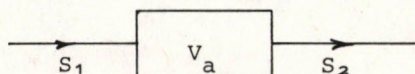
$$V_a = \{v_a, v_a^2, \dots, v_a^n\}$$

$$v_a^x \cdot v_a^y = v_a^{x+y}$$

$$v_a^x \cdot v_a^{n-x} = v_a^n$$

The set of states of automaton consist of the V_a set of functions, and in this case V_a maps the input into the output.

$$X = S_1; \quad Y = S_2; \quad Z = V_a$$



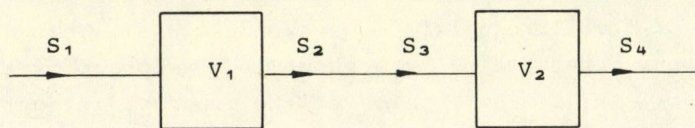
If the input and the output are given in a construction-form, then together (A) the input construction and the output one achieve

a structure with $\alpha\beta$ properties by connections through a set of maps.

$$S_1 S_2 = S^*$$

$$S^* V_a = A$$

It is possible to connect two or more automaton in series.



$$S_1 S_2 S_3 S_4 V_1 V_2$$

It is appropriate to define cyclic groups on all the irreducible equivalence classes of the input construction and the output one, thus the elements of the free semigroup generated by these cyclic groups as functions are defined on the full construction of the original one.

Analogously, it is possible to generate an $\alpha\beta$ structure by giving the relations on the set of functions. All elements of this construction are maps. The domain is the full construction belonging to the automaton, but the images will not become real elements of the construction.

To avoid this, let us define a metric space on the set of maps in order that the automaton should be able to pass from any state into that one which is the nearest and at the same time the image becomes a real element of the construction. Then the automaton will continue its work in this new state.

$$V = \{V_\alpha : V_\alpha = (v_1^{x1}, v_2^{x2}, \dots, v_m^{xm})\}$$

$$\mu(V_\alpha, V_\beta) = \sum_{i=1}^m t_i$$

$$t_j = \begin{cases} |x_{j\alpha} - x_{j\beta}|, & \text{if } |x_{j\alpha} - x_{j\beta}| \leq M_j/2, \\ M_j - |x_{j\alpha} - x_{j\beta}| & \text{otherwise.} \end{cases}$$

M_j is the number of elements of K_j .

The state transition function can be replaced by this metric space. This is far more preferable in the case of a large number of elements.

REFERENCES

1. Műszaki kémiai rendszerek szerkezete. (The Structure of Technical Chemistry Systems) MTA MŰKKI, Veszprém, 1974.
2. MOORE, E.F.: Automata Studies. Princeton University Press, Princeton, N.J., 1956.

РЕЗЮМЕ

Авторы занимались алгебраическим методом изучения различных операций и процессов, проводимых в одинаковом оборудовании, в одинаковой системе оборудований. Истолковался алгебраический автомат (S_b, S_k, S_v, \dots) , где множества S_b - входное, S_k - выходное и S_v - множество состояния, которые обладают характерными для системы свойствами, а далее $\lambda: S_b \times S_v \rightarrow S_k$ и метрика истолкованная через структуру S_v .

Функция $S_b \times S_v \rightarrow S_v$, описывающая изменения состояния алгебраического автомата становится определяемой через μ .

α и β структура определенных автоматов служит для анализа и синтеза систем.

THE BUILDING UP OF THE STRUCTURE OF THE QUANTITATIVE
ALGEBRAICAL AUTOMATONS IN THE TECHNICAL CHEMISTRY

T. BLICKLE and J. GYENIS

(Research Institute for Technical Chemistry of the
Hungarian Academy of Sciences, Veszprém)

The authors show the possibility of the building up the structure of the quantitative automaton in technical chemistry. Four sets are defined, and by making their elements correspond to the structure of the material systems, the structure of the quantitative automaton can be constructed. There is also a possibility to construct the structure of chemical operational systems from the structure of automaton.

Earlier papers on this subject [1-2] established that the structure constructed on the set of material properties is the structure of the one component material. The elements of this structure S_1 can be written as follows:

$$S_i = c_j b_k l_m d_n f_o T_p P_r \quad (1)$$

where $s_i \in S_1$.

From the above mentioned structure the periodical structures of the combined material systems can be established by means of linking relations, defining the type of connections between the components. The elements of these periodical structures, e.g. in the case of two components, can be described by the following expression:

$$s_i = (c_j b_k \beta_l \varphi_m c_n b_o \beta_p) k_r d_s f_t u_v P_v \quad (2)$$

where $s_i \in S_2$.

From the structure of the one component material a structure of algebrical automaton can be constructed with the aid of a cyclic unary operation defined for the structure of the chemical technological transformations [3]. The structure of automaton has the following feature: from a set of given input elements s_i it can produce such output elements s_j , which are also the elements of the structure of the material systems. The expression

$$s_i s_v s_j \in A_1 \quad (3)$$

represents an element of the structure of automaton A_1 , where $s_i, s_j \in S_1$, and s_v is an element of the structure of chemical technological transformations.

The most of the transformations in technical chemistry cannot be explained on the structure of the simple one component material, e.g. the exchange of the homogeneous connection (see absorption or extraction) takes place between two phases, and at least one of these phases consists of two or more components.

For establishing a structure of automaton in that any chemical technological operation is defined, it is necessary to form the union of the structures of the material systems of one, two or more components:

$$S = S_1 \cup S_2 \cup \dots \cup S_n \quad (4)$$

and the structure of automaton can be constructed from the elements of the power set S^* of the resulted set S :

$$s_i^* s_v s_j^* \in A \quad (5)$$

where $s_i^*, s_j^* \in S^*$ and $s_v \in S_v$.

The linkage between s_i^* and s_j^* is given by s_v , if there is a real structure element of the automaton, which is able to produce s_j^* from s_i^* .

If the input and output is given, an element of this structure of automaton can be constructed, e.g. from the following parts:

$$s_i^* = \{C_1\beta_2T_{20}P_5, (C_2\beta_3 \Rightarrow C_3\beta_2)T_{200}P_5\} \quad (6)$$

$$s_j^* = \{(C_1\beta_2 \Leftrightarrow C_3\beta_2)T_{40}P_5, C_2\beta_3T_{100}P_5\} \quad (7)$$

$$s_{v_i} = v_8^2 v_5^1 v_9^4 v_8^4 \quad (8)$$

where v_8^2 , v_5^1 , v_9^4 and v_8^4 represent the mixing of the phases, the heat exchange between the phases, the exchange of the homogeneous connection between the components and the separation of the phases, respectively.

The resulted element can be written in the usual form of algebraical mapping:

$$v_8^2 v_5^1 v_9^4 v_8^4: \begin{pmatrix} C_1\beta_2T_{20}P_5 & 0 & (C_2\beta_3 \Rightarrow C_3\beta_2)T_{200}P_5 \\ (C_1\beta_2 \Leftrightarrow C_3\beta_2)T_{40}P_5 & 0 & C_2\beta_3T_{100}P_5 \end{pmatrix} \quad (9)$$

THE STRUCTURE OF THE QUANTITATIVE AUTOMATONS

Let us consider a set G_1 , the elements of which are rational functions of time:

$$g_i(t) \in G_1 \quad (10)$$

Let the usual addition (denoted by $+$) be an operation defined on the set G_1 , with an unambiguous (but not mutual) correspondence between the elements of the sets S and G_1 . Let the operation of the outer direct multiplication be defined as follows:

If $g_i(t)$ and $g_j(t)$ correspond to s_i and s_j , respectively, and their outer direct product is written by:

$$g_i(t)s_i \circ g_j(t)s_j \quad (11)$$

then this corresponds to the following operation:

$$g_i(t) + g_j(t) \quad \text{and} \quad s_i \circ s_j \quad (12)$$

where \circ is the designation of the outer direct multiplication and at the same time that of the contact operation of the phases s_i and s_j , in the structure of the material systems.

Thus an element of the structure of automaton can be written in the following form:

$$s_{v_i} : \begin{pmatrix} g_1(t)c_1 \circ g_2(t)(c_2 \Rightarrow c_3) \\ g_3(t)(c_1 \Leftrightarrow c_3) \circ g_4(t)c_2 \end{pmatrix} \quad (13)$$

which is the qualitative description of the material streams in the continuous type unit operation.

Evidently there are limitations regarding the correspondence between the elements of the sets S and G_1 , because of the conservation of component and chemical element masses, i.e.:

$$\sum g_i^b(t) + \sum g_j^k(t) = 0 \quad (14)$$

where $g_i^b(t)$ and $g_j^k(t)$ are the inflow and outflow material streams, respectively. If there is a local change of the masses in the operational unit, the equation must also be completed with a third term.

For the batchwise operation type unit the elements of the structure of the quantitative automaton can be obtained by defining a set G_2 , the elements of which are rational numbers. In this case the elements of the set S must be completed with the time t , resulting in a set S' , and the correspondence between the elements of these two sets S' and G_2 must be considered. An element

of the resulting structure of automaton is e.g.:

$$s_{V_i} : \left(\begin{array}{l} g_1 c_1(t_0) \circ g_2(c_2 \Rightarrow c_3)(t_0) \\ g_3(c_1 \Leftrightarrow c_3)(t_v) \circ g_4 c_2(t_v) \end{array} \right) \in A_2 \quad (15)$$

where t_0 and t_v are the moments of the beginning and the finishing of the operation, respectively.

Analogously a set G_3 can be defined, the elements of which having a form:

$$\tilde{g}_i = \int_{t_i}^{t_j} g_i(t) dt \quad g_i \in G_3 \quad (16)$$

Using the elements of the sets S and G_3 , the summary mass balance of the continuous type operation can be obtained. And by defining a set G_4 , the elements of which having a form:

$$g'_i(t) = \frac{dg_i}{dt} \quad g'_i \in G_4 \quad (17)$$

where g_i is the time function of the mass change of the phases found in the operational unit, the structure of automaton describes the differential mass balance of the batchwise type operation.

In the above mentioned cases the conservation of mass can be expressed by equations analogous to the Equation (14).

In the semicontinuous operation, where one of the materials is introduced continuously into the unit, while the other one in a batchwise manner, the structure of automaton can be established as follows:

The elements of the $G_1 * G_4$ or $G_2 * G_3$ product are made to correspond to the elements of the $S * S'$ product. Thus the elements of the structure of automaton take the following forms:

$$s_{V_i} : \left(\begin{array}{l} g_1(t)c_1 \circ g_2(t)c_2 \\ g_3(t)c_3 \circ g_4(t)c_4 \end{array} \right) \quad (18)$$

$$s_{vi} : \begin{pmatrix} g_1 c_1 & 0 & g_2 c_2(t_0) \\ g_3 c_3 & 0 & g_4 c_4(t_v) \end{pmatrix} \quad (19)$$

where in the first case $g_i(t)$ gives the amount of the material streams entering or discharging by convection or conduction, or the intensity of the material sources or sinks, and $g'_i(t)$ gives the rate of the reduction or accumulation of the components, flowing in or out in a batchwise manner.

In the expression (19) the elements involve information about the summarized mass balance of a chemical technological operation.

THE CONSTRUCTION OF THE STRUCTURE OF CHEMICAL OPERATIONAL SYSTEMS

Let $s_{vi}^* s_j^*$ be an element of the structure of automaton constructed on the power set S^* , and let ψ be a mapping, by which the union of s_i^* and s_j^* is mapped onto a set of periodical structure elements consisting of the given combinations of the sections of $s_i^* \cup s_j^*$.

For example if s_i^* is natural gas (c_1) containing petrol vapour (c_2) and fuel oil (c_3) contacting with the gas, while s_j^* is liquid petrol dissolved in fuel oil and pure natural gas, i.e.:

$$s_i^* = c_1 \beta_3 \Rightarrow c_2 \beta_2 \cup c_3 \beta_2 \quad (20)$$

$$s_j^* = c_1 \beta_3 \cup c_2 \beta_2 \Leftrightarrow c_3 \beta_2 \quad (21)$$

then $\psi(s_i^* \vee s_j^*) = \{c_1 \beta_3 \Rightarrow c_2 \beta_2 \Rightarrow c_3 \beta_2$ (i.e. petrol and fuel oil vapor in natural gas), $c_1 \beta_3 \Rightarrow c_2 \beta_2 \rightarrow c_3 \beta_2$ (i.e. fuel oil spray in the gas mixture), $c_2 \beta_2 \Rightarrow c_3 \beta_2 \Rightarrow c_1 \beta_3$ (i.e. dissolved natural gas in the fuel oil containing liquid petrol) $c_2 \beta_2 \Leftrightarrow c_3 \beta_2 \Rightarrow c_1 \beta_3 \rightarrow c_1 \beta_3 \Rightarrow c_2 \beta_2$ (i.e. gas bubbles in the liquid), etc.}

The elements $s_{vi}^* s_j^*$ completed by the mapping $\psi(s_i^* \vee s_j^*)$ also results structure elements:

$$s_{vi} : \begin{pmatrix} s_i^* \\ s_j^* \end{pmatrix} \psi(s_i^* \cup s_j^*) \in Z \quad (22)$$

which gives information about the inlet and outlet materials, as well as the material system existing inside of the operational unit.

If the structure of the operational units (denoted by M) is known, the product $M * Z = R$ gives all the information mentioned above, as well as the properties of the operational unit. Thus the product set R is the structure of the chemical operational systems.

SYMBOLS USED

A	structure of automatons
b	biological structure
c	chemical structure
d	size of the particles
f	form of the particles
G_1, G_2, G_3, G_4	sets, defined by this paper
g	the elements of the sets G
k	crystallic structure
M	structure of the operational units
P	pressure
R	structure of the chemical technological systems
S_1, S_2, \dots, S_n	structure of the materials consisting of one, two, or more components, respectively
s	the elements of the structures S
s_v	the elements of the structures of the chemical technological transformations
T	temperature
t	time
v	chemical technological transformations, e.g.
v_5^1	heat exchange
v_8^2	the mixing of the phases
v_8^4	the separation of the phases
v_9^4	the exchange of the homogeneous connection between the components

β state of matter, e.g.

β_1 solid

β_2 liquid

β_3 gas

φ the type of connection between the components and the appearance of the phases. The elements of this:

\Rightarrow homogeneous connection

\rightarrow heterogeneous connection

(the arrows are directed from the component determining the appearance of the phase)

Subscripts

i, j, \dots, v the $i^{\text{th}}, j^{\text{th}}, \dots, v^{\text{th}}$ properties or element

b inlet

k outlet

o beginning

v finishing

REFERENCES

1. Műszaki kémiai rendszerek szerkezete. MTA Műszaki Kémiai Kutató Intézet Tudományos Eredményei II. (The structure of systems in technical chemistry. The scientific results of the Research Institute of Technical Chemistry Vol. II.) Veszprém, 1974.
2. BLICKLE, T. and Mrs. BÁTOR, E.: Hung. J. Ind. Chem., 4, Suppl. 37 (1976)
3. BLICKLE, T. and BEZEGH, A.: Hung. J. Ind. Chem., 4, Suppl. 51 (1976)

РЕЗЮМЕ

Авторами излагаются возможности создания автоматических структур, построенных на многокомпонентных материальных системах и дающих количественное описание.

Авторы дают соответствия между полученными автоматическими структурами и общими уравнениями баланса.

Структуры систем, соответствующих техническим химико-технологическим системам можно создать специальным изображением, истолкованным на основе множества степеней материальных систем, и композицией автоматических структур и структур процессионных единиц.

APPLICABILITY OF SYSTEM STRUCTURES IN THE
TECHNICAL CHEMISTRY

T. BLICKLE

(Research Institute for Technical Chemistry of the
Hungarian Academy of Sciences, Veszprém)

Application of structures theory in technical chemistry is shown by a simple example.

Starting from four chemical components the separation methods of two-component systems can be determined with the aid of the structures theory.

The application of a structure system in technical chemistry will be shown by a simple example. A two-component system will be separated in two steps by an auxiliary material:

1. the auxiliary material and the first component form a two-component system, while the other component leaves the system;
2. separation of the two-component system.

The second step by itself can be applied for the separation of a two-component system. Thus the two possibilities for separation are as follows:

1. by auxiliary material in two steps;
2. without auxiliary material in one step.

The scheme of the process is shown on Figure 1. Indices on the left side represent the place in the process. The meanings are summarized in Table 1.

Table 1

<u>c</u> <u>chemical structure</u>	<u>v</u> <u>change</u>
c ₁ water	v ₁ separation
c ₂ sulphuric acid	v ₂ exchange
c ₃ air	v ₃ separation and heat exchange
c ₄ silica gel	v ₄ exchange and heat conduction
<u>β</u> <u>state</u>	<u>h</u> <u>procedure</u>
β ₁ solid	h ₁ liquid tank
β ₂ liquid	h ₂ film
β ₃ gas	h ₃ rotary film
	h ₄ foam
<u>d</u> <u>size</u>	h ₅ fixed layer
d ₁ no characteristic size	h ₆ vibrated layer
d ₂ mean size 0.1 mm	h ₇ fluidized layer
d ₃ mean size 0.2 mm	
<u>T</u> <u>temperature</u>	<u>i</u> <u>heat transfer surface</u>
-10°C ≤ T ≤ 110°C	i ₁ no
	i ₂ pipe coil in the apparatus
	i ₃ wall of the apparatus
<u>P</u> <u>pressure</u>	<u>j</u> <u>separating plate</u>
0.1 atm ≤ P ≤ 1 atm	j ₁ none
	j ₂ perforated
	j ₃ slotted

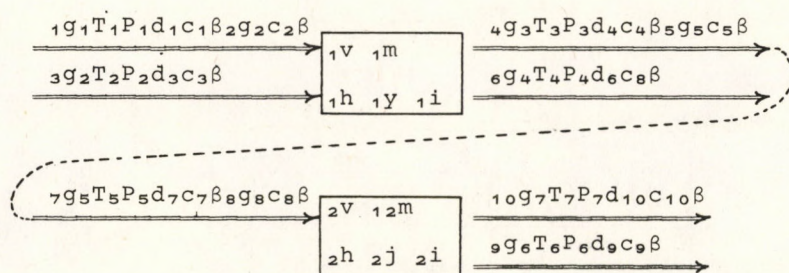


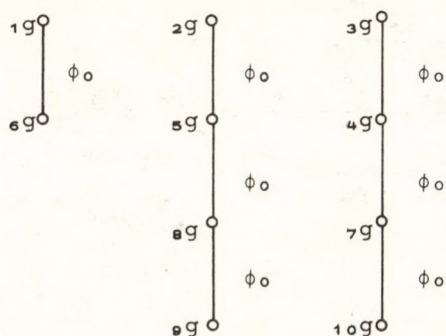
Figure 1

Thus e.g. g_{c2} the output flow of the second unit is H_2SO_4 . The number of object classes in the structure are as follows:

g	10
T	7
P	7
d	7
c	10
β	10
v	2
m	2
h	2
i	2
j	2

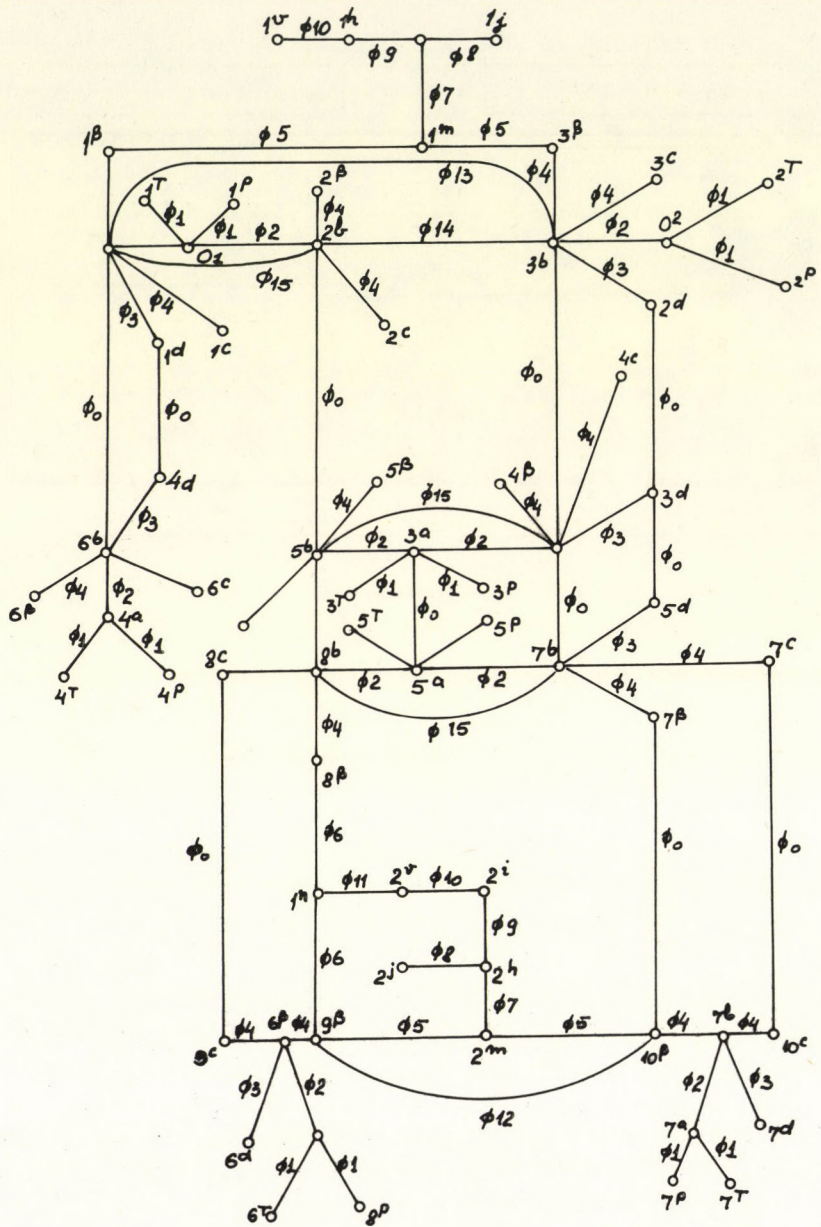
61

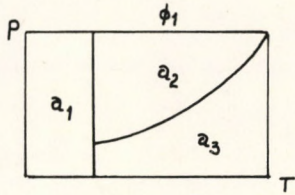
The structures form four structures: three are formed by the 10 g object classes (Figure 2) one by the other ones (Figure 3).



ϕ_x is the relation matrices, ϕ_0 is equality, the other ϕ_x are shown by Table 2. The "a" auxiliary object class is defined by the ϕ_1 , the "b" by the ϕ_4 , the "m" by the ϕ_5 , and the "n" by the ϕ_6 . The relationships determine the complete structure.

The following tasks can for example by determined: one





	β_1	β_2	β_3
ϕ_4	c_1	b_1	b_2
	c_2	0	b_4
	c_3	0	0
	c_4	b_6	0

	b_1	b_2	b_3	b_4	b_5	b_6
ϕ_2	a_1	1	0	0	1	1
	a_2	0	1	0	1	1
	a_3	0	0	1	1	1

	β_1	0	m_1	m_2
ϕ_5	β_2	m_1	0	m_3
	β_3	m_2	m_3	0

	d_1	0	1	1	1	0
ϕ_3	d_2	1	0	0	0	0
	d_3	1	0	0	0	1

	β_1	n_1	n_2	n_3
ϕ_6	β_2	n_1	n_1	n_2
	β_3	n_2	n_2	n_1

	h_1	h_2	h_3	h_4	h_5	h_6	h_7
ϕ_7	m_1	1	0	1	0	1	1
	m_2	0	0	0	0	1	1
	m_3	0	1	1	1	0	0

	v_1	v_2	v_3	v_4
ϕ_{10}	i_1	1	1	0
	i_2	0	0	1
	i_3	0	0	1
ϕ_{11}	n_1	0	0	1
	n_2	1	1	0

	j_1	1	1	1	1	1	1
ϕ_8	j_2	0	0	0	1	0	0
	j_3	0	0	0	1	0	0

	i_1	1	1	1	1	1	1
ϕ_9	i_2	1	0	0	1	1	1
	i_3	1	1	1	1	1	1

	$10\beta_1$	$10\beta_2$	$10\beta_3$
ϕ_{12}	β_1	0	1
	β_2	0	0
	β_3	1	1

Table 2 a

element of the ($1g \ 1T \ 1P \ 1d \ 1h \ 1\beta \ 2g \ 2c \ 2v$) object class is given and structures being its multiplies are the two-step separations.

One element of the ($7g \ 5T \ 5P \ 5d \ 7c \ 7\beta \ 8g \ 8c \ 8\beta$) object class is given and elements of ($7g \ 5T \ 5P \ 5d \ 7c \ 7\beta \ 8g \ 8c \ 8\beta \ 2v \ 2m \ 2h \ 2i.. \ 2j \ 9g \ 6T \ 6P \ 6d \ 9c \ 10g \ 7T \ 7P \ 7d \ 10c \ 10\beta$) object class being multiples determine the single-step separations.

The determination is carried out according to [1].

REFERENCES

1. VERESS, G., BLICKLE, T. and GALBAVY, M.: Hung. J. Ind. Chem. 4, Suppl. 43 (1976)

РЕЗЮМЕ

Автором показана применимость теории структур в технической химии на конкретном примере. Исходя из четырех химических компонентов с помощью теории структур им определены возможные осуществимые методы разделения двухкомпонентных систем.

COMPUTER ALGORITHM FOR THE DETERMINATION OF THE
STRUCTURE OF CHEMICAL COMPOUNDS

T. BLICKLE* and B. NOVÁK**

(*Research Institute for Technical Chemistry of the
Hungarian Academy of Sciences, Veszprém

**Veszprém University of Chemical Engineering, Veszprém)

The number of possible structural formulae of compounds containing a given number of atoms usually increases to a large extent with the increased number of atoms and thus their determination by manual methods becomes increasingly difficult.

An algorithm developed for the construction of structural formulae by computer is shown. The main procedures of a computer algorithm are then discussed and following an analysis of the results, the possibilities of application and further development are also outlined.

One main field of structure theoretical investigations is the study of the material transformations (technological mappings) realized in chemical technological systems.

Within this field one problem to be solved is the description of mapping realized by a given technological system (analysis of the system).

The other task is to determine the technological mappings resulting from the desired final products when the raw materials are given (synthesis of the system). In order to built up the technological system, first of all the determination of the com-

pounds that can be formed from the given elements and compounds must be determined. The starting elements and compounds are given by their formula. In addition, possible valencies of the occurring elements are given and the task is to determine the possible structural formulae from these.

The number of structural formulae of compounds constructable from given atoms rapidly increases with the increased number of atoms and thus the application of a computer to solve this problem seems to be useful.

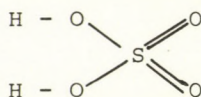
The earlier structures of theoretical results and methods were used as a starting base.

A graph (compound graph) is co-ordinated to the structural formula of the compound. From the viewpoint of a calculation technique, this graph can suitably be treated by its point matrix. This matrix will in future be referred to as the structural matrix.

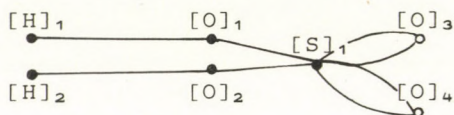
Valencies of atoms in the compound are summarized in the valency vector.

The above mentioned technique is illustrated by an example.

The structural formula of sulphuric acid is as follows:



The corresponding compound graph:



The identification symbols of the atoms are to be found at the graph points.

The elements of the structural matrix determine the number of bonds between the single atoms. For this reason the matrix is symmetrical and the main diagonal contains only 0.

The structural matrix

the valency vector

[S]₁ [O]₁ [O]₂ [O]₃ [O]₄ [H]₁ [H]₂

$$\begin{array}{l}
 [S]_1 \\
 [O]_2 \\
 [O]_2 \\
 [O]_3 \\
 [O]_4 \\
 [H]_1 \\
 [H]_2
 \end{array}
 \begin{bmatrix}
 0 & 1 & 1 & 2 & 2 & 0 & 0 \\
 1 & 0 & 0 & 0 & 0 & 1 & 0 \\
 1 & 0 & 0 & 0 & 0 & 0 & 1 \\
 2 & 0 & 0 & 0 & 0 & 0 & 0 \\
 2 & 0 & 0 & 0 & 0 & 0 & 0 \\
 0 & 1 & 0 & 0 & 0 & 0 & 0 \\
 0 & 0 & 1 & 0 & 0 & 0 & 0
 \end{bmatrix}
 \begin{bmatrix}
 6 \\
 2 \\
 2 \\
 2 \\
 2 \\
 1 \\
 1
 \end{bmatrix}$$

Sum of a line in the matrix determines the valency of the given atom.

To reach our goal the above method has to be passed inversely. Let our task be the following. One sulphur, four oxygen and two hydrogen atoms are given. Which are the constructable structural formulae if the valencies permitted are as follows:

S	6, 4, 0
O	2, 0
O	2, 0
O	2, 0
O	2, 0
H	1, 0
H	1, 0

The 0 valencies here mean that even compounds that do not contain given atoms must be listed.

The structural formulae have to be determined in matrix form: for all combinations of given valencies all possible fills of structural matrix must be determined so that:

1. the matrix is symmetrical;
2. the main diagonal contains only 0;
3. the sum of any line is equal to the adequate element of the valency vector;
4. the given chemical restrictions are fulfilled (e.g. the sulphur and the hydrogen cannot be bonded).

An algorithm constructed to solve this problem starts with the construction of the first valency vector. The valency vector is also changed by using the repeated new combinations of valencies belonging to the atoms of given chemical elements.

The existence of at least one compound graph having this valency system is investigated for every valency vector.

The fills of matrix that belong to a realizable valency vector are given by the following recursive method:

1. to the first line of the $n \times n$ matrix to be filled an $n-1$ decomposition (combination) of the first element of the valency vector that is permitted by the restrictions.

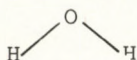
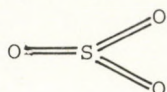
2. Transforming the line and subtracting the adequate values from the elements of the valency vector, the procedure is continued by the construction of all possible fills belonging to the remained valency vector of the still unfilled $(n-1) \times (n-1)$ matrix. The lowest 2×2 matrix can be filled only in one manner. The complete structural matrix is gained following this fill.

3. If all possible fills of a matrix of lower level are gained, the valency vector regains the used values and the procedure is continued by fill a matrix of a higher level.

One part of the solution to the given example:

$$\begin{array}{cccccccc}
 & \text{S} & \text{O} & \text{O} & \text{O} & \text{O} & \text{H} & \text{H} \\
 \text{S} & \left[\begin{array}{cccccccc} 0 & 2 & 2 & 2 & 0 & 0 & 0 & 0 \end{array} \right] & \left[\begin{array}{c} 6 \\ 2 \\ 2 \\ 2 \\ 2 \\ 1 \\ 1 \end{array} \right] & \left| \begin{array}{c} \left[\begin{array}{c} 0 \\ 0 \\ 0 \\ 0 \\ 2 \\ 1 \\ 1 \end{array} \right] \\ \dots \\ \left[\begin{array}{c} 2 \\ 1 \\ 1 \end{array} \right] \end{array} \right. & \left[\begin{array}{c} 0 \\ 0 \\ 0 \\ 0 \\ 2 \\ 1 \\ 0 \end{array} \right]
 \end{array}$$

The corresponding structural formulae:



The algorithm investigates the coherence of the gained compound graph and if the incoherent ones are not needed they are left out.

The matrices constructed thus represent different, (non isomorphous) labelled (numbered) graphs. The labels have not importance regarding the chemical structure and so only the compound graphs differing from the earlier listed unlabelled graphs must be taken into consideration.

The isomorphism of the compound graphs was investigated by the variation of canonic labelling modified for compound graphs that is known from the literature of computation technique.

The computer programme was written in Algol language. The programme was run on the ODRA 1204 computer of the Veszprém University of Chemical Engineering. Structural formulae of different compounds were determined as examples. These compounds were the following: inorganic compounds (with SO_4H_2 formula), organic compounds (with CO_2H_2 formula), carbohydrates (with C_nH_n , C_nH_{2n} ,

C_nH_{2n+2} formula) and usual graphs (as special compound graphs, the points of which are atoms of the some chemical element). The results gained by the algorithm agree well with the literature data.

The algorithm generates structural formulae constructable combinatorically from given atoms of given valencies in accordance with our goal. The model does not take into consideration the arrangement of atoms in space and thus structural formulae that cannot be realized because of limitations in bond distances and angles are to be found among the listed ones.

For this reason the further development and complement of the algorithm seems to be necessary in order to make it possible to study constructed structural formulae in space, i.e. finally the listing of stereoisomers by computer.

РЕЗЮМЕ

Число возможных структурных формул соединений, содержащих данное число атомов, с увеличением числа атомов обычно быстро увеличивается. Таким образом перечисление их ручными методами слишком трудно.

Авторами изложен алгоритм для вычислительного составления структурных формул. Излагаются главные способы вычислительного алгоритма, анализ результатов, и возможности применения и развития.

DETERMINATION OF STOICHIOMETRIC EQUATIONS CONSTRUCTABLE
FROM GIVEN COMPOUNDS

T. BLICKLE and J. SZÉPVÖLGYI

(Research Institute for Technical Chemistry of the
Hungarian Academy of Sciences, Veszprém)

The construction and optimization of reaction series describing given technology are of considerable importance both from a theoretical point of view and for the production engineer. With a knowledge of the compounds involved in the process, stepwise construction of reaction series becomes possible on the basis of the theoretical consideration of systems.

The first step of this construction is reviewed here, namely the method for the determination of stoichiometrically, then chemically independent equations in the knowledge of the compounds involved in the processes. The developed method can be applied for the determination of the equilibrium constants and apparent rate constants of reactions occurring in the given system.

The method of theoretical treatment systems developed at the Research Institute for Technical Chemistry of the Hungarian Academy of Sciences can also mainly be applied for chemical processes. One of the possible fields of application is the determination of the structure of chemical compounds using a computer, while the other field is the determination of stoichiometric equations and possible reaction paths, then starting from these the description of complicated reaction series.

The latter case is reviewed here and the method for the determination of the possible stoichiometric equations will be shown through a simple example.

Let us consider the system described by the following matrix:

$$\begin{array}{c}
 \begin{array}{c} \text{O} \\ \text{H} \\ \text{C} \end{array}
 \begin{bmatrix}
 \text{O}_2 & \text{H}_2 & \text{CO} & \text{CO}_2 & \text{H}_2\text{O} \\
 2 & 0 & 1 & 2 & 1 \\
 0 & 2 & 0 & 0 & 2 \\
 0 & 0 & 1 & 1 & 0
 \end{bmatrix}
 \end{array} \quad (1)$$

As it can be seen the above matrix determines compounds consisting of oxygen and/or hydrogen and/or carbon.

The first task is to give stoichiometrically independent equations in the case of these compounds.

Determination of the base of stoichiometrical equations actually means the following. Let us consider in the system given by matrix (1) two independent equations, e.g.:

$$[\text{H}_2 + \frac{1}{2} \text{O}_2 = \text{H}_2\text{O}] = \text{S}_1 \quad (2)$$

and

$$[\text{C} + \text{O}_2 = \text{CO}_2] = \text{S}_2 \quad (3)$$

Let us define the addition of S_1 and S_2 as follows:

$$\text{S} = (\text{S}_1 + \text{S}_2) = (\text{H}_2 + \text{C} + \frac{3}{2} \text{O}_2) = (\text{H}_2\text{O} + \text{CO}_2) \quad (4)$$

If the set of real numbers as the operator range is added to the S set gained above and the elements of the S set are multiplied with a given element of this number set this can be interpreted as follows:

$$g(a + b) = ga + gb \quad (5)$$

then a linear space is gained and by determining its minimum base that of stoichiometric equations is gained.

Determination takes place in the following manner: let us select from matrix (1) a quadratic matrix corresponding to the number of chemical elements, i.e. lines of original matrix, so

that it will not be singular, i.e. it will not have 0 line. Such a matrix is e.g. the following:

$$\begin{array}{c}
 \text{O}_2 \quad \text{H}_2 \quad \text{CO} \\
 \begin{array}{c} \text{O} \\ \text{H} \\ \text{C} \end{array} \begin{bmatrix} 2 & 0 & 1 \\ 0 & 2 & 0 \\ 0 & 0 & 1 \end{bmatrix}
 \end{array} \quad (6)$$

Let us add the remaining columns of matrix (1) one after the other to matrix (6) and multiply the matrix so gained with a column matrix and set the product equal to 0. Then let us carry out the operations according to the rules of matrix multiplication.

For example let us add to matrix (6) the fourth column of matrix (1):

$$\begin{bmatrix} 2 & 0 & 1 & 2 \\ 0 & 2 & 0 & 0 \\ 0 & 0 & 1 & 1 \end{bmatrix} \begin{bmatrix} x_1 \\ y_1 \\ z_1 \\ -1 \end{bmatrix} = 0 \quad (7)$$

Carrying out the multiplication:

$$2x_1 + z_1 = 2$$

$$2y_1 = 0$$

$$z_1 = 1$$

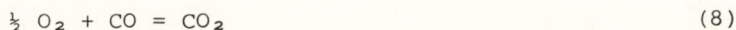
that is

$$x_1 = \frac{1}{2}$$

$$y_1 = 0$$

$$z_1 = 1$$

This means that the first basic equation is the following:



Completely similarly, carrying out operations when the fifth column of matrix (1) is added to matrix (6) and the second basic equation is gained:



The determination of the existing reaction equations from these basic equations represents the following task, however, these equations cannot be the multiples of each other. Construction is carried out with the aid of operation interpreted as follows:

$$g_1 \begin{pmatrix} \frac{1}{2} O_2 & CO \\ & CO_2 \end{pmatrix} \odot g_2 \begin{pmatrix} \frac{1}{2} O_2 & H_2 \\ & H_2O \end{pmatrix} =$$

$$= \begin{pmatrix} \frac{1}{2} (g_1 + g_2) O_2 & g_1 CO & g_2 H_2 \\ & g_1 CO_2 & g_2 H_2O \end{pmatrix} \quad (10)$$

In Equation (10) g_1 and g_2 are the elements of the earlier mentioned set of real numbers, while mappings in the brackets represent basic equations and resultant mapping determinable from those, respectively. In the resultant mapping of Equation (10) the coefficients are g_1 , g_2 and $(g_1 + g_2)$. If the sign of these coefficients is positive then the compounds in the mapping remain on their original place, i.e. compounds in the antecedent are further in the antecedent, and compounds in the successor remain in the successor; if the coefficients are equal to 0 then the given compound does not appear in the mapping, while at negative coefficients the given compound moves over from the antecedent to the successor and vice versa.

Now let us define a structure of elements constructed from the following elements of A, B and C sets, respectively.

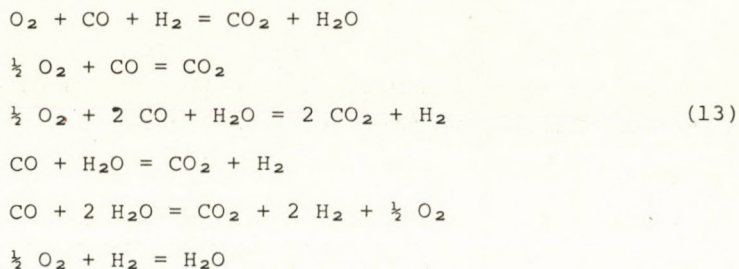
A		B		C	
a_1	$g_1 > 0$	b_1	$g_2 > 0$	c_1	$(g_1 + g_2) > 0$
a_2	$g_1 = 0$	b_2	$g_2 = 0$	c_2	$(g_1 - g_2) = 0$
a_3	$g_1 < 0$	b_3	$g_2 < 0$	c_3	$(g_1 + g_2) < 0$

(11)

Elements of the structure are the following:

$$\begin{array}{lll}
 a_1 & b_1 & c_1 \\
 a_1 & b_2 & c_1 \\
 a_1 & b_3 & c_1 \\
 a_1 & b_3 & c_3 \\
 a_1 & b_3 & c_3 \\
 a_2 & b_1 & c_1 \\
 a_2 & b_2 & c_2 \\
 a_2 & b_3 & c_3 \\
 a_3 & b_1 & c_1 \\
 a_3 & b_1 & c_2 \\
 a_3 & b_1 & c_3 \\
 a_3 & b_2 & c_3 \\
 a_3 & b_3 & c_3
 \end{array} \tag{12}$$

Neglecting the trivial case ($a_2b_2c_2$), 12 elements will remain. From these 2-2 are inverse of each other (e.g. $a_1b_1c_1$ and $a_3b_3c_3$ or $a_2b_1c_1$ and $a_2b_3c_3$) so suitably only one of them must be taken into account. So 6 independent elements of structure exist, i.e. in the given system 6 independent stoichiometric equations can be given. These equations are the following:



Whether the reaction leads to equilibrium or not at a given reaction was so far not taken into consideration. Let us consider two equilibrium reactions. For these the following equation is valid:

$$(S_i K_i) \odot (S_j K_j) = S_k K_k \tag{14}$$

where S_i and S_j are two independent, equilibrium stoichiometric equations

K_i and K_j are equilibrium constants of these equations.

If

$$S_k = S_i \odot S_j \quad (15)$$

then K_k i.e. the equilibrium constant of the new stoichiometric equation is equal to the following expression:

$$K_k = K_i \cdot K_j \quad (16)$$

Let us consider the following case as an example: a mixture of CO and O₂ is burned in a reactor. Let g_2 be mass stream of oxygen and g_3 that of carbon monoxide. What will be the composition of the gas stream leaving the reactor in the case of equilibrium?

The system can be described by the following expression:

$$\begin{aligned} & \begin{pmatrix} g_2 \text{ O}_2 & 0 & g_3 \text{ CO} \\ g_2 \text{ O}_2 & 0 & g_3 \text{ CO} \end{pmatrix} \oplus \begin{pmatrix} \frac{1}{2} g_1 \text{ O}_2 & 0 & g_1 \text{ CO} \\ & g_1 \text{ CO}_2 & \end{pmatrix} = \\ & = \begin{pmatrix} g_2 \text{ O}_2 & 0 & g_3 \text{ CO} \\ (g_2 - \frac{1}{2} g_1) \text{ O}_2 & 0 & (g_3 - g_1) \text{ CO} & 0 & g_1 \text{ CO}_2 \end{pmatrix} \end{aligned} \quad (17)$$

The real task is the determination of the value of g_1 . It can be determined knowing the equilibrium constant of the process. The equilibrium constant is as follows:

$$K = \frac{\frac{g_1}{g_3 + g_2 - \frac{1}{2} g_1}}{\left(\frac{g_2 - \frac{1}{2} g_1}{g_3 + g_2 - \frac{1}{2} g_1} \right)^{\frac{1}{2}} \left(\frac{g_3 - g_1}{g_3 + g_2 - \frac{1}{2} g_1} \right)} \quad (18)$$

After suitable transformations, supposing that $x = \frac{g_1}{g_3}$ and selecting value of g_2 so that $g_2 = \frac{g_3}{2}$ then following expression is gained:

$$K = \frac{x (3 - x)^{\frac{1}{2}}}{(1 - x)^{\frac{3}{2}}} \quad (19)$$

Expressing the value of x from Equation (19) g_1 , i.e. the mass stream of CO₂ leaving the system can be determined. It is easy to

realize that an expression similar to Equation (19) can be gained calculating for opposite direction reaction.

Another problem is how to take into account the kinetics of the reactions. As a primary approximation let us suppose that the 6 reactions described earlier can take place kinetically. Applying a simple formal treatment, e.g. in the case of the following reaction:



the kinetical equation has the form:

$$q_2 = k_1 \cdot c_{\text{O}_2} \cdot (c_{\text{CO}})^{\frac{1}{2}} - k_2 \cdot c_{\text{CO}_2} \quad (21)$$

where q_2 is the "reaction stream" of given reaction;

k_1, k_2 the rate constants;

$c_{\text{O}_2}, c_{\text{CO}}, c_{\text{CO}_2}$ the actual concentrations.

A similar formal equation can be described for all reactions. Then two elements are selected: at least one of them is present in all equations. In this case such elements are e.g. H_2 and O_2 . The reaction co-ordinates of these elements are taken in all equations, and having expressed them two equations are gained with as many various unknown quantities as the number of reactions taken into consideration. In the given case 6 unknown quantities appear in the equations. This means that in order to determine the kinetical expressions describing the system we have to know 4 reaction streams.

The determination of the reaction rate constants is needed to give the reaction streams. The rate constants can be determined from the data of the measurements carried out in a batch system. Let us consider that 12 data were measured. At first data of the first 6 measurements are taken and 6 k values are calculated from these. Then data of 2-7, 3-8, etc., measurements are taken, and 6-6 k values are also determined from these. At length the agreement of these k values is checked.

The method has a major advantage, namely all the reactions occurring in the system are certainly taken into consideration. If

any of the studied reaction cannot be realized because of kinetical causes, its rate constant will be 0.

Complicated reaction series can be constructed by 4 mappings which are the following:

- mappings relating to the mixing of the reaction components; in a homogeneous system mixing takes place spontaneously
- mapping relating to chemical reactions and discussed earlier
- mappings relating to the heat transfer
- mappings relating to the separation of the produced components.

Optimization of the reaction series constructed by the above mappings must be carried out for every reaction concerning temperature and measure of separation.

The described method can easily be utilized with the use of computers and this is especially advantageous for the determination of possible equations and rate constants in the case of complicated systems.

РЕЗЮМЕ

Построение и оптимизация ряда химических реакций, описывающих данную технологию, имеет важное значение и с теоретической, и с технологической точки зрения. Исходя из основ теории систем, можно построить ряд реакций постепенно, зная соединения, участвующие в процессе. Авторами излагаются два первых шага этого построения: метод определения стехиометрически, а далее химически независимых уравнения, в случае если известны исходные соединения. Полученный метод может быть применен и при равновесных реакциях.

SYSTEM OF BALANCE EQUATIONS

T. BLICKLE

(Research Institute for Technical Chemistry of the
Hungarian Academy of Sciences, Veszprém)

A complete balance equation system of technical chemical processes can be given by a description of the balance equations for continuous object classes occurring in the structure of materials.

The complete balance equation system gained in this manner is shown.

Conservation of mass and energy for technical chemical systems can be summarized in the following equations:

$$\sum_i \sum_j \nabla (\rho_{j,i} \underline{v}_i - K_{j,i} \nabla \rho_{j,i}) + \sum_i \sum_j \frac{\partial \rho_{j,i}}{\partial t} = 0 \quad (1)$$

and

$$\sum_i \sum_k \nabla (\hat{\rho}_{k,i} \underline{v}_i - K_i \nabla \hat{\rho}_{k,i}) + \sum_i \sum_k \frac{\partial \hat{\rho}_{k,i}}{\partial t} = 0 \quad (2)$$

where

- i is the index of the summarization according to phases
- j that for components
- k that for energies.

If $\nabla \underline{v}_i = 0$ and $K_{j,i}$ and K_i are constant in the geometrical space, the conservation equations are valid even in the following form:

$$\sum_i \sum_j -K_{j,i} \nabla^2 \rho_{j,i} + \sum_i \sum_j \underline{v}_i \nabla \rho_{j,i} + \sum_i \sum_j \frac{\partial \rho_{j,i}}{\partial t} = 0 \quad (3)$$

and

$$\sum_i \sum_k -K_i \nabla^2 \hat{\rho}_{k,i} + \sum_i \sum_k \underline{v}_i \nabla \hat{\rho}_{k,i} + \sum_i \sum_k \frac{\partial \hat{\rho}_{k,i}}{\partial t} = 0 \quad (4)$$

If Equation (1) or (2) are decomposed to equations described for the phases (according to index i) the mass transfer numbers having a sum equal to zero appear.

If Equation (1) or (3) and the equations given for the phases are decomposed to equations described for the component (according to index j) the source members having a sum equal to zero appear. The sum of the source members that is related to the chemical elements is naturally also equal to zero.

If Equations (2) or (4) are decomposed according to the phases the energy transfer members having a sum equal to zero appear.

If Equations (2) or (4) and equations according to the phases are decomposed to equations described for the energies (according to index k) the energy transformation members having a sum equal to zero appear. If the equations of all energies are not given in the equations of the energies, transformation members of not regarded energies appear as energy sources or absorbers.

Correlations originated from decomposition of conservation equations will also be termed balance equations.

In a description of the technical chemical systems, the energy will be suitable decomposed to the following species:

- compression energy; its intensive parameter is the pressure (p);
- heat energy; its intensive parameter is the temperature (T);
- motion energy; its intensive parameter is the velocity (\underline{v});
- chemical energy;
- surface energy.

The intensive parameter of the chemical energy is the chemical potential. The balance equation is usually not given for the chemical energy and thus its transformation members are interpreted as sources and absorbers in balance equations of thermal and compression energies.

Separated balance equations is not given even for the surface energy primarily used for the characterization of dispersions. For solid/gas and solid/liquid dispersions three parts of the surface energy vis. that being proportional to the surface, the length of edges and number of corners are distinguished, i.e.

$$E_f = a_1 \bar{f}N + a_2 \bar{d}N + a_3 N \quad (5)$$

Spherical particles are usually assumed for gas/liquid, liquid/gas and liquid/liquid dispersions. However, the changes in the phase size distribution of one, two or three parameters even in this case can be described by balance equations of numericality, characteristic linear size and surface. In balance equations of extensive quantities characterizing the dispersion, the specific numericality (n^*), the specific size (d^*) and the specific surface (f^*) may appear as intensive quantities of density character.

The E_k extensive quantity of different energies, if the distribution in space and time of the corresponding η_k in parameter is uniform (homogeneous), can be given as follows:

$$\bar{E}_k = \bar{f}_k(\eta_k) \quad (6)$$

In the case of the inhomogeneous distribution of intensive characteristics, the determination of the energy content and an assessment of the exact distribution of η_k is often troublesome. For this reason, let us decompose into two parts the E_k energy content being characteristic for inhomogeneous distribution of η_k as follows:

$$\tilde{E}_k = \bar{E}_k - E_k^I \quad (7)$$

where:

$$E_k^I = \overline{f_k(\eta_k)} - f_k(\bar{\eta}_k) \quad (8)$$

is the inhomogeneity energy part belonging to the k^{th} energy type. E_k^I decreases monotonously with decreased inhomogeneity of η_k distribution, while for homogeneous η_k distribution $E_k^I = 0$.

If the \tilde{E}_k energy contents as function of η_k is approximated by power series:

$$E_k^I = b_2(\overline{\eta_k^2} - \bar{\eta}_k^2) + b_3(\overline{\eta_k^3} - \bar{\eta}_k^3) + \dots + b_m(\overline{\eta_k^m} - \bar{\eta}_k^m) \quad (9)$$

Consequently, the $\eta(\vartheta)$ distribution may be characterized by the following inhomogeneity moments:

$$\left. \begin{aligned} I_n &= \frac{1}{\theta} \int_0^\theta (\eta - \bar{\eta})^n d\vartheta \\ \bar{\eta} &= \frac{1}{\theta} \int_0^\theta \eta d\vartheta \\ n &= 2, 3, \dots, m \end{aligned} \right\} \quad (10)$$

The $\eta(\vartheta)$ can be approximated with desired accuracy if inhomogeneity moments of adequate number are given as it was proved by us. There is an accordance of one to one between the $\overline{\eta_k^n} - \bar{\eta}_k^n$ expressions and the inhomogeneity moments.

Generally it can be proved that any balance equation of extensive technical chemical characteristics - that originated from the decomposition of (1) and (2) conservation equations - can be decomposed with given accuracy to m balance equations being valid for $\bar{\Gamma}^n$ ($n = 1, 2, \dots, m$) type variable constructed from Γ intensive characteristics belonging to the ψ extensive quantity.

Finally let us investigate the number of quantities describing the technical chemical system of F phase and C component. In a general sense, let us regard two components to be different if they differ in chemical structure, crystal structure or form.

A phase of C component may be characterized by the following parameters: intensive quantities (p, T, \underline{v}) corresponding to the

energies taken into account, concentration of C-1 component, total mass of phase, and if the phase is a dispersed one, even the parameters characterizing the dispersion (n^* , d^* , f^*) must be given. So if variables $\bar{\Gamma}^n$ ($n = 1, 2, \dots, m$) type are applied the number of describing quantities:

$$F(C - 1)m + F \cdot 6 \cdot m + F$$

i.e. a system of F phase and C component may be described from the technical chemical viewpoint by $F((C + 5)m + 1)$ balance equations.

SYMBOLS USED

a	constant
b	constant
C	number of components
d^*	specific linear size (m/m^3)
\bar{d}	energy ($kg\ m^2/s^2$)
\bar{E}	energy of homogeneous phase ($kg\ m^2/s^2$)
\tilde{E}	energy of inhomogeneous phase ($kg\ m^2/s^2$)
E^I	inhomogeneity energy part ($kg\ m^2/s^2$)
F	number of phases
f^*	specific surface (m^2/m^3)
\bar{f}	mean surface (m^2)
K	conductivity (m^2/s)
n^*	specific numericality (ℓ/m^3)
N	numericality
p	pressure ($kg/m\ s^2$)
t	time (s)

T	temperature (K)
\underline{v}	linear velocity (m/s)
Γ	characteristic intensive quantity belonging to ψ extensive quantity
η	intensive characteristics belonging to E energy
ϑ	space - time variable
θ	space - time range
ρ	mass density (kg/m ³)
$\hat{\rho}$	energy density (kg/m s ²)
ψ	extensive technical chemical quantity

The i,j,k,m,n indexes are positive real numbers.

The $\bar{}$ sign usually represents mean value.

РЕЗЮМЕ

Записав уравнения балланса для классов непрерывных объектов, имеющих в структуре материалов получаем целую систему уравнений балланса технических химических процессов.

Автором приводится полученная им целая система уравнений балланса.

INVESTIGATIONS OF NUMERICALITY OF CHANGES IN FLUIDIZED
BED ATOMIZATION-GRANULATION PROCESSES

B. CSUKÁS, T. BLICKLE and Z. ORMÓS

(Research Institute for Technical Chemistry of the
Hungarian Academy of Sciences, Veszprém)

The building up granulation is an operation increasing sizes and decreasing numericality i.e. numericality of particle set decreases during transformation of particle size distribution. Description of process is not possible by the usual transport equations, because the numericality, the transported characteristic is an extensive amount.

The authors report on investigation of change in numericality during batch granulation by fluidization and atomization and their activity aimed at determination of differential equation describing source member of numericality balance equation is described as well.

Size-altering processes (e.g. grinding, and granulation etc.) are characterized by changes of the phase-size distribution. Taking the dispersion as a discontinuous phase, the number of the "required but sufficient" parameters, defining the quality and the degree of the dispersity, can be taken as the additional degree of freedom of the dispersion. The additional degree of freedom of the dispersion is ν if the number of parameters characterizing the $z(x)$ density function of the phase-size distribution is ν or if the $z(x)$ density function is characterized by ν moments as follows:

$$\mu_i = \int_0^{\infty} z(x) x^i dx \quad (1)$$

and $i = 1, 2, 3, \dots v$. The additional degree of freedom of dispersions of practical significance is generally 2 or 3.

The appropriately selected physical quantities corresponding to the 3 additional degrees of freedom are:

- the numericality (N),
- the linear size (D), and
- the surface area (F).

The numericality, linear size and surface area are all extensive quantities, but allow for the derivation of intensive, density-like quantities based on unit volumes:

- the specific numericality ($n = \frac{N}{V}$):
- the specific size ($d = \frac{D}{V}$), and
- the specific surface area ($f = \frac{F}{V}$).

The total volume of the disperse phase or the total volume of the continuous phase including the dispersion can be taken for V reference volume. The specific quantities (n , d and f) can be equally well determined from the parameters and the moments of the $z(x)$ distribution function.

A Damköhler type balance equation can be derived, based on the equation of continuity, to characterize the changes of numericality, size and surface (the procedure obviously also requires the introduction of a source term). The convective numericality, size and surface flows can always be related to certain mass (or volume) flows.

The treatment outlined above is demonstrated on the example of the fluidized bed atomization-granulation process.

The fluidized bed atomization-granulation process is best characterized by saying that a granulating liquid (generally containing the binder as well) is atomized into the fluidized bed composed of the solid raw materials and of the fluidizing gas. Agglomerates are formed in the bed from the wetted particles and the solvent is evaporated yielding in granules held together by

solid binding bridges. The granulate produced in the fluidized bed displays a characteristic particle size distribution that can be well characterized by the two parameter lognormal distribution function, therefore $v = 2$.

Consequently, the granulation process can be described by two balance equations which, considering the physical model, best relate to the numericality and surface area.

Assuming that the fluidized bed is totally mixed, the integral form of the balance equations reads as follows:

$$\dot{V}_O n_O = \dot{V}_1 n_1 = \frac{d(V_r n)}{dt} + V_r q_n \quad (2)$$

and:

$$\dot{V}_O f_O = \dot{V}_1 f_1 + \frac{d(V_r f)}{dt} + V_r q_f \quad (3)$$

In batch operation the V_r volume of the bed increases due to the decreasing bulk density of the bed, therefore either the average density values or, more advantageously, the specific numericality and specific surface area values by mass have to be applied.

In both cases the source terms:

$$- \frac{dn}{dt} = q_n \quad (4)$$

and

$$- \frac{df}{dt} = q_f \quad (5)$$

are applied to describe the system.

As far as the studies on the source terms are concerned, results of the batch granulation experiments were evaluated by two independent methods. A Leitz-Classimate type particle size analyzer was applied to determine the particle size distribution of the granules of smaller size (composed of lactose-starch mixture).

Two equations were used to determine the specific numericality and specific surface area values from the ϕ_i moments of the

$$\phi(r) = \frac{F(r)}{4 r^2 \pi} \quad (6)$$

distribution function as follows:

$$n = \frac{\phi_1^2}{2 \pi \phi_2 \phi_3} \quad (7)$$

and

$$f = \frac{2 \phi_1}{\phi_2} \quad (8)$$

The numericality and surface area values of the granules of greater size (made of quicksand) were evaluated from the parameters of the lognormal distribution function approximating the size distribution as follows:

$$n = \frac{6}{\pi a^3 e^{\frac{9}{2} b^2}} \quad (9)$$

and

$$f = \frac{6}{a e^{\frac{5}{2} b^2}} \quad (10)$$

The wetting and drying properties of the two materials used differ significantly: quicksand dries instantaneously while the lactose-starch material accumulates 3-6 weight % solvent during the formation of the granulate. Fig. 1 presents the plot of numericality - time function for the quicksand granulate. The numericality decreases with increasing time according to an S curve, passing an inflection point and the first derivate at the $t = 0$ point is probably zero. The same tendency is observed with the surface area - time function as well (cf. Fig. 2). Decrease of the numericality and the surface area well approximated by a declining exponential function from the inflection point on. To interpret the phenomenon, it has to be noted that for fluidized bed atomization-granulation process the $t = 0$ time instant is the time when the atomization of the granulating liquid is started. Conditions necessary for the appropriate agglomeration are built up only with

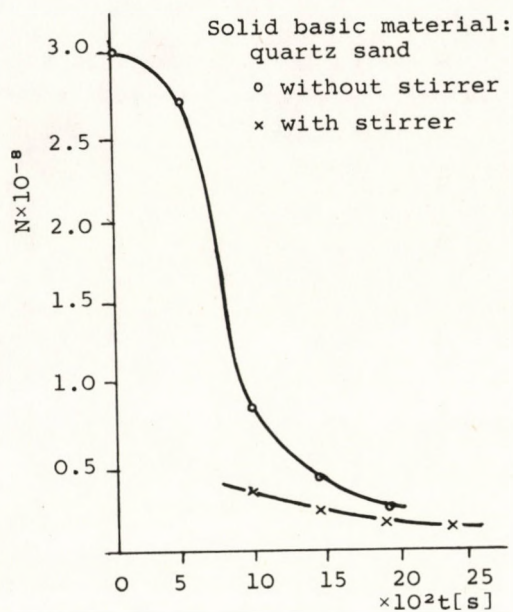


Figure 1

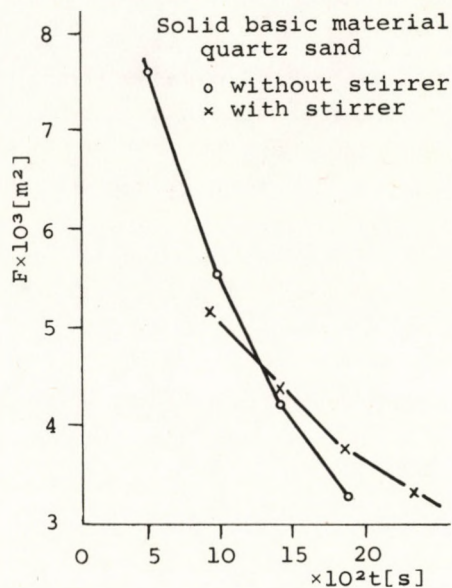


Figure 2

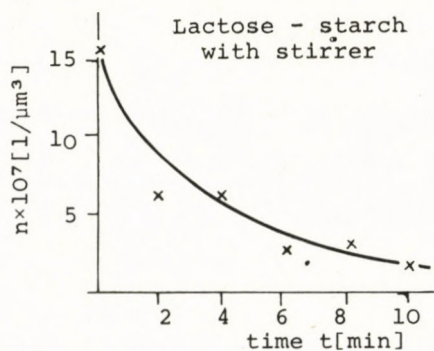


Figure 3

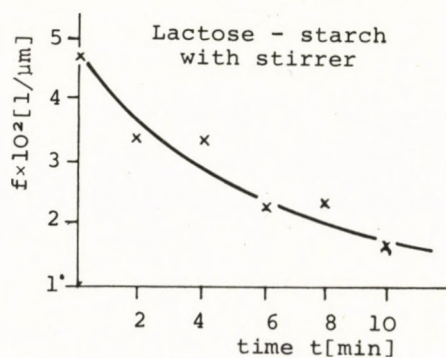


Figure 4

a certain time delay, due to the good drying properties of quicksand, while part of the vetted particles undergoes spontaneous deactivation.

Fig. 3 presents the specific numericality plotted against time while Fig. 4 shows the specific surface area vs time plot for the lactose-starch mixture. An exponential behaviour is noted in both cases and the derivate assumes the highest value for $t \rightarrow 0$. The drying rate is lower for the lactose-starch mixture, as it is for most of the materials to be granulated, therefore the duration of the induction period is negligible. Based on Fig. 5 and 6, the source terms (4) and (5) are defined by the following apparent kinetic expressions,

$$\frac{dn}{dt} = -k_1 (n - n_\infty) \quad (11)$$

$$(t = 0 \rightarrow n = n_0)$$

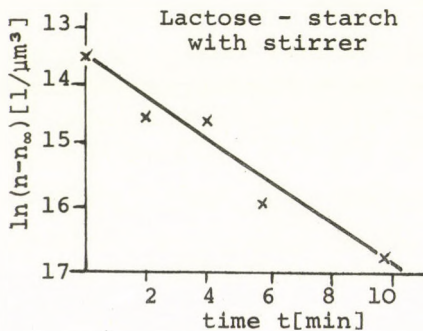


Figure 5

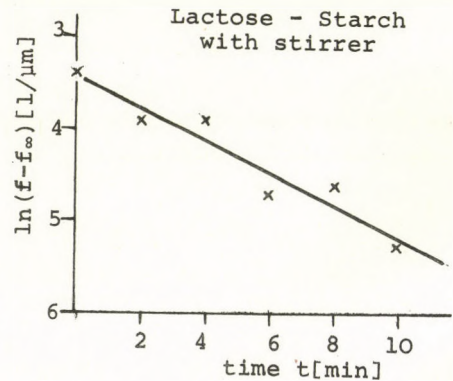


Figure 6

and

$$\frac{df}{dt} = -k_2 (f - f_\infty) \quad (12)$$

$$(t = 0 \rightarrow f = f_0)$$

respectively.

The following differential equation system takes into consideration the activation (in the example given for numericality):

$$\left. \begin{aligned} \frac{dn^*}{dt} &= k_3 - k_4 n^* - q_n \\ - \frac{dn}{dt} &= q_n \end{aligned} \right\} \quad (13)$$

where:

n^* is the numericality of the activated particles,

k_1 is the negative source characterizing the atomization,

k_2 is the negative source characterizing the spontaneous deactivation,

q_n is the negative source characterizing the agglomeration.

If the q_n and q_f source terms, as well as the residence time distribution are known, the continuous granulation can easily be calculated. For example, assuming that Equation (11) and (12) are valid and the fluidized bed is totally mixed, the numericality and the surface area read as:

$$n = \int_0^\infty \frac{n - n_\infty}{n_0 - n_\infty} e^{-k_1 t} \cdot \frac{1}{\tau} e^{-\frac{t}{\tau}} dt = \frac{n - n_\infty}{1 + k_1 \tau} + n_\infty \quad (14)$$

$$f = \int_0^\infty \frac{f - f_\infty}{f_0 - f_\infty} e^{-k_2 t} \cdot \frac{1}{\tau} e^{-\frac{t}{\tau}} dt = \frac{f_0 - f_\infty}{1 + k_2 \tau} + f_\infty \quad (15)$$

SYMBOLS USED

a	parameter of the lognormal distribution function,
b	parameter of the lognormal distribution function,
d	specific size (m/m^3),
D	characteristic linear size (m),
f	specific area (m^2/m^2),
F	area (m^2),
k_j	constant,
n	specific numericality (l/m^3),
N	numericality,
q	source term,
r	radius of the particle (m),
t	time (s),
V	volume (m^3)
V_r	volume of the fluidized bed (m^3),
\dot{V}	volumetric flow (m^3/s)
$z(x)$	phase-size distribution of the dispersion,
μ_i	i -th moment of the $z(x)$ function,
ν	additional degree of freedom of the dispersion,
$\bar{\tau}$	average residence time (s),
$\phi(r)$	particle-size distribution according to Equation (6)
ϕ_i	i -th moment of the $\phi(r)$ function.

РЕЗЮМЕ

Грануляция надстраиванием является операцией, увеличивающей размер и уменьшающей численность, т.е. при трансформации распределения размера зерен численность множества зерен уменьшится. Описание процесса обычными уравнениями транспорта невозможно, т.к. транспортируемый параметр - численность - является экстенсивным.

Авторами изложены исследования по изменению численности при грануляции с помощью периодической флюидизации - распыления, и сообщают о работе, связанной с определением дифференциального уравнения, описывающего источник уравнения баланса, относящегося к численности.

CHANGE OF NUMEROSITY DURING MILLING

L. MISKIEWICZ and L. FÓNAI

(Research Institute for Technical Chemistry of the
Hungarian Academy of Sciences, Veszprém)

Kinetic model of grinding process which was constructed on the basis of uniform view necessary for theoretical treatment of systems was studied.

Balance equation of numerosity flow makes possible a new treatment of grinding process. The members (source, inlet and exit numerosity flow) of balance equation are functions of some characteristic sizes. The mean or characteristic size can be given from the kinetical equation.

The indication of the type of distribution, the equivalent average particle diameter and the dispersion is generally accepted to characterize milling products. However, even with the knowledge of these characteristic features the kinetic investigation of the milling process is very difficult.

One of the aims of the system theory research work carried out at the Research Institute for Technical Chemistry is to elaborate a unified treatment of the transport and dimensional change processes. The results of the theoretical investigations justified the view that the balance equations can also be stated for the change of numerosity superficial area and inhomogeneity [1].

In this study, using the results mentioned above, the change in the number of particles was considered theoretically, then the model was compared with the results of the milling tests.

Balance Equations

On the basis of the drawing shown in Fig. 1 the differential balance equations can be stated - also assuming the mixing - for the whole milling process occurring in the mill as well as for the volume, mass, superficial area and numerical flux.

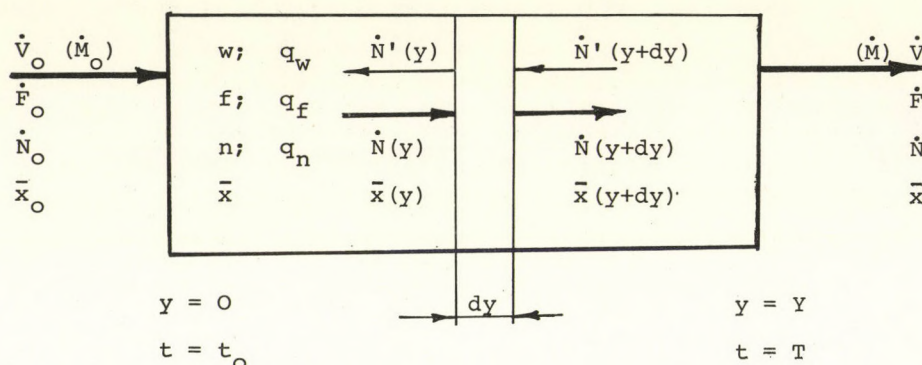


Fig. 1

$$KF \frac{\partial^2 n}{\partial y^2} - \dot{V} \frac{\partial n}{\partial y} + \frac{w}{Y} \frac{\partial n}{\partial t} - \frac{w}{Y} q_n = 0 \quad (1)$$

Now let us define the notion of the specific numerosity and the specific numerosity proportion. The milling was studied in a steady state set in volume or mass flux:

$$\frac{dw}{dt} = 0 \quad (2)$$

Assuming that during the comminution the specific volume - or the real density of the material is constant, the process can be considered to be sourceless for the volume flux, i.e. the change in the number of particles being in the partial volumes de-

pends upon some characteristic size of the particle mass being in the same place:

$$n = \frac{W}{\bar{x}^3} \quad (3)$$

The specific numerosity is the number of particles being in unit volume:

$$\hat{n} = \frac{n}{W} = \frac{1}{\bar{x}^3} \quad (4)$$

The theoretical and experimental results justified the view that the milling process tends towards the equilibrium state (\bar{x}_∞) [2], i.e. the specific numerosity proportion tends towards a maximum value (\hat{n}_∞). So the specific numerosity proportion expresses the rate between the changing specific numerosity and the equilibrium specific numerosity:

$$\alpha = \frac{\hat{n}}{\hat{n}_\infty} = \frac{n}{n_\infty} = \left(\frac{\bar{x}_\infty}{\bar{x}} \right)^3 \quad (5)$$

Stating and assessing the Equation (1) by using the specific numerosity proportion the next equation is given:

$$\frac{KF}{\dot{V}} \frac{\partial^2 \alpha}{\partial y^2} + \frac{\partial \alpha}{\partial y} + \frac{F}{\dot{V}} \frac{\partial \alpha}{\partial t} - \frac{F}{\dot{V} n_\infty} q_\alpha = 0 \quad (6)$$

The differential Equation (6) is a model of an open system, continuous run, unsteady state milling process which also takes the longitudinal mixing into account. From the general equation the particular cases of the milling process can be deduced:

- in the case of complete mixedness

$$K = \infty$$

- if there is no mixing

$$K = 0$$

- in the case of a continuous run, open system, unsteady state milling process:

$$\frac{\partial \alpha}{\partial t} = 0$$

- in the case of an intermittent run, closed system, unsteady state milling process:

$$\frac{\partial^2 \alpha}{\partial y^2} = 0; \quad \frac{\partial \alpha}{\partial y} = 0$$

The experiments were carried out in an intermittent run, closed system vibro-mill, therefore the mathematical model could be justified below:

$$\frac{d\alpha}{dt} - \frac{1}{n_{\infty}} q_{\alpha} = 0 \quad (6.1)$$

The condition of the solution of the differential Equation (6.1) is to know the dimensional change kinetics of the milling. The kinetic model is deduced theoretically by using the fundamental principles of crystallography leaving the power decreasing effect of the lattice defects and micro-cracks out of consideration. The kinetic model is the next:

$$\bar{x}(t) = \frac{\bar{x}_{\infty} t + \bar{x}_0 H}{t + H} \quad (7)$$

The constant H involves material, crystal geometric and operating features.

In the case of fulfillment of the conditions in Equations (2) and (3), transforming Equation (7) is given:

$$q_{\alpha} = n_{\infty} \dot{H} (\alpha^{1/3} - \alpha^{2/3})^2 \quad (8)$$

where \dot{H} is given by the next formula:

$$\dot{H} = \frac{3}{H} \frac{\alpha_0^{1/3}}{(1 - \alpha_0^{1/3})}$$

Replacing the value of q_α into Equation (6.1) and considering the next boundary conditions:

$$t = 0 \Rightarrow \alpha = \alpha_0$$

as a solution is gained:

$$\alpha(t) = \left[\frac{t + H}{t + \frac{1}{\alpha_0^{1/3}} \cdot H} \right]^3 \quad (9)$$

The experimental, and calculation results are summed up in Table 1. These data are shown in Fig. 2 and Fig. 3.

Table 1

$$H = 36 \text{ s}$$

$$\bar{x}_0 = 240 \text{ } \mu\text{m}$$

$$\bar{x} = 4.5 \text{ } \mu\text{m}$$

t (s)	\bar{x}_s (μm)	$\alpha(\bar{x}_s)$	\bar{x} (μm) (calculated by Eq.7.)	α (calculated by Eq.9.)
300	43	1.146×10^{-3}	29.70	3.48×10^{-3}
600	17	1.854×10^{-2}	17.83	1.61×10^{-2}
900	11.8	5.546×10^{-2}	13.56	3.65×10^{-2}
1200	11.0	6.846×10^{-2}	11.36	6.21×10^{-2}
1500	11.0	6.846×10^{-2}	10.02	9.06×10^{-2}
1800	7.9	1.84×10^{-1}	9.12	1.20×10^{-1}
2100	7.8	1.92×10^{-1}	8.47	1.50×10^{-1}
2400	7.9	1.84×10^{-1}	7.98	1.79×10^{-1}
3000	7.3	2.34×10^{-1}	7.29	2.35×10^{-1}
3600	7.4	2.25×10^{-1}	6.83	2.86×10^{-1}

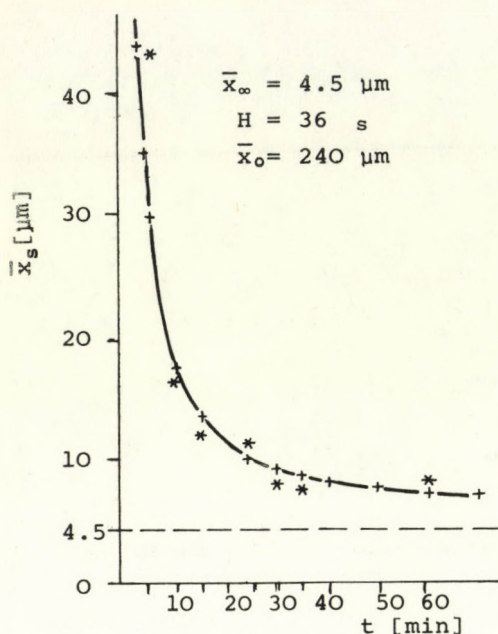


Fig. 2. Characteristic dimension as a function of grinding time on the basis of weight distribution data

* experimental data
 + values calculated theoretically

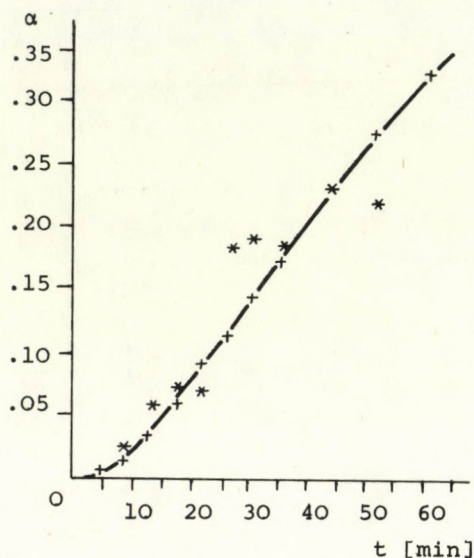


Fig. 3. Specific numerosity proportion as a function of grinding time on the basis of weight distribution data

* values calculated from measurements
 + values calculated theoretically

SYMBOLS USED

F premix surface (m^2)
 H combined constant (s)
 $\frac{O}{H}$ combined constant ($1/\text{s}$)

K	mixing factor (m^2/s)
Y	length of the milling apparatus (m)
n	numerosity
n_0	starting numerosity
n_∞	equilibrium numerosity
\hat{n}	specific numerosity ($1/\text{m}^3$)
\hat{n}_∞	equilibrium specific numerosity ($1/\text{m}^3$)
t	time (s)
\bar{x}	characteristic size (m)
q_n	numerosity source ($1/\text{s}$)
q_α	numerosity proportion source ($1/\text{s}$)
y	co-ordinate along the length of the milling apparatus (m)
w	real volume of the ground material (m^3)
α	numerosity proportion
\dot{V}	volume flow rate (m^3/s)

REFERENCES

1. BLICKLE, T.: A kémiai újabb eredményei (New Results in Chemistry) Vol. 16. Műszaki Könyvkiadó, Budapest, 1973.
2. BEKE, B.: Aprításelmélet (The Theory of Desintegration) Akadémiai Kiadó, Budapest, 1963.

РЕЗЮМЕ

Авторы занимаются изучением кинетической модели, построенной по единому замыслу необходимому для легкого с точки зрения - системы - техники проведения процесса помола.

Уравнение баланса, написанное для потока многочисленности, дает возможность нового анализа процесса помола. Один член уравнения баланса (источник, входящий и выходящий поток многочисленности) зависят от некоторого характерного размера. Зная кинетическое уравнение можно определить средний или характерный размер.

ANALYSIS OF GRINDING KINETICS AND THE CHANGE OF
PARTICLE SIZE DISTRIBUTION AND NUMERICALITY IN A JET-MILL

T. BLICKLE, Mrs. J. MENYHÁRT and T. VIRÁG

(Research Institute for Technical Chemistry of the
Hungarian Academy of Sciences, Veszprém)

Change of particle structure and relative number of particles was investigated in jet mill at different pressures of grinding gas in the case of different model materials by the aid of R-R-B function and the Kolmogorov-Fay-Zselev monogram technique. On the basis of multigrade grinding change of relative particle number as function of time was determined. This function can be applied for elaboration of equation describing batch and continuous grinding.

The particle size distribution curve results of some granulometric analysis are primarily used to characterize granulous materials produced by comminution. Grinding kinetic investigations have also mainly been restricted to the study of the size reduction of a particle or a fraction of particles of a given size in a period of time.

Starting from the particle size distribution curves and making further calculations, the number of the produced particles can be evaluated and by this means further conclusions can be drawn on the efficiency of the milling and the evolution of the rate of comminution.

Investigations were carried out with regard to the jet-milling, using an 80 mm diameter Fryma laboratory size jet-mill with intermittent running, in such a way that the same charge was fed into the mill seven times. In this way, a milling process was considered in which the comminution was continuous within each milling stage and the successive seven stages took place in a total residence time of $\tau_1 - \tau_7$.

The test materials were:

- aplite of Fehérvár ①
- sand of Fehérvárcsurgó ⑦
- sand of Pécsvárad ⑭
- cement clinker ⑳

each of them very hard raw material of the silicate industry. Fractions of 100-200 μm of the test materials were chosen for the jet-milling experiments. The particle size analysis of the milling product was completed by a Leitz-Classimat microscope.

To characterize the milling process, the R-R-B function was used, which is highly favourable to qualitatively evaluate the milling process and its outgrowths [1].

As the integral concerning the number of particles originating in a united period of time which can be deduced from the equations, R-R-B gives real values only in a certain range of the uniformity factor, therefore the Kolmogorov-Rényi equation was chosen as a basis for the calculations.

According to Kolmogorov the number of particles related to each particle size shows a log-normal distribution [2].

In the form of the Gauss distribution function, at milling, the quantities proportional to the particle size get into the exponent.

$$N(x) = \frac{1}{\sqrt{2\pi} \cdot b \cdot x} e^{-\frac{(\ln x - \ln a)^2}{2b^2}} \quad (1)$$

Where \underline{a} is the average particle size, \underline{b} is the deviation of the normal distribution (by particle number).

Utilizing the Kolmogorov-Rényi results [3] Fáy and Zselev elaborated, by graph-technical solutions, an evaluation method [4], which is easy treatable in practice, to represent the weight distribution, the superficial area distribution, and the number distribution function in one graph, then by means of the nomogram, the specific superficial area and the specific particle number could be evaluated by a relatively simple calculation method. Fig. 1 was made by using these results.

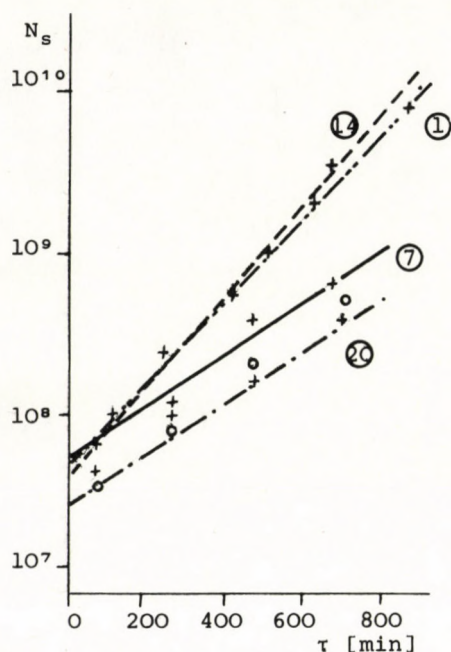


Fig. 1. (1) aplite of Fehérvár
(7) sand of Fehérvár-csurgó
(14) sand of Pécsvárad
(20) cement clinker
 $p\delta = 16$ att

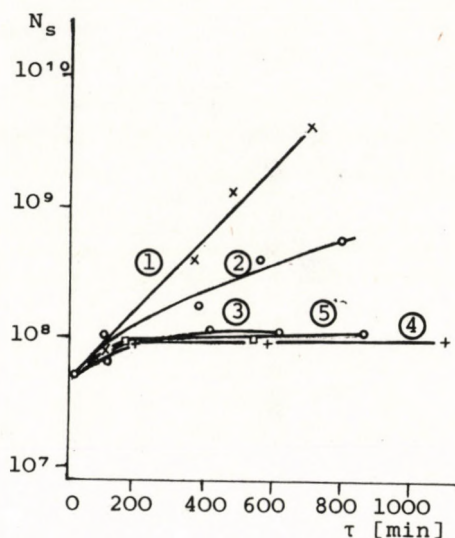


Fig. 2. Aplite of Fehérvár
(1) $p\delta = 16$ att
(2) $p\delta = 14$ att
(3) $p\delta = 12$ att
(4) $p\delta = 9$ att
(5) $p\delta = 6$ att

In Figure 1 the specific particle number (obtained in units of particle number per kilogram) - milling period function is

shown, calculated from the experiments carried out with 16 kg/cm² milling gas pressure.

It can be seen that the optimum milling gas pressure is that at which the change of the particle number as a function of time gives a straight line. Decreasing the milling gas pressure the kinetic energy of the particles provided by the gas is insufficient to ensure the constant milling rate so the milling equilibrium will set in a very short time.

The findings concerning the change of the numericality as a function of time are well supported by those curves showing the relation between the degree of milling and the particle size. These curves are shown in Figure 3 in case of aplite of Fehérvár.

In order to be able to characterize the jet-mill as a grinding apparatus from the point of technical chemistry system theory, the function of $N = \psi(t)$ has to be defined.

As a starting point, the degree of milling as a function of time was analyzed. The degree of milling is defined as follows:

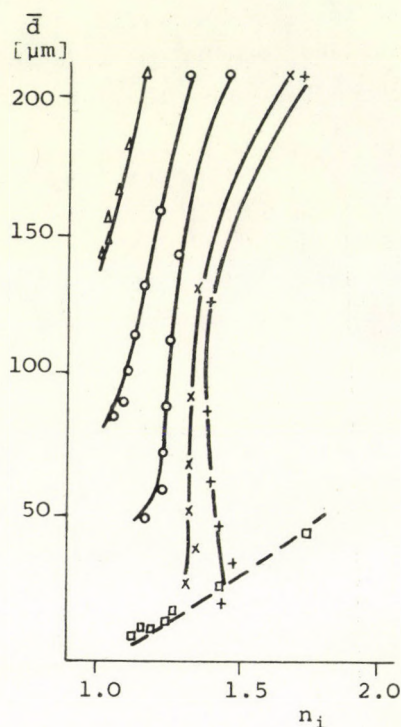


Fig. 3. Aplite of Fehérvár

	\bar{d}_0
+ 16 att	207.7 μm
x 14 att	207.7 μm
o 12 att	207.7 μm
• 9 att	207.7 μm
Δ 6 att	207.7 μm
◻ 16 att	44.6 μm

$$n_i(t, \Delta t) = \frac{\bar{d}(t)}{\bar{d}(t + \Delta t)} \quad (2)$$

To approach the relationship between the degree of milling and the milling period, a differential quantity $v(t)$ is introduced:

$$\begin{aligned} v(t) &= \lim_{\Delta t \rightarrow 0} \frac{\bar{d}(t + \Delta t) - \bar{d}(t)}{\bar{d}(t + \Delta t)\Delta t} = \\ &= \frac{\frac{d}{dt} \bar{d}(t)}{\bar{d}(t)} = \frac{d}{dt} \ln \bar{d}(t) \end{aligned} \quad (3)$$

If Δt is fairly minor the next relationship exists between $v(t)$ and $n_i(t + \Delta t)$:

$$v(t) = \frac{1 - n_i(t, \Delta t)}{\Delta t} \quad (4)$$

(at milling $v < 0$, at agglomerating $v \geq 0$).

So $v(t)$ seemingly depends upon Δt , but in case of little Δt very slightly.

The function $v(t)$ can be determined by utilizing the experimental results from Kolmogorov's particle size distribution curves. However, it is more reasonable to work instead of this with the function $v(\bar{d})$ which is obtained by choosing \bar{d} measured at a moment of t as an independent variable instead of Δt . On the basis of Figure 4 knowing the milling period of Δt the function $v(\bar{d})$ is directly and simply evaluated from Equation (4).

If the points of the curves of Figure 3 are taken at the same moment of the milling period then by transforming linearly the curves of n_i the curves of v are obtained. It can be seen that in this case (with high milling pressure) n_i is approximately independent of \bar{d} so v can be taken as a constant.

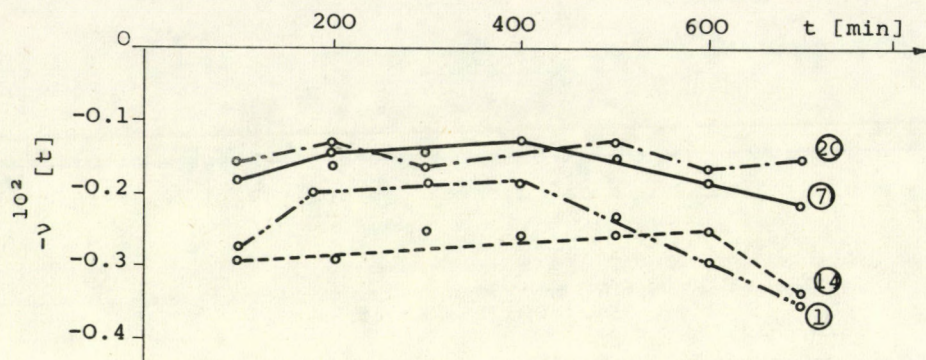


Fig. 4. (1) - aplite of Fehérvár; (14) - sand of Pécsvárad
(7) - sand of Fehérvárcsurgó; (20) - cement clinker

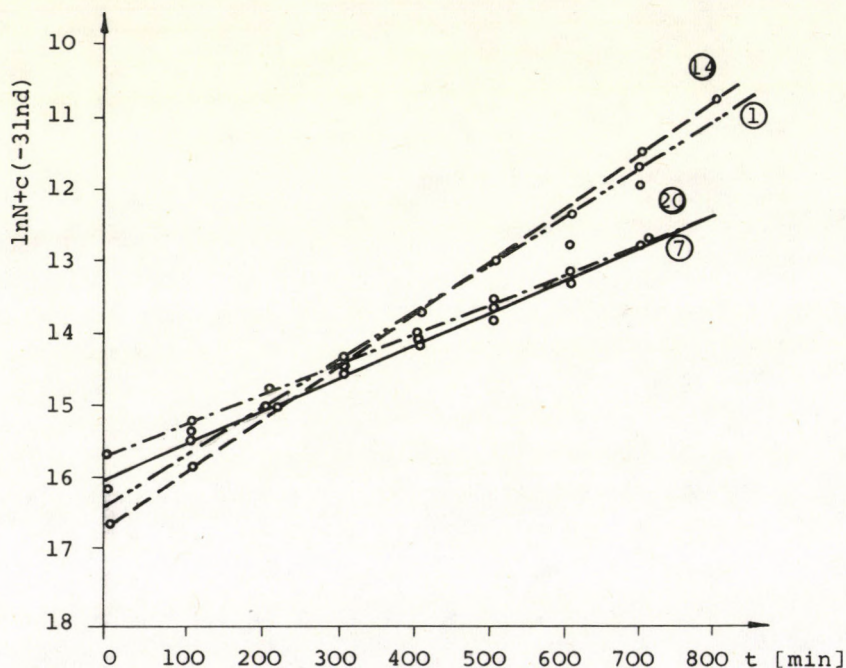


Fig. 5. (1) - $v = -0.223 \cdot 10^{-2}$; (14) - $v = 0.24 \cdot 10^{-2}$
(7) - $v = -0.15 \cdot 10^{-2}$; (20) - $v = -0.14 \cdot 10^{-2}$

Let us change over the particle diameter as an independent variable to the particle number:

$$\hat{N} = \alpha \cdot \bar{d}^{-3} \quad (5)$$

$$v = -\frac{1}{3} \frac{d}{dt} \ln \hat{N} \quad (6)$$

Showing the relationship between the milling period of time and the quantity $-\ln \hat{N} + c(-3 \ln \bar{d})$ the straight lines shown in Figure 5 are obtained from which the values of v are evaluated for each material. The values of v taken from Figure 4 and calculated by using the relationship between Equations (5) and (6), respectively, show good agreement so the value of v can indeed be considered as a constant.

In the case of intermittent running the function $\hat{N} = \psi(t)$ can be calculated by integrating Equation (6):

$$\hat{N}(t) = N_{(0)} \cdot e^{-3vt} \quad (7)$$

In Figure 1 the calculated values are drawn in (with a sign 0) and there is good conformity to the numerical curve determined by the measurements.

Consequently the particle number increases exponentially. At the same time, it means that the particle number is a source in the system:

$$q(N) = -3 v N \quad (8)$$

On the basis of the foregoing the balance equation of a totally mixed system is:

$$\tilde{N}_0 = \tilde{N}_k + \frac{dN}{dt} - q(N) \quad (9)$$

changing over to a volumetric flow rate:

$$V\mu_0 = W[q(N)](\mu) = V\mu_k + W \frac{d\mu}{dt}$$

in intermittent system:

$$W \frac{du}{dt} = 0$$

REFERENCES

1. BEKE, B.: Aprításelmélet, Szilikátkémiai monográfiák (The Theory of Desintegration, Monographies in Silicate Chemistry), Akadémiai Kiadó, Budapest, 1964.
2. KOLMOGOROV, A.N.: Über das logarithmisch-normale Verteilungsgesetz der Dimensionen bei Zehrstückelung. Dokladi Akademii Nauk S.S.S.R., 31, 99 (1941).
3. RÉNYI, A.: Épitőanyag, 2, 177 (1950).
4. FÁY, G., ZSELEV, B.: Energia és Atomtechnika 13, 333 (1960).

РЕЗЮМЕ

Авторы изучали изменение структуры зерен и удельного числа зерен в струевой мельнице при разных давлениях мелющего газа с помощью соотношения Р-Р-Б, и техники номограмма КОЛМОГОРОВА - ФАЙ - ЖЕЛЕВА.

Зная это изменение, они определили функцию, описывающую изменение во времени удельного числа зерен. С помощью этой функции можно выработать уравнение, используемое для описания периодического и непрерывного помола.

THE GENERAL TREATMENT OF PROCESSES WITH INHOMOGENEITY
VARIATION

T. BLICKLE and T. VAJDA

(Research Institute for Technical Chemistry of the
Hungarian Academy of Sciences, Veszprém)

In the paper it is investigated whether the

$$\sigma^2 = \frac{1}{V} \int_{(V)} (u - \bar{u})^2 d^3r$$

amount (where \bar{u} is the average in space of potential, V is the volume of the system) measuring inhomogeneity of $u(x,y,z,t)$ potential in the general transport system satisfies some kind of universal equation from which it can be determined independently the relating potential.

In previous publications a study was made in one-dimension, symmetric [1] and in three-dimension, fully general [2] cases of the behaviour of the mean square deviation from the space mean value of the potential during the diffusive homogenization of a supposed initial potential distribution $\phi(x)$ in a closed system (in the case [1]). This quantity used for measuring the potential inhomogeneity of the system is termed in the following, the dispersion σ^2 . It has been shown that the dispersion versus time can be given in the form of the exponential series:

$$\sigma^2(t) = \sum_{k=1}^{\infty} A_k e^{-\lambda_k t} \quad (1)$$

where:

$$A_k = \frac{1}{2} \left[\frac{1}{L} \int_{-L}^L \varphi(s) \cos \frac{k\pi}{L} s ds \right]^2 \quad (2a)$$

$$\lambda_k = 2 a^2 \left(\frac{k\pi}{L} \right)^2 \quad (2b)$$

($2L$ is the length of the system, a^2 is related to the conductivity coefficient), and so the course of the dispersion is - as shown in Figure 1 - predominantly exponential. All this follows from the fact that the λ_k values form a monotonously increasing sequence. It was also established that the dispersion exactly satisfies only the infinite first order differential equation system involving the partial sums according to (1) and the linear description of the logarithmic dispersion according to Figure 1 leads to accurate results only in the case of higher t values.

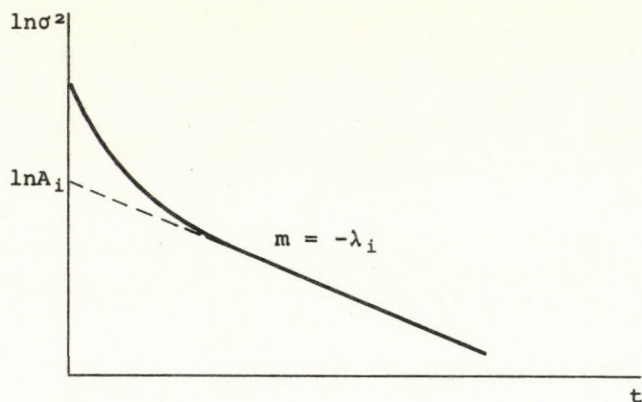


Figure 1

The aim of this work is to give a phenomenological approximate differential equation of the dispersion which is satisfactorily perspicuous (no system, linear) and describes the exact dispersion over the complete interval of the independent variable with a satisfactory accuracy. Let us therefore consider the following trivial equality:

$$\frac{d\sigma^2}{dt} = \frac{\frac{d\sigma^2}{dt}}{\sigma^2} \sigma^2 = -k(t)\sigma^2 \quad (3)$$

where k denotes the differential quotient of the dispersion in time divided by the dispersion. By substituting (1) into (3) the behaviour of the function coefficient k can be established on the basis of (2a) - (2b); by starting from a certain value λ_0 it tends asymptotically to the value $\lambda_\infty \equiv \lambda_1$.

On the basis of the above, the coefficient k is modelled by the following function form:

$$k(t) = (\lambda_0 - \lambda_\infty) e^{-\mu t} + \lambda_\infty \quad (4)$$

By substituting (4) into (3) the differential equation describing the dispersion is as follows:

$$\frac{d\sigma^2}{dt} = -[(\lambda_0 - \lambda_\infty) e^{-\mu t} + \lambda_\infty] \sigma^2 \quad (5)$$

The initial condition of Equation (5) is $\sigma^2(t=0) = \sigma_0^2$, whose value may be obtained only by measurement. The value λ_0 of the differential quotient of the dispersion normalized to unity at the point $t = 0$ can be obtained exclusively by measurement. λ_∞ and A_1 respectively can be determined both by measurement and in the knowledge of the conductivity coefficient of the diffusion problem respectively in the knowledge of the initial potential distribution by calculation (2a) - (2b). The value A_1 is required for the interpretation of μ that has not been studied so far.

Let us now solve the differential Equation (5). After the reparation of the variables and after integration we have:

$$\ln \frac{\sigma^2}{\sigma_0^2} = - \frac{\lambda_0 - \lambda_\infty}{\mu} (1 - e^{-\mu t}) - \lambda_\infty t \quad (6)$$

where the initial condition was utilized; or from (6):

$$\sigma^2 = \sigma_0^2 \exp \left[- \frac{\lambda_0 - \lambda_\infty}{\mu} (1 - e^{-\mu t}) - \lambda_\infty t \right] \quad (7)$$

The value of the still undetermined parameter μ can be derived by the following consideration: let us require from the solution of the approximative differential Equation (7) that its logarithm shows the same asymptotic behaviour as (1). This means that - on the basis of Figure 1 - the asymptote must intersect the ordinate axis at point $\ln A_1$ (the slope of $m = -\lambda_\infty$ is already as necessary) and so by utilizing (6) and on the basis of geometrical considerations it is true that:

$$\ln \sigma_0^2 - \ln A_1 = \frac{\lambda_0 - \lambda_\infty}{\mu}$$

giving:

$$\mu = \frac{\lambda_0 - \lambda_\infty}{\ln \frac{\sigma_0^2}{A_1}} \quad (8)$$

Finally by substituting (8) into (7), and after the rearrangement, the final form of the solution is obtained as:

$$\sigma^2(t) = A_1 e^{-\lambda_\infty t} \left(\frac{\sigma_0^2}{A_1} \right)^{-\frac{\lambda_0 - \lambda_\infty}{\ln \frac{\sigma_0^2}{A_1}} t} e^{\frac{\lambda_0 - \lambda_\infty}{\ln \frac{\sigma_0^2}{A_1}} t} \quad (9)$$

Summing up the above results it can be stated that the approximate solution (9) meets the following requirements:

- 1) It starts from the same point, with an identical tangent in $t=0$ and its logarithm tends to the asymptote of the same slope in the limes $t \rightarrow +\infty$, as the exact dispersion function;
- 2) The intersection points of the asymptotes with the ordinate axis also coincide.

The course of the approximative solution can be studied on Figure 2 by the given parameter values. The phenomenological description also gives a completely reassuring result according to this figure.

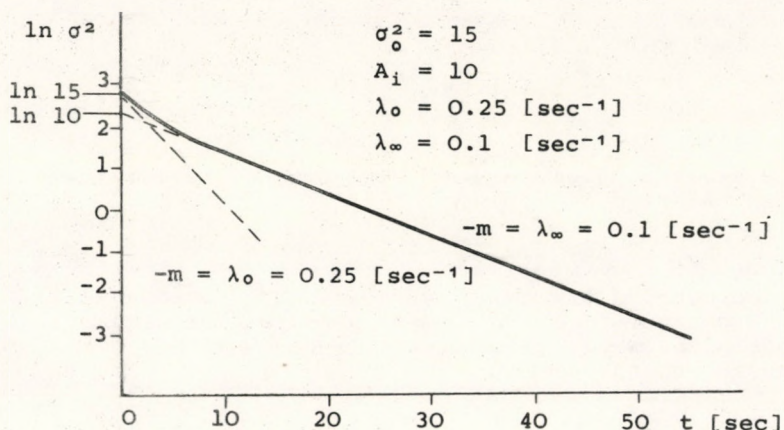


Figure 2

REFERENCES

1. MTA Műszaki Kémiai Kutató Intézet Tudományos Eredményei II. 5.1. 9. Szórás forrás, Veszprém, 1974. (Research Institute for Technical Chemistry of the Hungarian Academy of Sciences. Scientific Results II. 5.1. 9. Dispersion, Source. Veszprém, 1974).
2. BLICKLE, T., SEITZ, K., VAJDA, T.: Behaviour of the inhomogeneity of potential functions describing conductive transport processes in closed systems. Magyar Kémikusok Lapja (to be published).

РЕЗЮМЕ

Автором изучается : удовлетворяет-ли какому-нибудь универсальному уравнению параметр

измеряющий неоднородность $u(x, y, z, t)$ по потенциалу совершенно - общей транспортной системы (где \bar{u} : среднее значение потенциала по объему, V - объем системы), из которого (уравнения) его можно определить независимо от потенциала.

STUDIES ON INHOMOGENEITY IN A QUASI-STEADY-STATE SYSTEM

T. BLICKLE, B. LAKATOS, Gy. FLÓRIÁN and Gy. BUCKSKY

(Research Institute for Technical Chemistry of the
Hungarian Academy of Sciences, Veszprém)

The technical chemical systems theory defines the inhomogeneity in addition to the usual parameters in order to describe the chemical operations unambiguously. These characteristics of deviation can be interpreted according to space and time. Inhomogeneity in time and its close connection with mixing were also investigated.

The empty tube reactor was chosen as a model and at the input and output of the reactor, the inhomogeneity was determined by the method of periodic disturbance.

The algebraic description of technical chemical systems gives structures of these systems and connections among the properties, i.e. it shows how the system can be elaborated to realize a given technical chemical assignment [1, 2].

However, the fulfilment of a technical chemical assignment not only means the realization of certain changes, but also the manner in which they occur to certain extent. Therefore, certain quantitative functions must be interpreted on those qualitative properties that determine the connections among the parameters corresponded to the structural elements of the algebraic description [1].

Depending on the concrete assignment, usually the mass, the concentrations of different components, the temperature and the momentum are chosen as parameters. However, the interpretation of numericality [1] and the introduction of the inhomogeneity squares in space and time to characterize the distribution of the above parameters in space and time, are often necessary to the complete description.

Let $c = c(x, t)$ designate the concentration of a given component in a practically unidimensional operational unit of L length. In order to characterize the special distribution, the following inhomogeneity square is introduced:

$$I_v^2(t) = \frac{1}{L} \int_0^L [c(x, t) - \bar{c}(t)]^2 dx \quad (1)$$

where

$$\bar{c}(t) = \frac{1}{L} \int_0^L c(x, t) dx \quad (2)$$

is the mean value.

At a fixed x point the inhomogeneity square in time is defined as follows:

$$I_t^2(x) = \lim_{t \rightarrow \infty} \frac{1}{t} \int_0^t [c(x, \tau) - \bar{c}(x)]^2 d\tau \quad (3)$$

where

$$\bar{c}(x) = \lim_{t \rightarrow \infty} \frac{1}{t} \int_0^t c(x, \tau) d\tau \quad (4)$$

If the concentration changes periodically, i.e. $c(x, t) = c(x, t+T)$ where T designates the cycle time:

$$I_t^2(x) = \frac{1}{T} \int_0^T [c(x, \tau) - \bar{c}(x)]^2 d\tau \quad (5)$$

and

$$\bar{c}(x) = \frac{1}{T} \int_0^T c(x, \tau) d\tau \quad (6)$$

For a concentration changing according to regular sinusoidal wave:

$$c(x, t) = A(x) \sin[\omega t + \alpha(x)] + \bar{c}(x) \quad (7)$$

Replacing Eq. (7) to Eq. (5) after simple calculation, the following expression is gained:

$$I_t^2(x) = \frac{A^2(x)}{2} \quad (8)$$

If a completely mixed system is disturbed by a concentration change that may be described by Eq. (7), the c_1 outlet concentration - ignoring the need to designate the dependence on x space co-ordinate - will be determined by the following ordinary differential equation of first order:

$$\bar{t} \frac{d c_1(t)}{dt} + c_1(t) = A \sin(\omega t + \alpha) + \bar{c} \quad (9)$$

The solution of Eq. (9) after the decay of transient member - quasi-steady - state operation - has the following form:

$$c_1(t) = \frac{A}{\sqrt{1 + \omega^2 \bar{t}^2}} \sin(\omega t + \alpha + \varphi) + \bar{c} \quad (10)$$

where:

$$\varphi = - \arctg \omega \bar{t} \quad (11)$$

in the phase lag caused by the system.

Calculating the inhomogeneity square of the output sign from Eq. (10):

$$I_{t1}^2 = \frac{I_t^2}{1 + \omega^2 \bar{t}^2} \quad (12)$$

where $I_t^2 = A^2/2$.

If more such identical systems are connected in series, the inhomogeneity square of the input sign from the i^{th} element of the cascade is as follows:

$$I_{tn}^2 = \frac{I_t^2}{(1 + \omega^2 \bar{t}^2)} \quad (13)$$

Let us now assume that the mean residence time for an incompletely mixed system of x length that may be described by a unidimensional model is the following:

$$\frac{V}{Q} = n\bar{t} \quad (14)$$

where n is exactly the mixing unit number characterizing the mixing conditions in the system [3], i.e.:

$$n = nx_0 \quad (15)$$

Assuming S = the constant cross section in the studied system when Eqs. (14) and (15) are compared, the following equation is gained:

$$\bar{t} = \frac{Sx_0}{Q} \quad (16)$$

i.e. the volume of one mixing unit is equal exactly to the n^{th} part of the total volume of the studied system.

Substituting Eqs. (15) and (16) into Eq. (13):

$$I_{tn}^2 = I_t^2(x) = \left(1 + \frac{\omega^2 x_0^2 S^2}{Q^2}\right)^{\frac{x}{x_0}} \cdot I_t^2(0) \quad (17)$$

where $I_t^2 = I_t^2(0)$ is the inhomogeneity square of the input sign.

After simple transformations the following correlation is gained from Eq. (17):

$$\ln \frac{I_t^2(x)}{I_t^2(0)} = -kx \quad (18)$$

where

$$k = \frac{\ln \left(1 + \frac{\omega^2 x_0^2 S^2}{Q^2}\right)}{x_0} \quad (19)$$

The differential form of Eq. (18) is expressed by the following ordinary differential equation:

$$\frac{d I_t^2(x)}{dx} = -k I_t^2(x) \quad (20)$$

with the $I_t^2(x=0) = I_t^2$ initial condition.

As it can be seen for the system fulfilling the above conditions, the inhomogeneity square in time decreases exponentially along the axis of the system and the characteristic parameter for the change is k quantity determined by Eq. (19) that depends on the frequency of the input sign, the length of mixing, the diameter of the system and volumetric flow transporting the concentration sign.

In the experiments aimed at controlling Eq. (18) the flow of the binary mixture in smooth tubes was investigated.

The scheme of the experimental apparatus is shown on Fig. 1.

During the experiments, water was mixed with a sodium chloride solution of sinusoidal mass flow in a hydrocyclone. The experiments were evaluated on the basis of the input and output concentration signs in accordance with Eq. (18), i.e. the inhomogeneity squares in time of the input and output signs were calculated and the natural logarithm of their ratio was plotted against the length of the measuring section.

In the experiments, the length of tube, its diameter and the frequency of the periodical concentration sign were the varying parameters.

Results of experiments are shown in Figures 2-4.

A summarized result of the experiments is shown in Fig. 2. As it can be seen, the approximation (18) fits well and for all diameters the inhomogeneity square in time decreases exponentially along the length of the tube.

However, the change of the inhomogeneity square in time is not only determined by the length of the tubes, but the diameter

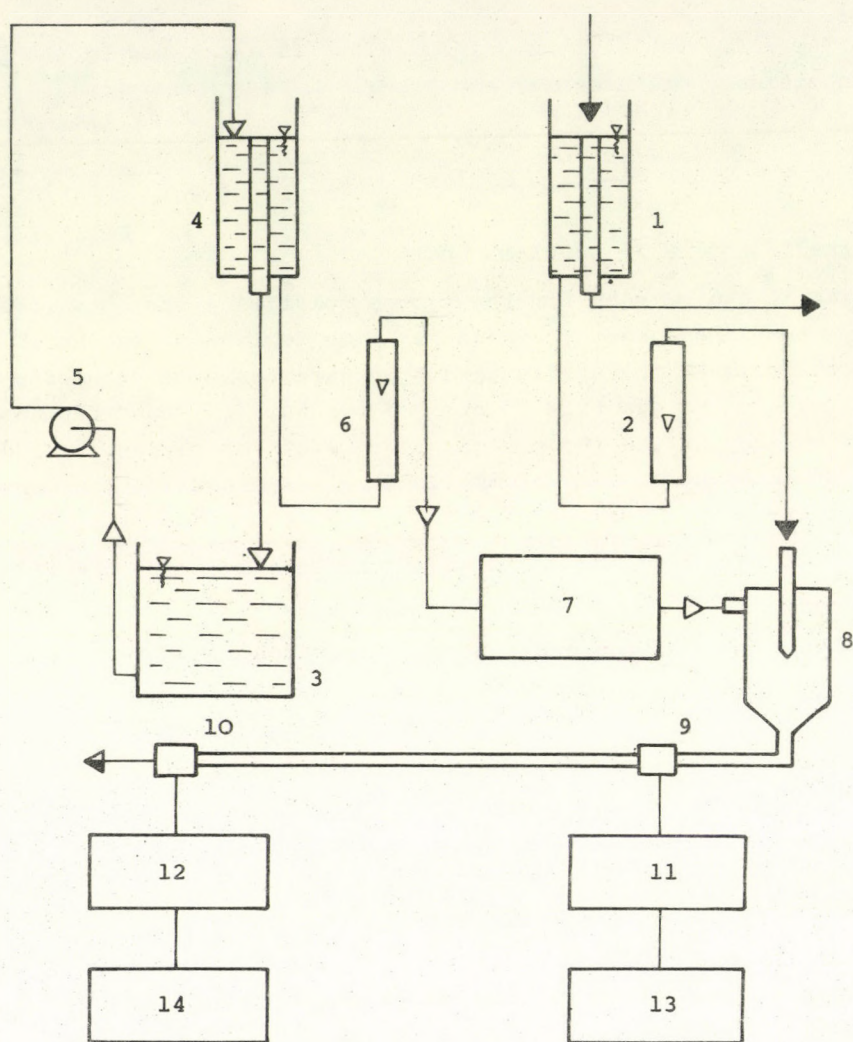


Fig. 1. 1,4 - feed tanks, 2,6 - rotameters, 3 - reservoir, 5 - pump, 7 - peristaltic pump, 8 - mixing unit, 9,10 - detectors, 11,12 - conductivity meters, 13,14 - recorders. Δ - tap water, Δ - sodium chloride solution, Δ - diluted sodium chloride solution.

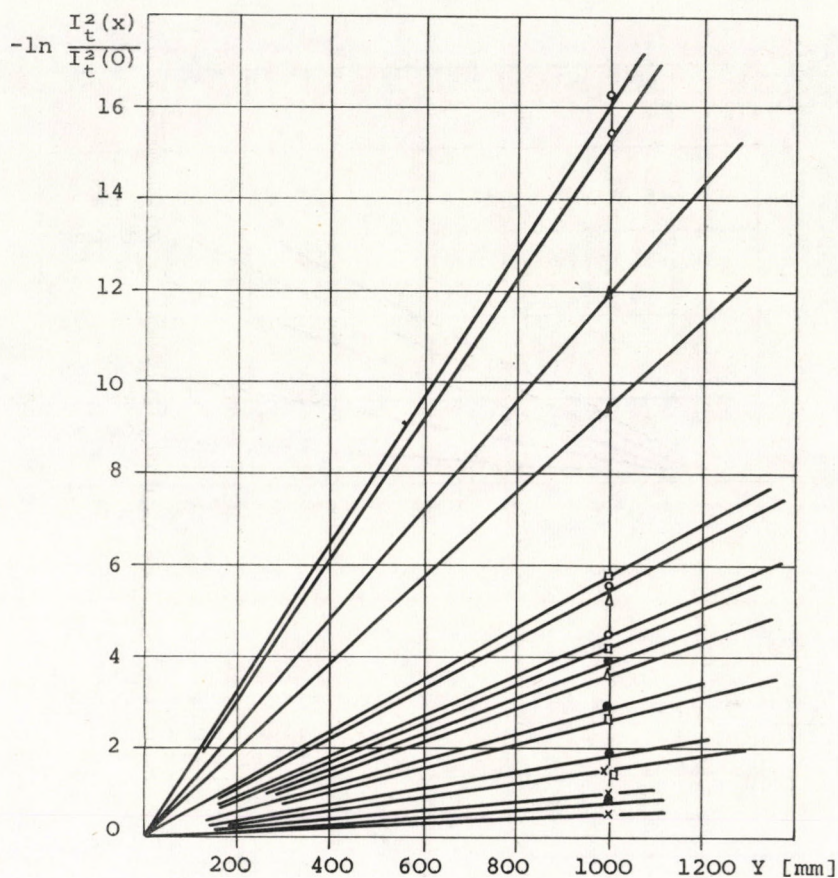


Figure 2 x - ϕ 5 mm; \bullet - ϕ 6 mm; \square - ϕ 7 mm; Δ - ϕ 9 mm;
 \circ - ϕ 10 mm

and frequency are also of major importance. At constant tube length, the inhomogeneity square in time decreases with the increased diameter.

Effect of the frequency on the inhomogeneity square in time can be seen in Figure 4 showing the increase of the measure of change - i.e. the k constant - with increased frequency.

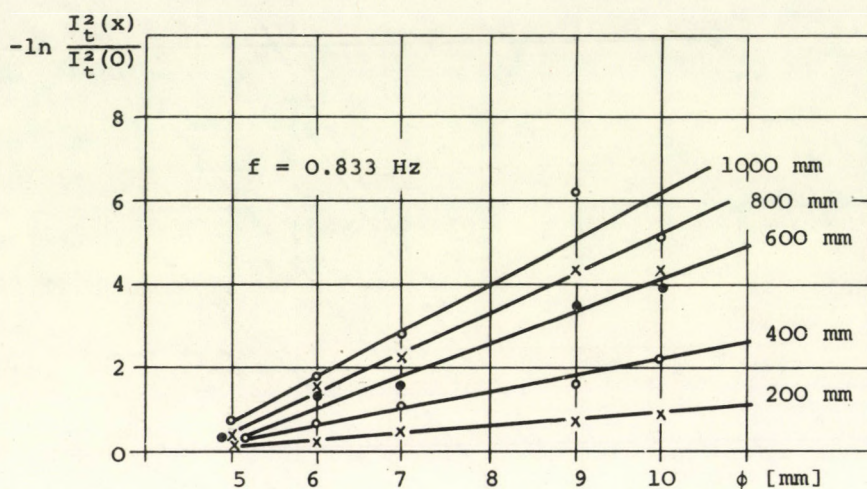


Figure 3

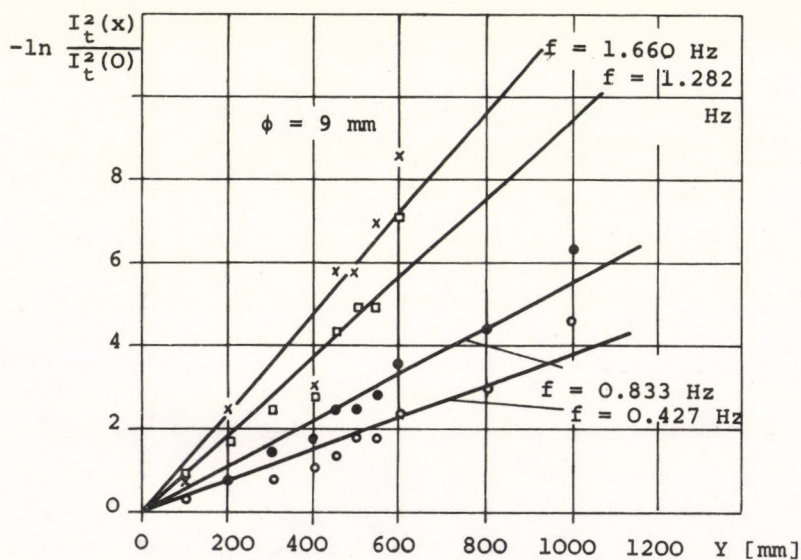


Figure 4

Finally it should be mentioned that the linear tendency of the dependence on diameter and frequency originated from the small studied frequency and diameter ranges and thus only small changes in the k values could be investigated and as a first approximation it can be regarded as linear.

SYMBOLS USED

c	concentration ($\text{mole} \cdot \text{m}^{-3}$)
x	local co-ordinate (m)
t	time (s)
L	length of apparatus (m)
I_v^2	special inhomogeneity square
I_t^2	inhomogeneity square in time
T	cycle time (s)
A	amplitude ($\text{mole} \cdot \text{m}^{-3}$)
α	phase (rad)
c_i	output concentration of the i^{th} cascade element ($\text{mole} \cdot \text{m}^{-3}$)
ϕ	phase lag (rad)
ω	radian frequency (s^{-1})
n	mixing unit number; number of cascade elements
V	volume (m^3)
Q	volumetric flow ($\text{m}^3 \cdot \text{s}^{-1}$)
x_0	mixing unit length (m)
S	cross-section (m^2)
k	Eq. (19)
F	mean residence time (s)

REFERENCES

1. BLICKLE, T. (Ed.): Structure of technical chemical systems (in Hungarian). MTA MÜKKI Tudományos Eredményei, Veszprém, 1974.
2. SEITZ, K., BLICKLE, T.: The structure of systems (1974-2. Dept. of Math., Karl Marx University of Economics, Budapest).
3. SEITZ, K., TÖRÖS, R.: Acta Chim. Acad. Sci. Hung., 62, 19 (1969).

РЕЗЮМЕ

В теории систем технической химии - для однозначного описания химического процесса - истолковывается понятие неоднородности. Этот параметр, характеризующий отклонение, исследуется по времени и по объему. Авторы изучали неоднородность по времени и тесную ее связь со смешением.

Моделью служил пустой трубчатый реактор, а методом периодической помехи определили неоднородность у входа и у выхода реактора.

VARIANCE ANALYSIS IN A GAS-SOLID
FLUIDIZED BED

E. MONOSTORI and T. BLICKLE

(Research Institute for Technical Chemistry of the
Hungarian Academy of Sciences, Veszprém)

Standard deviation in temperature of a gas passing through the fluidized layer in the case of periodic change in temperature is interpreted as follows:

$$\sigma^2 = \int_{PER} (T - T_{mean})^2 dt$$

Change of the standard deviation along the length of layer is discussed in the case of periodic inlet temperature sign.

According to the experiments carried out so far, the variance of the investigated feature - in this case the temperature of the fluidizing gas - seems to be suitable for describing by a certain means the dynamic behaviour of technical chemistry systems.

As a definition the variance of the gas temperature signal is represented by the following equation:

$$\sigma^2 = \frac{\int_t^{t+\tau} (T(z,t) - \bar{T})^2 dt}{\bar{T}^2} \quad (1)$$

It was assumed that the gas temperature performs a sustained oscillation of the τ period and that there is no reduction of

heat from the system. Relying upon these findings it can be written:

$$\frac{\int_t^{t+\tau} T(O,t)dt}{\tau} = \frac{\int_t^{t+\tau} T(L,t)dt}{\tau} = \bar{T} \quad (2)$$

That is to say the integral mean values of the inlet and outlet gas temperatures over the period are equals.

In accordance with this supposition, the change of variance in the fluidized bed was described by the next differential equation:

$$\frac{d\sigma^2}{dz} = -k \cdot \sigma^2 \quad (3a)$$

The solution of which - at a point $z=0$ and with a boundary condition of $\sigma^2 = \sigma_0^2$ - is:

$$\sigma^2 = \sigma_0^2 \cdot e^{-kz} \quad (3)$$

The k variance change factor depends upon the characteristics of the system. In accordance with the experiments carried out so far k depends upon the height of the bed L , the gas velocity v and the frequency of the gas temperature signal ω , namely $k = k(\omega, L, v)$.

Knowing the gas temperature signal at the gas inlet point ($z=0$) the variance can be evaluated. The chosen incoming signal is a sinus function:

$$T(O,t) = \bar{T} + A_b \cdot \sin \omega t \quad (4)$$

where \bar{T} is the mean value of the oscillating gas temperature. With this the value of the variance at the point of $z=0$ is:

$$\sigma_0^2 = \frac{\int_t^{t+\tau} (\bar{T} + A_b \cdot \sin \omega t - \bar{T})^2 dt}{\bar{T}^2} = \frac{A_b^2}{\bar{T}^2} \frac{\pi}{\omega} \quad (5)$$

Assuming that the heat loss of the bed is zero as well as no feeding and carrying out of granulous material, the outlet gas temperature signal at the point of $z=0$ is given by the next equation:

$$T(L,t) = \bar{T} + A_k \cdot \sin(\omega t + \varphi) \quad (6)$$

The variance of the outlet signal can be evaluated in a similar manner as above:

$$\sigma^2 = \frac{\int_t^{t+\tau} (\bar{T} + A_k \cdot \sin(\omega t + \varphi) - \bar{T})^2 dt}{\bar{T}^2} = \frac{A_k^2 \pi}{\bar{T}^2 \omega} \quad (7)$$

Substituting Equations (5) and (7) into Equation (3), after the rearrangement it can be written:

$$\frac{\sigma^2}{\sigma_0^2} = \frac{A_k^2}{A_b^2} = \left(\frac{A_k}{A_b} \right)^2 = e^{-kL} \quad (8)$$

and

$$\ln \left(\frac{A_k}{A_b} \right)^2 = -kL \quad (9)$$

On the basis of Equation (9), the experimental data were processed in the form of tables in which, in addition to the material and operational features, the angular frequency ω , the values of $-\ln \frac{A_k}{A_b}^2$ and the values of k evaluated at different points are given. In the last two columns of the tables, the values of the axial section and the rise of the straight lines are given which can be drawn through the points belonging together.

On the basis of Equation (9) such curves can be drawn which show the changing of k as a function of ω and the parameter of which is the height of the bed L , and L_2 , respectively. With different values of ω the rates of amplitudes were determined experimentally in case of a given bed height L and from these the values of k can be evaluated.

Table 1.

material: activated carbon

particle size: $d = 0.8-0.63$ (mm)air flow rate: $0.37 \text{ kg/m}^2\text{s}$

$L_1 = 30$ (mm)			$L_2 = 60$ (mm)		b	$m \times 10^2$
ω (ℓ/s)	$-\ln \left(\frac{A_k}{A_b} \right)^2$	$k_1 \times 10^2$ (ℓ/mm)	$-\ln \left(\frac{A_k}{A_b} \right)^2$	$k_2 \times 10^2$ (ℓ/mm)	(ℓ)	(ℓ/mm)
0.0135	1.2037	0.04	1.7016	0.02	-0.26	0.01
0.0203	1.5316	0.05	2.2702	0.03	-0.2	0.02
0.0287	1.8554	0.06	2.7349	0.04	0.0	0.02
0.0354	2.1170	0.07	3.0901	0.05	+0.2	0.03
0.0502	2.6325	0.08	3.6497	0.06	0.58	0.03
0.0563	2.7489	0.09	3.9529	0.06	0.56	0.04
0.0634	2.9998	0.10	4.2687	0.07	0.70	0.04

Table 2.

material: activated carbon

particle size: $d = 0.8-0.63$ (mm)air flow rate: $0.29 \text{ kg/m}^2\text{s}$

$L_1 = 30$ (mm)			$L_2 = 60$ (mm)		b	$m \times 10^2$
ω (ℓ/s)	$-\ln \left(\frac{A_k}{A_b} \right)^2$	$k_1 \times 10^2$ (ℓ/mm)	$-\ln \left(\frac{A_k}{A_b} \right)^2$	$k_2 \times 10^2$ (ℓ/mm)	(ℓ)	(ℓ/mm)
0.0064	1.4280	0.04	1.4220	0.02	1.44	0.00
0.0142	1.9500	0.06	2.2440	0.03	1.66	0.00
0.0201	2.3250	0.07	2.8920	0.04	1.76	0.01
0.0269	2.7210	0.09	3.4920	0.05	1.96	0.02
0.0354	3.1170	0.10	3.9420	0.06	2.28	0.02
0.0422	3.3000	0.11	4.3020	0.07	2.30	0.03
0.0496	3.6210	0.12	4.6860	0.07	2.56	0.03
0.0564	3.7500	0.12	5.0460	0.08	2.46	0.04

Table 3

material: sea-sand

particle size: $d = 0.59-0.21$ (mm)air flow rate: $0.71 \text{ kg/m}^2\text{s}$

$L_1 = 30$ (mm)			$L_2 = 60$ (mm)		b	$m \times 10^2$
ω	$-\ln \left(\frac{A_k}{A_b} \right)^2$	$k_1 \times 10^2$	$-\ln \left(\frac{A_k}{A_b} \right)^2$	$k_2 \times 10^2$		
(ℓ/s)		(ℓ/mm)		(ℓ/mm)	(ℓ)	(ℓ/mm)
0.0066	0.9063	0.03	1.3303	0.02	0.52	0.01
0.0139	1.5087	0.05	2.2082	0.03	0.80	0.02
0.0207	2.0357	0.06	2.8560	0.04	1.20	0.02
0.0280	2.5575	0.08	3.3933	0.05	1.72	0.02
0.0352	2.9432	0.09	3.9529	0.06	1.94	0.03
0.0414	3.2915	0.10	4.3901	0.07	2.21	0.03

Table 4

material: sea-sand

particle size: $d = 0.59-0.21$ (mm)air flow rate: $0.58 \text{ kg/m}^2\text{s}$

$L_1 = 30$ (mm)			$L_2 = 60$ (mm)		b	$m \times 10^2$
ω	$-\ln \left(\frac{A_k}{A_b} \right)^2$	$k_1 \times 10^2$	$-\ln \left(\frac{A_k}{A_b} \right)^2$	$k_2 \times 10^2$		
(ℓ/s)		(ℓ/mm)		(ℓ/mm)	(ℓ)	(ℓ/mm)
0.0064	1.1243	0.03	1.7356	0.02	0.52	0.02
0.0142	1.6587	0.05	2.9356	0.04	0.40	0.04
0.0205	2.1153	0.07	3.7050	0.06	0.52	0.05
0.0280	2.6550	0.08	4.3584	0.07	0.96	0.05
0.0353	3.0770	0.10	4.8929	0.08	1.22	0.06
0.0421	3.5133	0.11	5.3186	0.08	1.70	0.06

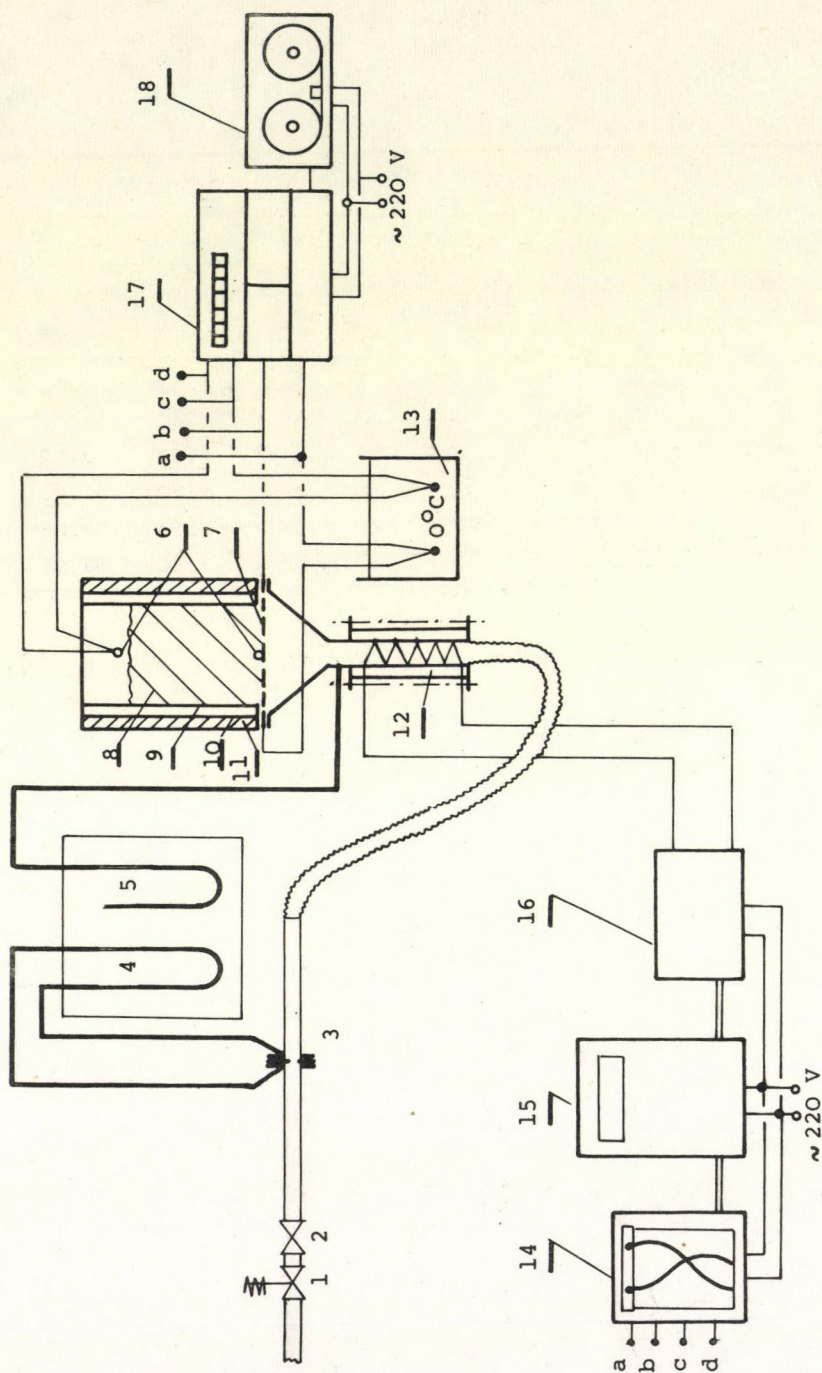


Figure 1

- | | | |
|-----------------------------|-----------------------|---------------------------|
| 1 - Pressure reducing valve | 8 - Fluidized bed | 14 - Compensograph |
| 2 - Valve | 9 - Inner wall | 15 - Regulating drive |
| 3 - Orifice | 10 - Outer wall | 16 - Sinus-sign generator |
| 4-5.- Manometers | 11 - Heat insulation | 17 - Digital voltmeter |
| 6 - Thermometers | 12 - Heating elements | 18 - Tape recorder |
| 7 - Grid | 13 - Thermostat | |

Experiments

The experimental apparatus is shown in Figure 1. The air flow through the pressure reducing valve (1) and the regulating valve (2) and the orifice (3) goes into the electric heater (12). The periodically changing voltage of the electric heater is supplied by the electromechanic sinus-sign generator (16). The generator and the paper-delivery roll of the compensograph are driven by the variable-speed drive (15). The inlet and outlet temperature signals are joined to the compensograph, enabling the visual observation of the signals.

The temperature of the air coming from the electric heater periodically changes according to the frequency. The inlet and outlet air temperatures of the fluidized bed are measured by the thermocouple (7) and (6), respectively. In order to minimize the heat losses the apparatus is double-insulated. The outer insulation (11) is slag-wool and between the walls (10) and (9) there is air insulation. To minimize the heat capacity of the apparatus its inner wall was made from bronze plate of 0.2 mm thickness.

The voltages of the thermocouples are measured by the digital voltmeter (17) and these values are recorded by the tape-recorder (18) so the data are suitable for processing by a computer.

Test materials were activated carbon and sea-sand with a well-defined fraction of particle diameter. The experiments were carried out with two kinds of bed height, 30 and 60 mm, and with a bed diameter of 100 mm. The air flow-rate was chosen to gain a homogeneous well-fluidized bed. The experiments were reproduced with different, altogether six kinds of angular frequency.

Results

From the tape-recorded experimental data the zero-harmonic, in conformity with Equation (2) was evaluated by Fourier-analysis.

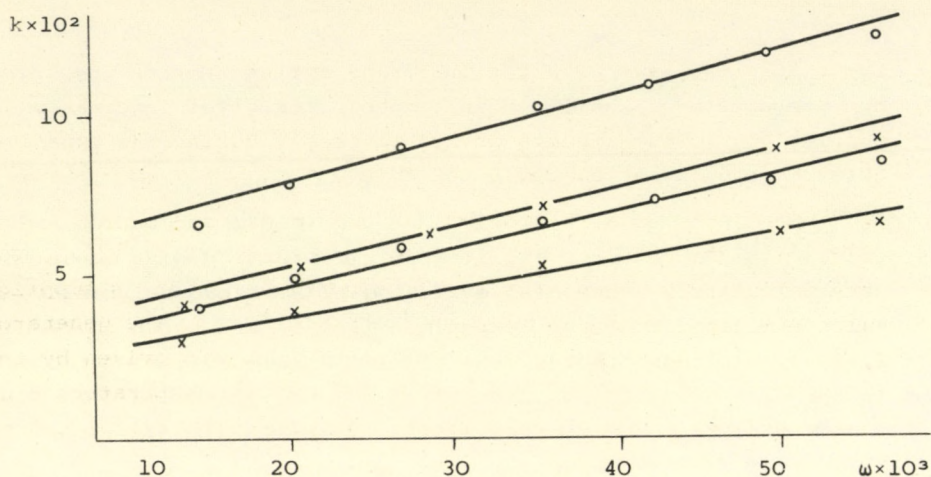


Fig. 2. Activated carbon. $d = 0.8 - 0.63$ mm
 air flow rate: x - $0.37 \text{ kg/m}^2\text{s}$
 o - $0.29 \text{ kg/m}^2\text{s}$

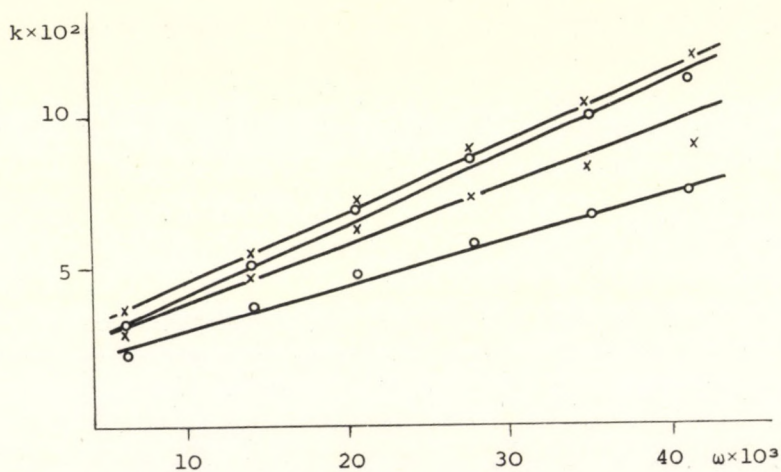


Fig. 3. Sea sand. $d = 0.59 - 0.21$ mm
 air flow rate: o - $0.71 \text{ kg/m}^2\text{s}$
 x - $0.58 \text{ kg/m}^2\text{s}$

Fulfilling the same with the inlet and outlet temperature signals, the comparison of the two mean temperatures gives information concerning about the amounts of heat losses. During the experiments this amount did not exceed 6 per cent.

The fundamental harmonics of the inlet and outlet signals, from which the rates of amplitudes in conformity with Equation (9) were calculated, were also evaluated by Fourier-analysis. The results evaluated from the experimental data are shown in Tables 1, 2, 3, 4. In these tables the angular frequency is the parameter. In the case of this representation, a value of k is evaluable to each point. Representing these values of k as a function of ω Figures 2 and 3 were gained, where the parameter is the height of the bed L .

From the results attained so far it can be concluded that the variance change factor k must not be regarded as a constant, but it involves a relationship. It is intended to carry out further theoretical and experimental work to investigate this.

SYMBOLS USED

σ^2	variance
$T(z,t)$	gas temperature ($^{\circ}\text{C}$)
\bar{T}	integral mean temperature ($^{\circ}\text{C}$)
τ	period (s)
t	time (s)
z	height co-ordinate (m)
L	height of the bed (m)
k	variance change factor
v	gas velocity (m/s)
ω	angular frequency (1/s)

A_b amplitude

A_k amplitude

РЕЗЮМЕ

Квадратичное отклонение температуры газа, проходящего через псевдооживленный слой, при периодическом изменении температуры, - описывается следующим выражением:

Автором изучается изменение квадратичного отклонения по длине слоя в случае периодического входного температурного сигнала.

STUDIES ON THE APPLICABILITY OF THE MOMENTUM METHOD FOR
TRANSFER CONDITIONS DURING THE SEPARATION OF HOMOLOGOUS
HYDROCARBON SERIES

T. BLICKLE and T. VIRÁG

(Research Institute for Technical Chemistry of the
Hungarian Academy of Sciences, Veszprém)

In order to characterize the mass transfer between multicomponent systems, numerous transfer coefficients and equilibrium constants - which can be measured in practice with difficulty - have to be given. An attempt is made to simplify the system of equations describing the mass transfer relating to components and to decrease the number of material constants to be measured.

Moments of component distribution were defined. Conservation of moments follows from the law of the conservation of material and transport equations, and similar to component transfer equations are also valid for the change of moments. The number of independent parameters is reduced to two by these assumptions and thus the problem can be treated much more simply.

The differential equation systems describing the separation of multicomponent systems, similar to the homologous hydrocarbons by selective separation wall, contain too many empirical factors that have to be determined experimentally, e.g. the transfer coefficients and equilibrium constants. The picture in the case under review becomes more complicated, because the change of these parameters as the function of concentration must also be taken into account.

In this paper the possibility of decreasing the parameters that must be determined by experiments has to be discussed if it is not intended to calculate the change in time for all the components, but only determine those certain parameters that will characterize the concentration distribution.

Let us assume the mixture consisted of n components. The concentration of the i^{th} component is c_i . The k^{th} moment of this concentration distribution is defined as follows:

$$M_k = \sum_{i=1}^n i^k c_i \quad (k = 0, 1, 2, \dots) \quad (1)$$

As it can be proved, the c_i concentration values can be calculated from the first n moments, however, in practice the usual concentration distribution is appropriately determined by a few moments, much less than n .

On this basis the description of the concentration distribution seemed to be practical by the moments and the necessary assumptions were investigated that are needed to derive relatively simple equations describing the changes of moments in time from equations giving the transfer of the different components.

The fact that the moments are homogeneous linear functions of the concentrations has a basic role in the simplification, i.e. the conservation of moments follows from the conservation of different components.

$$V_1 M_k^{(1)}(t) + V_2 M_k^{(2)}(t) = V_1 M_k^{(1)} \quad (k = 0, 1, 2, \dots) \quad (2)$$

If the transfer coefficients and equilibrium constants of different components depend on the concentrations in the system to a much greater extent than the quality of the component, then equations relating to the change of moments in time and being similar to the above mentioned ones are originated from the equations describing the transfer.

$$V_2 \frac{d M_k^{(2)}(t)}{dt} = -\beta [M_k^{(2)}(t) - K M_k^{(1)}(t)] \quad (k = 0, 1, 2, \dots) \quad (3)$$

where

$$\beta = \beta[M_a^{(1)}(t); M_1^{(1)}(t); \dots; M_a^{(2)}(t); M_1^{(2)}(t); \dots] \quad (4)$$

$$K = K[M_a^{(1)}(t); M_1^{(1)}(t); \dots; M_a^{(2)}(t); M_1^{(2)}(t); \dots] \quad (5)$$

The initial conditions of Eq. (3) can be given from those of the original equation.

$$M_k^{(1)}(0) = M_a^{(1)}; M_k^{(2)}(0) = 0 \quad (k = 0, 1, 2, \dots) \quad (6)$$

Introducing

$$\frac{M_k^{(2)}(t)}{M_k^{(1)}} = m_k(t) \quad (7)$$

Eqs. (2) and (3) can be described in simpler form as follows:

$$\frac{d m_k(t)}{dt} = -\beta \left[\left(\frac{K}{V_1} + 1 \right) m_k(t) - \frac{K}{V_2} \right] \quad (k = 0, 1, 2, \dots) \quad (8)$$

Eqs. (8) are valid for all $k = 0, 1, 2, \dots$ values. The $k = 0$ equation is subtracted from $k = 1, 2, \dots$ equations.

$$\frac{d(m_k(t) - m_0(t))}{dt} = -\beta \left(\frac{K}{V_1} + 1 \right) [m_k(t) - m_0(t)] \quad (k = 1, 2, \dots) \quad (9)$$

The $k = 2, 3, \dots$ equations are then divided by the $k = 1$ equation. The following simple differential equations are gained:

$$\frac{d[m_k(t) - m_0(t)]}{d[m_1(t) - m_0(t)]} = \frac{m_k(t) - m_0(t)}{m_1(t) - m_0(t)} \quad (k = 2, 3, \dots) \quad (10)$$

Their solution:

$$m_k(t) - m_0(t) = c_k [m_1(t) - m_0(t)] \quad (k = 2, 3, \dots) \quad (11)$$

The c_k coefficients can be determined from the initial conditions. The above equation means that by fixed initial conditions, the original problem has only two free parameters, the m_0 and m_1 moments. All moments may be expressed by these two moments. The two moments can be determined from Eq. (8) if the K and m_2 , m_3 variables are replaced by values determined from Eq. (11). Thus the following differential equation system is gained:

$$\frac{d m_0(t)}{dt} = - \beta(m_0, m_1) \left[\left(\frac{K(m_0, m_1)}{V_1} + 1 \right) m_0(t) - \frac{K(m_0, m_1)}{V_2} \right] \quad (12)$$

$$\frac{d m_1(t)}{dt} = - \beta(m_0, m_1) \left[\left(\frac{K(m_0, m_1)}{V_1} + 1 \right) m_1(t) - \frac{K(m_0, m_1)}{V_2} \right]$$

In a general case, Eq. (12) can be solved by the method applied earlier. The second equation in (12) is divided by the first:

$$\frac{d m_1}{d m_0} = \frac{\left(\frac{K(m_0, m_1)}{V_1} + 1 \right) m_1 - \frac{K(m_0, m_1)}{V_2}}{\left(\frac{K(m_0, m_1)}{V_1} + 1 \right) m_0 - \frac{K(m_0, m_1)}{V_2}} \quad (13)$$

This is an ordinary differential equation and m_1 can be determined as a function of m_0 . Replacing this by the first equation in (12), an ordinary differential equation is gained from that dependence of m_0 calculated on the time:

$$\frac{d m_0(t)}{dt} = - \beta(m_0) \left[\left(\frac{K(m_0)}{V_1} + 1 \right) m_0(t) - \frac{K(m_0)}{V_2} \right] \quad (14)$$

It should be observed that the β does not appear in Eq. (13) determining the $m_1(m_0)$ function. So it does not affect the concentrations in the system, only the change of concentrations in time.

The solution of the problem becomes much simpler if K and β depend only on m_0 or m_1 or their difference. In the first case, Eq. (12) is not connected so they can be solved separately, while in the second case the solution is given by Eq. (9) for $k = 1$.

Applying this method, the number of K and β variables in the two functions describing the material properties characterizing the process can be reduced from $2n+1$ to two by the single assumption which represents an enormous simplification regarding the measurements. The validity of this assumption will be controlled by the experiments which are still being carried out.

РЕЗЮМЕ

Для характеристики массопередачи между многокомпонентными системами требуется много таких данных (напр. коэффициенты передачи, константы равновесия) которые слишком трудно измерить. Авторы попытались упростить систему уравнений массопередачи (для компонентов) с помощью некоторых опущений. Таким образом число измеряемых материальных констант уменьшалось.

Определялись моменты распределения компонентов. Из принципа сохранения вещества следует сохранение моментов, и на изменение моментов действительны уравнения, аналогичные уравнениям, написанных для компонентов. Эти предположения уменьшают число независимых параметров до двух, и таким образом проблему можно разрешить гораздо легче.

ALGEBRAIC INVESTIGATION OF THE CONNECTION OF BATCH AND
CONTINUOUS OPERATIONAL UNITS

G. VERESS* and A. CZULEK**

(*Department Team of the Hungarian Academy of Sciences,
(Budapest Technical University), Budapest

**Research Institute for Computation and Automation
of the Hungarian Academy of Sciences)

Four different types of operational units are interpreted according to their method of operation, namely: batch, continuous, differentiating and integrating. The connection of these operational units is limited. The rules of connection of the different operational units is described by an exact mathematical model, the idea of "category" known in the algebra.

On the basis of the algebraic discussion of the connection rules between the operational units, the simple investigation of the connection of a large number of possibilities becomes possible by computer.

The construction of possible alternatives of complex systems consisting of different subsystems is an important question both from designing and controlling points of view, if it is taken into account that the different subsystems usually can be connected in accordance with given rules.

An arbitrary connection of the operational units cannot be realized for complex chemical industrial systems constructed from batch and continuous operational units, i.e. the number of possible connections is limited.

In the following, the possible connections of differently operating operational units will be described by algebraic methods

and thus a large number of connection alternatives can be investigated simply, algorithmically.

Types of operational units

The chemical operational units can be classified from different points of view. For the definition of batch and continuous operational unit, the interpretation of BENEDEK and LÁSZLÓ [1] is accepted, however, it is narrowed further. In the construction of a complex chemical system - regarding the connection of operational units as subsystems - the most important property is the type of mass flow into and from the operational unit. Two extreme types of mass flow are distinguished: in batch flow the movement of the material can be regarded as an instantaneous moment, while in the continuous flow the material moves continuously. (This classification can, of course, be widened and numerous physical conditions must be fulfilled to bring about a real flow.)

On the basis of the above mentioned classification of the input and output flows, the following four types of operational units can be distinguished.

<div>Place of flow</div> <div>Operational unit</div>	input	output
batch (B)	batch	batch
continuous (C)	continuous	continuous
integrating (I)	continuous	batch
differentiating (D)	batch	continuous

These four operational units - being basic types with respect to the input and output flows - cannot be connected arbitrarily. The possible connections will be given in algebraic form.

The term "category"

A well known term in modern algebra is the category, however, it is still interpreted in different manners (e.g. [2]). The category is a class consisting of objects and mappings, and has the following properties:

a) one object pair of the category corresponds one to one to every mapping;

b) the product of the mappings is interpreted, if the last object of the first mapping is the same as the first one in the second mapping, and in this case the object pair belonging to the product of the mappings consists of the first object of the first mapping and the last object of the second mapping;

c) the multiplication of the mapping is associative;

d) a "unit mapping" belongs to all mappings, i.e. a mapping having the same objects.

A special operator structure of the structure theory

It is easy to see [3] that the \otimes operation [4] interpreted in the structure theory of technical chemical systems - that is now becoming widespread - as a special part of a greater algebraic description, has the same properties as the category.

Algebraic description of the connection of operational units

Let b denote the batch flow, and c the continuous one. In this case, the operational units can be regarded as the following mappings and object pairs respectively:

batch: $B(b,b)$

continuous: $C(c,c)$

integrating: $I(c,b)$

differentiating: $D(b,c)$

On the basis of the above interpretation, the connection rules for the operational units can be interpreted as a product of the mappings in the category theory and an operation of the structure theory, respectively.

The relationships of the objects and mappings are shown on Fig. 1, where the circles represent the objects, and the arrows the mappings.

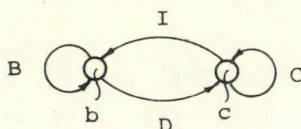


Figure 1

Following from the algebraic rules of category or structure theory, the possible connections of operational units are shown as follows:

	B	D	I	C
B	B	D	-	-
D	-	-	B	D
I	I	C	-	-
C	-	-	I	C

As it can be seen from the above multiplication table, only 8 of the possible 16 connections are permitted. According to the meaning, the "unit mapping" of b object is B , while that for c object is C .

On the basis outlined above, the following types of operational units can be distinguished:

$$\text{homogeneous batch: } B = \pi_i B^i$$

$$\text{quasi-homogeneous batch: } B = \pi_i B^i \cdot \pi_j (D \cdot I)^j$$

homogeneous continuous: $C = \pi_i C^i$

quasi-homogeneous continuous: $C = \pi_i C^i \cdot \pi_j (I D)^j$

heterogeneous: $X = \pi_k (\pi_i B^i \cdot D \cdot \pi_j C^j \cdot I)^k$

It should be mentioned that the above discussion can also be widened for more inputs and outputs, and then the operational unit is interpreted as a complex of more mappings.

Example

In order to illustrate the process outlined above, let us study the chemical industrial process given in Fig. 2.

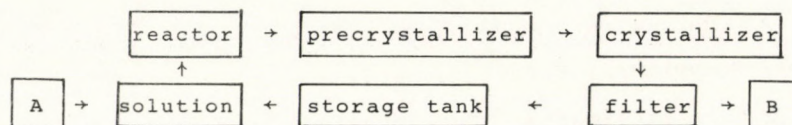


Figure 2

If for example the reactor is assumed to be a continuous one, the crystallizer and the storage tank are batch units and the precrystallizer can be integrated only in accordance with the algebraic rules. The filter can operate only batchwise, while the dissolving tank is a differentiating unit. The "A" operational unit may be only batch or differentiating, while the "B" operational unit may be batch or differentiating.

Final remarks

With the above - primarily illustrative - method of thinking the aim was to direct attention to the possibility of the algebraic discussion of connections among subsystems. The above ideas enable different generalizations to be made.

The first step in such generalization is that the characterization of the flow in the operational units can be described with more than two objects in accordance with the different flow rates and types.

A further possibility for the application of these ideas is represented by the algebraic discussion of possible reaction paths and the use of these algebraic methods for process planning by computer in the case of simulation programmes of a module system.

Naturally, the proposed algebraic method is generally applicable for the algorithmic construction of complex systems from subsystems.

REFERENCES

1. BENEDEK, P. and LÁSZLÓ, A.: A vegyészmérnöki tudomány alapjai. Műszaki Könyvkiadó, Budapest, 1964.
2. FUCHS, L.: Algebra (Kézirat) Tankönyvkiadó, Budapest, 1969. pp. 145-148.
3. BLICKLE, T.: private communication. 1975.
4. BLICKLE, T.: Műszaki kémiai rendszerek szerkezete. MTA MÜKKI Tudományos Eredményei II., Veszprém, 1974. pp. 18-25.

РЕЗЮМЕ

Авторами истолковываются следующие процессионные единицы: периодического, непрерывного, дифференцирующего и интегрирующего действия. Связь между этими процессионными единицами не может быть - любой, число разрешенных связей определено. Правила присоединения между процессионными единицами разного типа действия описаны с помощью понятия "категория", известного в алгебре, и с помощью точной математической моделью.

DETERMINATION OF THE OPTIMUM TECHNOLOGICAL PROCEDURE

T. BLICKLE and Mrs. E. BÁTOR

(Research Institute for Technical Chemistry of the
Hungarian Academy of Sciences, Veszprém)

The changes of the properties that build up the structure of materials are modellized by technical chemical mappings. A partial algebraic structure of two operations are interpreted on the set of mappings, and with the aid of this algebraic structure, the series of mappings modellizing changes taking place in the most complicated processes are build up. The cost functions interpreted on the mappings make the determination of an optimal series of mappings possible.

The method developed for the generation of a partial algebraic structure interpreted on a set of mappings can be applied for the determination of the optimum technological procedure.

In the case of a given technological task, the initial mappings, their cost functions, the connecting elements between the mappings and the system of demands belonging to the given task are given for all steps of the possible procedures. The generated mapping gives initial materials and final products. Quantitative parameters appearing in the initial mappings, but which do not appear in the generated mapping are parameters selectable independently and the cost function can be affected by them. On the basis of the cost functions, the optimum procedure and optimum values of the independent parameters can be given.

The application of the method will be shown in the case of the separation of a homogeneous system consisting of two components.

The task is given by the following mapping:

$$l_1 = \left[\begin{array}{l} g_1 c_1 \Rightarrow g_2 c_2 \\ g_1 c_1 \Rightarrow g_3 c_2 \text{ o } (g_2 - g_3) c_2 \end{array} \right] \quad (1)$$

The homogeneous system to be separated is in the antecedent of mapping (c_1 and c_2 are the components to be separated; g_1 and g_2 are their quantity or mass stream; while the \Rightarrow sign symbolizes the homogeneous connection between the components.)

The originating material system in the case of partial separation is given in the successor of mapping; the principle of conservation of matter is taken into consideration in the g values. (Sign o symbolizes different material streams.)

In order to determine the optimum separation method a search has to be made for elementary mappings by which the (1) originating mapping can be constructed by \oplus and \Uparrow operations. (Operation \oplus means that mappings take place one after the other, while operation \Uparrow corresponds to recirculation.)

From the numerous possibilities of the construction of (1) originating mapping two cases will now be discussed:

1. the homogeneous system of two components is separated in one step, and the elementary mapping is equal to the originating mapping (1).

2. An auxiliary material containing a given amount from one of the components to be separated is given to the homogeneous system:

$$l_{2a} = \left[\begin{array}{l} g_1 c_1 \Rightarrow g_2 c_2 \text{ o } g_4 c_3 \Rightarrow g_5 c_2 \\ g_1 c_1 \Rightarrow g_3 c_2 \text{ o } g_4 c_3 \Rightarrow (g_5 + g_2 - g_3) c_2 \end{array} \right] \quad (2)$$

then the c_2 component will be separated from the auxiliary material:

$$l_{2b} \left[\begin{array}{l} g_6 c_3 \Rightarrow g_7 c_2 \\ g_6 c_3 \Rightarrow g_8 c_2 \text{ o } (g_7 - g_8) c_2 \end{array} \right] \quad (3)$$

Operations \oplus and \Uparrow can be carried out between mappings (2) and (3) if g values of similar components in the successor of l_{2a} and antecedent of l_{2b} , and in successor of l_{2b} and antecedent of l_{2a} are equal, respectively.

So the connecting elements of l_{2a} and l_{2b} mappings are the following:

$$g_6 = g_4 \quad (4)$$

$$g_7 = g_5 + g_2 - g_3 \quad (5)$$

$$g_8 = g_5 \quad (6)$$

Replacing connecting elements into the l_{2b} mapping and carrying out operations, the following originating mapping is gained:

$$l_{2a} = \Uparrow (l_{2a} \oplus l_{2b}) \quad (7)$$

$$l_2 = \Uparrow \left\{ \begin{aligned} & \left[\begin{aligned} g_1 c_1 &\Rightarrow g_2 c_2 \circ g_4 c_3 \Rightarrow g_5 c_2 \\ g_1 c_1 &\Rightarrow g_3 c_2 \circ g_4 c_3 \Rightarrow (g_5 + g_2 - g_3) c_2 \end{aligned} \right] \oplus \\ & \oplus \left[\begin{aligned} g_4 c_3 &\Rightarrow (g_5 + g_2 - g_3) c_2 \\ g_4 c_3 &\Rightarrow g_5 c_2 \circ (g_2 - g_3) c_2 \end{aligned} \right] \end{aligned} \right\} \quad (8)$$

$$l_2 = \begin{bmatrix} g_1 c_1 \Rightarrow g_2 c_2 \\ g_1 c_1 \Rightarrow g_3 c_2 \circ (g_2 - g_3) c_2 \end{bmatrix} \quad (9)$$

From comparison of (1) and (9) mappings it can be seen that the two methods of separation have the same result, however, the costs of their realization are different, because different cost functions belong to each initial mapping.

$$l_1 \triangleq N_1 \quad (10)$$

$$l_{2a} \triangleq N_{2a} \quad (11)$$

$$l_{2b} \triangleq N_{2b} \quad (12)$$

$$l_2 \triangleq N_2 \quad (13)$$

In the case of a given separation problem, values of g_1 , g_2 and g_3 originate from the task itself, at the separation in two steps the independently selectable parameters are g_4 and g_5 and so the cost of realization can be affected.

In the general description of the cost functions belonging to the given mappings the fact has to be taken into consideration that cost of separation is proportional to:

- amounts of materials to be separated,
- measure of separation, i.e. concentrations,
- economical coefficients.

Cost of separation in one step is the following:

$$N_1 = (g_1 + g_2)a_1 \left[\frac{1}{C_1 - C_\infty} - \frac{1}{C_0 - C_\infty} \right] \quad (14)$$

Cost of separation with auxiliary material:

$$N_2 = N_{2a} + N_{2b} \quad (15)$$

$$N_{2a} = (g_1 + g_2 + g_4 + g_5)a_2 \left[\frac{1}{C_1 - C_{S1}} - \frac{1}{C_0 - C_{S1}} \right] \quad (16)$$

$$N_{2b} = (g_4 + g_5 + g_2 - g_3)a_3 \left[\frac{1}{C_{S1} - C_{S\infty}} - \frac{1}{C_{S0} - C_{S\infty}} \right] \quad (17)$$

Concentrations in the cost functions can be given by the aid of g values:

$$C_0 = \frac{g_2}{g_1 + g_2} \quad (18)$$

$$C_1 = \frac{g_3}{g_1 + g_3} \quad (19)$$

$$C_{S0} = \frac{g_5 + g_2 - g_3}{g_4 + g_5 + g_2 - g_3} \quad (20)$$

$$C_{S_1} = \frac{g_5}{g_4 + g_5} \quad (21)$$

Let us introduce the recirculation ratio, as follows:

$$X = \frac{g_5}{g_1 + g_2} \quad (22)$$

In this case, the minimum value of N_2 cost has to be determined as the function of C_{S_1} and X , because parameters selectable independently can be found in these parameters. Comparing the minimum cost with the value of N_1 , the more economical separation method, of the homogeneous system can be selected. Investigation can also be carried out for different auxiliary materials, giving the cost parameter and value of C_{S_∞} for each auxiliary material. In this manner, the suitable choice of auxiliary material also becomes possible.

The two methods selected as examples for the separation of homogeneous systems, cannot be applied for all materials and auxiliary materials, because the following restrictions relating to the phase system have to be taken into consideration

- a) the solid homogeneous system and gas mixture cannot be separated in one step,
- b) the solid homogeneous system cannot be separated by solid auxiliary material,
- c) the solid component cannot be gasified from the solution,
- d) the homogeneous gas mixture cannot be separated by gaseous auxiliary material.

If a computer programme is given for the shown method, then the initial mappings, the cost functions and an inlet vector have to be given for all the separation tasks. The vector is the following:

$$[C_0, C_1, C_\infty, (g_1 + g_2), C_{S_1}, \dots, C_{S_\infty}, a_1, a_2, a_{S_1}, \dots, a_{S_n}] \quad (23)$$

On the basis of the system of conditions given for the phases, the computer selects the applicable methods and auxiliary materials, calculates the costs for these and comparing the cost minima, determines the suitable auxiliary material and the value of the recirculation rate and C_{S_1} in the case of a minimum separation cost.

SYMBOLS USED

a_1, a_2, a_3	cost parameters
c_1, c_2	components to be selected
c_3	auxiliary material
C_0	concentration of c_2 component in the homogeneous system
C_1	concentration of c_2 component after the separation
C_∞	concentration limit theoretically determining the measure of the separation
C_{S_0}	concentration of c_2 component in the auxiliary material before the separation
C_{S_1}	concentration of c_2 component in the recirculating auxiliary material
C_{S_∞}	concentration limit determining the separation of the auxiliary material

РЕЗЮМЕ

Авторы дают исходные изображения, относящиеся к ним расходные функции, соединяющие элементы между изображениями, и систему требований задания для каждого шага возможных способов при конкретном технологическом задании. Генерированное изображение дает исходные и конечные материалы. Количественные показатели, присутствующие только в исходных изображениях, (а в генерированных нет) являются параметрами, которые можно произвольно выбрать, и с помощью которых можно влиять на расход. По расходным функциям определяется оптимальный метод и оптимальное значение произвольного параметра.

SUITABLE CHOICE BETWEEN THE METHODS OF CRYSTALLIZATION

Mrs. S. HALÁSZ and C. JUHÁSZ

(Research Institute for Technical Chemistry of the
Hungarian Academy of Sciences, Veszprém)

The paper reviews theoretical method systems for the suitable selection between different possibilities of crystallization.

Structure elements constructed from discrete objects are given as functions in the crystallization task, material properties and cost parameters. Ranges of varying parameters belonging to different crystallization methods are determined.

Two methods were developed to select systems of a similar purpose, which achieve different crystallization tasks.

1. According to the first method the demands relating to the product are given as discrete objects and methods of realization also correspond as discrete objects.

The structure of the methods of realization is constructed on four object classes, namely:

A - auxiliary operations

- a₁ indirect cooling
- a₂ direct cooling by gas
- a₃ cooling by mixing of cool and warm solutions
- a₄ evaporation in vacuum
- a₅ vaporization
- a₆ "salting out" with liquid
- a₇ "salting out" with steam

B - processes

- b₁ mechanical mixing
- b₂ tube reactor with rotating screw
- b₃ fluidization
- b₄ rotary film
- b₅ bubble column
- b₆ foam (froth) column
- b₇ spouted bed
- b₈ pulsated partition wall

C - character of heat transfer surface

- c₁ there is no heat transfer surface
- c₂ heat transfer through wall
- c₃ heat transfer through inserted surface (e.g. tube)

D - role of gas

- d₁ there is no gas
- d₂ the gas is recirculated
- d₃ the gas is not recirculated

On the basis of data in literature and on our experience [1, 2, 3] we could determine elements which could be co-exist with others and those which could not. In this manner, 61 different combinations can be given from a,b,c and d elements allowing each other mutually. These individual combinations correspond to one method of crystallization, e.g. a₁b₁c₂d₁ means the following method of realization:

crystallization with indirect cooling mechanical mixing, applying heat transfer surface, but not using gas.

The property classes of the structure of the demands relating to crystallization were as follows:

α - mean relative crystal size

The elements are sections which can correspond to the different procedures. These elements are relative, i.e. they express e.g. the mean particle size of crystals produced by

the pulsated partition wall process is about 8 times larger compared to that produced by the rotary film process [4, 5].

α_1	1 -1.5	to b_1 procedure belongs	α_6, α_7
α_2	2.5-3.2	b_2 - " -	α_2
α_3	3.7-4.5	b_3 - " -	$\alpha_4, \alpha_5, \alpha_6$
α_4	4.5-5.0	b_4 - " -	α_4
α_5	5.0-5.2	b_5 - " -	α_7, α_8
α_6	5.2-6.0	b_6 - " -	α_3, α_4
α_7	6.0-7.7	b_7 - " -	$\alpha_6, \alpha_7, \alpha_8$
α_8	7.7-8.7	b_8 - " -	α_8

β - central scattering of size distribution

The elements are intervals of scattering, through the size intervals (these elements were gained from analysis of the particle size distribution curves of products produced by different procedures)

$$\beta_1 - \beta_8$$

γ - adhesion of crystals on the heat transfer surface

- γ_1 there is no adhesion
- γ_2 slightly adhere
- γ_3 adhere
- γ_4 strongly adhere

δ - gas tolerance of solution

- δ_1 it cannot be contacted with gas
- δ_2 can be contacted with inert gas
- δ_3 can be contacted with any gas

Relations between the methods of crystallization and the $\alpha, \beta, \gamma, \delta$ demands and material properties are known so the two structures can be composed. In this manner, the suitable methods of achieving the production of a crystalline product of a given particle size and homogeneity can be determined. However, this system of requirements in its present form does not contain economical decisions.

2. According to the second method functions and costs can correspond to the structure elements. As the first step of optimization the value of the free parameters is determined, by which the cost of the given structure element is the smallest. Then the optimized structure elements of a similar purpose will be compared and the one having the smallest cost will be selected as the method of realization.

In the case of technical chemical systems the minimum cost depends on:

the material properties,
and the cost factors.

For this reason, in the space of material properties and cost factors, a structure element having the minimum cost can be given to every point of the space. (Dimension of the space is determined by the sum of the numbers of the cost factors material properties.)

In the illustrative example, let our task be crystallization of the given particle size from solution. However, the task is not solved according to the structure elements.

Let the two crystallization methods be A and B, while G is a granulation procedure. (In this case, the optimization of intermediate parameters is shown in the example. The intermediate parameter is the particle size after crystallization, i.e. before granulation. This size is not limited contrary to the final one. Optimization must be carried out ensuring minimum total cost of the two operations.)

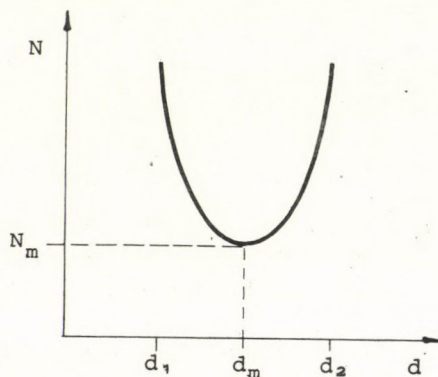


Figure 1

At first let us determine the cost separately. By the experiments, certain particle size ranges can correspond to the different crystallization procedures. These ranges are connected with costs of procedures (Figure 1).

The particle size of the product which can be produced by a given procedure with the greatest probability prospectively is found in the middle of the range.

For this reason, the cost functions of the crystallization methods are approximated by parabola having a minimum value determined by $\frac{d_1+d_2}{2}$ and the characteristic cost of procedure.

The cost of the crystallization procedure A:

$$N = a_1 x^2 + a_2 x + a_3 \quad (1)$$

The cost of the crystallization procedure B:

$$N' = a'_1 x^2 + a'_2 x + a'_3 \quad (2)$$

The cost of the granulation procedure G:

$$N_g = b_1 x_e (x_e - x) \quad (3)$$

where: $a_1, a_2, a'_1, a_3, a'_3, b_1$ are cost factors

x is the particle size of the product to be granulated

x_e final size

Let the following notations be introduced:

$$\hat{N} = \frac{N - N_m}{a_1} ; \quad N' = \frac{N' - N_m}{a_1} ; \quad \hat{N}_g = \frac{N_g}{a_1}$$

$$c = \frac{N'_m - N_m}{a_1} ; \quad c = \frac{b_1}{a_1}$$

(By division with a_1 a space of three dimensions is gained instead of a four dimension one.)

The cost function as they are expressed to the extreme:

$$\text{Procedure A: } N = (x - x_m)^2 \quad (4)$$

$$\text{Procedure B: } N' = (x - x'_m)^2 + c_1 \quad (5)$$

$$\text{Procedure G: } N_g = c_2 x_e (x_e - x) \quad (6)$$

$$\text{Procedure A + G: } (N + N_g)_m = x_e^2 \left(c_2 - \frac{c_2^2}{4} \right) - c_2 x_m x_e \quad (7)$$

$$\text{Procedure B + G: } (N' + N_g)_m = x_e^2 \left(c_2 - \frac{c_2^2}{4} \right) - c_2 x_e x'_m + c_1 \quad (8)$$

$$x_0 = \frac{c_2 x_e}{2} + x_m$$

N_g is valid only for granulation and for: $x_e > x_0$

When the different possibilities are compared, the costs are equalized and the limit curves - where one or the other method of realization is more economical - are determined (Figures 2 and 3).

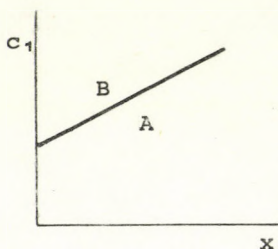


Figure 2

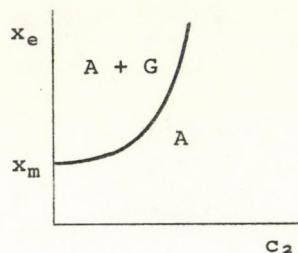


Figure 3

1. A and B

$$(x_e - x_m)^2 = (x_e - x'_m)^2 + c_1 \quad (9)$$

$$c_1 = 2 x_e (x'_m + x_m) + (x_m^2 - x'^2_m) \quad (10)$$

2. A and A+G

$$(x_e - x_m)^2 = x_e^2 \left(c_2 - \frac{c_2^2}{4} \right) - c_2 x_m x_e \quad (11)$$

$$x_e = \frac{2 x_m}{2 - c_2} \quad (12)$$

3. B and B+G

$$(x - x'_m)^2 = x_e^2 \left(c_2 - \frac{c_2^2}{4} \right) - c_2 x_e x_m \quad (13)$$

$$x_e = \frac{2 x'_m}{2 - c_2} \quad (14)$$

3. A+G and B+G

$$x_e^2 \left(c_2 - \frac{c_2^2}{4} \right)^2 - c_2 x_m x_e^2 = x_e \left(c_2 - \frac{c_2^2}{4} \right) - c_2 x_e x'_m + c_1 \quad (15)$$

$$c_1 = c_2 x_e x'_m - x_m \quad (16)$$

5. A and B+G

$$(x_e - x_m^2) = x_e^2 \left(c_2 - \frac{c_2^2}{4} \right) - c_2 x_e x'_m + c_1 \quad (17)$$

$$c_1 = x_e^2 \left(1 - c_2 + \frac{c_2^2}{4} \right) + x_e (c_2 x'_m - 2 x_m) + x_m^2 \quad (18)$$

6. B and A+G

$$(x_e - x'_m)^2 + c_1 = x_e \left(c_2 - \frac{c_2^2}{4} \right) - c_2 x_m x_e \quad (19)$$

$$c_1 + x_e^2 \left(1 + c_2 - \frac{c_2^2}{4} \right) + x_e (2 x'_m - c_2 x_m) + x_m^2 \quad (20)$$

Introducing the following designations:

$$c_3 = \frac{c_1}{x_m^2}; \quad y = \frac{x_e}{x_m}; \quad c_4 = \frac{x'_m}{x_m}$$

and replacing them into Equations (10, 12, 14, 16, 18 and 20):

$$1. \quad c_3 = 2 y(c_4 - 1) + 1 - c_4^2 \quad (21)$$

$$2. \quad y = \frac{2}{2 - c_2} \quad (22)$$

$$3. \quad y = \frac{2 c_4}{2 - c_2} \quad (23)$$

$$4. \quad c_3 = c_2 y(c_4 - 1) \quad (24)$$

$$5. \quad c_3 = y^2(1 - c_2 + \frac{c_2^2}{4}) + y(c_2 c_4 - 2) + 1 \quad (25)$$

$$6. \quad c_3 = y^2(1 + c_2 - \frac{c_2^2}{4}) + y(2 c_4 - c_2) + c_4^2 \quad (26)$$

Expressing the costs of the different methods of realization with these constants the following expressions are gained:

$$\underline{A} \quad \hat{N} = x_m^2(y - 1)^2 \quad (27)$$

$$\underline{B} \quad \hat{N}' = x_m^2(y - c_4)^2 + x_m^2 c_3 \quad (28)$$

$$\underline{A+G} \quad (\hat{N} + \hat{N}_g)_m = x_m^2 y^2 (c_2 - \frac{c_2^2}{4}) - c_2 x_m^2 y \quad (29)$$

$$\underline{B+G} \quad (\hat{N}' + \hat{N}_g)_m = x_m^2 (y - c_4)^2 + x_m^2 y^2 (c_2 - \frac{c_2^2}{4}) - c_2 x_m^2 y \quad (30)$$

Normalizing the costs to x_m^2 :

$$\frac{\hat{N}}{x_m^2} = \phi_1 ; \quad \frac{\hat{N}'}{x_m^2} = \phi_2 ; \quad \frac{(\hat{N} + \hat{N}_g)_m}{x_m^2} = \phi_3 ; \quad \frac{(\hat{N}' + \hat{N}_g)_m}{x_m^2} = \phi_4$$

that is:

$$\underline{A} \quad \phi_1 = (y - 1)^2 \quad (31)$$

$$\underline{B} \quad \phi_2 = (y - c_4)^2 + c_3 \quad (32)$$

$$\text{A+G} \quad \phi_3 = y^2 \left(c_2 - \frac{c_2^2}{4} \right) - c_2 y \quad (33)$$

$$\text{B+G} \quad \phi_4 = y^2 \left(c_2 - \frac{c_2^2}{4} \right) + c_3 - c_2 c_4 y \quad (34)$$

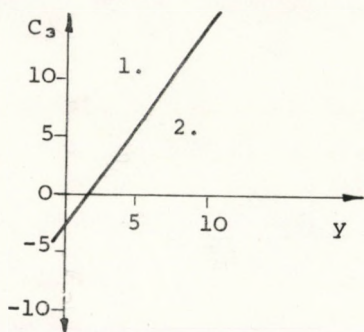
Let c_4 be equal to 2. This means that we have a space of three dimensions: c_3, c_2, y . Following from the mathematical expressions, c_2 may vary only between 0 and 2.

Replacing the $c_4 = 2$, and $c_2 = 2$

then $c_4 = 2$, and $c_2 = 1$

and $c_4 = 2$ and $c_2 = 0$

The space is cut into planes. Two cases are shown on Figures 4 and 5 respectively.



$$c_4 = 2; c_2 = 2$$

ϕ_1 is greater than ϕ_2 if c_3 $2y - 3$ i.e. then the 2nd method of crystallization is better compared to the 1st one.

Figure 4

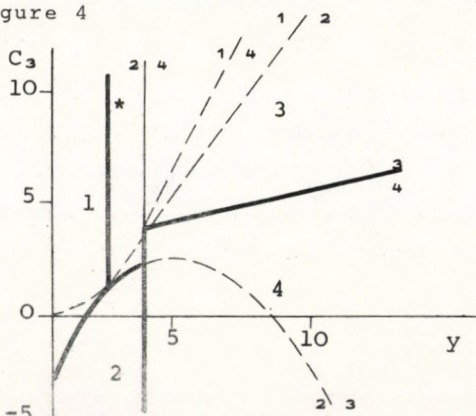


Figure 5

$$c_4 = 2; c_2 = 1$$

*the best one is 3
the second is 4
the third is 2
the worst is 1

A certain sequence of goodness can be determined by the aid of Figure 5. What is the situation in a given task? From the optimization, e.g. the 3rd method is derived as the best one. If by chance the discrete demands would not be satisfied by this method, a selection can be made between methods 4 and 2, and the task is now realized economically.

The problem becomes unidimensional when the values of the parameters are fixed and we have one variable, the final size (Figure 6).

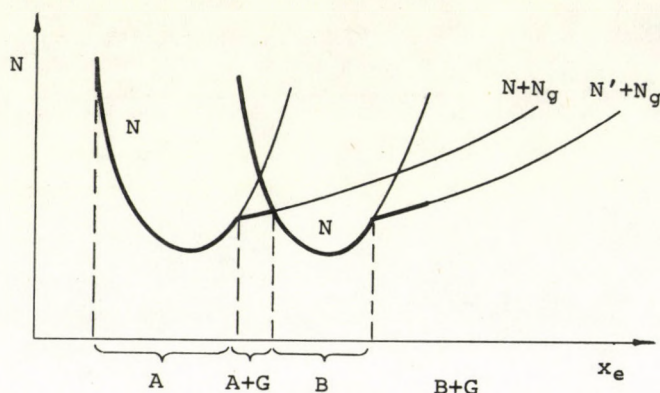


Figure 6

If two variables are free, surfaces are gained, etc.

The essence of the second method was shown by a simple example. The complete solution is naturally gained if this method is applied to the system of demands described in the first method.

The aim of our further activity is to determine the optimum structure elements applicable for the solution of crystallization problems.

REFERENCES

1. MULLIN, J.W.: Crystallization. Butterworths, London, 1961.
2. BAMFORTH, A.W.: Industrial Crystallization. Leonard-Hill, London, 1965.
3. HALÁSZ, S.: Kristályosítás. MTA Műszaki Kémiai Kutató Intézet Tudományos Eredményei. Veszprém, 1973.
4. BABOS, B., SIMON, E. and BUCSKY, Gy.: Proceedings of the 2 nd Conference on Applied Physical Chemistry Vol. 2. 237 (1971)
5. GYENIS, J., BLICKLE, T.: Hung. J. Ind. Chem. 3, 265 (1975)

РЕЗЮМЕ

Авторами представляется структурно - теоритический метод целесообразного выбора между разными способами кристаллизации.

В зависимости от кристаллизационных задач, материальных свойств и расходных показателей определяются структурные элементы, построенные из дискретных объектов. Определяется область переменных параметров, относящихся к отдельным кристаллизационным способам.

Решение объясняется на конкретном примере.

COMPUTER ALGORITHM FOR THE SELECTION OF SUITABLE
CRYSTALLIZATION PROCEDURES

M. GALBÁVY*, T. BLICKLE** and G. VERESS***

(* Computer Technology and Automation Research Institute
of the Hungarian Academy of Sciences, Budapest

**Research Institute for Technical Chemistry of the
Hungarian Academy of Sciences, Veszprém

***Department Team of the Hungarian Academy of Sciences
(Budapest Technical University), Budapest)

An important practical result in the sphere of system theoretical research of technical chemical systems is the procedure constructed for the selection of suitable crystallization procedures. A computer programme system was developed in order to make the practical application of the formerly elaborated method easier.

Using the above described computer programme, the rapid selection of suitable crystallization procedures and wide-range application of the method become possible.

In the field of the structural research of technical chemical systems, the algorithm prepared for the selection of suitable crystallization procedures represents a very important practical result. In order to make the practical application easier, a computer algorithm was developed, and with its use the selection of the suitable crystallization procedures becomes possible and the method can be widely applied.

The main point of the algorithm will be shown through the following example: how can a crystalline product be produced satisfying a given demand and what is the suitable crystallization procedure to realize the task. The problem in structural theoretical representation is as follows: the optimum structural element of the structure of the crystallization methods is sought with regard to a given element of the structure of the crystallization parameters, determined by the demands and material constants.

I. The structure of the crystallization methods is given by the following four object classes:

- A - the auxiliary operations of crystallization
- B - the crystallization procedures
- C - the character of heat transfer
- D - the role of the gas

where the elements of A are as follows:

- a₁ - indirect cooling
- a₂ - cooling by evaporation
- a₃ - cooling by direct mixing of the cold and warm solutions
- a₄ - evaporation in vacuum
- a₅ - evaporation
- a₆ - "salting out" by liquid
- a₇ - "salting out" by gas

The elements of B

- b₁ - mechanical mixing
- b₂ - tube reactor with rotating screw
- b₃ - fluidization
- b₄ - rotary film
- b₅ - bubble column

- b_6 - foam column
- b_7 - gas geyser
- b_8 - pulsated separation wall

The elements of C

- c_1 - no heat transfer surface
- c_2 - heat transfer through a wall
- c_3 - heat transfer through an insert (tube)

The elements of D

- d_1 - no gas
- d_2 - gas recirculation
- d_3 - no gas recirculation

II. The structure of crystallization parameters contain parameters related to crystallization problems. The object classes for this task were as follows:

- α - mean relative crystal size
- β - central scattering of the size distribution
- γ - the adhesive properties of crystals on the heat transfer surface
- δ - gas resistance of the solution
- μ - relative economy of the auxiliary processes

where elements of α are the

- α_1
- .
- .
- particle size ranges
- .
- .
- α_8

elements of β β_1

.

. scattering ranges (through the size ranges)

.

 β_7 elements of γ γ_1 - no adhesive γ_2 - less adhesive γ_3 - adhesive γ_4 - strongly adhesiveelements of δ δ_1 - cannot be contacted with gas δ_2 - can be contacted with inert gas δ_3 - can be contacted with any gas

elements of μ are given by the different possibilities of decision, e.g.:

 $\mu_1 = a_1$ the best $\mu_2 = a_2$ the best, etc.

In order to generate the structure the relations between the elements of different objects must be given. These relations corresponded to Boole matrices, where e.g. the elements of AD matrix:

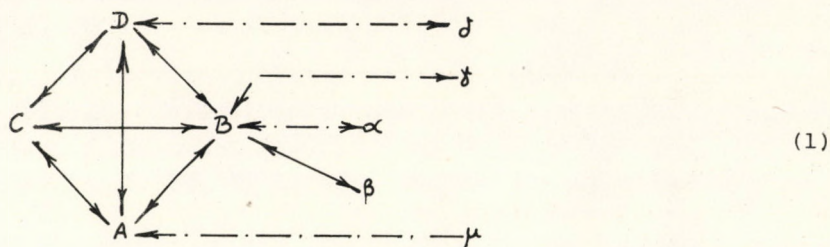
$$(ad)_{ij} = \begin{cases} 1 & \text{if there is connection between the elements of} \\ & a_i \text{ and } d_j \\ 0 & \text{otherwise} \end{cases}$$

So

$$(A, D) = \begin{matrix} & d_1 & d_2 & d_3 \\ \begin{matrix} a_1 \\ a_2 \\ a_3 \\ a_4 \\ a_5 \\ a_6 \\ a_7 \end{matrix} & \begin{bmatrix} 1 & 1 & 1 \\ 0 & 1 & 1 \\ 1 & 1 & 1 \\ 1 & 0 & 0 \\ 0 & 1 & 1 \\ 1 & 1 & 1 \\ 0 & 1 & 1 \end{bmatrix} \end{matrix}$$

In this manner all dual relations between the elements of classes are given. The elements of the structure of the crystallization parameters cannot be given because only a few connections between the object classes of the two structures are known.

In the concrete task, the following connections were known:



where \leftrightarrow represents known relations between the object classes of similar structure
 \leftrightarrow represents known relations between the object classes of two structures.

A ternary connection $(A \wedge C \Rightarrow \gamma)$ also existed among the given relations so it was transformed by an auxiliary connection $- B \wedge C = \phi$ to dual relations and the following system of connections were gained:



This connection system is described in matrix form:

	A	Φ	D	α	β	γ	δ	μ
A		x	x					
Φ	x		x	x	x	x		
D	x	x					x	
α		x						
β		x						
γ		x						
δ			x					
μ	x							

As it can be seen, some elements of the matrix are absent, i.e. these connections must be determined as the first step in solution of the task.

Analgorism was prepared that determines the missing elements by the multiplication of Boole matrices. The multiplication factors can be read from Fig. 2 on the basis of the connections. For example: the relation between Φ and δ is not known. We can reach δ from Φ through D: $(\Phi, \delta) = (\Phi, D) \times (D, \delta)$, where \times represents the Boole multiplication of the two Boole matrices.

If the wanted element cannot be reached through a cross multiplication then similar multiplication of 3 matrices must be carried out, e.g.:

$$(\delta, \mu) = [(\delta, D) \times (D, A)] \times (A, \mu)$$

$$\underbrace{\hspace{1.5cm}}_{(\delta, A)} \quad \times (A, \mu)$$

As the connection matrix is symmetrical the main diagonal can be filled out.

Be the following task with the above relation conditions regarded:

It is known that the material

γ_3 - is adhesive

δ_3 - can be contacted with any gas

The demand is:

α_3 - particle size

α_6 - scattering

We have to determine which is the

A - auxiliary operation of crystallization

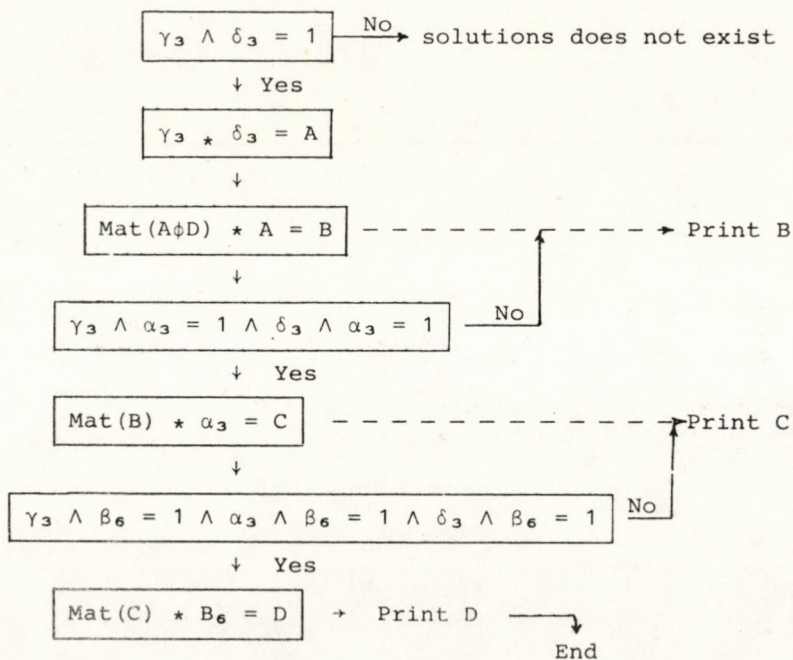
B - crystallization procedure

C - heat transfer surface

D - role of gas

that can be applied.

The algorithm for the given task is as follows:



where $A\phi D$ is the part of relation matrix. It should be remembered that ϕ is an auxiliary connection to eliminate the ternary relation. For this reason, following the solutions, retransformation to the ABCD object classes is necessitated.

As it can be seen from the flow diagram of the algorithm, it may occur that when introducing a new condition a not permitted connection is reached (the condition is not fulfilled). In this case the task is completed by printing the last, still permitted connection.

The programmes were made on SIMULA language for a CDC-3300 computer.

The connection matrix contained 51 lines and columns. The missing parts were calculated within 1 minute. The calculation period of the concrete example was 22 seconds.

The algorithms can be well applied in practice and eliminate calculation that becomes very complicated for more object classes.

РЕЗЮМЕ

Одним из важных практических результатов исследований структуры систем технической химии является способ выбора целесообразных, кристаллизационных процессов.

С целью облегчения практического применения разработанного ранее способа была составлена вычислительная программная система для выбора целесообразных кристаллизационных процессов.

Излагаемая вычислительная программа позволяет производить быстрый выбор целесообразных кристаллизационных процессов и дает широкое применение метода.

OPTIMIZATION OF SALTING OUT CRYSTALLIZATION

Mrs. E. SIMON and R. TÖRÖS

(Research Institute for Technical Chemistry of the
Hungarian Academy of Sciences, Veszprém)

The physical and mathematical model of a salting out crystallization process is given and on the basis of its solution by computer a nomogram and an approximating equation are determined. With the aid of this equation, knowing the material constants and cost functions, the cost of salting out belonging to optimum operation can be calculated. The method makes it possible to compare the different solvents and salting out reagents from an economical point of view and can be applied for economical decision making between auxiliary operations of crystallization.

The term "salting out" means the generation of crystals by the effect of a component decreasing the solubility. Applying the different solubility of compounds in a different solvent and solvent mixtures, the salting out effect can be ensured by adding another solvent (salting out reagent) to the material to be separated and dissolved in a given solvent and thus the solubility of the material is decreased. The extent of solubility decrease depends on the quantity and solution power of the salting out reagent. For salting out under isothermal conditions, the solubility of the salt is determined by Equation (1):

$$c_x = a_3 e^{-a_2 x} + a_3 \quad (1)$$

where

c_x - solubility of the salt in 100 g solvent

x - salting out reagent-solvent ratio

a_1, a_2 and a_3 - material constants

In practice water is usually applied as the solvent, while the most frequently used salting out reagents are the following: ethyl alcohol, methyl alcohol, isopropyl alcohol, acetone and their mixtures. The following viewpoints are usually taken into account in the selection of salting out reagent:

- it has to be mixed well with the original solvent in the desired concentration range;
- it has to dissolve the material to be separated as slightly as possible;
- the salting out reagent must have been regenerated from the final mother lye (e.g.: by distillation).

The optimization method proposed can be applied for a continuous series of operational units that consists of a solvent, a crystallizer and regenerator of the salting out reagent (Figure 1).

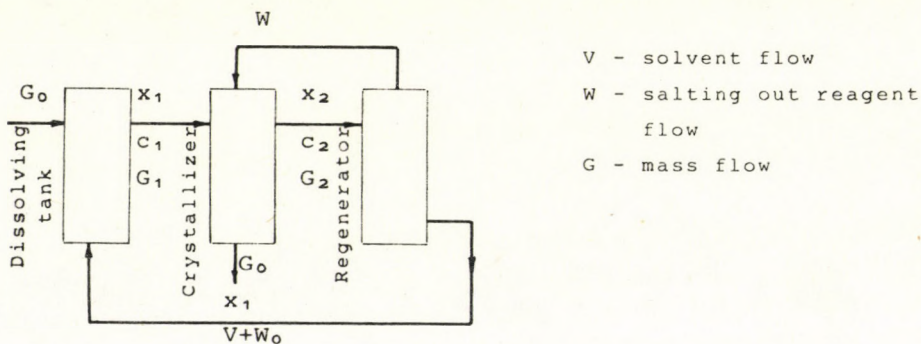


Figure 1

In the solvent G_0 solid material is dissolved. The solution entering the crystallizer contains salt of G_1 quantity, the con-

centration is c_1 and that of the salting out reagent is x_1 , because depending on the separation even the solvent leaving the regenerator contains salting out reagent. In the crystallizer on the effect of W salting out reagent G_0 crystal is separated. The solution leaving the system contains salt of G_2 quantity and the concentration of the salting out reagent increases to x_2 . For the regenerator, the top product is assumed to be clear; it does not contain solvent.

The cost function for the above model is given by Equation (2):

$$N = (\psi_3 + \psi_4 N_{SZ}) \frac{V + W_0 + W}{G_0} \quad (2)$$

The cost is related to the unit quantity of the product and is assumed to be proportional to the mass of the moving solvent.

ψ_3 - cost factor containing costs of solution moving, dissolver and crystallizer;

ψ_4 - cost factor of separation;

N_{SZ} - as it can be seen from Equation (3) takes into account the changes in the separation costs depending on the degree of separation.

$$N_{SZ} = \frac{1}{x_1 - x_\infty} - \frac{1}{x_2 - x_\infty} \quad (3)$$

where

x_∞ - concentration of the salting out reagent in the bottom product for the best possible separation;

x_1 - the actual concentration in the bottom product;

x_2 - concentration of the salting out reagent in the inlet solution.

The optimization method used can determine the operational conditions ensuring the lowest operational cost. In the discussed model - if the product of a given quantity is produced - two parameters can be chosen independently: the recirculation of the

salting out reagent that affects the x_2 value and the degree of separation that determines x_1 . So the optimization is carried out according to these parameters.

The quantity of salt separated in the crystallizer is the following:

$$G_0 = G_1 - G_2 \quad (4)$$

The input and output solvent concentrations:

$$c_1 = \frac{G_1}{V + W_0} = a_1 \cdot e^{-a_2 x_1} + a_3 \quad (5)$$

$$c_2 = \frac{G_2}{V + W_0 + W} = a_1 \cdot e^{-a_2 x_2} + a_3 \quad (6)$$

where

$$x_1 = \frac{W_0}{V} \quad x_2 = \frac{W + W_0}{V}$$

Replacing Equations (3)-(6) to the cost function and performing the possible transformations the cost is gained as a function of x_1 and x_2 :

$$N = \varphi_4 \frac{\left(\frac{\varphi_3}{\varphi_4} + \frac{1}{x_1 - x_\infty} - \frac{1}{x_2 - x_\infty} \right) (1 + x_2)}{(1 + x_1) (a_1 \cdot e^{-a_2 x_1} + a_3) - (1 + x_2) (a_1 \cdot e^{-a_2 x_2} + a_3)} \quad (7)$$

On the basis of the following considerations, the technical optimum for x_2 can be given. The value of x_2 changes depending on the input ratio of W salting out reagent and with increased x_2 the salt content in the solution changes through a minimum value. From Equation (6) the salt content of the solvent:

$$\frac{G_2}{V} = (1 + x) (a_1 \cdot e^{-a_2 x_2} + a_3) \quad (8)$$

For its minimum value

$$\frac{a_3}{a_1} = e^{-a_2 x_M} [a_2(1 + x_M) - 1] \quad (9)$$

where x_M means x_2 value belonging to the minimum. So x_M is constant for a given system and can be determined by Equation (9). It is not certain that the economical optimum is reached at x_M , however, with its aid the salting out reagent range in question is narrowed.

In order to transform the cost function further constants are defined:

$$b_1 = a_2(1 + x_M) \quad (10)$$

$$b_2 = a_2(x_M - x_\infty) \quad (11)$$

$$A = \frac{\varphi_3}{\varphi_4} \cdot (x_M - x_\infty) \quad (12)$$

and passing on new variables taking into account x_M :

$$\varphi = \frac{x_2 - x_1}{x_M - x} \quad 0 < \omega < 1 \quad (13)$$

$$\omega = \frac{x_M - x_2}{x_M - x_2 + x_1 - x} \quad 0 < \varphi < 1 \quad (14)$$

The extreme of cost function given by Equations (10)-(14) has been determined and the result was the following:

$$\hat{y} = \frac{\hat{A} + \frac{1}{1 - \varphi - \eta} - \frac{1}{1 - \eta}}{e^{b_2 \eta + \varphi} - e^{b_2 \eta} - \varphi B} \quad (15)$$

where

$$\eta = \omega(1 - \varphi)$$

$$y = N \frac{a_1 b_2}{a_2 \varphi_4 e^{a_2 x_M}}$$

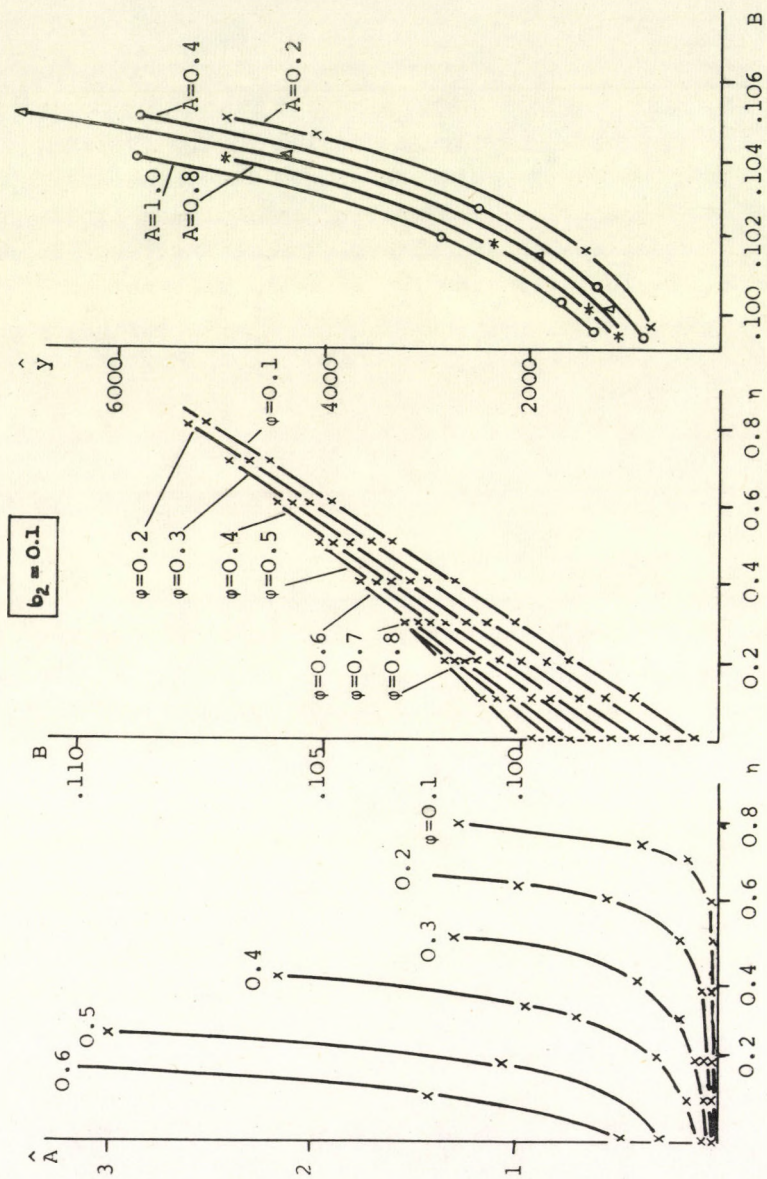


Figure 2

$$B = \frac{(b_1 - 1)b_2}{b_1}$$

Taking into account the possible ranges of parameters in Eq. (15) this was solved by computer. For different b_2 values nomograms shown in Figure 2 were gained. Using these nomograms, - at first - in the knowledge of the solubility data of the studied system and the cost functions constants b_2 , B and \hat{A} can be determined. The latter two values give the \hat{y} value on the nomogram. Using the other two nomograms the connection of η and φ can be determined at \hat{A} and B , and the intersection of the curves marks out the $\eta - \varphi$ pair belonging to the optimum cost and from these η and φ values the operational x_1 and x_2 values can be calculated.

The effect of the different salting out reagents on the cost can be read directly from the nomogram, because they have an effect on the b_2 , B and \hat{A} values of the material properties.

The summary of the results is as follows: by this method the x_1 , x_2 cost belonging to the optimum operation can be given in the knowledge of the material constants (a_1 , a_2 , a_3 , x_M , x_∞) and the cost factors (φ_3 , φ_4). Equation (15) makes it possible to compare the different solvents and salting out reagents from an economical point of view and can even be applied for economical decisions relating to the auxiliary operations of salting out.

РЕЗЮМЕ

Авторами излагается физическая и математическая модель процесса. На основании решения этой модели, проведенного на вычислительной машине, составляется номограмма и приближенное уравнение, с помощью которых - зная материальные постоянные и расходные показатели - можно определить затраты на отсоливание при оптимальной эксплуатации. Метод позволяет экономически сопоставить различные растворители и средства отсоливания, и применим при решении о выборе различных процессов с экономической точки зрения.

STRUCTURE THEORETICAL STUDY OF ABSORPTION-DESORPTION SYSTEMS SEPARATING GAS MIXTURES

O. BORLAI and E. NAGY

(Research Institute for Technical Chemistry of the
Hungarian Academy of Sciences, Veszprém)

In the absorption-desorption systems numerous variations of absorbers can be constructed. These variations can be defined by functions. By the aid of these functions at a given inlet concentration the exit concentrations can be calculated for any variation.

The absorption-desorption cycle can be applied for the separation of gas mixtures. Such a cycle can be realized, e.g. by the aid of a dynamic foam layer. In this case, both in the absorber

and in the desorber a dynamic foam layer is formed and the liquid recirculates between the two foam layers [1]. The scheme of the cycle is shown on Fig.1. In the case of isotherms which can be approximated linearly and assuming a complete mixing, a simple recirculation model can be constructed. The amounts transferred according to the model are as follows [1].

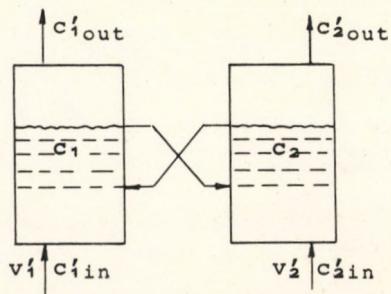


Figure 1

If $K = K' \rightarrow \infty$, then

$$Q = v_1'(c_{1in}' - c_{1out}') \quad (1)$$

$$Q = v_2'(c_{2out}' - c_{2in}') \quad (2)$$

$$Q = \beta_1 F_1 (c_{out}' - H_1 c_1) \quad (3)$$

$$Q = \beta_2 F_2 (H_2 c_2 - c_{2out}') \quad (4)$$

$$Q = w(c_1 - c_2) \quad (5)$$

By the experimental data [2] in the foam layer the mixing is not complete, i.e. $0 < K < \infty$. For this reason Equations (3) and (4) are replaced by differential equations of second order.

A concentration simplex can be given by the aid of Equations (1) - (5). Using this simplex - when gas velocities on both sides and inlet concentration are known - outlet concentration of gas can be calculated.

Each absorption and desorption apparatus is dividable in many layers which can be connected in direct, counter and cross-flow. The latter is realisable by cross-flow both of the gas and liquid.

With regard to the connecting possibility - leaving out of consideration the mixed ones - five cases of layer connection are distinguished. Let a_j represent the connection possibilities of absorbers and \bar{a}_j that of the desorbers.

a_1 or $\bar{a}_1 = 1$ layer (no direct-current connection of layers)

a_2 or $\bar{a}_2 =$ direct-current connection of layers in the absorption and desorption apparatus, respectively

a_3 or $\bar{a}_3 =$ counter-current connection of layers in the absorption and desorption apparatus, respectively

a_4 or $\bar{a}_4 =$ cross-current connection of the gas phase in the absorption apparatus, respectively

a_5 or $\bar{a}_5 =$ cross-current connection of the liquid phase in the absorption and desorption apparatus, respectively.

The absorbers and similarly desorbers can be connected in series and parallel. The parallel connection always increases only the amount (in calculation it means multiplication).

b_1 or \bar{b}_1 = where there is no parallel connection - the multiplier is 1.

b_2 or \bar{b}_2 = the absorbers and desorbers are parallel connected, the multiplier is the number of parallel branches, r and \bar{r} , respectively.

At the connection in series of absorbers and desorbers five cases of connection can also be distinguished.

d_1 or \bar{d}_1 = where there is no connection in series (single absorber or desorber)

d_2 or \bar{d}_2 = direct-current connection of absorbers and desorbers, respectively

d_3 or \bar{d}_3 = counter-current connection of absorbers and desorbers, respectively

d_4 or \bar{d}_4 = cross-current connection of gas phase in the series of absorbers and desorbers, respectively

d_5 or \bar{d}_5 = cross-current connection of liquid phase in the series of absorbers and desorbers, respectively.

The liquid recirculation block can be formed by connection of absorber or absorbers in series with desorbers or desorbers in series. The blocks can also be connected parallel and in series. The blocks naturally can be connected through the gas phase because of the liquid recirculation cycle.

c_1 = where there is no parallel connected block, the multiplier is 1.

c_2 = the blocks are parallel connected, the multiplier is the number of blocks connected parallel, s .

The cases of connection in series of blocks are the following:

g_1 = no connection in series

g_2 = direct-current connection of blocks

g_3 = counter-current connection of blocks

g_4 = cross-current connection of gas phase on absorber side of block series

g_5 = cross-current connection of gas phase on desorber side of block series.

Number of variations when absorbers are connected: $a_j \times b_i \times d_h = 50$, while at desorber connections: $\bar{a}_j \times \bar{b}_i \times \bar{d}_h = 50$, i.e. within the block: $50 \times 50 = 2,500$. Taking into account connection methods of blocks the number of variations: $2,500 \times e_p \times g_q = 2,500 \times 2 \times 5 = 25,000$. In the following, calculation of these numerous variations on the basis of structural theoretical consideration, will be shown.

An organizing algorithm was developed for carrying out calculations comprising comprehending all variations and this algorithm makes the calculation of the outlet concentrations possible in any variation if inlet mass streams and concentrations are known. The organizing algorithm is based on the fact that concentration simplexes can be described from Equations (1)-(5) and these simplexes express the ratio of the differences in the inlet and outlet concentrations. Equations (3) and (4) were solved for direct, and counter-current in the case of $0 < K' < \infty$ gas mixing, and the latter solution was used when the algorithm was constructed, because this solution also involves the case of almost complete mixing. Very complicated differential equations were gained for gas and liquid cross-current. These equations are still not solved, for this reason in the case of cross-current connections solutions of approximately complete mixing can be found in the algorithm.

The following general equation can be given for the layers of absorption apparatus:

$$a_j = f_j A_j^n + f_z \quad (6)$$

The meaning of symbols:

a_j	f_1	f_2	n	A_j
a_1 1 layer	1	0	1	$A_1 = A_3$
a_2 direct-current	1	0	n	$\frac{1}{A_2} = 1 + \frac{B_a (1 + \phi_2) (1 + \sqrt{1 + 4 B_a \phi_2 B'_K})}{(1 + \phi_2) B'_K 2 [1 - \exp - \frac{1 + \sqrt{1 + 4 B_a \phi_2 B'_K}}{2 B'_K}]}$
a_3 counter-current	1	0	n	$A_3 = \frac{\{\exp[\frac{1}{2 B'_K} (1 + \sqrt{1 + 4 B_a \phi_2 B'_K})]\} \frac{2 B_a B'_K}{1 + \sqrt{1 + 4 B_a \phi_2 B'_K}} + 1 - 1\}}{1 + \frac{1}{2} (1 + \sqrt{4 B_a \phi_2 B'_K})}$
a_4 cross-current of gas	$1 + \frac{\phi_2}{n}$	$\frac{\phi_2}{n}$	n	$A_4 = \frac{1 + \phi_2 B_a}{1 + B_a (1 + \phi_2)}$
a_5 cross-current of liquid	$1 + \frac{1}{n \phi_2}$	$-\frac{1}{n \phi_2}$	n	$A_5 = \frac{1 + B_a}{1 + B_a (1 + \phi_2)}$

Similar equations can be described for layers of desorption apparatus, of course, changing the symbols, e.g. $a_1 = \bar{a}_1$ etc.

$$\bar{a}_j = f_j \bar{A}_j^n + f_2 \quad (7)$$

Connection in series of absorbers can also be described in the following equation:

$$d_h = D_h \quad (8)$$

Similarly for connection in series of desorbers:

$$\bar{d}_h = \bar{D}_h \quad (9)$$

The symbols used have the following meanings:

d_h	D_h	\bar{d}_h	\bar{D}_h
$d_1 \left. \begin{array}{l} \\ \end{array} \right\} D_2$	$\frac{1 - a_j^m}{1 + \phi_2}$	$\bar{d}_1 \left. \begin{array}{l} \\ \end{array} \right\} \bar{D}_2$	$\frac{\bar{a}_j^m - 1}{\bar{\phi}_2 + \bar{a}_j^m}$
$d_3 \quad D_3$	$\frac{1 - a_j^m}{1 - \phi_2 a_j^m}$	$\bar{d}_3 \quad \bar{D}_3$	$\frac{\bar{a}_j^m - 1}{(1 - \bar{\phi}_2) \cdot \bar{a}_j^m}$
$d_4 \quad D_4$	$\frac{m + \phi_2 - (m + \phi_2) \left(\frac{\phi_2 + a_j}{1 + \phi_2} \right)^m}{m(1 + \phi_2)}$	$\bar{d}_4 \quad \bar{D}_4$	$\frac{\left(\frac{\bar{\phi}_2 + \bar{a}_j}{1 + \bar{\phi}_2} \right)^{\bar{m}} - 1}{\left(\frac{\bar{\phi}_2 + \bar{a}_j}{1 + \bar{\phi}_2} \right)^{\bar{m}} - \frac{1 - \bar{m}}{1 + \frac{\bar{m}}{\bar{\phi}_2}}}$
$d_5 \quad D_5$	$\frac{1 + m\phi_2 - (1 + \phi_2) \left(\frac{1 + \phi_2 a_j}{1 + \phi_2} \right)^m}{(1 + \phi_2)m\phi_2}$	$\bar{d}_5 \quad \bar{D}_5$	$\frac{\left(\frac{1 + \bar{a}_j \bar{\phi}_2}{1 + \bar{\phi}_2} \right)^{\bar{m}} (+\bar{m}\bar{\phi}_2) - (1 + \bar{m}\bar{\phi}_2)}{\left(\frac{1 + \bar{a}_j \bar{\phi}_2}{1 + \bar{\phi}_2} \right)^{\bar{m}} (1 + \bar{m}\phi_2) - (1 - \bar{m}\phi_2^2)}$

d_1 no connection in series; d_2 direct-current connection;
 d_3 counter-current connection; d_4 cross-current connection
of gas phase; d_5 cross-current connection of liquid phase

Connecting the absorber and desorber to a recirculation block:

$$E = 1 + (\bar{\phi}_2 + \phi_2) \frac{D \bar{D}}{D - \bar{D}} \quad (10)$$

In the case of connection in series of blocks:

g_q	G_q
g_1 no connection in series	$G_2 = E^k$
g_2 direct-current connection	
g_3 counter-current connection	$G_3 = (\phi_1 E^k - 1) / (\phi_1 - E^k)$
g_4 cross-current connection of absorber gas phase	$G_4 = \frac{\phi_1 + k \left(\frac{\phi_1 + E}{\bar{\phi}_1 + 1} \right)^k - \phi_1}{k}$
g_5 cross-current connection of desorber gas phase	$G_5 = \frac{\left(\frac{1 + \phi_1 E}{1 + \bar{\phi}_1} \right)^k (1 + k \phi_1) - 1}{k \phi_1}$

The outlet gas connection to be calculated, if the value of G_q is known, is the following:

$$c_{1 \text{ out}} = \frac{c_{1 \text{ in}} (1 + \phi_1 \cdot G) + c'_{1 \text{ in}} (\phi_1 - \phi_2 G)}{1 + \phi_1} \quad (11)$$

$$c_{2 \text{ out}} = \frac{c_{1 \text{ in}} (1 - G) - c_{2 \text{ in}} (\phi_1 - G)}{1 + \phi_1} \quad (12)$$

As it can be seen the 25,000 variations can be calculated with the aid of six: equations selected for the given case from 25, i.e. 1,000 times fewer equations. A computer programme was worked out and checked for their utilization.

SYMBOLS USED

a	connection in series of layers in the absorber
\bar{a}	connection in series of layers in the desorber
b	parallel connection of absorbers
\bar{b}	parallel connection of desorbers
c_1	component concentration in the liquid phase of absorber
c_2	component concentration in the liquid phase of desorber
c_1^g	component concentration in the gas phase of absorber
c_2^g	component concentration in the gas phase of desorber
d	connection in series of absorbers
\bar{d}	connection in series of desorbers
e	parallel connection of blocks
g	connection in series of blocks
h, i, j	subscripts (1, 2, ...)
k	number of blocks connected in series
m	number of absorbers connected in series
\bar{m}	number of desorbers connected in series
n	number of absorber layers connected in series
\bar{n}	number of desorber layers connected in series
p, g	subscripts (1, 2, ...)
r	number of absorbers connected parallel
\bar{r}	number of desorbers connected parallel
s	number of blocks connected parallel
v_1^g	volumetric flow rate of gas phase in the absorber (m^3/h)
v_2^g	volumetric flow rate of gas phase in the desorber (m^3/h)
w	volumetric flow rate of recirculating liquid (m^3/h)

B_a	$\frac{\beta F}{w}$
B'_k	$\frac{k'F}{v'L}$
F'	cross section of gas phase flow (m^2)
F_1	gas-liquid contact surface in the absorber (m^2)
F_2	gas-liquid contact surface in the desorber (m^2)
H_1	Henry constant in the absorber
H_2	Henry constant in the desorber
K	mixing coefficient of liquid (m^2/h)
K'	mixing coefficient of gas (m^2/h)
L	height of foam layer (m)
Q	amount of transferred material (kg/h)
B_1	mass transfer coefficient in the absorber (m/h)
B_2	mass transfer coefficient in the desorber (m/h)

Subscripts

in	inlet
out	outlet

REFERENCES

1. BORLAI, O., BLICKLE, T.: Proc. 2nd Conf. on Appl. Phys. Chem. Vol. 2. p. 439. Akadémiai Kiadó, Budapest, 1971.
2. FILKA, J.: Doctor techn. Thesis (in Hungarian) Veszprém University of Chemical Engineering, Veszprém, 1974.

РЕЗЮМЕ

В абсорбционно - десорбционных газоразделяющих системах можно составить много вариаций оборудования, принимая во внимание методы связи прямого и перекрестного тока в слоях и аппаратах в газе и жидкости, и параллельную и последовательную связь аппаратов. Эти вариации можно задать с помощью меньшего (примерно на 2 порядка) числа функций. С помощью этих функций - зная входную концентрацию - можно вычислить выходную концентрацию любой вариации связи.

OPTIMIZATION OF ABSORPTION-DESORPTION
SYSTEMS

O. BORLAI and E. NAGY

(Research Institute for Technical Chemistry of the
Hungarian Academy of Sciences, Veszprém)

A cost function was interpreted for the absorption-desorption system. This cost function contains costs of amortization, gas pumping and liquid circulation. Connection variations having better one comparing to them can be determined and eliminated. In this manner number of variations for which the cost function has to be applied decreases considerably.

A computer program applicable for determination of optimum parameters and selection of the most economical one from the possible methods of realization was developed.

The structure theoretical treatment of absorption-desorption systems to a large extent simplifies functions expressing different possibilities of connection. The 25,000 methods of connection can be described by 25 functions [1]. The cost functions relating to different connections can be constructed similarly and knowing them the optimum connection method at a given concentration ratio - which has the smallest value of cost function - can be determined.

In the following, the cost functions, their change at different connection methods and the determination of their optimum value are presented. The cost function of one layer, then that of multilayer apparatuses, series of apparatuses, block and series of

blocks will be given. At parallel connections, if the measurements of apparatuses are similar, the costs are summarized, i.e. these connections do not give new cost functions so the four connection method (direct-current, counter-current, gas cross-current, and liquid cross-current) mean both on the absorption and desorption side $4 \times 4 - 4 \times 4$ variations. The connection of blocks has 4 variations, i.e. number of cost functions is $16 \times 16 \times 4 = 1,024$. Naturally this is also a large number and extreme value of cost function, taking into account the fact that all the variations can be determined most suitably by computer. There is no necessity, however, to calculate all the variations, because with the aid of the treatment elaborated, solutions that were originally uneconomic can be selected.

The cost function for one layer contains the cost of amortization, gas passing through and liquid circulation. The cost parameter (indicated by sign φ ; determines the cost ratio relating to the unit of weight of the investigated apparatus) depending on the characteristic size and thus the diameter and length of apparatus. It means that, e.g. with increased diameter, the change of cost as the function of weight is not linear, but the cost changes to a greater extent. The tendency of change is similar with regard to the height of layer. This means that the costs for one layer are as follows:

Amortization cost:

$$N_{am} = 2\varphi_1(1 + \alpha_4 D^2)D^2 + \varphi_2(1 + \alpha_5 D^2)D^2 + \varphi_3(1 + \alpha_6 D)D \cdot (1 + \alpha_1 Y_0)Y_0 \quad (1)$$

where the first member is the cost of the two covering plates

the second member is the cost of the separating element

the third member is the cost of the mantle.

D = diameter of apparatus (m)

Y_0 = height of layer (m)

As it can be seen in the first two members, dependence of φ on the diameter is expressed by $\varphi(1 + \alpha D^2)$ while in the third mem-

ber, where amortization cost changes linearly with the diameter, this dependence is expressed by $\varphi_3(1 + \alpha_6 D)$. The α parameters are so called penalty parameters, their values depend on the form and type of apparatus.

Similarly the costs can be given of gas and liquid passing through, being proportional to the quantities passed through and the pressure drop in the layer. The function of the costs caused by the pressure drop is not linear, so a penalty parameter can also be used here.

Similarly the cost of gas passing through:

$$N_{\text{gas}} = b_1 v' (1 + \alpha_2 \Delta p'_0) \Delta p'_0 \quad (2)$$

and that of liquid passing through, respectively:

$$N_{\text{liq}} = b_2 v (1 + \alpha_3 \Delta p_0) \Delta p_0 \quad (3)$$

In Equations (2) and (3) $\Delta p'_0$ and Δp_0 are pressure drops of gas and liquid, v' , v are the velocities, α is a penalty factor and b_1 and b_2 are cost ratio of energy.

Taking into account the above mentioned, a given operational and connection method can be constructed from the cost function of one layer. It has to be taken into account that the cost of gas and liquid passing through and that of amortization also change depending on the connection.

Generally, taking into account the connection methods, the following cost function can be given:

$$\begin{aligned} N = & 2\varphi_1 (D^2 + \alpha_4 D^4) m k m_1 k_1 + \varphi_2 (D^2 + \alpha_5 D^4) n m k m_1 k_1 + \varphi_3 (D + \alpha_6 D^2) (Y_0 + \alpha_1 Y_0^2 n) n m k m_1 k_1 + \\ & + b_1 v' \Delta p'_0 (\omega_3 + \omega_4 \omega_5 \alpha_2 \Delta p'_0) \omega_6 m_1 k_1 + b_2 v \Delta p_0 (\omega_1 \omega_2 + \alpha_3 \omega_1 \omega_2^2 \Delta p_0) k m_1 k_1 + \\ & + 2\bar{\varphi}_1 (\bar{D}^2 + \bar{\alpha}_4 \bar{D}^4) \bar{m} k \bar{m}_1 k_1 + \bar{\varphi}_2 (\bar{D}^2 + \bar{\alpha}_5 \bar{D}^4) \bar{n} \bar{m} k \bar{m}_1 k_1 + \bar{\varphi}_3 (\bar{D} + \bar{\alpha}_6 \bar{D}^2) (\bar{Y}_0 + \alpha_1 Y_0^2 \bar{n}) \bar{n} \bar{m} k \bar{m}_1 k_1 + \\ & + \bar{b}_1 \bar{v}' \Delta p'_0 (\bar{\omega}_3 + \bar{\omega}_4 \bar{\omega}_5 \bar{\alpha}_2 \bar{\Delta p}'_0) \bar{\omega}_6 \bar{m}_1 k_1 + \bar{b}_2 \bar{v} \bar{\Delta p}_0 (\bar{\omega}_1 \bar{\omega}_2 + \bar{\alpha}_3 \bar{\omega}_1 \bar{\omega}_2^2 \bar{\Delta p}_0) k \bar{m}_1 k_1 \end{aligned}$$

n = number of layers, m = number of apparatuses (m = connected in

series, m_1 = parallel connected), k = number of blocks (k = connected in series, k_1 = parallel connected).

The cost function also contains costs of the desorption side. The ω and $\bar{\omega}$ values in the cost function, which in all cases are determined by number of layers and apparatuses are positive integers with exception of one connection, and change depending on the connection of layers, apparatuses and blocks, respectively. The ω and $\bar{\omega}$ values are shown in Table 1. Values of the connection of blocks are also given in the Table 1.

Table 1. Values of ω at different connections in the case of absorption

(The $\bar{\omega}$ values relating to desorption are equal to the adequate ω values, while instead of n , values of \bar{n} and \bar{m} have to be given)

apparatus layer	direct- -current	counter- -current	gas cross- -current	liquid-cross- -current
direct and	$\omega_1 = 0$	0	0	0
	$\omega_2 = 0$	0	0	0
counter- -current	$\omega_3 = nm$	nm	n	nm
	$\omega_4 = n^2m^2$	n^2m^2	n^2	n^2m^2
counter- -current	m	m	m	l
	n	n	n	n
	nm	nm	n	nm
	n^2m^2	n^2m^2	n^2	n^2m^2
gas cross- -current	0	0	0	0
	0	0	0	0
	m	m	l	m
	m^2	m^2	l	m^2
liquid cross- -current	m	m	m	l
	$(1 + n)/2$	$(1 + n)/2$	$(1 + n)/2$	$(1 + n)/2$
	nm	nm	n	nm
	n^2m^2	n^2m^2	n^2	n^2m^2

Connections of blocks

direct-current:	$\omega_5 = k$	$\omega_6 = k$	$\bar{\omega}_5 = k$	$\bar{\omega}_6 = k$
counter-current:	$\omega_5 = k$	$\omega_6 = k$	$\bar{\omega}_5 = k$	$\bar{\omega}_6 = k$
abs. gas cross- -current:	$\omega_5 = 1$	$\omega_6 = 1$	$\bar{\omega}_5 = k$	$\bar{\omega}_6 = k$
des. gas cross- -current	$\omega_5 = k$	$\omega_6 = k$	$\bar{\omega}_5 = 1$	$\bar{\omega}_6 = 1$

The optimization essentially means the determination of the connection method at given n , \bar{n} , m and k values giving the smallest concentration simplex, i.e. from the view point of the mass transfer, is the best and at the same time operational costs must be minimum. As it was mentioned, with the aid of this method, connection possibilities, which are uneconomic or do not satisfy the technological demands, can easily be selected. As examples some ideas are mentioned:

- a) the cost of gas passing through is the smallest at gas cross-current, for this reason this connection method can be advantageous with technologies having a low gas lifting height, e.g. flue gas.
- b) The cost of the liquid passing through is zero at the changing connection and at the gas cross-current connection.
- c) The amortization cost can be compared in a simple manner with the energy costs. The application of a smaller diameter assumes an increased length. The optimum values of the diameter and length are evidently determined by the ratio of the energy cost and amortization cost.

Similarly to the aforementioned, numerous other economical and technological points of view can be taken into consideration. So optimization must be carried out only for the remaining variations of connection.

Let us design the functions to be studied separately for the absorption and desorption side:

$$\begin{aligned}
 N_a &= F_a(n, m, k) \\
 N_d &= F_d(\bar{n}, \bar{m}, k) \\
 \phi &= F_\phi(n, \bar{n}, m, \bar{m}, k)
 \end{aligned}
 \tag{6}$$

where ϕ is the ratio of the difference between the outlet and inlet gas concentrations.

From parameters in the cost function and concentration simplex, the outlet concentration at the absorption side determines the outlet concentrations at the desorption side, because a block means a closed system for the liquid phase, i.e. if n and \bar{n} are regarded as independent ones, then m determines the value of \bar{m} .

Taking into account the aforesaid, optimization can be carried out according to the following principle. At first let us optimize the number of layers. At the given m and k values, that of ϕ concentration simplex and cost functions are determined as the function of the change in the number of the layers. From the gained connection, the selected methods ensure the lowest operation cost at the given ϕ value. A similar procedure is also followed at the desorption. Thus the minimum values of n and \bar{n} are gained at given m and k values. Now the cost function contains only m and k as variables:

$$N = N_{a_m}(m, k) + N_{d_m}(m, k) \quad (7)$$

The optimization is carried out similarly to m and k . Thus the connection method, carrying out the given task with lowest cost, is gained. Minimum values of single variables, however, were determined at arbitrary fixed values of the other two variables, so there is no certainty that the ratio of n, \bar{n}, m and k is optimum. For this reason a controlling calculation has to be carried for this connection method by changing the values of n, \bar{n}, m and k .

РЕЗЮМЕ

Истолковывается расходная функция для абсорбционно - десорбционно газоразделительной системы. Эта расходная функция содержит затраты на амортизацию, на прогон газа и циркуляцию жидкости. Можно определить и элиминировать варианты связи, лучше которых всегда можно найти. Таким образом значительно (примерно на 1 порядок) уменьшается число вариантов, для которых нужно применять расходную функцию.

Была выработана программа для вычислительной машины, применимая для определения оптимальных параметров и для выбора наиболее экономичного способа из всех возможных при данных условиях.

DEVELOPING COST FUNCTION OF ROTARY
DRUM VACUUM FILTERS

Mrs. M. PÉTER and G. RÁTKAI

(Research Institute for Technical Chemistry of the
Hungarian Academy of Sciences, Veszprém)

Assuming incompressible sludge, the cost function was defined for immersed multicell vacuum filter with outer filtration surface.

Basic filtration and balance equations valid for the given system are summarized in a form being most convenient for the construction of cost function.

Having defined the cost function an optimum was determined as the function of pressure drop during filtration. Relative costs are expressed from this cost function, which relate to the amount of slurry, filtrate and sludge, respectively.

The application of rotary drum filters is not only widely used in the chemical industry, but also in other industries (e.g. paper-making, and waste-water treatment, etc.). The types of rotary drum filters can be categorized into three mean groups: gravity, pressure and vacuum rotary drum filters. Among them, the use of the rotary drum filters is the most frequent, therefore the cost function of this filter type is reviewed here.

Many different rotary drum vacuum filter designs are known and their operational characteristics also influenced the development of costs, therefore, as a preliminary it was reasonable to fix the characteristics of the system studied.

For the design of the filter, the following suppositions were made: the filter medium is equipped on the external surface of the drum, the drum is a multiple compartment, and is an immersed type (no top feed filter). The type of the cake discharge mechanism (scraper or belt type dischargers) does not play a significant role.

From the point of view of the operational features it is assumed that the filter cake is non-compressible and that the filtration is carried out by a common filter medium (without precoating). Taking into consideration the fact that if the cake or the filtrate is a precious product, the final formulas are expressed separately and the cost function is also expressed with reference to the amount of the slurry to be filtered. The matter of washing was not studied, but on the other hand, the influence of the flocculation could be considered by means of the characteristic particle size.

The basic relationships valid for this system are as follows.

The filtration time is

$$\tau = \frac{\alpha}{360 n} \quad (1)$$

where n is the number of revolutions of the drum (1/s)

α is the immersion angle (grade).

The amount of filtrate is:

$$V = \frac{D \cdot \pi \cdot \alpha}{360} \cdot \ell_D \cdot \sqrt{\frac{\Delta p \tau}{C \mu}} \quad (2)$$

where D is the diameter of the drum (m)

μ is the dynamic viscosity of the liquid (kg/m s)

ℓ_D is the length of the drum (m)

Δp is the pressure drop the filtration (N/m²)

C is a filtration coefficient (1/m²)

In the most general form used in literature [1, 2] the filtration coefficient is:

$$C = \frac{K K_x}{2} \quad (3)$$

where K is a coefficient depending upon the porosity and the sphericity of the filter cake and the characteristic particle size:

$$K = \frac{f_1(\epsilon)}{f_2(\psi)} \cdot \frac{1}{d_e^2} \quad (4)$$

where ϵ is the porosity of the cake (m^3/m^3)

ψ is the sphericity (m^2/m^2)

d_e is the characteristic particle size (m)

and

$$K_x = \frac{x \cdot \rho_l}{(1 - \epsilon) \rho_s (1 - x) - \epsilon \rho_l x} \quad (5)$$

where x is the solid concentration in the slurry ($\frac{\text{kg solid}}{\text{kg slurry}}$)

ρ_l is the density of the liquid (kg/m^3)

ρ_s is the density of the dry solid material (kg/m^3)

Relying upon these findings, if the dependence on the characteristic particle size is to be considered, the filtration coefficient can be written in the following forms:

$$C = A \frac{1}{d_e^2} \quad (6)$$

or

$$C = B \frac{K_x}{d_e^2} \quad (6a)$$

where

$$A = \frac{f_1}{f_2} \frac{K_x}{2}$$

and

$$B = \frac{1}{2} \frac{f_1}{f_2}$$

Taking into account these findings the filtrate capacity is:

$$L = \frac{V}{\tau} = F_D \sqrt{n} \sqrt{\frac{\Delta p d_e^2}{A \mu}} \sqrt{\frac{\epsilon}{360}} \quad (7)$$

where F_D is the filter area of the drum (m^2).

The produced (dry) cake capacity is given by the next equation:

$$S = F_D \cdot \ell_i \cdot n \cdot \rho_s (1 - \epsilon) \quad (8)$$

where ℓ_i is the thickness of the discharged cake (m).

Assuming that the solid content of the filtrate is zero (according to RUDOLF [3] the solid content of the filtrate ranges in an order of mg/m^3) the material balance for the solid material and the filtrate will be:

$$Z x = S \quad (9)$$

$$Z(1 - x) = L \rho_\ell + F_D \cdot \ell_i \cdot n \cdot \epsilon \cdot \rho_\ell \quad (10)$$

where Z is the fed capacity of the slurry (kg/s).

On the basis of these, the thickness of the cake deposited on the drum will be given by the next equation:

$$\ell_i = \frac{L}{F_D \cdot n} \left[\frac{x \cdot \rho_\ell}{(1 - \epsilon) \rho_s (1 - x) - \epsilon \rho_\ell x} \right] \quad (11)$$

Developing the cost function, the filtration pressure drop Δp is chosen as a basic variable, since drawing the two components of the cost as a function of Δp (the annual depreciation of the capital cost and the annual operating cost) their changes show opposite trends (Figure 1).

The capital cost as a function of Δp has a decreasing tendency, since a higher pressure drop will result, working out a given filtration job, using a filter with less filter area. The annual operating cost has an opposite tendency as a higher pres-

sure drop requires a vacuum pump with higher operating cost. (According to PURCHAS [5] the total operating cost of the rotary drum vacuum filter is dominated - at least to an extent of 70 per cent - by the operating cost of the vacuum pump). Taking into account that the ultimate pressure drop, even theoretically, can at best be equal with the atmospheric pressure (p_o) the operating cost function, at a point of $\Delta p = p_o$, tends towards infinity underlining, of course, only in the case of rotary drum vacuum filters.

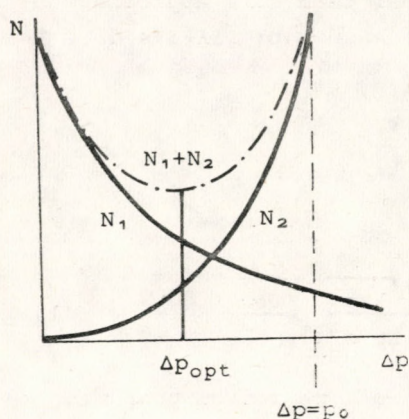


Figure 1

will be as follows:

$$N = N_1 + N_2 \quad (12)$$

where N_1 is the annual depreciation of the capital cost (without considering any interest, but this point does not influence the theoretical development of this method).

$$N_1 = \frac{K_1 \cdot F_D + K'_1}{t} \quad (13)$$

and expressing F_D from Equation (7)

$$N_1 = f(\Delta p) = \frac{K_1}{t} \frac{L}{\sqrt{n}} \sqrt{\frac{K \cdot L}{\Delta p d_g^2}} \sqrt{\frac{360}{a}} + \frac{K'_1}{t} \quad (13a)$$

where K_1 is the capital cost of the rotary drum vacuum filter per quadrate meter (Ft/m^2)

t is the time of depreciation (years)

In the formula the capital cost of the drum filter is taken as a linear function of the filter area. It is not certain that this supposition is absolutely correct, but the dependence of K_1 on F_D cannot be so divergent from linear that this approach would be unacceptable. For example, on the basis of PERRY's data [4] $K_1 \approx 608 F_D + 3,000$ (\$).

The annual operating cost is:

$$N = \frac{K_2}{(p_0 - \Delta p)} F_D \quad (14)$$

and

$$N_2 = f(\Delta p) = \frac{K_2}{(p_0 - \Delta p)} \frac{L}{\sqrt{n}} \sqrt{\frac{A \cdot \mu}{\Delta p d_e^2}} \sqrt{\frac{360}{\alpha}} \quad (14a)$$

where K_2 is the annual operating cost of the vacuum pump with reference to the absolute pressure affecting in the suction duct of the vacuum pump and the filter area:

$$K_2 = \frac{Ft \frac{N}{m^2} \text{ (absolute pressure in the suction duct)}}{\text{year} \times m^2 \text{ (filter area)}}$$

The cost coefficient K_2 , in addition to the dependence on the highness of the vacuum, also depends on the extent of the filter area, since the required volumetric delivery of the vacuum pump is proportional to the filter area. According to PURCHAS the delivery of the vacuum pump ranges between the values of 0.3 and 1.5 m³/min·m² filter area.

In accordance with the above findings the cost function is:

$$N = \left(\frac{K_1}{t} + \frac{K_2}{p_0 - \Delta p} \right) \frac{L}{\sqrt{n}} \sqrt{\frac{A \cdot \mu}{\Delta p d_e^2}} \sqrt{\frac{360}{\alpha}} + \frac{K'_1}{t} \quad (15)$$

From Equation (15) by extreme value calculation the optimum pressure drop is:

$$\Delta p_{opt} = p_0 + \frac{3}{2} \frac{K_2 t}{K_1} - \sqrt{\frac{2 p_0 K_2 t}{K_1} + \frac{9}{4} \frac{K_2^2 t^2}{K_1^2}} \quad (16)$$

Substituting it into Equation (15):

$$N_{\min} = \left(\frac{K_1}{t} + \frac{K_2}{p_o - \Delta p_{\text{opt}}} \right) \frac{L}{\sqrt{n}} \sqrt{\frac{A \mu}{\Delta p_{\text{opt}} d_e^2}} \sqrt{\frac{360}{\alpha}} + \frac{K_1^2}{t} \quad (17)$$

Finally referring the cost function to the amounts of slurry, filtrate and cake:

$$\begin{aligned} \frac{N_{\min}}{Z} &= \left(\frac{K_1}{t} + \frac{K_2}{p_o - \Delta p_{\text{opt}}} \right) \sqrt{\frac{360}{\alpha \cdot n}} \cdot \sqrt{\frac{B \cdot \mu}{\Delta p_{\text{opt}} \cdot d_e^2}} \cdot \\ &\cdot \sqrt{\frac{x(1 - \varepsilon) \rho_s (1 - x) - \varepsilon \rho_\ell x^2}{\rho_s^2 \cdot (1 - \varepsilon)^2 \cdot \rho_\ell}} + \frac{K'}{t \cdot Z} \left[\frac{\text{Ft/year}}{\text{kg/s}} \right] \quad (18) \end{aligned}$$

$$\begin{aligned} \frac{N_{\min}}{L} &= \left(\frac{K_1}{t} + \frac{K_2}{p_o - \Delta p_{\text{opt}}} \right) \sqrt{\frac{360}{\alpha \cdot n}} \sqrt{\frac{B \cdot \mu}{\Delta p d_e^2}} \cdot \\ &\cdot \sqrt{\frac{x \rho_\ell}{(1 - \varepsilon) \cdot \rho_s (1 - x) - \varepsilon \rho_\ell x}} + \frac{K'}{t \cdot L} \left[\frac{\text{Ft/year}}{\text{m}^3/\text{s}} \right] \quad (19) \end{aligned}$$

$$\begin{aligned} \frac{N_{\min}}{S} &= \left(\frac{K_1}{t} + \frac{K_2}{p_o - \Delta p_{\text{opt}}} \right) \sqrt{\frac{360}{\alpha \cdot n}} \sqrt{\frac{B \cdot \mu}{\Delta p_{\text{opt}} d_e^2}} \cdot \\ &\cdot \sqrt{\frac{(1 - \varepsilon) \rho_s (1 - x) - \varepsilon \rho_\ell x}{\rho_s^2 (1 - \varepsilon) x \cdot \rho_\ell}} + \frac{K'}{t S} \left[\frac{\text{Ft/year}}{\text{kg/s}} \right] \quad (20) \end{aligned}$$

Developing this calculation method the fact was neglected that the filtration pressure drop Δp is made up of two parts: the pressure drop of the cake and the pressure drop of the drum which substantially is a constant. If this negligence is not acceptable, then the two parts of the pressure drop have to be separated and the optimizing procedure has to be made according to this. However, this does not create any mathematical problem.

REFERENCES

1. BROWNELL, L.E.: Chem. Eng. Progr. 43, 537, 601, 703 (1974).
2. BROWN, G.G.: Unit Operations. London (1951).
3. RUDOLF, H.: Chemie Ing. Technik 42, 241 (1970).
4. PERRY, J.H.: Vegyész-mérnökök Kézikönyve (Chemical Engineers' Handbook) Budapest, 1968.
5. PURCHAS, D.B.: Industrial Filtration of Liquids Leonard Hill, London (1967).

РЕЗЮМЕ

Авторами была разработана расходная функция для погруженного, многокамерного вакуумного, барабанного фильтра, с внешней фильтрующей поверхностью, предполагалось, что шлам неожидан.

Излагаются основные уравнения фильтрования действительные для данной системы и уравнения баланса в виде, удобном для составления расходной функции.

Составив расходную функцию, авторы определили оптимум расходов в зависимости от падения давления при фильтровании, а потом из полученного таким образом уравнения определяют удельные расходы на единицу количества пульпы, фильтрата и шлама.

STUDIES ON COMPLEX SYSTEMS

T. BLICKLE*, K. SEITZ** and Mrs. E. VASANITS-VARGA*

(*Research Institute for Technical Chemistry of the
Hungarian Academy of Sciences, Veszprém

**Budapest Technical University)

In a complex system two chemical works producing similar final products are studied.

The changes occurring in the system are described by adequate mappings containing cost functions. The resultant mapping of complex systems is determined by a series of mappings to which the profit of the whole system belongs. The optimum graph of the complex system can be constructed if the values of the independent mass flows are changed by a computer so that at given cost factors the profit of the system has a maximum value. The advantage and applicability of the constructed algorithm, e.g. for studying investment and development activities were also examined.

The system to be investigated consisted of two factories producing the same final product. The changes in the material properties, the states within the system and outside, and the geographical displacement relating to the complex system were studied. The outer system is formed by the purchase of the raw material and the sale of final product. In the inner system, the technological mappings and the possible transportation between the two factories were investigated.

In the system the changes are described by mappings containing the cost functions. The series of mappings gives the resulting

mapping of the complex system and the profit of the whole system corresponding to it. The goal of investigations was to determine the optimum set of the complex system that gives the maximum profit.

1. The general determination of mappings

The changes in the elements of three object classes studied in the complex system are described by the appropriate mappings (see Table 1).

Object classes	Elements of object classes	Change	Mappings
A	a_i : materials	v_a : technological change	l_a : technological mapping (1)
L	L_i : geographical places	transportation between the factories $L_1 - L_2$	l_b : mapping of transport (2)
\emptyset	\emptyset_1 : state within the system	$\emptyset_2 - \emptyset_1$: purchase of raw material	l_c : mapping of raw material purchase (3)
	\emptyset_2 : state outside the system	$\emptyset_1 - \emptyset_2$: sale of final product	l_d : mapping of final product sale

The N specific cost function belonging to the given change can be corresponded to the mappings.

The mappings in Table 1 can generally be given by the (1)-(4) expressions:

a) the technological mapping

$$l_a = v_a : g_a \begin{bmatrix} n_1(a_1, L_1, \emptyset_1) \circ n_2(a_2, L_1, \emptyset_1) \\ n_3(a_3, L_1, \emptyset_1) \circ n_4(a_4, L_1, \emptyset_1) \end{bmatrix} \Delta - N_a(g_a) \quad (1)$$

where g_a is the largest common divider of the adequate mass flows;

$-N_a(g_a)$ the technological operational cost depending on the mass flows; it is negative;

b) the mapping of the transport

$$l_b = g_b \begin{bmatrix} a_1 L_1 \emptyset_1 \\ a_1 L_2 \emptyset_1 \end{bmatrix} \Delta - N_b = -\beta_b g_b \quad (2)$$

where g_b the transported mass flow

$-N_b$ the cost of the negative sign for the transport that depends linearly on the mass flow (see β_b transport cost factor).

c) the mapping of raw material purchase

$$l_c = g_c \begin{bmatrix} a_1 L_1 \emptyset_2 \\ a_1 L_1 \emptyset_1 \end{bmatrix} \Delta - N_c(g_c) = -\beta_c g_c \quad (3)$$

where g_c quantity of raw material;

$-N_c$ the cost of the negative sign for the raw material purchase;

β_c specific price of raw material;

d) the mapping of final product sale

$$l_d = g_d \begin{bmatrix} a_{3L_1\emptyset_1} \\ a_{3L_1\emptyset_2} \end{bmatrix} \Delta N_d g_d = \beta_d g_d \quad (4)$$

where g_d quantity of final product;

N_d the positive selling price of the final product that changes linearly with the quantity of the final product;

β_d specific selling price of the final product.

The resulting mapping of the complex system contained only those raw materials and final products that are in \emptyset_2 state, i.e. outside the system. The resulting mapping, at the same time expressed the profit of the whole system that arose and the result of the single costs. In this manner the law of mass conservation is valid for the complex system: the result of the mass flows for all the structure elements being in \emptyset_1 state, i.e. within the system will be 0. As a consequence of the fulfilment of conservation law values of single mass flows can be expressed as a function of the free mass quantities from the algebraic equations described for the mass flows of different structure elements. The goal of optimization for the complex system is to determine by computer algorithm the $g_i(\text{opt})$ optimum values of the free mass flows that ensure a maximum profit for the complex system.

2. Application of the organizing system

The complex system discussed in this paper consists of two nitric acid plants operating at two different L_1 and L_2 places. During the preparation of the organizing programme it was sufficient to give only the l_a technological mappings because from these all mappings automatically resulted. For the raw materials

of technological mapping (1), the mapping of raw material purchase (3) and for the products, the mapping of final product sale (4) must be given. The mapping of transport (2) must be described for the final product of the technological mapping relating to the first plant and for the raw material of the technological mapping of the second plant. So all mappings needed for the optimization of the complex system are gained together with the adequate cost functions.

Then according to the fulfilment of the law of conservation, the suitable mass flows are expressed as functions of the free mass quantities by the collection the structure elements containing \emptyset_1 . The optimum mass flow values belonging to the maximum profit of the whole system are subsequently determined.

The advantage of such an organizing system construction is that any change can be investigated later by additional adequate mapping without the reconstruction of the whole organizing system. The effect of any cost factor affecting the profit of the complex system can be determined simply by the constructed organizing programme. Thus the effect of the price change for the raw material and final product can be followed with attention and the production can rapidly be retooled to optimum mass flow adjusting to the changed cost factors. In addition, the economical system is applicable for preliminary economical calculations in the case of a given development or investment problem.

Furthermore the prepared organizing programme can be used in the study of another complex system being of isomorphous mapping comparing to the studied system.

РЕЗЮМЕ

В сложной системе авторы изучали два химических завода, производящих тождественные конечные продукты.

Изменения, происходящие в системе описываются соответствующими изображениями, содержащими расходные функции. Суммарное отображение получается из ряда отображений, сопряжением пользы всей системы, в целом. Оптимальная часть сложной системы получается, если программа изменяет значение свободовыбранных токов так, чтобы польза системы была максимальной, при данных расходных параметрах. Излагается преимущество и применимость выработанного алгоритма, напр. в случае изучения проблемы развития и инвестификации.

CONTENTS

BLICKLE, T.: Preface	1
BLICKLE, T., SEITZ, K., JUHÁSZ, C. and Mrs. FONÓD-LAKOS, A.: Algebraic Study of Structures	3
SEITZ, K. and GREGA, B.: Recent Results in the Theory of Semigroups of Type α	13
SEITZ, K. and BLICKLE, T.: Application of Outer Direct Products of Semigroups in the Study of Structures	17
SEITZ, K. and BALÁZS, J.: Investigation of the Structure of the Semigroup $(\hat{F}^+x\hat{F}^+, \otimes)$ and of the Partial Semigroup (F^+xF^+, \odot) of the Partial Algebraic Structure $S(\hat{F}^+x\hat{F}^+, \odot, \otimes)$	21
SZÉP, J. and SEITZ, K.: Recent Results in the Theory of Partial Semigroups	27
JUHÁSZ, C.: Continuous Structures	31
BLICKLE, T. and Mrs. E. BÁTOR: Description of Material Systems by Continuous Structure	37
VERESS, G., BLICKLE, T. and GALBAVY, M.: Computer Algorithms for the Investigation of Structures of Systems in Che- mical Engineering	43
BLICKLE, T. and BEZEGB, A.: Algebraic Automaton of Construc- tions	51
BLICKLE T. and GYENIS, J.: The Building Up of the Structure of the Quantitative Algebraical Automatons in the Technical Chemistry	57
BLICKLE, T.: Applicability of System Structures in the Technical Chemistry	65
BLICKLE, T. and NOVÁK, B.: Computer Algorithm for the Determi- nation of the Structure of Chemical Compounds	73
BLICKLE, T. and SZÉPVÖLGYI, J.: Determination of Stoichiometric Equations Constructable from Given Compounds	79
BLICKLE, T.: System of Balance Equations	87
CSUKÁS, B., BLICKLE, T. and ORMÓS, Z.: Investigations of Nume- ricality of Changes in Fluidized Bed Atomization-Granula- tion Prozesses	93
MISKIEWICZ, L. and FÓNAI, L.: Change of Numericality During Milling	101
BLICKLE, T., Mrs. MENYHÁRT, J. and VIRÁG, T.: Analysis of Grinding Kinetics and the Change of Particle Size Distribution and Numericality in a Jet-Mill	109
BLICKLE, T. and VAJDA, T.: The General Treatment of Processes with Inhomogeneity Variation	117
BLICKLE, T., LAKATOS, B., FLÓRIÁN, Gy. and BUCSKY, Gy.: Studies on Inhomogeneity in a Quasi-steady-state System	123
MONOSTORI, E. and BLICKLE, T.: Variance Analysis in a Gas-Solid Fluidized Bed	133

BLICKLE, T. and VIRÁG, T.: Studies on the Applicability of the Momentum Method for Transfer Conditions During the Separation of Homologous Hydrocarbon Series	143
VERESS, G. and CZULEK, A.: Algebraic Investigation of the Connection of Batch and Continuous Operational Units .	149
BLICKLE, T. and Mrs. E. BÁTOR: Determination of the Optimum Technological Procedure	155
Mrs. HALÁSZ, S. and JUHÁSZ, C.: Suitable Choice between the Methods of Crystallization	161
GALBAVY, M., BLICKLE, T. and VERESS, G.: Computer Algorithm for the Selection of Suitable Crystallization Procedures	173
Mrs. SIMON, E. and TÖRÖS, R.: Optimization of Salting out Crystallization	181
BORLAI, O. and NAGY, E.: Structure Theoretical Study of Absorption-Desorption Systems Separating Gas Mixture .	189
Mrs. PÉTER, M. and RÁTKAI, G.: Developing Cost Function of Rotary Drum Vacuum Filters	205
BLICKLE, T., SEITZ, K. and Mrs. VASANITS-VARGA, E.: Studies on Complex Systems	213